

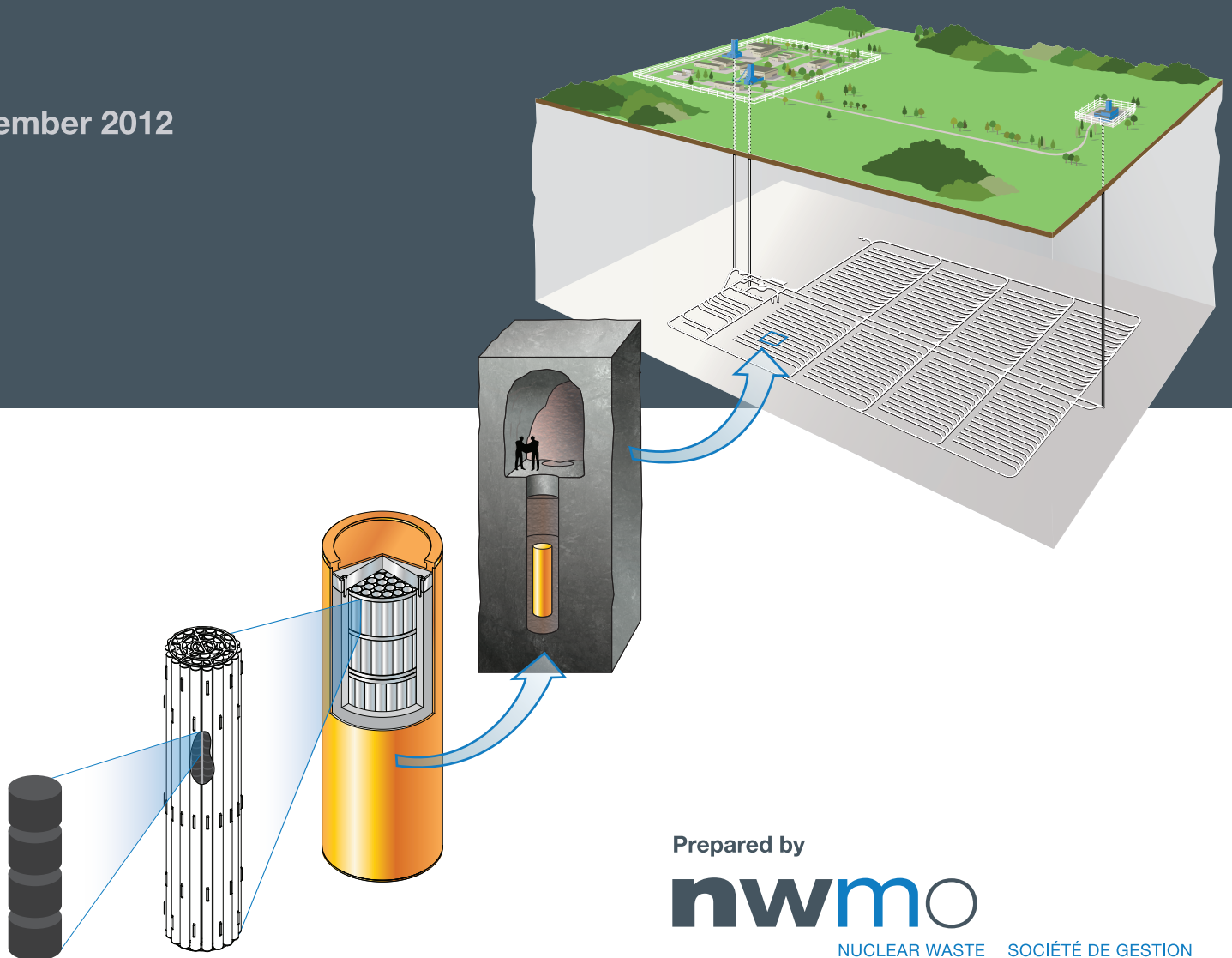
Adaptive Phased Management Used Fuel Repository Conceptual Design and Postclosure Safety Assessment in Crystalline Rock



Pre-Project Report

NWMO TR-2012-16

December 2012



Prepared by

nwmo

NUCLEAR WASTE
MANAGEMENT
ORGANIZATION

SOCIÉTÉ DE GESTION
DES DÉCHETS
NUCLÉAIRES

Nuclear Waste Management Organization
22 St. Clair Avenue East, 6th Floor
Toronto, Ontario
M4T 2S3
Canada

Tel: 416-934-9814
Web: www.nwmo.ca

Adaptive Phased Management

**Used Fuel Repository Conceptual Design and
Postclosure Safety Assessment in Crystalline Rock**

Pre-Project Report

NWMO TR-2012-16

December 2012

Prepared by:

Nuclear Waste Management Organization

EXECUTIVE SUMMARY

The Nuclear Waste Management Organization (NWMO) is responsible for the implementation of Adaptive Phased Management (APM), the federally-approved plan for safe long-term management of Canada's used nuclear fuel. Under the APM plan, used nuclear fuel will ultimately be placed within a deep geological repository in a suitable rock formation.

The repository and its surroundings comprise a system that is designed to protect people and the environment through multiple barriers. These barriers include the ceramic used fuel, long-lived corrosion resistant containers, engineered sealing materials and the surrounding geosphere.

Safety is a priority for the implementation of the APM program. To support the focus on safety, the NWMO conducts a wide range of complementary activities, including research, design development, technology demonstration and safety assessment, which are necessary to assess the performance of the multi-barrier repository concept at timeframes relevant to illustrating long-term safety.

A site selection process is currently underway to identify a safe site in an informed and willing host community. The process of site selection will take several years. As potentially suitable sites are identified with interested communities, detailed field studies and geoscientific site characterization activities will be conducted to assess whether the APM multi-barrier repository concept could be safely implemented to meet rigorous regulatory requirements.

At this very early stage in the process, before specific sites have been identified for examination, it is useful to conduct generic studies to illustrate the long-term performance and safety of the multi-barrier repository system within various geological settings.

This report provides an illustrative case study of the current multi-barrier design and postclosure safety of a deep geological repository in a hypothetical crystalline Canadian Shield setting. The purpose of this case study is to present a postclosure safety assessment methodology to illustrate how Canadian Nuclear Safety Commission (CNSC) expectations, documented in CNSC Guide G-320, Assessing the Long Term Safety of Radioactive Waste Management, are satisfied. For a licence application for a candidate site, a full safety case would be prepared that would include more information on the design and postclosure safety, as well as a detailed description of the geosphere, an environmental assessment, and an operational safety assessment.

Geosphere

A hypothetical geosphere was derived, in part, from historic experience gained in the Canadian Nuclear Fuel Waste Management Program. It was developed for the purpose of this illustrative case study while the NWMO proceeds with the APM siting process and selection of a preferred site in an informed and willing host community. While the hypothetical site represents one example of a possible crystalline rock setting, a range of characteristics are described for alternative settings that are considered in the safety assessment to both illustrate an approach to assess long-term safety and the functionality of various barrier systems.

The long-term safety and performance of a used fuel repository will rely in part on the geologic setting that surrounds the repository. The geosphere will provide a geomechanically and geochemically stable environment. Geomechanical stability enables safe excavation and placement of the containers and engineered barrier system, and isolates the containers from a

wide range of future human and natural events. A stable geochemical environment supports the container durability and minimizes radionuclide mobility. The ability of the geosphere to support these attributes will be dependent on site-specific conditions.

For the purposes of this illustrative assessment, the hypothetical geosphere is divided into three groundwater systems, which are assumed to have the following characteristics:

1. The shallow groundwater system, located near surface between 0 and 150 m below ground surface, is predominately driven by local and sub-regional scale topographic changes. The groundwater velocities in the shallow zone are sufficiently high that mass transport is primarily by advection. The groundwater in this zone is fresh and oxygen-rich with a low total dissolved solids concentration.
2. The intermediate groundwater system between 150 and 700 m below ground surface is a transition zone from fresh and oxygen-rich to more mineralized and becoming chemically reducing with depth. At the hypothetical site, the shift from oxidizing to reducing conditions occurs at a depth of about 150 m. In the intermediate groundwater system, larger domains of low permeability rock tend to decrease mass transport rates.
3. In contrast with the shallow and intermediate groundwater systems, the groundwater in the deep system below 700 m has a higher total dissolved solids concentration and fluid densities, and is under chemically reducing conditions. The groundwater velocity in the rock mass is very small.

Design Concept

The current conceptual design for crystalline rock consists of a repository constructed at a depth of approximately 500 m below surface. The repository contains a network of placement rooms with in-floor boreholes for the base case inventory of 4.6 million used fuel bundles encapsulated in about 12,800 long-lived used fuel containers. The container design consists of a copper outer vessel, or shell, that encloses a steel inner vessel. The outer copper shell provides effective resistance to container corrosion under deep geological conditions, while the inner steel vessel provides strength for the container to withstand expected hydraulic and mechanical loads, including earthquakes and glaciation.

Each borehole in the floor along the placement room centerline has a used fuel container surrounded by a clay-based sealing material of highly-compacted bentonite buffer disks, rings and gap-fill pellets. The placement room above the boreholes is filled with backfill materials such as a bentonite/sand mixture and other sealing materials. Bentonite and sand are durable natural materials that are expected to maintain their properties over the long term. Bentonite is a type of clay that swells on contact with water, resulting in its natural self-sealing property.

Postclosure Safety Assessment

The primary safety objective for the deep geological repository is the long-term containment and isolation of the used nuclear fuel. The safety of the repository would be based on a combination of the geology, engineered design, careful operations, and quality assurance processes including review and monitoring. Safety assessment provides a quantitative evaluation of the overall performance of the repository system and its impact on human health and on the environment. In this respect it is able to identify features or processes that contribute to an understanding and confidence in long-term repository safety.

This illustrative case study focuses on long term or postclosure safety. This is the period after the repository has been filled with used fuel containers, and has been sealed off and closed. Consistent with CNSC Guide G-320, the study identifies scenarios, models and methods for evaluating safety, with which to assess dose consequences and the influence of uncertainties. The results are compared against interim acceptance criteria for protecting persons and the environment.

The assessment does not try to predict the future, but instead examines the consequences for a range of scenarios, from likely to unlikely to “what if”. The likely scenarios are considered under the heading of “Normal Evolution Scenario.”

Normal Evolution Scenario

The normal evolution scenario presented in this report is based on a reasoned extrapolation of the reference case site and repository characteristics over time, consistent with the expectations of CNSC Guide G-320. The report describes why the used fuel copper containers are expected to remain intact over the timeframe of interest. For the purpose of the reference case normal evolution scenario, a small number of containers are assumed to be placed in the repository with undetected defects in the copper shell. Conservatively, these containers are assumed to be positioned within a placement room associated with the shortest travel time through the geosphere to the surface biosphere. The anticipated effects of glaciations on the assessment are also described.

The postclosure safety assessment adopts scientifically informed, physically realistic assumptions for processes and data that are understood and can be justified on the basis of the results of research and/or future site investigation. Where there are high levels of uncertainty associated with processes and data, conservative assumptions are adopted and documented to allow the impacts of uncertainties to be bounded.

For the reference case safety assessment, the primary contributor to the public dose over the long term from an assumed small number of defective used fuel containers is the instant release fraction of Iodine-129, a long-lived radionuclide in used fuel that is non-sorbing in the geosphere. The calculated peak dose for the reference case is about 910 times lower than the interim dose acceptance criterion of 0.3 mSv per year for the normal evolution scenario and occurs at about 100,000 years after closure. The long time to peak dose is due, in part, to the combined performance of the repository barrier systems including the robustness of the long-lived containers, the integrity of the engineered sealing systems and the near-field rock surrounding the repository.

Sensitivity Analyses and Bounding Assessments

Recognizing that there are uncertainties associated with the future evolution of a repository, the NWMO has varied a number of important parameters and assumptions, completed bounding assessments and has developed a number of hypothetical “what-if” scenarios to explore the influence of parameter and scenario uncertainty in assessing long-term safety. This approach is consistent with CNSC Guide G-320 on the use of different assessment strategies.

Key parameters that could potentially affect long-term safety are varied in sensitivity cases to understand the impact of uncertainties in these parameters:

- An increase in fuel dissolution rate by a factor of 10;
- An increase of radionuclide instant release fractions to 10%;

- A range of rock mass hydraulic conductivities that cover a factor of 1,000;
- A decrease in distance between the repository and an assumed transmissive fracture from 25 m to 10 m;
- An increase in container degradation by increasing the assumed undetected container defect area by a factor of 10; and
- A decrease in geosphere sorption with a coincident increase in radionuclide solubility limits.

Some parameters are also pushed beyond the reasonable range of variations in bounding assessments. In these cases, parameters are completely ignored by setting their values to zero or by removing physical limits for the following:

- An increase in radionuclide solubility in groundwater by ignoring solubility limits;
- A decrease in radionuclide sorption in the geosphere by ignoring sorption; and
- A decrease in radionuclide sorption in the near field by ignoring sorption.

The results from the sensitivity analysis and the bounding assessments conducted as part of this illustrative case study are shown in Figure E1.

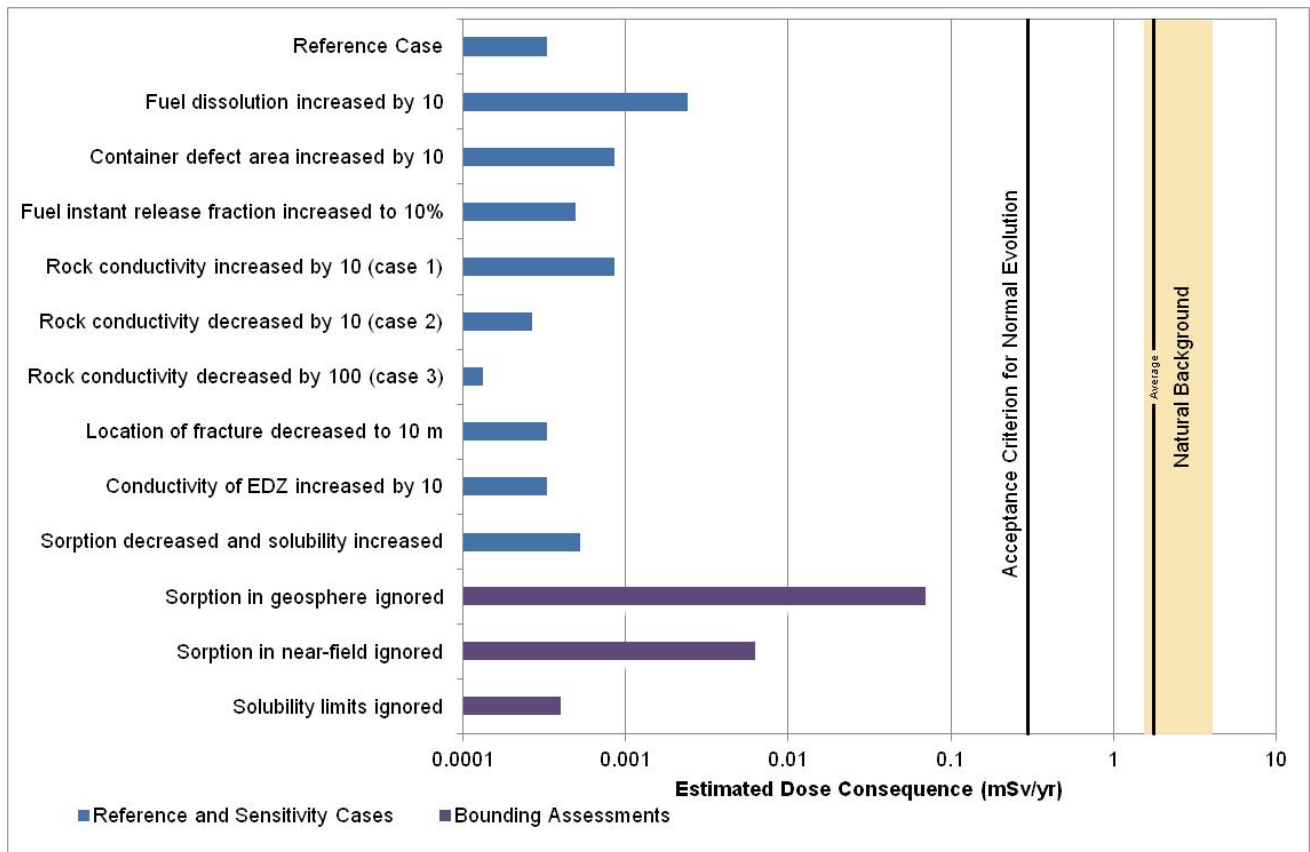


Figure E1: Results from Sensitivity Analysis and Bounding Assessments

The sensitivity analyses show that the impact on dose is small when key parameters are varied. As shown in Figure E1, the parameter with the most significant impact on dose is from the dissolution of ceramic used fuel. This is because the bulk of the radionuclides are retained within the used fuel, which is a low-solubility solid. The dose consequence when the fuel dissolution is increased by a factor of 10 is assessed to be 7.3 times greater than the reference case value.

The bounding assessments show a noticeable increase in dose when sorption in the geosphere is ignored, as well as when sorption in the near field is ignored (see Figure E1). When sorption is ignored in the geosphere, peak dose is increased to 210 times the reference case value and occurs at ~48,000 years (versus 100,000 years in the reference case).

Recognizing the importance of parameters such as used fuel dissolution and sorption as shown in this case study, NWMO maintains active research programs in these areas to continue to improve our understanding of these processes. Nevertheless, the peak dose rate to a member of the public is still estimated to be about 130 times lower than the interim dose acceptance criterion of 0.3 mSv per year.

All the previous results were obtained through deterministic analyses. A further understanding of uncertainties can be obtained through probabilistic modelling. In the present illustrative case study, a probabilistic analysis was conducted on the contaminant release and transport parameters. A total of 120,000 simulations were examined to identify a 95th percentile peak dose rate. The dose consequence in this case is assessed to be 4 times greater than the reference case. This remains 230 times below the interim dose acceptance criterion of 0.3 mSv per year.

Disruptive Scenarios

A number of disruptive or “what-if” scenarios are identified by examining possible failure mechanisms. These scenarios are assessed to evaluate the potential impact of major barrier failures on safety, in accordance with CNSC Guide G-320. The disruptive event scenarios considered in this illustrative case study include:

- Container failures at 60,000 years;
- Container failures at 10,000 years;
- Container failure at 10,000 years with varying hydraulic conductivity; and
- Failure of seals.

The container failure scenarios (i.e., all containers fail at 60,000 years and a variation where all containers fail at 10,000 years due to some unanticipated effect of glaciations such as beyond-design mechanical loading or unexpected changes in groundwater chemistry) indicate a significant increase in the peak dose results. However, the peak doses remain below the interim dose acceptance criterion of 1 mSv per year for disruptive scenarios.

The results also reveal that there is low sensitivity to peak dose to the assumed failure time of all used fuel containers in the reference case geosphere. This occurs primarily as the assumed container failure time is longer than the short-lived fission product decay time. The remaining actinides and most of the remaining long-lived fission products are sorbed within the clay-based

engineered barriers and natural barrier of the enclosing rock mass so that the peak dose rate does not substantially change between these two cases.

The peak results are found to be more sensitive when varying the geosphere hydraulic conductivity at the same time as having all the containers fail at 10,000 years. When the hydraulic conductivity is increased by a factor of 10, the peak dose rate is 1.7 times above the disruptive events interim dose acceptance criterion of 1 mSv per year and it occurs at 17,000 years. This result suggests that a candidate site with a rock mass hydraulic conductivity on the order of 4×10^{-10} m/s or higher would have the potential to exceed the interim dose acceptance criterion for disruptive scenarios.

And finally, a stylized analysis was completed for inadvertent human intrusion. This scenario is a special case, as recognized in CNSC Guide G-320, since it bypasses all the multiple barriers put in place, and therefore the associated dose consequence could exceed the regulatory dose limit. The results show a potential dose to the drill crew, and to a site resident, from early intrusion, exceeds the dose limit. However, the likelihood of this event occurring is very small due to placing the used fuel containers deep underground in a location with institutional controls in place for a period of time, no economically viable mineral resources, and no potable groundwater resources. Normal deep drilling practices (e.g., control of drilling fluids, use of gamma logging, etc.) will also tend to reduce consequences relative to those estimated here. Although the likelihood of human intrusion cannot be readily defined, it will be very low. The annual risk of health effects from human intrusion is estimated to be less than 1 in 100,000 per year.

Conclusion

This report describes the reference design for a deep geological repository in crystalline rock and provides an illustrative postclosure safety assessment approach which is structured, systematic and consistent with CNSC Guide G-320. The illustrative assessment includes a description of the repository system, systematically identifies scenarios, models and methods for evaluating safety, uses different assessment strategies, addresses uncertainty, and compares the results of the assessment with interim acceptance criteria.

The postclosure safety assessment shows, for the normal evolution scenario and associated sensitivity cases, that all radiological and non-radiological interim acceptance criteria are met with substantial margins during the postclosure period. This result is consistent with previous assessments of a deep geological repository in Canada, as well as with safety assessment studies by other national radioactive waste management organizations.

TABLE OF CONTENTS

	<u>Page</u>
EXECUTIVE SUMMARY	i
1. INTRODUCTION.....	1
1.1 Purpose and Scope	1
1.2 Background and Project Overview	2
1.3 APM Project Phases	3
1.3.1 Siting and Preparing for Construction	5
1.3.2 Site Preparation and Construction	5
1.3.3 Operation	5
1.3.4 Extended Monitoring	6
1.3.5 Decommissioning	6
1.4 Repository Timeframes	8
1.4.1 Preclosure Period.....	8
1.4.2 Postclosure Period	8
1.5 Relevant Legislation	11
1.5.1 CNSC Regulatory Requirements	11
1.5.2 Transportation of Used Nuclear Fuel	13
1.5.3 Canadian Codes and Standards	14
1.5.4 Safeguards.....	14
1.5.5 Traditional Knowledge.....	15
1.5.6 International Guidance	15
1.6 Safety Case	16
1.6.1 Safety Case Context	16
1.6.2 Safety Strategy.....	17
1.6.3 Deep Geological Repository System	19
1.6.3.1 Geology.....	19
1.6.3.2 Waste Characteristics	21
1.6.3.3 Design	21
1.6.3.4 Institutional Controls	21
1.6.4 Safety Assessment	22

1.6.5	Management of Uncertainties	22
1.6.6	Iterative Approach	22
1.6.7	Integration of Safety Arguments.....	23
1.6.8	Stakeholder and Regulatory Involvement	25
1.6.9	Management System	26
1.7	International Status of Deep Geological Repositories	27
1.8	Report Structure and Content	28
1.9	References for Chapter 1	30
2.	DESCRIPTION OF A HYPOTHETICAL SITE	33
2.1	Introduction.....	33
2.2	Conceptual Model for Hypothetical Site.....	33
2.2.1	Descriptive Geologic Site Model	33
2.2.1.1	Geologic Description.....	33
2.2.1.2	Surface Features	34
2.2.1.2.1	Topography	34
2.2.1.2.2	Surface Hydrology.....	37
2.2.1.3	Discrete Fracture Network	37
2.2.2	Descriptive Hydrogeologic Site Model	39
2.2.2.1	Groundwater Systems	39
2.2.2.2	Hydraulic Parameters	40
2.2.2.3	Paleohydrogeology Boundary Conditions.....	43
2.2.3	Descriptive Geochemical Site Model	44
2.2.3.1	Geochemical Conditions at the Hypothetical Site	47
2.2.3.2	Microbial Conditions in Crystalline Environments	49
2.2.3.3	Colloids	50
2.2.3.4	Sorption.....	51
2.3	Sub-Regional Scale Hydrogeologic Modelling	51
2.3.1	Modelling Strategy	51
2.3.2	Computational Models	52
2.3.3	System Performance Measures.....	54
2.3.4	Sub-Regional Scale Conceptual Model	54
2.3.4.1	Model Domain and Spatial Discretization	54
2.3.4.2	Model Parameters.....	54

2.3.4.3	Flow Boundary Conditions	54
2.3.4.4	Initial Conditions and Solution of Density-dependent Flow.....	55
2.3.5	Sub-regional Scale Analyses	57
2.3.5.1	Reference Case Simulation	57
2.3.5.2	Temperate Transient Sensitivity Cases	63
2.3.5.3	Paleohydrogeologic Sensitivity Cases	70
2.4	Summary and Conclusions	81
2.5	References for Chapter 2	82
3.	USED FUEL CHARACTERISTICS.....	87
3.1	Used Fuel Description	87
3.1.1	Used Fuel Type and Amount	87
3.1.2	Geometry	87
3.1.3	Burnup and Linear Power	89
3.1.4	Effect of Irradiation	90
3.2	Radionuclide and Chemical Element Inventory.....	94
3.3	References for Chapter 3	101
4.	REPOSITORY FACILITY – CONCEPTUAL DESIGN.....	103
4.1	General Description.....	103
4.2	Surface Facilities	105
4.3	Used Fuel Container.....	108
4.4	Used Fuel Packaging Plant.....	109
4.4.1	Transport Cask Receiving and Unloading.....	110
4.4.2	Module Handling Cells	110
4.4.3	Empty Used Fuel Container Receiving	111
4.4.4	Used Fuel Container Transport within the Plant	111
4.4.5	Fuel Handling Operations	113
4.4.6	Used Fuel Container Processing	113
4.4.6.1	Inerting Station.....	113
4.4.6.2	Welding Station.....	115
4.4.6.3	Machining and NDT Stations	116
4.4.6.4	Handling of Defective Containers	117
4.4.7	Filled Used Fuel Container Storage Cell.....	118
4.4.8	Used Fuel Container Dispatch Hall	118

4.5	Buffer, Backfill and Seals	125
4.5.1	General Description	125
4.5.1.1	Buffer	126
4.5.1.2	Backfill	127
4.5.1.3	Gap Fill.....	129
4.5.1.4	Concrete	129
4.5.1.5	Grout	130
4.5.1.6	Asphalt.....	130
4.6	Sealing Materials Production Plants	131
4.7	Shafts and Hoists	133
4.8	Underground Facility Design	133
4.8.1	Placement Room Geometry and Spacing.....	139
4.8.2	Ventilation System	140
4.9	Repository Construction	140
4.10	Repository Operation	143
4.11	Extended Monitoring	151
4.12	Decommissioning	151
4.12.1	Sealing of Underground Horizontal Openings.....	151
4.12.2	Sealing of Shafts	151
4.12.3	Decommissioning of Monitoring Wells and Sealing of Geological Boreholes	152
4.13	References for Chapter 4	153
5.	LONG-TERM EVOLUTION OF THE MULTIPLE BARRIER SYSTEM	155
5.1	Conceptual Model for the Repository Environment	157
5.1.1	Repository-induced Disturbances	157
5.1.1.1	Excavation Damage Zone.....	158
5.1.1.2	Repository Saturation	159
5.1.2	Changes due to Presence of Waste Placed in the Repository	160
5.1.2.1	Temperature	160
5.1.2.2	Near-Field Chemistry	161
5.1.2.3	Gas Generation.....	162
5.2	Used Fuel	163
5.2.1	Radioactive Decay	164
5.2.2	Changes in Temperature	165

5.2.3	Changes in the UO ₂	167
5.2.3.1	Radionuclide Diffusion	167
5.2.3.2	Changes in the Oxidation State of Fuel	167
5.2.3.3	Build Up of He Gas	167
5.2.3.4	Alpha Radiation Damage	168
5.2.4	Changes in the Zircaloy Cladding	168
5.2.4.1	Zircaloy Creep and Rupture.....	169
5.2.4.2	Uniform Corrosion (Oxidation) of Cladding	169
5.2.4.3	Hydrogen Absorption and Zircaloy Embrittlement	169
5.2.4.4	Delayed Hydride Cracking	170
5.2.4.5	Stress Corrosion Cracking	170
5.2.4.6	Pellet Swelling and Cladding “Unzipping”	170
5.2.5	Other Processes	171
5.2.5.1	Criticality	171
5.2.5.2	Hydraulic Processes	171
5.2.5.3	Mechanical Stresses.....	171
5.2.5.4	Biological Processes.....	171
5.2.6	Confidence and Uncertainties	171
5.3	Evolution of a Used Fuel Container	172
5.3.1	Evolution of Intact Containers	172
5.3.1.1	Irradiation of Container Materials.....	173
5.3.1.2	Changes in Container Temperature.....	174
5.3.1.3	Changes to Mechanical Integrity.....	177
5.3.1.3.1	Early Conditions	177
5.3.1.3.2	Effects of Hydrostatic and Buffer Swelling Pressures	177
5.3.1.3.3	Effects of Glacial Loading.....	178
5.3.1.3.4	Effect of Seismic Stresses.....	178
5.3.1.3.5	Effect of Creep	179
5.3.1.4	Effect of Chemical Processes Inside the Container.....	180
5.3.1.5	Effect of Chemical Processes Outside the Container	181
5.3.1.5.1	Uniform Corrosion	182
5.3.1.5.2	Localized Corrosion.....	187
5.3.1.5.3	Stress Corrosion Cracking	187

5.3.1.5.4	Microbiologically Influenced Corrosion.....	189
5.3.1.6	Summary.....	189
5.3.2	Evolution of a “Breached Used Fuel Container”.....	190
5.3.2.1	Description of Repository Conditions Prior to Saturation for a “Breached Container”.....	191
5.3.2.2	Description of Post-Saturation Processes for a “Breached Container”.....	192
5.3.2.3	Anaerobic Corrosion of the Steel Vessel.....	193
5.3.2.4	Galvanic Corrosion.....	193
5.3.2.5	Plastic Deformation and Rupture of the Copper Shell.....	194
5.3.2.6	Plastic Deformation of the Steel Vessel.....	196
5.3.2.7	Corrosion and Deformation of Zircaloy Cladding.....	197
5.3.2.8	Dissolution of Used Fuel Matrix.....	198
5.3.2.9	Radionuclide Release from the Fuel Pellets.....	200
5.3.2.10	Fate of Released Radionuclides.....	201
5.3.3	Confidence and Uncertainties.....	201
5.4	Evolution of Buffer, Backfill and Seals.....	204
5.4.1	Changes during Saturation and Development of Swelling Pressure.....	204
5.4.2	Temperature Changes.....	208
5.4.3	Chemical Changes.....	210
5.4.4	Changes due to Biological Processes.....	210
5.4.5	Radiation.....	213
5.4.6	Sorption.....	213
5.4.7	Vertical Movement of Containers.....	213
5.4.8	Erosion and Colloid Formation.....	214
5.4.9	Confidence and Uncertainties.....	214
5.5	Long-term Natural Evolution of the Geosphere.....	216
5.5.1	Geological Disturbances.....	216
5.5.1.1	Seismicity and Seismic Hazard Assessment.....	217
5.5.1.2	Fault Rupture and Reactivation.....	217
5.5.1.3	Volcanism.....	217
5.5.2	Climate Change (Glaciation).....	218
5.5.2.1	Glacial Erosion.....	218
5.5.2.2	Glacial Loading.....	219

5.5.2.3	Permafrost Formation (Changes in Groundwater Recharge)	220
5.5.3	Confidence and Uncertainties	226
5.6	Summary	227
5.7	References for Chapter 5	227
6.	SCENARIO IDENTIFICATION AND DESCRIPTION	237
6.1	The Normal Evolution Scenario	238
6.1.1	External FEPs	238
6.1.2	Internal FEPs	247
6.1.3	Description of the Normal Evolution of the Repository System.....	247
6.1.3.1	Events Occurring for Intact Containers	247
6.1.3.2	Events Occurring for Defective Containers.....	251
6.2	Disruptive Event Scenarios	252
6.2.1	Identification of Disruptive Scenarios	252
6.2.2	Description of Disruptive Event Scenarios	272
6.2.2.1	Inadvertent Human Intrusion Scenario	272
6.2.2.2	Shaft Seal Failure Scenario	272
6.2.2.3	Fracture Seal Failure Scenario	273
6.2.2.4	Poorly Sealed Borehole Scenario.....	273
6.2.2.5	Undetected Fault Scenario	273
6.2.2.6	All Containers Fail Scenario.....	273
6.2.2.7	Container Failure	274
6.3	References for Chapter 6	274
7.	POSTCLOSURE SAFETY ASSESSMENT	277
7.1	Interim Acceptance Criteria	278
7.1.1	Interim Acceptance Criteria for the Radiological Protection of Persons.....	278
7.1.2	Interim Acceptance Criteria for the Protection of Persons from Hazardous Substances	279
7.1.3	Interim Acceptance Criteria for the Radiological Protection of the Environment	280
7.1.4	Interim Acceptance Criteria for the Protection of the Environment from Hazardous Substances	282
7.2	Scope	282
7.2.1	Analysis Cases for the Normal Evolution Scenario	282
7.2.2	Analysis Cases for Disruptive Event Scenarios	290

7.2.3	Analyses for Miscellaneous Modelling Parameters.....	291
7.2.4	Analysis Exclusions.....	296
7.3	Conceptual Model.....	297
7.3.1	Used Fuel Containers	299
7.3.2	Engineered Barriers	302
7.3.3	Geosphere	303
7.3.4	Biosphere.....	304
7.4	Computer Codes.....	307
7.5	Analysis Methods and Key Assumptions	313
7.5.1	Overall Approach	313
7.5.2	Radionuclide and Chemical Toxicity Screening Model	316
7.5.3	Detailed Flow and Transport Models	319
7.5.3.1	Sub-Regional Model	322
7.5.3.2	Site-Scale Model.....	326
7.5.3.3	Repository-Scale Model.....	334
7.5.4	System Model	340
7.5.4.1	Radionuclide Source Term	341
7.5.4.2	Repository Model.....	342
7.5.4.3	Geosphere Model	344
7.5.4.4	Biosphere Model.....	355
7.6	Results of Radionuclide and Chemical Hazard Screening Analysis	360
7.7	Results of Detailed 3D Groundwater Flow and Transport Analysis	361
7.7.1	Sub-Regional Model.....	362
7.7.1.1	Flow Results	363
7.7.1.1.1	Reference Case	363
7.7.1.1.2	Sensitivity to Changes in Geosphere Hydraulic Conductivity...	365
7.7.1.1.3	Sensitivity to Discrete Fracture Modelling	370
7.7.2	Site-Scale Model.....	371
7.7.2.1	Flow Results	371
7.7.2.1.1	Reference Case	371
7.7.2.2	Radionuclide Transport Results.....	379
7.7.2.2.1	Location of the Well and Defective Containers	379
7.7.2.2.2	Reference Case	381

7.7.2.2.3	Sensitivity to Changes in Geosphere Hydraulic Conductivity...	387
7.7.2.2.4	Sensitivity to Fracture Location	406
7.7.2.2.5	Sensitivity to Spatial Resolution and Time Step Size.....	409
7.7.2.2.6	Other Sensitivity Cases	413
7.7.2.2.7	Effect of Barriers on Radionuclide Transport	415
7.7.3	Repository-Scale Model	417
7.7.3.1	Flow Results	417
7.7.3.1.1	Reference Case	417
7.7.3.2	Radionuclide Transport Results.....	420
7.7.3.2.1	Reference Case	421
7.8	Results of System Modelling	429
7.8.1	Transport Model Verification	429
7.8.2	Deterministic Analysis	434
7.8.2.1	Reference Case	434
7.8.2.2	Sensitivity to a Degraded Physical Barrier.....	436
7.8.2.3	Sensitivity to a Degraded Chemical Barrier	441
7.8.2.4	Sensitivity to a Higher Geosphere Hydraulic Conductivity.....	447
7.8.3	Probabilistic Analysis	451
7.8.3.1	All Parameters Simultaneously Varied.....	451
7.9	Disruptive Event Scenarios	458
7.9.1	Inadvertent Human Intrusion.....	459
7.9.1.1	Description.....	459
7.9.1.2	Model and Assumptions.....	462
7.9.1.3	Results	465
7.9.2	All Containers Fail	470
7.9.2.1	Model and Assumptions.....	471
7.9.2.2	Results	471
7.9.3	Shaft Seal Failure.....	476
7.9.3.1	Model and Assumptions.....	476
7.9.3.2	Results	476
7.9.4	Fracture Seal Failure.....	476
7.9.4.1	Model and Assumptions.....	476
7.9.4.2	Results	477

7.10	The Effects of Glaciation	477
7.10.1	Description of the Glacial Cycle	477
7.10.2	Hydrogeological Modelling	480
7.10.3	Transport Modelling	484
7.10.4	Biosphere Model and Dose Calculations	485
7.10.5	Applicability to the Pre-Project Review	489
7.11	Other Considerations	490
7.11.1	Complementary Indicators for the Radiological Assessment.....	491
7.11.2	Radiological Protection of the Environment	496
7.11.3	Protection of Persons and the Environment from Hazardous Substances ...	499
7.11.3.1	Contaminants from the Used Fuel Bundles	499
7.11.3.2	Copper Container Chemical Hazard Assessment	504
7.11.3.3	Complimentary Indicators	507
7.11.4	The Effects of Gas Generation.....	508
7.11.4.1	Gas Generation from Metals and Organics	509
7.11.4.2	Gas Generation from Radiolysis and Decay.....	510
7.11.4.3	Volatilization of H ₂ S	510
7.11.4.4	Gas Release and Migration	511
7.11.4.5	Evaluation of Potential Gas Generation Impacts	513
7.12	Summary and Conclusions	515
7.12.1	Scope Overview	515
7.12.2	Results for the Normal Evolution Scenario	517
7.12.3	Results for the Disruptive Event Scenarios.....	521
7.12.4	Conclusion	522
7.13	References for Chapter 7	522
8.	TREATMENT OF UNCERTAINTIES	531
8.1	Approach	531
8.2	Key Uncertainties	534
8.3	References for Chapter 8	535
9.	NATURAL ANALOGUES	537
9.1	Analogues for Used Nuclear Fuel	537
9.1.1	Natural Uranium Deposits	537
9.1.2	Natural Fissioned Uranium.....	539

9.1.3	Roll-Front Uranium Deposits	541
9.1.4	Fractured Uranium Deposits	541
9.2	Analogues for Barriers	541
9.2.1	Metals.....	541
9.2.2	Copper	542
9.2.3	Iron	542
9.2.4	Clays	543
9.3	Analogue for Geosphere	545
9.4	Natural Analogue Summary.....	545
9.5	References for Chapter 9	546
10.	QUALITY ASSURANCE	549
10.1	Introduction	549
10.2	Used Fuel Repository Conceptual Design and Postclosure Safety.....	549
10.2.1	APM Safety Case Project Quality Plan	549
10.2.2	Examples of Peer Review and Quality Assurance	550
10.2.3	Future Safety Case Quality Assurance	551
10.3	References for Chapter 10	551
11.	SUMMARY AND CONCLUSIONS	553
11.1	Purpose of the Pre-Project Report.....	553
11.2	Repository System	554
11.2.1	Geologic Description of the Hypothetical Site	554
11.2.2	Used Fuel.....	555
11.2.3	Design Concept.....	555
11.3	Safety Assessment.....	556
11.3.1	Assessment Strategies	558
11.3.2	Modelling Tools and Computer Codes.....	558
11.3.2.1	Key Assumptions and Conservatisms in Modelling	559
11.3.3	Normal Evolution Scenario.....	561
11.3.3.1	Results from Sensitivity Analyses and Bounding Assessments	563
11.3.3.2	Results from the Probabilistic Analysis	565
11.3.3.3	Results from Complimentary Indicators	566
11.3.4	Disruptive Events Scenarios	566
11.4	Future Work.....	568

11.5	Conclusion	569
11.6	References for Chapter 11	569
12.	SPECIAL TERMS	571
12.1	Units	571
12.2	Abbreviations and Acronyms	572

LIST OF TABLES

	<u>Page</u>
Table 1-1: CNSC Regulatory Documents Applicable to the APM Project	12
Table 1-2: International Guidance Applicable to the APM Project	15
Table 1-3: Status of National Plans for High-Level Waste	27
Table 1-4: Pre-Project Report Content Mapped to CNSC Guide G-320	29
Table 2-1: Physical Hydrogeological Parameters	42
Table 2-2: Hydromechanical Coupling Parameters	43
Table 2-3: CR-10 Porewater Parameters	48
Table 2-4: Geosphere Redox Conditions	49
Table 2-5: Table of Sub-regional Scale Simulations	53
Table 3-1: Used Fuel Parameters	88
Table 3-2: Radionuclide Decay Chains Included in the Radiological Assessment	95
Table 3-3: List of Potentially Significant Chemically Toxic Elements and Radionuclide Decay Chains Included in the Hazardous Substance Assessment	95
Table 3-4: Inventories of Radionuclides of Interest in UO ₂ Fuel for 220 MWh/kgU Burnup and 30 Years Decay Time	97
Table 3-5: ORIGEN-S: Pickering Fuel Inventory Comparison	99
Table 3-6: Inventories of Chemical Elements of Interest in UO ₂ Fuel for 220 MWh/kgU Burnup and 30 Years Decay Time	100
Table 4-1: APM Facility Number and Description	107
Table 4-2: Reference Copper Vessel Parameters	109
Table 4-3: Reference Steel Vessel Parameters	109
Table 4-4: Physical Composition and As-Placed Properties of Potential Clay-Based Sealing System Components	128
Table 4-5: Composition of Various Concretes Proposed for Repository Use	130
Table 4-6: Sealing Materials Attributes	131
Table 4-7: Proposed Sealing System for Shafts	152
Table 5-1: General Parameters	156
Table 5-2: Processes with a Potential Influence on the Near-field Geosphere	157
Table 5-3: Processes with a Potential Influence on the Evolution of Used Fuel Bundles ...	163
Table 5-4: Processes with a Potential Influence on the Evolution of Containers	173
Table 5-5: Typical Instant-release Fractions for Selected Radionuclides	200
Table 5-6: Processes with a Potential Influence on the Evolution of Buffer/Backfill/Seals .	205

Used Fuel Repository Conceptual Design and Postclosure Safety Assessment in Crystalline Rock

Document Number: NWMO TR-2012-16

Revision: 000

Class: Public

Page: xx

Table 5-7:	Processes with a Potential Influence on the Geosphere	216
Table 6-1:	Status of External FEPs for the Normal Evolution of the Repository System	240
Table 6-2:	External FEPs Potentially Compromising Arguments Relating to the Long-Term Safety	253
Table 6-3:	Internal FEPs Potentially Compromising Arguments Relating to Long-Term Safety.....	261
Table 6-4:	Potential Failure Mechanisms and Associated Scenarios	267
Table 6-5:	Additional Scenarios Considered in Other Safety Assessments	271
Table 7-1:	Interim Acceptance Criteria for the Protection of Persons and the Environment from Non-Radiological Impacts	280
Table 7-2:	Interim Acceptance Criteria for the Radiological Protection of the Environment.....	281
Table 7-3:	Sensitivity Cases for the Normal Evolution Scenario.....	285
Table 7-4:	Analysis Cases for Disruptive Event Scenarios	292
Table 7-5:	Modelling Parameter Cases	295
Table 7-6:	RSM, Version RSM110.....	310
Table 7-7:	SYVAC3-CC4, Version SCC4.09	311
Table 7-8:	FRAC3DVS-OPG, Version 1.3	312
Table 7-9:	HIMv2.0	313
Table 7-10:	Screening Model Geosphere Zone Properties	317
Table 7-11:	Cases Considered for the Radionuclide and Chemically Hazardous Element Screening Assessment.....	318
Table 7-12:	Deep Groundwater Composition	319
Table 7-13:	Data for Effective Diffusion Coefficients	320
Table 7-14:	Data for Sorption Coefficients (K_d).....	321
Table 7-15:	Data for Material Porosity and Tortuosity	322
Table 7-16:	Property Descriptors for Flow Model Layers.....	323
Table 7-17:	Site-Scale Model: Flow Model Properties.....	330
Table 7-18:	Repository-Scale Model: Flow Model Properties	335
Table 7-19:	Instant-release Fractions for Selected Radionuclides	341
Table 7-20:	Container Distribution by Repository Sector.....	349
Table 7-21:	Surface Water Discharge Areas	356
Table 7-22:	Soil Properties	357
Table 7-23:	Climate and Atmosphere Parameters.....	358
Table 7-24:	Human Lifestyle Data	359

Table 7-25:	Summary of Screened in Radionuclides and Chemically Hazardous Elements for Each Case Considered.....	360
Table 7-26:	List of Potentially Significant Radionuclides	361
Table 7-27:	List of Potentially Significant Chemically Hazardous Elements	361
Table 7-28:	Fracture Distance Sensitivity: Results for I-129 Transport.....	409
Table 7-29:	Site-Scale Transport Sensitivity Cases.....	413
Table 7-30:	Comparison of Peak Transport Rates to the Geosphere.....	431
Table 7-31:	Comparison of Peak Release Rates to the Surface	432
Table 7-32:	Radionuclide Dose Pathways for the Reference Case	436
Table 7-33:	Result Summary for Defective Physical Barrier Sensitivity Cases.....	441
Table 7-34:	Result Summary for Defective Chemical Barrier Sensitivity Cases	447
Table 7-35:	Statistical Information Concerning the Distribution of the Peak Dose Rate	454
Table 7-36:	Average and Median Peak Dose Rates for Individual Radionuclides.....	455
Table 7-37:	Human Intrusion Pathways Considered in Recent Safety Assessments.....	461
Table 7-38:	Common Parameters for Human Intrusion Scenario	464
Table 7-39:	Exposure Specific Parameters for Human Intrusion Scenario.....	465
Table 7-40:	Results for All Containers Fail at 10,000 Years - Sensitivity to Geosphere Hydraulic Conductivity	475
Table 7-41:	Time History for Reference Glacial Cycle.....	480
Table 7-42:	Reference Values for Indicators	492
Table 7-43:	Comparison of Reference Case Concentrations with Interim Acceptance Criteria for the Radiological Protection of Non-human Biota	496
Table 7-44:	Comparison of No Sorption in Geosphere Sensitivity Case Concentrations with Acceptance Criteria for the Radiological Protection of Non-human Biota ..	497
Table 7-45:	Comparison of All Containers Fail at 60,000 years Disruptive Event Scenario Concentrations with Interim Acceptance Criteria for the Radiological Protection of Non-human Biota	498
Table 7-46:	SYVAC3-CC4 - Concentration Quotients for the Reference Case	500
Table 7-47:	SYVAC3-CC4 - Concentration Quotients for the No Solubility Limits Case	502
Table 7-48:	SYVAC3-CC4 - Concentration Quotients for the All Containers Fail Case.....	504
Table 7-49:	SYVAC3-CC4 - Concentration Maximum Impurity Levels in Copper and Estimated Impurity Element Concentration Quotients for Well Water	507
Table 7-50:	Erosion Fluxes out of the Geosphere	508
Table 7-51:	Result Summary	519
Table 7-52:	Effect of Geosphere Hydraulic Conductivity on the All Containers Fail at 10,000 Years Scenario	522

Table 11-1:	Summary and Key Findings from Sensitivity Analyses and Bounding Assessments	564
Table 11-2:	Summary of Key Findings from Disruptive Events	567

LIST OF FIGURES

	<u>Page</u>	
Figure 1-1:	Illustration of Deep Geological Repository Concept	4
Figure 1-2:	Illustrative APM Implementation Schedule for Planning Purposes	7
Figure 1-3:	Perspective of Past Events and Expected Future Events in Earth's History Including Repository Events	10
Figure 1-4:	Components of the Safety Case	18
Figure 1-5:	Iterative Process for Developing the Safety Case	24
Figure 1-6:	Site Evaluation Process	26
Figure 2-1:	Regional Watershed Boundary and Sub-regional Domain Boundary	35
Figure 2-2:	Sub-regional Watershed including Topography and Surface Hydrology	36
Figure 2-3:	Fracture Network Model Elements	38
Figure 2-4:	Distribution of Fracture Zones	38
Figure 2-5:	Rock Mass and Fracture Zone Conductivity Profile	41
Figure 2-6:	GSM Outputs from Simulation nn2008 for the Grid Cell Containing the Sub-Regional Modelling Domain	45
Figure 2-7:	GSM Outputs from Simulation nn2778 for the Grid Cell Containing the Sub-Regional Modelling Domain	46
Figure 2-8:	Upper Boundary of Total Dissolved Solids Concentrations (g/L) versus Depth...	56
Figure 2-9:	Block Cut View of Steady-State Freshwater Heads.....	58
Figure 2-10:	Initial Total Dissolved Solids Distribution	59
Figure 2-11:	Freshwater Heads for Transient Coupled Density-Dependent Flow and Transport after One Million Years	59
Figure 2-12:	Environmental Heads for Transient Coupled Density-Dependent Flow and Transport after One Million Years.....	60
Figure 2-13:	TDS Distribution after Coupled Density-Dependent Flow and Transport for One Million Years	60
Figure 2-14:	Reference Case Porewater Velocity Magnitudes	61
Figure 2-15:	Reference Case Péclet Number	61

Figure 2-16:	The Ratio of the Vertical Component of Velocity to Velocity Magnitude.....	62
Figure 2-17:	Reference Case Mean Life Expectancies.....	62
Figure 2-18:	Ratio of Velocity Magnitudes of Steady-State Groundwater Flow to Density-Dependent Flow Case	64
Figure 2-19:	Ratio of MLEs of Steady-State Groundwater Flow to Density-Dependent Flow Case	65
Figure 2-20:	TDS Distribution after Coupled Density-Dependent Flow and Transport for One Million Years	65
Figure 2-21:	Difference in Freshwater Heads between Reference Case and Simulation using Initial TDS Distribution from McMurry (2004)	66
Figure 2-22:	Velocity Magnitude Ratios of McMurry (2004) TDS Distribution Simulation to Reference Case Simulation	66
Figure 2-23:	Ratio of MLEs of McMurry (2004) TDS Distribution Simulation to Reference Case Simulation.....	67
Figure 2-24:	Difference in Freshwater Heads between a Simulation using an Increased Rock Mass Hydraulic Conductivity and Reference Case	67
Figure 2-25:	The Total Dissolved Solids Concentrations at One Million Years for an Increased Rock Mass Hydraulic Conductivity.....	68
Figure 2-26:	Ratio of Pore Velocity Magnitudes.....	68
Figure 2-27:	MLE Ratio of Increased Rock Mass Hydraulic Conductivities Simulation Relative to Reference Case Simulation	69
Figure 2-28:	Cumulative Density Function of Mean Life Expectancy within Repository Outline for Temperate Sensitivity Cases	69
Figure 2-29:	Tracer Migration after 120 Thousand Years for Reference Case Paleohydrogeologic Scenario (fr-base-paleo)	72
Figure 2-30:	A Cumulative Density Function of 5% Isochlor Depth for Paleohydrogeologic Sensitivity Cases.....	73
Figure 2-31:	Tracer Migration at 120 Thousand Years for the nn2778 Paleoclimate Boundary Conditions (fr-base-paleo-nn2778).....	73
Figure 2-32:	Tracer Migration at 120 Thousand Years for nn2008 Paleoclimate Boundary Conditions and a Loading Efficiency of 1 (fr-base-paleo-le1)	74
Figure 2-33:	Tracer Migration at 120 Thousand Years for nn2008 Paleoclimate Boundary Conditions and a Loading Efficiency of 0 (fr-base-paleo-le0)	74
Figure 2-34:	Tracer Migration at 120 Thousand Years for nn2008 Paleoclimate Boundary Conditions	75
Figure 2-35:	Péclet Number versus Time for the Reference Case Paleohydrogeological Scenario (fr-base-paleo)	76
Figure 2-36:	Péclet Number versus Time for the nn2778 Paleoclimate Boundary Conditions (fr-base-paleo-nn2778)	77

Figure 2-37:	Péclet Number versus Time for nn2008 Paleoclimate Boundary Conditions and a Loading Efficiency of 1 (fr-base-paleo-le1)	78
Figure 2-38:	Péclet Number versus Time for nn2008 Paleoclimate Boundary Conditions and a Loading Efficiency of 0 (fr-base-paleo-le0)	79
Figure 2-39:	Péclet Number versus Time for nn2008 Paleoclimate Boundary Conditions	80
Figure 3-1:	Typical CANDU Fuel Bundle	89
Figure 3-2:	Typical Microstructure of Unirradiated and Irradiated UO ₂ Fuel	91
Figure 3-3:	Grain Growth in Irradiated UO ₂ Fuel	92
Figure 3-4:	Segregation of Metallic Fission Products from UO ₂ Fuel	92
Figure 3-5:	Illustrative Distribution of Some Fission Products and Actinides within a Used-Fuel Element	94
Figure 4-1:	Illustration of an APM Facility in Crystalline Rock	104
Figure 4-2:	APM Surface Facilities Layout	106
Figure 4-3:	Copper Used-fuel Container and Fuel Basket	108
Figure 4-4:	Shielded Frame and Air-cushion Transporter	112
Figure 4-5:	Inerting Station	114
Figure 4-6:	Welding Station	114
Figure 4-7:	Friction Stir Welding of a Copper Lid	115
Figure 4-8:	Machining Station	116
Figure 4-9:	Non-destructive Testing Station	116
Figure 4-10:	Used Fuel Packaging Plant – Container Transfer Level	119
Figure 4-11:	Used Fuel Packaging Plant – Operation Level	121
Figure 4-12:	Used Fuel Packaging Plant – Cross-Section	123
Figure 4-13:	Illustrative Tunnel Plug in a Hydraulically Active Region	126
Figure 4-14:	Example of a Closed-Die Forging Press	132
Figure 4-15:	Underground Repository Layout	135
Figure 4-16:	Placement Room Longitudinal Section	137
Figure 4-17:	Placement Room Geometry	139
Figure 4-18:	In-floor Borehole Drilling Equipment	142
Figure 4-19:	In-floor Borehole Drilling	142
Figure 4-20:	Legend for Container Placement Equipment	144
Figure 4-21:	Placement Room and In-floor Borehole Cross-Section	145
Figure 4-22:	Container Placement – Sequence of Operations	146
Figure 5-1:	Illustrative Example of the Range of Temperature Variation over Time in a Placement Room	161

Figure 5-2:	Evolution of the Repository Environment from an Initial Warm, Oxidizing Period to a Prolonged Cool, Anoxic Phase.....	162
Figure 5-3:	Radioactivity of Used CANDU Fuel with a Burnup of 220 MWh/kgU.....	164
Figure 5-4:	Amounts of Key Long-Lived Radionuclides in Used Fuel (220 MWh/kg U burnup)	165
Figure 5-5:	Heat Output of a Used Fuel Container with Time	166
Figure 5-6:	Equivalent Volume of Gas at Normal Temperature and Pressure Produced in a CANDU Fuel Element (220 MWh/kgU burnup).....	168
Figure 5-7:	Illustrative Container Cooling Profiles at Three Generalized Locations within a Repository.....	175
Figure 5-8:	Illustrative Variation in Container Surface Temperature over Time for Various Container Designs and Fuel Loading Characteristics	176
Figure 5-9:	Schematic Representation of the Loading History in a Repository.....	178
Figure 5-10:	Reaction Scheme for the Uniform Corrosion of Copper in Compacted Bentonite Saturated with O ₂ -containing Chloride Solution.....	186
Figure 5-11:	Early Evolution of Conditions in a Container with a Small Defect in Copper Shell.....	192
Figure 5-12:	Possible Damage by Iron Oxide Expansion	195
Figure 5-13:	Radiation Dose Rate in Water at the Fuel Surface (220 MWh/kgU Burnup)	199
Figure 5-14:	Hydraulic Conductivity and Swelling Pressure Variation with Porewater Salinity and Effective Montmorillonite Dry Density	206
Figure 5-15:	Thermal Conductivity of 50:50 wt% Bentonite-Sand Buffer (BSB) and of Highly-Compacted Bentonite (HCB).....	208
Figure 5-16:	Temperature versus Time for Three Placement Room Spacings for the In-Floor Borehole Placement Method in the Crystalline Geosphere.....	209
Figure 5-17:	Effect of Water Activity on Aerobic Culturability in Compacted Bentonite	212
Figure 5-18:	Simulated Evolution of Ice Sheet Load.....	220
Figure 5-19:	Aquifers Commonly Found within Regions of Permafrost	221
Figure 5-20:	Simulated Expansion of Hudson Bay Coastline during Glacial Melting.....	222
Figure 5-21:	A Cumulative Density Function of 5% Isochlor Depth for Paleohydrogeologic Sensitivity Cases.....	224
Figure 5-22:	Péclet Number versus Time for the Reference Case Paleohydrogeological Scenario (fr-base-paleo).....	225
Figure 6-1:	External, Repository and Contaminant Factors / FEPs	238
Figure 6-2:	Total Thermal Power of the Repository (Average 220 MWh/kgU Burnup)	248
Figure 7-1:	General Conceptual Model for Defective Containers	298
Figure 7-2:	Conceptual Model for the Waste Form and Container	299

Figure 7-3:	Radiation Dose Rate in Water at the Fuel Surface (220 MWh/kgU Burnup)	301
Figure 7-4:	Conceptual Model for the Geosphere	303
Figure 7-5:	Conceptual Model for the Constant Biosphere	305
Figure 7-6:	Environmental Transfer Model Describing Critical Group Exposure Pathways .	307
Figure 7-7:	Main Computer Codes	308
Figure 7-8:	FRAC3DVS-OPG Model Domains and Basic Features at the Hypothetical Site	315
Figure 7-9:	Sub-Regional Model: EPM Fracture Network and Vertical Hydraulic Conductivity Profile	324
Figure 7-10:	Sub-Regional Model: DFN Fracture Network and Vertical Hydraulic Conductivity Profile	324
Figure 7-11:	Sub-Regional Model: Well Location and Near-Surface Fracture System	325
Figure 7-12:	Site-Scale Model: Coordinate System and Domain Boundary	327
Figure 7-13:	Site-Scale Model: Plan Section	328
Figure 7-14:	Site-Scale Model: Vertical Hydraulic Conductivity Profile	329
Figure 7-15:	Site-Scale Model: Property Assignment on Vertical Cross-Section through Placement Room Seal	331
Figure 7-16:	Site-Scale Model: Property Assignment on Vertical Cross-Section through Main Shaft	331
Figure 7-17:	Site-Scale Model: Property Assignment on Plan View through Placement Rooms	332
Figure 7-18:	Site-Scale Model: 3D Visualization of Reference Case Head Boundary Conditions on Vertical Model Boundaries	333
Figure 7-19:	Repository-Scale Model: 3D Visualization of Domain Elements	334
Figure 7-20:	Repository-Scale Model: 3D View of Repository Room, Tunnel Seals and Three Assumed Defective Containers	335
Figure 7-21:	Repository-Scale Model: Plan View of Sealing Arrangement in Rooms and Tunnel	336
Figure 7-22:	Repository-Scale Model: Vertical Slice along Placement Drift (Y = 0 m)	337
Figure 7-23:	Repository-Scale Model: Vertical Slice through Placement Drift Room Seal (X = 60.5 m)	337
Figure 7-24:	Repository-Scale Model: 3D View Showing Defective Container Source Nodes	338
Figure 7-25:	Repository-Scale Model: 3D View of Reference Case Head Boundary Conditions	339
Figure 7-26:	Radionuclide Release Rates from Three Defective Containers	340
Figure 7-27:	Fuel Dissolution Rate	342

Figure 7-28:	SYVAC3-CC4 Repository Model	343
Figure 7-29:	Origin and Discharge Locations of Advective Transport Pathways for a Well Demand of 911 m ³ /a	346
Figure 7-30:	Repository Sectors and Surface Discharge Locations.....	348
Figure 7-31:	Representative Transport Pathways for the Repository Sectors	350
Figure 7-32:	SYVAC3-CC4 Transport Network Showing Connectivity	353
Figure 7-33:	Sub-Regional Model - Reference Case Advective Velocity and Hydraulic Head at Repository Elevation	363
Figure 7-34:	Sub-Regional Model - Reference Case Vertical Advective Velocity at Repository Elevation.....	364
Figure 7-35:	Sub-Regional Model - Reference Case Advective Velocity and Hydraulic Head on a Vertical Slice through the Well	365
Figure 7-36:	Sub-Regional Model - Hydraulic Conductivity Increase by a Factor of 10: Advective Velocity and Hydraulic Head at Repository Elevation	366
Figure 7-37:	Sub-Regional Model - Hydraulic Conductivity Increase by a Factor of 10: Advective Velocity and Hydraulic Head on a Vertical Slice through the Well	366
Figure 7-38:	Sub-Regional Model - Hydraulic Conductivity Decrease by a Factor of 10: Advective Velocity and Hydraulic Head at Repository Elevation	367
Figure 7-39:	Sub-Regional Model - Hydraulic Conductivity Decrease by a Factor of 10: Advective Velocity and Hydraulic Head on a Vertical Slice through the Well	368
Figure 7-40:	Sub-Regional Model - Hydraulic Conductivity Decrease by a Factor of 100: Advective Velocity and Hydraulic Head at Repository Elevation	369
Figure 7-41:	Sub-Regional Model - Hydraulic Conductivity Decrease by a Factor of 100: Advective Velocity and Hydraulic Head on a Vertical Slice through the Well	369
Figure 7-42:	Sub-Regional Model - Discrete Fracture Network Sensitivity Case Comparison of Velocities and Hydraulic Heads in the Rock Mass at Repository Elevation...	370
Figure 7-43:	Site-Scale Model - Comparison of Hydraulic Heads With Sub-Regional Model at Repository Elevation (-135 mASL)	372
Figure 7-44:	Site-Scale Model - Comparison of Hydraulic Heads With Sub-Regional Model Hydraulic Heads at Repository Elevation	373
Figure 7-45:	Site-Scale Model - Advective Velocities in TDZ Layer.....	374
Figure 7-46:	Site-Scale Model - Advective Transport Pathways	375
Figure 7-47:	Site-Scale Model - Advective Transport Time to the Surface or Water Supply Well.....	376
Figure 7-48:	Site-Scale Model - Advective Transport Discharge Zones	377
Figure 7-49:	Site-Scale Model - Mean Life Expectancy	378
Figure 7-50:	Site-Scale Model - Potential Well Locations	380
Figure 7-51:	Site-Scale Model - Potential Contaminant Source Locations	380

Figure 7-52:	Site-Scale Model - Effect of Different Source Locations on I-129 Transport	381
Figure 7-53:	Site-Scale Model - Reference Case I-129 Concentration at 10,000 Years.....	382
Figure 7-54:	Site-Scale Model - Reference Case I-129 Concentration at 50,000 Years.....	383
Figure 7-55:	Site-Scale Model - Reference Case I-129 Concentration at 500,000 Years.....	384
Figure 7-56:	Site-Scale Model – Reference Case I-129 Concentration at 1 Million Years.....	385
Figure 7-57:	Site-Scale Model – Reference Case 3D View of I-129 Plume at 1 Million Years	386
Figure 7-58:	Site-Scale Model - Reference Case Radionuclide Transport to Well	387
Figure 7-59:	Site-Scale Model - Hydraulic Conductivity Increase by a Factor of 10: I-129 Concentration at 1 ka	388
Figure 7-60:	Site-Scale Model - Hydraulic Conductivity Increase by a Factor of 10: I-129 Concentration at 10 ka	389
Figure 7-61:	Site-Scale Model - Hydraulic Conductivity Increase by a Factor of 10: I-129 Concentration at 50 ka	390
Figure 7-62:	Site-Scale Model - Hydraulic Conductivity Increase by a Factor of 10: I-129 Concentration at 100 ka	391
Figure 7-63:	Site-Scale Model - Hydraulic Conductivity Increase by a Factor of 10: I-129 Concentration at 500 ka	392
Figure 7-64:	Site-Scale Model - Hydraulic Conductivity Increase by a Factor of 10: Radionuclide Transport to Well.....	393
Figure 7-65:	Site-Scale Model - Hydraulic Conductivity Increase by a Factor of 10: C-14 Concentration at 10 ka	394
Figure 7-66:	Site-Scale Model - Hydraulic Conductivity Increase by a Factor of 10: C-14 Concentration at 50 ka	395
Figure 7-67:	Site-Scale Model - Hydraulic Conductivity Decrease by a Factor of 10: I-129 Concentration at 10 ka	397
Figure 7-68:	Site-Scale Model - Hydraulic Conductivity Decrease by a Factor of 10: I-129 Concentration at 100 ka	398
Figure 7-69:	Site-Scale Model - Hydraulic Conductivity Decrease by a Factor of 10: I-129 Concentration at 500 ka	399
Figure 7-70:	Site-Scale Model - Hydraulic Conductivity Decrease by a Factor of 10: I-129 Concentration at 1 Ma	400
Figure 7-71:	Site-Scale Model - Hydraulic Conductivity Decrease by a Factor of 100: I-129 Concentration at 50 ka	402
Figure 7-72:	Site-Scale Model - Hydraulic Conductivity Decrease by a Factor of 100: I-129 Concentration at 100 ka	403
Figure 7-73:	Site-Scale Model - Hydraulic Conductivity Decrease by a Factor of 100: I-129 Concentration at 500 ka	404

Figure 7-74:	Site-Scale Model - Hydraulic Conductivity Decrease by a Factor of 100: I-129 Concentration at 1 Ma	405
Figure 7-75:	Site-Scale Model – Effect of Hydraulic Conductivity on I-129 Transport to the Well.....	406
Figure 7-76:	Site-Scale Model - Fracture Location Sensitivity Plan View	407
Figure 7-77:	Site-Scale Model - Fracture Location Sensitivity Vertical Cross-Section View ..	408
Figure 7-78:	Site-Scale Model - Fracture Location Sensitivity I-129 Transport.....	408
Figure 7-79:	Sub-Regional Model - Spatial Convergence Sensitivity Comparison of Head Contours	410
Figure 7-80:	Site-Scale Model - Spatial Convergence Sensitivity I-129 Plume.....	411
Figure 7-81:	Site-Scale Model - Spatial Convergence Sensitivity I-129 Transport to the Well.....	412
Figure 7-82:	Site-Scale Model - Time Step Convergence Sensitivity - I-129 Transport to the Well.....	413
Figure 7-83:	Site-Scale Model - I-129 Transport in Sensitivity Cases.....	414
Figure 7-84:	FRAC3DVS-OPG - I-129 Transport through Barriers	415
Figure 7-85:	FRAC3DVS-OPG - Ca-41 Transport through Barriers	416
Figure 7-86:	FRAC3DVS-OPG - U-238 Transport through Barriers	416
Figure 7-87:	Transport Surface for the Repository Release	417
Figure 7-88:	Repository-Scale Model - Head at TDZ Elevation	418
Figure 7-89:	Repository-Scale Model - Advective Velocities in TDZ Layer.....	418
Figure 7-90:	Repository-Scale Model - 3D View of Advective Velocity Magnitudes	419
Figure 7-91:	Repository-Scale Model - Advective Transport Pathways.....	420
Figure 7-92:	Repository-Scale Model - Boundary Volume for Calculation of Radionuclide Releases into the Geosphere	421
Figure 7-93:	Repository-Scale Model - I-129 Concentration at 10 ka	422
Figure 7-94:	Repository-Scale Model - I-129 Concentration at 100 ka	423
Figure 7-95:	Repository-Scale Model - I-129 Concentration at 500 ka	424
Figure 7-96:	Repository-Scale Model - I-129 Concentration at 1 Ma	425
Figure 7-97:	Repository-Scale Model - U-238 Concentration at 1 Ma	426
Figure 7-98:	Repository-Scale Model – Cs-135 Concentration at 100 ka.....	427
Figure 7-99:	Repository-Scale Model - Transport Rates for I-129, C-14, Cl-36, Ca-41, Cs-135 and Sn-126.....	428
Figure 7-100:	Repository-Scale Model - Transport Rates for U-234 and U-238	428
Figure 7-101:	Comparison of SYVAC3-CC4 and FRAC3DVS-OPG Transport of I-129, C-14, Cl-36, Ca-41, Sn-126 and Cs-135 to the Geosphere.....	430

Figure 7-102: Comparison of SYVAC3-CC4 and FRAC3DVS-OPG Transport of U-234 and U-238 to the Geosphere	430
Figure 7-103: Comparison of SYVAC3-CC4 and FRAC3DVS-OPG Transport of I-129, C-14, Cl-36 Ca-41 and Cs-135 to the Surface.....	432
Figure 7-104: Comparison of SYVAC3-CC4 and FRAC3DVS-OPG Transport of I-129 and Sn-126 to the Surface for Three Container Failures in Sector 1.....	433
Figure 7-105: SYVAC3-CC4 – Reference Case Total Dose Rate	434
Figure 7-106: SYVAC3-CC4 – Reference Case Individual Radionuclide Dose Rates.....	435
Figure 7-107: SYVAC3-CC4 - Sensitivity to a Factor of 10 Increase in Fuel Dissolution Rate.....	437
Figure 7-108: SYVAC3-CC4 - Sensitivity to a Factor of 10 Increase in Container Defect Area	438
Figure 7-109: SYVAC3-CC4 - Sensitivity to All Instant Release Fractions Set to 10 Percent .	439
Figure 7-110: SYVAC3-CC4 - Result Summary for Defective Physical Barrier Sensitivity Cases	440
Figure 7-111: SYVAC3-CC4 – Sensitivity to No Sorption in the Geosphere.....	442
Figure 7-112: SYVAC3-CC4 – Sensitivity to No Solubility Limits.....	443
Figure 7-113: SYVAC3-CC4 – Sensitivity to No Sorption in the Near Field.....	444
Figure 7-114: SYVAC3-CC4 – Sensitivity to Low Sorption in the Geosphere with Coincident High Solubility Limits.....	445
Figure 7-115: SYVAC3-CC4 - Summary for Defective Chemical Barrier Sensitivity Cases	446
Figure 7-116: SYVAC3-CC4 - Comparison of C-14, Ca-41, Cl-36, Cs-135, I-129, Sn-126 Release Rates to the Surface for Geosphere Hydraulic Conductivity Increased by a Factor of 10	448
Figure 7-117: SYVAC3-CC4 - Total Dose Rate for Geosphere Hydraulic Conductivity Increased by a Factor of 10	449
Figure 7-118: SYVAC3-CC4 - Radionuclide Dose Rates for Geosphere Hydraulic Conductivity Increased by a Factor of 10	450
Figure 7-119: SYVAC3-CC4 - Distribution of Container Failures for 120,000 Simulations	452
Figure 7-120: SYVAC3-CC4 - Distribution of the Peak Dose Rate for Simulations with at Least One Defective Container.....	453
Figure 7-121: SYVAC3-CC4 - Average Dose Rate With 95% Confidence Bounds.....	456
Figure 7-122: SYVAC3-CC4 - Dose Rate Percentile Bands.....	457
Figure 7-123: General Sequence of Events for Inadvertent Human Intrusion	460
Figure 7-124: Inadvertent Human Intrusion - General Conceptual Model	463
Figure 7-125: Inadvertent Human Intrusion - Exposure as a Function of Intrusion Time.....	466
Figure 7-126: Inadvertent Human Intrusion - Exposure Pathway Doses for Drill Crew	467

Figure 7-127: Inadvertent Human Intrusion - Exposure Pathway Dose Rates for Resident	467
Figure 7-128: Dose Rate to Resident as a Function of Arrival Times Assuming Intrusion Occurs 300 Years after Closure	468
Figure 7-129: Effect of Rn-222 and Short-Lived Daughters in Groundshine Pathway on Resident Exposure	469
Figure 7-130: All Containers Fail at 60,000 Years - Dose Rate	472
Figure 7-131: All Containers Fail at 60,000 Years – Contributing Radionuclides	473
Figure 7-132: Sensitivity - All Containers Fail at 10,000 Years - Dose Rate.....	474
Figure 7-133: Sensitivity to Geosphere Hydraulic Conductivity - All Containers Fail at 10,000 Years - I-129 Transport to the Well.....	475
Figure 7-134: Permafrost Depth and Ice Sheet Thickness for Simulation nn2778	478
Figure 7-135: Comparison of Ice Sheet Height for the Reference Glacial Cycle with Simulation nn2778	479
Figure 7-136: Comparison of Permafrost Depths for the Reference Glacial Cycle with Simulation nn2778	479
Figure 7-137: Hydrogeological and Transport Model Domain for Glaciation Study	481
Figure 7-138: Average Vertical Component of Velocity	483
Figure 7-139: Cumulative Average Vertical Advective Flow Distance	484
Figure 7-140: I-129 Mass Flow Rate and Cumulative Mass Flow from the Glaciation Study ..	486
Figure 7-141: I-129 Dose Rate with Glacial Cycles	488
Figure 7-142: Total Dose Rate with Glacial Cycles.....	488
Figure 7-143: SYVAC3-CC4 – Reference Case Results for Complementary Indicators	493
Figure 7-144: SYVAC3-CC4 – Distribution of Complementary Indicators	495
Figure 7-145: SYVAC3-CC4 - Concentration Quotients for the Reference Case	500
Figure 7-146: SYVAC3-CC4 - Concentration Quotients for the No Solubility Limits Case	501
Figure 7-147: SYVAC3-CC4 - Concentration Quotient for the All Containers Fail Case	503
Figure 7-148: FRAC3DVS-OPG - Cu Concentration Over the Repository Site	505
Figure 7-149: FRAC3DVS-OPG - Cu Transport to the Surface	506
Figure 9-1: Cigar Lake Ore Deposit	538
Figure 9-2: Naturally Occurring Fission Reactor	540
Figure 9-3: Copper Analogues	542
Figure 9-4: Bentonite Clay	544
Figure 9-5: 1.5 Ma Sequoia-like Tree Stumps at Dunarobba, Italy	545
Figure 11-1: Illustration of Radionuclide Transport in the Repository System	562

THIS PAGE HAS BEEN LEFT BLANK INTENTIONALLY

1. INTRODUCTION

1.1 Purpose and Scope

The purpose of this report is to show how the conceptual repository design and safety assessment approach addresses general Canadian Nuclear Safety Commission (CNSC) staff expectations, including those of CNSC Guide G-320, Assessing the Long Term Safety of Radioactive Waste Management (CNSC 2006). It presents a case study that illustrates the Nuclear Waste Management Organization's (NWMO) approach to conducting a safety assessment of a repository for used CANada Deuterium-Uranium reactor (CANDU) fuel within a hypothetical Canadian Shield setting. As part of the case study, a reference Adaptive Phased Management (APM) facility is described and assessed. The APM facility is a self-contained complex with a combination of surface and underground engineered structures designed to provide multiple isolation barriers and passive systems to provide long-term containment and isolation. It consists of the surface facilities and the Deep Geological Repository (DGR). The approach, methods and tools for conducting a postclosure safety assessment, which contribute to the repository safety case, are fully described. The results of the safety assessment for a hypothetical site are presented to illustrate the multi-barrier deep geological repository concept and provide evidence of how Canadian regulatory requirements can and will be met.

A licence application to prepare the site and to construct a used fuel repository will be supported by a safety case. A safety case is defined as the integration of arguments and evidence that describe, quantify and substantiate the safety, and the level of confidence in the safety, of the deep geological repository and associated facilities. It includes the collection of scientific and technical arguments and evidence in support of the safety of the APM facility covering the site characterization and geosynthesis, the design, construction and operation of the facility, the assessment of radiation risk during operation and postclosure, and quality assurance of all safety-related work associated with the facility.

This definition is consistent with the CNSC Guide G-320 as well as international guidance. The International Atomic Energy Agency (IAEA) also provides guidance in SSG-23 – Safety Case and Safety Assessment for the Disposal of Radioactive Waste (IAEA 2012), where it notes that the primary objective of a safety case is to allow for informed decisions to be made that are commensurate with the lifecycle phase of the project.

The level of detail in the current study is consistent with the pre-project stage of the APM facility and is not a full safety case. It considers a hypothetical site for a deep geological repository in crystalline rock, and therefore does not include a geosynthesis. It identifies and analyzes key scenarios, but does not assess all possible scenarios associated with the safety case for an actual site. The current study builds upon previous safety studies that were completed by Atomic Energy of Canada Limited (AECL) and Ontario Power Generation.

Site-specific information will be used in a licence application for a selected site for the APM facility. However, at this pre-project stage and in place of site-specific information, data representing a crystalline Canadian Shield setting are used to illustrate how the postclosure safety assessment can be carried out consistent with Canadian regulatory requirements.

A preclosure safety assessment is not included in the present report. However preclosure safety, including transportation safety, and conventional safety, will be assessed as part of a

licence application for a future-selected site. A special project arrangement has been agreed to by NWMO and the CNSC that includes a CNSC review of the design concepts for the APM (CNSC and NWMO 2008). NWMO's request for a regulatory review of this pre-project report is consistent with CNSC Guide G-320 which states that:

"It is up to the applicant to determine an appropriate methodology for achieving the long term safety of radioactive waste based on their specific circumstances; however, applicants are encouraged to consult with CNSC staff throughout the pre-licensing period on the acceptability of their chosen methodology."

This review is similar to other CNSC pre-project reviews conducted for new nuclear power plants.

1.2 Background and Project Overview

Investigations into the long-term management of used nuclear fuel have a long history in Canada. The deep geological repository concept was identified at the start of the Canadian nuclear program. In 1977, a task force commissioned by Energy, Mines and Resources Canada recommended burial in geological formations with a preference for crystalline rock of the Canadian Shield, but noted that other rock types such as sedimentary rock and salt should also be studied (Hare et al. 1977). Also in 1978, the Porter Commission for Electricity Planning in Ontario recommended that an independent committee be established. The committee would be tasked with reporting progress on waste disposal research and demonstration, to support additional power plant capacity in Ontario. Subsequently, the governments of Canada and Ontario initiated the Canadian Nuclear Fuel Waste Management Program in 1980.

Based on this Canadian program and parallel international work, the concept for a deep geological repository was developed by AECL. The work included an underground research laboratory in Manitoba, in which approaches and materials were tested. The AECL concept was then submitted for review by a federal independent environmental assessment panel. For this review, AECL completed two case studies illustrating the deep geological repository concept in crystalline Canadian Shield settings. AECL submitted its Environmental Impact Statement to the federal review panel in 1994. In 1998, the panel made a number of recommendations and identified the following key conclusions (CEAA 1998):

- *"From a technical perspective, safety of the AECL concept has been on balance adequately demonstrated for a conceptual stage of development, but from a social perspective, it has not.*
- *As it stands, the AECL concept for deep geological disposal has not been demonstrated to have broad public support. The concept in its current form does not have the required level of acceptability to be adopted as Canada's approach for managing nuclear fuel wastes."*

After 1995, research on the deep geological repository concept continued under Ontario Power Generation funding. As part of this, Ontario Power Generation completed a case study identified as the "Third Case Study" in 2004, which considered a third hypothetical Canadian Shield site and used current design concepts, data and assessment methodologies (Gierszewski et al. 2004).

The NWMO was created by Canada's nuclear energy generators as a requirement of the *Nuclear Fuel Waste Act* in 2002, which largely incorporated the recommendations from the earlier federal review panel. It required the NWMO to study possible approaches, recommend an approach, and then implement the approved plan for the long-term management of Canada's used nuclear fuel.

In 2005, based on extensive discussions across Canada, the NWMO recommended the APM approach, which consists of both a technical method and a management system. Its key attributes include:

- Ultimate centralized containment and isolation of used nuclear fuel in an appropriate geological formation;
- Phased and adaptive decision-making; and
- Citizen engagement throughout all phases of implementation.

Following the 2007 decision by the Government of Canada to support the recommended approach, the NWMO collaboratively developed with Canadians an approach for the implementation of APM. The NWMO is implementing this approach that is consistent with Canadian federal government policy and with international best practice in its development of a deep geological repository.

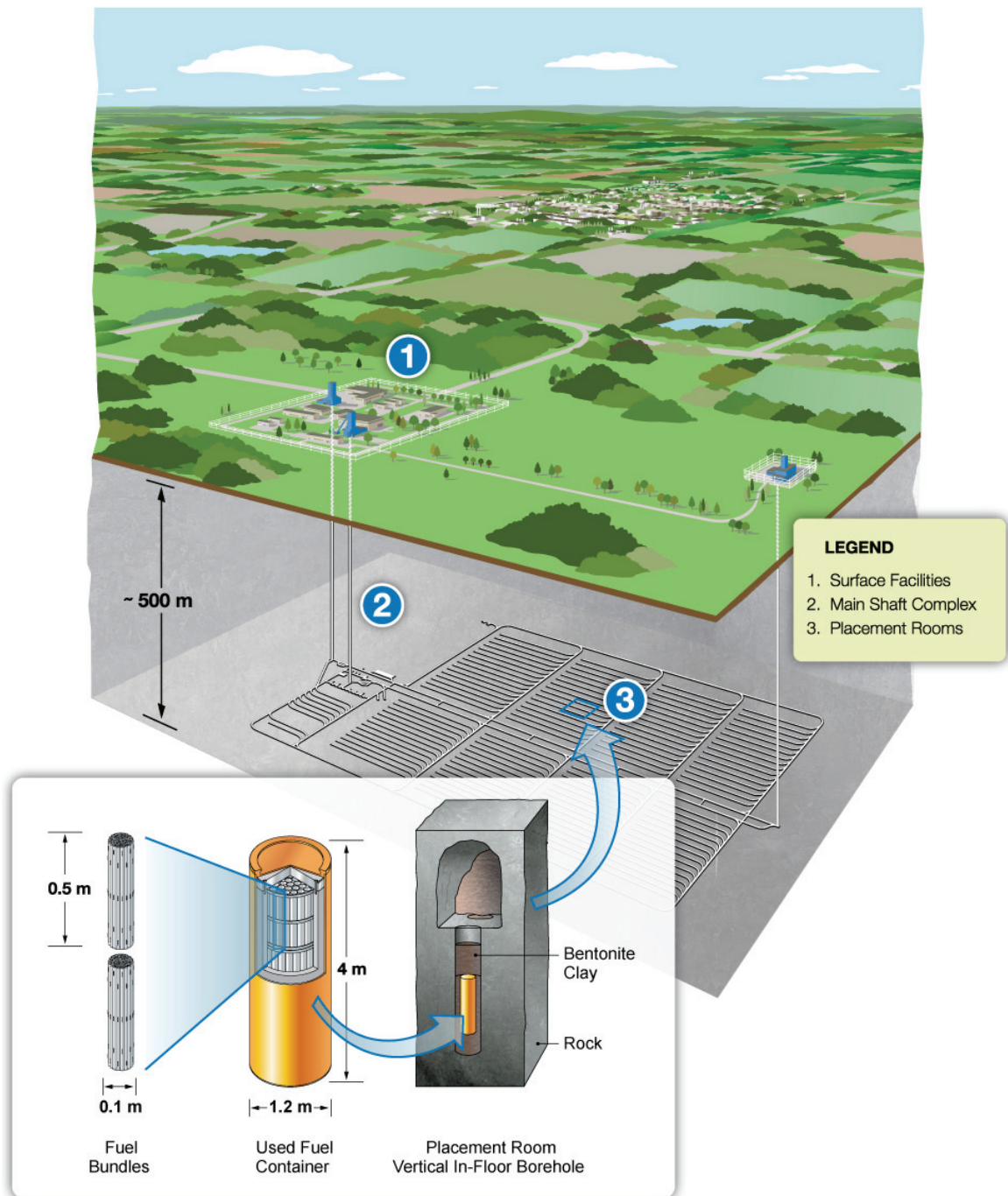
APM includes the development of a deep geological repository, associated surface facilities and a used fuel transportation system. The repository system is a multiple-barrier concept designed to safely contain and isolate used nuclear fuel over the long term. The current conceptual design in crystalline rock consists of a repository constructed for a reference inventory of 4.6 million used CANDU fuel bundles at a depth of approximately 500 metres. It contains a network of placement rooms with in-floor boreholes for used fuel containers (see Figure 1-1). The actual depth of the repository will depend on geologic characteristics at the selected site, along with other design features and safety considerations.

Used fuel will be loaded into licensed transport casks at the interim storage facilities at the reactor sites and transported to the deep geological repository facility where it will be repackaged in corrosion-resistant containers for placement underground. In the reference concept for crystalline rock, the used fuel containers will be transferred underground via a shaft, placed in in-floor boreholes and surrounded by clay material, with the remaining void spaces backfilled and sealed.

1.3 APM Project Phases

The APM project is divided into phases that are linked to the major licensing activities for a nuclear facility in Canada. NWMO is committed to a step-wise decision-making process and will only proceed to the next step after careful consideration and with societal support. Assumed progress through the phases of APM is based on a number of assumptions and decisions, which may differ in terms of scope of work and timing of activities.

This section briefly describes the phases of APM, along with the milestones and the assumed timeline associated with each, providing context for the broader implementation plan. The timeline illustrating these phases is provided in Figure 1-2. The legal framework that governs these licensing activities is further described in Section 1.5.



Note: This figure is not to scale.

Figure 1-1: Illustration of Deep Geological Repository Concept

1.3.1 Siting and Preparing for Construction

The Site Selection Process was launched by the NWMO in 2010 after a dialogue with interested Canadians. It has been designed to identify an informed and willing host community for the APM facility and to ensure that the site selected to host the facility will safely contain and isolate used nuclear fuel. The Site Selection Process is a nine-step process based on social and technical considerations. Site screening criteria have been established to ensure that documented safety criteria are defined at an early step in the siting process. These criteria will be used in the site evaluations, which include studies to confirm site suitability that could support a future licence application. Section 1.6.3 of this report highlights the evaluation factors used in the process. The timeframe associated with completing surface and subsurface investigations at a candidate site is about 5 years.

An application for a licence to prepare the site and to construct the facility will be submitted for a selected site. Licences are issued under the *Nuclear Safety and Control Act*. Licences can only be issued once an environmental assessment has been completed and a series of steps in the CNSC's licensing process have been completed. This phase of the project is expected to last five years or more and will begin by submitting a project description to the CNSC. Subsequently, a Preliminary Safety Report, an Environmental Impact Statement (EIS) and other supporting documents, will demonstrate compliance with the regulatory requirements as set out in the *Nuclear Safety and Control Act* and its associated regulations, as well as in the EIS Guidelines.

1.3.2 Site Preparation and Construction

On receipt of the licence to prepare the site and construct the facility, the site will be prepared for construction by clearing, site grading, installing fencing, installing temporary construction services, and establishing a stormwater management system. The first phase of construction will be to excavate the shafts and an underground demonstration facility. This phase is expected to last about five years, the time needed to sink the shafts, construct the demonstration facility, complete the detailed design and update the safety case. It is described in more detail in Chapter 4.

After the final design is completed, the construction of the full-scale underground repository and associated surface facilities can begin. The purpose of this construction phase is to excavate and erect all of the facilities necessary for the operation of the repository. This phase is expected to last about five years.

Therefore, the total site preparation and construction phase could be about 10 years.

1.3.3 Operation

The operation of the repository will only begin once a licence to operate the facility has been issued. Operation will consist of receiving used nuclear fuel transported to the site, re-packaging the used fuel into long-lived containers, placing the used fuel containers in the repository, and continued underground development. All activities will be executed in compliance with the supporting documents used to obtain the operating licence.

For a reference used fuel inventory of 4.6 million used CANDU fuel bundles, these operational activities are expected to last about 40 years. The actual duration of repository operation will depend on the total inventory of used fuel to be managed at the site and the timing of its production, transportation considerations and other operational factors.

1.3.4 Extended Monitoring

Following placement of used fuel in the repository, a period of monitoring is assumed to continue for an extended period of time. The duration of extended monitoring will be decided in collaboration with a future society. For planning purposes, the period of extended monitoring is assumed to be up to 70 years.

Towards the end of the extended monitoring period (i.e., during the last five years), a detailed decommissioning plan will be prepared, the detailed design of the shaft sealing system will be finalized, and an application to decommission the facility will be submitted to the CNSC.

1.3.5 Decommissioning

Decommissioning will only begin once a licence to decommission has been issued. It is expected that an Environmental Assessment to cover decommissioning activities will also be needed prior to the issuance of a decommissioning licence. The decommissioning of the facility will include sealing of access tunnels and shafts, and removal of surface facilities. The site will be restored to a defined end-state that will depend largely on future plans for the site (e.g., industrial, forestry, park, or wilderness). For planning purposes, the period of decommissioning is assumed to be 30 years.

A formal licence to abandon the facility could be obtained once the decommissioning and monitoring results have confirmed that it is acceptable to release the facility from CNSC regulatory control. An application for this licence will include a decommissioning end-state report and other supporting licensing documents. It is anticipated that appropriate institutional controls will be put in place at that time.

Used Fuel Repository Conceptual Design and Postclosure Safety Assessment in Crystalline Rock

Document Number: NWMO TR-2012-16

Revision: 000

Class: Public

Page: 7

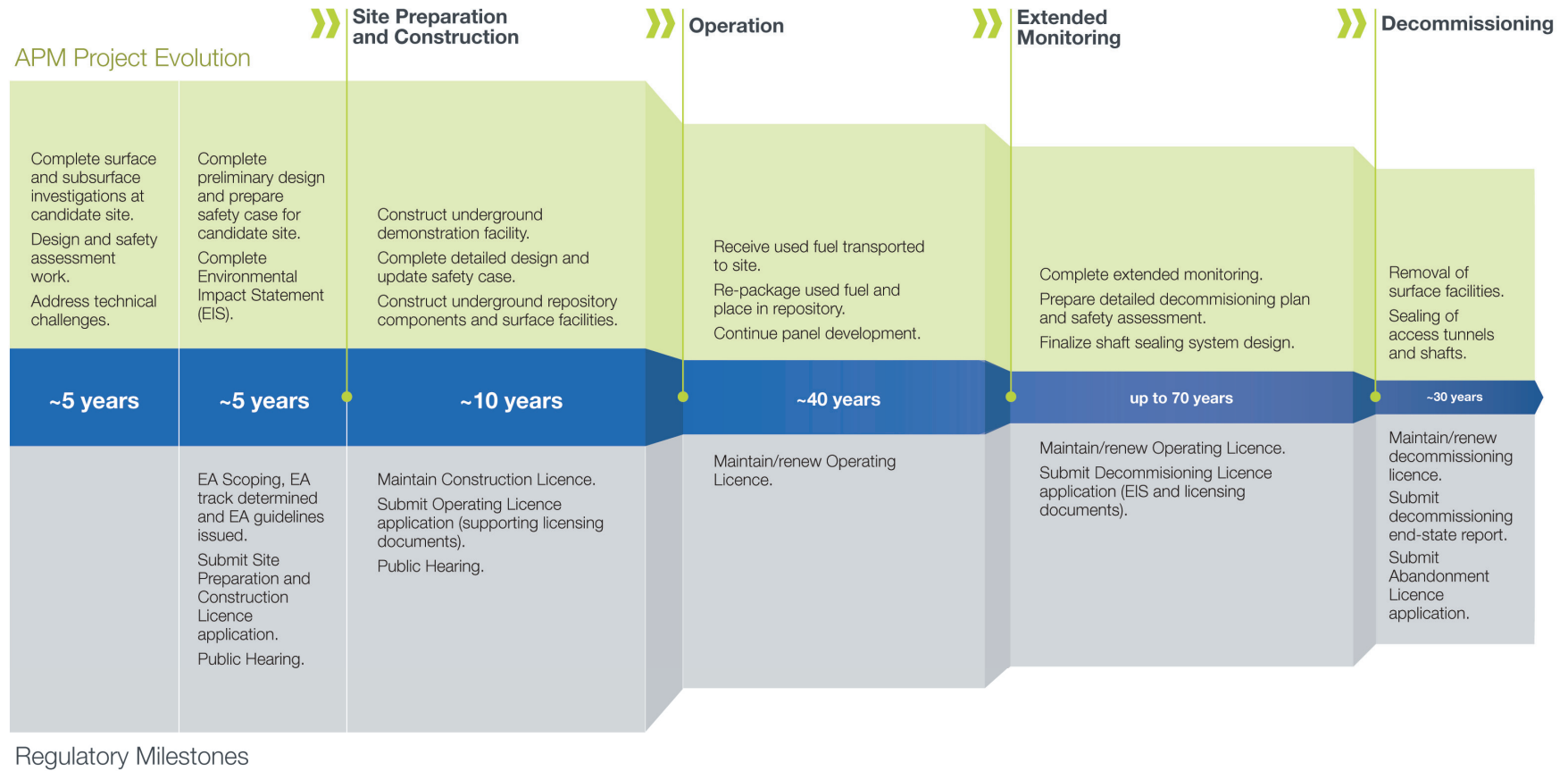


Figure 1-2: Illustrative APM Implementation Schedule for Planning Purposes

1.4 Repository Timeframes

In this safety assessment the potential impact of a repository is assessed in accordance with the CNSC Policy P-290 (CNSC 2004), which requires that, “the assessment of future impacts of radioactive waste on the health and safety of persons and the environment encompasses the period of time when the maximum impact is predicted to occur.” In discussing the long-term evolution of a repository system, it is helpful to consider a sequence of timeframes during which certain events or processes dominate in the postclosure period.

1.4.1 Preclosure Period

The preclosure period is intended to cover the activities described in Sections 1.3.1 to 1.3.5 and is assumed to last up to about 150 years (see Figure 1-2).

During this time, the reference inventory of 4.6 million used nuclear fuel bundles will be transported to the APM facility, encapsulated in approximately 12,800 long-lived used fuel containers, transferred to the underground repository and surrounded by clay-based sealing materials. The total radioactivity will increase as more used fuel is placed in the repository, and then start to decrease due to radioactive decay.

1.4.2 Postclosure Period

The postclosure period starts at the end of decommissioning, after the shafts have been sealed and the surface facilities have been dismantled.

In the postclosure period, the site is assumed to remain under institutional controls for a period of time. Based on CNSC Guide G-320 (CNSC 2006), and IAEA Safety Series No. 111-F (IAEA 1995), institutional controls can be defined as, “the control of residual risks at a site (by a designated Institution or Authority) after it has been decommissioned.” These controls can include both active measures (requiring activities on the site such as monitoring and maintenance) and passive measures (that do not require activities on the site, such as land use restrictions, as well as measures taken to support societal memory). Such measures should prevent inappropriate land use, including drilling, deep excavation, or disruption of the shaft seals.

Although there is no specific date beyond which institutional controls or societal memory will not be effective, it is assumed for safety assessment purposes that these institutional controls or societal memory are effective for about 300 years.

The postclosure period is described in four timeframes. Each of the timeframes is also described in this section. To provide context for these timeframes, Figure 1-3 highlights timescales for relevant past events and expected future events in the Earth’s history.

1 - 1,000 years

At the beginning of this time, the facility is decommissioned. Distinct physical and chemical differences exist between the various components of the repository, and between the repository and the geosphere. The containers reach their peak temperature. Slow saturation of the repository by groundwater occurs, which is accompanied by swelling of bentonite sealing materials. Especially during the first 500 years, radioactivity and heat in the used fuel decrease significantly due to the decay of most of the fission products.

1,000 - 60,000 years

This time period represents conditions with no glaciation coverage of the site. During this period, the initial sharp physical and chemical gradients around the repository slowly diminish. The surrounding crystalline rock reaches its peak temperature and largely cools back down to natural ambient temperatures. Surface conditions are likely to change reflecting human activities and natural evolution, possibly in response to climate change. Although the overall climate is likely to remain temperate, climate changes could include global warming in the near term, and the advent of cooler climate in the long term.

60,000 - 1,000,000 years

Over this timescale, the main perturbations in the system cease to be repository-driven. Instead, there are regional-scale changes in the geosphere that in turn may be transmitted to the repository. In particular, during this timeframe, climate change initiated by broad changes in solar insolation patterns may occur leading to initiation of a new glaciation cycle. Based on past history, several cycles of glaciation are likely to occur over the next million years.

1,000,000 years and beyond

Beyond this timescale, the repository will be a relatively passive feature of the geosphere, in quasi-equilibrium with the surrounding rock. The dominant processes will be regional perturbations to the geosphere that in turn affect the repository. Over this longer time period, the changes will include slow-acting tectonic forces, and cumulative erosion or deposition processes.

In the safety analysis presented in this report, the discussion of the evolution of a repository focuses on the interval covered by the first three postclosure timeframes, i.e., up to one million years. It will be during this period that the differences between the natural environment and an engineered repository for used fuel are noticeable. Long before major changes will be apparent at times beyond one million years, the total amount of radioactivity in the waste will have diminished to the point that it is similar to that of a naturally occurring uranium ore body.¹ As part of the safety case prepared for an actual candidate site, geoscientific arguments and evidence supporting the long-term stability and resilience to change of a crystalline rock environment would also be presented.

¹ With 70,000 Mg of uranium, it will be smaller than large ore bodies like Cigar Lake and MacArthur River in Saskatchewan.

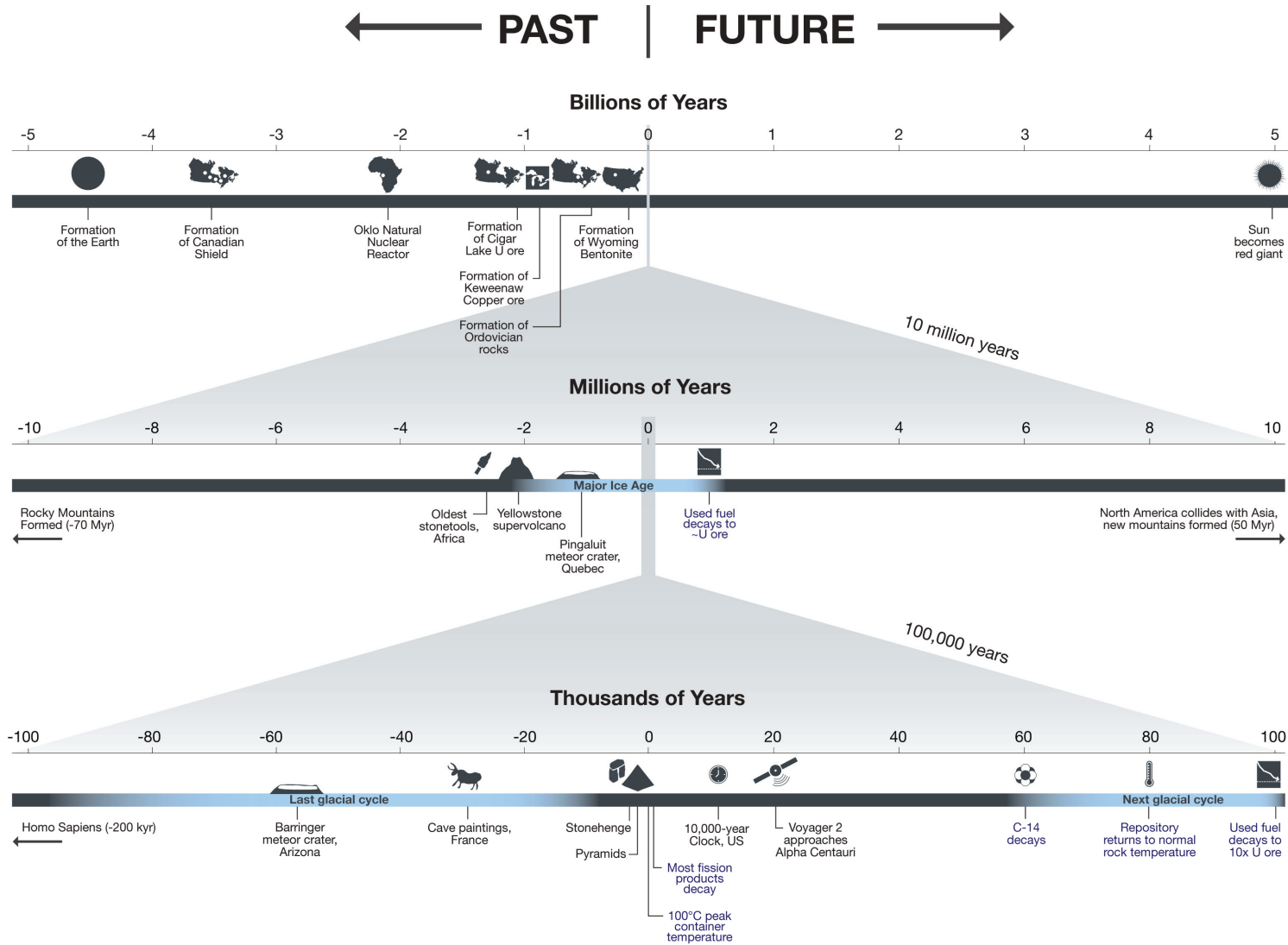


Figure 1-3: Perspective of Past Events and Expected Future Events in Earth’s History Including Repository Events

1.5 Relevant Legislation

This section presents the regulatory requirements under the *Nuclear Safety and Control Act* and its associated regulations, as well as the international guidance on safety of a deep geological repository.

The intention is for the deep geological repository to meet or exceed all regulatory requirements and to be consistent with international practices during site preparation, construction, operation, and beyond.

1.5.1 CNSC Regulatory Requirements

In accordance with paragraph 2(g) of *Nuclear Safety and Control Act* and paragraph 1(e) of the Class I Nuclear Facilities Regulations, the repository is a Class 1B nuclear facility.

Paragraph 26(e) of the Act states that, “subject to the Regulations, no person shall, except in accordance with a licence...prepare a site for, construct, operate, modify, decommission or abandon a nuclear facility”. The following licences are required over the life of the repository:

- Site Preparation Licence;
- Construction Licence;
- Operating Licence;
- Decommissioning Licence; and
- Abandonment Licence.

The detailed requirements to obtain a licence are described in Section 3 of the General Nuclear Safety and Control Regulations and in Sections 3, 4 and 5 of the Class I Nuclear Facilities Regulations. Other applicable regulations include the Nuclear Security Regulations, Radiation Protection Regulations, Packaging and Transport of Nuclear Substances Regulations, which apply to all nuclear facilities, and the Uranium Mines and Mills Regulations – due to similarities of some aspects of the APM facility (i.e., deep geological repository) to a mining project.

In addition to the regulations, a number of CNSC regulatory documents in the following categories are also applicable:

- Regulatory policies – describe general principles applied by the CNSC in their review;
- Regulatory documents and standards – establish regulatory standards; and
- Regulatory guides – set out regulatory expectations.

In Canada, the primary regulatory requirements and expectations for the assessment of long-term safety of radioactive waste management are given in the CNSC Policy P-290 (CNSC 2004) and CNSC Guide G-320 (CNSC 2006) and these are the focus of this pre-project report. These and other regulatory documents that will apply to the APM project in support of a future licence application are listed in Table 1-1.

Table 1-1: CNSC Regulatory Documents Applicable to the APM Project

Document Number	Title
Pre-project Report	
P-290	Managing Radioactive Waste (CNSC 2004)
G-320	Assessing the Long Term Safety of Radioactive Waste Management (CNSC 2006)
Licence Application	
P-119	Policy on Human Factors
P-211	Compliance
P-223	Protection of the Environment
P-299	Regulatory Fundamentals
P-325	Nuclear Emergency Management
R-72	Geological Considerations in Siting a Repository for Underground Disposal of High-Level Radioactive Waste
G-129 Rev.1	Keeping Radiation Exposures and Doses "As Low as Reasonably Achievable (ALARA)"
G-205	Entry to Protected and Inner Areas
G-206	Financial Guarantees for the Decommissioning of Licensed Activities
G-208	Transportation Security Plans for Category I, II or III Nuclear Material
G-217	Licensee Public Information Programs
G-219	Decommissioning Planning for Licensed Activities
G-221	A Guide to Ventilation Requirements for Uranium Mines and Mills
G-225	Emergency Planning at Class I Nuclear Facilities and Uranium Mines and Mills
G-274	Security Programs for Category I or II Nuclear Material or Certain Nuclear Facilities
G-276	Human Factors Engineering Program Plans
G-278	Human Factors Verification and Validation Plans
S-296/ G-296	Environmental Protection Policies, Programs and Procedures at Class I Nuclear Facilities and Uranium Mines and Mills
RD-327/ GD-327	Nuclear Criticality Safety
RD-336/ GD-336	Accounting and Reporting of Nuclear Material
RD-353	Testing the Implementation of Emergency Measures
RD-363	Nuclear Security Officer Medical, Physical, and Psychological Fitness

Note: Current versions of the CNSC regulatory documents can be found on the CNSC website (www.cnsccsn.gc.ca).

CNSC Policy P-290 (CNSC 2004) identifies the need for long-term management of radioactive waste and hazardous waste arising from licensed activities. The principles espoused by CNSC Policy P-290 that relate to long-term management are the following:

- The management of radioactive waste is commensurate with its radiological, chemical, and biological hazard to the health and safety of persons and the environment, and to national security;
- The assessment of future impacts of radioactive waste on the health and safety of persons and the environment encompasses the period of time when the maximum impact is predicted to occur; and
- The predicted impact on the health and safety of persons and the environment from the management of radioactive waste is no greater than the impact that is permissible in Canada at the time of the regulatory decision.

Key objectives for long-term management are *containment* and *isolation* of the waste, in accordance with the CNSC Guide G-320 (CNSC 2006). The guide states that:

“containment can be achieved through a robust design based on multiple barriers providing defence-in-depth. Isolation is achieved through proper site selection and, when necessary, institutional controls to limit access and land use”.

CNSC Guide G-320 identifies expectations for *“developing a long term safety case that includes a safety assessment complemented by various additional arguments based on:*

1. *Appropriate selection and application of assessment strategies;*
2. *Demonstration of system robustness;*
3. *The use of complementary indicators of safety; and*
4. *Any other evidence that is available to provide confidence in the long term safety of radioactive waste management.”*

Guidance is also provided for defining acceptance criteria and performing long-term assessments that includes considerations for: selection of methodology, assessment context, system description, assessment timeframes, assessment scenarios, assessment models, and the interpretation of results.

A mapping that shows how the content of this report is consistent with aspects of CNSC Guide G-320 is shown in Table 1-4 and described in more detail in Chapter 11.

1.5.2 Transportation of Used Nuclear Fuel

The safe and secure transportation of used nuclear fuel is regulated through a comprehensive multi-agency framework of regulations, oversight, and inspections. The process builds on the roles of federal, provincial, and local agencies.

The regulatory oversight of safe transportation of used nuclear fuel in Canada is jointly shared by the CNSC and Transport Canada. Transport Canada's *Transportation of Dangerous Goods Regulations*, and the *Transportation of Dangerous Goods Act*, and CNSC's *Packaging and Transport of Nuclear Substances Regulations*, associated with *Nuclear Safety and Control Act*, and the *Nuclear Security Regulations* apply to all persons who handle, offer for transport, transport or receive nuclear substances.

Transport Canada and CNSC regulations follow the IAEA regulations (TS-R-1) for the safe transport of radioactive materials and cover certification of the package used to transport the used fuel, the licence to transport, the security planning, training requirements for the shipper and the transporter, emergency response planning, and communications. These are in addition to the normal commercial vehicle and rail operating regulations and are similar to those used internationally. Packages designed for the transport of used nuclear fuel require certification by the CNSC before they can be used in Canada.

The provinces are responsible for developing, maintaining, and operating the highway infrastructure and for inspecting the commercial vehicles and their drivers. Local governments provide law enforcement and emergency response to incidents. The interaction and cooperation between these agencies facilitates comprehensive regulation and oversight of all transportation of used nuclear fuel.

1.5.3 Canadian Codes and Standards

A number of Canadian codes and standards apply to a deep geological repository project. Compliance with these will be demonstrated in the future in support of a licence application. For example, requirements exist in the following areas and include the following:

- Civil structures will comply with the National Building Code of Canada and the National Fire Code of Canada;
- Electrical installations and components will be in accordance with the Canadian Electrical Code and associated Canadian Standards Association (CSA) standards;
- The management system will comply with the CSA N286 series of standards as well as ISO 9001;
- The environmental management and monitoring programs will comply with the CSA N288 series of standards as well as ISO 14001; and
- The occupational health and safety management programs will comply with the CSA Z1000 standard.

Some regulatory requirements from the provincial jurisdiction will also be applicable. For example, the health and safety program will comply with provincial Occupational Health and Safety Requirements. Although there is presently no specific site and therefore no specific province identified, for purposes of this study some provincial regulations or criteria may be adopted to provide more specific context. For example, while Canadian Drinking Water Quality guidelines are generally used to assess water quality, in some cases in this study the criteria have been based on more complete provincial standards, such as the Ontario water quality objectives (MoEE 1994) and the soil, groundwater and sediment standards (MoE 2011).

1.5.4 Safeguards

Canada's international safeguards obligations are the result of treaty commitments (IAEA 1970, IAEA 1972, and IAEA 2000). The specific legal requirements to implement these commitments come in the form of licence conditions that are included in a CNSC licence. Compliance with these requirements will be demonstrated in support of a future licence application.

1.5.5 Traditional Knowledge

NWMO respects the status and rights of First Nations and understands that interweaving of Aboriginal Traditional Knowledge in the implementation of APM helps to build relationships with Aboriginal peoples and benefits the long-term management of used nuclear fuel. Early in the project this includes recognizing the importance of water, the relationships between various aspects of the environment as well as the health, trade and spiritual needs of people. The NWMO's Site Selection Process will look to Aboriginal peoples as practitioners of Traditional Knowledge to be active participants in the process, and to share that knowledge with the NWMO to the extent they wish to in order to help guide the decisions involved in site selection and ensure safety and the long-term well-being of the community. The NWMO will seek to engage in discussions with Traditional Knowledge holders to ensure that the factors and approaches used to assess the site appropriately interweave Traditional Knowledge and western science throughout the steps in the siting process.

1.5.6 International Guidance

The development and safety of deep geological repositories has been the subject of international attention by the IAEA and the Nuclear Energy Agency for many years.

A number of technical documents are available that provide guidance on best international practices with respect both to achieving safety, and on the demonstration of safety. Particular international documents relevant to development and safety for a repository are listed in Table 1-2.

Table 1-2: International Guidance Applicable to the APM Project

Document Number	Title
IAEA SSR-5	Disposal of Radioactive Waste
IAEA SSG-23	The Safety Case and Safety Assessment for Radioactive Waste Disposal
ICRP 103	The 2007 Recommendations of the International Commission on Radiological Protection
Case Study	European Pilot Study on the Regulatory Review of the Safety Case for Geological Disposal of Radioactive Waste – Case Study: Uncertainties and their Management (Vigfusson et. al 2007)

Note: The latest version of international guidance can be found on the associated agency's website (www.iaea.org, www.icrp.org).

1.6 Safety Case

CNSC Guide G-320 states “*Demonstrating long term safety consists of providing reasonable assurance that waste management will be conducted in a manner that protects human health and the environment. This is achieved through the development of a safety case, which includes a safety assessment complemented by various additional arguments*”.

The safety case has been defined in Section 1.1 as: the integration of arguments and evidence that describe, quantify and substantiate the safety, and the level of confidence in the safety, of the deep geological repository and associated facilities. It includes the collection of scientific and technical arguments and evidence in support of the safety of the repository covering the site characterization and geosynthesis, the design, construction and operation of the repository, the assessment of radiation risk during operation and postclosure, and quality assurance of all safety-related work associated with the repository.

This report documents components of a safety case, but not a full safety case, as discussed later, representing information at a very early stage before a site has been selected. The report contains a description of these various components, and in some cases, an illustration of how the design of the repository will meet Canadian regulatory requirements and will be consistent with international practice.

CNSC Guide G-320 (CNSC 2006) recommends following a structured approach for preparing a safety case and safety assessment. The safety assessment is defined as: the process of systematically analyzing the hazards associated with the facility, and the ability of the site and design to provide the safety functions and meet technical requirements.

The most recent international guidance is included in the IAEA’s SSG-23 (IAEA 2012). This guidance is used to present the safety case components for this study. The guidance also acknowledges applying the concept of defence in depth to disposal facilities by stating that: “*the host environment shall be selected, the engineered barriers of the disposal facility shall be designed... to ensure that safety is provided by means of multiple safety functions. Containment and isolation of the waste shall be provided by means of a number of physical barriers of the disposal system. The performance of these physical barriers shall be achieved by means of diverse physical and chemical processes...The capability of the individual barriers...shall be demonstrated. The overall performance of the disposal system shall not be unduly dependent on a single safety function.*” It further recommends that the number and extent of required barriers depends on the type of waste and should be commensurate with the hazard potential of the waste, in accordance with the graded approach.

Figure 1-4 is largely consistent with the IAEA’s components of a safety case (IAEA 2012). This figure is used to illustrate the current phase and to identify the further phases that will be included as part of a project at the final selected site. The discussion of each of these components is included in this section.

1.6.1 Safety Case Context

The Canadian regulatory framework presented in Section 1.5 provides the context for a deep geological repository safety case.

The primary *safety objective* of the deep geological repository is:

to provide safe long-term management of used fuel without posing unreasonable risk to the environment or health and safety of humans.

This objective is consistent with the *Nuclear Safety and Control Act* (subparagraph 9(a) (i)) and IAEA guidance (IAEA 2011), which notes that the geological disposal of radioactive waste is aimed at:

- Containing the waste until most of the radioactivity, and especially that associated with shorter-lived radionuclides, has decayed;
- Isolating the waste from the biosphere and substantially reducing the likelihood of inadvertent human intrusion into the waste;
- Delaying any significant migration of radionuclides to the biosphere until a time in the far future when much of the radioactivity will have decayed; and
- Ensuring that any levels of radionuclides eventually reaching the biosphere are such that possible radiological impacts in the future are acceptably low.

As described in Section 1.1, this study presents a conceptual design and illustrative safety assessment for a deep geological repository at a hypothetical site. The level of detail is consistent with the pre-project stage, i.e., before a final site has been selected, and sufficient to support a CNSC review with respect to the approach and methodology. It is not a full safety case. It considers a hypothetical site, and therefore does not include a geosynthesis. It identifies and analyzes key scenarios, but does not assess all relevant scenarios.

1.6.2 Safety Strategy

Used nuclear fuel is hazardous for long periods of time and its characteristics are used as an input to the design of the repository. The safety strategy is to provide long-term containment and isolation through the use of multiple barriers and passive systems, including in particular a stable and robust geosphere. The geosphere has characteristics that will also delay significant migration of radionuclides to ensure that the impacts in the future are acceptably low.

In this study, a set of safety relevant features are assumed to be present in this hypothetical site. The geological features will need to be affirmed at any future candidate site as part of the Site Selection Process (NWMO 2010). The design concept includes engineered barriers that have properties that also allow a set of safety functions to be fulfilled.

The geological characteristics and the engineered barrier's safety functions are consistent with the concept of defence in depth and are further described in the following section on the deep geological repository system.

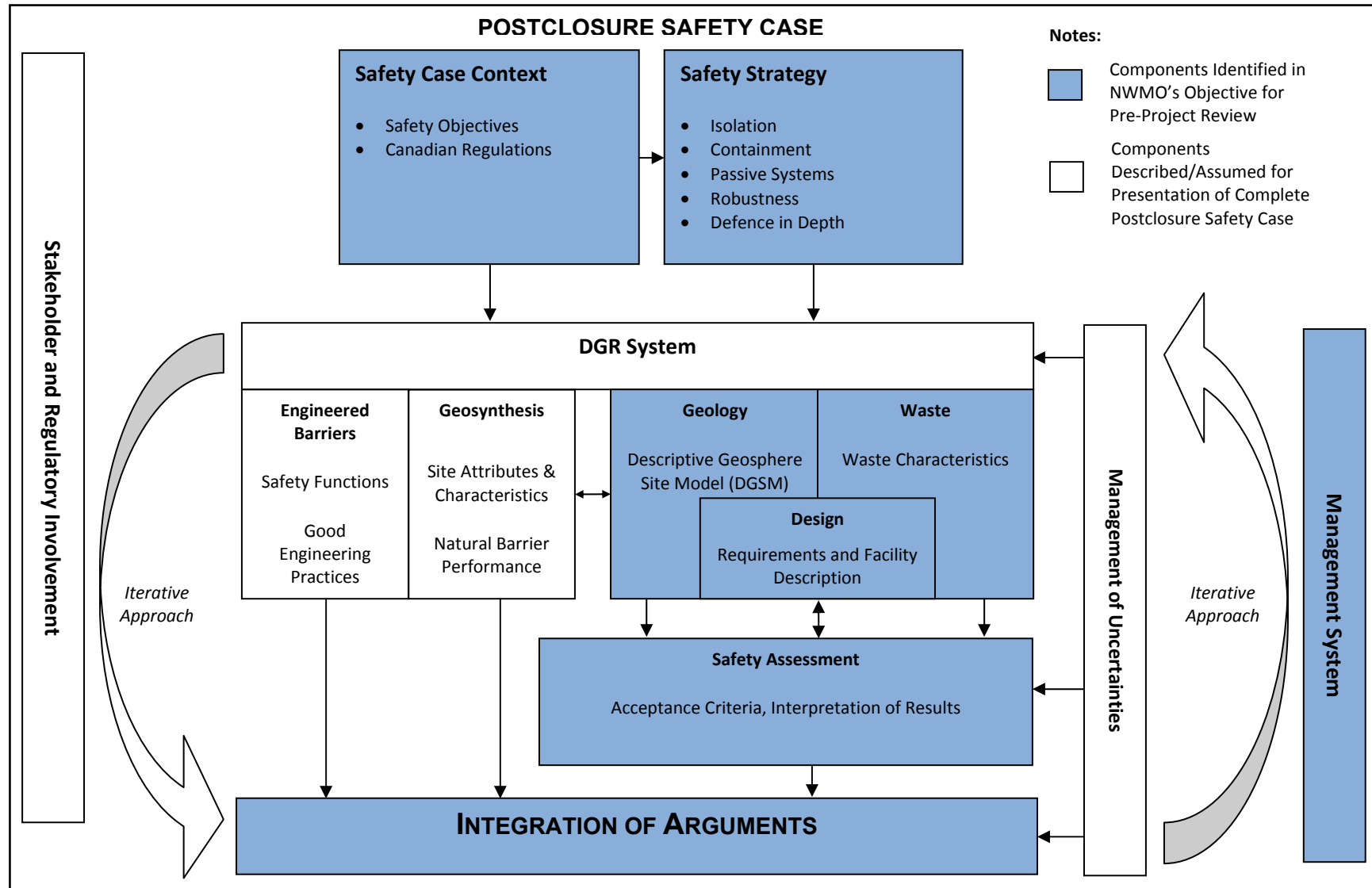


Figure 1-4: Components of the Safety Case

1.6.3 Deep Geological Repository System

The DGR system includes the DGR facility, its geological setting, and the surrounding surface environment. The system includes the engineered and the natural barriers that provide containment and isolation of the waste. The repository system includes the waste, containers, sealing systems and the near-field geosphere around the repository.

Figure 1-4 represents the system across three main areas for which safety arguments are presented: 1) the geology, 2) the waste characteristics, and 3) the design. This section includes a summary of the type of information that needs to be considered.

In this study for a hypothetical site, no specific description of communities is considered, although that will be important for any candidate site.

1.6.3.1 Geology

The information that describes the geological setting of the repository is used to guide the design of the DGR facility and as an input into the safety assessment. The geoscience program for a future candidate site will be designed to support the safety case and to produce:

- A Descriptive Geosphere Site Model (DGSM) that will describe, assess and interpret geoscientific data as it relates to site-specific geologic, hydrogeochemical, hydrogeologic and geomechanical characteristics and attributes; and
- A Geosynthesis that will provide a geoscientific explanation of the overall understanding of site characteristics, attributes and evolution as they relate to demonstrating long-term performance and safety.

The DGSM is defined as: a description of the present day three-dimensional physical and chemical characteristics of a specific site as they relate to implementation of the repository concept. For the purpose of the pre-project report and for conducting the illustrative safety assessment, this type of information is presented in Chapter 2.

The safety strategy identified that long-term containment and isolation is provided through the use of multiple barriers and passive systems, including in particular a stable and robust geosphere. The evidence to support the safety case arguments will be presented in the Geosynthesis for a candidate site that examines the past, present, and future evolution of the site. The Geosynthesis is defined as: the assembly of all the geologically-based evidence relevant to the repository safety case; the integration of multi-disciplinary geoscientific data relevant to the development of a descriptive conceptual geosphere model; and explanation of a site-specific descriptive geosphere model within a systematic and structured framework.

The NWMO's siting process (NWMO 2010) includes technical evaluations of a candidate site. The evaluation factors (listed in Section 1.6.8) in this process identify the following key geological site attributes.

- The depth of the host rock formation should be sufficient for isolating the repository from surface disturbances and changes caused by human activities and natural events.

- The volume of available competent rock at repository depth should be sufficient to host the repository and provide sufficient distance from active geological features such as zones of deformation or faults and unfavourable heterogeneities.
- The mineralogy of the rock, the geochemical composition of the groundwater and rock porewater at repository depth should not adversely impact the expected performance of the repository multi-barrier system.
- The hydrogeological regime within the host rock should exhibit low groundwater velocities.
- The mineralogy of the host rock, the geochemical composition of the groundwater and rock porewater should be favourable to retarding radionuclide movement.
- The host rock should be capable of withstanding mechanical and thermal stresses induced by the repository without significant structural deformation or fracturing that could compromise the containment and isolation functions of the repository.
- Current and future seismic activity at the repository site should not adversely impact the integrity of the repository system during operation and in the very long term.
- The expected rates of land uplift, subsidence and erosion at the repository site should not adversely impact the containment and isolation functions of the repository.
- The repository should not be located within rock formations containing economically exploitable natural resources such as minerals and other valuable commodities as known today.
- The repository is not located within geological formations containing groundwater resources at repository depth that could be used for drinking, agriculture or industrial uses.

It is noted that site characterization activities for an actual site in crystalline rock would include a thorough and systematic assessment of such features as, for example, major fractures and natural resource potential in the proximity of the repository. The assessment findings would be documented in the DGSM and in the Geosynthesis prepared for a candidate site, described above. For the purpose of the pre-project report, the key attributes assumed for the hypothetical site in the Canadian Shield are:

- The repository is located at a depth of 500 m;
- There is sufficient volume of rock at the site and depth to host the repository;
- Groundwater at repository depth has low salinity;
- Groundwater at repository depth provides a chemically reducing environment and a low concentration of potentially corrosive agents;
- The host rock is capable of withstanding mechanical and thermal stresses;
- Seismic activity is low, consistent with general Canadian Shield conditions;
- Rates of land uplift, subsidence and erosion at the site are low enough that they will not adversely impact the isolation of the repository; and
- The host rock formations do not contain groundwater or economically exploitable natural resources at repository depth.

1.6.3.2 Waste Characteristics

The waste characteristics are an input to the safety assessment and guide the design of the DGR facility. In addition, the waste has safety features that are identified in the safety case as follows:

- The used nuclear fuel is a durable uranium oxide (UO₂); it will dissolve very slowly under the chemical conditions within a failed container.
- Most of the initial radioactivity is held within the UO₂ grains, where it can only be released as the used fuel dissolves.

The waste characteristics are further described in Chapter 3.

1.6.3.3 Design

The design is largely guided by the geological characteristics and features of a candidate site and also by the characteristics of the waste that will be placed in the repository. For the pre-project report, a hypothetical crystalline site on the Canadian Shield is considered. Representative characteristics of the crystalline site are used to guide specific repository design requirements which include engineered barriers to fulfill specific safety functions. Design requirements are used as an input to the safety assessment.

The safety strategy acknowledges that properties of the engineered barriers will allow safety functions to be fulfilled. This includes the following design characteristics:

- The used fuel container has a design life of at least 100,000 years under the geomechanical and chemical repository conditions expected to exist within the repository; and
- The container is surrounded by a layer (approximately 30 cm) of dense bentonite-based clay that inhibits groundwater movement, has self-sealing capability, inhibits microbial activity near the container, and retards contaminant transport.

The repository design is described in Chapter 4 at a conceptual level of detail. The description focuses on the underground portions relevant to postclosure safety.

The purpose of the design concept presented here is to provide information to support the postclosure safety assessment. This design concept is expected to be further refined once a site has been selected and site specific information becomes available.

1.6.3.4 Institutional Controls

Institutional controls have been described in Section 1.4.2 where it is stated that institutional controls are assumed for a period of time. The safety feature associated with this assumption includes: institutional controls will limit the potential for human encounter with the repository in the near term after closure.

And finally, Chapter 5 discusses the evolution of the deep geological repository system, including how the different components of the system will interact with each other and the environment in the long term, consistent with CNSC Guide G-320 (CNSC 2006).

1.6.4 Safety Assessment

The safety assessment has been defined as: the process of systematically analyzing the hazards associated with the facility, and the ability of the site and design to provide the safety functions and meet technical requirements. As noted in the scope of this report, it focuses on the illustrative postclosure safety assessment, which is discussed in detail in Chapter 7. The scenarios, assessment tools and methods and assessment results are presented. Both radiological and non-radiological impacts are assessed and the safety assessment results are compared against acceptance criteria.

1.6.5 Management of Uncertainties

The report describes the assessment of uncertainties associated with numerical analyses at a level that is reasonable for a conceptual design at a hypothetical site. The discussion is consistent with the CNSC guidance for analyzing uncertainties and addresses such things as: degree of conservatism, conceptual model uncertainty, parameter value uncertainty, and scenario uncertainty. The illustrative safety assessment provides examples of approaches used to assess and understand the relevance of uncertainties in scientific knowledge, data or analysis that support statements of reliability in calculated repository performance.

As noted in Section 1.6.3.1, the geoscience program for a future candidate site will be designed to support the safety case and to produce a Descriptive Geosphere Site Model and a Geosynthesis.

The site model and geosynthesis will be developed in the phased site characterization work program. The work program will allow for the iterative development, testing and refinement of a site-specific model that will contribute to managing uncertainties in scientific understanding, data or models.

The iterative approach described below also highlights how the assessment of uncertainties will be incorporated in the process of developing a safety case for a future candidate site.

1.6.6 Iterative Approach

Consistent with international guidance, the NWMO plans to use an iterative approach in the strategies for management, site characterization, design and assessments of a candidate site. The documentation process to support this iterative approach is included in Figure 1-5. On the left hand side of this figure, two key documents that will support licence applications and that will document the safety case are identified as the Preliminary Safety Report and Final Safety Report.

As noted in Section 1.6.3.3, the design concept presented is illustrative and intended for the safety assessment methodology to be demonstrated. The actual design is expected to be refined once a specific site has been selected, site-specific information becomes available, and design optimization is implemented.

Furthermore, once a site has been selected, Figure 1-5 assumes that the characterization and engineered design programs will go through iterations based on increased knowledge of site

characteristics and safety assessment input during detailed site investigations. A few iterations are expected during the phase of detailed investigations.

Some of the key activities in this approach include:

- National and international peer reviews;
- Using site characterization results as an input to repository design and safety assessment, and in building the safety case;
- Conducting complementary geoscience analogue studies to assist with the explanation of geoscience phenomena related to, and to enhance confidence in, the understanding of long-term repository safety;
- Using proven technology in the design;
- Using the results of safety assessment, in particular the preclosure safety assessment and occupational radiation dose ALARA² assessment and conventional safety considerations in the design;
- Continuing to make use of a range of safety and performance indicators in safety analyses; and
- Assessing associated uncertainties and identification of any significant deficiencies in scientific understanding, data or analysis that might affect the analysis results that are presented.

1.6.7 Integration of Safety Arguments

The safety arguments will be integrated as part of a complete safety case. These arguments will be supported by evidence and multiple lines of reasoning gathered in the site characterization work program and documented in a Geosynthesis for a candidate site.

For the purpose of this report and to present the illustrative safety assessment, a number of safety arguments have been assumed in Section 1.6.3. These assumptions are made to show how site characteristics or attributes and safety functions are used to illustrate the robustness of a multi-barrier system.

The assessment results presented in Chapter 7 will be used to support safety arguments resulting from the postclosure assessment.

² ALARA: As low as reasonably achievable, social and economical factors taken into account.

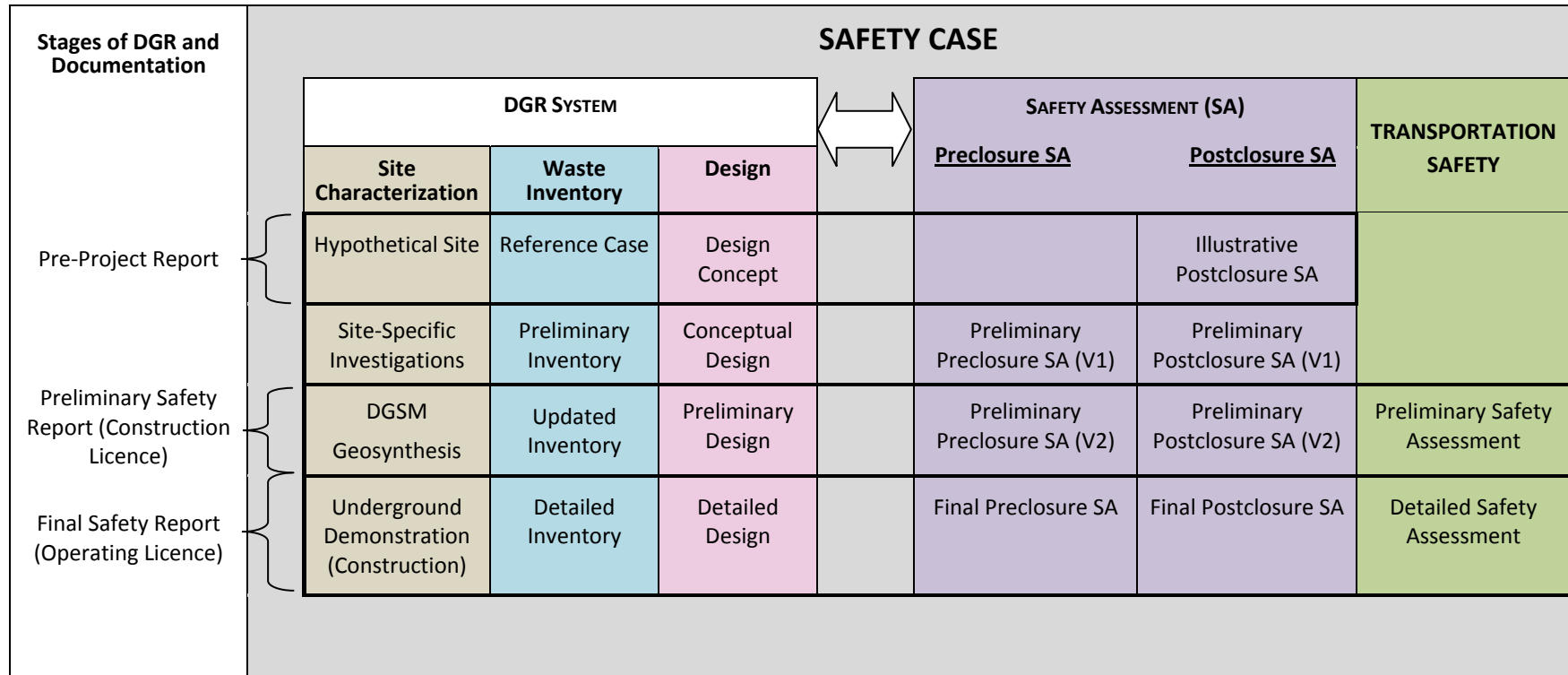


Figure 1-5: Iterative Process for Developing the Safety Case

1.6.8 Stakeholder and Regulatory Involvement

As noted in Section 1.1, the purpose of this report is to present a case study involving an illustrative safety assessment of a deep geological repository in a representative crystalline Canadian Shield setting for a pre-project regulatory review. This is being conducted under a special project arrangement between the CNSC and the NWMO (CNSC and NWMO 2008).

This report considers a hypothetical site, so there are no direct stakeholders. However, it will be available to the public and may be of interest to communities as part of the site selection process.

This report and illustrative safety assessment have been conducted in parallel with activities in the NWMO APM site selection process. This section shows how both of these activities are consistent and also confirms that technical evaluation stages are built into the process to select a candidate site.

As noted in the project overview, a site selection process was designed to identify an informed and willing host community for a deep geological repository for the long-term management of Canada's used nuclear fuel. It is a nine-step process developed to reflect the values, concerns and priorities expressed by Canadians, which are detailed by the NWMO (2010). The guiding principles that are embedded in the site selection process include:

- To focus decision-making on safety;
- To meet or exceed regulatory requirements;
- To find an informed and willing host community;
- To focus siting on the provinces directly involved in nuclear fuel cycle; and
- To acknowledge the right for a community to withdraw from the process.

Furthermore, it identifies site evaluation factors with which the suitability of a candidate site to host an APM repository will be assessed (see Figure 1-6). These factors include the list of geoscientific attributes identified in Section 1.6.3.1 and the following attributes:

- The containment and isolation characteristics (e.g., geological, hydrogeological, chemical, and mechanical) of the host rock;
- The long-term stability of the site to ensure that containment and isolation of the repository will not be unacceptably affected by future geological processes and climate changes including earthquakes and glacial cycles;
- Surface and underground characteristics of the site are favourable for the repository's construction, operation, closure, and long-term performance;
- Future human activities are not likely to disrupt containment and isolation of the repository;
- The characteristics of the site should be amenable to site characterization and site data interpretation activities; and
- The site should have a route that exists or is amenable to being created that enables the safe and secure transportation of used fuel from storage sites to the repository site.

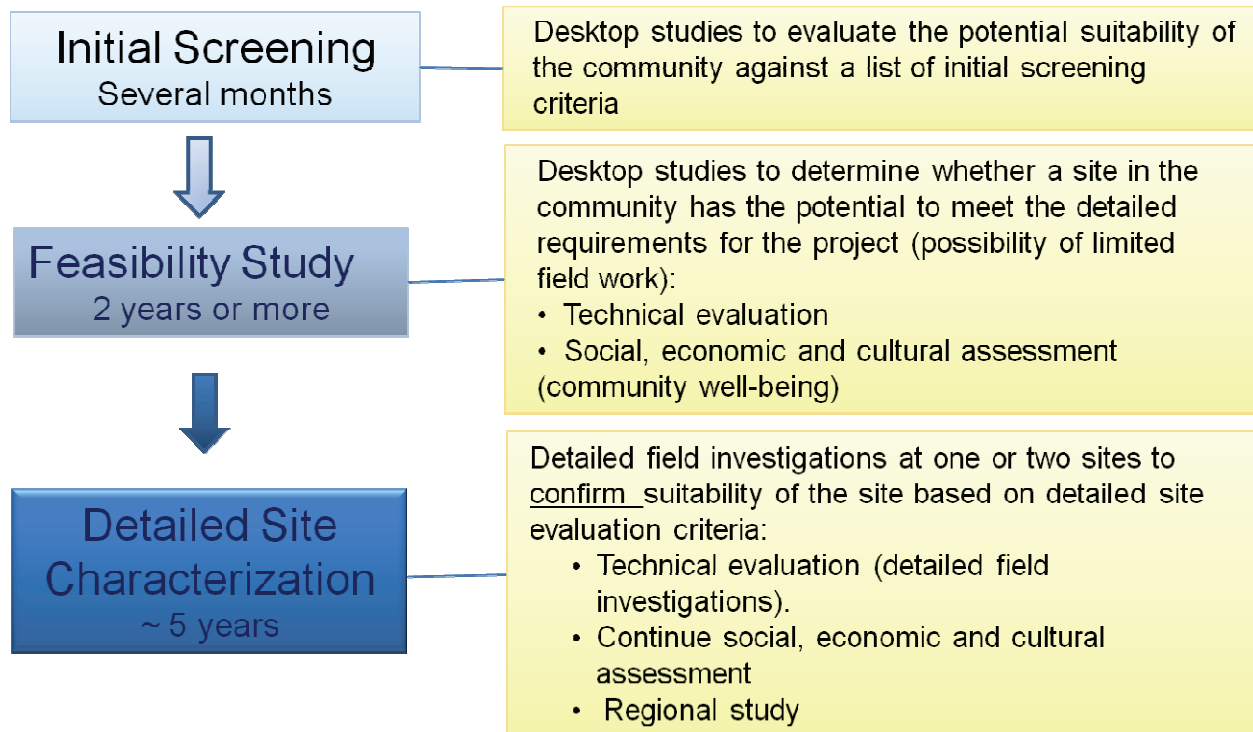


Figure 1-6: Site Evaluation Process

The stakeholder and regulatory involvement activities associated with the siting process were initiated in 2010 and are ongoing.

1.6.9 Management System

The management system includes a project quality plan under which the APM design and safety assessment update has been executed. The project quality plan was developed specifically for this phase of the work. The plan includes the following elements:

- The project organization and responsibilities;
- NWMO and project-specific governance;
- Quality requirements;
- Verification requirements;
- Requirements for consultant or contractor quality management system;
- Records requirements;
- Program's periodic assessment activities; and
- Annual assessment activities.

Chapter 10 describes the elements of the project quality plan in more detail.

1.7 International Status of Deep Geological Repositories

The concept of using a deep geological repository for long-term management of used fuel is consistent with other national plans for high-level waste as summarized in Table 1-3. In-service dates for other geological repository projects have been included, where available.

Table 1-3: Status of National Plans for High-Level Waste

Country	National Plan for High-Level Waste	Potential Rock Type	Repository Status
Finland	Geological Repository	Crystalline Rock	- Willing host community selected - Underground demonstration facility under construction at repository site - 2012: plan construction licence application - 2020: plan in-service date
Sweden	Geological Repository	Crystalline Rock	- Willing host community selected - Underground demonstration facility operating at generic site - 2011: construction licence application - 2025: plan in-service date
France	Geological Repository	Sedimentary Rock	- General geological region identified - Underground demonstration facility operating at generic site - 2025: plan in-service date
UK	Geological Repository	Crystalline Rock	- 2075: plan in-service date
Germany	Geological Repository	Salt, Crystalline, and Sedimentary Rock	- No fixed date
Japan	Geological Repository	Crystalline and Sedimentary Rock	- Generic underground research facilities under construction - 2040: plan in-service date
Switzerland	Geological Repository	Sedimentary Rock	- Underground demonstration facility operating at generic site - 2040: plan in-service date
USA	Geological Repository	To be decided	- Blue Ribbon Panel recommendations issued
China	Geological Repository	Crystalline Rock	- 2050: plan in-service date

1.8 Report Structure and Content

The structure of this pre-project review report is as follows:

- Chapter 1 Introduction: An overview of the APM project and the context for the report.
- Chapter 2 Description of a Hypothetical Site: Information related to a hypothetical site is presented.
- Chapter 3 Used Fuel Characteristics: Information on the reference fuel bundle adopted in the postclosure safety assessment is presented.
- Chapter 4 Repository Facility – Conceptual Design: Description of conceptual design for a deep geological repository.
- Chapter 5 Long-Term Evolution of the Multiple Barrier System: Description of the deep geological repository system, including the interaction of different components of the system.
- Chapter 6 Scenario Identification and Description: Description of the systematic scenario identification process used to identify Normal Evolution and Disruptive Event Scenarios.
- Chapter 7 Postclosure Safety Assessment: Provides an evaluation of potential impacts during Normal Evolution and Disruptive Event Scenarios.
- Chapter 8 Treatment of Uncertainties: Description of scenario, model and data uncertainties.
- Chapter 9 Natural Analogues: Description of natural analogues that illustrate material integrity and identification of the role of site-specific analogues.
- Chapter 10 Quality Assurance: Description of the APM quality assurance plan.
- Chapter 11 Summary and Conclusions: Summary of information presented in the pre-project report and overall conclusion on meeting the pre-project report objective.
- Chapter 12 Special Terms: Includes units, abbreviations and acronyms.

The IAEA's structured approach presented in the recent guidance on the Safety Case and Safety Assessment for the Disposal of Radioactive Waste (IAEA 2012) was used to describe the components of a safety case in Section 1.6. This guidance is complimentary to the CNSC Guide G-320 and its structure is used to present the information in this report. To illustrate how the content of G-320 is captured in this report, a mapping of the pre-project report sections to the content in G-320 is included in Table 1-4.

Table 1-4: Pre-Project Report Content Mapped to CNSC Guide G-320

G-320 Content	Relevant Section(s) in Report
Developing a Long-Term Safety Case	
Safety Assessment	Chapter 7
Use of Different Assessment Strategies	Section 7.2
Robustness and Natural Analogues	Chapters 7 and 9
Use of Complementary Indicators to Safety	Section 7.11.1
Defining Acceptance Criteria	
Overview	Section 7.1
Criteria for Protection of Persons and the Environment	Section 7.1
Performing Long-Term Assessments	
Selection of Appropriate Methodology	Section 7.4
Assessment Context	Section 7.2
System Description	Chapters 2, 3, 4, and 5
Assessment Time Frames	Section 6.1.3
Assessment Scenarios	Chapter 6
Developing and Using Assessment Models	Sections 7.5, 7.6, 7.7 and 7.8
Interpretation of Results	
Comparing Assessment Results with Acceptance Criteria	Section 7.12
Analyzing Uncertainties	Chapter 8

1.9 References for Chapter 1

- CEAA. 1998. Report of the Nuclear Fuel Waste Management and Disposal Concept Environmental Assessment Panel. Canadian Environmental Assessment Agency. Ottawa, Canada.
- CNSC. 2004. Regulatory Policy P-290: Managing Radioactive Waste. Canadian Nuclear Safety Commission. Ottawa, Canada.
- CNSC. 2006. Regulatory Guide G-320: Assessing the Long Term Safety of Radioactive Waste Management. Canadian Nuclear Safety Commission. Ottawa, Canada.
- CNSC and NWMO. 2008. Special Project Arrangement between the Canadian Nuclear Safety Commission and the Nuclear Waste Management Organization. Canadian Nuclear Safety Commission and Nuclear Waste Management Organization. April 1, 2008.
- Gierszewski, P., J. Avis, N. Calder, A. D'Andrea, F. Garisto, C. Kitson, T. Melnyk, K. Wei and L. Wojciechowski. 2004. Third-Case Study – Postclosure Safety Assessment. Ontario Power Generation Report 06819-REP-01200-10109-R00. Toronto, Canada.
- Hare, F.K., A.M. Aikin and J.M. Harrison. 1977. The Management of Canada's Nuclear Wastes. Report for Energy, Mines and Resources Canada EP77-6. Minister of Energy, Mines and Resources. Ottawa, Canada.
- IAEA. 1970. Treaty on the Non-Proliferation of Nuclear Weapons. International Atomic Energy Agency INFCIRC/140. Vienna, Austria.
- IAEA. 1972. Agreement Between the Government of Canada and the International Atomic Energy Agency for the Application of Safeguards in Connection with the Treaty on the Non-Proliferation of Nuclear Weapons. International Atomic Energy Agency INFCIRC/164. Vienna, Austria.
- IAEA. 1995. IAEA Safety Series: The Principles of Radioactive Waste Management. International Atomic Energy Agency. Safety Fundamentals IAEA 111-F. Vienna, Austria.
- IAEA. 2000. Protocol Additional to the Agreement between Canada and IAEA for the Application of Safeguards in Connection with the Treaty on the Non-Proliferation of Nuclear Weapons. International Atomic Energy Agency INFCIRC/164/Add. 1. Vienna, Austria.
- IAEA. 2011. IAEA Safety Standards: Disposal of Radioactive Waste. International Atomic Energy Agency. Specific Safety Requirements IAEA SSR-5. Vienna, Austria.
- IAEA. 2012. IAEA Safety Standards: The Safety Case and Safety Assessment for the Disposal of Radioactive Waste. International Atomic Energy Agency. Specific Safety Guide IAEA SSG-23. Vienna, Austria.

MoEE. 1994. Water Management Policies Guidelines Provincial Water Quality Objectives of the Ministry of Environment and Energy. Ministry of Environment and Energy. Ontario, Canada.

MoE. 2011. Soil, Groundwater and Sediment Standards for Use under Part XV.1 of the Environmental Protection Act. Ontario Ministry of Environment. Ontario, Canada.

NWMO. 2010. Moving Forward Together: Process for Selecting a Site for Canada's Deep Geological Repository for Used Nuclear Fuel. Nuclear Waste Management Organization. Toronto, Canada.

Vigfusson, J., J. Maudoux, R. Raimbault, K.-J. Röhlig and R.E. Smith. 2007. Geological Disposal of Radioactive Waste – Case Study: Uncertainties and their Management. European Pilot Study on the Regulatory Review of the Safety Case for Geological Disposal of Radioactive Waste.

THIS PAGE HAS BEEN LEFT BLANK INTENTIONALLY

2. DESCRIPTION OF A HYPOTHETICAL SITE

2.1 Introduction

The purpose of this chapter is to describe the characteristics of a hypothetical crystalline site that could be encountered during geoscientific site characterization activities on the Canadian Shield. The description is provided in-lieu of geoscientific information that would be derived through site-specific surface and sub-surface investigations. The intent is to provide information necessary to support an illustrative safety assessment, the focus of which is to demonstrate a methodology to assess the postclosure safety of a deep geological repository for Canada's used nuclear fuel in a crystalline geosphere at an approximate depth of 500 m.

Although the data represent a hypothetical Shield site, the information is consistent with reported values obtained from site-specific investigations during the Canadian Nuclear Fuel Waste Management Program on the Canadian Shield (Garisto et al. 2010, Sykes et al. 2004, 2009, Normani et al. 2007). The following sections describe characteristic surface Shield features through the presentation of descriptive geologic (Section 2.2.1), hydrogeologic (Section 2.2.2) and geochemical (Section 2.2.3) site models. The site models are used as a basis for numerical simulations that are intent on illustrating groundwater system behaviour and evolution at time frames relevant to the long-term performance of a deep geological repository. The numerical groundwater simulations are described in Section 2.3.

2.2 Conceptual Model for Hypothetical Site

The following section describes the geosphere model for hypothetical crystalline site, including information on: the site geology, surface features (topography and hydrology), hydrogeological and geochemical conditions. The long-term stability and natural evolution of the geosphere, including potential geological disturbances (e.g., seismicity) and climate change are discussed in Chapter 5, Section 5.5.

2.2.1 Descriptive Geologic Site Model

The geologic site model describes the geologic composition and structural features of the geosphere, and provides the basis for geoscientific understanding of the current conditions, as well as its past evolution.

2.2.1.1 Geologic Description

The geology of the site is defined by a layer of Quaternary-aged glacial drift and, lake and river sediments (consisting of clay, silt and sand), up to 10 m depth, overlying crystalline rock of the Canadian Shield. The Canadian Shield consists of a variety of igneous and metamorphic rock types, including volcanic, plutonic, metasedimentary and gneissic (Hoffman 1988, Card 1990). Exposed bedrock areas range from several km² to hundreds of km². The crystalline rocks vary in composition from gabbros and diorites (which contain many mafic minerals) to granites and granodiorites (which contain mostly felsic minerals). The crystalline rocks for this case study consist of granodiorite and granite, as well as tonalite, and are Archean in age (OGS 2000). The granitic rocks are composed of microcline, plagioclase and quartz, with minor biotite and trace amounts of opaques, epidote, muscovite, chlorite and sphene.

The geothermal gradient is 12 °C/km, as is typical for the Canadian Shield (Perry et al. 2010).

For the purposes of this case study, the geology is divided into three rock mass permeability zones and three fracture zones: shallow, intermediate and deep, as described in Section 2.2.2.2. Physical characteristics, including the density and porosity of the geosphere, are also described in Section 2.2.2.2.

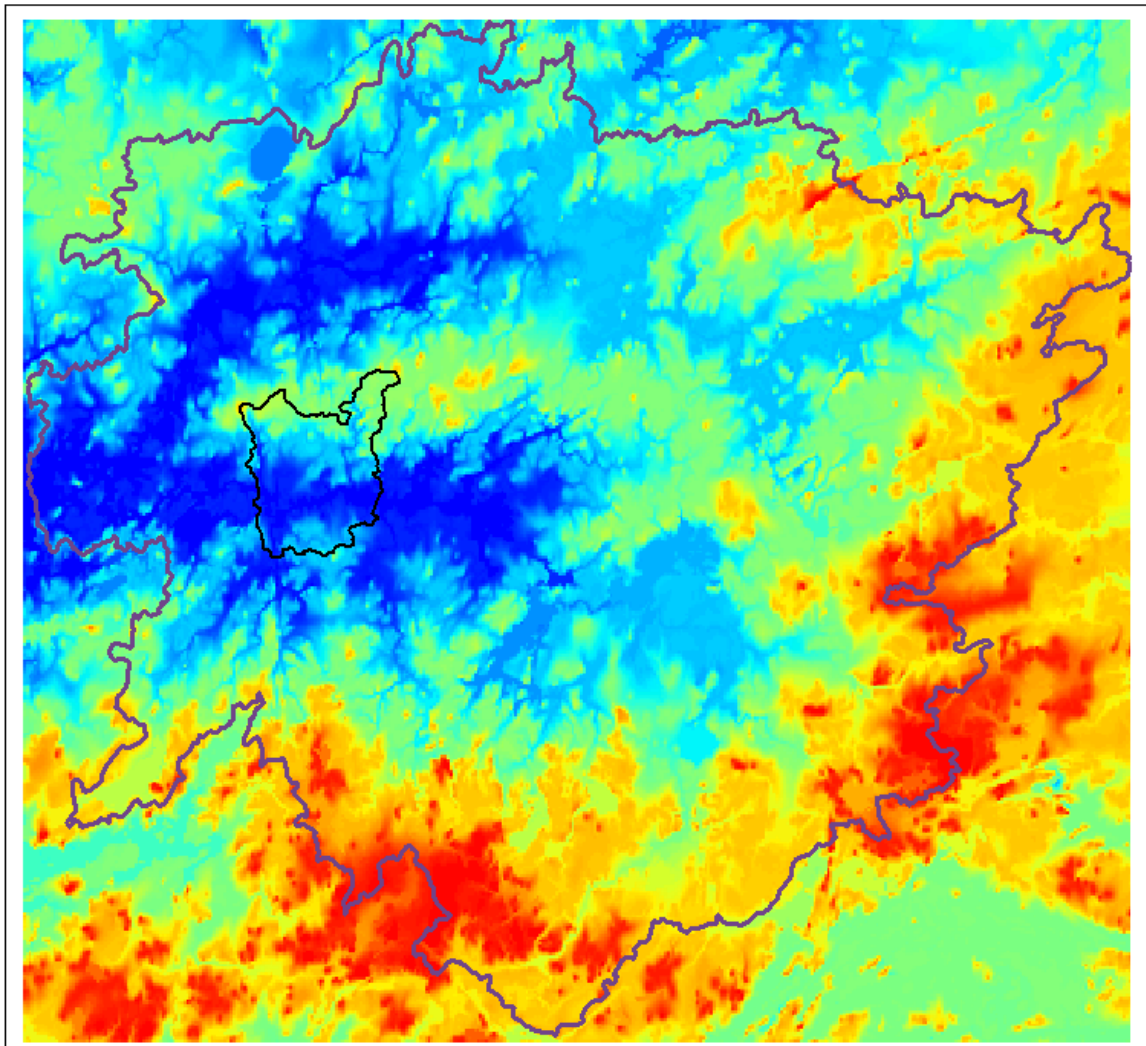
2.2.1.2 Surface Features

2.2.1.2.1 Topography

A representative regional area encompassing a watershed with Shield topography was selected for this case study, and is shown in Figure 2-1 with an area of 5734 km². The average topographic gradient across the domain is estimated at 0.007. Within this region, an illustrative sub-regional area has been selected to provide a basis for the postclosure safety assessment (refer to Figure 2-1 and Figure 2-2). The boundaries for the sub-regional domain were selected to correspond with surface and groundwater divides, which represent planes across which groundwater flow is not expected.

The top surface of the domain was defined by a 50 m Digital Elevation Model (DEM) interpolated from an NRCAN 0.75 second resolution DEM using ArcGIS. Due to hydrologic irregularities introduced during digitization, it was necessary to adjust the elevations of water features, such as lakes, rivers, and wetlands, to ensure hydrologic consistency amongst features. Paper National Topographic System (NTS) map sheets for the region provided the basis for the adjustment.

The sub-regional watershed and hydrogeologic conditions are described in Section 2.3 and in Sykes et al. (2004). Detailed topography for the sub-regional site is shown in Figure 2-2. The sub-regional watershed corresponds to topographic divides to the north and south, and local topographic highs along other perimeter boundaries.



Topography (mASL)

High : 462.88
Low : 333.02

— Sub-regional Watershed Boundary
— Regional Watershed Boundary



0 5 10 20 30
Kilometers

Note: Elevation is given in metres Above Sea Level (mASL).

Figure 2-1: Regional Watershed Boundary and Sub-regional Domain Boundary

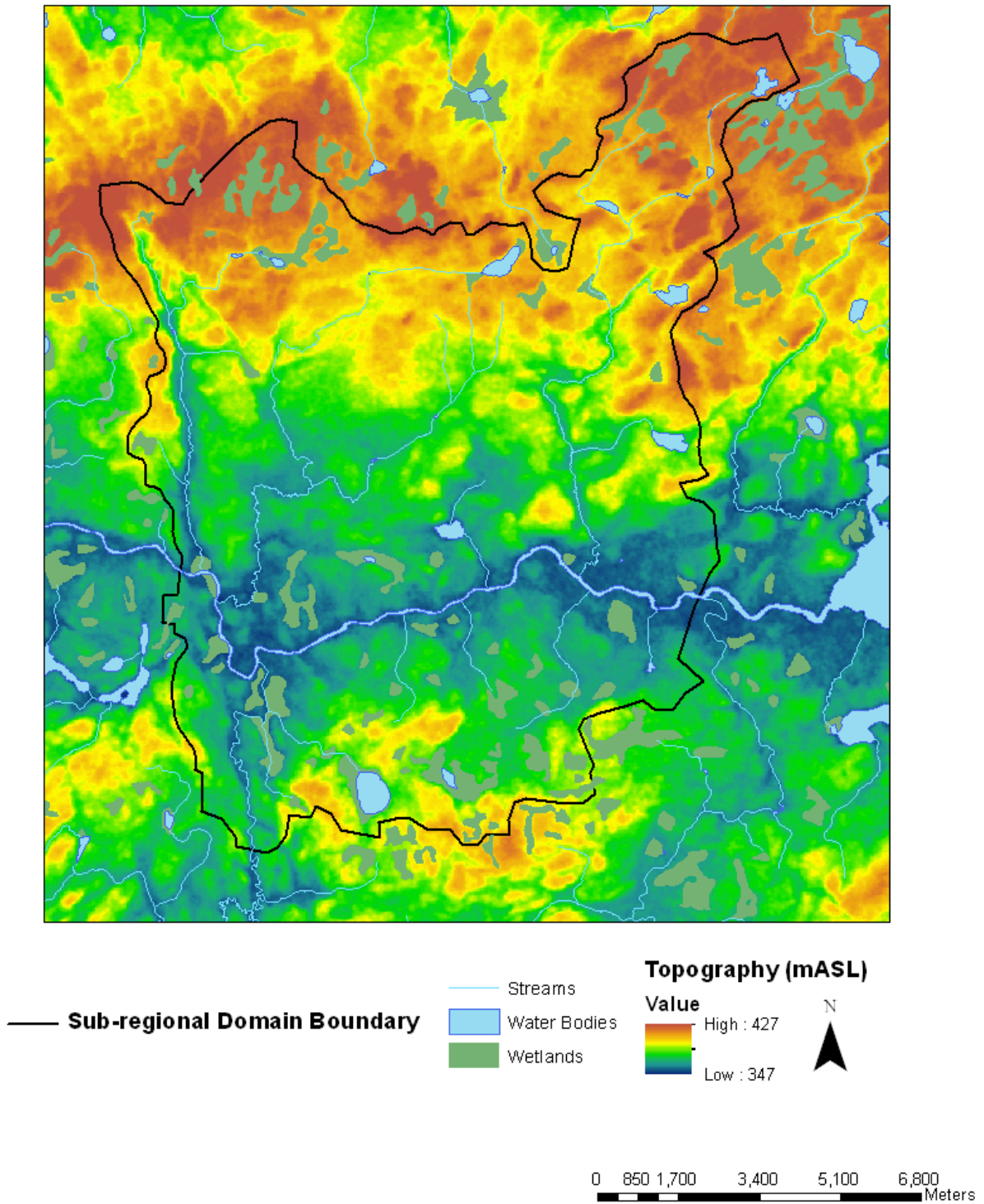


Figure 2-2: Sub-regional Watershed including Topography and Surface Hydrology

2.2.1.2.2 Surface Hydrology

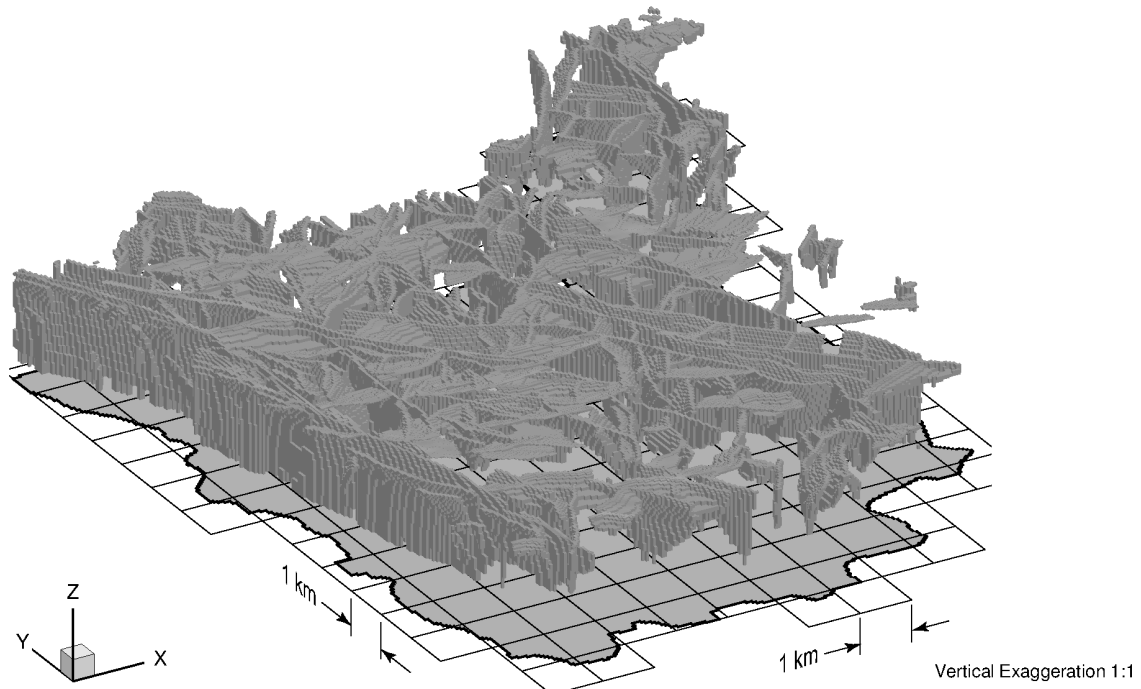
The surface-water features, along with the domain boundary, are also shown in Figure 2-2. The east-west trending river corresponds with a topographic low. This river divides the domain and will act as the convergence point for local surface water patterns. The sub-regional watershed contains smaller rivers that flow into the main east-west trending river, as well as wetlands.

2.2.1.3 Discrete Fracture Network

Srivastava (2002) generated a fracture network model for a sub-regional area of the Canadian Shield that was used in the Third Case Study (Garisto et al. 2004). The fracture network was based on a surface lineament analysis that coincided with surface drainage features, and extended underground using a geostatistical fracture propagation process that respected fracture statistics from the Canadian Shield. The network included all fractures with scale length larger than about 500 m.

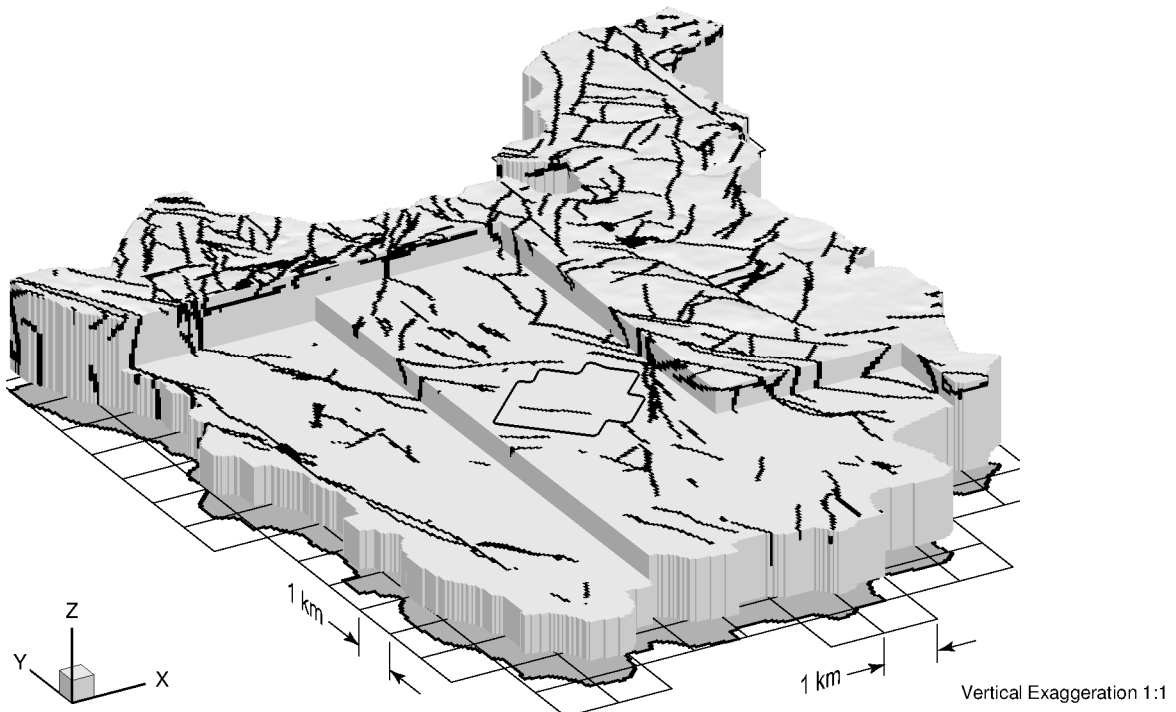
The fracture network model created by Srivastava (2002) was informed by a combination of site-specific lineament data and statistical parameter distributions obtained from studies of the Whiteshell Research Area (WRA) on the Canadian Shield. The conditioning data used to determine the fracture distribution and characteristics are from Sikorsky et al. (2002). The conditioning data used would be typical of that available during initial surface based site characterization activities. Near the surface of the crystalline rock site, the fracture zones can be grouped into either subvertical fractures or low-dip fracture sets. The low-dip fracture zones truncate against the subvertical fracture zones. At depth, the low-dip fracture zones will not be frequent and the sub-vertical fracture zones will tend to converge, resulting in a decrease in fracture density with depth (Srivastava 2002).

The distribution and locations of the fracture zone elements, as applied in the numerical groundwater model (see Section 2.3), are shown in Figure 2-3 and Figure 2-4. The fracture zone network consists of a large number of intersecting features within the first few hundred metres, and significantly fewer features (larger and/or more vertical) extending to greater depths. Characterizing fracture zones with a high degree of detail can be difficult. Major fracture zones can be identified at surface, but the location and distribution of smaller fracture zones, as well as their interconnectedness, will be less certain.



Note: Figure is based on Srivastava (2002)

Figure 2-3: Fracture Network Model Elements



Note: Figure is based on Srivastava (2002). Cut away sections are at 500 metres below ground surface (mBGS) and 1000 mBGS.

Figure 2-4: Distribution of Fracture Zones

2.2.2 Descriptive Hydrogeologic Site Model

Groundwater flow paths and residence times within a crystalline groundwater system are governed to a large extent by site-specific conditions. Key factors influencing groundwater movement include the nature, spatial variability and anisotropy of the permeability field (comprised of the rock matrix and transmissive structural discontinuities), the direction and magnitude of hydraulic gradients resulting from topographic and spatial fluid density differences, and hydraulic boundary conditions. Hydraulic gradients on the Canadian Shield are often on the order of 10^{-3} due to the low topographic relief (Sykes et al. 2009, Ophori et al. 1995). With respect to the latter, at longer time scales, external perturbations, such as hydromechanical ice-sheet loading and permafrost, can influence groundwater system evolution.

The hydrogeologic system at a specific crystalline site, including the existing fracture systems, would be investigated as part of detailed site characterization activities. For the hypothetical crystalline site considered in this study, the conceptual hydrogeological model, including information on the groundwater systems and hydraulic parameters, is described in this section.

2.2.2.1 Groundwater Systems

In the hypothetical Canadian Shield site, three groundwater systems are considered: shallow, intermediate and deep. These systems are identified, in part, by rock mass hydraulic conductivities, as observed at Atikokan and the WRA, as well as groundwater total dissolved solids (TDS) concentrations and redox conditions (a detailed, geochemical conceptual model is presented in Section 2.2.3). The primary characteristics for the three groundwater systems are tabulated in Table 2-1 and described below. For the purpose of this study, the hydraulic conditions were assumed to be hydrostatic with respect to the variable density fluids.

Shallow Groundwater System (0-150 mBGS)

The shallow groundwater system, located near surface, is predominately driven by local- and sub-regional-scale topographic changes. Within this system, groundwater flow reflects, in part, the heterogeneous three-dimensional network of near-surface vertical and horizontal fracture zones. Meteoric water, in the form of rain or snowmelt, initially recharges the groundwater system by infiltration in fractures from topographic highs, and flows near the surface before discharging into streams or rivers, lakes, swamps or bogs associated with local topographic lows. The velocities in the shallow groundwater zone result in advection dominating contaminant transport processes (Normani et al. 2007). The average travel time for groundwater to recharge, and then subsequently discharge, in the shallow zone is typically less than 1,000 years. The groundwater in the shallow groundwater zone is fresh and oxygen-rich, with low TDS concentrations (further discussion of which can be found in Section 2.2.3).

Intermediate Groundwater System (150-700 mBGS)

The groundwater in the intermediate groundwater system transitions from fresh and oxygen-rich, to more mineralized and chemically reducing with depth. At the hypothetical site, the shift from oxidizing to reducing conditions occurs at around 150 mBGS. In the intermediate groundwater system, larger domains of low permeability rock tend to decrease mass transport rates.

Deep Groundwater System (>700 mBGS)

In contrast with the shallow and intermediate groundwater zones, the groundwaters in the deep system have higher total dissolved solids concentrations and, hence, fluid densities. Geochemical redox potential is reducing. The increased fluid density will influence both energy gradients within the groundwater regime and vertical upward movement of groundwater between the shallow/intermediate and deep groundwater zones (Park et al. 2009).

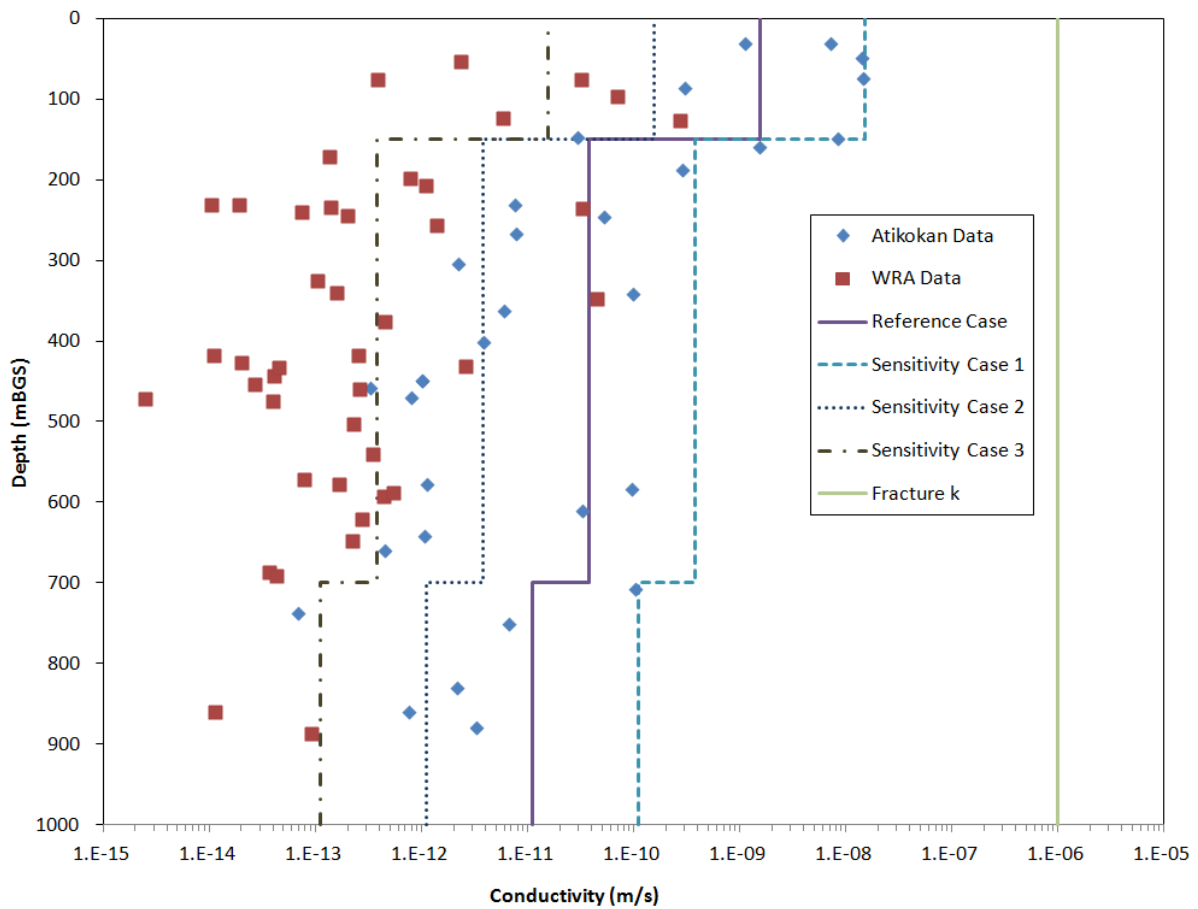
2.2.2.2 Hydraulic Parameters

Rock mass hydraulic conductivity data from Canadian Shield research sites in the WRA (Stevenson et al. 1996) and Atikokan (Ophori and Chan 1996) were used to define hydraulic conductivity versus depth profiles for the hypothetical site. The hydraulic conductivity versus depth profiles were grouped into three depth ranges based upon observable trends in the rock mass data. When organized in this manner, the data indicate a trend of decreasing rock mass hydraulic conductivity with depth (Sykes et al. 2004).

The hydraulic conductivity of fracture zones in crystalline rock has a high degree of influence on the development and evolution of groundwater systems at depth (Normani et al. 2007). For this case study, however, the fracture hydraulic conductivity is assumed to be 10^{-6} m/s (≈ 30 m/a) and independent of depth. For the purpose of this illustrative case study, smaller fractures and joints are accounted for by the effective hydraulic conductivity assigned to the rock mass between the fracture zones.

The rock mass and fracture zone hydraulic conductivity profiles are plotted versus depth in Figure 2-5. The key hydraulic parameters (hydraulic conductivity, specific storage, fluid density, rock porosity and effective diffusion coefficients¹) for the hypothetical site are provided in Table 2-1. At 500 m below ground surface, the reference hydraulic conductivity in the rock mass surrounding the repository is assumed to be 4×10^{-11} m/s (≈ 0.001 m/a). Based upon Young's Moduli, Poisson's Ratio and fluid density, the calculated specific storage for the shallow, intermediate and deep groundwater zones is $1 \times 10^{-7} \text{ m}^{-1}$.

¹ The effective diffusion coefficients were calculated using the following relationship: $D_e = \tau n D_o$, where τ represents the tortuosity of the rock matrix and n represents the porosity. D_o represents the free-water diffusion coefficient for brine. The effect of temperature on effective diffusion coefficients is not considered.



Note: WRA data are from Stevenson et al. (1996). Atikokan data are from Ophori and Chan (1996).

Figure 2-5: Rock Mass and Fracture Zone Conductivity Profile

Table 2-1: Physical Hydrogeological Parameters

Zone	Layer	Depth (mBGS)	Thickness (m)	Hydraulic Conductivity (m/s)				Bulk Density (kg/m ³)	Porosity (-)	Specific Storage (m ⁻¹)	Effective Diffusion Coeff. (m ² /s)	Redox Conditions
				Ref. Case	Sens. Case 1	Sens. Case 2	Sens. Case 3					
Shallow Groundwater Zone	Sediment	0 – 10	0 – 10	1x10 ⁻⁵	1x10 ⁻⁵	1x10 ⁻⁵	1x10 ⁻⁵	1250	0.5	1x10 ⁻⁷	1x10 ⁻¹²	Oxidizing
	Overburden	0 – 10	0 – 10	1x10 ⁻⁸	1x10 ⁻⁸	1x10 ⁻⁸	1x10 ⁻⁸	1537	0.42			
	Rock Mass Permeability Zone 1	10 – 150	140	2x10 ⁻⁹	2x10 ⁻⁸	2x10 ⁻¹⁰	2x10 ⁻¹¹	2700	0.003			
	Shallow Fracture Zone	10 – 150	140	1x10 ⁻⁶				2400	0.1			
Intermediate Groundwater Zone	Rock Mass Permeability Zone 2	150 – 700	550	4x10 ⁻¹¹	4x10 ⁻¹⁰	4x10 ⁻¹²	4x10 ⁻¹³	2700	0.003	1x10 ⁻⁷	1x10 ⁻¹²	Reducing
	Intermediate Fracture Zone	150 – 700	550	1x10 ⁻⁶				2400	0.1			
Deep Groundwater Zone	Rock Mass Permeability Zone 3	700 – 1500	800	1x10 ⁻¹¹	1x10 ⁻¹⁰	1x10 ⁻¹²	1x10 ⁻¹³	2700	0.003	1x10 ⁻⁷	1x10 ⁻¹²	Reducing
	Deep Fracture Zone	700 – 1500	800	1x10 ⁻⁶				2400	0.1			

Notes: The porosity value of 0.003 represents the rock matrix porosity. The porosity value of 0.1 represents the porosity of the fracture zone. Bulk density values taken from Davison et al. (1994), App. D. Porosity values taken from Davison et al. (1994), App. D. Effective diffusion coefficient for Iodide taken from Vilks et al. (2004).

Additional parameters are required to perform mass transport simulations and hydro-mechanically coupled paleohydrogeological simulations.

The parameters required for hydro-mechanical paleohydrogeologic simulations are provided in Table 2-2. For the reference case, the fluid modulus is calculated to be 3600 MPa based on a pressure of 14.7 MPa, a temperature of 20°C and a fluid density of 1200 kg/m³ (Batzle and Wang 1992). The grain modulus of 50 GPa for crystalline rock was obtained from Lau and Chandler (2004). Given a Poissons Ratio of 0.25 and a specific storage of 1x10⁻⁷ m⁻¹, the Young's Modulus is calculated to be 51.8 GPa. The resulting Biot coefficient² is 0.309, with a loading efficiency of 0.59. A loading efficiency of 1.0 is specified for glacial drift.

Table 2-2: Hydromechanical Coupling Parameters

Simulation Case	Youngs Modulus (GPa)	Grain Modulus (GPa)	Biot Coefficient	Specific Storage (m ⁻¹)	Loading Efficiency (-)
Reference Case	51.8	50.0	0.309	1.00x10 ⁻⁷	0.59
Biot Coefficient = 1.0	51.8	Infinity	1.0	1.99x10 ⁻⁷	0.95
Biot Coefficient = 0.5	37.5	50.0	0.5	1.92x10 ⁻⁷	0.68

2.2.2.3 Paleohydrogeology Boundary Conditions

Paleohydrogeological simulations are used to illustrate the long-term evolution and stability of the geosphere to external perturbations. Glaciation is expected to be the largest external perturbation to which a repository would be subject.

Over the past 900,000 years, the crystalline rocks of the Canadian Shield have been subjected to nine glaciation events, each lasting for a period of approximately 100,000 years (Peltier 2002). During the last glacial advance and retreat, up to 4 km of ice overrode the Canadian Shield. In assessing the long-term stability and evolution of groundwater systems at depth in a crystalline rock site in the Canadian Shield, the loading and unloading of the geosphere by the glacier will represent one of the most significant perturbations from the current conditions.

The University of Toronto (UofT) Glacial Systems Model (GSM) provides the hydraulic and mechanical paleoclimate boundary conditions and permafrost depths for the paleohydrogeologic simulations (Peltier 2006). Paleoclimate simulation nn2008 represents a single example of a

² According to Wang (2000), "The Biot-Willis parameter α is the ratio of increment of fluid content to change in bulk volume when the pore fluid remains at constant pressure [...]. It would be exactly one if all of the bulk strain were due to pore volume change (i.e., the solid phase is incompressible). It is less than one for a compressible solid phase because the change in bulk volume is greater than the change in pore volume by the amount of the change in the solid volume."

The loading efficiency term ζ [dimensionless] acts as a source/sink term that will increase or decrease fluid pressure based upon a change in vertical stress. Further information on the loading efficiency term can be found in Therrien et al. (2010).

glacial cycle, as predicted by the GSM. A plot of various nn2008 GSM outputs for the grid cell containing the sub-regional modelling domain is shown in Figure 2-6. These outputs include ice thickness, meltwater production rate, lake depth, permafrost depth, and ice-sheet basal temperature relative to the pressure melting point of ice. Only the ice thickness and permafrost depth outputs are applied to the paleohydrogeologic groundwater simulations. Similarly, the alternate paleoclimate simulation, nn2778, GSM model outputs for the grid cell containing the sub-regional modelling domain are shown in Figure 2-7. The main difference between the two glaciation scenarios is the duration of permafrost during the 121 thousand year GSM simulation; the length of time nn2778 is subject to permafrost conditions is less than that of nn2008. The paleoclimate boundary conditions presented in Figure 2-6 and Figure 2-7 are applied to the paleoclimate simulations described in Section 2.3.5.3. A permafrost hydraulic conductivity of 5×10^{-11} m/s, from McCauley et al. (2002) as determined experimentally for frozen soils, was applied.

2.2.3 Descriptive Geochemical Site Model

The groundwater chemistry of the crystalline rocks in the Canadian Shield site shows a general pattern in chemical evolution with respect to depth or distance along the flow path (Gascoyne and Kamineni 1994). Singer and Cheng (2002) suggest, in general, that within the Canadian Shield there are two main groundwater systems: a shallow fresh water system (0-150 m) and an underlying deep system with increased groundwater salinity. Although crystalline rocks occupy vast geographic distances, it is unlikely that shallow groundwater systems have the same extent (Singhal and Gupta, 2010).

The transition between the shallow and deep systems is, in part, a function of the occurrence, frequency and interconnectivity of discrete fractures and fracture zones within the rock mass. In the deeper regions of the groundwater system, the hydraulic conductivity of the rock mass tends to decrease as the structural discontinuity frequency and interconnectivity diminish (Stevenson et al. 1996, see Figure 2-5).

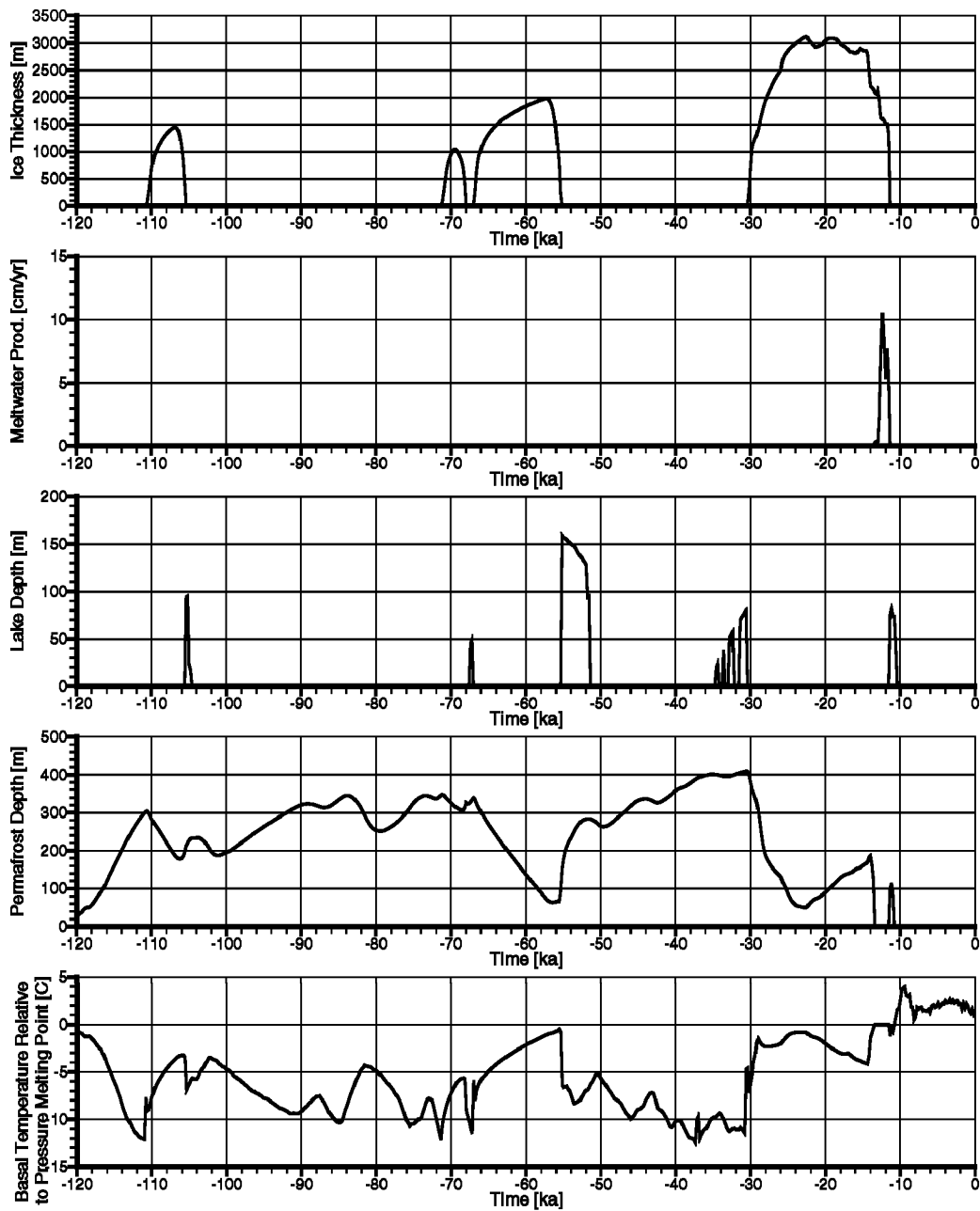


Figure 2-6: GSM Outputs from Simulation nn2008 for the Grid Cell Containing the Sub-Regional Modelling Domain

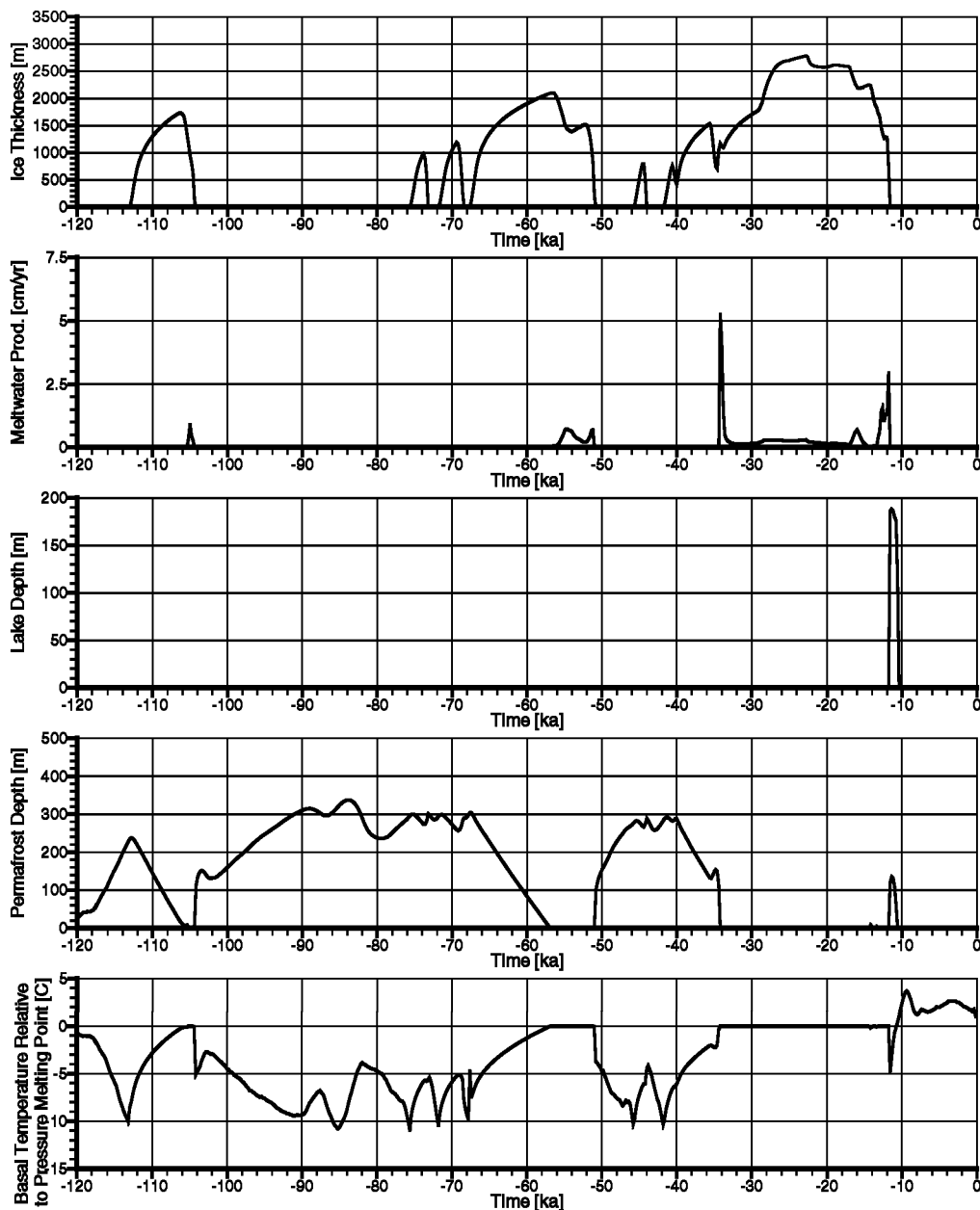


Figure 2-7: GSM Outputs from Simulation nn2778 for the Grid Cell Containing the Sub-Regional Modelling Domain

In low temperature environments, dissolution rates are very low for the major rock-forming minerals in granitic rocks. The most abundant chemical components in groundwater in granitic rocks are the cations Ca, Na, and Mg, and the anions HCO_3 , SO_4 , and Cl (Bucher and Stober 2000). Cations such as K, Al, Si, and Fe, which are important components of the most abundant minerals in the rock, are less abundant in solution because they tend to be associated with relatively insoluble secondary minerals. Groundwater geochemistry is modified over time and space by rock-water interactions, mixing with other waters in the system, and by microbially-mediated reactions. In crystalline rocks, vertical zoning in groundwater chemical

composition has been reported from several areas, with a progression from dilute near-surface waters, to brackish waters and, in some instances, to saline waters at depths ≥ 500 m (Singhal and Gupta 2010, and references therein).

Information on the geochemical conditions collected as part of detailed site characterization activities would be combined with available regional information to define site-specific conditions. The geochemical conditions in the shallow, intermediate and deep groundwater systems assumed for the hypothetical site (Section 2.2.2.1) are described below. The microbial conditions and expected colloid concentrations in groundwaters within crystalline settings are also described.

2.2.3.1 Geochemical Conditions at the Hypothetical Site

The geochemical conditions described here pertain to both the groundwater present in fractures and to porewaters within the rock matrix.

Shallow Groundwater System (0-150 mBGS)

McMurry et al. (2003) reported that shallow groundwaters in crystalline rock generally are dilute and oxidizing. The pH values are buffered by carbonate equilibria to near-neutral pH values of about 6 to 8. Reactions with organic material and bacteria tend to consume dissolved oxygen rapidly along the flow path, promoting reducing conditions in the subsurface within tens of metres, in most cases (Gascoyne 1997). The shallow groundwaters in the crystalline rocks of the hypothetical Canadian Shield site remain largely separate from stagnant, geochemically distinct groundwaters at depth, consistent with data collected from actual Canadian Shield environments.

Intermediate Groundwater System (150-700 mBGS)

With increased depth, rock-water interactions, such as the precipitation and dissolution of calcite and ion exchange on clay minerals, cause the groundwaters to become slightly more mineralized (e.g. McMurry 2004, Gascoyne and Kamenini 1994). Hydrolysis reactions, particularly those involving amphiboles and plagioclase feldspar, in some cases, cause pH values to increase to about 9 for granitic rocks, or to about 10 for rocks such as gabbros, which contain large amounts of Ca-rich plagioclase. Reactions with ferrous minerals, sulphides, reduced sulphur aqueous species, and dissolved organics promote and maintain reducing conditions. Many of these redox reactions are microbially-mediated. The depth of the redox divide is typically 150 mBGS (Gascoyne 2000).

Gascoyne et al. (1988) investigated the saline brines within several Precambrian plutons and identified a chemical transition around 300 m depth, marked by a rapid rise in total dissolved solids (TDS). This was attributed to advective mixing above 300 m, with a shift to diffusion-controlled transport below that depth. It was noted that major fracture zones within the bedrock can, where present, extend the influence of advective processes to greater depth. In the deeper regions, groundwater transport in the rock matrix tends to be very slow, resulting in long residence times (Gascoyne and Kamineni 1993, Gascoyne 2004).

A reference groundwater composition, CR-10 (Table 2-3), has been defined to represent the saline groundwater conditions at the depth of the hypothetical repository (500 mBGS). It is based on the understanding that the typical groundwater chemistry at this depth in crystalline rock is Na-Ca-Cl or Ca-Na-Cl saline water under reducing conditions (McMurry 2004,

Gascoyne and Kamenini 1994). The CR-10 water was derived from the WRA reference water WN-1M, which, in turn, was derived from data at depths ranging from 350-800 mBGS at the WRA in crystalline rocks of the Canadian Shield (Gascoyne 1988; McMurry 2004).

CR-10 is a Ca-Na-Cl type water with a TDS concentration of 11.3 g/L and is under reducing conditions. The density of the groundwater is 1.006 kg/L. The concentration of key chemical solutes is shown in Table 2-3.

The reducing environment at depth is, in part, the result of microbial reactions involving organic carbon, and rock-water interactions between dissolved oxygen and iron- and sulphur-rich minerals (see Table 2-4). These reactions consume dissolved oxygen, resulting in a reducing groundwater environment (Davison et al. 1994). The assumed colloid concentration in groundwater at repository depth is 0.34 mg/L (Davison et al. 1994). Further discussion of colloids can be found in Section 5.4.8.

Table 2-3: CR-10 Porewater Parameters

Composition	CR-10
pH	7.0
Environment type	Reducing
Eh (mV)	-200
Density	1.006
Solutes (mg/L)	
Na	1900
K	15
Ca	2130
Mg	60
HCO ₃	70
SO ₄	1000
Cl	6100
Br	-
Sr	25
Li	-
F	2
I	-
B	-
Si	5
Fe	1
NO ₃	<1
PO ₄	0
TDS	11,300

Note: The charge balance error (CBE) for water CR-10 in Table 2-3 is 0.08%

Table 2-4: Geosphere Redox Conditions

Depth(mBGS)	Redox Condition
0-10	Oxidizing
10-150	Oxidizing
150-300	Reducing
300+	Reducing

Deep Groundwater System (>700 mBGS)

Groundwater research carried out at the Atomic Energy of Canada Limited (AECL) Underground Research Lab (URL) found that groundwaters and seepage waters in the crystalline rocks at depths of 300 to 1000 m possessed TDS concentrations values ranging between 3 and 90 g/L (Gascoyne 2000, Gascoyne 2004). However, as summarized in Stotler et al. (2012), TDS concentrations exceeding 250 g/L have been reported in some regions of the Canadian Shield at depths below 500 m. There are a number of potential sources of salinity, including: prolonged interactions of pore fluids with the rock, salt enrichment by freezing or evaporation, and mixing with hydrothermal saline fluids that may have persisted in fractures for hundreds of millions of years. In crystalline rocks that were adjacent to, or covered by, marine waters at some time in the geological past, there is also evidence that seawater or evaporative brines have migrated into the fractures along regional flow paths (Bottomley et al. 1999).

In-situ diffusion experiments, conducted within low-permeability crystalline rock, estimated effective diffusion coefficients (D_e) for iodide in the range of 1.4×10^{-13} m²/s to 1.1×10^{-12} m²/s. Evidence obtained during the in-situ experiments did not identify an apparent trend related to sample depth or stress conditions (Vilks et al. 2004). An effective diffusion coefficient value of 1×10^{-12} m²/s is applied at the hypothetical site (as listed in Table 2-1). To achieve this D_e value, zonal tortuosity values were calculated using porosity and a brine diffusion coefficient (NaCl at 1 mol/L) of 1.5×10^{-9} m²/s (Weast 1983). For paleohydrogeologic simulations with a tracer, the free-water diffusion coefficient for the tracer (H₂¹⁸O) of 2.7×10^{-9} m²/s in Singh and Kumar (2005) was used with the tortuosity value previously calculated. Longitudinal dispersivity values for brine and tracer transport, and for mean life expectancy (MLE)³, are set to 120 m, while both transverse horizontal and transverse vertical dispersivities were set to 12 m. Smaller dispersivity values resulted in numerical artifacts and oscillations in the transport and MLE solutions.

2.2.3.2 Microbial Conditions in Crystalline Environments

Cell densities in Canadian groundwaters have been reported between 10^3 and 10^5 cells/mL (Stroes-Gascoyne and West, 1997). Microbial metabolism requires a carbon source, terminal electron donor and terminal electron acceptor. Additional nutrients required for growth and

³ Mean Life Expectancy (MLE): Mean Life Expectancy is the mean time for discharge of a non-decaying, non-sorbing solute from a given point in the groundwater system based upon advective-dispersive mass transport.

maintenance include N, P, S, K, Mg, Na, Ca and Fe, as well as a suite of other trace elements. Subsurface microbial communities are capable of using an array of terminal electron accepting processes. The dominant species in a given environment tend to be those bacteria that generate the most energy from the available nutrient sources. As summarized by Sherwood Lollar (2011), acetogens are often the dominant component of the population in the Canadian Shield, followed by iron-reducing and sulphate-reducing bacteria and methanogens (using either dissolved inorganic carbon or acetate). In addition, studies of Canadian Shield groundwaters have shown microbial assemblages containing heterotrophic aerobes and anaerobes, denitrifying, N₂-fixing and iron-precipitating bacteria (Jain et al. 1997).

Microbial processes in the geosphere that are relevant to a DGR for used nuclear fuel are summarized in Humphreys et al. (2010) and Sherwood Lollar (2011). The consumption of oxygen by aerobic microbial activity has been identified as the most significant effect of microorganisms on base scenario processes related to the evolution of the geosphere (McMurry et al. 2003). Microbial processes play an important role in O₂ reduction in the subsurface and are able to catalyze reactions that would not otherwise take place at low temperatures (SKB 2006). Oxygen is a versatile electron acceptor and is energetically favourable for many microorganisms. As summarized in SKB (2006), several in-situ and laboratory experiments have demonstrated the consumption of oxygen in granitic environments. These studies have shown that there is a substantial increase in microbial activity where surface water containing O₂ encounters stagnant groundwater systems, and that the time scale for complete microbial oxygen reduction in typical fractures is on the order of a few days (SKB 2006). In crystalline rock environments, oxygen concentrations have been shown to decrease with depth due to microbial processes. For example, at the crystalline site of Olkiluoto, Finland, oxygen concentration decreases have been correlated to methanotrophic (methane metabolizing) bacteria, suggesting that these bacteria could constitute an effective barrier against oxygen intrusion in the presence of methane (Pedersen 2006).

Gas production is a natural abiotic and biotic process in crystalline rock environments (Sherwood Lollar et al. 1993a, 1993b, 2007). From a microbial energy production perspective, methane and hydrogen are perhaps the most important deep subsurface gases. Methane concentrations ranging from 1 µM to 18,600 µM have been reported in Canadian Shield and Fennoscandian Shield groundwaters (Sherwood Lollar et al. 1993a, 1993b). The fixation of CO₂ to organic molecules by autotrophic methanogens and acetogens under anaerobic conditions is an important process in the deep subsurface resulting in the formation of methane and acetate, respectively. This provides a renewable source of organic carbon to continually fuel the consumption of oxygen (if present) in the deep subsurface (SKB 2006). Hydrogen is a versatile electron donor in subsurface environments. H₂ concentrations tend to increase in deeper, more saline fracture waters (Sherwood Lollar et al. 2007). Between 2 µM and 1600 µM of hydrogen in groundwater from Canadian Shield and Fennoscandian Shield rocks has been reported (Sherwood Lollar et al. 1993a, 1993b). Hydrogen from deep geological processes contributes to the redox stability of deep groundwater by acting as an electron donor for microbial metabolism (Pedersen 2000).

2.2.3.3 Colloids

Particles between 1 to 1 x 10⁻³ µm are termed colloids and include both inorganic mineral particles (in particular clays) and organic particles, such as microbial cells, viruses or organic matter (Hallbeck and Pedersen 2008). They are suspended in groundwater and are sufficiently

small so that interfacial forces are significant controls on their transport and fate. Depending on their composition and physical characteristics, among other factors, colloids may be transported at approximately the same velocity as groundwaters.

Colloids typically are present in low concentrations (less than 1 mg/L) in groundwaters (McMurry et al. 2003). The natural colloid concentration in deep groundwaters in the Canadian Shield is expected to be low. See, for example, data from Whiteshell and Atikokan on total colloids (Davison et al. 1994, Vilks and Bachinski 1997, Vilks et al. 1998) and also on organic colloids in Fennoscandian Shield groundwaters (Andersson 1999). In such settings, the assumed reference natural colloid concentration in deep groundwaters is between 0.2 and 0.4 mg/L. The concentration of colloids in the near-field geosphere is influenced to some extent due to repository-related changes in temperature and interactions with clay and cementitious sealing materials as well as groundwater salinity.

2.2.3.4 Sorption

The sorption of radionuclides onto mineral surfaces within the geosphere is a potential mechanism for slowing the transport of radionuclides from repository depth to the surface environment. There are many factors that impact radionuclide sorption processes in the geosphere, such as rock type, mineral surface area, groundwater salinity, pH, redox conditions, temperature, the presence or absence of complexing ligands, and radionuclide concentration. The sorption partition coefficient (K_d) of radionuclides is used to describe their sorption behaviour. In fractures, the presence of alteration minerals will generally result in higher sorption capacities (K_d values) than in non-altered rock (Byegård et al. 2008, Crawford et al. 2006).

Sorption of radionuclides is generally reduced in groundwaters with high salinity (Vilks 2009). In particular, radionuclides that are retarded by cation exchange mechanisms (i.e., Cs and Sr) are more strongly adsorbed in groundwaters with lower ionic strengths (Byegård et al. 2008, Crawford et al. 2006). This effect is not as important for either the elements that adsorb by surface complexation, or for the moderately saline groundwater conditions at repository level for this hypothetical Canadian Shield site. Sorption coefficients for the hypothetical site considered in this study are presented in Chapter 7.

2.3 Sub-Regional Scale Hydrogeologic Modelling

In order to illustrate the role of key geosphere parameters and processes, such as rock mass permeabilities and groundwater salinity, on geosphere and groundwater system stability at repository depth, a suite of sub-regional scale numerical groundwater models were developed. The following sections describe the strategy behind the modelling conducted.

2.3.1 Modelling Strategy

The behaviour, stability and resilience to change of the geosphere at repository depth is illustrated through the use of 13 comparative sensitivity cases, contrasted with a reference case based upon the conceptual model described in Section 2.2. In the sensitivity cases, key geosphere parameters are varied to illustrate the role they play in influencing groundwater flow and mass transport. The reference case and the geosphere parameters varied in the sensitivity cases are shown in Table 2-5.

The reference case simulates current site conditions at the sub-regional scale and it includes groundwater salinity distributions to allow simulation of density-dependent flow. For the purpose of this illustrative case study, the discrete fracture network realization is simulated as an equivalent porous media representation.

Sensitivity cases, in which the distribution of total dissolved solids are varied, are conducted to examine the role of spatially variable groundwater densities on hydraulic gradients, groundwater velocities, groundwater system stability and dominant mass transport processes. The hydraulic conductivity of the rock mass is also varied within an expected range of uncertainty to illustrate the sensitivity of estimated groundwater performance measures and, in particular, designation of mass transport regimes.

The purpose of the paleohydrogeologic scenarios is to assess the influence of a glacial event on groundwater system stability. In particular, the simulations explore transient hydraulic gradients, groundwater velocities, and the depth of penetration by glacial recharge, which are relevant to illustrating long-term DGR safety. The paleohydrogeologic boundary conditions are varied to include cold and warm based glaciers in order to illustrate groundwater system resilience to external perturbations. In addition to the cold and warm based glaciers, the hydrogeologic surface boundary conditions are varied to illustrate the effect of the surface recharge boundary condition.

The effect of hydromechanical coupling during paleohydrogeologic scenarios is investigated in two ways: i) the loading efficiency is varied from the calculated reference value to 0 in order to illustrate the role of hydromechanical coupling; and, ii) the Biot coefficient is varied from 1.0 to 0.5 to illustrate the role of the assumed grain compressibility groundwater system response.

2.3.2 Computational Models

The numerical groundwater modelling was performed using FRAC3DVS-OPG v1.3.0. FRAC3DVS-OPG (Therrien et al. 2010) is a computational model capable of solving three-dimensional variably-saturated groundwater flow and solute transport in discretely-fractured media. The model includes a dual porosity formulation while discrete fractures are represented as idealized two-dimensional parallel plates, or as fracture zones defined by hydraulic conductivity and width. The numerical solution to the governing equations is based on implementations of both the control volume finite element method and the Galerkin finite-element method. The FRAC3DVS-OPG version of the model couples fluid flow with salinity transport through fluid density, which is dependent on the total dissolved solids concentration. Details of the FRAC3DVS-OPG model that are pertinent to the study are described in Therrien et al. (2010) and in Normani et al. (2007). FRAC3DVS-OPG is developed and maintained as nuclear grade software in a Quality Assurance framework in accordance with NWMO Technical Computing Software Procedure document number NWMO-PROC-EN-0002.

Important attributes of FRAC3DVS-OPG include: its ability to describe arbitrary combinations of porous, discretely fractured and dual porosity media; its flexible pre- and post-processing capabilities; the accurate handling of fluid and mass exchanges between fracture zones and matrix, including matrix diffusion effects and solute advection in the matrix; fluid and solute mass balance tracking; and, adaptive time-stepping schemes with automatic generation and control of time steps. Additional attributes, added in previous work supported by the NWMO and OPG, include sub-gridding and sub-timing capabilities (Guvanaseen 2007; Park et al. 2008a). Additionally, algorithms to estimate performance measures of groundwater age and life expectancy for the domain groundwater are also present (Cornaton and Perrochet 2006a, 2006b; Park et al. 2008b).

2.3.3 System Performance Measures

The safety case for a potential deep geological repository will rely, in part, on the ability of the geosphere to provide a long-term barrier to solute transport. The behaviour and stability of the groundwater flow and transport regimes found at repository depth can be illustrated by determining and quantifying what impact, if any, the variability of model parameters will have upon the model results. By demonstrating and determining the sensitivity of the model to perturbations in model parameters, insight into the understanding of groundwater system behaviour influencing deep geological repository performance can be obtained.

Common measures of the performance of a groundwater system include the flow state variables of equivalent freshwater head or environmental head and the derived porewater velocity, the solute concentration for a conservative tracer, the Péclet number⁴ (Bear 1988, Huysmans and Dassargues 2005) and, as shown in Normani et al. (2007), mean life expectancy (MLE) and groundwater age. Life expectancy is estimated by determining the Probability Density Function (PDF) for the time required for water particles at a spatial position in a groundwater system to reach outflow points. Particles can migrate to the boundary by both advection and hydrodynamic dispersion; particles at a given point in the system will not follow the same path to the boundary due to hydrodynamic dispersion. In this case study, the first moment of the PDF for life expectancy is estimated with the value being expressed as the MLE. Groundwater age of water particles at a spatial position can be determined by the PDF for time elapsed since the water particles entered the system from a boundary.

2.3.4 Sub-Regional Scale Conceptual Model

2.3.4.1 Model Domain and Spatial Discretization

The top surface of the domain was defined by a 50 m Digital Elevation Model (DEM) interpolated from an NRCAN 0.75 second resolution DEM using ArcGIS. Further description of the DEM and corrections made can be found in Section 2.2.1.2. The lateral boundaries were chosen to be coincident with topographic divides.

2.3.4.2 Model Parameters

The physical hydrogeological parameters are given in Section 2.2.2.2, Table 2-1. The approach used to define these additional parameters is described below.

2.3.4.3 Flow Boundary Conditions

For the solution of the groundwater flow equation, a specified head (Dirichlet) boundary condition is applied to all surface nodes to set the head equal to elevation. Zero flux boundary conditions are applied to both the lateral and bottom boundaries of the modelling domain. For simulations involving coupled density-dependent flow and transport of brine, a Dirichlet boundary condition equal to the TDS value at the bottom of the modelling domain is applied to all bottom nodes, and a mixed (Cauchy) boundary condition with zero concentration for recharging waters is applied to all surface nodes. A tracer representing recharge waters is used

⁴ Péclet Number: The Péclet number is used to assess transport mechanisms and is estimated by comparing rates of advection to diffusion.

in the paleohydrogeologic simulations and its boundary conditions are set to zero concentration for all bottom nodes and a concentration of unity using a Cauchy boundary condition for all surface nodes.

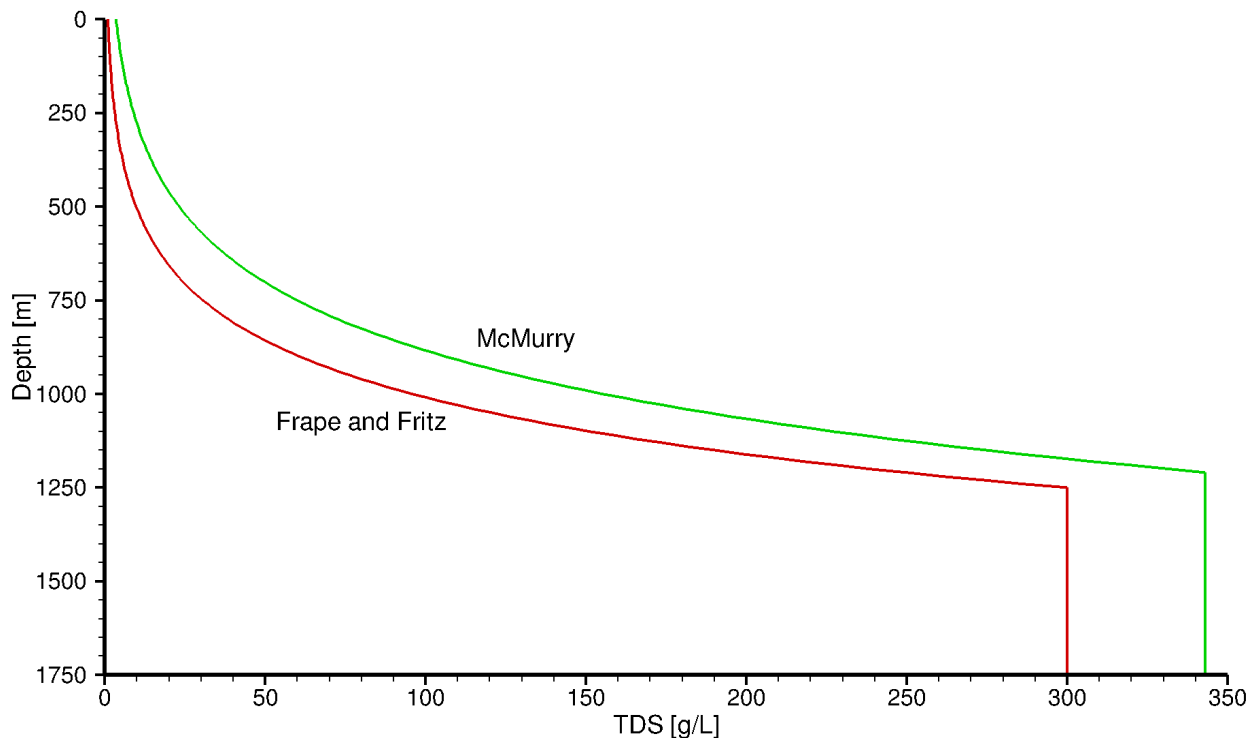
2.3.4.4 Initial Conditions and Solution of Density-dependent Flow

Salinity plays an important role with regard to fluid flow at repository depth. An increase in the concentration of TDS will result in an increase in the fluid density, which will then act as an inhibitor of active flow at depth (Park et al. 2009). The methodology for developing a solution for density-dependent flow is described in the following paragraphs.

In the absence of a source term for salinity, a transient analysis is required to determine a pseudo-equilibrium solution at a time, t , for density-dependent flow. The analysis requires the specification of an initial distribution throughout the spatial domain for both freshwater heads and TDS concentrations. In a transient analysis, the initial prescribed salinity distribution is allowed to evolve to a new state that reflects the boundary conditions, hydraulic properties and transport properties of the sub-regional scale domain. For the coupled density-dependent flow and transport system, fresh water can recharge at the surface, reducing the TDS concentration in the shallow groundwater system. The time to flush TDS from a fracture zone or the matrix is a function of the hydraulic conductivity of the unit and the energy potential of the displacing fluid as compared to the energy potential of the fluid being displaced. Fluids with lower total dissolved solids, such as recharging water, will have a lower energy potential when compared to higher total dissolved solids fluids with the same elevation and pressure. Therefore, for low-permeability regions with a relatively high TDS concentration, the time to flush the region or displace the fluids can be very long (millions of years). Complete flushing may only occur as a result of diffusion because energy gradients and/or low permeabilities may yield low fluid fluxes that may not be sufficient for advective displacement to occur. In using this method to synthesize a spatial salinity distribution, the total mass of dissolved solids and its distribution in the model domain is assumed to be known and will be a maximum initially because there are no internal sources to generate dissolved solids resulting from rock-water interaction. With this approach, as time progresses, the dissolved solids will gradually reduce as the groundwater discharges from the system.

The initial condition for TDS must specify concentrations at all nodes in the modelling domain. A depth-dependent initial TDS distribution was applied, based on Frappe and Fritz (1987), for the reference case, and based on McMurtry (2004) for sensitivity case 1. A plot of TDS with depth for both curves is provided in Figure 2-8. The curves shown in Figure 2-8 represent an upper bound for the TDS distributions on which they were based.

A linear relationship is assumed between fluid density and TDS such that a fluid density of 1200 kg/m^3 is equal to 300 g/L. Further discussion of the linear relationship between fluid density and TDS can be found in Normani et al. (2007).



Note: Figure is based on McMurry (2004) and Frape and Fritz (1987).

Figure 2-8: Upper Boundary of Total Dissolved Solids Concentrations (g/L) versus Depth

For this study, the final freshwater head distribution for the reference case analysis was calculated using the following three-step process.

- i) The distribution of freshwater heads was calculated for density-independent steady-state flow.
- ii) A TDS concentration distribution was assigned throughout the domain as an initial condition using the procedure described in the preceding paragraph. The density-independent freshwater heads were allowed to equilibrate to the assigned TDS distribution in a transient analysis, while not allowing the TDS distribution to evolve. This step allowed the freshwater heads to reflect the variation of fluid density as specified by the initial TDS distribution.
- iii) The TDS distribution was allowed to vary with the freshwater heads in a one million year transient analysis.

After one million years, the model, having been allowed to reach pseudo-equilibrium between freshwater heads and TDS distribution, produces a salinity distribution that is compatible with the fracture network model, boundary conditions, geochemical framework and, hence, the flow domain. Generally, pseudo-equilibrium is reached when then the model TDS reasonably matches field measurements (for detailed discussion, see Normani 2009). In recharge areas, brine will be flushed because of a combination of the absence of a source term for brine and the effect of meteoric recharge. This is contrasted with discharge locations, which tend to transport higher concentration brines from deeper in the groundwater system. Both the freshwater heads

and brine concentrations at one million years are used as the initial conditions for the paleohydrogeologic simulations.

2.3.5 Sub-regional Scale Analyses

2.3.5.1 Reference Case Simulation

The reference case is comprised of multiple simulations, beginning with steady-state groundwater flow. The steady-state freshwater heads, as a block-cut view, are shown in Figure 2-9. The fresh-water steady-state heads shown are calculated without the influence of density, and, as stated above, represent the first step in simulating density-dependent flow and transport. The EPM fracture zone network is shown in two block-cuts, at approximately 500 mBGS and 1000 mBGS. The freshwater heads at depth are controlled by the major east-west trending river that crosses the modelling domain.

To perform density-dependent groundwater simulations, an initial TDS concentration is needed. A depth-dependent TDS profile, according to Frappe and Fritz (1987) (Figure 2-8), is applied to the model domain to yield the distribution shown in Figure 2-10.

In order to allow TDS to migrate and to flush out of higher hydraulic conductivity zones due to meteoric recharge, a transient coupled density-dependent flow and transport one million year simulation is performed, as described in Section 2.3.4.4. The freshwater heads from the one million year simulation are shown in Figure 2-11, and the corresponding environmental heads are shown in Figure 2-12. Freshwater heads increase with an increase in fluid density and include the effects of both topographic and density gradients. To determine vertical gradients, environmental heads are calculated, which compensate for the density gradients and yield heads that are independent of fluid density. Environmental heads can only be compared along a vertical profile, as discussed in Lusczynski (1961). The distribution of TDS concentrations after one million years of simulation time are shown in Figure 2-13. Meteoric waters recharging into the shallow groundwater system reduce TDS concentrations in recharge areas, and along some fracture zones. Shallower portions of the groundwater system are more affected than the intermediate and deep groundwater systems, which retain high TDS concentrations at the end of the one million year simulation.

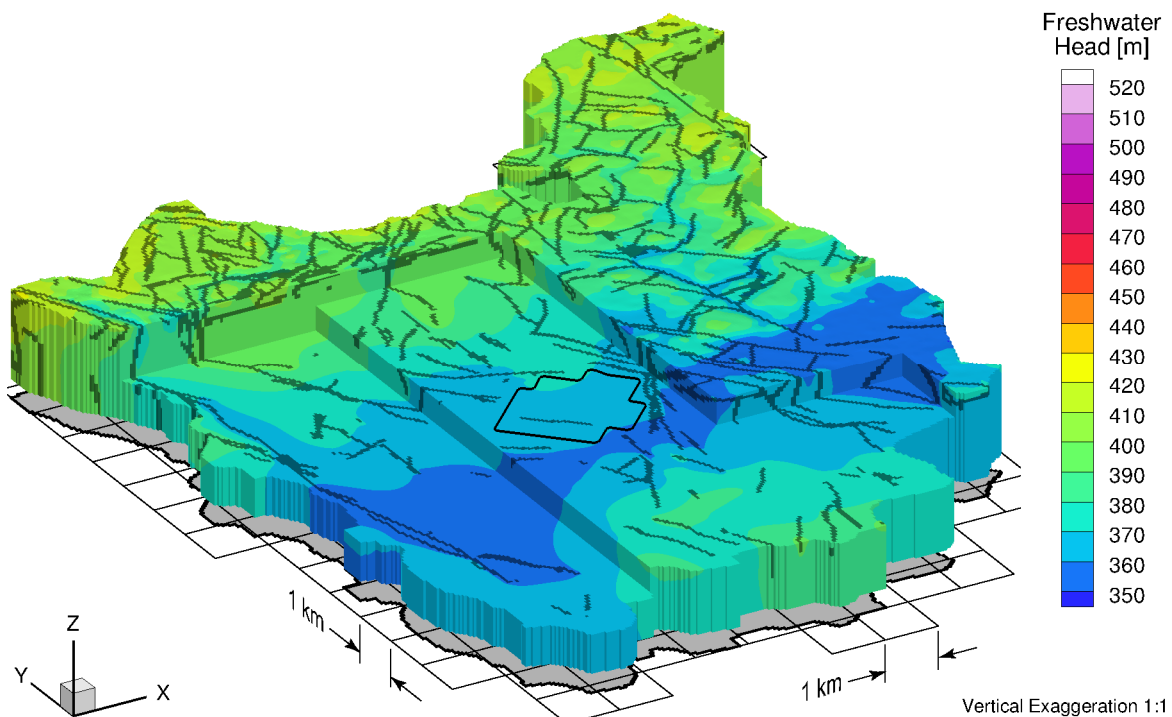
Porewater velocity magnitudes are shown in Figure 2-14. The highest velocities occur within fracture zones and in the more permeable shallow groundwater system. Velocity magnitudes tend to decrease with increasing depth, generally due to the decreasing hydraulic conductivity with depth. In the repository footprint, the porewater velocity magnitudes are between 10^{-2} and 10^{-3} m/a, except within or immediately adjacent to a fracture zone. A cross-sectional plot through the repository that depicts the vertical distribution of estimated Péclet numbers for the reference case simulation is provided in Figure 2-15. With respect to this figure, the estimated Péclet numbers shown represent ranges in which advective (>5), advective-dispersive (5 to 0.4) and diffusive (0.4) mass transport processes most influence solute migration (Bear 1988).

Within the repository footprint at 500 mBGS typical Péclet numbers are on the order of 10^{-2} with associated porewater velocities in the range 10^{-3} m/a. The higher Péclet numbers associated with the fractures, as shown in Figure 2-15, reflect the influence of the higher hydraulic conductivities within the discrete structural features.

The ratio of the vertical component of velocity to velocity magnitude for the domain is shown in Figure 2-16. The figure can be used to determine the predominant direction of the calculated

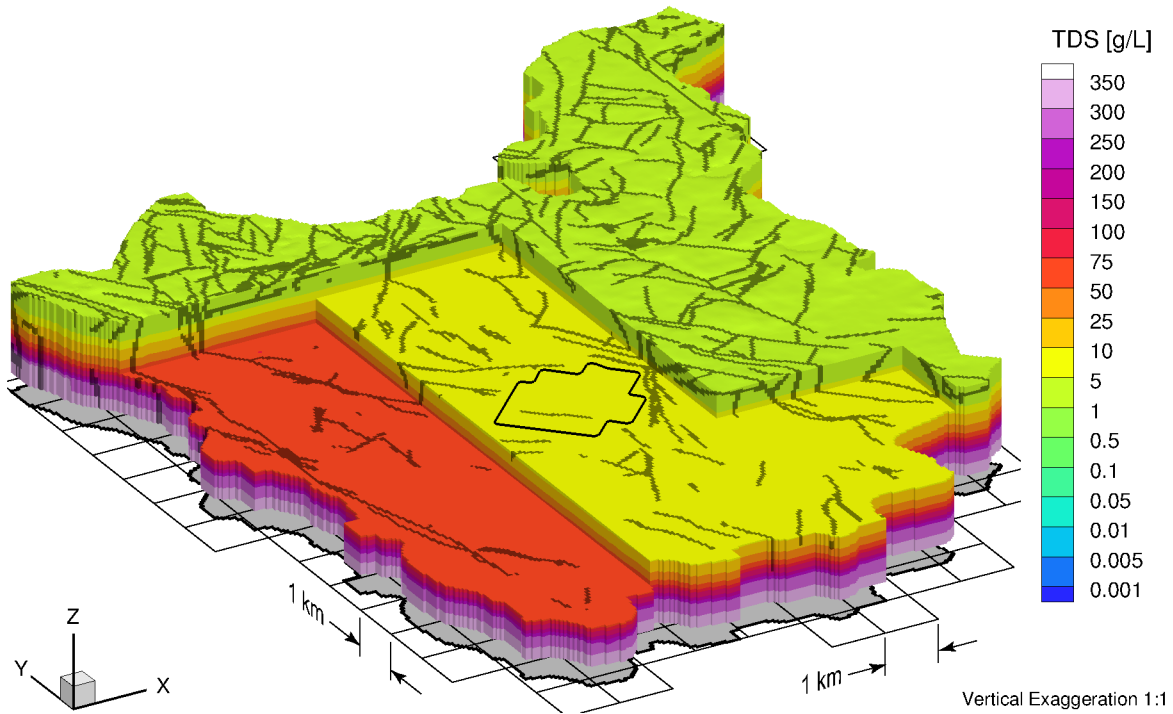
velocity vectors of the sub-regional scale model. The vertical component of the velocity vector will equal the velocity magnitude only when there are no horizontal components to the velocity vector; the ratio of the vertical component of the velocity vector to the velocity magnitude will be positive 1.0 for solely upward velocity and negative 1.0 for solely downward velocity. In the figure, blue corresponds to zones where the vertically downward velocity components dominate, white to zones where horizontal velocity components dominate the velocity vector, and red to zones where the velocity vectors are dominated by vertically upward components. Transition zones also are evident in the figure. It is important to note that the figures cannot be used to interpret velocity magnitude; they can only be used to interpret the direction of the calculated velocity vectors at a given location. This figure should be referred to in conjunction with Figure 2-14, which shows the porewater velocity magnitudes. Within the repository outline, upward velocities are associated with surface discharge areas, and downward velocities are associated with surface recharge areas.

The performance measure selected for the evaluation of the groundwater system at repository depth is the MLE, as shown in Figure 2-17. The shallow groundwater system has significantly shorter mean life expectancies compared to the deep groundwater system. The areas of surficial recharge versus discharge can be identified in the figure because the recharge areas have a high MLE while the discharge areas have low MLEs. The MLEs within the repository outline are between ten thousand years and ten million years, depending on the proximity to surface discharge areas. Mean life expectancies are lower in regions near fracture zones, due primarily to their higher hydraulic conductivity.



Note: Cut-aways occur at 500 mBGS and 1000 mBGS. The black outline in the centre of the figure delineates the repository footprint.

Figure 2-9: Block Cut View of Steady-State Freshwater Heads



Note: Figure is as per Frape and Fritz (1987).

Figure 2-10: Initial Total Dissolved Solids Distribution

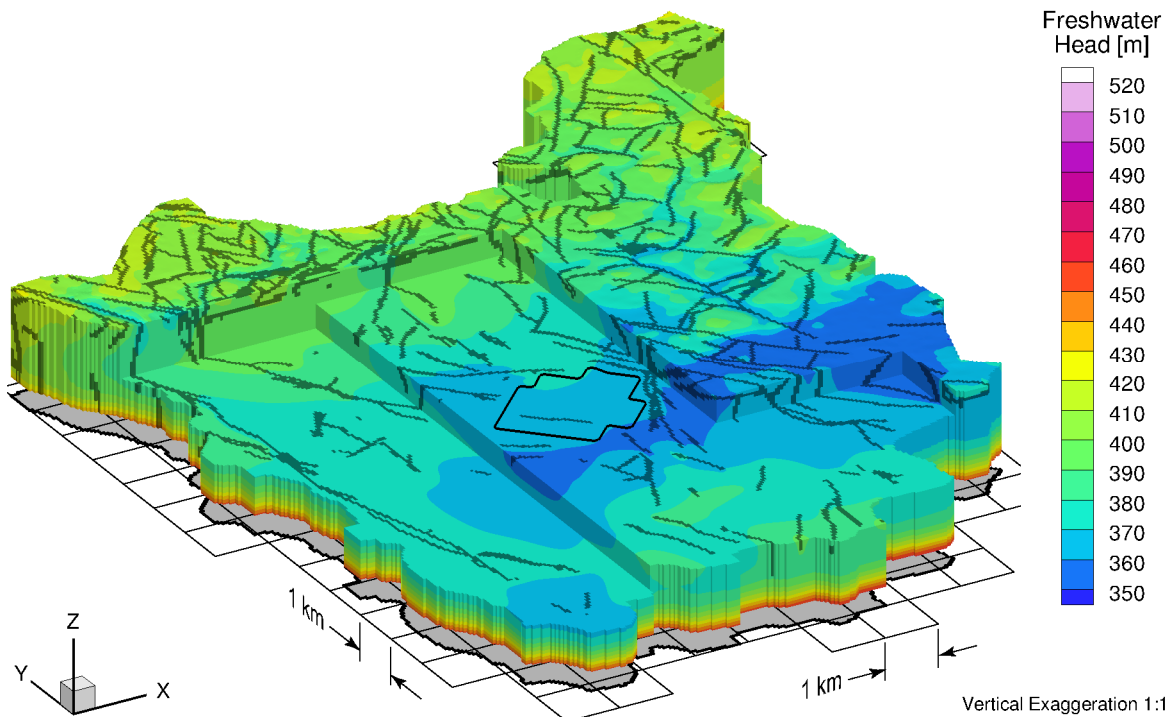


Figure 2-11: Freshwater Heads for Transient Coupled Density-Dependent Flow and Transport after One Million Years

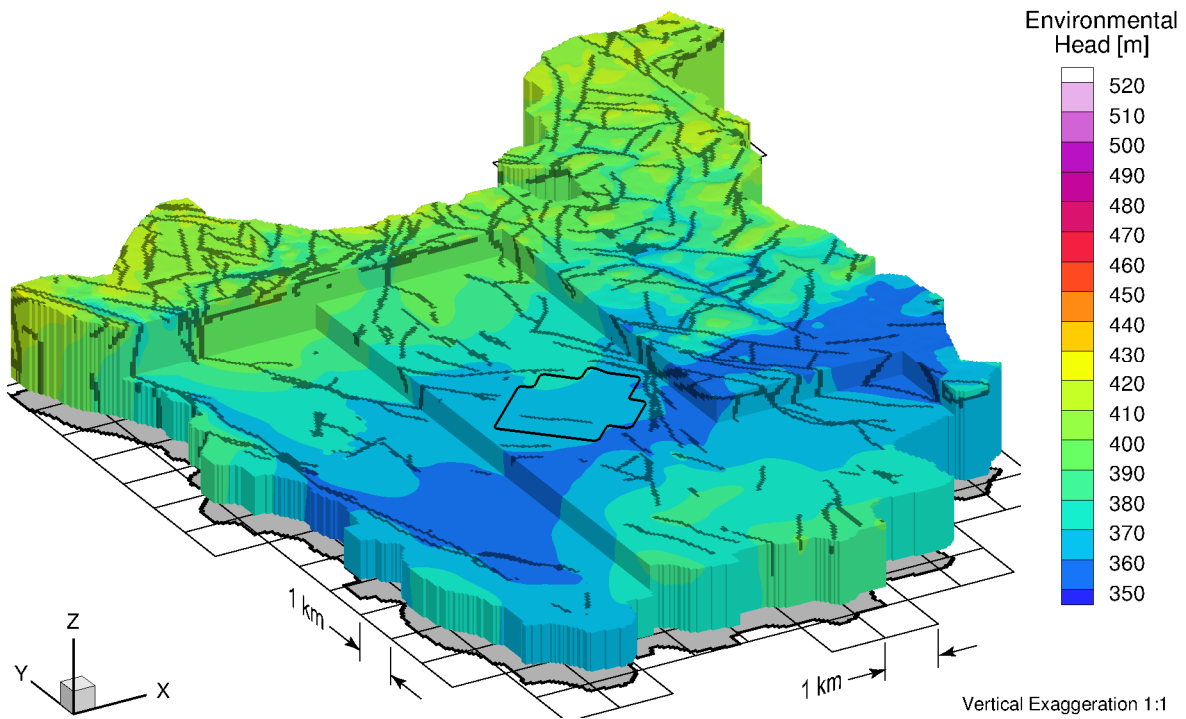


Figure 2-12: Environmental Heads for Transient Coupled Density-Dependent Flow and Transport after One Million Years

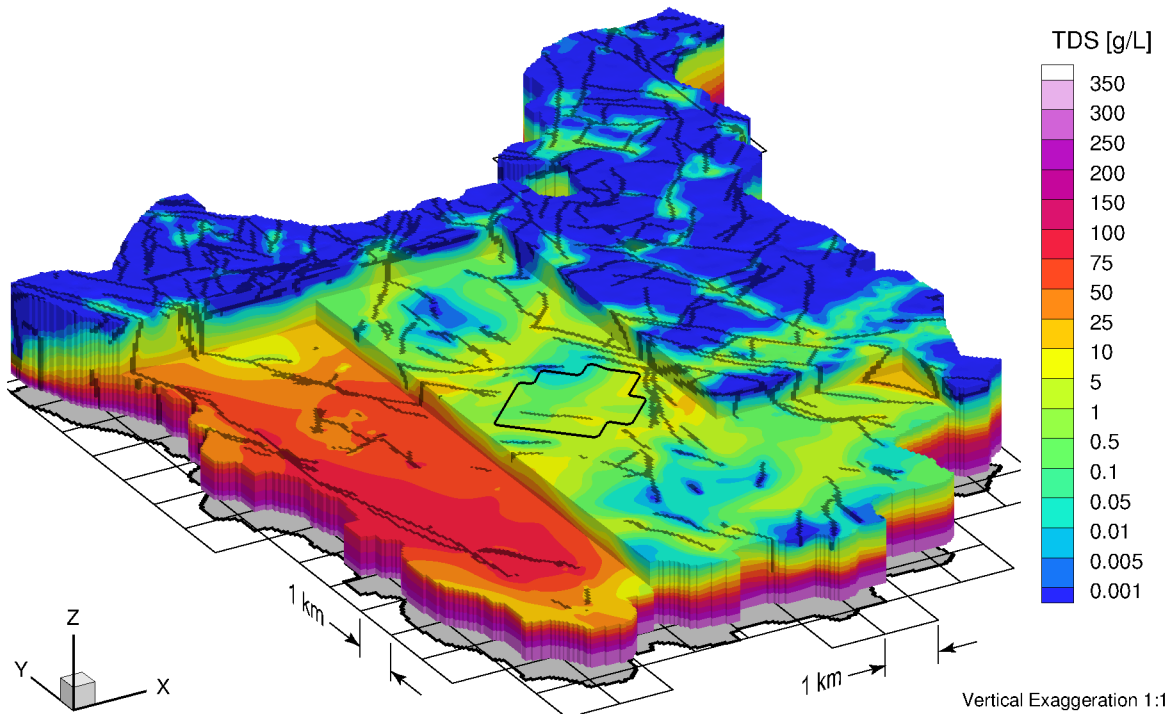


Figure 2-13: TDS Distribution after Coupled Density-Dependent Flow and Transport for One Million Years

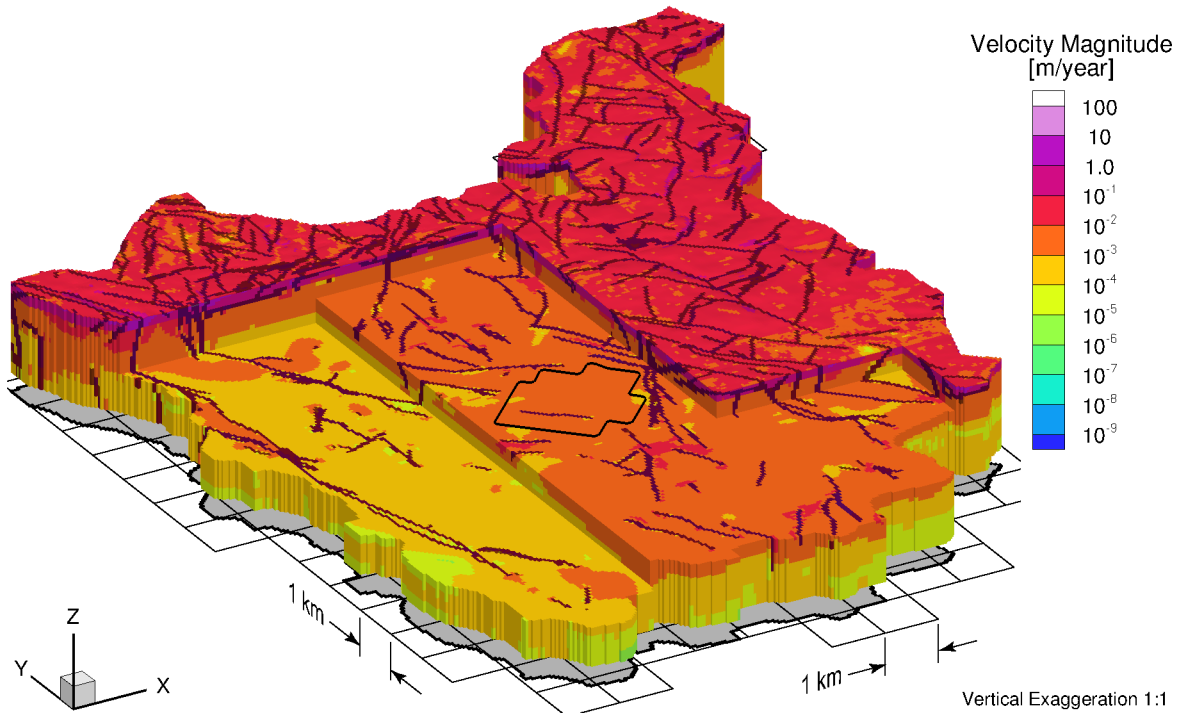
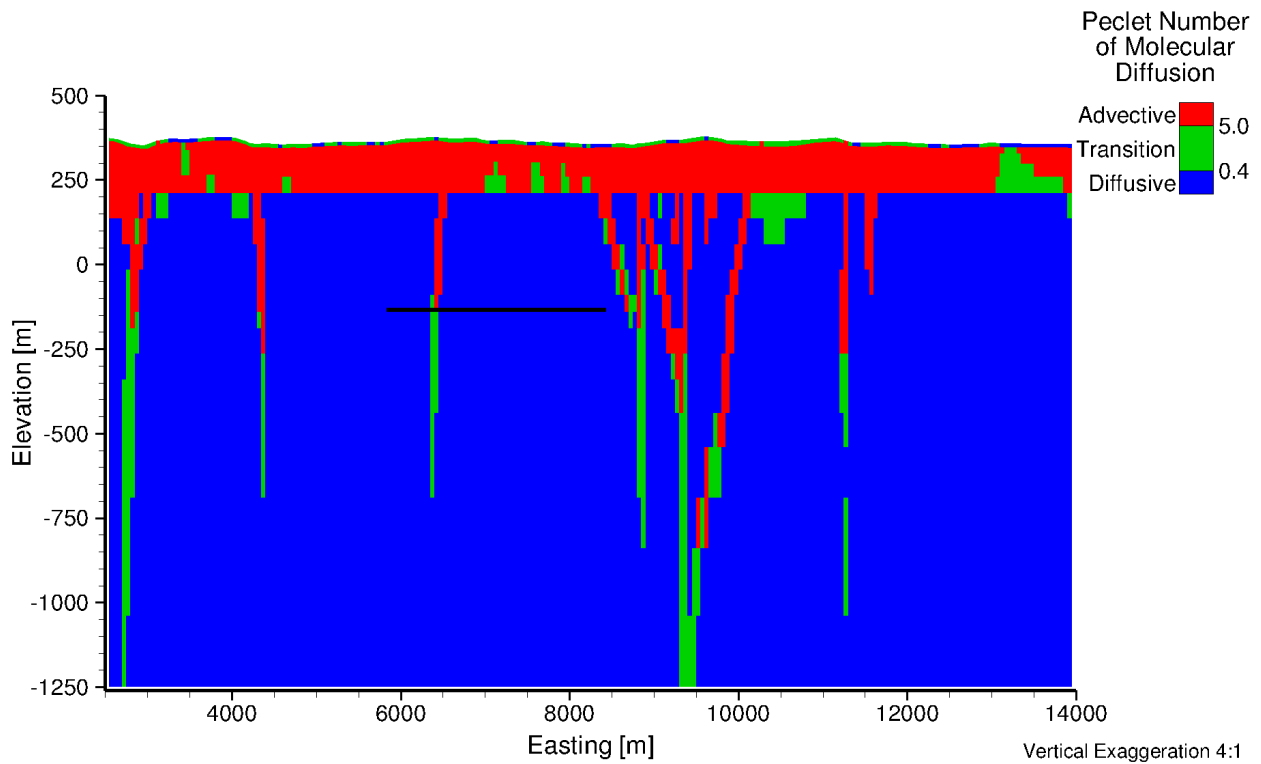


Figure 2-14: Reference Case Porewater Velocity Magnitudes



Note: The solid black line indicates the location of the repository.

Figure 2-15: Reference Case Péclet Number

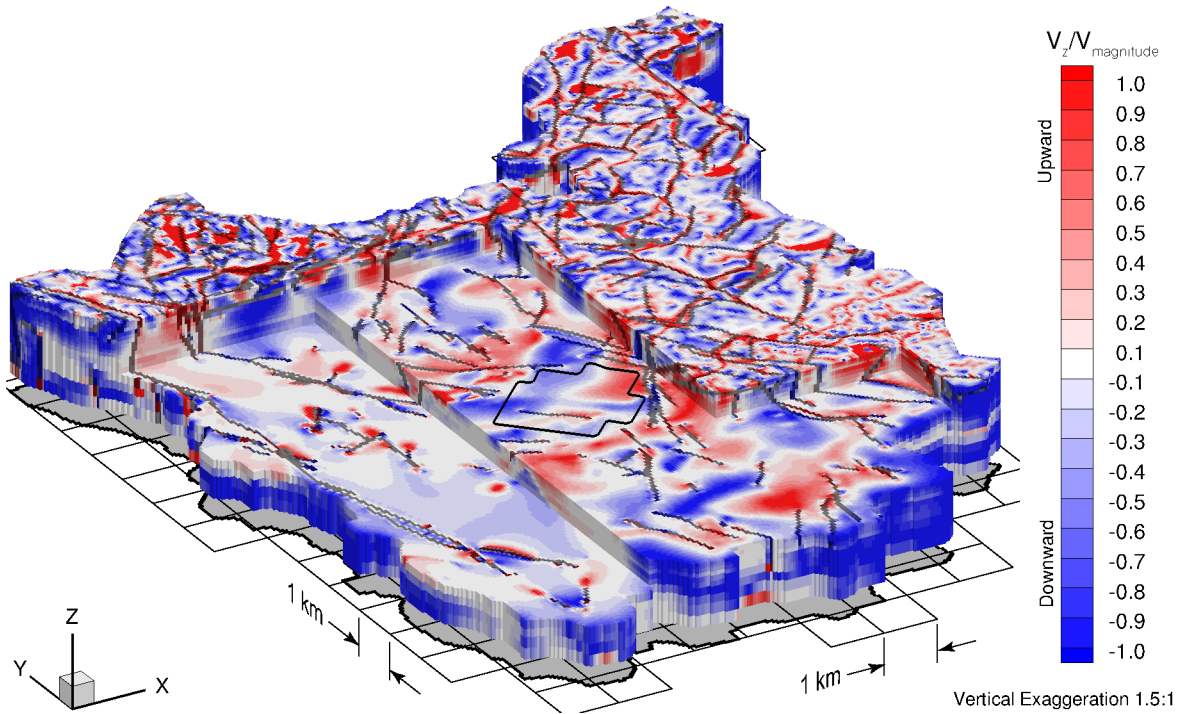


Figure 2-16: The Ratio of the Vertical Component of Velocity to Velocity Magnitude

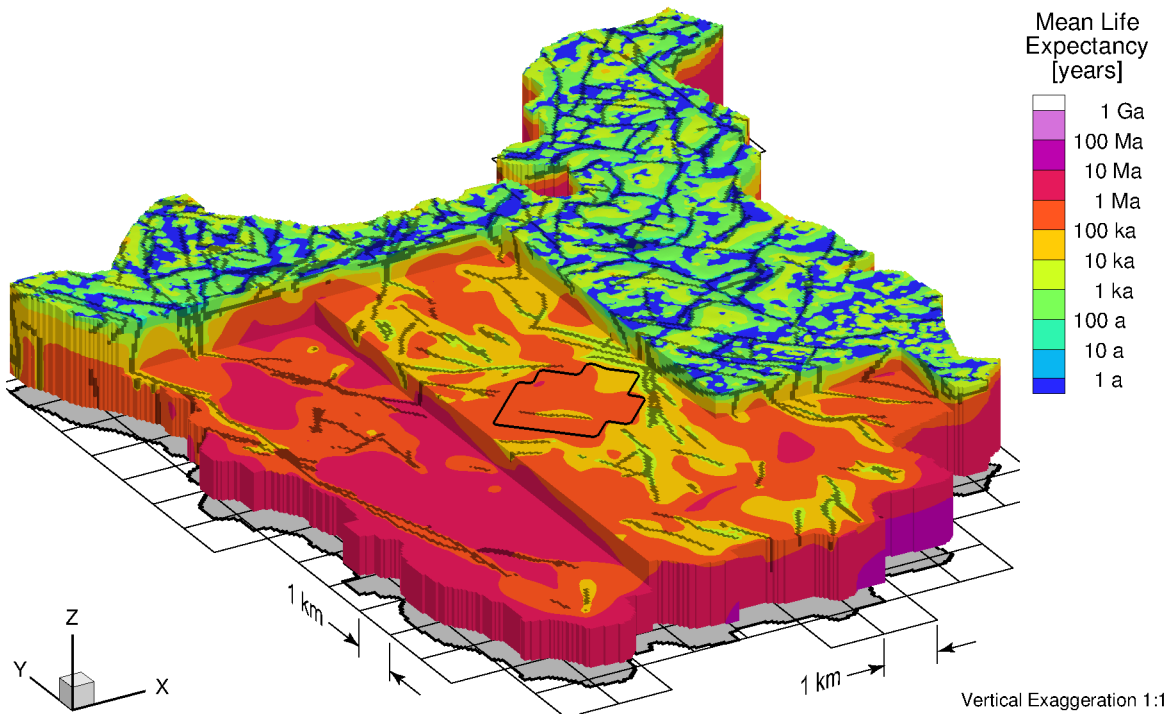


Figure 2-17: Reference Case Mean Life Expectancies

2.3.5.2 Temperate Transient Sensitivity Cases

Although the inclusion of coupled density-dependent flow and transport can be computationally burdensome, it is an important physical attribute of the groundwater system, both from a geochemical and hydrogeologic perspective. The impact of density-dependent flow is investigated by comparing porewater velocity magnitudes and mean life expectancies between a steady-state groundwater flow simulation and the one million year transient density-dependent flow simulation. Figure 2-18 shows the porewater velocity ratio on a logarithmic scale whereby a number greater than unity indicates porewater velocities in the steady-state model are greater than in the density-dependent flow. Porewater velocities are generally greater without brine present; however, in some portions of the domain, the velocities can be less. The increased velocities in the density-dependent case will coincide with changes in TDS adjacent to deep fracture zones. One cannot, a priori, assume steady-state flow without brine is a conservative approach to modelling groundwater systems because velocities can be both greater and lesser than the case without salinity. This is shown in Figure 2-18 both at repository level and in deeper portions of the groundwater system. Calculating the ratio of MLE between a steady-state freshwater system without brine and the one million year transient brine simulation, as shown in Figure 2-19, shows changes across the domain within an order of magnitude. The 50th percentile MLE for the repository footprint for the reference case without salinity is 2.9×10^5 years, compared to the 50th percentile MLE for the reference case including salinity, which is 3.8×10^5 years. However, within the repository footprint, the MLEs are generally reduced in freshwater simulations. In the deeper portions of the groundwater system, especially along or near fracture zones, mean life expectancies can be an order of magnitude less for the freshwater simulation when compared to the brine simulation. In general, the average MLE will be greater for scenarios including salinity.

Implementation of the TDS profile from McMurry (2004) generally increases the total dissolved solids throughout the domain, relative to that observed for the TDS profile of Frapre and Fritz (1987) (Figure 2-8). The total dissolved solids concentrations at one million years are shown in Figure 2-20. Figure 2-21 shows the difference in freshwater heads relative to the reference case freshwater heads. Freshwater heads generally increase throughout the lower portion of the domain due to higher pore fluid densities in the case using the TDS profile from McMurry (2004). Pore velocity magnitudes are shown in Figure 2-22. Generally, the ratios are close to unity. Within the repository footprint, both increases and decreases in the predicted porewater velocity magnitude ratio occur between the McMurry (2004) TDS simulation and the reference case simulation. Greater variation is observed when comparing the reference case transient brine simulation to the steady-state freshwater simulation (Section 2.3.5.1). Changes in MLE are also expected, and the ratios are shown in Figure 2-23. Throughout the repository footprint, the mean life expectancies generally increase, although only marginally, to a 50th percentile MLE value of 4.5×10^5 years, compared to a 50th percentile MLE of 3.8×10^5 years for the reference case. Depending on the distribution of TDS, some portions of the domain show greater increases or decreases in MLE ratios when compared to the reference case. The increased TDS defined by McMurry (2004) leads to a slight increase in geosphere stability compared to the reference case, as indicated by the estimated MLEs and porewater velocities.

Increasing the rock mass hydraulic conductivities by an order of magnitude significantly affects the groundwater system. The difference in freshwater heads between sensitivity case 1 and the reference case are shown in Figure 2-24. Within the repository footprint, freshwater heads generally increase, while, near the bottom of the domain, decreases are noted. Higher

hydraulic conductivities allow the groundwater system to transport higher TDS brines from depth to the intermediate groundwater system in a shorter period of time. Because the transient simulations allow both TDS and freshwater heads to evolve over a period of one million years, greater movement of brines occurs in the groundwater system with higher porewater velocities. The TDS concentrations at one million years for the sensitivity case are shown in Figure 2-25. The TDS is generally lower than for the reference case shown in Figure 2-13.

The ratio of porewater velocities between sensitivity case 1 and the reference case are shown in Figure 2-26. Porewater velocities generally increase by an order of magnitude within the rock mass, but little change occurs within the fracture zones because the EPM calculated fracture zone hydraulic conductivities are dominated by the fracture hydraulic conductivity of 1×10^{-6} m/s. The MLE ratios shown in Figure 2-27 generally indicate a decrease in the MLE values of approximately one order of magnitude for the sensitivity case, resulting in a 50th percentile MLE for the repository of 3.7×10^4 years.

Figure 2-28 shows a cumulative density function of MLE within the repository for the temperate sensitivity cases. The most discernible difference is the impact of the hydraulic conductivity in sensitivity case 1. The inclusion of salinity and density-dependent flow generally tends to increase the MLE within the repository.

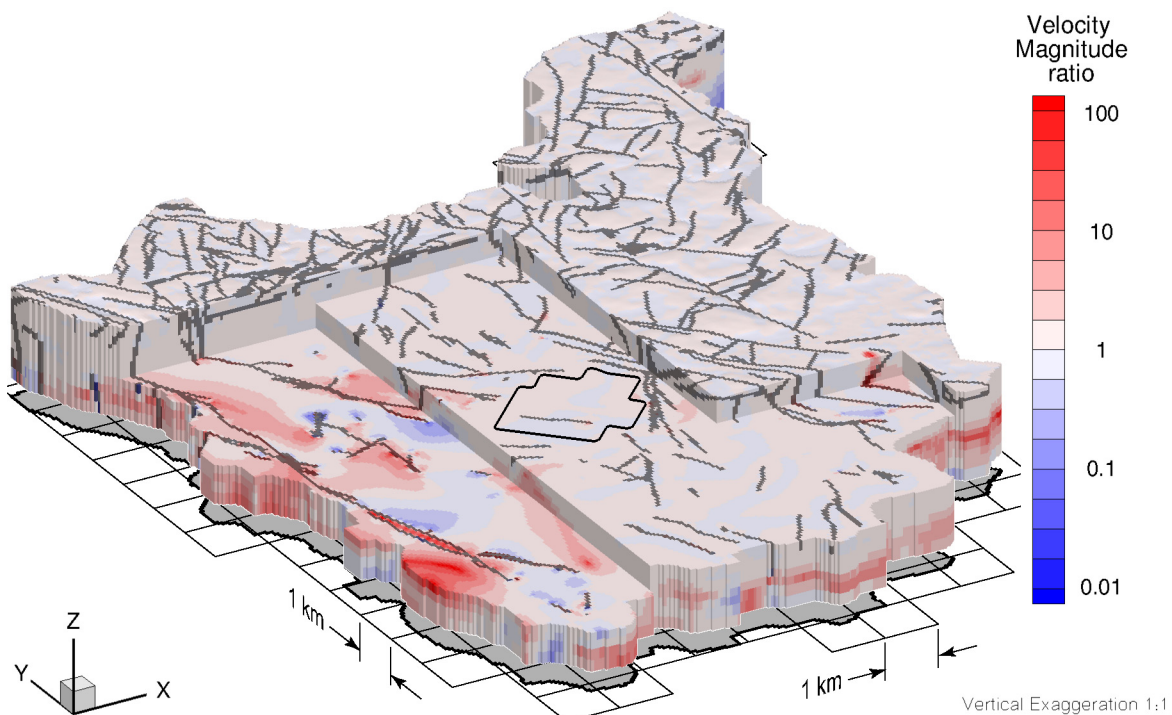


Figure 2-18: Ratio of Velocity Magnitudes of Steady-State Groundwater Flow to Density-Dependent Flow Case

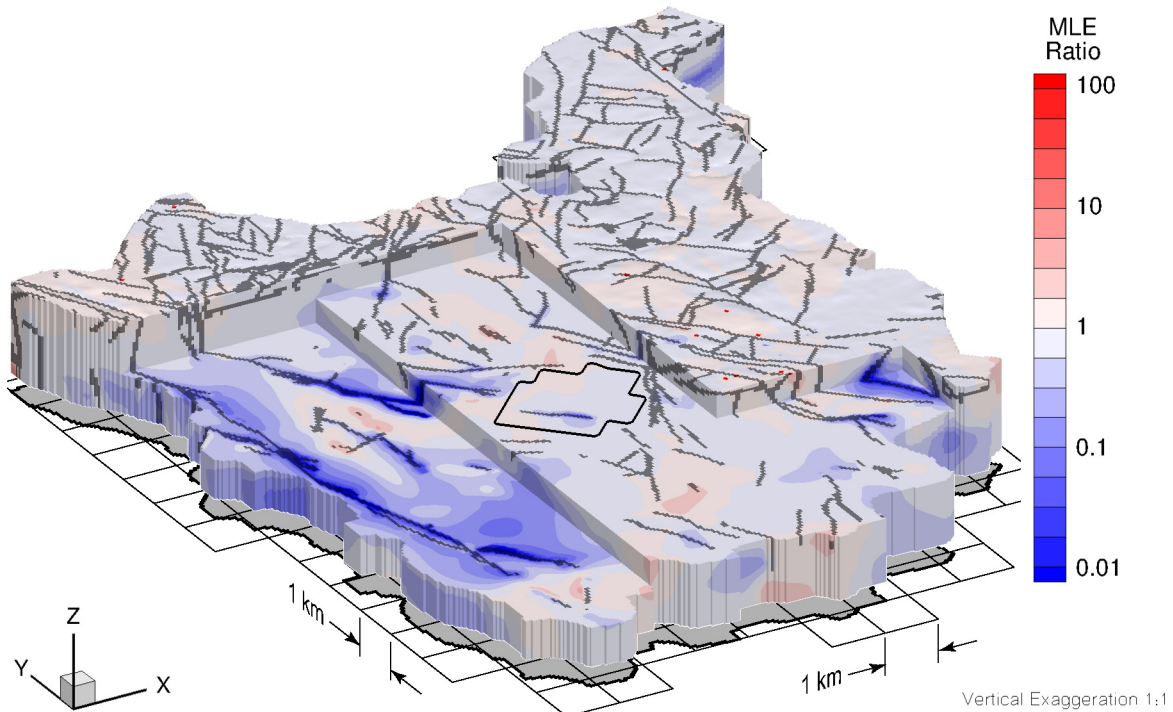
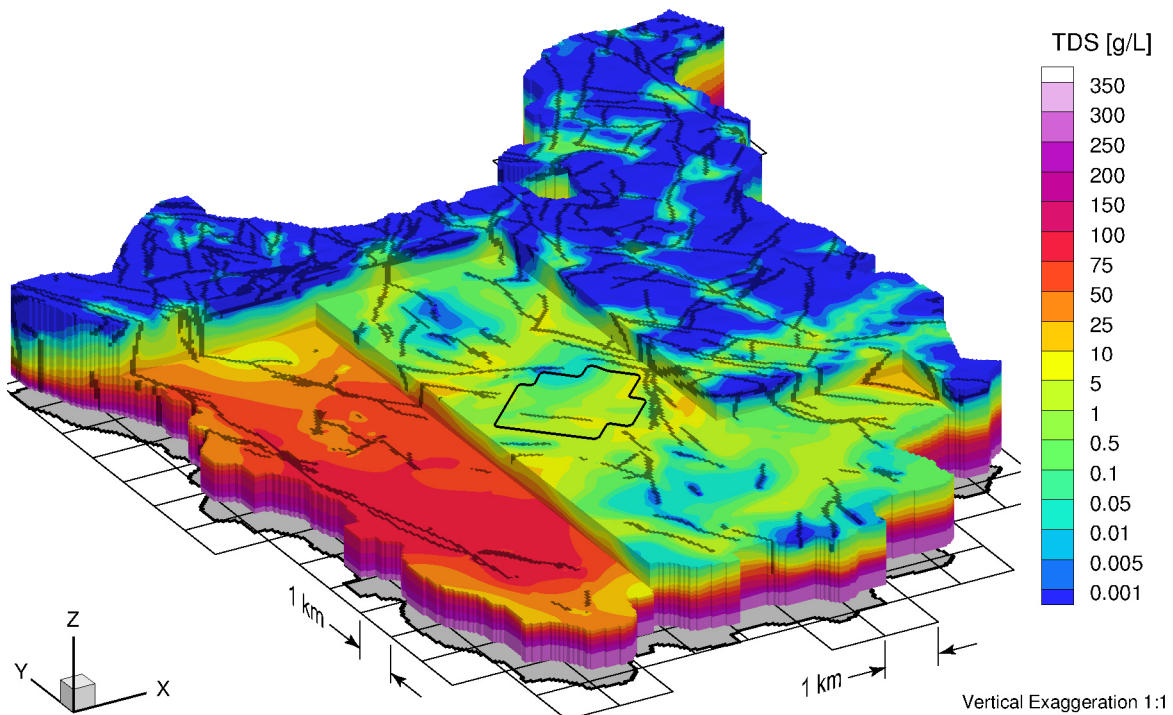


Figure 2-19: Ratio of MLEs of Steady-State Groundwater Flow to Density-Dependent Flow Case



Note: Initial TDS distribution from McMurry (2004) was used in this simulation.

Figure 2-20: TDS Distribution after Coupled Density-Dependent Flow and Transport for One Million Years

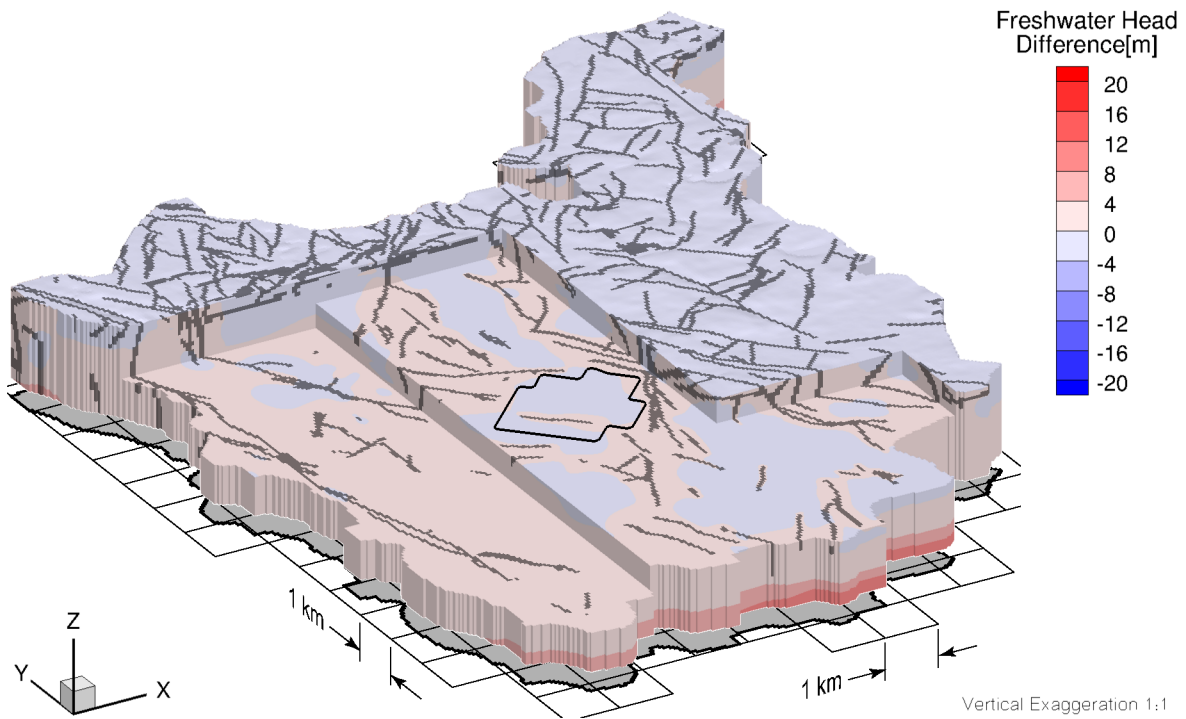


Figure 2-21: Difference in Freshwater Heads between Reference Case and Simulation using Initial TDS Distribution from McMurry (2004)

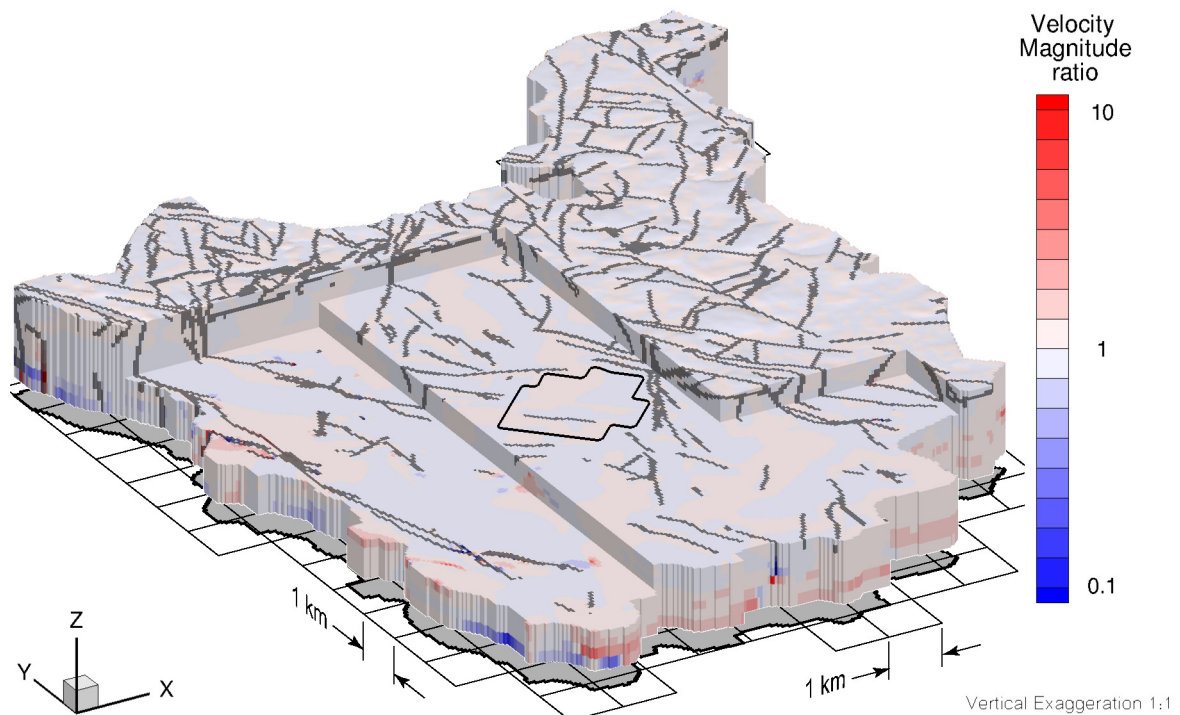


Figure 2-22: Velocity Magnitude Ratios of McMurry (2004) TDS Distribution Simulation to Reference Case Simulation

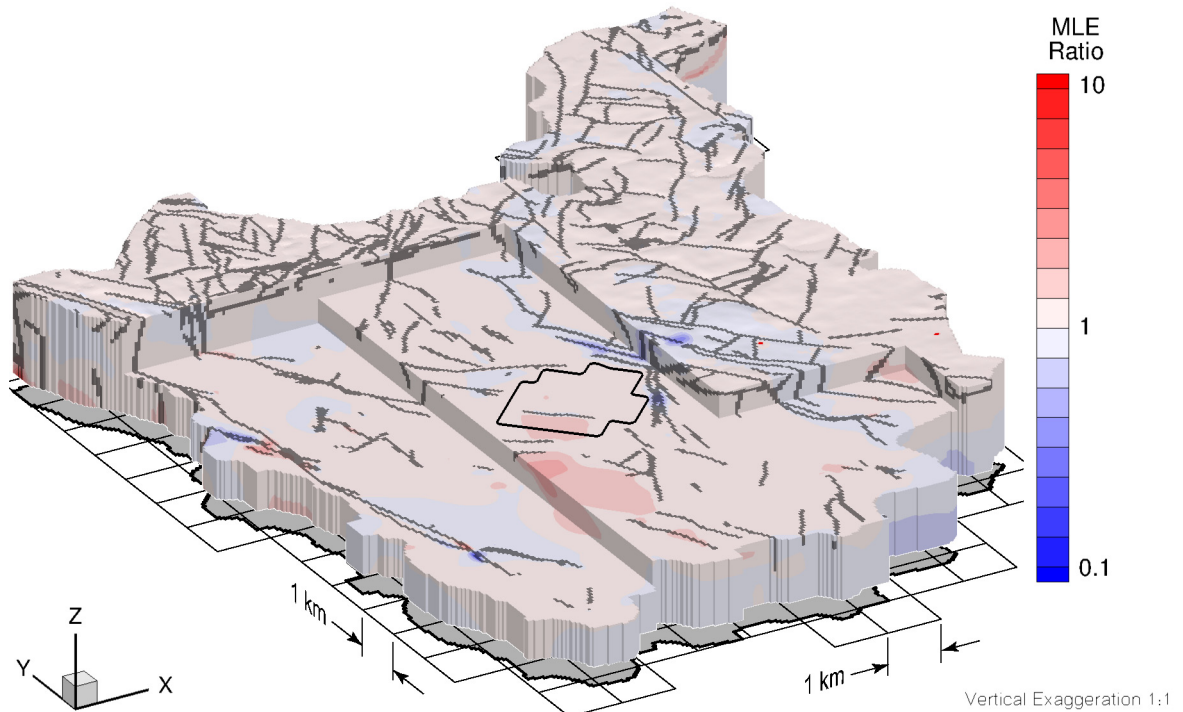


Figure 2-23: Ratio of MLEs of McMurry (2004) TDS Distribution Simulation to Reference Case Simulation

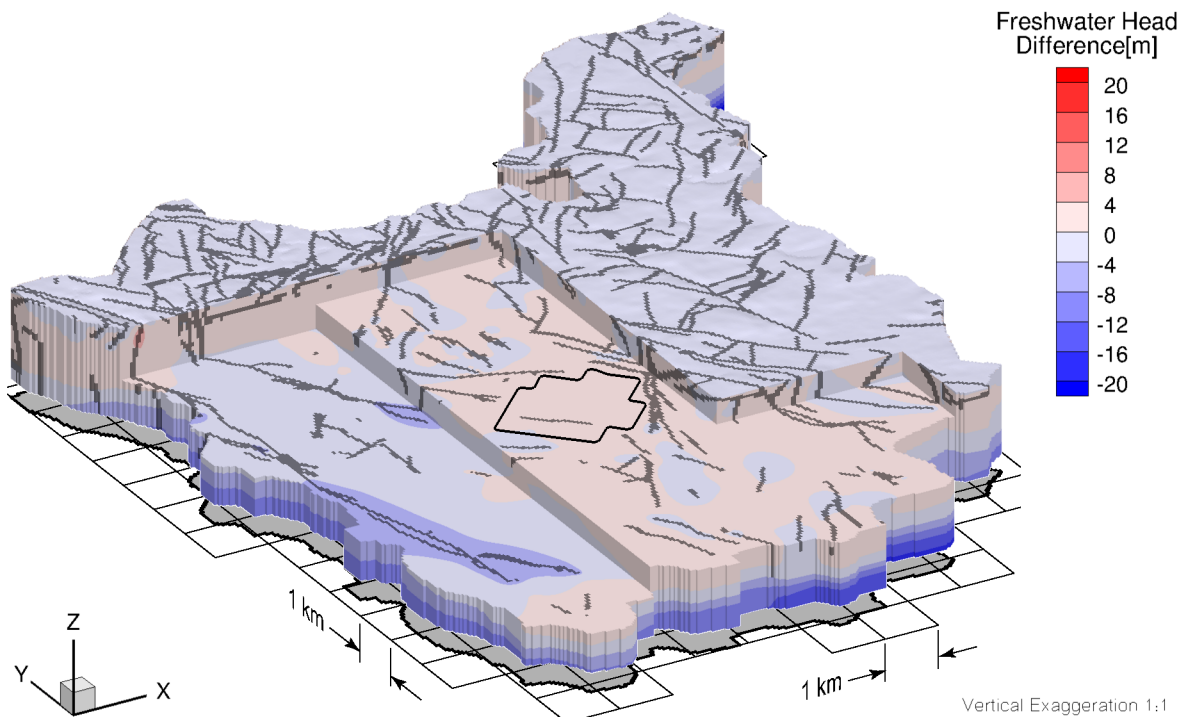


Figure 2-24: Difference in Freshwater Heads between a Simulation using an Increased Rock Mass Hydraulic Conductivity and Reference Case

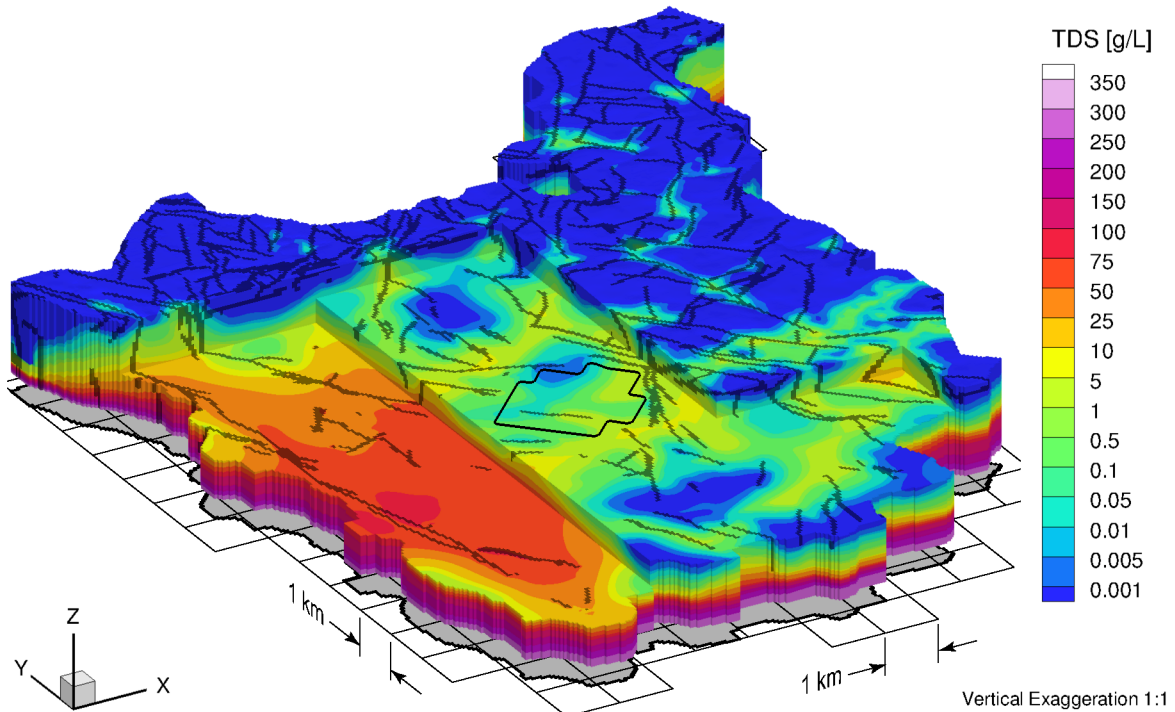
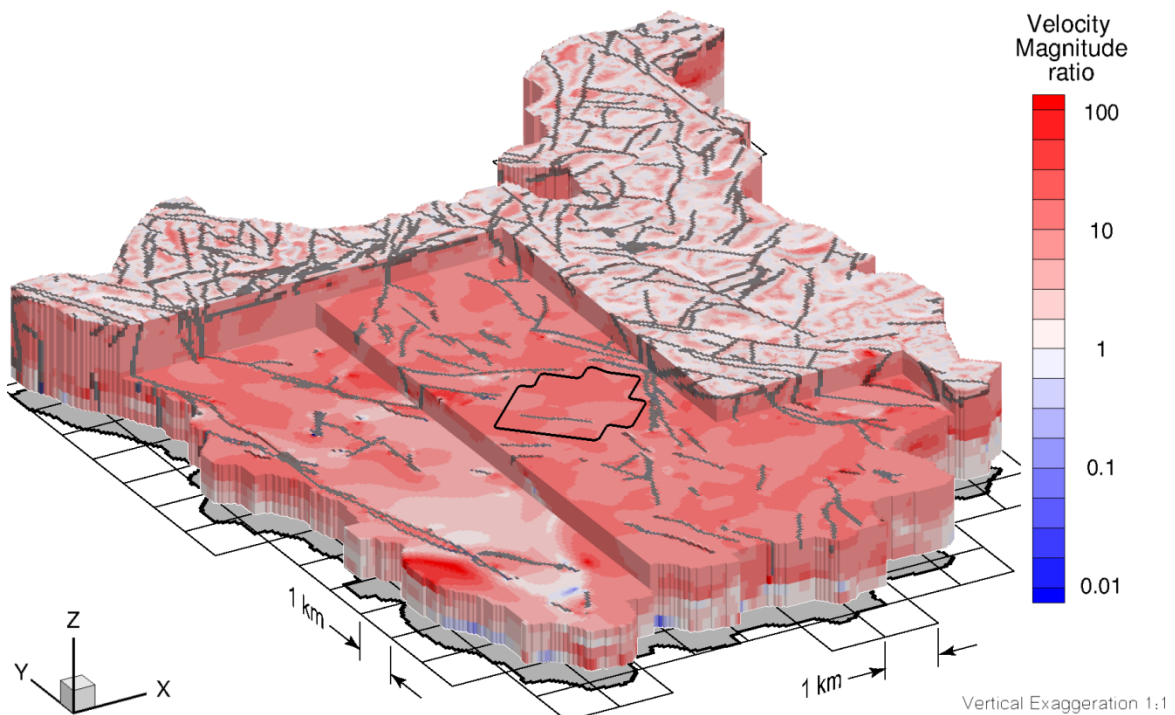


Figure 2-25: The Total Dissolved Solids Concentrations at One Million Years for an Increased Rock Mass Hydraulic Conductivity



Note: Ratio of sensitivity case using an increased rock mass hydraulic conductivity relative to the reference case.

Figure 2-26: Ratio of Pore Velocity Magnitudes

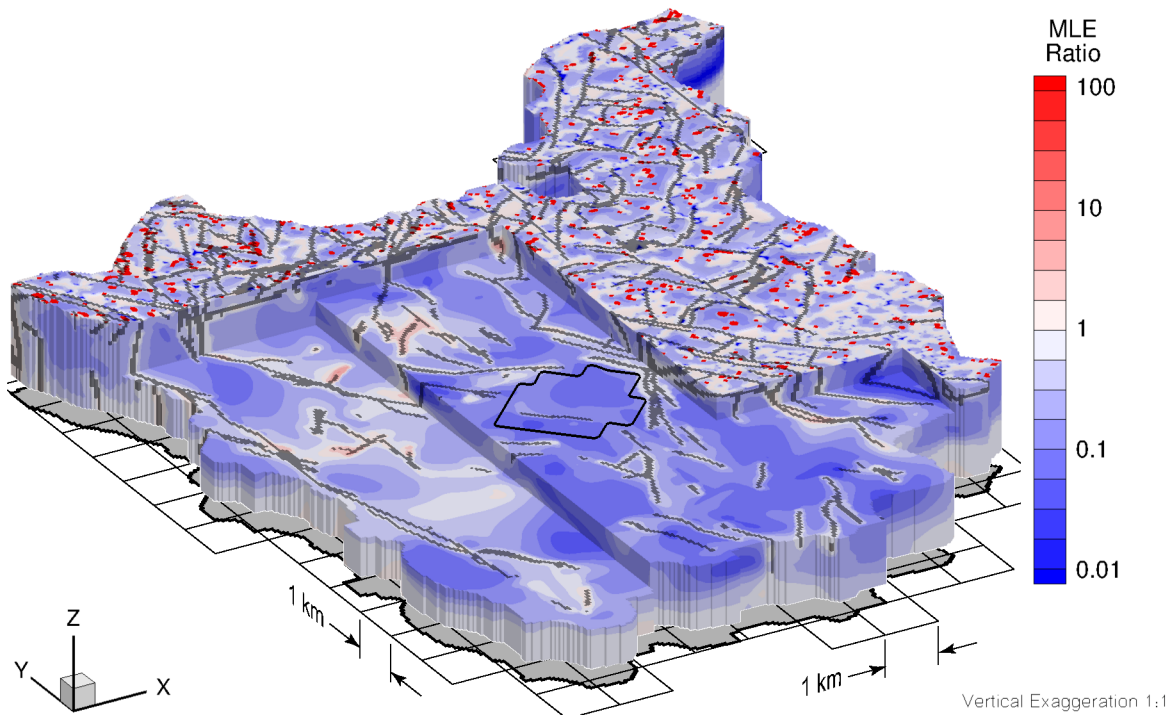


Figure 2-27: MLE Ratio of Increased Rock Mass Hydraulic Conductivities Simulation Relative to Reference Case Simulation

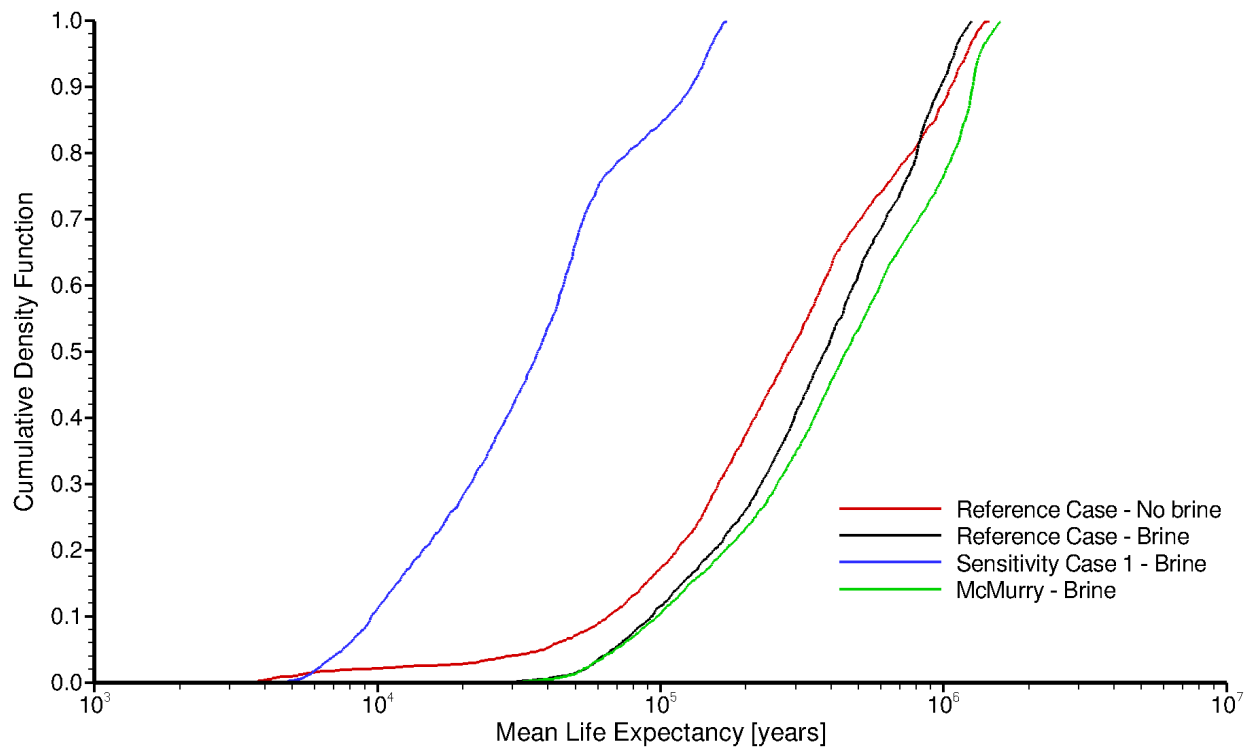


Figure 2-28: Cumulative Density Function of Mean Life Expectancy within Repository Outline for Temperate Sensitivity Cases

2.3.5.3 Paleohydrogeologic Sensitivity Cases

A total of ten paleohydrogeologic simulations were performed to investigate the role of varying paleoclimate boundary conditions and the characterization of hydromechanical coupling. These simulations are summarized in Table 2-5. The reference case model is used as the basis for all simulations and the initial conditions for both freshwater heads and brine distribution come from the pseudo-equilibrium brine simulation at one million years, as described in Section 2.3.5.1.

The performance measure chosen to compare the paleohydrogeologic simulations is the movement of a conservative unit tracer applied with a Cauchy boundary condition at the top surface of the model domain. This tracer represents the migration of recharge waters into the groundwater system over the course of a 120 thousand year simulation. Comparisons between simulations are made using block-cut three-dimensional figures, as well as calculating the cumulative density function of tracer depth at a 5% isochlor⁵. The 5% isochlor represents a pore fluid containing 5% recharge water; it provides an indication of recharge water migration into the subsurface, which can be used to compare alternative paleohydrogeologic scenarios. The 5% isochlor illustrates a potential depth of penetration of glacial meltwater. However, the dissolved oxygen content of these waters will likely be consumed within the shallow groundwater system by mineralogical and/or microbial reactions (see also Section 2.2.3.2).

The tracer migration at 120 thousand years for the paleohydrogeologic reference case simulation (fr-base-paleo) is shown in Figure 2-29. Deeper migration can occur in fracture zones; however, it depends on whether that portion of the fracture zone is associated primarily with a recharge area or a discharge area. The portion of the domain within the repository outline shows a variation in tracer concentration of approximately 50% at the fracture zone within the footprint to less than 5% elsewhere. The 50th percentile of tracer depth (5% isochlor) for the reference case results in a depth of 666 m. Higher concentrations are generally associated with recharge areas and fracture zones. A cumulative density function of 5% isochlor depth for this case is shown in Figure 2-30. All other simulations are plotted on the same figure for comparison purposes.

As discussed in Section 2.2.2.3, multiple plausible paleoclimate reconstructions can be developed from the UofT GSM model (Peltier 2006). The reference case paleohydrogeologic simulation uses paleoclimate simulation nn2008, representing a cold based ice-sheet condition with extensive permafrost. An alternate paleoclimate simulation nn2778 (fr-base-paleo-nn2778) represents a greater extent of ice-sheet coverage over the domain, but less permafrost is predicted to form in subsurface over the 120 thousand year simulation period. Figure 2-31 shows the tracer migration at 120 thousand years for the nn2778 paleoclimate boundary conditions. In comparison to the reference case simulation, there is a significant increase in the depth to which the tracer migrates, 889 mBGS versus 666 m in the reference case, as shown in Figure 2-30. Increased migration results from less permafrost and more ice-sheet advance/retreat cycles.

The top surface hydraulic boundary condition can be varied as various percentages of ice-sheet thickness. The reference case uses 100% of ice-sheet thickness in calculating the equivalent

⁵ Isochlor: The 5% isochlor illustrates the migration of recharge waters into the groundwater system over the course of a 120,000 year glacial cycle and conservatively represents the distribution of a pore fluid containing 5% recharge water.

freshwater head. One paleohydrogeologic scenario for each of 0%, 30%, and 80% (named fr-base-paleo-0, fr-base-paleo-30, and fr-base-paleo-80, respectively) of ice-sheet thickness were performed; the CDF versus depth relationship for tracer migration is shown in Figure 2-30. For the 0% case, representing zero fluid pressure, slightly deeper migration than the reference case (699 mBGS) is noted and is attributed to the ice-sheet unloading rates being greater than loading rates. The 30% and 80% cases result in CDF versus depth relationships that are very similar to the reference case (665 mBGS and 649 mBGS, respectively).

In addition to the surface hydraulic boundary condition, an equally important parameter is the one-dimensional loading efficiency. The loading efficiency is calculated based on the pore fluid and rock matrix compressibilities (see also Section 2.2.2.2). In the reference case simulation, the one-dimensional loading efficiency is calculated to be 0.59 for the rock mass. In two paleohydrogeologic sensitivity scenarios, the one-dimensional loading efficiencies are set to zero (fr-base-paleo-le0) and unity (fr-base-paleo-le1) while maintaining the specific storage at $1 \times 10^{-7} \text{ m}^{-1}$. The purpose of these sensitivity cases is to illustrate the role of the one-dimensional loading efficiencies. Both the loading efficiency and specific storage values are affected by the choice of Biot coefficient. The following sensitivity cases investigate the role of the Biot coefficient on hydromechanical coupling. For a Biot coefficient of 1.0 (fr-base-paleo-biot10), a one-dimensional loading efficiency of 0.95 results, while a Biot coefficient of 0.5 (fr-base-paleo-05) yields a one-dimensional loading efficiency of 0.68. In both Biot simulations, the specific storage approximately doubles from the reference case value. The final simulation (fr-base-paleo-0-le1) uses a loading efficiency of unity and a 0% of ice-sheet thickness equivalent freshwater head for the surface hydraulic boundary condition. For the nn2008 paleoclimate boundary conditions, fr-base-paleo-le1 (Figure 2-32) represents the shallowest predicted tracer migration, to a depth of 640 mBGS, while fr-base-paleo-le0 (Figure 2-33) represents the deepest, reaching a depth of 722 mBGS. As the one-dimensional loading efficiency is decreased, vertical gradients increase because in-situ pore pressures are reduced during ice-sheet loading for the same 100% of ice-sheet thickness equivalent freshwater head surface hydraulic boundary condition. Similar to the comparison between fr-base-paleo-0 and fr-base-paleo, deeper migration, to a depth of 751 mBGS, occurs in the fr-base-paleo-0-le1 (Figure 2-34) simulation when compared to fr-base-paleo-le1 (shown in Figure 2-30 and Figure 2-32). Again, the deeper tracer migration is attributed to the greater ice-sheet unloading rates compared to the loading rates, thereby producing larger vertically downward gradients due to a zero pressure hydraulic surface boundary condition.

Insight into the depth of penetration by glacial meltwaters within the sub-regional groundwater domain is based on the spatial distribution of the 5% isochlor for 10 paleohydrogeologic simulations. Within the discretely fractured groundwater system average depths of penetration ranged between approximately 640 and 890 mBGS. Within the rock matrix at the repository horizon for the reference case simulation, tracer meltwater concentrations range between approximately 0% to 25%. Significantly higher meltwater concentrations occurred to greater depth (>1000m) within the discrete higher permeability fracture zones. Although predicted glacial meltwater recharge depths may approach the repository level, it is expected that groundwater conditions will remain reducing.

Plots of the Péclet number versus time at five locations within the repository footprint (centre and four corners) for the reference case paleohydrogeologic scenario (fr-base-paleo) are shown in Figure 2-35. These results illustrate the stability of geosphere during glacial advances and retreats. The grey regions in the figure represent upward groundwater movement. Through the

duration of the glacial cycle, diffusion is the dominant transport mechanism for the reference case scenario. Select sensitivity cases illustrating the Péclet numbers versus time are also shown in Figure 2-36, Figure 2-37, Figure 2-38, and Figure 2-39. The figures were chosen, based upon the 5% isochlor migration CDF plot shown in Figure 2-30, to show the widest range of results. As illustrated in Figure 2-36 and Figure 2-37, diffusion remains the dominant transport mechanism for the duration of the glacial cycles. The combination of using either a loading efficiency of 0 (Figure 2-38) or a loading efficiency of 1 and a 0% of ice-sheet thickness equivalent freshwater head for the surface hydraulic boundary condition (Figure 2-39) result in Péclet numbers reaching the transition region, where advection and diffusion both occur on equal orders. It is worth noting that the Péclet numbers reach the transition region during periods of downward groundwater movement.

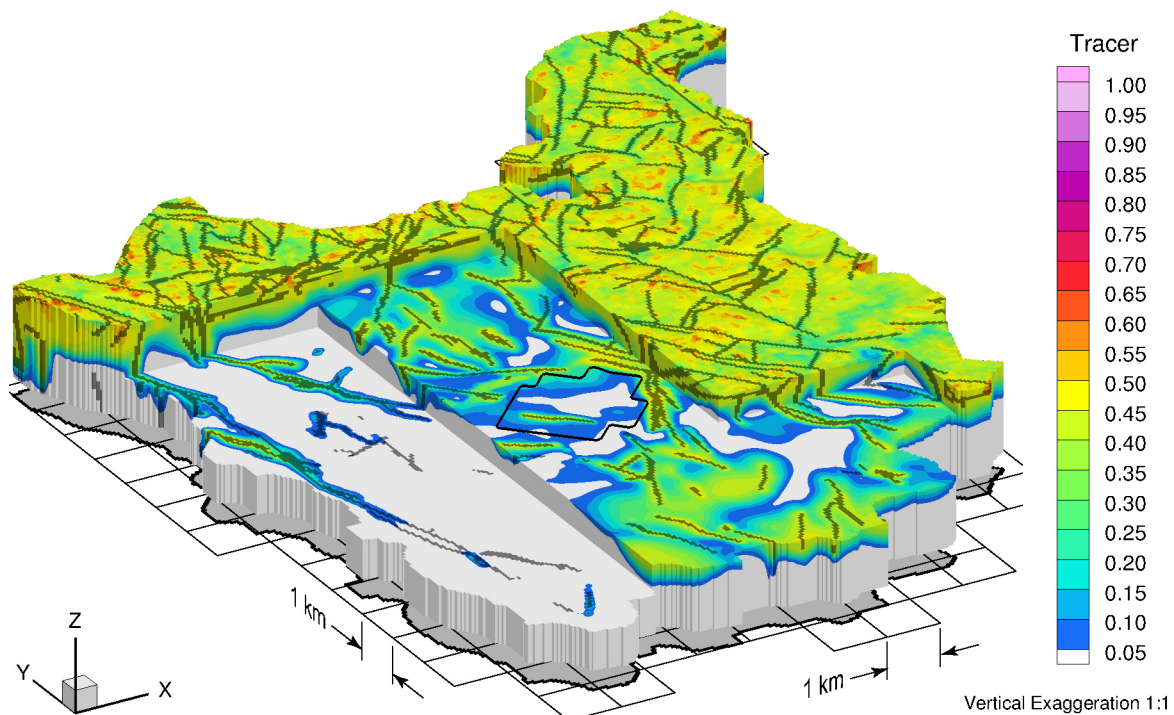


Figure 2-29: Tracer Migration after 120 Thousand Years for Reference Case Paleohydrogeologic Scenario (fr-base-paleo)

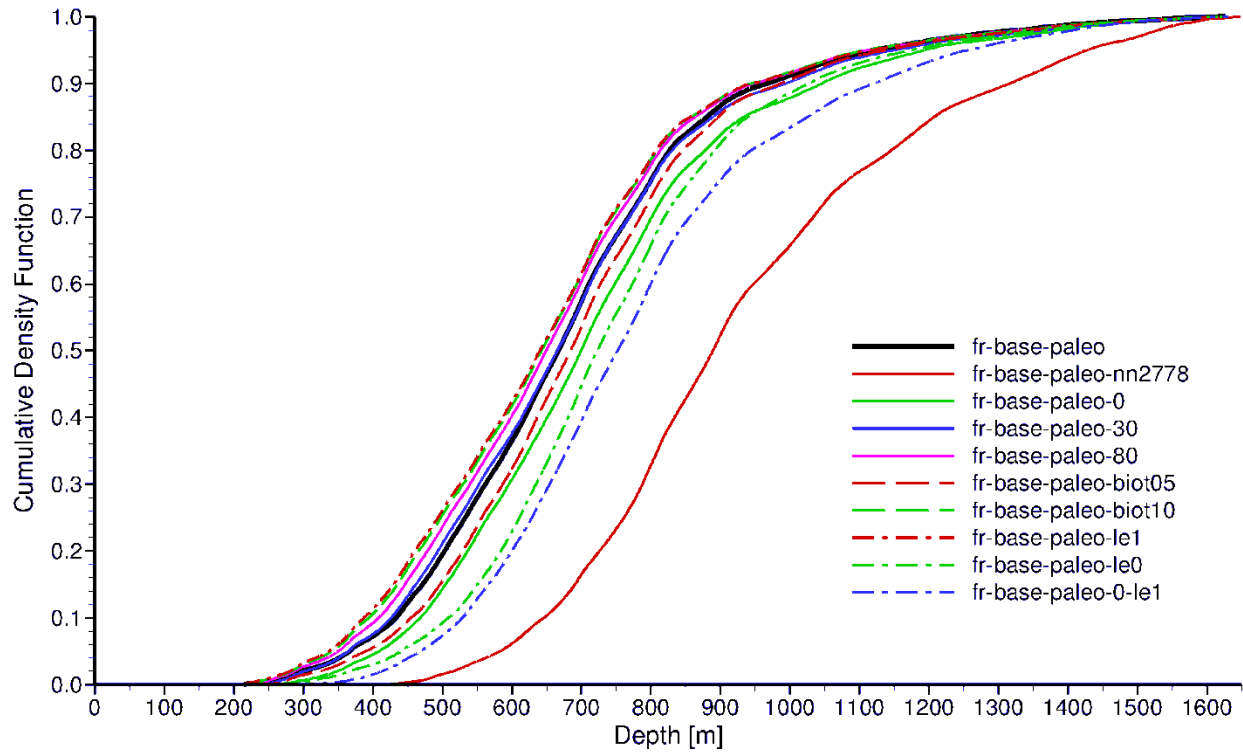


Figure 2-30: A Cumulative Density Function of 5% Isochlor Depth for Paleohydrogeologic Sensitivity Cases

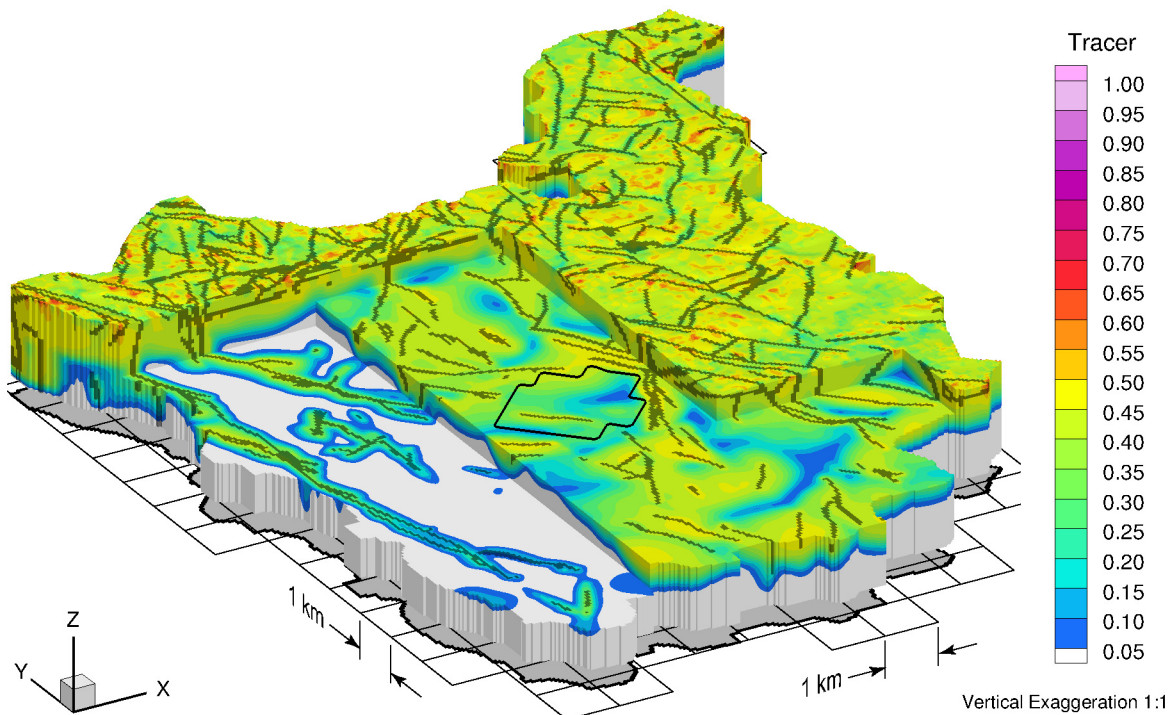


Figure 2-31: Tracer Migration at 120 Thousand Years for the nn2778 Paleoclimate Boundary Conditions (fr-base-paleo-nn2778)

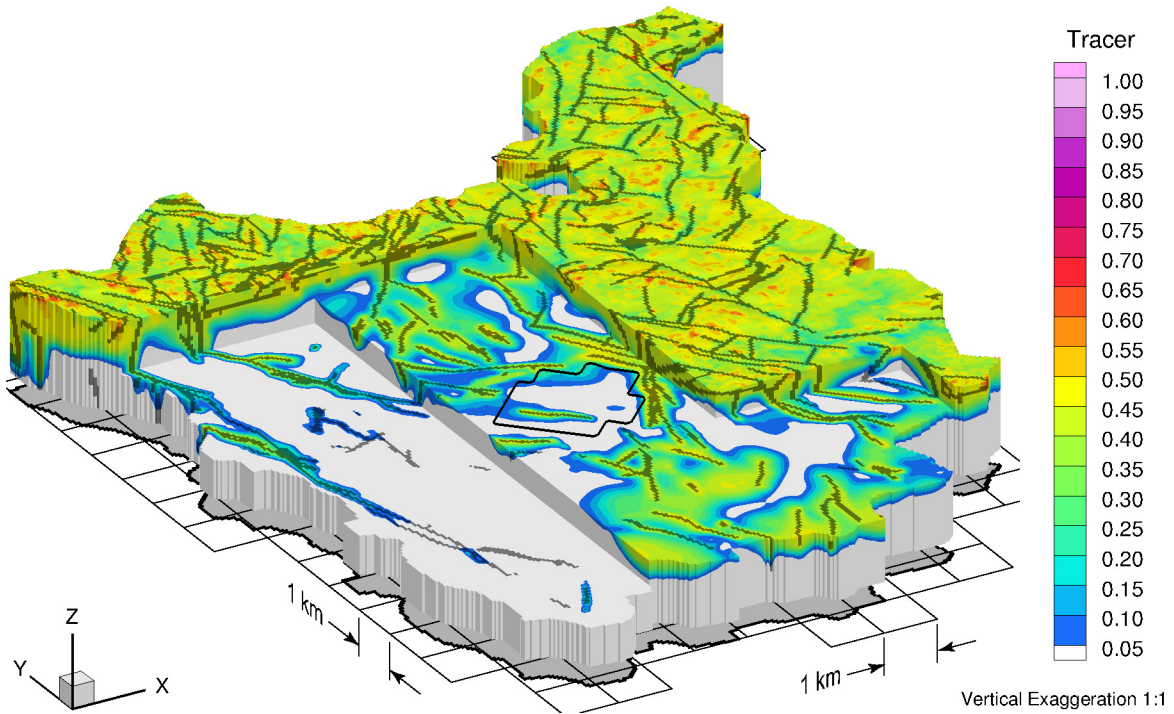


Figure 2-32: Tracer Migration at 120 Thousand Years for nn2008 Paleoclimate Boundary Conditions and a Loading Efficiency of 1 (fr-base-paleo-le1)

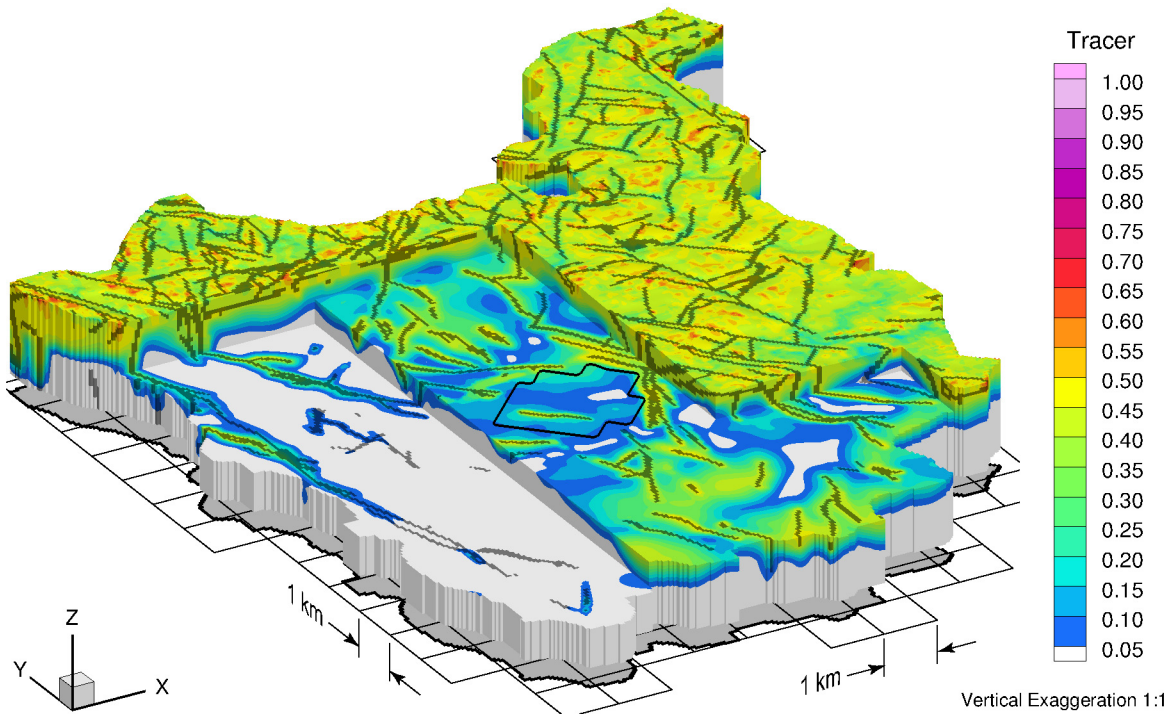
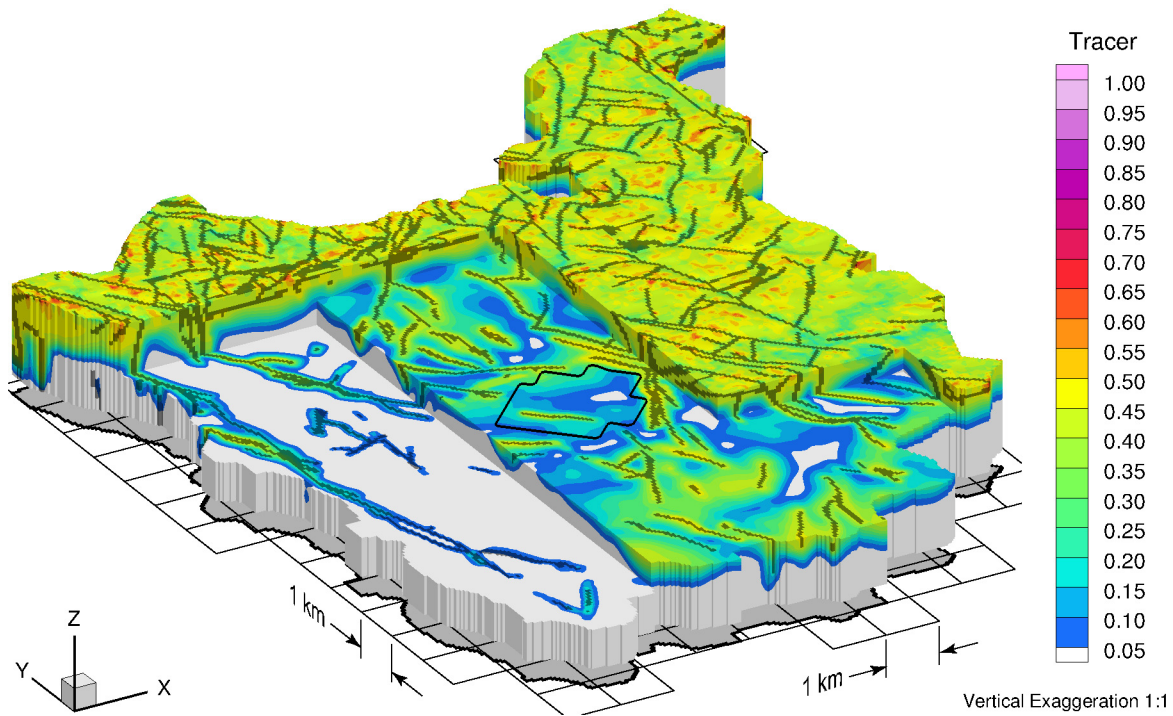


Figure 2-33: Tracer Migration at 120 Thousand Years for nn2008 Paleoclimate Boundary Conditions and a Loading Efficiency of 0 (fr-base-paleo-le0)



Note: Results for simulation using a loading efficiency of 1 and a 0% of ice-sheet thickness equivalent freshwater head for the surface hydraulic boundary condition (fr-base-paleo-0-le1).

Figure 2-34: Tracer Migration at 120 Thousand Years for nn2008 Paleoclimate Boundary Conditions

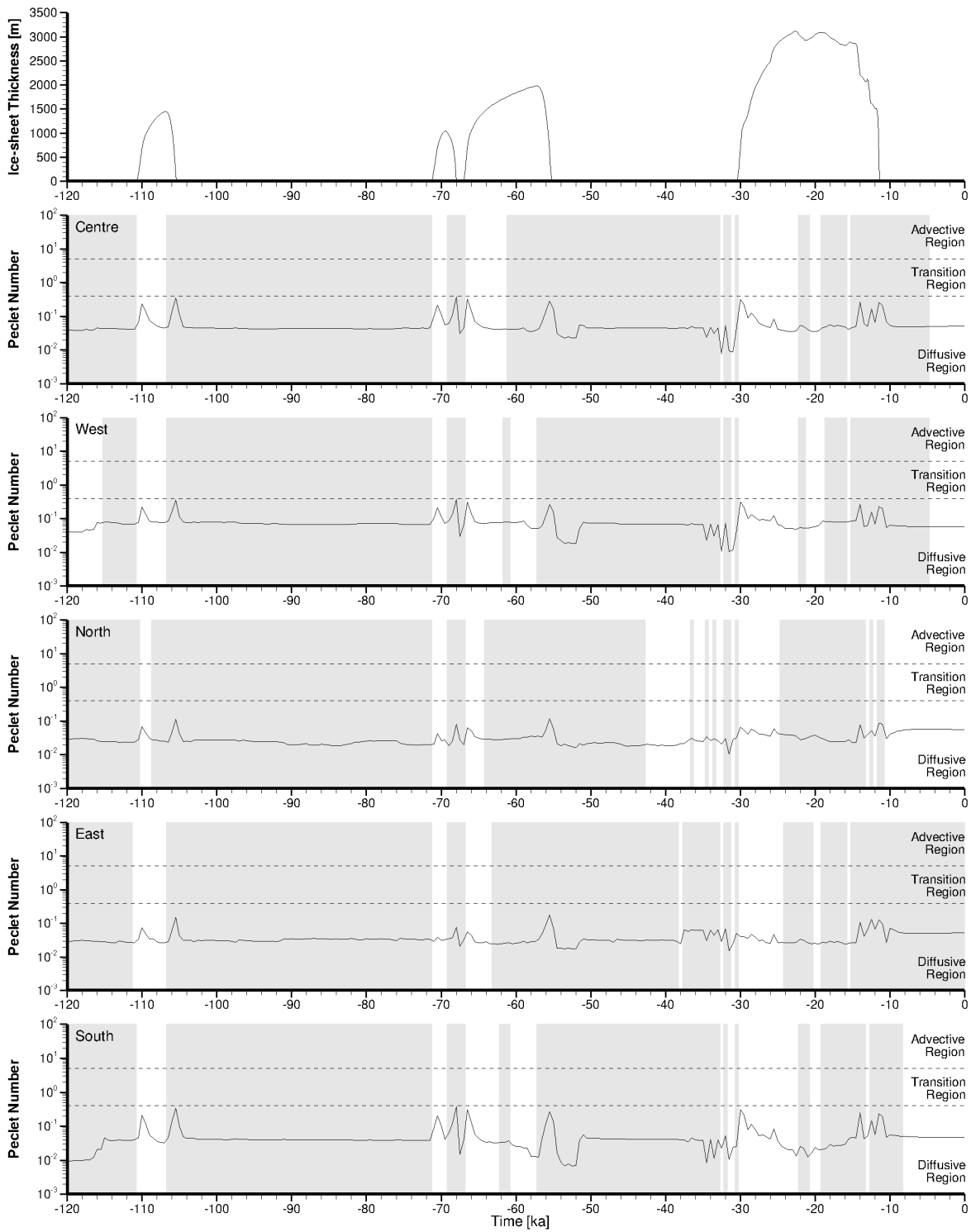


Figure 2-35: Péclet Number versus Time for the Reference Case Paleohydrogeological Scenario (fr-base-paleo)

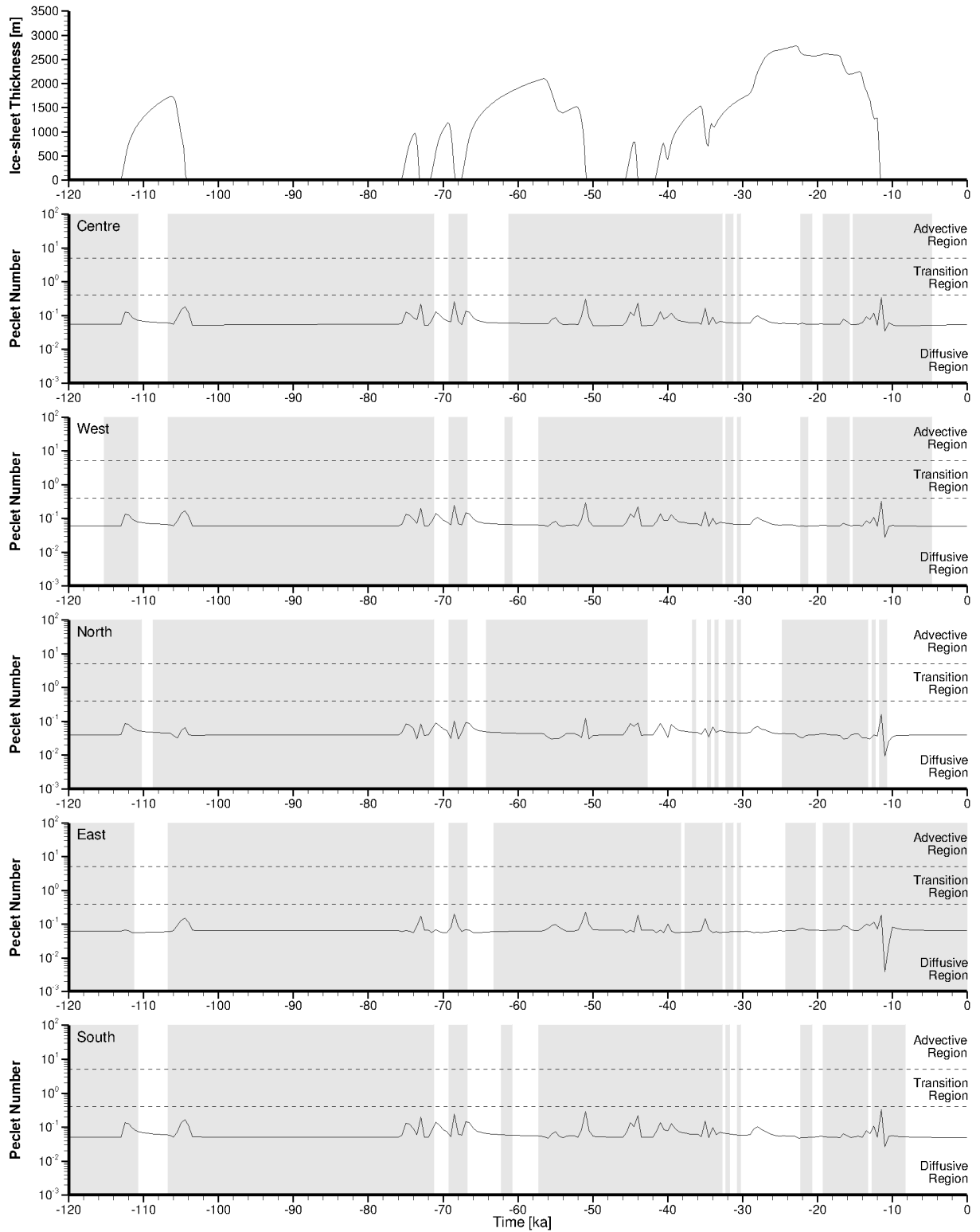


Figure 2-36: Péclet Number versus Time for the nn2778 Paleoclimate Boundary Conditions (fr-base-paleo-nn2778)

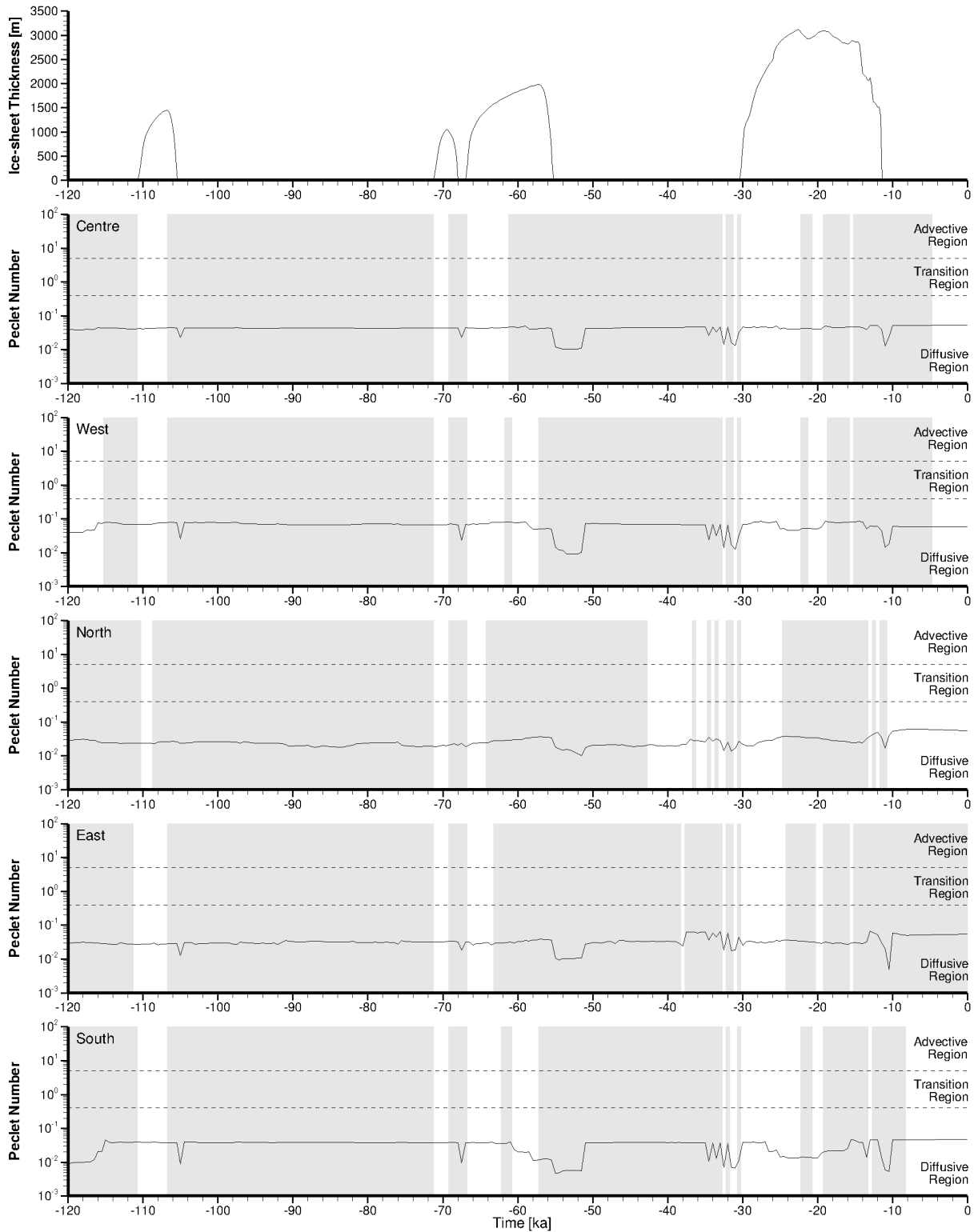


Figure 2-37: Péclet Number versus Time for nn2008 Paleoclimate Boundary Conditions and a Loading Efficiency of 1 (fr-base-paleo-le1)

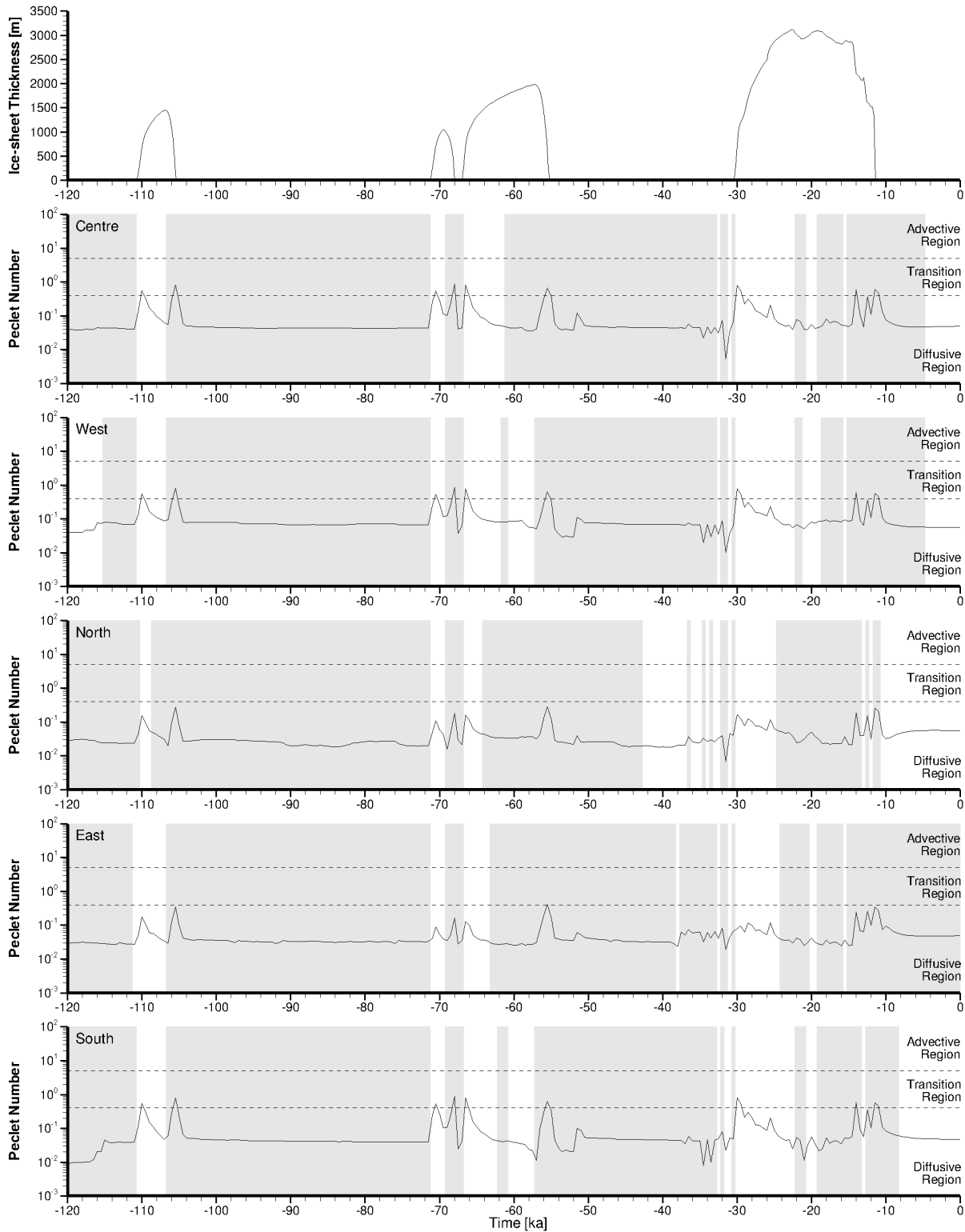
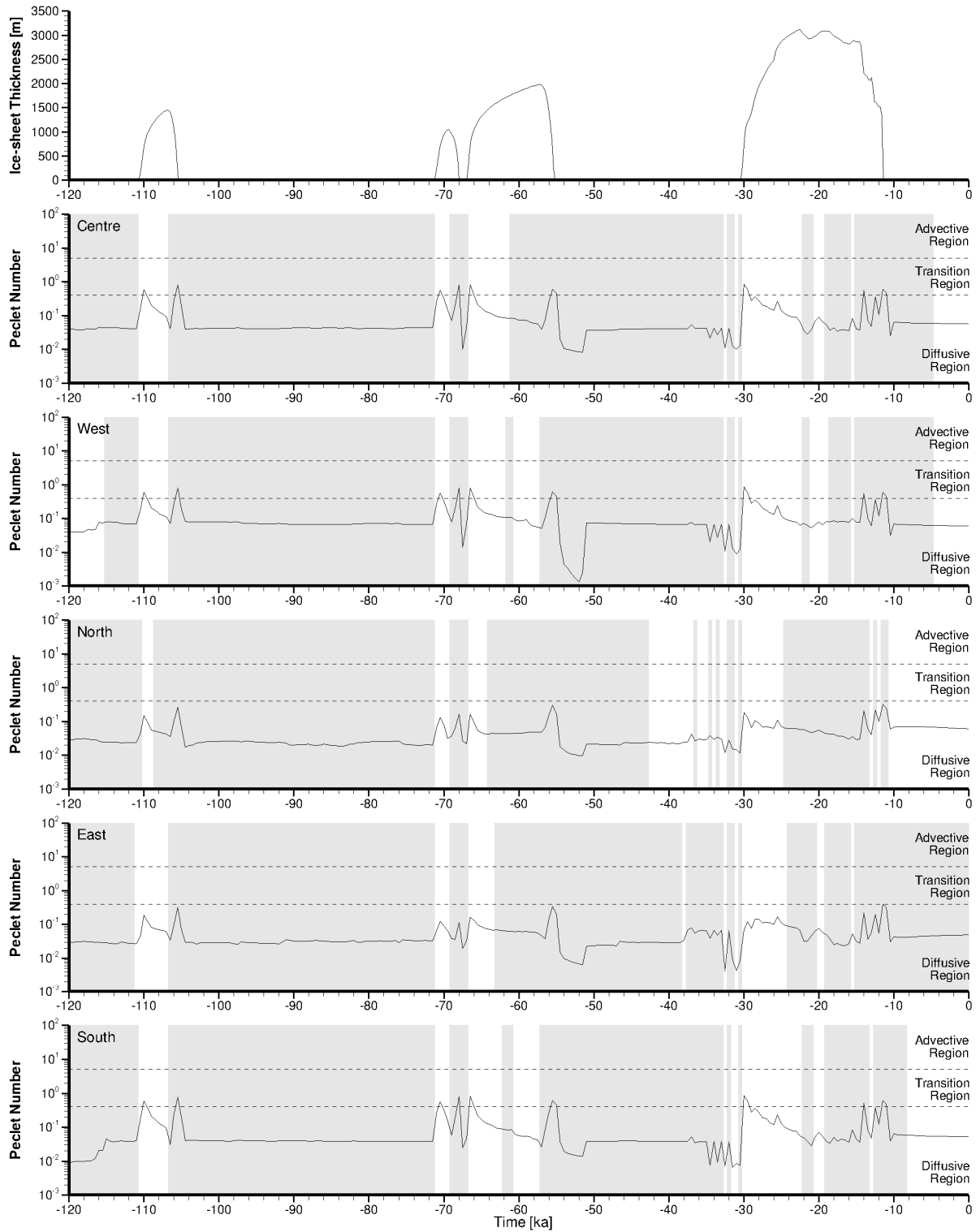


Figure 2-38: Péclet Number versus Time for nn2008 Paleoclimate Boundary Conditions and a Loading Efficiency of 0 (fr-base-paleo-le0)



Note: This simulation used a loading efficiency of 1 and a 0% of ice-sheet thickness equivalent freshwater head for the surface hydraulic boundary condition (fr-base-paleo-0-le1).

Figure 2-39: Péclet Number versus Time for nn2008 Paleoclimate Boundary Conditions

2.4 Summary and Conclusions

This chapter describes a geosphere dataset for a hypothetical crystalline site on the Canadian Shield. The dataset was developed from historical work conducted during the Canadian Nuclear Fuel Waste Management Program on the Canadian Shield, as summarized, in part, by Sykes et al. (2004, 2009) and Normani et al. (2007). The geosphere data set described in this chapter was provided for the purpose of performing an illustrative postclosure safety assessment. Three groundwater systems are considered: shallow, intermediate and deep. The behaviour of the groundwater systems during temperate and glacial conditions was explored through a suite of 14 sensitivity cases.

The hydrogeological domain for the geosphere described in this chapter is divided into three groundwater systems: shallow (0 – 150 mBGS), intermediate (150 – 700 mBGS) and deep (700 - 1500 mBGS). These systems are identified, in part, by rock mass hydraulic conductivities, as observed at the Atikokan and the Whiteshell Research Area, as well as groundwater total dissolved solids concentrations and redox conditions. The shallow groundwater zone occurs in the upper 150 m and comprises glacial sediment overlying a relatively permeable fractured rock mass. In the shallow system, groundwater is considered to be fresh and oxygen-rich. The intermediate groundwater system is a transition zone in which the groundwater becomes progressively more mineralized and reducing with depth. Within the deep groundwater system, groundwater conditions are saline and reducing. With increasing depth, the general increase in salinity and decrease in rock mass hydraulic conductivities leads to improved groundwater system stability at time frames relevant to repository safety. Péclet numbers and mean life expectancies were used as illustrative performance measures to gain insight into the processes most influencing mass transport. For an assumed reference case, the shallow groundwater system is advective, whereas at greater depths, the low permeability rock mass and decreased interconnectivity of the fracture network decreases mass transport rates. Further groundwater system stability occurs as a result of salinity gradients within the intermediate and deep groundwater systems.

Paleohydrogeological simulations were used to illustrate the long-term evolution and stability of the geosphere and groundwater systems to external perturbations. The distribution and duration of permafrost at the repository location play a role in governing the depth to which meltwater penetrates. Paleohydrogeologic simulations suggest that glacial meltwaters may recharge to depths of 640 to 890 mBGS. The depth of recharge estimated within the more permeable discrete fractures can exceed 1000 mBGS. Glacial recharge penetrating below the shallow groundwater system is not expected to be oxygenated or influence redox conditions at the repository horizon. For the paleohydrogeologic sensitivity cases performed, the glacial perturbations did not materially change mass transport rates at repository depth.

2.5 References for Chapter 2

- Andersson, J. 1999. SR97 Data and data uncertainties. SKB Technical Report TR-99-09. Stockholm, Sweden.
- Batzle, M. and Z. Wang. 1992. Seismic properties of pore fluids. *Geophysics* 57(11), 1396–1408.
- Bear, J. 1988. *Dynamics of Fluids in Porous Media*. Dover edition. Dover Publications Inc., New York, USA.
- Bottomley, D.J., A. Katz, L.H. Chan, A. Starinsky, M. Douglas, I.D. Clark and K.G. Raven. 1999. The origin and evolution of Canadian Shield brines: evaporation or freezing of seawater? New lithium isotope evidence from the Slave craton. *Chemical Geology* **155**, 295-320.
- Bucher, K. and I. Stober. 2000. The Composition of Groundwater in the Continental Crystalline Crust. In *Hydrogeology of Crystalline Rocks*. Kluwer Academic Publishers, Netherlands, 141-175.
- Byegård, J., E. Selnert and E.L. Tullborg. 2008. *Bedrock Transport Properties, Data Evaluation and Retardation Model, Site Descriptive Modeling SDM-Site Forsmark*. Swedish Nuclear Fuel and Waste Management Company Report SKB R-08-98. Stockholm, Sweden.
- Card, K.D. 1990. A review of the Superior Province of the Canadian Shield, a product of Archean accretion. *Precambrian Research* **48**, 99-156.
- Cornaton, F., and P. Perrochet. 2006a. Groundwater age, life expectancy and transit time distributions in advective-dispersive systems: 1. generalized reservoir theory, *Advances in Water Resources*, 29(9), 1267–1291.
- Cornaton, F., and P. Perrochet. 2006b. Groundwater age, life expectancy and transit time distributions in advective-dispersive systems; 2. reservoir theory for sub-drainage basins, *Advances in Water Resources*, 29(9), 1292–1305.
- Crawford J., I. Neretnieks and M. Malmström. 2006. *Data and Uncertainty Assessment for Radionuclide Kd Partitioning Coefficients in Granitic Rock for Use in SR-Can Calculations*. Swedish Nuclear Fuel and Waste Management Company Report SKB R-06-75. Stockholm, Sweden.
- Davison, C.C., T. Chan, A. Brown, M. Gascoyne, D. Kamineni, G. Lodha, T. Melnyk, B.W. Nakka, P. O'Connor, D. Ophori, N. Scheier, N. Soonawala, F. Stanchell, D. Stevenson, G. Thorne, T. Vandergraaf, P. Vilks and S. Whitaker. 1994. *The Disposal of Canada's Nuclear Fuel Waste: The Geosphere Model for Postclosure Assessment*. Atomic Energy of Canada Limited Report AECL-10719, COG-93-9. Pinawa, Canada.
- Frape, S.K. and P. Fritz. 1987. Geochemical trends for groundwaters from the Canadian Shield. In *Saline Water and Gases in Crystalline Rocks* (P. Fritz and S.K. Frape, eds.). Number 33 in Geological Association of Canada Special Paper, 19–38.

- Garisto, F., J. Avis., T. Chshyolkova, P. Gierszewski, M. Gobien, C. Kitson, T. Melnyk, J. Miller, R. Walsh and L. Wojciechowski. 2010. Glaciation Scenario: Safety Assessment for a Used Fuel Geological Repository. Nuclear Waste Management Organization Report NWMO TR-2010-10. Toronto, Canada.
- Garisto, F., A. D'Andrea, P. Gierszewski and T. Melnyk. 2004. Third Case Study – Reference Data and Codes. Ontario Power Generation Report 06819-REP-01200-10107-R00. Toronto, Canada.
- Gascoyne, M. and D.C. Kamineni. 1993. The hydrogeochemistry of fractured plutonic rocks in the Canadian Shield. *Applied Hydrogeology*, 2, 43-49.
- Gascoyne, M. and D.C. Kamineni. 1994. The Hydrogeochemistry of Fractured Plutonic Rocks in the Canadian Shield. *Applied Hydrogeology*, 2, 43-49.
- Gascoyne, M. 1997. Evolution of redox conditions and groundwater composition in recharge-discharge environments on the Canadian Shield. *Hydrogeological Journal* 5, 4-18.
- Gascoyne, M. 1988. Reference Groundwater Composition for a Depth of 500 m in the Whiteshell Research Area – Comparison with Synthetic Groundwater WN-1. Atomic Energy of Canada Limited Report AECL TR-463. Pinawa, Canada.
- Gascoyne, M. 2000. Hydrogeochemistry of the Whiteshell Research Area. Ontario Power Generation, Nuclear Waste Management Report 06819-REP-01200-10033-R00. Toronto, Canada.
- Gascoyne, M. 2004. Hydrogeochemistry, groundwater ages and sources of salts in a granitic batholith on the Canadian Shield, southeastern Manitoba. *Applied Geochemistry* 19, 519-560.
- Guvanasen, V. 2007. FRAC3DVS-OPG Enhancements: Subgridding, Hydromechanical Deformation and Anisotropic Molecular Diffusion. Nuclear Waste Management Organization Report NWMO TR-2007-05. Toronto, Canada.
- Hallbeck, L. and K. Pedersen. 2008. Explorative Analyses of Microbes, Colloids, and Gases together with Microbial Modelling. Site Description Model SDM-Site Laxemar. Swedish Nuclear Fuel and Waste Management Company Report SKB TR-08-109. Stockholm, Sweden.
- Hoffman, P.F. 1988. United plates of America, the birth of a craton Early Proterozoic assembly and growth of Laurentia. *Annual Review of Earth and Planetary Sciences* 16, 543-603.
- Humphreys, P.N., J.M. West, and R. Metcalfe. 2010. Microbial effects on repository performance. Prepared by Quintessa Ltd. for the Nuclear Decommissioning Authority, Oxfordshire, United Kingdom. Report No. QRS-1378Q-1.
- Huysmans, M. and A. Dassargues. 2005. Review of the use of Peclet numbers to determine the relative importance of advection and diffusion in low permeability environments. *Hydrogeology Journal* 13, 895–904.

- Jain, D.K., S. Stroes-Gascoyne, M. Providenti, C. Tanner and I. Cord. 1997. Characterization of microbial communities in deep groundwater from granitic rock. *Canadian Journal of Microbiology* 43, 272-283.
- Lau, J.S.O. and N.A. Chandler. 2004. Innovative laboratory testing. *International Journal of Rock Mechanics & Mining Sciences* 41(8), 1427-1445.
- Luszczynski, N.J. 1961. Head and flow of ground water of variable density. *Journal of Geophysical Research* 66(12), 4247–4256.
- McCauley, C. A., D. M. White, M. R. Lilly, and D. M. Nyman. 2002. A comparison of hydraulic conductivities, permeabilities and infiltration rates in frozen and unfrozen soils. *Cold Regions Science and Technology* 34(2), 117–125.
- McMurry, J. 2004. Reference Water Compositions for a Deep Geologic Repository in the Canadian Shield. Ontario Power Generation Report 06819-REP-01200-10135-R01, Toronto, Canada.
- McMurry, J., D.A. Dixon, J.D. Garroni, B.M. Ikeda, S. Stroes-Gascoyne, P. Baumgartner and T.W. Melnyk. 2003. Evolution of a Canadian Deep Geologic Repository: Base Scenario. Ontario Power Generation Report 06819-REP-01200-10092-R00. Toronto, Canada.
- Normani, S.D., Y.-J. Park, J.F. Sykes and E.A. Sudicky. 2007. Sub-Regional Modelling Case Study 2005-2006 Status Report. Nuclear Waste Management Organization Report NWMO TR-2007-07. Toronto, Canada.
- Normani, S.D. 2009. Paleoevolution of Pore Fluids in Glaciated Geologic Settings. Ph.D. Thesis, Department of Civil Engineering, University of Waterloo. Ontario, Canada.
- Ontario Geological Survey (OGS). 2000. Bedrock Geology of Ontario. ERLIS Data Set 6, Queens Printer for Ontario. ISBN 0-7778-9309-6. Ontario, Canada.
- Ophori, D.U., D.R. Stevenson, M. Gascoyne, A. Brown, C.C. Davison, T. Chan, and F.W. Stanchell. 1995. Revised Model of Regional Groundwater Flow of the Whiteshell Research Area: Summary. AECL-11286.
- Ophori, D.U. and T. Chan. 1996. Regional Groundwater Flow in the Atikokan Research Area: Model Development and Calibration. Atomic Energy of Canada Limited Report AECL-11081, COG-93-183. Pinawa, Canada.
- Park, Y.-J., E.A. Sudicky, S. Panday, J.F. Sykes and V. Guvanasen. 2008a. Application of implicit sub-time stepping to simulate flow and transport in fractured porous media. *Advances in Water Resources*, 31(7), 995-1003.
- Park, Y.-J., F.J. Cornaton, S.D. Normani, J.F. Sykes and E.A. Sudicky. 2008b. Use of groundwater lifetime expectancy for the performance assessment of a deep geologic radioactive waste repository: 2. Application to a Canadian Shield environment. *Water Resources Research*, 44.
- Park, Y. J., E. A. Sudicky, and J. F. Sykes. 2009. Effects of Shield brine on the safe disposal of waste in deep geologic environments. *Advances in Water Resources* 32, 1352–1358.

- Pedersen, K. 2006. Microbiology of transitional groundwater of the porous overburden and underlying shallow fractured bedrock aquifers in Olkiluoto 2004, Finland. POSIVA Working Report 2006-09.
- Pedersen, K. 2000. Microbial processes in radioactive waste disposal. SKB TR-00-04.
- Peltier, W.R. 2002. A Design Basis Glacier Scenario. Ontario Power Generation Report 06819-REP-01200-10069-R00. Toronto, Canada.
- Peltier, W.R. 2006. Boundary conditions data sets for spent fuel repository performance assessment. Ontario Power Generation, Nuclear Waste Management Division Report 06819-REP-01200-10154-R00. Toronto, Canada.
- Perry, C., C. Rosieanu, J.-C. Mareschal and C. Jaupart. 2010. Thermal Regime of the Lithosphere in the Canadian Shield. Canadian Journal of Earth Sciences, 47, 389-408.
- Sherwood Lollar, B. 2007. Hydrogeologic controls on episodic H₂ release from Precambrian fractured rocks – Energy for deep subsurface life on Earth and Mars. Astrobiology, 7(6): 971-986.
- Sherwood Lollar, B. 2011. State of Science Review: Far-field microbiological considerations relevant to a Deep Geological Repository for used nuclear fuel. Nuclear Waste Management Organization Report No. TR-2011-09, Toronto, ON.
- Sherwood Lollar, B., S.K. Frape, P. Fritz, S.A. Macko, J.A. Welhan, R. Blomqvist and P.W. Lahermo. 1993a. Evidence for bacterially-generated hydrocarbon gas in Canadian and Fennoscandian Shield rocks. Geochimica et Cosmochimica Acta, Vol. 57:5073-5085.
- Sherwood Lollar, B., S.K. Frape, S.M. Weise, P. Fritz, S.A. Macko and J.A. Welhan. 1993b. Abiogenic methanogenesis in crystalline rocks. Geochim. Cosmo. acta, Vol. 75:5087-5097.
- Sikorsky, R.I., M. Serzu, D. Tomsons and J. Hawkins. 2002. A GIS-based Methodology for Lineament Interpretation and its Application to a Case Study at AECL's Whiteshell Research Area in Southeastern Manitoba. Ontario Power Generation Report 06819-REP-01200-10073-R00, Toronto, Canada.
- Singer S.N. and C.K. Cheng. 2002. An Assessment of the Groundwater Resources of Northern Ontario. Hydrogeology of Ontario Series (Report 2). Ministry of the Environment: Environmental Monitoring and Reporting Branch. Page 255. Ontario, Canada.
- Singh, B.P. and B. Kumar. 2005. Isotopes in Hydrology, Hydrogeology, and Water Resources. Narosa Publishing House Pvt. Ltd., New Delhi, India.
- Singhal, B.B.S. and R. P. Gupta. 2010. Chapter 13: Hydrogeology of Crystalline Rocks. In Applied Hydrogeology of Fractured Rocks. Springer Science and Business Media. 237-255.
- SKB. 2006. Geosphere process report for the safety assessment of SR-Can. Swedish Nuclear Fuel and Waste Management Company Report TR-06-19. Stockholm, Sweden.

- Srivastava, R.M. 2002. Probabilistic Discrete Fracture Network Models for the Whiteshell Research Area. Ontario Power Generation Report 06819-REP-01200-17001-R00. Toronto, Canada.
- Stevenson, D.R., E.T. Kozak, C.C. Davison, M. Gascoyne and R.A. Broadfoot. 1996. Hydrogeologic Characteristics of Domains of Sparsely Fractured Rock in the Granitic Lac du Bonnet Batholith, Southeastern Manitoba, Canada. Atomic Energy of Canada Limited Report AECL-11558, COG-96-17. Pinawa, Canada.
- Stotler, R.L., S.K. Frappe, T. Ruskeeniemi, P. Pitkänen and D.W. Blowes. 2012. The interglacial–glacial cycle and geochemical evolution of Canadian and Fennoscandian Shield groundwaters. *Geochimica et Cosmochimica Acta* 76, 45-67.
- Stroes-Gascoyne, S., and J.M. West. 1997. Microbial studies in the Canadian nuclear fuel waste management program. *FEMS Microbiology Reviews*, 20: 573-590.
- Sykes, J.F., S.D. Normani, E.A. Sudicky and R.G. McLaren. 2004. Sub-regional Scale Groundwater Flow within an Irregularly Discretely Fractured Canadian Shield Setting. Ontario Power Generation Report 06819-REP-01200-10133-R00. Toronto, Canada.
- Sykes, J.F., S.D. Normani, M.R. Jensen and E.A. Sudicky. 2009. Regional-scale groundwater flow in a Canadian Shield setting. *Canadian Geotechnical Journal*, 46(7), 813–827.
- Therrien, R., R. G. McLaren, E. A. Sudicky, S.M. Panday, and, V. Guvanasen. 2010. FRAC3DVS-OPG: A Three-Dimensional Numerical Model Describing Subsurface Flow and Solute Transport. User's Guide. Groundwater Simulations Group, University of Waterloo, Waterloo, Ontario, Canada.
- Vilks, P., N.H. Miller and F.W. Stanchell. 2004. Phase II In-Situ Diffusion Experiment. Ontario Power Generation Report 06819-REP-01200-10128-R00. Toronto, Canada.
- Vilks, P. 2009. Sorption in Highly Saline Solutions – State of the Science Review. Nuclear Waste Management Organization Report NWMO TR-2009-18. Toronto, Canada.
- Vilks, P., F. Caron and M. Haas. 1998. Potential for the formation and migration of colloidal material from a near-surface waste disposal site. *Applied Geochemistry* 13: 31-42 (AECL-11935).
- Vilks, P. and D. Bachinski. 1997. Natural colloids in groundwater from granite and their potential impact on radionuclide transport. Atomic Energy of Canada Limited Report AECL-11635, COG-96-311-I. Pinawa, Canada.
- Wang, H.F. 2000. Theory of Linear Poroelasticity with Applications to Geomechanics and Hydrogeology. Princeton University Press. Princeton, USA.
- Weast, R.C. (Ed.). 1983. CRC Handbook of Chemistry and Physics. 64th edition. CRC Press, Inc., Boca Raton, Florida, USA.

3. USED FUEL CHARACTERISTICS

3.1 Used Fuel Description

3.1.1 Used Fuel Type and Amount

The used fuel waste form is a post-discharge natural uranium UO₂ CANDU fuel bundle.

The hypothetical repository is assumed to contain 4.6x10⁶ bundles, which is the total reference used fuel inventory projected over the expected lifetime of the current fleet of Canadian CANDU power reactors (Garamszeghy 2011)¹.

There are a few variant CANDU fuel bundle designs, in particular the 28-element bundle, the 37-element standard bundle, and the 37-element long length bundle. Some older bundles do not have CANLUB, which is a thin graphite coating between the fuel pellet and the fuel sheath. Sensitivity studies by Tait et al. (2000) indicate that the radionuclide inventory per unit mass of fuel is not sensitive to these different designs, and so the standard 37-element (Bruce) fuel bundle is selected as the reference as it will be the most common bundle.

The age of the fuel when placed in the repository will vary. Because the earliest bundles date back to 1970 and because the repository is unlikely to open before 2035, some fuel will be over 60 years old. The older the fuel, the lower the residual thermal power and the lower the radiation fields. For this pre-project review, all fuel bundles are assumed to have an out-of-reactor decay time of 30 years.

Table 3-1 summarizes the characteristics of the reference used fuel. These are further discussed below.

3.1.2 Geometry

Fuel pellets formed from natural uranium UO₂ are placed inside a fuel sheath made of a zirconium-tin alloy (Zircaloy-4) with a thin CANLUB graphite coating on the inside. The ends of the sheath are closed by a welded zirconium alloy plug to produce a sealed fuel element. Fuel elements are welded to zirconium alloy end plates to form a fuel bundle as shown in Figure 3-1.

¹ Includes refurbishment of Bruce A, Darlington, Point LePreau and Gentilly-2. No further refurbishment of Pickering or Bruce B. No new build reactors. Should Gentilly-2 not proceed with refurbishment, the projected used fuel inventory would be reduced to about 4.4x10⁶ bundles.

Table 3-1: Used Fuel Parameters

Parameter	Value	Comment
Waste Form	37-element UO ₂ fuel bundle	Standard fuel element from Bruce and Darlington stations
Mass U/bundle	19.25 kg	Initial mass (before irradiation)
Mass Zircaloy/ bundle	2.2 kg	Includes cladding, spacers, end plates
Initial U-235	0.72 wt%	Natural uranium is used in OPG CANDU fuel
Burnup	220 MWh/kgU	Highest OPG station-average burnup in Tait et al. (2000). More recent data suggest that the highest average burnup for any OPG station is 200 MWh/kgU (Garisto et al. 2012)
Power Rating	455 kW/bundle	Nominal mid-range value
Fuel Age (when placed in repository)	30 years	e.g., 10 years in pools, 20 years in dry storage
Fuel Pellet Geometric Surface Area	8.47 cm ²	Surface area of undamaged pellet (37 element design)

Note: From Tait et al. (2000).

The number of pellets in a fuel element, and the number and dimensions of the fuel elements in a fuel bundle depend on the particular CANDU reactor. The most common bundle contains 37 fuel elements, each of which is 13.1 mm diameter and 486 mm long. This fuel bundle weighs 23.9 kg, of which 21.7 kg is UO₂ and 2.2 kg is Zircaloy (Tait et al. 2000).

Upon discharge, less than 0.1% of the bundles have minor damage or defects (such as pinhole failures in the fuel sheaths) (Tait et al. 2000). Analysis of the integrity of used fuel bundles indicates that they are unlikely to fail during storage (Freire-Canosa 2011). A small percentage may have increased susceptibility to integrity failure during subsequent transport to permanent storage. While the specific value may be relevant to the packaging plant design, the postclosure safety assessment is not sensitive to this value since no credit is taken for fuel bundle integrity.

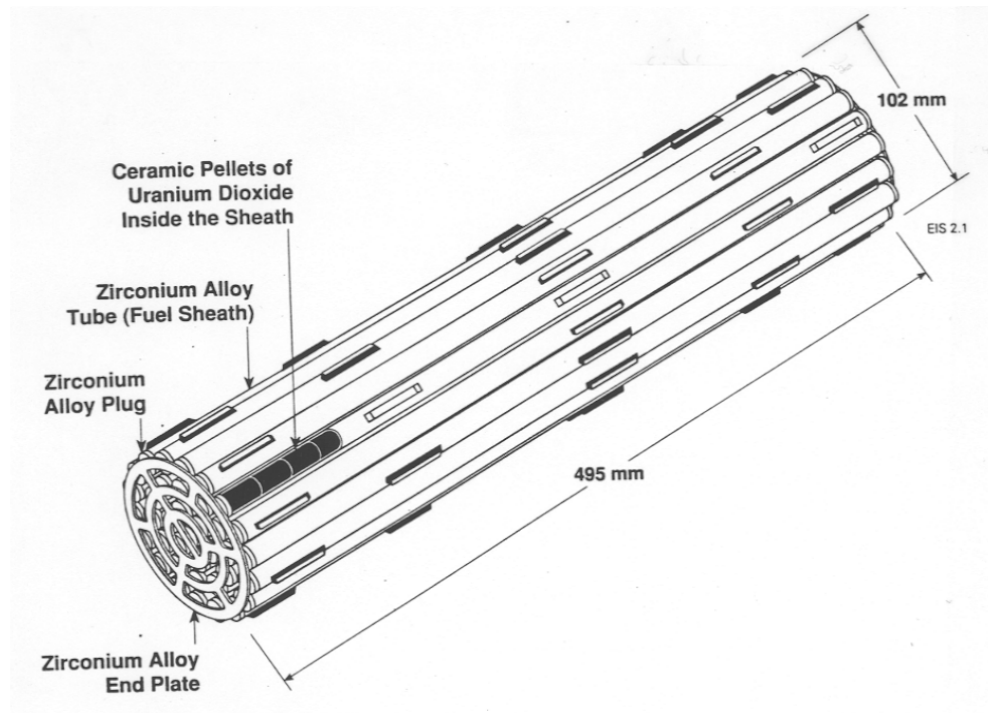


Figure 3-1: Typical CANDU Fuel Bundle

3.1.3 Burnup and Linear Power

The radioactivity level, heat generation rate, and bundle composition are all affected by the fuel burnup. This in turn depends on many factors including the type of reactor, the location of the bundle in the core, the bundle residence time, and bundle shifts that occur during fuelling operations. Although each bundle has a unique irradiation history, used fuel from all CANDU reactors is similar enough that it is not necessary to know individual detailed characteristics to assess the overall behaviour of the used fuel assemblies in the repository.

The typical burnup range for CANDU fuel is about 120 to 320 MWh/kg U (99th percentile, Tait et al. 2000, Wilk and Cantello 2006) with some exceptional fuel elements experiencing burnups as high as 706 MWh/kg U (Wilk and Cantello 2006). Tait et al. (2000) recommend a reference mean burnup value of 220 MWh/kg U based on the highest station-averaged mean burnup. Wilk and Cantello (2006) show that the 220 MWh/kgU value exceeds the median burnup for all OPG stations. At this level, about 2% of the initial uranium is converted into other elements.

The other major irradiation parameter that characterizes used fuel is linear power, which is the energy production rate per unit length. Tait et al. (2000) considered a power range of 200 to 900 kW/bundle (10-50 kW/m) as typical for the power range within which most CANDU bundles operate during their reactor lifetimes. The power level primarily affects the operating temperatures, which typically range from around 400°C on the outside of the fuel sheath to between 800°C and 1700°C in the fuel centreline, well below the melting temperature of 2800°C.

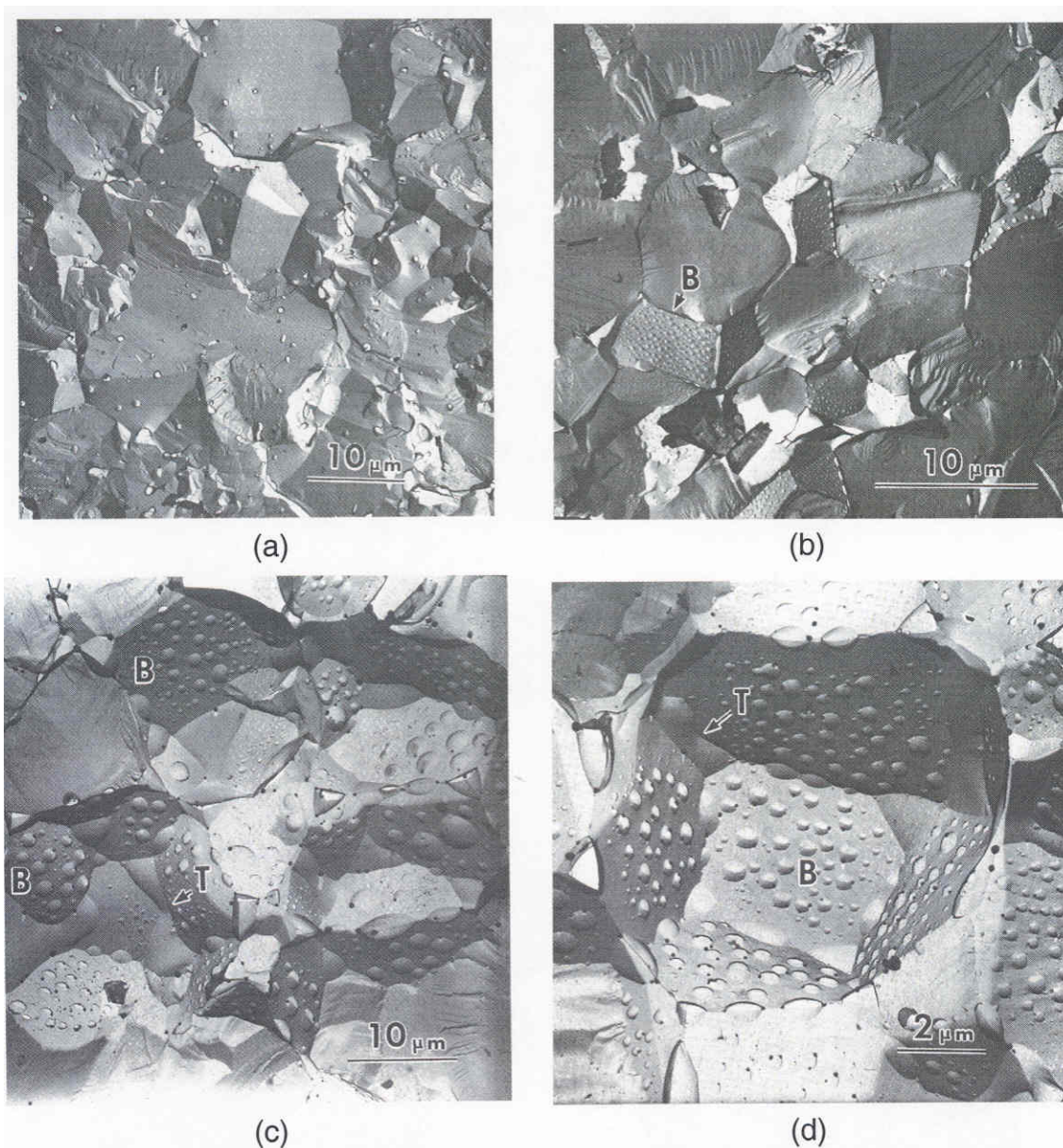
Tait et al. (2000) have calculated that the differences in radionuclide inventories between typical minimum and maximum power levels (200 and 900 kW/bundle) are generally less than about 2% for the same burnup. Tait et al. (2000) therefore used a mid-range value of 455 kW/bundle for reference inventory calculations.

In summary, a burnup level of 220 MWh/kg U and a power level of 455 kW/bundle are therefore used to calculate radionuclide inventories.

3.1.4 Effect of Irradiation

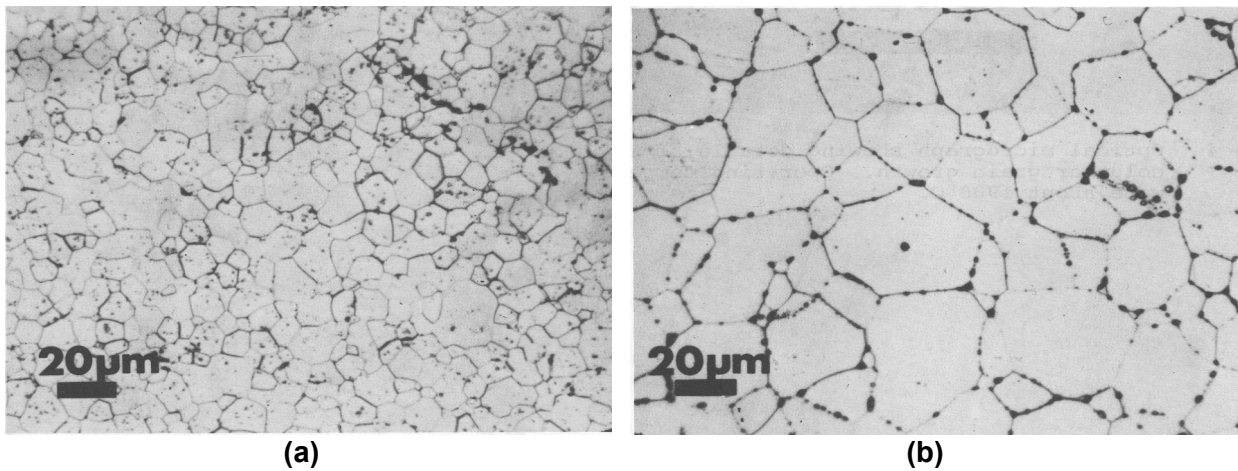
The fuel undergoes a number of microstructural changes during irradiation, as illustrated by the sequence of photographs in Figure 3-2. Unirradiated fuel has a cohesive, interlocking microstructure and many grains have some internal sintering porosity from the fuel fabrication process. During irradiation, the sintering porosity is largely eliminated, boundaries between individual grains become more distinct, and some volatile elements diffuse out of the fuel grains to form fission gas bubbles at the interfaces between grains. At linear power ratings higher than approximately 50 kW/m (i.e. higher than achieved in most CANDU bundles), the fission gas bubbles enlarge and begin to coalesce, leading in some cases to the formation of gas tunnels along grain boundaries.

Unirradiated fuel pellets are very fine-grained, but at linear power ratings higher than approximately 50 kW/m equiaxial grain growth occurs in the pellet interior where temperatures are highest (Figure 3-3). Grain growth is typically accompanied by the diffusion and segregation of non-volatile fission products, some of which form small metallic particles at grain boundaries as shown in Figure 3-4.



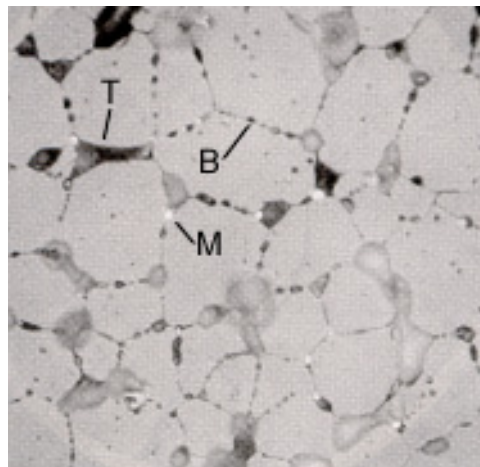
- Notes: a) Typical microstructure of unirradiated UO_2 . Small inclusions = sintering porosity.
b) Irradiated at low power ($< 45 \text{ kW/m}$). Note loss of sintering porosity and development of small intergranular fission gas bubbles (B).
c) Irradiated at higher power ($\geq 50 \text{ kW/m}$), showing growth of fission gas bubbles (B) and initiation of tunnels (T).
d) Magnified view of irradiated higher power fuel. Note the grain-edge tunnels (T) and the development of fission gas bubbles (B) on all faces of the "pull-out" of a single grain.
Ref.: Hastings (1982)

Figure 3-2: Typical Microstructure of Unirradiated and Irradiated UO_2 Fuel



- Notes: a) Unirradiated UO_2 . Note sintering porosity in grain interiors.
 b) Irradiated UO_2 at low burnup and high power (20 MWh/kg U at 50 kW/m). Note increase in grain size, loss of sintering porosity, and formation of fission gas bubbles and tunnels along boundaries.
 Ref.: Hastings (1982)

Figure 3-3: Grain Growth in Irradiated UO_2 Fuel



Ref: Novak and Hastings (1991)

- Notes: Optical micrograph of polished and etched UO_2 fuel irradiated to very high burnup (770 MWh/kg U at 52 kW/m), showing small white particles at grain boundaries (M) that are formed from incompatible metals such as Mo, Ru, and Pd that have diffused out of the UO_2 grains. Well-developed fission gas bubbles (B) and tunnels (T) are also present at grain boundaries. Scale is approximately same as shown for Figure 3-3.

Figure 3-4: Segregation of Metallic Fission Products from UO_2 Fuel

Compared to fresh bundles, used bundles contain new elements (approximately 2% by mass), including fission products, activation products and actinides other than uranium. Of these, more than ~95% remain within the UO_2 lattice very close to the location of their formation (Garisto et al. 2012, and references therein).

As indicated in Figure 3-5, the species produced can be grouped according to their chemical behaviour into the following categories (Kleykamp 1985):

1. Species such as He, Kr, Ar, Cs and I that are gaseous or somewhat volatile at fuel operating temperatures (i.e., 400-1700°C). Due to their relatively high diffusion coefficients, during reactor operation a small fraction of each species migrates out of the fuel grains and into fuel element void spaces (i.e., into the fuel sheath gap and into cracks in the fuel pellets). At the same time, another small fraction moves to the grain boundaries within the fuel pellets and forms fission gas bubbles. The remainder (roughly 95%) of the fission gases are held in the UO_2 crystal lattice.
2. Species such as the metals Mo, Ru, and Pd that are non-volatile but have a low solubility in UO_2 . At high in-reactor temperatures, small quantities of these species can diffuse from the fuel grains and segregate as metallic alloy phases at grain boundaries, particularly in areas of UO_2 grain growth. The majority of incompatible species remain trapped within the fuel grains due to their low diffusion coefficients in UO_2 at fuel operating temperatures.
3. Species that are compatible with UO_2 , including the lanthanide elements and actinides such as Pu, Am, Np. These elements can substitute chemically for uranium in UO_2 , and the atoms are then structurally bound as trace elements in the UO_2 crystal lattice.

The Zircaloy-4 fuel sheath consists of more than 98 wt% Zr and approximately 1.5 wt% Sn, with a number of other elements present as impurities (Tait et al. 2000). During irradiation, the cladding receives a neutron fluence of around 10^{25} n/m² (Truant 1983). The irradiated metal cladding is a fine-grained material (grain size typically 10 μm , thickness typically 0.4 mm) with neutron activation products, such as C-14, Ni-59 and Ni-63, present at concentrations less than 1 mg/kg Zr. Due to the low temperature of the cladding during irradiation (<400°C), activation products in the Zircaloy cannot diffuse any significant distance from the site of their formation, and they are therefore likely to be distributed uniformly throughout the metal. While in-reactor, coolant pressure causes the fuel cladding to collapse onto the fuel pellets, the heat generated in the fuel causes the pellets to expand slightly into an hourglass shape, which leads to the formation of minor cylindrical ridges in the cladding. This effect is more pronounced at high linear power and when fuel is in the reactor for long times.

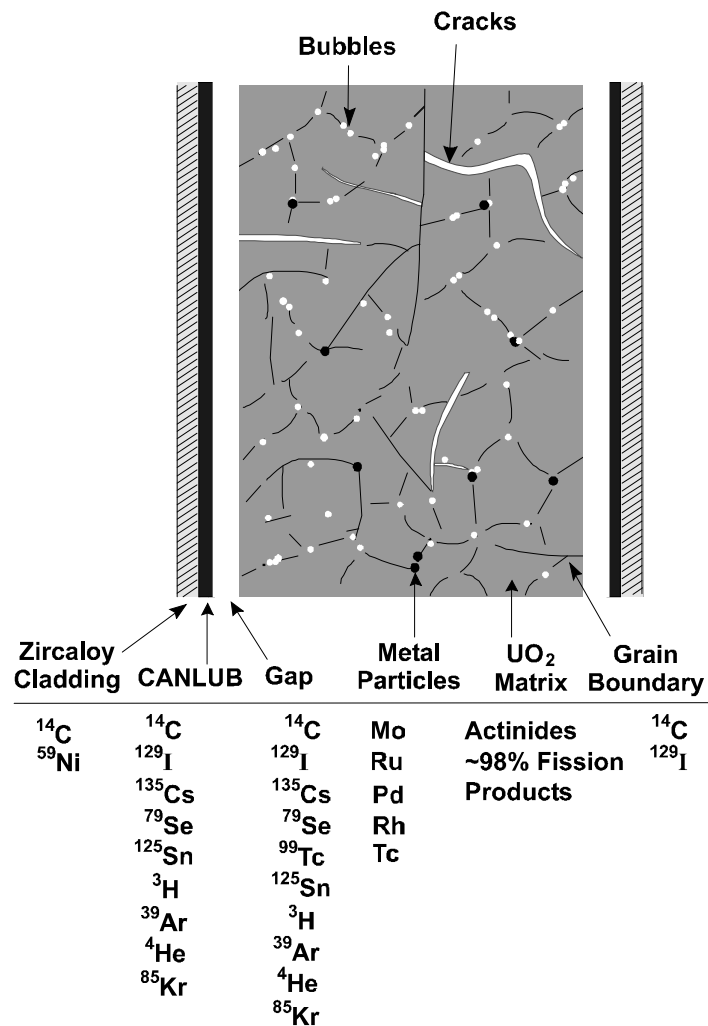


Figure 3-5: Illustrative Distribution of Some Fission Products and Actinides within a Used-Fuel Element

3.2 Radionuclide and Chemical Element Inventory

At the time of discharge the used fuel contains many hundreds of radionuclides; however, following placement in a deep geological repository only a small fraction poses a potential radiological risk to humans or to the environment. The subset of radionuclides of potential concern for safety assessment is identified via a screening analysis.

The screening analysis is described in Chapter 7. The analysis identifies 25 radionuclides of potential concern. However, parents and progeny of the screened in radionuclides are also included to ensure that ingrowth is adequately accounted for in the system model so 39 radionuclides are represented in total. The radionuclide decay chains included in the radiological assessment are shown in Table 3-2.

Table 3-2: Radionuclide Decay Chains Included in the Radiological Assessment

Single Nuclides	Cl-36, I-129, C-14, Cs-135, Ca-41, Ni-59, Se-79
Chains	
Neptunium Series	Am-241 → Np-237 → Pa-233 → U-233 → Th-229 → Ra-225 → Ac-225
Uranium Series	Pu-242 → U-238 → Th-234 → U-234 → Th-230 → Ra-226 → Rn-222 → Pb-210 → Bi-210 → Po-210
Actinium Series	Pu-239 → U-235 → Th-231 → Pa-231 → Ac-227 → Th-227 → Ra-223
Thorium Series	Pu-240 → U-236 → Th-232 → Ra-228 → Th-228 → Ra-224
Misc	Sn-126 → Sb-126

At the time of discharge the used fuel also contains essentially the entire periodic table of elements from hydrogen to californium; however, only a small fraction of these could pose a chemical toxicity risk to humans or to the environment. As is the case for radionuclides, the subset of chemical elements of potential concern is identified via a screening analysis.

The screening analysis is described in Chapter 7. The results identify 16 elements of potential concern, where multiple isotopes of an element are considered as one element. In addition, the element As is added for historical reasons. Some of these screened in elements (e.g., Pb, Ag, and Te) are generated by radioactive decay of parent progeny. Consequently, to ensure that in-growth is properly accounted for in the system model 21 additional nuclides and their decay chains are included. The chemical elements of concern along with the required decay chains are shown in Table 3-3.

Table 3-3: List of Potentially Significant Chemically Toxic Elements and Radionuclide Decay Chains Included in the Hazardous Substance Assessment

Elements*	As, Ce, Cd, Co, Cr, Eu, Hg, I, La, Nd, P, Pr, Y
Chains*	
Actinium Series	Pu-239 → U-235 → Th-231 → Pa-231 → Ac-227 → Th-227 → Ra-223 → Pb
Thorium Series	Pu-240 → U-236 → Th-232 → Ra-228 → Th-228 → Ra-224 → Pb
Uranium Series	Pu-242 → U-238 → Th-234 → U-234 → Th-230 → Ra-226 → Rn-222 → Pb-210 → Bi-210 → Po-210 → Pb
Misc	Pd 107 → Ag, Sn-126 → Te

It should be noted that it is the total concentration of a potentially chemically toxic element in the biosphere that is important for the hazardous substance assessment. For example, the total uranium concentration in a particular biosphere medium is the sum of the concentrations of all the uranium isotopes.

Table 3-4 lists all the radionuclides included in either Table 3-2 or Table 3-3 together with their half lives, their inventories at the assumed time of placement in the repository, and various uncertainties associated with the inventories. The inventories are from Tait et al. (2000);

however, corrections to the inventories were made to account for the difference in the bundle average and “ring sum” inventories if differences exceeded +1%, as described in Garisto et al. (2012).

It should be emphasized that what is important for the safety assessment is the uncertainty in the total radionuclide inventory in a container with 360 fuel bundles which (based on the central limit theorem) would be much smaller than the uncertainty in the inventory of a single fuel bundle. Thus, it is these uncertainties that are shown in Table 3-4.

Uncertainty arises due to the accuracy of the ORIGEN-S calculations when compared against measurements (σ_{OR}), and due to the use of an average power rating (σ_{PR}) in the calculation of initial radionuclide inventories. The latter uncertainty is small for the radionuclides of interest except for Cs-135 (Garisto et al. 2012).

There is no need to account for the uncertainty arising from calculating the inventories at a burnup of 220 MWh/kgU because this burnup is 10% higher than the average burnup from any of the OPG generating stations (Garisto et al. 2012). Thus, since inventories generally increase with burnup (Tait et al. 2000), the calculated inventories are conservative.

Validation studies (Tait et al. 1995) indicate that ORIGEN-S predictions generally agree with measured actinide and fission product inventories, with the residual uncertainty in many cases related more to the accuracy of the measurements. A comparison of measured and predicted values for a Pickering fuel bundle is shown in Table 3-5.

More recent comparisons by SKB (2010) for PWR fuel, indicates that the ratio of measured to ORIGEN calculated inventories is 1.01 for U and Pu isotopes; 1.01 for fission products and 1.11 for actinides other than U and Pu. Again, the agreement is good and within the uncertainty of the measured data.

Further information on the derivation of the uncertainties is available in Garisto et al. (2012).

Table 3-6 lists the chemical elements included in Table 3-3 together with their inventories at the assumed time of placement in the repository, and various uncertainties associated with the inventories. The inventory of an element is equal to the sum of the inventories of the long-lived isotopes of the element.

The inventories are from Tait et al. (2000). However, corrections to the inventories were made to account for the difference in the bundle average and “ring sum” inventories if differences exceeded +1%, as described in Garisto et al. (2012). Also, for Eu, the inventory includes the inventory of a short-lived precursor (Sm-151).

Table 3-4: Inventories of Radionuclides of Interest in UO₂ Fuel for 220 MWh/kgU Burnup and 30 Years Decay Time

Nuclide	Half-life* [a]	Inventory [moles/kgU initial]	σ_{OR} [%]	σ_{PR} [%]	σ_{Total} [%]
Ac-225	2.738E-02	1.662E-14	-	-	NA1
Ac-227	2.177E+01	1.573E-11	2.5	-	2.5
Am-241	4.326E+02	1.155E-3	15	-	15
Bi-210	1.372E-02	5.296E-18	-	-	NA1
C-14	5.700E+03	5.60E-06	-	-	NA2
Ca-41	1.020E+05	2.354E-06	7	-	7.0
Cl-36	3.010E+05	5.42E-06	-	-	NA2
Cs-135	2.300E+06	2.675E-04	7	3	7.6
I-129	1.570E+07	4.228E-04	7	-	7.0
Ni-59	7.600E+04	6.438E-06	-	-	NA3
Np-237	2.144E+06	1.708E-04	20	-	20
Pa-231	3.276E+04	3.820E-08	2.5	-	2.5
Pa-233	7.385E-02	5.901E-12	-	-	NA1
Pb-210	2.220E+01	8.604E-15	55	-	55
Pd-107	6.500E+6	6.901E-4	7	-	7
Po-210	3.789E-01	1.463E-16	-	-	NA1
Pu-239	2.411E+04	1.123E-02	3	-	3
Pu-240	6.561E+03	5.339E-03	4	-	4.0
Pu-242	3.735E+05	4.257E-04	7	-	7.0
Ra-223	3.129E-02	2.243E-14	-	-	NA1
Ra-224	1.002E-02	1.099E-12	-	-	NA1
Ra-225	4.079E-02	2.460E-14	-	-	NA1
Ra-226	1.600E+03	2.354E-12	55	-	55
Ra-228	5.750	8.370E-13	-	-	NA1
Rn-222	1.047E-02	1.541E-17	-	-	NA1
Sb-126	3.381E-02	2.462E-12	-	-	NA1
Se-79	2.950E+05	1.762E-05	7	-	7.0
Sn-126	2.300E+05	5.182E-05	7	-	7.0
Th-227	5.114E-02	3.620E-14	-	-	NA1
Th-228	1.912	2.097E-10	-	-	NA1
Th-229	7.340E+03	4.783E-09	20	-	20
Th-230	7.538E+04	1.636E-08	55	-	55

Nuclide	Half-life* [a]	Inventory [moles/kgU initial]	σ_{OR} [%]	σ_{PR} [%]	σ_{Total} [%]
Th-231	2.911E-03	2.944E-14	-	-	NA1
Th-232	1.405E+10	2.095E-03	4	-	4
Th-234	6.598E-02	6.091E-11	-	-	NA1
U-233	1.592E+05	3.608E-05	20	-	20
U-234	2.455E+05	2.089E-04	50	-	50
U-235	7.038E+08	7.238E-03	2.5	-	2.5
U-236	2.342E+07	3.501E-03	4	-	4
U-238	4.468E+09	4.125E+00	0	-	0

Notes:

NA1 = Nuclide assigned a constant inventory because it has a short half-life.

NA2 = Nuclide inventory is assigned a uniform distribution. For C-14, the inventory is between 2.45×10^{-6} and 8.75×10^{-6} moles/kgU and for Cl-36 the inventory is between 9.86×10^{-7} and 9.86×10^{-6} moles/kgU. Table shows the median value, which is not from Tait et al. (2000).

NA3 = Nuclide assigned a constant inventory because it is formed by activation of impurity in the fuel, and impurity levels were assigned high values in Tait et al. (2000).

*Half-life from ENDF/B VII.1 (Chadwick et al. 2011) and converted as required using $365.25 \text{ days} = 1 \text{ year}$.

Table 3-5: ORIGEN-S: Pickering Fuel Inventory Comparison

Isotope	Measured¹ (Bq/kgU)	ORIGEN-S (Bq/kg U)	Ratio (meas/calc)
Cm-244	7.12E+08 ± 15%	7.44E+08	0.96 ± 0.14
Am-241	1.86E+10 ± 20%	1.92E+10	0.97 ± 0.19
Np-237	1.00E+05 ± 20%	8.51E+05	1.17 ± 0.23
H-3	2.07E+09 ± 7%	2.23E+09	0.92 ± 0.06
Sr-90	4.86E+11 ± 4%	5.03E+11	0.97 ± 0.04
Tc-99	1.08E+08 ± 10%	1.50E+08	0.72 ± 0.07
Ru-106	8.72E+07 ± 5%	2.52E+08	0.35 ± 0.02
Sb-125	2.20E+09 ± 18%	2.56E+09	0.86 ± 0.16
I-129	2.44E+05	3.62E+05	0.67
Cs-134	4.16E+09 ± 7%	4.03E+09	1.03 ± 0.07
Cs-137	8.05E+11 ± 5%	7.88E+11	1.02 ± 0.05
Eu-154	8.14E+09 ± 5%	9.07E+09	0.90 ± 0.04
Eu-155	3.35E+09 ± 8%	3.13E+09	1.07 ± 0.09
Isotope	Measured (g/kg U)	ORIGEN-S (g/kg U)	Ratio (meas/calc)
U-233	< 0.01	2.22E-07	--
U-234	0.0339 ± 55%	0.0423	0.8 ± 0.44
U-235	1.64 ± 2.4%	1.64	1.00 ± 0.02
U-236	0.802 ± 3.7%	0.813	0.99 ± 0.04
U-238	983.5 ± 0.01%	983.5	1.00 ± 0.0
Pu-238	0.0058 ± 5.6%	0.0053	1.10 ± 0.06
Pu-239	2.69 ± 2.5%	2.72	0.99 ± 0.03
Pu-240	1.22 ± 37%	1.25	0.98 ± 0.04
Pu-241	0.134 ± 9%	0.142	0.95 ± 0.09
Pu-242	0.094 ± 6.8%	0.0972	0.97 ± 0.07

Notes:

From Tait et al. (1995), Pickering fuel bundle with average burnup of 221 MWh/kgU and average outer-element linear power of 43 kW/m.

¹ Analytical uncertainty expressed as a percentage.

Table 3-6: Inventories of Chemical Elements of Interest in UO₂ Fuel for 220 MWh/kgU Burnup and 30 Years Decay Time

Element	Main Source ¹	Inventory [moles/kgU initial]	σ_{OR} [%]	σ_{PR} [%]	σ_{Total} ² [%]
Ag	FP	3.348E-4	7	-	7.0
As	Imp	4.024E-5	-	-	NA1
Cd	FP	1.928E-4	7	-	7.0
Ce	FP	4.766E-3	7	-	7.0
Co	Imp	3.099E-4	-	-	NA1
Cr	Imp	9.635E-4	-	-	NA1
Eu	FP	1.895E-4	6.5	-	6.5
Hg	Imp	6.719E-6	-	-	NA1
I	FP	5.372E-4	7	-	7.0
La	FP	2.459E-3	7	-	7.0
Nd	FP	7.562E-3	7	-	7.0
P	Imp	1.935E-3	-	-	NA1
Pb	Imp	4.824E-4	-	-	NA1
Pr	FP	2.181E-3	7	-	7.0
Te	FP	1.048E-3	7	-	7.0
Y	FP	1.327E-3	7	-	7.0

Notes:

¹ Source of chemical element in fuel is either fission product (FP) or impurity in fuel (Imp).² NA1 = Nuclide assigned a constant inventory because it is formed by activation of impurity in the fuel, and impurity levels were assigned high values in Tait et al. (2000).

3.3 References for Chapter 3

- Chadwick, M.B., M. Herman, P. Obložinský, M.E. Dunn, Y. Danon, A.C. Kahler, D.L. Smith, B. Pritychenko, G. Arbanas, R. Arcilla, R. Brewer, D.A. Brown, R. Capote, A.D. Carlson, Y.S. Cho, H. Derrien, K. Guber, G.M. Hale, S. Hoblit, S. Holloway, T.D. Johnson, T. Kawano, B.C. Kiedrowski, H. Kim, S. Kunieda, N.M. Larson, L. Leal, J.P. Lestone, R.C. Little, E.A. McCutchan, R.E. MacFarlane, M. MacInnes, C.M. Mattoon, R.D. McKnight, S.F. Mughabghab, G.P.A. Nobre, G. Palmiotti, A. Palumbo, M.T. Pigni, V.G. Pronyaev, R.O. Sayer, A.A. Sonzogni, N.C. Summers, P. Talou, I.J. Thompson, A. Trkov, R.L. Vogt, S.C. van der Marck, A. Wallner, M.C. White, D. Wiarda, P.G. Young. 2011. ENDF/B-VII.1 Nuclear data for science and technology: Cross Section, Covariances, Fission Product Yields, and Decay Data. *Nuclear Data Sheets*: 112-12, 2887-2996 (2011).
- Freire-Canosa, J. 2011. Used Fuel Integrity Program: Summary Report. Nuclear Waste Management Organization Report NWMO TR-2011-04. Toronto, Canada.
- Garamszeghy, M. 2011. Nuclear Fuel Waste Projections in Canada - 2011 Update. Nuclear Waste Management Organization Report NWMO TR-2011-25. Toronto, Canada.
- Garisto, F., M. Gobien, E. Kremer and C. Medri. 2012. Fourth Case Study: Reference Data and Codes. Nuclear Waste Management Organization Report NWMO TR-2012-08. Toronto, Canada.
- Hastings, I.J. 1982. Structures in Irradiated UO₂ Fuel from Canadian Reactors. Atomic Energy of Canada Limited Report AECL-MISC-249. Chalk River, Canada.
- Kleykamp, H. 1985. The chemical state of the fission products in oxide fuels. *Journal of Nuclear Materials* 131, 221-246.
- Novak, J. and I.J. Hastings. 1991. Ontario Hydro Experience with Extended Burnup Power Reactor Fuel. Atomic Energy of Canada Limited Report AECL-10388. Chalk River, Canada.
- SKB. 2010. Spent Nuclear Fuel for Disposal in the KBS-3 Repository. Swedish Nuclear Fuel and Waste Management Company Report SKB TR-10-13. Stockholm, Sweden.
- Tait, J.C., I.C. Gauld and A.H. Kerr. 1995. Validation of the ORIGEN-S code for predicting radionuclide inventories in used CANDU fuel. *Journal of Nuclear Materials* 223, p. 109-121.
- Tait, J.C., H. Roman and C.A. Morrison. 2000. Characteristics and Radionuclide Inventories of Used Fuel from OPG Nuclear Generating Stations, Volumes 1 and 2. Ontario Power Generation Report 06819-REP-01200-10029. Toronto, Canada.
- Truant, P.T. 1983. CANDU Fuel Performance: Power Reactor Experience. Atomic Energy of Canada Limited Report AECL-MISC-250, Rev. 1. Chalk River, Canada.
- Wilk, L. and G. Cantello. 2006. Used Fuel Burnups and Power Ratings for OPG Owned Used Fuel. Ontario Power Generation Report 06819-REP-01300-10121. Toronto, Canada.

THIS PAGE HAS BEEN LEFT BLANK INTENTIONALLY

4. REPOSITORY FACILITY – CONCEPTUAL DESIGN

4.1 General Description

The APM facility is a self-contained complex that includes an underground repository for used CANDU fuel and a number of surface facilities designed to support the construction and operation of the repository. The primary function of the surface facilities is to receive used fuel that is shipped from reactor-site storage facilities, place it in durable used fuel containers and transfer the containers to the underground repository. The reference used fuel container is designed with a corrosion-resistant copper barrier and an inner supporting steel vessel to provide long-term containment of the fuel in the repository (SNC-Lavalin 2011a).

A repository site has not been selected, but the assumptions made for development of the site model reflect the properties of crystalline rock found in the Canadian Shield. Therefore, a generic repository design is described here for the purpose of preparing an illustrative postclosure safety assessment for a hypothetical APM facility in crystalline rock. Two key safety concepts on which the repository design is based are the multiple barrier system for containment of the fuel, and passive safety. In this case, passive safety means that once the operational phase is complete and the repository is backfilled and sealed, no further actions are needed to ensure its safety.

For the purpose of this study, the repository is assumed to be constructed in crystalline rock at a depth of 500 m. In the repository the used fuel containers will be surrounded by engineered, clay-based sealing materials that will provide protection against mechanical, chemical and biological agents that could cause container damage. The function of the repository engineered barriers also includes creating both a chemical and physical environment that would limit the mobility of contaminants under the conditions of postulated scenarios that deviate from the expected, normal evolution of the repository.

The used fuel container, the sealing systems surrounding the container and the rock mass in which the repository is constructed provide multiple protective barriers that are capable of containing and isolating the used fuel indefinitely.

The underground repository consists of several panels of used fuel containers in placement rooms, which are connected to the surface via a network of access tunnels and three vertical shafts. The containers are placed in vertical boreholes drilled into the floor along the axis of the placement room.

An illustration of an APM facility in crystalline rock is shown in Figure 4-1.

Monitoring systems for verification of safety performance are provided as part of the repository system design. Retrieval of the fuel containers is another design feature of the APM repository. These two capabilities of the repository design are discussed further in reports by SNC-Lavalin (2011a) and Villagran (2012).

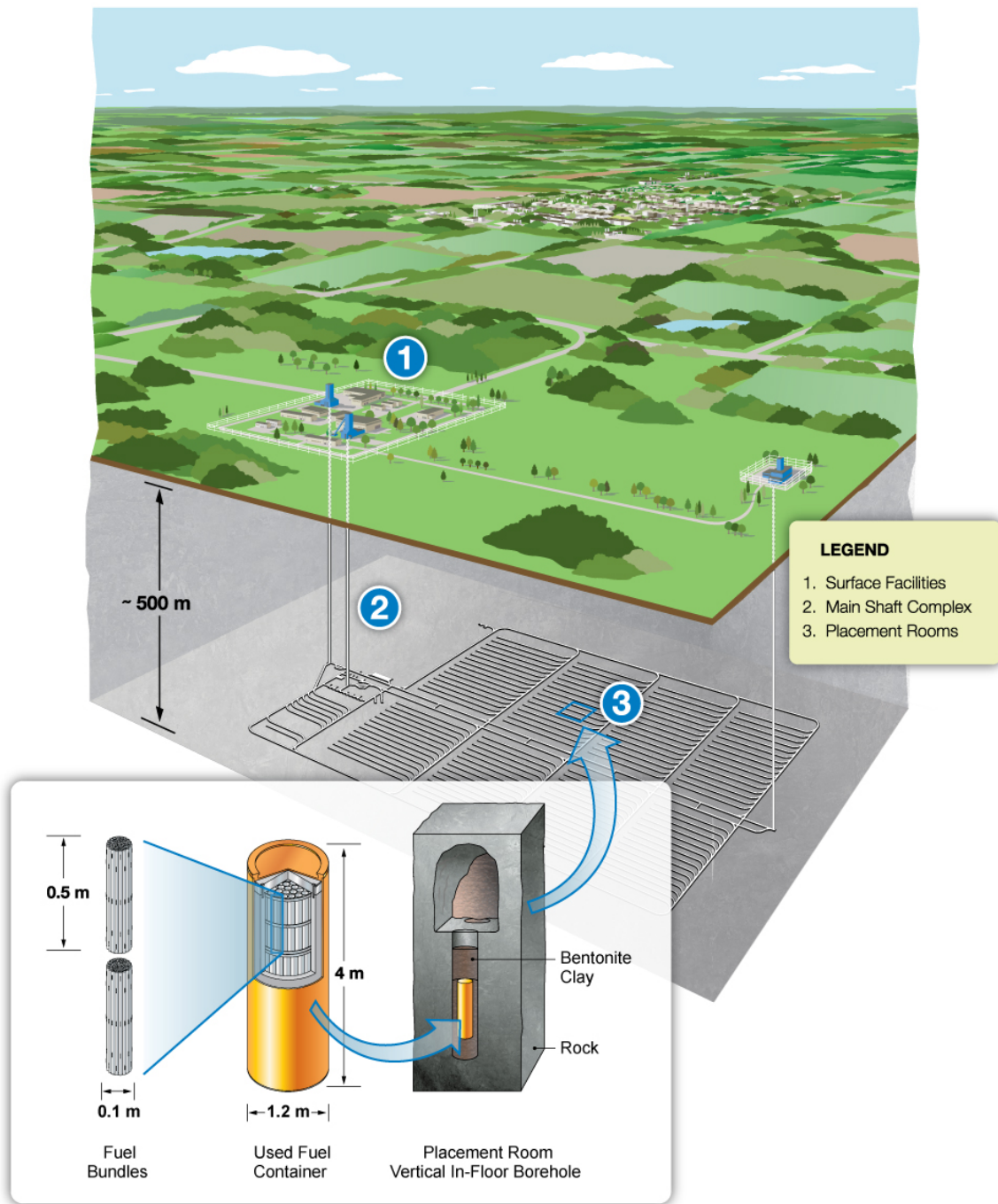


Figure 4-1: Illustration of an APM Facility in Crystalline Rock

4.2 Surface Facilities

The APM facility requires a dedicated surface area of about 600 m by 550 m for the surface buildings and about 100 m by 100 m for the ventilation exhaust shaft located about 2 kilometres from the main facility. The APM facility also requires an off-site storage area of about 700 m by 700 m for the excavated rock; its location would be selected in consultation with the community and surrounding region. The surface water run-off from the excavated rock will be monitored and appropriate effluent control procedures will be implemented based on the monitoring results.

The site layout is shown in Figure 4-2; individual buildings and other surface facilities are listed Table 4-1. The site is surrounded by a perimeter fence; and the facilities within this perimeter are arranged into two areas:

- a) the Protected Area, which is a high-security zone; and
- b) the Balance of Site, a zone which includes facilities that do not require high security.

The main facilities included in the Protected Area are the Used Fuel Packaging Plant (UFPP), the main shaft and service shaft buildings as well as the auxiliary building, quality control offices, laboratory, radioactive waste handling facilities, switchyard, transformer area and powerhouse. All activities pertaining to handling and storage of used nuclear fuel are conducted in the UFPP. A detailed description of the UFPP and its operation is given in Section 4.4.

The Balance of Site zone includes the administration building, the fire hall, the ventilation shaft building, as well as ancillary facilities such as the cafeteria, garage, warehouse, water and sewage treatment plants, and helicopter pad. Fuel and water storage tanks and an air compressor building are also found in the Balance of Site, as well as the aggregate plant, concrete batch plant and the sealing materials compaction plant.

The aggregate plant will produce material for the concrete batching plant and sealing materials compaction plant. The concrete batching plant will produce the concrete mixes required for specific functions in the repository, including the low-heat, high-performance (LHHP) concrete required for the bulkheads to be placed at entrance of the filled container placement rooms and for other repository seals. At the sealing materials compaction plant, raw materials from the aggregate plant and externally sourced lake clay and bentonite will be mixed to produce dense backfill blocks, light backfill, compacted bentonite blocks and gap-fill material required for used fuel container placement and for sealing of the placement rooms.

A number of other support buildings and structures including offices, laboratory facilities and the common services required in a self-sufficient industrial site are also included in the site; a complete list is given in Table 4-1.

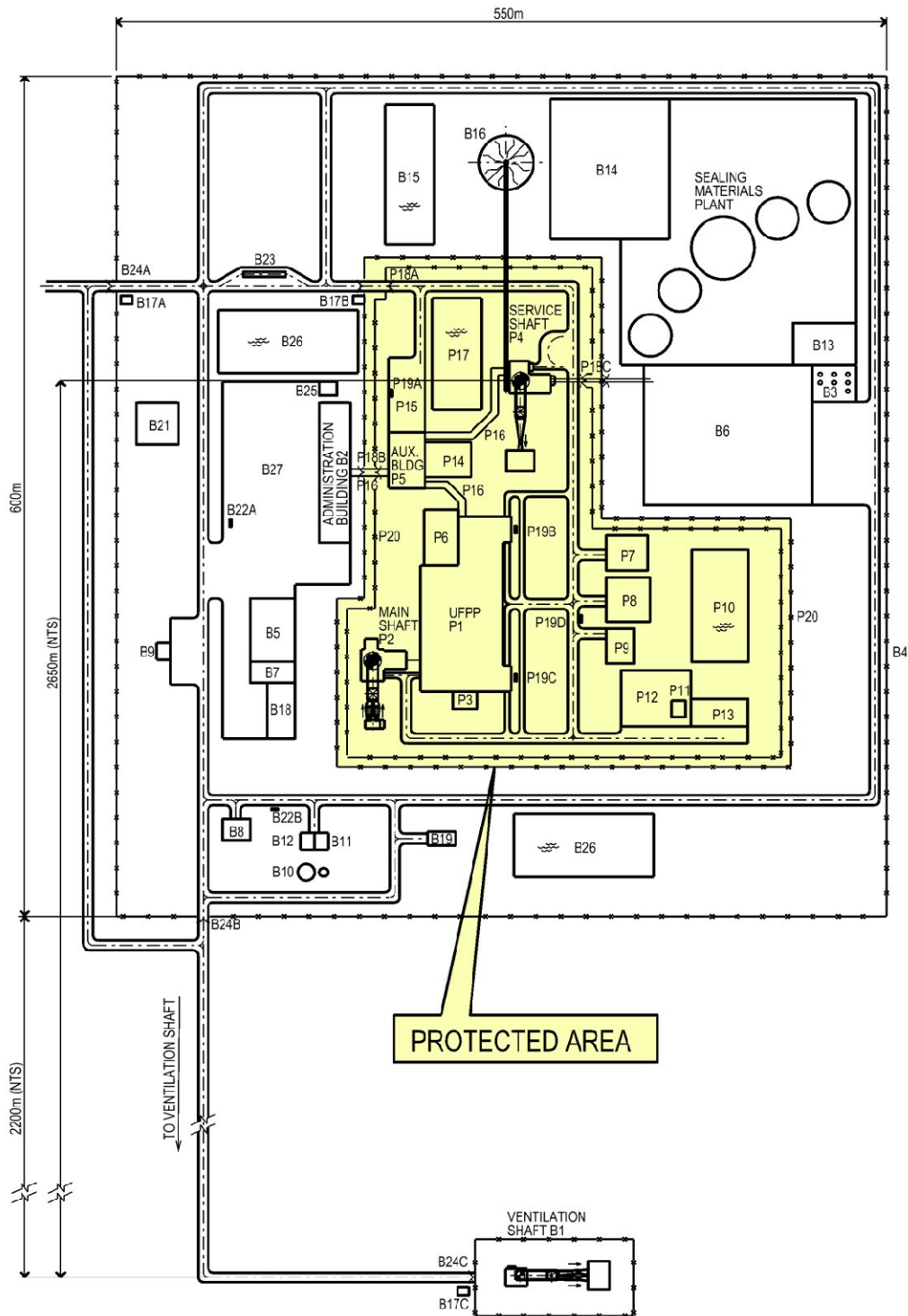


Figure 4-2: APM Surface Facilities Layout

Table 4-1: APM Facility Number and Description

Area	Protected Area	Area	Balance of Site
P1	Used Fuel Packaging Plant	B1	Ventilation Shaft Complex
P2	Main Shaft Complex	B2	Administration Building including Firehall and Cafeteria
P3	Stack	B3	Sealing Material Storage Bins
P4	Service Shaft Complex	B4	Perimeter Fence
P5	Auxiliary Building	B5	Garage
P6	Active Solid Waste Handling Facility	B6	Sealing Materials Compaction Plant
P7	Waste Management Area	B7	Warehouse and Hazardous Materials Storage Building
P8	Active Liquid Waste Treatment Building	B8	Air Compressor Building
P9	Low-Level Liquid Waste Storage Area	B9	Fuel Storage Tanks
P10	Stormwater Retention Pond	B10	Water Storage Tanks
P11	Switchyard	B11	Water Treatment Plant
P12	Transformer Area	B12	Pump House
P13	Powerhouse	B13	Concrete Batch Plant
P14	Quality Control Offices and Laboratory	B14	Aggregate (Rock Crushing) Plant
P15	Parking Area	B15	Process Water Settling Pond
P16	Covered Corridor / Pedestrian Routes	B16	Waste Rock Stockpile
P17	Mine Dewatering Settling Pond	B17	Guardhouse
P18	Security Checkpoint	B18	Storage Yard
P19	Bus Shelters	B19	Sewage Treatment Plant
P20	Double Security Fence	B20	Not Used
		B21	Helicopter Pad
		B22	Bus Shelters
		B23	Weigh Scale
		B24	Security Checkpoints
		B25	Security Monitoring Room
		B26	Storm water Retention Ponds
		B27	Parking Area

4.3 Used Fuel Container

The reference used fuel container design used for this study is the IV-25 copper container. It consists essentially of two vessels: an inner carbon-steel vessel that provides the required mechanical strength and outer copper vessel that provides a durable corrosion barrier. The capacity of the IV-25 copper container is 360 used CANDU fuel bundles for a fuel mass of 8,640 kg. The inner vessel wall thickness is 100 mm and it is designed to sustain a maximum external isotropic pressure of 45 MPa, which is a conservative estimate of the maximum loads the container would experience in the repository during a glaciation cycle, as a result of a 3 km thick ice sheet above the repository site.

The IV-25 container has been designed with a 25 mm thick outer copper shell for corrosion, fabrication and handling purposes. Under repository conditions, corrosion of the copper barrier is predicted to be less than 2 mm over a period of one million years (Kwong 2011), which is approximately the time required for the radioactivity of the used CANDU fuel to decay to levels comparable those of natural uranium deposits.

The used fuel bundles are arranged inside the container in six layers of 60 bundles each. They are loaded into the container in three baskets each holding two layers of 60 fuel bundles. An example of the container and basket are illustrated in Figure 4-3. The design parameters of the copper and the steel vessels are given in Table 4-2 and Table 4-3, respectively. The total mass of a loaded used fuel container is about 26,700 kg.

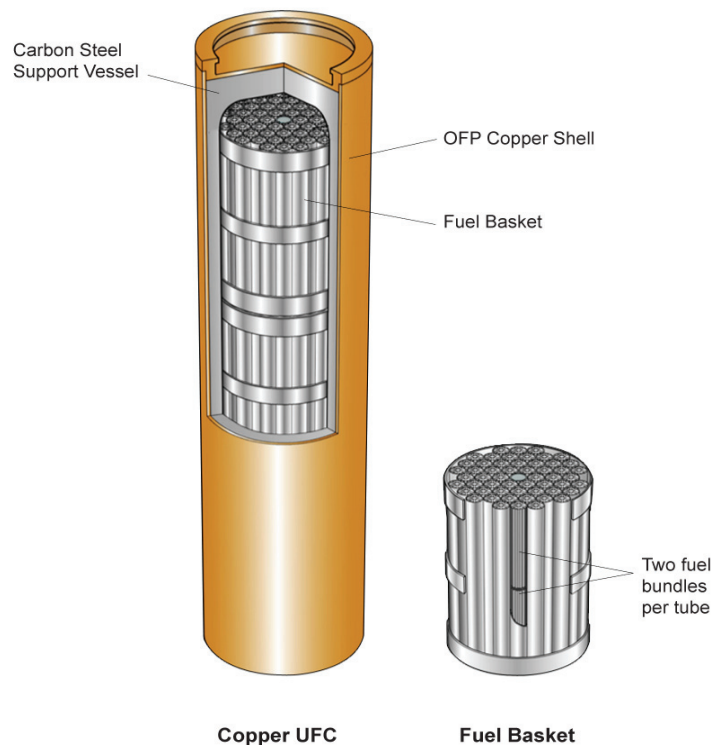


Figure 4-3: Copper Used-fuel Container and Fuel Basket

Table 4-2: Reference Copper Vessel Parameters

IV-25 Outer Copper Vessel	
Material	Oxygen-free, phosphorus-doped, high purity copper
Height	3,842 mm
Outside diameter	1,247 mm
Thickness (minimum)	25 mm
Mass of copper vessel	4,170 kg

Table 4-3: Reference Steel Vessel Parameters

IV-25 Inner Steel Vessel	
Material	ASTM ¹ A516 Gr 70 steel
Height	3,700 mm
Outside diameter	1,195 mm
Thickness (minimum)	102.5 mm
Mass of steel vessel	12,650 kg
Mass of 3 fuel baskets	1,240 kg

4.4 Used Fuel Packaging Plant

The Used Fuel Packaging Plant (UFPP) is a multi-storey building designed to receive the used fuel shipped from interim storage facilities, transfer the fuel bundles into long-lived used fuel containers, seal and inspect the containers for subsequent transfer to the underground repository. The UFPP concrete structure contains a number of cells where specialized operations requiring shielding and containment capability are conducted. The plant conceptual design is illustrated in a cross-section and two layout plans inserted towards the end of this section. These drawings are useful to visualize both the fuel handling operations and the loading and processing of used fuel containers.

¹ American Society for Testing and Materials.

The used fuel containers are assumed to be manufactured at a dedicated plant, separate from the APM facility and shipped to the UFPP, where they will be received at the receiving hall for empty used fuel containers. The used nuclear fuel is assumed to be shipped from interim storage facilities at the reactor sites in an irradiated fuel transport cask (IFTC).

The reference IFTC transportation package has a capacity of 192 fuel bundles, held in two used fuel storage modules containing 96 bundles each (SNC-Lavalin 2011b). The casks are received at the dedicated IFTC receiving and shipping hall. The process for transferring the used fuel from transport casks and placing it into used fuel containers consists of several major steps:

1. Receiving, unloading, decontamination and return of the IFTC;
2. Moving the received used fuel storage modules to the module handling cell and then to the fuel handling cell or, alternatively, placing them in a module storage pool;
3. Receiving and preparing new used fuel containers for loading;
4. Transferring the used fuel bundles from fuel storage modules to used fuel baskets;
5. Loading the fuel baskets into new used fuel containers;
6. Sealing and machining the container closure seal;
7. Inspecting the quality of the container closure seal; and
8. Placing used fuel container in a shielded transfer cask for transfer to the underground repository.

These operations and the associated features of the UFPP are described in the following sub-sections of this report.

4.4.1 Transport Cask Receiving and Unloading

The transport cask receiving and shipping hall is a dedicated area for transport cask handling and temporary storage, provided with an overhead crane, which is used initially used to unload the cask from the transport vehicle. Subsequently the transport cask impact limiter is removed and the cask is placed on a transfer pallet, which will move the cask along one of two processing lines. These two processing lines are identical and allow parallel unloading of casks and transfer of the used fuel storage modules either directly to the fuel handling cell or into a wet storage pool.

Transfer pallets that move on rails are used to move the transport casks from the cask receiving and shipping hall to a cask vent cell, and then to a docking position below the module handling cell (Figure 4-10 through to Figure 4-12). The transfer pallets are equipped with a scissors lift that enables the cask to be raised and docked at the module handling cell port.

The cask vent cell permits safe removal of the lid bolts and venting of the transport casks in a containment space. The vent cells are used also during dispatch of empty casks for replacing and fastening lid bolts, pressure testing lid seals and monitoring the cask surface for contamination. If necessary the transport casks can be decontaminated at the cask vent cell.

4.4.2 Module Handling Cells

From the vent cell the transport cask is moved to a cask docking cell, where it is connected to one of the two, parallel module handling cells. Once docked, the cask lid is removed and placed on the cell floor. The module handling cells provide the required radiation shielding and

containment to safely unload the fuel storage modules from the transport cask. The cells are equipped with lead glass windows and remotely-operated manipulators.

An overhead crane is used in each module handling cell for lifting and transferring modules between different positions in the cell. A module drying booth is also included in the fuel processing line to permit drying of the used fuel before it is transferred to the fuel handling cell. Alternatively, a fuel storage module in either of the two module handling cells can be moved into a module storage pool for interim storage before processing. The module storage pool provides buffer storage so that the fuel transfer and container loading operations can proceed without interruption.

4.4.3 Empty Used Fuel Container Receiving

Receiving and storage of new, empty used fuel containers takes place in a dedicated receiving hall located at ground floor level, that includes storage positions for 40 empty used fuel containers and 126 new, empty fuel baskets. The receiving hall has its own dedicated truck bay for unloading the new used fuel containers arriving at the UFPP.

The hall is equipped with a 30 tonne crane and a used fuel container preparation platform. The platform contains two parallel positions for inspection, installation of used fuel containers into sleeves, required to load the used fuel container into a shielded frame. Adjacent to the preparation platform are eight storage positions for sleeves, eight positions for empty baskets and four positions for pallets with empty used fuel containers in sleeves. The pallets are moved within the hall using an air-cushion transporter. Three new used fuel baskets are placed inside each fuel container prior to placing it in its docking position under the Fuel Handling Cell port.

4.4.4 Used Fuel Container Transport within the Plant

Both empty and full used fuel containers are moved in a Shielded Frame consisting essentially of a steel frame holding two telescopic, cylindrical shields vertically mounted on a steel platform. The bottom shield section can be raised and lowered by screw jacks, enabling a used fuel container to be raised and docked at the processing stations docking ports.

The top section is equipped with a gamma gate and is designed for airtight docking to the container ports at the used fuel container loading and processing stations. The shielded frame provides the required radiation shielding and effective isolation of the Fuel Handling Cell and the container processing stations from the used fuel container transfer area.

The shielded frames are moved between stations using an air-cushion transporter. The air-cushion transporter is equipped with steering wheels that remain in contact with the floor while the transporter is in the raised position, and can be controlled both manually and remotely. This technology is routinely used in industry as a safe and efficient means of moving heavy equipment. A shielded frame on an air-cushion transporter being used at SKB's Canister Laboratory in Sweden is shown in Figure 4-4.



© SKB International AB 2010

Figure 4-4: Shielded Frame and Air-cushion Transporter

Using air-cushion technology for moving the shielded frames allows the containers to be transported independently of each other and allows simultaneous, independent operation of all the processing stations. Other operational advantages of this used fuel container transport method include easy maintenance and faster recovery from equipment failure, minimizing the risk of production stops.

4.4.5 Fuel Handling Operations

The fuel handling cell is a shielded containment cell used for transferring used fuel bundles from storage modules into fuel baskets and for loading the filled fuel baskets into used fuel containers. To fulfill these tasks the cell is equipped with three fuel handling machines, lead glass windows, remote manipulators and vacuum cleaners. All equipment in the fuel handling cell is remotely operated. To enable loading of filled baskets into a container, the fuel handling cell has a docking port that connects it to the used fuel container transfer area.

During the fuel transfer operation from a module to a basket, the fuel bundle serial number is recorded for safeguard purposes. Damaged bundles can be placed in cans and/or loaded into baskets specially designed to accommodate damaged fuel.

The cell is also equipped with a crane for lifting used fuel modules and baskets. Within the cell, there are four positions for the temporary storage of modules, and one position for parking the containment door and inner vessel lid. The cell also has a dedicated area for the temporary storage of 12 filled or empty baskets. In the floor of the fuel handling cell, there is a port with a gamma gate leading to a waste management facility, which includes provisions for the decontamination and compaction of empty fuel storage modules.

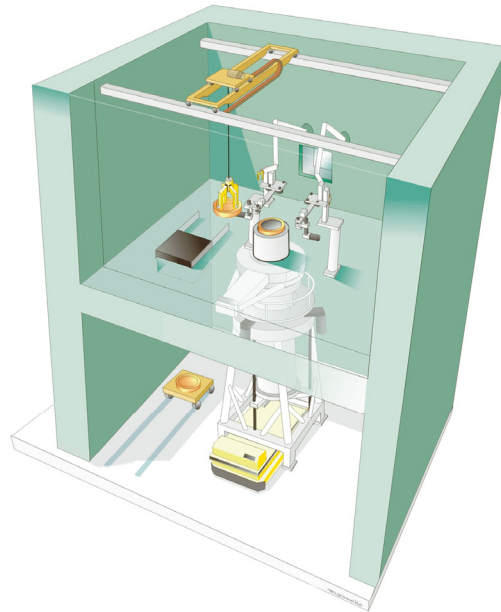
4.4.6 Used Fuel Container Processing

Once three fuel baskets are loaded into the used fuel container, the container inner lid is bolted on and the container is moved to other processing stations where a sequence of operations takes place to seal and test the container prior to its transfer to the underground repository. These operations, which take place at four separate processing stations, include backfilling the container with an inert gas, welding of the outer copper lid, machining the weld surface and non-destructive testing (NDT) of the weld. These processing stations are described below.

4.4.6.1 Inerting Station

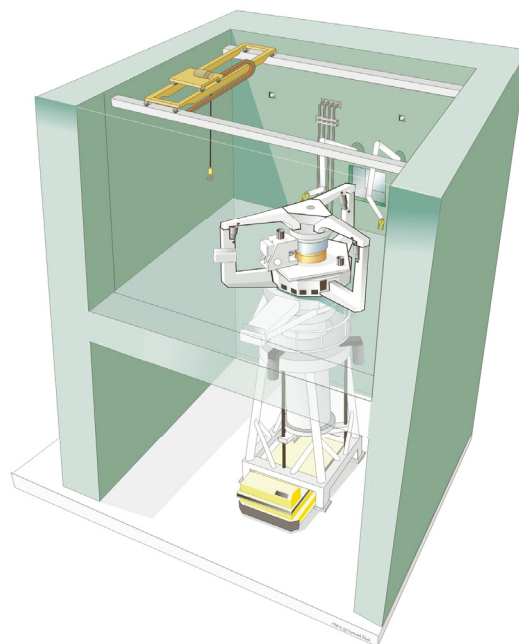
The inerting station is a radiation shielded cell that contains provisions for remotely bolting the inner vessel lid to the inner steel vessel. The station also houses equipment for removing the air contained in the inner vessel and backfilling the volume with an inert gas. This process is done via a valve in the inner vessel lid that can also be used for testing the leak-tightness of the lid. Containers are docked to the station in the same manner as described for the fuel handling cell. The inerting station is also equipped with a hatch and a crane for importing and moving container lids and any required equipment. Figure 4-5 shows a conceptual illustration of the inerting station.

After its inner volume is backfilled with an inert gas the container is moved to the welding station, illustrated in Figure 4-6, which has the required equipment for placing the copper lid on the container and welding it to the copper shell.



© SKB International AB 2010.

Figure 4-5: Inerting Station



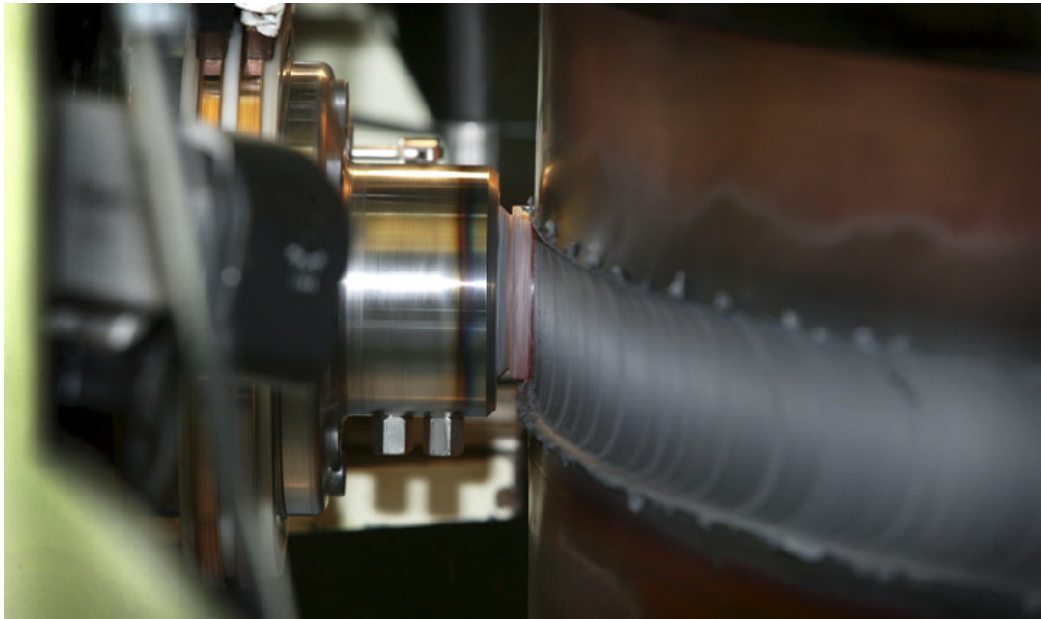
© SKB International AB 2010.

Figure 4-6: Welding Station

4.4.6.2 Welding Station

The selected method for welding the container copper lid to the container is Friction-Stir Welding (FSW). This method was originally developed for various industrial applications by The Welding Institute (TWI) in the United Kingdom, and adapted to this specific use by SKB. The process essentially consists of inserting a rotating metal tool in the lid-body joint at a perpendicular angle to the container surface and moving the tool along the circumference of the joint (Figure 4-7). The rotation of the welding tool around its own axis generates heat that effectively joins the lid and body of the container without melting of the metal. To execute this operation the container is held in a fixed position while the welding head assembly rotates around the container axis.

FSW has been extensively tested at SKB's Canister Laboratory and selected as the reference welding method for the Swedish spent fuel canisters after a thorough comparison with Electron-Beam Welding (EBW). FSW was found to be a more reliable process resulting in more uniform weld quality, and the properties of the resulting weld material were very close to those of the original OFP copper material. The FSW development program and the assessment results are documented in SKB 2007 and SKB 2008.



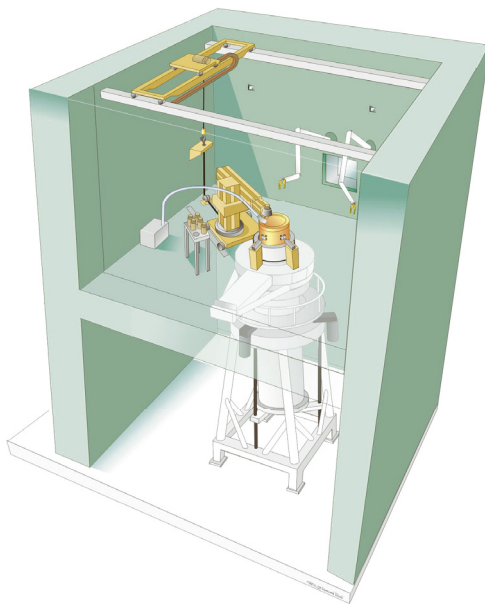
© SKB International AB 2010

Figure 4-7: Friction Stir Welding of a Copper Lid

4.4.6.3 Machining and NDT Stations

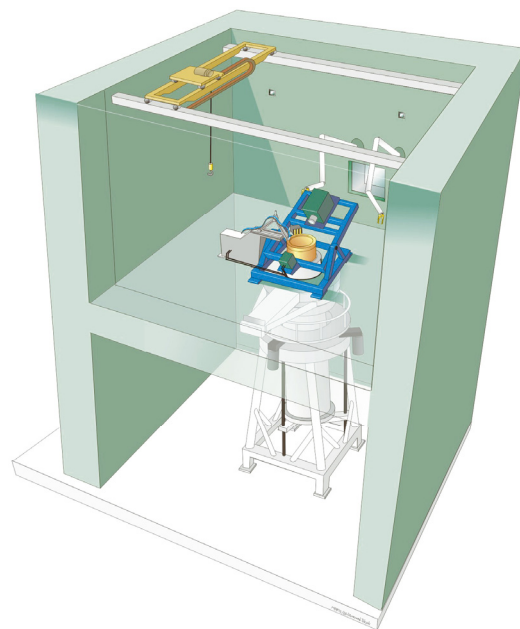
Following welding of the copper lid, the used fuel container is moved to a station where the weld surface is machined to achieve a finish similar to that of the rest of the container surface. This is required to ensure that the weld surface has a corrosion behaviour consistent with the rest of the copper shell as well as to facilitate non-destructive testing of the weld.

During machining, the equipment is rotated and the used fuel container is held in a fixed position (see Figure 4-8). The docking arrangements in the machining station are similar to those in the welding station. After this operation the container is moved to the non-destructive testing station, which contains equipment to conduct a minimum of two NDT examinations of the weld (see Figure 4-9). Two methods being considered are radiography (tomography) and ultrasonic testing. High-energy X-ray sources with very small focal spots and fast detectors with good time and spatial resolution allow the construction of good 3-D images in practical times. These weld examination methods are currently being assessed by Posiva (Finland) and SKB (Sweden), whose spent fuel container designs include a thick copper shell as corrosion barrier.



© SKB International AB 2010

Figure 4-8: Machining Station



© SKB International AB 2010

Figure 4-9: Non-destructive Testing Station

Both the stereoscopic radiographic method and ultrasound appear to provide satisfactory results (Sandlin 2010a, 2010b, 2010c). The stereographic radiography method has some limitations for detection of thin, planar defects; in this case ultrasonic testing is used to overcome the radiographic method limitations. Further tests on a larger sample of welds will be needed to achieve the required level of precision. Posiva is continuing work in the testing of container welds (Pitkanen 2010).

For design purposes, it is assumed that one out of 100 containers do not meet the specified quality requirements during non-destructive testing in the UFPP (SNC-Lavalin 2011a).

For postclosure safety assessment, it is assumed that one out of 5,000 containers have undetected defects based on a review of failure statistics for analogous nuclear components (Maak et al. 2001). This assumption is considered to be reasonable for safety assessment purposes, although a lower failure probability could likely be achieved.

Recently, an International Review Team was established by the Nuclear Energy Agency (NEA) to review SKB's postclosure safety case for a used fuel repository in Sweden (NEA 2012). The review was conducted by the NEA Secretariat on behalf of the Swedish Government. The International Review Team reviewed the methods developed by SKB for non-destructive testing of the container and the weld, and concluded that those methods have been verified to be able to detect inconsistencies and failures below the design limits of the safety case.

4.4.6.4 Handling of Defective Containers

Upon detecting a defect in a sealed used fuel container, the container processing at the UFPP is stopped and two separate actions are taken:

- I. The cause for the weld defects is investigated and resolved before loading and processing of new containers is allowed to proceed; and
- II. The defective container is opened, the loaded fuel baskets retrieved and the container is decontaminated and returned to the container factory for recycling of the materials.

To implement this second action, the container with the defective weld is moved from the NDT station the back to the machining station where the container weld is cut. Subsequently the copper lid is removed and the container is docked at the module handling cell where the three fuel baskets are extracted from the container, then both the lid and the container body are decontaminated and returned to the container factory for recycling.

After the cause for the weld defect is identified and the problem corrected, used fuel container processing is allowed to resume.

4.4.7 Filled Used Fuel Container Storage Cell

At the end of the used fuel container processing area opposite to the module handling cell there is a shielded area where full used fuel containers can be monitored and placed in temporary storage. This cell has 40 storage positions and is located above the container transfer area; it is equipped with four ports and a 30 tonne overhead crane capable of handling both empty and full used fuel containers.

Containers that have been successfully loaded, welded and inspected are then brought to an entrance port dedicated to the import/export of full containers. After a container is brought into the storage area it is either placed in a storage spot or monitored, decontaminated if required, and then transferred to the filled container dispatch cell. Containers requiring decontamination can be lowered using the overhead crane into a decontamination cell located below the floor level of the storage area.

4.4.8 Used Fuel Container Dispatch Hall

Adjacent to the loaded used fuel container storage cell is a dispatch hall, where the filled used fuel containers are placed into a shielded transfer cask for transfer to the repository. In the dispatch hall there is an airlock for the transfer casks arriving and departing on a rail wagon.

The used fuel container dispatch hall is equipped with an 80 tonne overhead crane and a working platform for inspection and cask preparation operations. The hall is also equipped with an air-cushion transporter and pallet for the transfer of a cask between the working platform and the filled used fuel container dispatch hall (see Figure 4-10 and Figure 4-12).

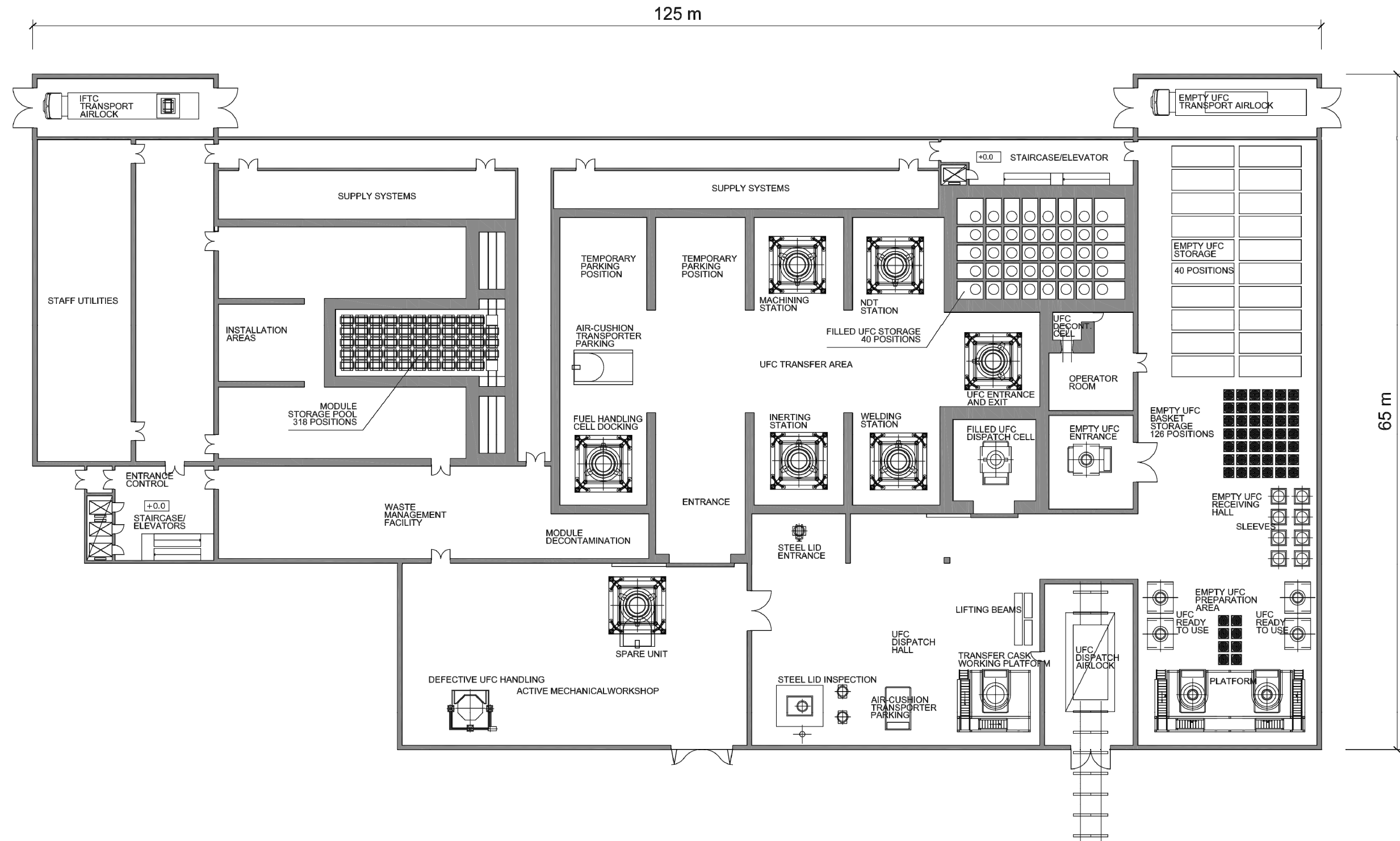


Figure 4-10: Used Fuel Packaging Plant – Container Transfer Level

THIS PAGE HAS BEEN LEFT BLANK INTENTIONALLY

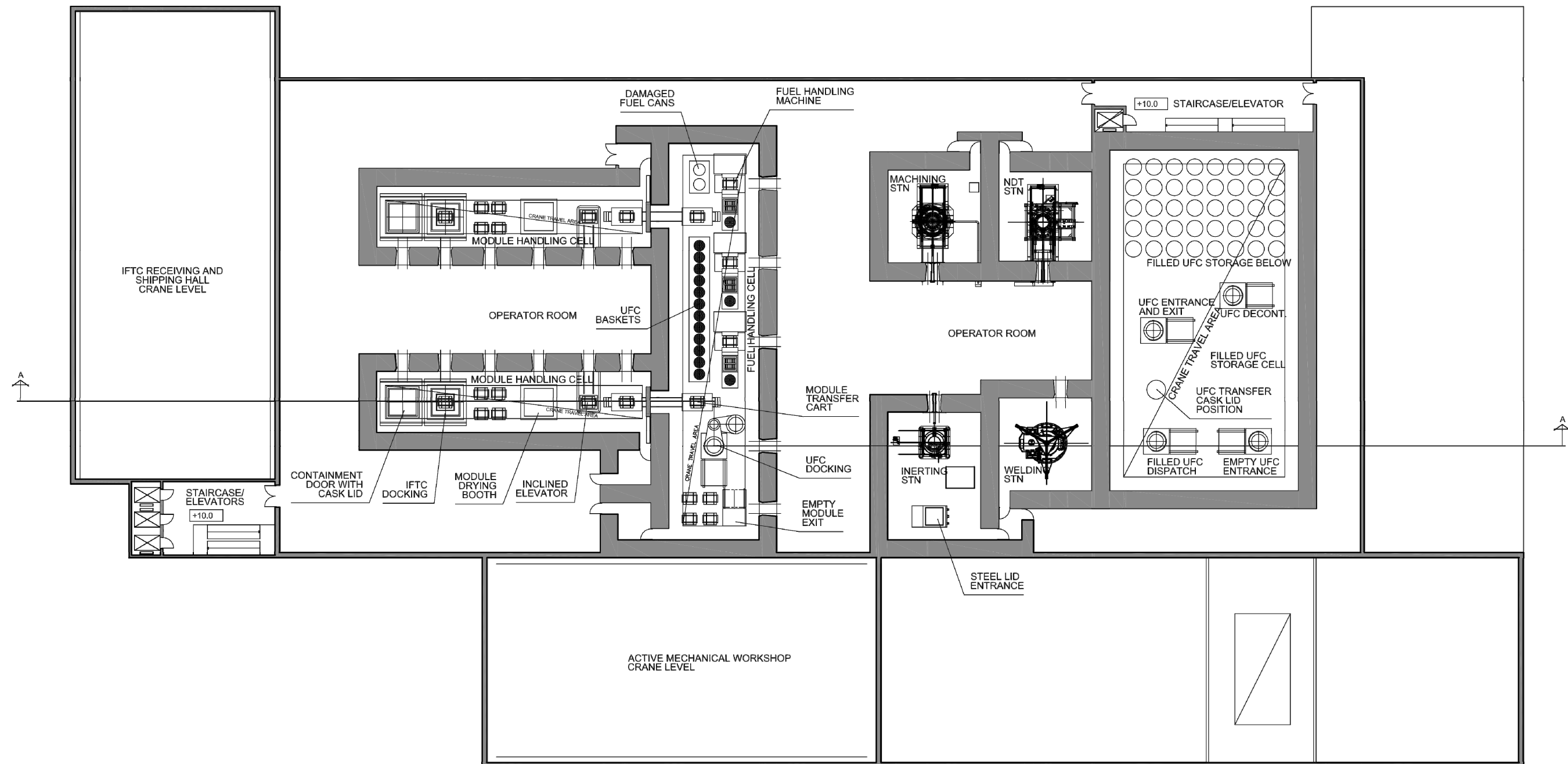


Figure 4-11: Used Fuel Packaging Plant – Operation Level

THIS PAGE HAS BEEN LEFT BLANK INTENTIONALLY

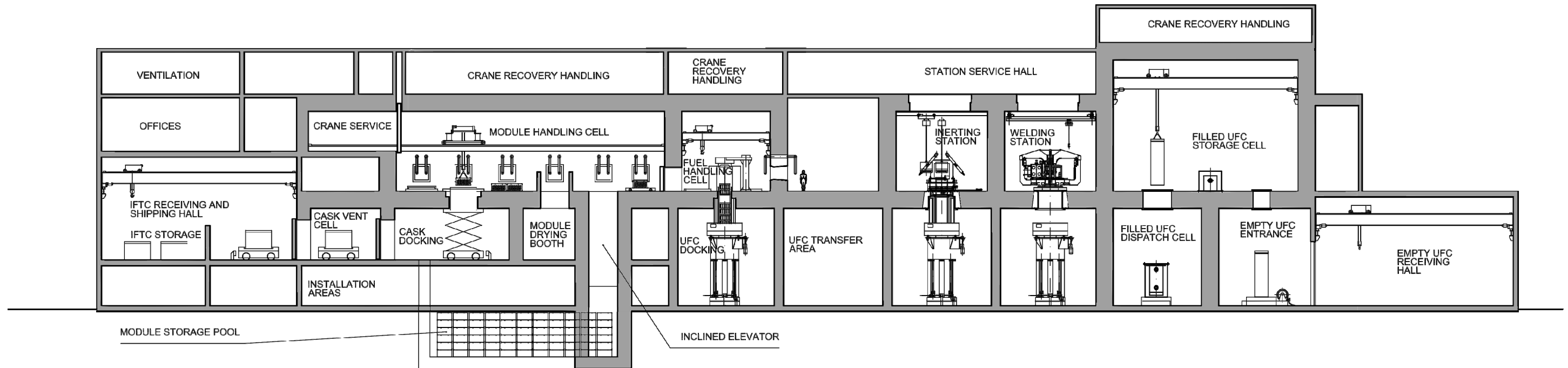


Figure 4-12: Used Fuel Packaging Plant – Cross-Section

THIS PAGE HAS BEEN LEFT BLANK INTENTIONALLY

4.5 Buffer, Backfill and Seals

4.5.1 General Description

The sealing system design concept presented in this report is generally based on previous studies that were summarized in McMurry et al. (2003). The main sealing and filling materials used in placement rooms consist of:

- Bentonite based buffer material that completely surrounds each used fuel container placed in the in-floor borehole; and
- Backfill, which is clay and a crushed rock aggregate used to fill in the remaining voids in the placement room.

Concrete floors, which will be removed during backfilling of the placement rooms, and minor amounts of light backfill materials are also used in the placement rooms, in addition to minor amounts of metal rock bolts and screens used to stabilize excavated walls and ceilings for worker safety. Iron rails, which would be used to guide remote handling equipment during the operations phase, will also be removed when the rooms are backfilled and sealed.

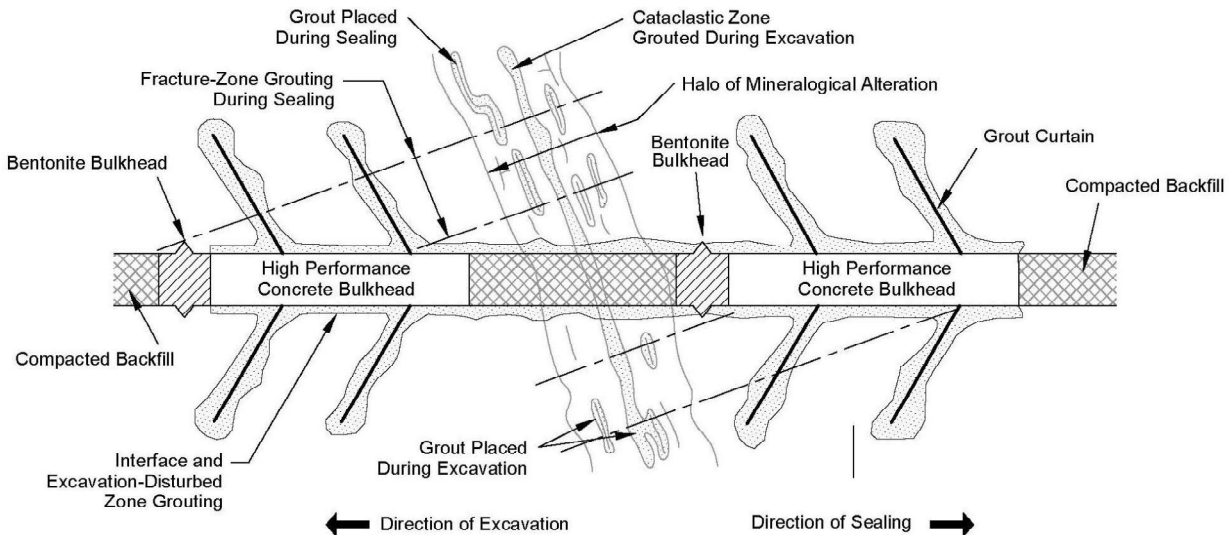
After a placement room has been filled, it would be closed off by the installation of a composite seal consisting of a buffer-type material and a thick bulkhead of low-heat, high-performance concrete (see Section 4.8). The purpose of the bulkhead is to provide mechanical restraint against the forces exerted by swelling clay seals. The bulkhead will further act to keep the sealing materials isolated in their intended positions while the access tunnels remain unfilled. The room closure would also permit physical isolation of the regions where container placement has been completed, improving security and permitting the continued use of the tunnels and access ways for ongoing repository operations in adjacent rooms. During decommissioning of the repository, the panel cross-cuts, access drifts, perimeter drifts, and shafts also would be backfilled and sealed. The most robust sealing arrangements for these excavations would be required at locations where tunnels or shafts intersect hydraulically active regions in the rock (Figure 4-13). The grouting shown in Figure 4-13 is discussed further in Section 4.5.1.5. It is in those regions where the seals and bulkheads would be required to withstand rapidly developing hydraulic pressures. A possible sealing system for the shafts is described in Section 4.12.2.

The approach for the shaft seal design focuses on the use of simple, relatively well understood and durable materials, and use of proven methodologies for placement. The shaft seal system consists primarily of a column of compacted bentonite/sand. Sand and bentonite are durable natural materials (see Chapter 9). An asphalt column or highly-compacted bentonite (HCB) may be placed above the first bentonite/sand layer to provide a redundant low permeability sealing material against upward or downward fluid flow. Concrete bulkheads could be used to provide structural components to the column and provide additional (early) sealing capability.

Siting, construction, and operation of a repository would require the drilling of numerous exploration and monitoring boreholes, including those drilled from the ground surface in the vicinity of the repository and boreholes drilled from within the repository into the adjacent rock. As part of the final closure of the repository, all boreholes would be sealed to ensure that there are no direct paths for water movement between the repository and the surface environment. The borehole seals would be composite seals made of bentonite, concrete, and grout, the

design of which can be adjusted as needed to compensate for hydraulically active regions in the adjacent rock.

As the repository saturates, the sealing materials swell, forming a dense, low-permeability seal around the container, isolating the placement rooms from access drifts, and isolating the repository level from the surface.



Note: Figure is not to scale.

Figure 4-13: Illustrative Tunnel Plug in a Hydraulically Active Region

4.5.1.1 Buffer

The buffer's sole constituent is bentonite (the commercial name given to a naturally occurring clay-rich sediment that is formed by the alteration of volcanic ash, McMurry et al. 2003). The main mineral phase in bentonite is montmorillonite, a smectitic clay mineral that has expandable layers when allowed access to free water and a high cation-exchange capacity. Montmorillonite is responsible for the most distinctive property of bentonite, which is that it can swell to several times its original volume when placed in fresh water. In a confined space, compacted bentonite expands on water uptake, and can apply a substantial swelling pressure on its confinement, which enhances its ability to seal fractures and to produce tight contacts with interfaces. Bentonite based materials also have the advantage of having a very low permeability, reducing mass transport in the vicinity of the container, and, at high density, provide an unfavourable environment for microbial activity.

Bentonite deposits from many parts of the world (e.g., Wyoming, Saskatchewan, Greece, India, China, Korea and Japan), have been characterized by various national programs for their potential use as buffer material in a deep geological repository. The proportion and composition

of montmorillonite varies with the source of the bentonite, with corresponding differences in swelling and mass transport properties. Bentonite that contains a high proportion of montmorillonite and whose main exchangeable cation is sodium (Na) (i.e., Na-bentonite) generally has the greatest swelling and sealing properties. Depending on its source, bentonite also contains some non-expandable clays, such as illite, and other minerals such as quartz, feldspars, calcite and gypsum, which generally are inert filler materials that do not actively affect buffer behaviour. Some bentonites are not chemically dominated by Na⁺ (e.g., Ca, Mg, Fe). These non-Na clays generally have a lower swelling capacity, higher hydraulic conductivity and some (e.g., Fe varieties) have the potential to interact adversely with their surroundings. It is also anticipated that ultimately Na-bentonites will evolve towards a calcium bentonite (Ca-bentonite) as ion exchange occurs with calcium-rich groundwaters. However for the critical period immediately following container placement, the buffer behaviour will be that of a Na-bentonite. Like Na-bentonites, Ca-bentonites exhibit a swelling capacity (< Na-varieties) and low permeability, making them suitable for use as buffer materials.

Important functions of the buffer in a deep geological repository are:

- To limit the container corrosion rate by inhibiting the movement and modifying the chemistry of groundwater in the vicinity of each container;
- To provide a thermally-conductive medium for heat transfer between the container and the geosphere;
- To keep the container in place, so its location remains at fixed coordinates in a room;
- To prevent damage to the container by acting as a mechanical buffer between the container and the rock; and
- To reduce the potential for microbially enhanced corrosion of the container by making the environment in the buffer unsuitable for microbial growth.

In the case of a breach of the container, other important functions of the buffer are:

- To limit the waste form dissolution rate by inhibiting the movement of groundwater;
- To retard the migration of dissolved contaminants and gases by limiting their movement to the slow process of diffusion and by enhancing their sorption; and
- To limit the solubility of certain contaminants by maintaining the pH of the groundwater around neutral conditions.

4.5.1.2 Backfill

McMurry et al. (2003) identifies two types of backfill in the repository, dense backfill and light backfill (Figure 4-16). Actual backfill compositions and their engineered physical properties will depend on the site-specific design requirements for a repository. Some of the general compositional features of the materials contemplated in this pre-project review are provided in Table 4-4. To provide for comparison of sealing materials prepared using different bentonite source materials and amounts, these relationships are expressed in terms of a parameter called the effective montmorillonite dry density, which normalizes bentonites and bentonite-sand mixtures in terms of their active component, montmorillonite clay.

Table 4-4: Physical Composition and As-Placed Properties of Potential Clay-Based Sealing System Components

	Dry density [kg/m ³]	Saturation [%]	Porosity [%]	Bulk density [kg/m ³]	Water content [kg/kg]	Effective montmorillonite dry density [kg/m ³]
Compacted bentonite (100% bentonite)	1610	65	41.3	1880	0.167	1465
Gap fill (100% bentonite)	1410	6	48.6	1439	0.021	1261
Light backfill (50:50 bentonite:granitic sand)	1240	33	53.7	1418	0.143	692
70% bentonite (70:30 bentonite:granitic sand)	1600	80	41.1	1930	0.205	1220
Dense backfill (5:25:70 bentonite:clay:aggregate)	2120	80	19.4	2276	0.074	376

Notes: These data assume relative solid densities of 2.75, 2.67, 2.65, and 2.62 for MX-80 bentonite (80% montmorillonite), non-montmorillonite clay, silica sand, and granite (aggregate), respectively. The density of water having 10 g/L salinity is 1005.8 kg/m³ at 20°C. Dry densities and saturations of the clay-based sealing materials are taken from SNC Lavalin (2011a); other properties are determined using calculations illustrated in Baumgartner (2006).

Dense backfill as currently formulated in Table 4-4 is a mixture of crushed rock (presumably taken from the repository excavations), naturally-occurring glacial lake clay and bentonite, installed as pre-compacted blocks to fill the majority of the placement tunnel volume. Important functions of dense backfill are:

- To provide load-bearing support to the rock after closure by filling most of the excavated space in rooms, tunnels, and shafts;
- To keep the buffer and containers securely in place in the placement rooms by resisting volumetric expansion of the buffer as it takes on water and develops a swelling pressure against the backfill above it; and
- To slow the movement of groundwater in the repository.

Light backfill provides many of the same functions as dense backfill. It contains less crushed rock and more bentonite than dense backfill, as indicated in Table 4-4. It would be used to fill the sides and upper (crown) regions of rooms and tunnels where it is not possible to place buffer or dense backfill blocks due to geometric or other constraints. Light backfill is likely to be placed pneumatically (“blown in”), and so it would not have as high a dry density as either the dense backfill or the buffer components.

Also note that light backfill has an initially high total porosity and has a much higher water content and lower density than either the buffer or dense backfill. The higher proportion of bentonite in light backfill compared to dense backfill is intended to give the lower density light backfill the ability to swell sufficiently when in contact with free water to ensure that adequately low permeability is maintained within the tunnels as soon as hydration is achieved.

4.5.1.3 Gap Fill

To facilitate the positioning of the precompacted buffer blocks in an in-floor placement hole, an approximately 50 mm wide gap (annulus) would be present between the buffer and the surrounding rock. A similar (~50 mm wide) gap would exist between the container and the buffer. To promote good thermal conductivity and to minimize density loss in the buffer as it swells into such gaps, the various small open spaces may be filled by an appropriate gap fill material, such as compacted bentonite pellets.

Gaps existing between backfill and the surrounding rock may also be filled with sand-bentonite material or perhaps precompacted bentonite pellets similar to those used to fill the buffer-rock gap (Figure 4-16). This type of fill is classified as light backfill, as discussed above in Section 4.5.1.2.

4.5.1.4 Concrete

Concrete is used throughout the repository for bulkheads, for floors where needed, and in various other shafts, drifts and cross-cuts as well as in construction of permanent bulkheads. The concrete would be mass-poured. It is intended that at least the concrete in the floors of the placement rooms, drifts and cross-cuts be removed as a component of the backfilling and decommissioning process.

Interactions between concrete and water in a repository have the potential over the long term to produce alkaline chemical conditions that are detrimental to the swelling properties of bentonite, and so a specialized low-heat, high-performance concrete has been developed (Table 4-5). Such a concrete has a much lower lime content than regular concrete, giving it a lower pH in reactions with water. This lower alkalinity would limit the potential for adverse chemical reactions within the repository. In addition, the low-heat, high-performance concrete generates less heat during curing than regular concrete, so the poured concrete would be less likely to crack due to thermal expansion and subsequent contraction during cooling.

Table 4-5: Composition of Various Concretes Proposed for Repository Use

Ingredients	Standard High-Perf. Concrete [kg/m ³]	Low-Heat High-Perf. Concrete [kg/m ³]	Cement Grout [kg/m ³]
Portland Cement	497 (CSA Type 50)	97 (CSA Type 50)	1208 - 950 (CSA Type 50)
Silica Fume	49.7	97	136 - 107
Fly Ash	0	0	0
Silica Flour	0	194	0
Superplasticizer	7.1	10.3	14 - 11
Fine Aggregate	703	895	0
Coarse Aggregate	1100	1040	0
Water	124	97	543 - 640
Water/Cement Ratio	0.23	0.5	0.4 - 0.6

Note: Table from McMurry et al. (2003).

4.5.1.5 Grout

Grouting is a short-term expedient that allows excavation and construction to be carried out in localized regions where groundwater inflow would otherwise be unacceptably high, or to limit seepage around or into engineered structures (Figure 4-13). Clay-based grouting materials may be an option under some conditions in a repository, but cement or silica-based grouts are more likely to be used. Although the amount of grout used in the rock around placement rooms likely would be minor, construction and closure of a repository nevertheless would involve the grouting of many cracks and fissures that would be ignored in most other types of underground engineering projects. To this end, low-viscosity cement grouts, grouts having a low cement content and silica rather than lime-bases have been developed for use in conditions anticipated to be encountered in a repository environment. One potential grout for use in a repository environment is presented in Table 4-5 (McMurry et al. 2003).

4.5.1.6 Asphalt

An asphalt column may form part of the shaft seals (Section 4.5.1). Asphalt has the ability to flow and make good contact with host rock. Immediately upon placement, the asphalt will create an effective barrier to water flow. The use of another low permeability sealing material provides an additional level of redundancy to the sealing system against upward or downward fluid flow. The reference asphalt mixture is based on a mix of asphalt compounds and aggregate, combined with a small porosity fraction to ensure low permeability and lime to reduce microbial activity.

4.6 Sealing Materials Production Plants

A number of engineered barriers are used as part of the repository system to isolate the used fuel containers from the rock and to inhibit the mobility of water and contaminants within the repository. These engineered barriers are manufactured on site, using clay, sand and crushed rock as their main components and are globally referred to as sealing materials. The primary barrier around the used fuel container is referred to as the buffer and consists of rings and blocks of compacted bentonite clay that are placed directly between the containers and the rock. Compacted bentonite is used also to construct seals that are placed at strategic locations in repository tunnels and shafts. The materials used as backfill or to construct seals at strategic points in the repository include:

- Highly-compacted bentonite (dense formed disks or rings to surround container).
- Light backfill (bentonite pellets pneumatically placed to fill voids in placement rooms).
- Gap fill (mechanically formed bentonite pellets pneumatically placed to fill the voids around the container and between the buffer and the rock).
- Dense backfill (bentonite-aggregate blocks designed to backfill placement rooms and tunnels); and,
- Low-heat high-performance concrete.

The clay-based sealing material's dimensions and composition are given in Table 4-6.

Table 4-6: Sealing Materials Attributes

Buffer / Backfill	
Buffer Rings	1.35 m inside diameter 1.87 metre outside diameter 0.50 m in height
Buffer Disks	1.87 metre outside diameter 0.50 m in height
Buffer Composition and Density	100% bentonite clay (MX-80 or equivalent) compacted to 1.6 Mg/m ³ dry density
Dense Backfill Composition and Density	5% bentonite, 25% lake clay, 70% granite aggregate, 2.1 Mg/m ³ dry density
Light Backfill Composition and Density	50/50 bentonite clay, granite sand, compacted in-situ to 1.2 Mg/m ³ dry density
Shaft Seal Composition and Density	70:30 bentonite clay, granite sand, either in blocks or compacted in-situ to 1.6 Mg/m ³ dry density
Concrete	Low-heat high-performance (LHHP) concrete

The repository surface facilities used produce sealing materials include an aggregate plant and rock crushing plant (Area B14), a concrete batch plant (Area B13) and a sealing material compaction plant with associated material storage bins (Areas B6 and B3).

The aggregate plant uses a portion of the excavated rock to manufacture products suitable for the concrete batch plant including sand and stone. Modified granular A (a graded crushed stone commonly used on roads) and fine sand for the compaction plant are also produced in the aggregate plant and used as a component of the sealing materials. Externally sourced raw materials required in the production of the various sealing materials include binders (Type 50 cement, sand fume and sand flour), bentonite and glacial lake clay. The concrete batch plant produces two different qualities of low-heat, high-performance concrete mixes, one used on the placement room floor and the other for the room closure bulkhead.

The compaction plant produces four different categories of clay based sealing material: dense backfill blocks and disks, light backfill, highly-compacted bentonite rings and disks, and gap fill. During decommissioning, the plant will produce the bentonite shaft seal materials. Asphalt seal mixes that may be required for sealing of shafts are assumed to be produced externally.

For logistics reasons the sealing materials facilities are situated outside the Protected Area but as close as possible to the service shaft. The sealing materials production equipment is based on conventional technologies. An example of the large presses that would be required for production of some of the bentonite components is shown in Figure 4-14. It is anticipated that two of these presses will be required in the facility for the production of buffer blocks and up to six presses may be required for making dense backfill blocks.



Figure 4-14: Example of a Closed-Die Forging Press

4.7 Shafts and Hoists

Access to the repository is via shafts serviced by hoisting facilities. Three shafts will be constructed, the main shaft, the service shaft, and the ventilation shaft (Figure 4-15) each serving specific functions during construction, operations and decommissioning of the repository facility. Their primary functions are the transport of materials and personnel, and providing ventilation to the repository. The shafts will be constructed using techniques that minimize host rock damage, to enhance the effectiveness of postclosure repository seals.

The shafts diameters are:

- Main shaft finished diameter of 7 metres;
- Service shaft finished diameter of 6.5 metres; and
- Ventilation shaft finished diameter of 6.5 metres.

The headframes for the three shafts will be of slip-formed concrete construction for a durable and easily maintainable structure. All the shafts will be concrete lined; the lining will be removed during decommissioning and closure of the facility.

The three shaft structures (including head frames and hoisting plants) provide a number of support functions during underground development, repository operation and decommissioning:

- The main shaft serves as the exclusive means for transfer of used fuel containers from the surface to the underground repository. Conversely, it could also be used for transfer of a retrieved used fuel container from the repository to the surface, if this was required. The main shaft also provides the fresh air supply to the underground.
- The service shaft serves as the principal conveyance for personnel, materials and equipment to the underground as well as for transport of excavated rock to the surface. It also provides some ventilation exhaust.
- The ventilation shaft, located about 2 km outside the main surface facilities fence is the primary exhaust shaft and serves also as emergency exit from the repository.

4.8 Underground Facility Design

For the purpose of preliminary design and safety studies for a hypothetical site in crystalline rock, the used fuel repository is assumed to be developed on a single level, at a depth of approximately 500 m. A possible layout of a repository designed to accommodate a reference inventory of 4.6 million used fuel bundles is shown in Figure 4-15. The actual layout for a selected repository site will be adapted to suit the specific site conditions. The geology of the hypothetical site used in this study is described in Chapter 2. The underground layout, which covers an area of about 6 km², assumes that the closest possible distance from a placement room to a water conducting fracture is 25 m.

The repository layout is generally a rectangular configuration, with two central access drifts and two perimeter access drifts connected by perpendicular tunnels (cross-cuts) that provide access to the used fuel container placement rooms. The placement rooms are grouped in panels, as shown in Figure 4-15.

The used fuel container placement rooms are a series of parallel tunnels arranged in eight panels. Within each panel, the placement rooms have a centre-to-centre spacing of 40 m, and each room has a single access from the corresponding cross-cut tunnel. The entrance to the room has a 50 m turning radius to facilitate the movement of the container transfer cask and related systems. The length of the rooms in the reference design is specified as 396 m and the in-floor boreholes in which the used fuel containers are placed have a center-to-center spacing of 4.2 m. The used fuel container density is designed to minimize the repository underground footprint while, at the same time, satisfying thermal design requirements. The repository includes provision for an underground demonstration facility located near the main and service shafts. This facility may be used to support long-term testing and demonstration of repository technology.

After used fuel container placement operations are completed in each placement room, the rails and concrete floor will be removed and the room will be filled with dense backfill blocks. Light backfill will be placed in the interstitial spaces and compacted in-situ to fill the residual volume between backfill blocks and the rock. The placement room design is described in further detail in Section 4.7.2.

A 6 m thick seal built with pre-compacted bentonite blocks and a 12 m concrete bulkhead will be used to seal the entrance to the placement room. The major components of a placement room are illustrated in Figure 4-16 (SNC-Lavalin 2011a). The borehole dimensions are determined by the used fuel container dimensions and the thickness of the buffer surrounding the containers, which is 35 cm. This results in an approximate borehole diameter of 2.0 m.

All underground openings (tunnels container placement rooms) will be excavated by drill and blast methods, with exception of the used fuel container placement boreholes, which will be drilled using a vertical boring machine. The placement rooms have a half-elliptical cross-section with nominal dimensions of 5.5 m wide by 5.5 m high as shown in Figure 4-17. Both, repository development (excavation) and used fuel container placement will be conducted on a panel by panel basis and, in a sequence that will provide suitable separation of these two major activities. The repository development/operation strategy will optimize efficiency while considering both, safety and operating factors (e.g., vehicle traffic and ventilation) as well as the potential interactions between repository development and operations.

The container placement operations will require first the installation of the buffer blocks in each borehole and then the transfer of a used fuel container to the borehole location and placement of the container in the borehole. These operations, which are discussed in further detail in Section 4.10, will be conducted in a retreating manner, starting at the blind end of the placement room, with the last container installed nearest to the placement room entrance.

When container placement and backfilling of the room are complete, a clay seal and a concrete bulkhead will be placed at the room entrance. The clay seal includes a wedge-shaped ring designed to interrupt the continuity of the excavation damage zone. The configuration of the engineered barriers is illustrated in Figure 4-16.

Within the boreholes, the containers are surrounded by highly-compacted buffer blocks in the shape of disks and rings, which form the primary isolation barrier between the container and the rock. This material is designed to inhibit groundwater flow and to adsorb several key chemical

species, therefore blocking or delaying their transport. The buffer also limits the viability of bacteria, preventing the biological production of corrosion agents such as sulphates.

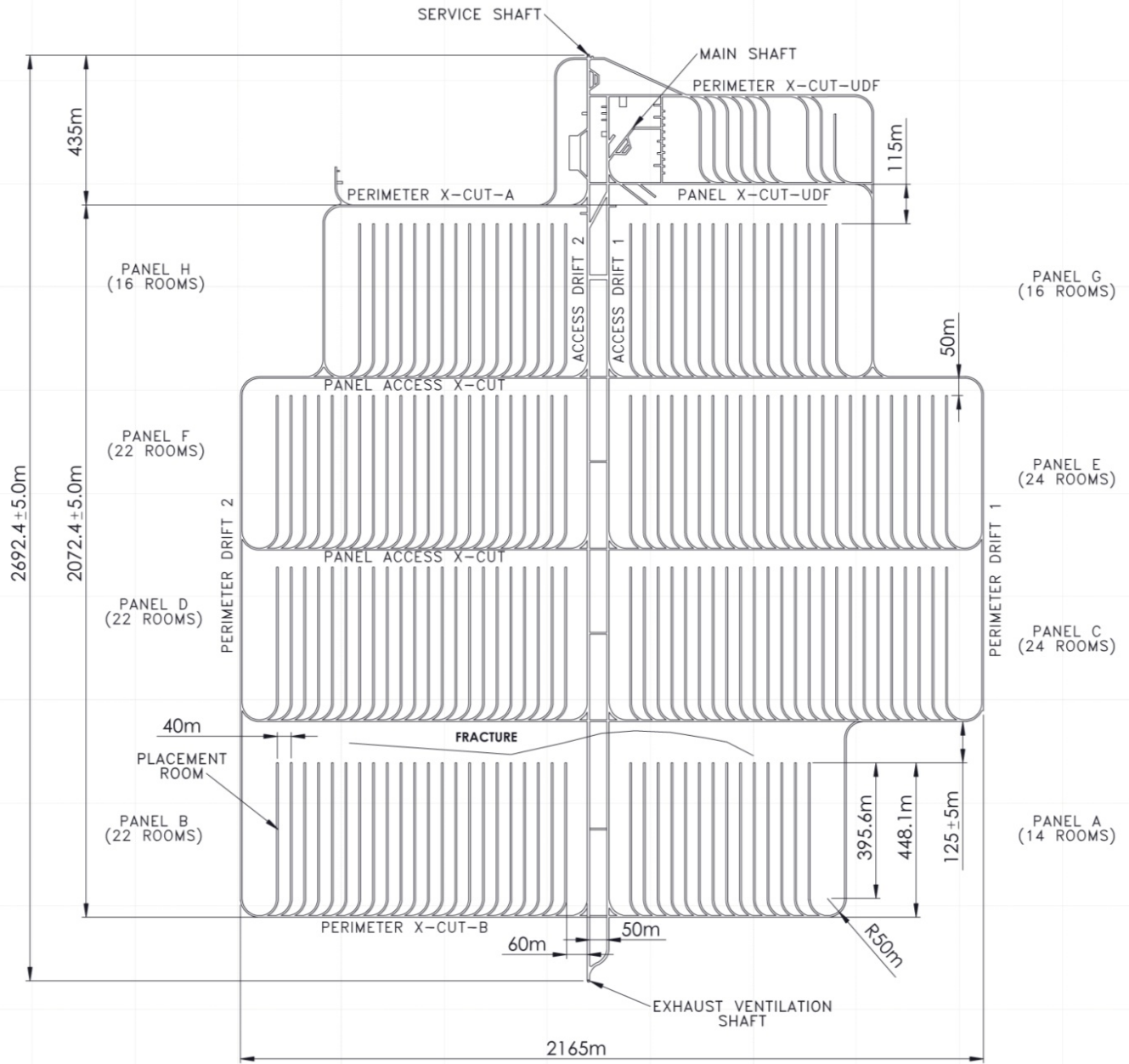


Figure 4-15: Underground Repository Layout

THIS PAGE HAS BEEN LEFT BLANK INTENTIONALLY

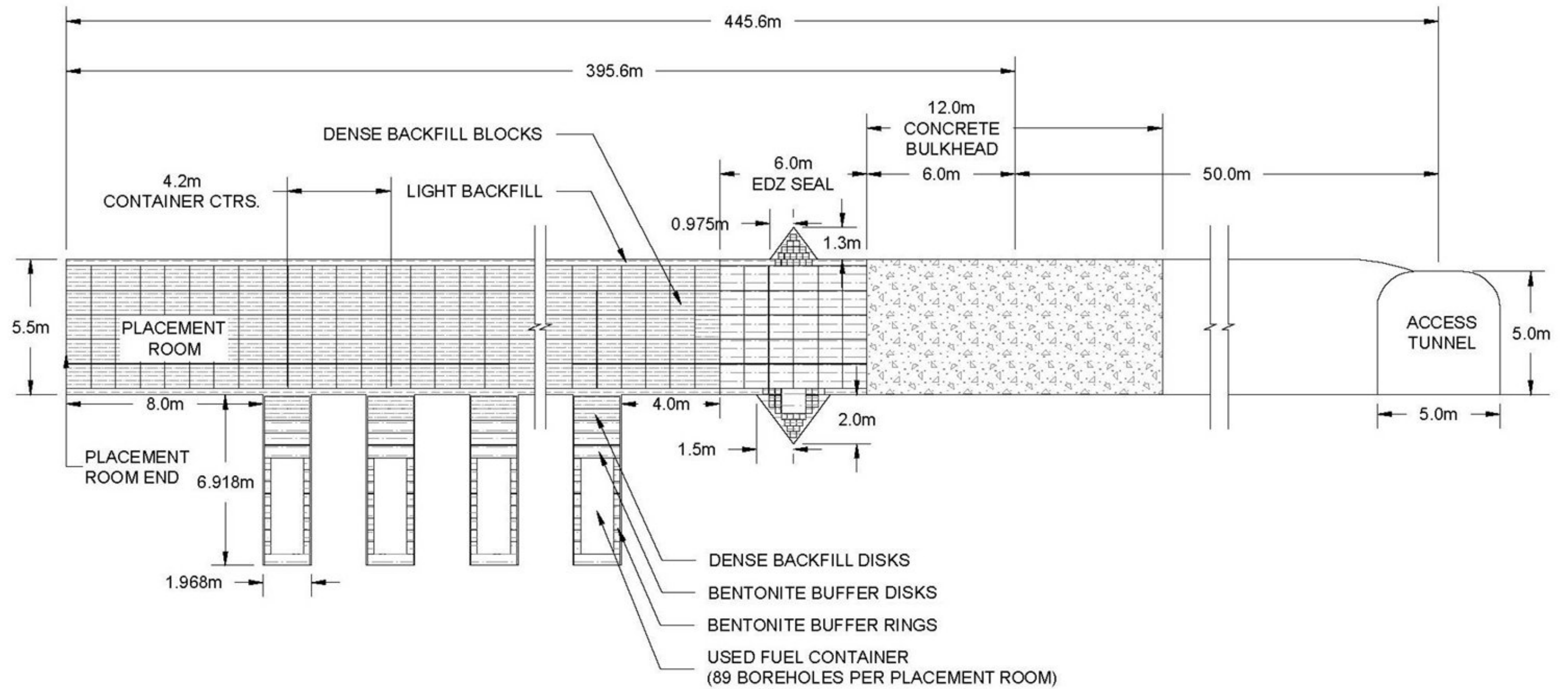


Figure 4-16: Placement Room Longitudinal Section

THIS PAGE HAS BEEN LEFT BLANK INTENTIONALLY

4.8.1 Placement Room Geometry and Spacing

The size of used fuel container, the borehole drilling equipment and the container placement equipment determine the placement room dimensions and profile. These factors and the need to minimize stresses (to maximize rock stability) were addressed by using a room cross-section geometry consisting of a half-ellipse with a height of 5.5 m and a maximum width of 5.5 m (Figure 4-17).

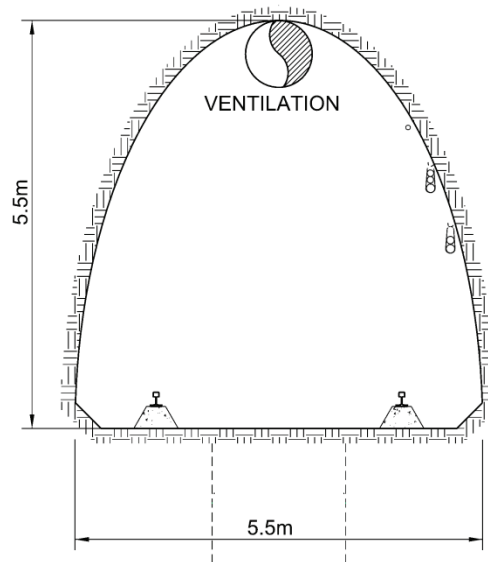


Figure 4-17: Placement Room Geometry

The placement rooms have been designed with a length of 396 metres and a curved entrance from the corresponding cross-cut with a 50 metres radius. The last 6 metres of the curved entrance and the first 12 metres of the placement room will also serve as the site for placement of a room clay seal and a concrete bulkhead after the container placement activities are completed in each room.

Thermal-hydraulic-mechanical (THM) analyses were conducted to establish the stress and temperature regimes for both the engineered barriers and the geosphere. The THM analysis results were used to optimize both room spacing and container spacing. These parameters were chosen to ensure that the temperature in a layer of buffer at least 250 mm thick will not exceed 100°C at any time. This value was chosen based on work by Wersin et al. (2007) which noted that at least 150°C is required for significant illitisation and cementation of the buffer. No notable changes have been observed in the buffer up to at least 120°C. To meet this requirement, the centre-to-centre spacing of placement rooms was conservatively set at 40 m and the centre-to-centre spacing of in-floor boreholes was set at 4.2 m.

Regardless of the in-floor borehole spacing, some excavation damage is expected to occur in the rock around the in-floor boreholes. The depth of this damage zone is expected to be larger around the borehole edge and have a minimum value at the mid-point between two in-floor boreholes. However, the maximum depth of the damaged zone along the room centerline is not expected to exceed a few tens of centimeters. The depth of the damage is also expected to decrease from the room centerline to the outer edges.

4.8.2 Ventilation System

The repository ventilation system utilizes the three shaft complexes and a combination of parallel airways for intake and exhaust. Underground booster fans, ventilation doors and dampers are used to control the airflow distribution. Since the primary repository ventilation system consists of relatively large airways, the overall circuit can be described as having relatively low resistance characteristics in a push-pull type network. Two parallel surface fresh air fans supply air (heated as required) to the main shaft. The fresh air supply reaches the repository level at the main shaft station and is split to the underground demonstration facility and the main repository itself. A portion of the exhaust air flow is routed to the service shaft by an exhaust booster fan, installed underground at the service shaft station. The return air is exhausted to atmosphere by one exhaust fan installed on the surface in the service shaft area.

Exhaust air from the repository area is routed to the ventilation shaft by two exhaust booster fans, installed underground in a parallel configuration at the shaft station. Return air is exhausted to atmosphere by two parallel exhaust fans installed on the surface in the ventilation shaft area. Air distribution in the repository is promoted through the use of fans and regulators. Fresh air will be distributed to the individual panels through axivane, or axial flow fans.

Individual placement rooms will be ventilated by axivane fans in an exhaust configuration, installed to remove air from the rooms and direct it into the exhaust circuit. Such fans will work with a ducting system to provide, by design, approximately 37.8 m³/s of air to the room face during room excavation. For used fuel container placement activities, the required supply flow per room for the reference design is expected to be 14 m³/s. The exhaust air from these fans will be carried to the panel exhaust drift, and then to underground booster exhaust fans.

The system will be operated to ensure that the underground work is performed in a fresh air supply stream with the exhaust being directed through unoccupied areas, going generally from clean areas towards operation areas. High-Efficiency Particulate (HEPA) filtration systems could be installed in the service shaft and ventilation shaft stations as stand-by systems that could be activated as required. Subsurface ventilation systems could also be equipped with air filtration systems if required, however, for the purpose of this conceptual design, stand-by HEPA filtration systems are assumed to be installed at the service shaft and ventilation shaft stations.

4.9 Repository Construction

Repository construction will be initiated after both a safety assessment and an environmental assessment have been completed and a construction licence has been obtained for the site. Initial site preparation activities, which include clearing and grading, establishing access roads and the installation of basic infrastructure systems would have been conducted earlier, under a site preparation licence. The site infrastructure required to support excavation, including

electrical delivery systems, headframes, ventilation and excavated rock management systems would follow after the construction licence is obtained.

Controlled construction methods will be used to minimize disturbances to the area surrounding the facility. The three shafts will be developed using a controlled drill and blast shaft sinking approach specifically designed to minimize the excavation damage zone. The shaft sinking process will involve the following steps:

- Collaring or starting the shaft;
- Setting up the equipment needed to sink the shaft;
- Sinking the shaft to its full depth using the drill and blast method; and
- Dismantling the equipment used for sinking.

Conventional blasting operations include drilling blast holes in a converging pattern designed to minimize the quantity of detonated explosive per volume of rock. In order to reduce damage to the perimeter of the opening, a larger number of blast holes with smaller individual explosive charges are used in the outer region of the shaft. This is usually referred to as contour wall blasting, and it will be used to minimize the thickness of the excavation damage zone. Between the blasting cycles, fumes are vented, scaling is done to remove loose rock and ground support is applied as required. This excavation method is expected to result in a rate of advance in the range of 2.5 metres to 3.5 metres per day.

Upon completion of the three shafts, the perimeter drifts will be excavated, defining the outline of the underground facility. The underground development required to support infrastructure will proceed in anticipation of the development of used fuel container placement rooms. The placement room panel development will be initiated along the cross-cut near the ventilation shaft and will continue in a retreating fashion towards the main shaft end of the repository. The repository panel development strategy will be designed to minimize any possible effects of the excavation activities on container placement operations. The excavation of new panels will take place as far as possible from the container placement operations.

Both, panel development and used fuel placement operations will move from the ventilation shaft end towards the main shaft end of the repository. Retreating towards the main shaft will minimize the need for personnel to enter or pass by completed repository areas. It will also ensure that all ventilation air from operating areas is routed directly to the exhaust shaft.

After development of a placement room has been completed, tracks to operate placement equipment will be installed on the floor. Each placement room panel will require about 3 years for development to be completed. Placement activities in each panel are expected to require from 3.5 to 4 years.

As the underground rooms are excavated, in-floor boreholes for placement of the used fuel containers will also be drilled. Drill and blast is not a suitable excavation method for the container placement boreholes due to the stringent requirements for geometry and integrity of the near-field rock. Therefore, a vertical boring machine is the favoured method to establish the boreholes. In-floor boreholes that do not meet rock quality and permeability requirements will be rejected and filled with highly-compacted bentonite. Figure 4-18 and Figure 4-19 illustrate the in-floor borehole equipment and operation.

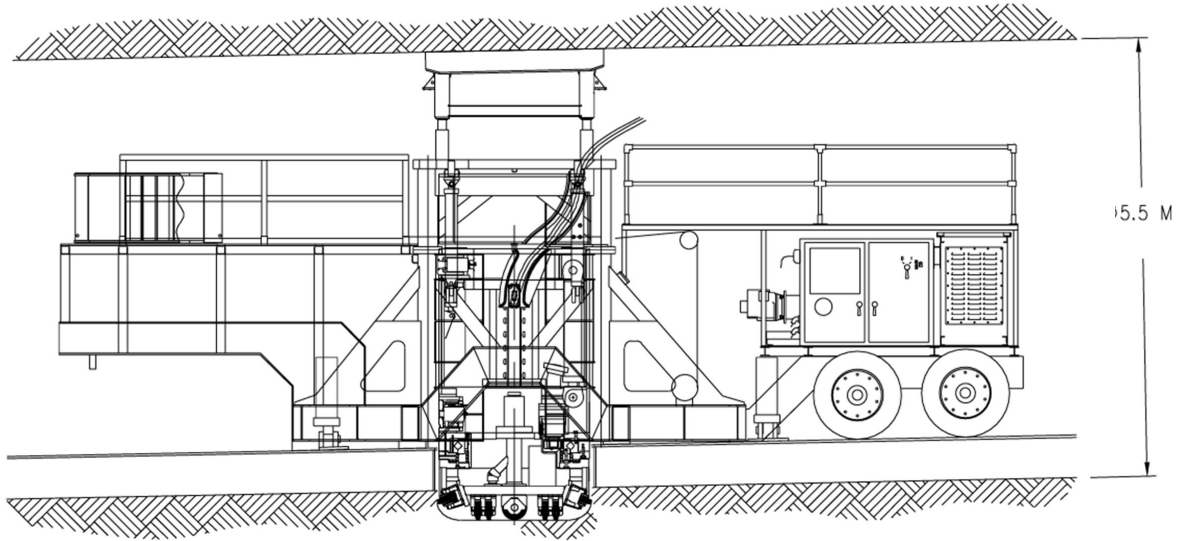


Figure 4-18: In-floor Borehole Drilling Equipment

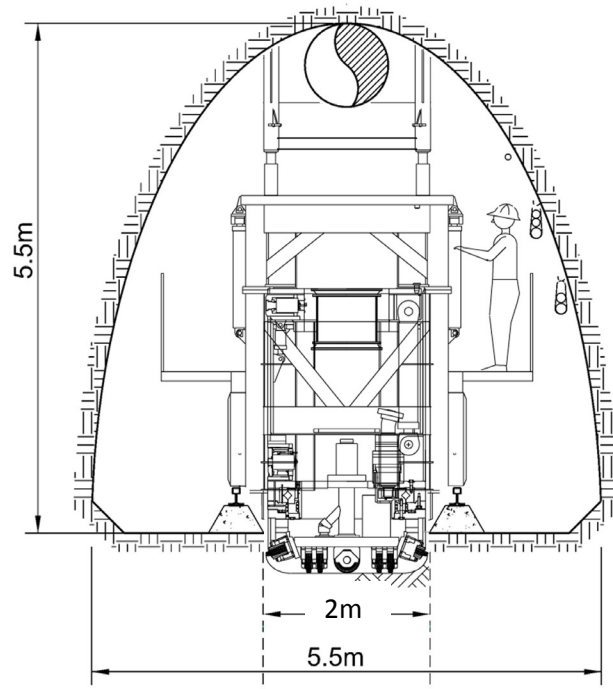


Figure 4-19: In-floor Borehole Drilling

4.10 Repository Operation

Prior to the start of container placement operations in a specific placement room all the required in-floor boreholes would have been excavated and would have temporary covers placed on them. The boreholes bottom will be levelled using in-situ compacted bentonite to provide a solid, flat base for the installation of bentonite discs and rings. Rails would have also been installed on the concrete floor to move heavy equipment, including the container transfer cask. The equipment required for the container placement operations is schematically illustrated in Figure 4-20. A summary description of the container placement operation is given below.

The placement machine is brought to the borehole location using a dedicated rail trolley and stationed at the selected borehole. Then, buffer discs and rings are transported by a rail trolley to the placement machine location. The buffer components are handled using a disk-placement shield, which is provided with a winch and handling tools in a shielded assembly to protect operators from radiation fields during the placement operation.

Using the disk-placement shield, the bottom buffer disk is placed on the floor of the borehole. Subsequently, using a similar process, eight buffer rings are placed in the borehole, defining the cavity where the container will reside. The geometry of the borehole is illustrated in Figure 4-21. Subsequently, the used fuel container transfer cask is moved into the room and transferred to the placement machine, which rotates the cask to a vertical position. Then, the cask shielded doors are opened and the placement machine lowers the container into the borehole.

After the container is in position inside the borehole, the transfer cask is removed and the rest of buffer rings are placed in the borehole. Subsequently, bentonite pellets are blown into the annulus between the buffer components and borehole wall, as well as between the used fuel container and the bentonite rings. The bentonite blowing equipment is then removed and three bentonite discs and two dense backfill discs are installed in the borehole. Following these operations the container placement machine is moved to a new borehole location and the above operations are repeated. The container placement sequence of operations is described in detail in Figure 4-22.

After completing the container placement operation, the placement machine is moved to the next borehole position and the section of track around the completed borehole and the related structures are removed. This segment of the placement room is then backfilled using dense backfill blocks and in-situ compacted light backfill. The light backfill is pneumatically placed in the interstitial spaces between the rock and backfill blocks and then mechanically compacted.

As the above described operations are repeated, the placement room will be backfilled in a retreating fashion towards the entrance. Upon completion of these activities, a 6 m thick bentonite seal will be placed to seal the entrance of the placement room. The seal will be constructed with pre-compacted bentonite blocks and will include a wedge-shaped ring designed to interrupt the continuity of the excavation damage zone (see Figure 4-16). The bentonite seal will be backed up by a 12 m long concrete bulkhead that will complete the closure of the placement room.

The repository operations will continue until all used fuel has been repackaged in used fuel containers, all used fuel containers placed into in-floor boreholes and all placement rooms sealed. This is expected to take 38 years for a used fuel inventory of 4.6 million bundles.

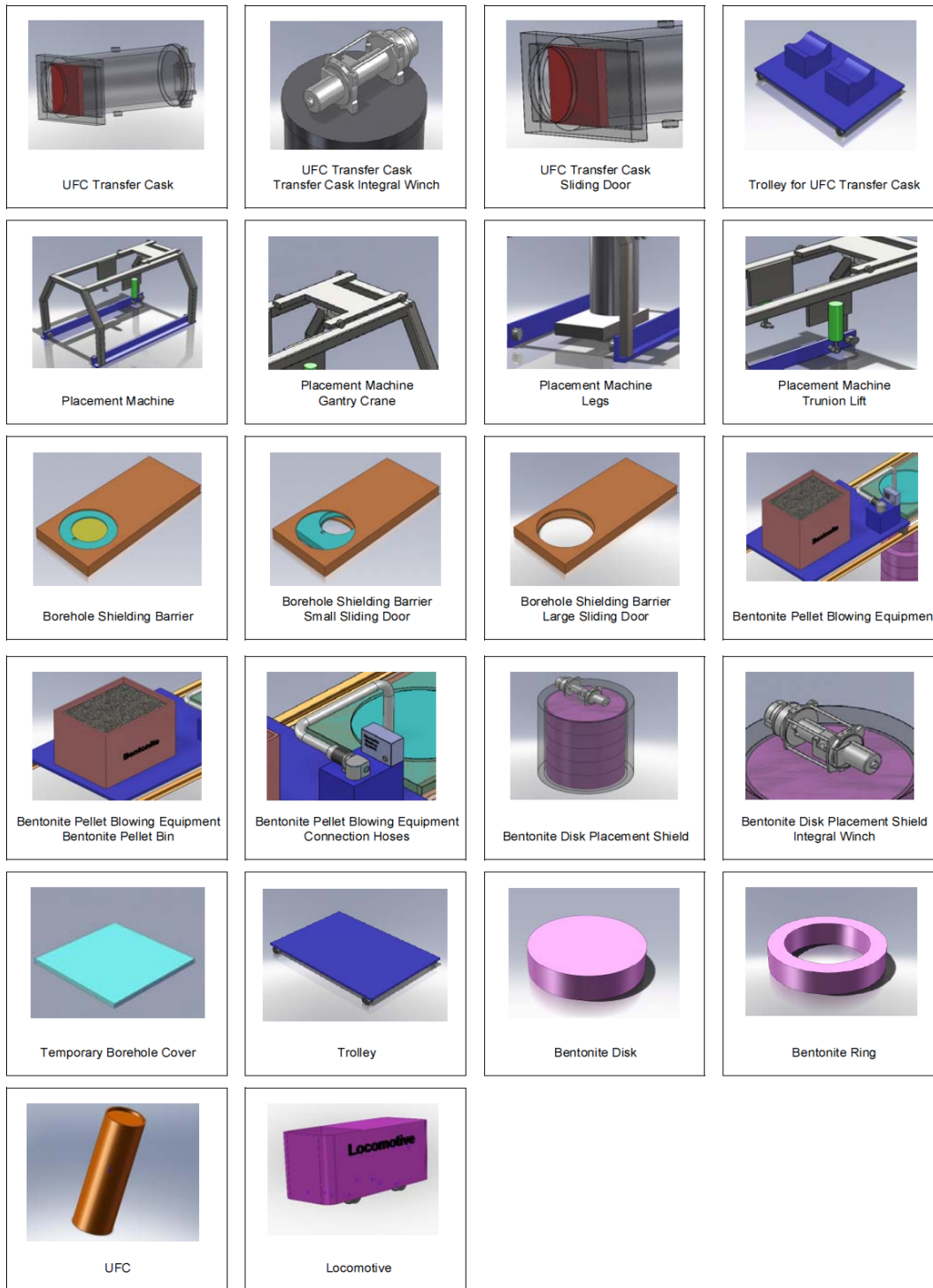
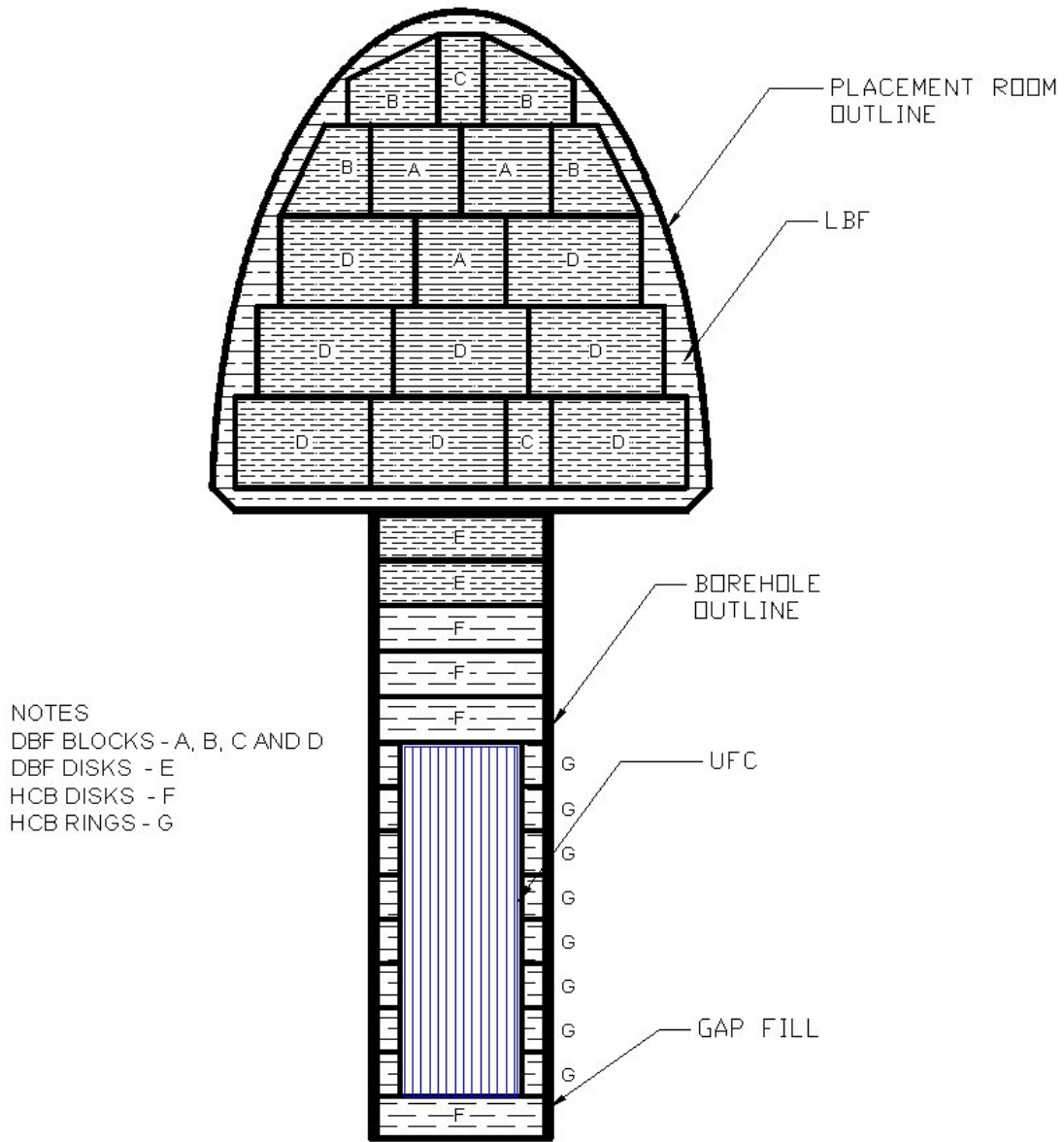


Figure 4-20: Legend for Container Placement Equipment



Note: Light Backfill (LBF), Dense Backfill (DBF), Highly Compacted Bentonite (HCB)

Figure 4-21: Placement Room and In-floor Borehole Cross-Section

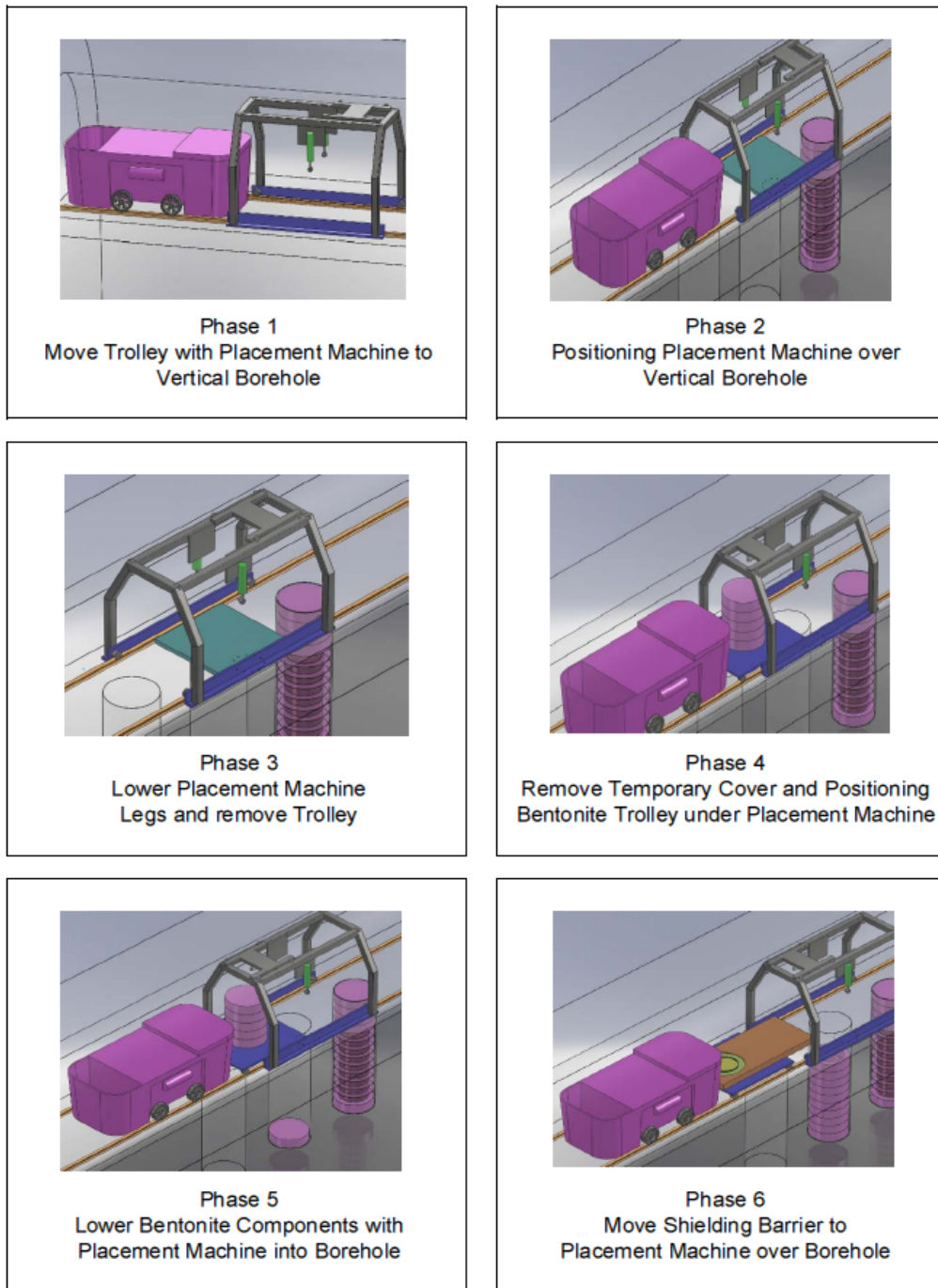


Figure 4-22: Container Placement – Sequence of Operations

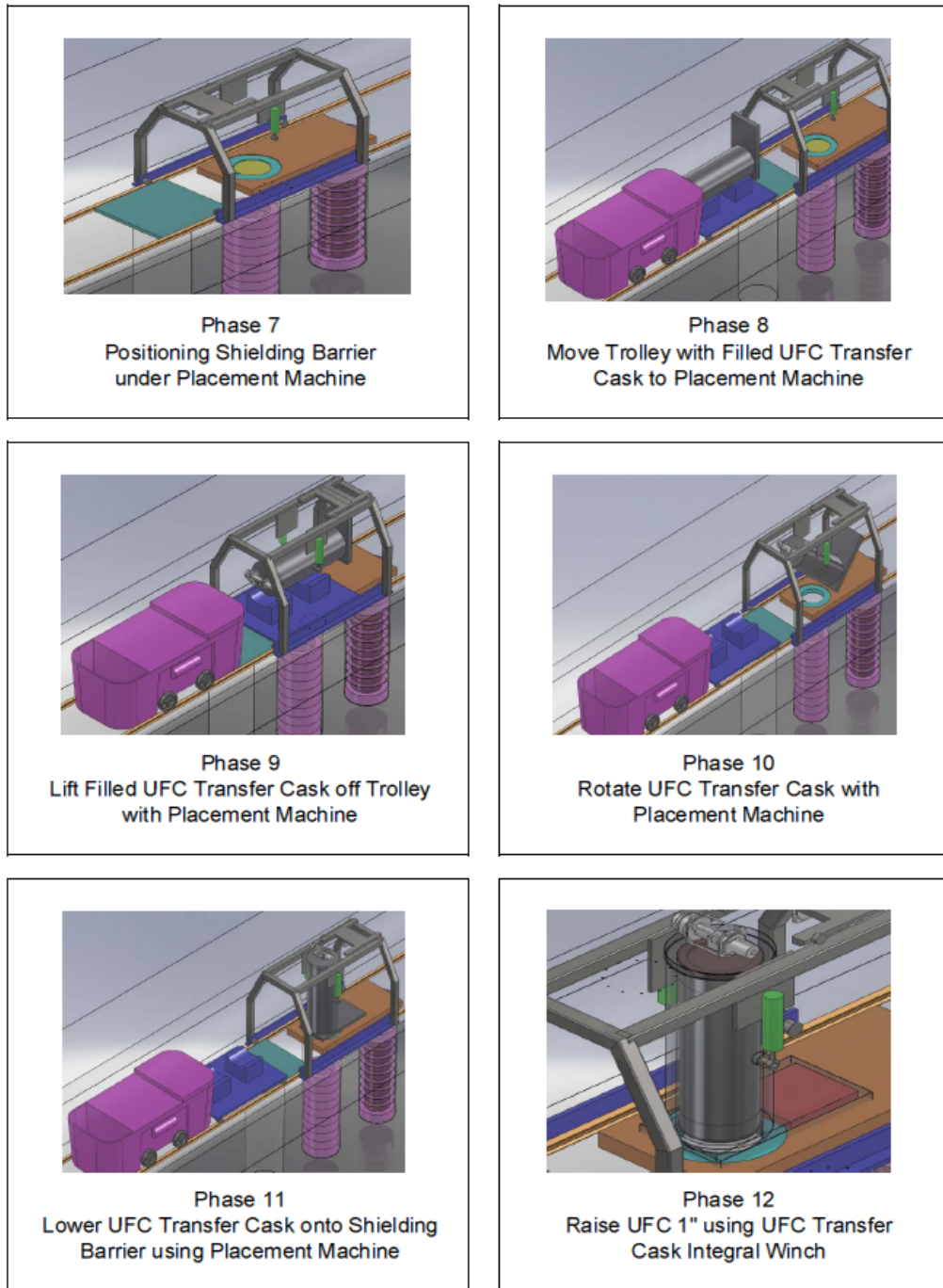
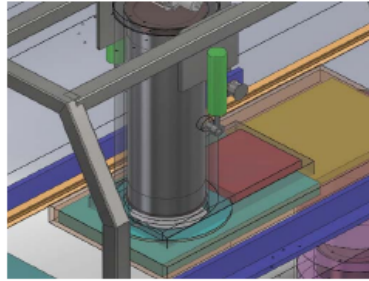
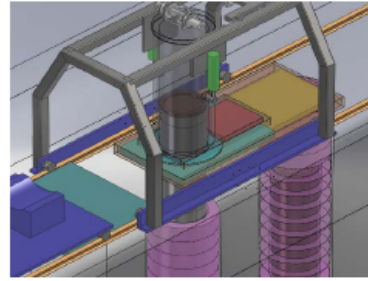


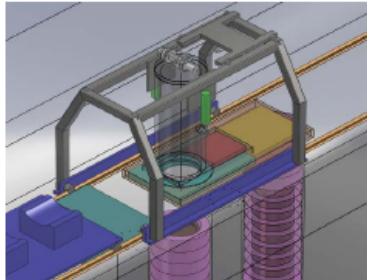
Figure 4-22: Container Placement – Sequence of Operations (continued)



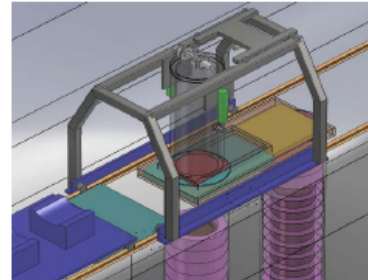
Phase 13
Open Shielding Barrier and UFC
Transfer Cask Sliding Door



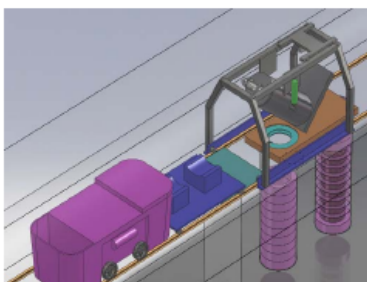
Phase 14
Lower UFC into Borehole



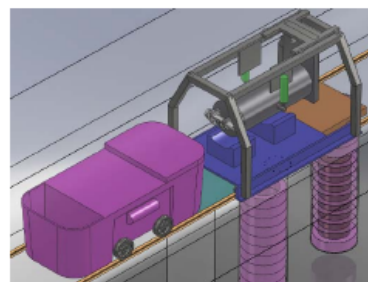
Phase 15
Use Tool to release UFC Clamp
and retract UFC Clamp



Phase 16
Close Shielding Barrier and UFC
Transfer Cask Sliding Door

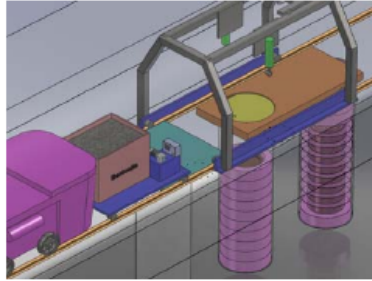


Phase 17
Lift and rotate UFC Transfer
Cask with Placement Machine

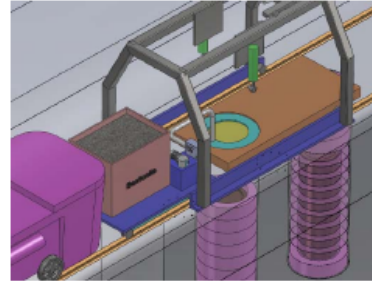


Phase 18
Lower UFC Transfer Cask on Trolley
and transport to Storage

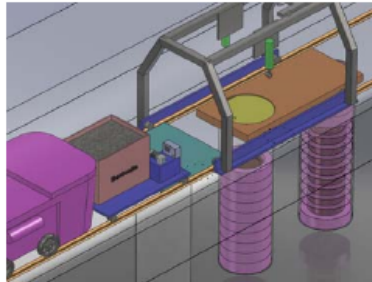
Figure 4-22: Container Placement – Sequence of Operations (continued)



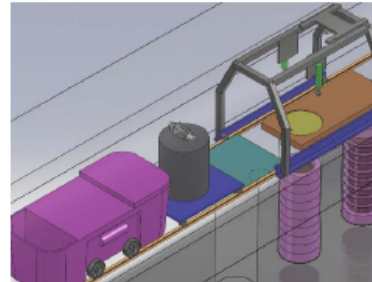
Phase 19
Move Trolley with Bentonite Pellet Blowing
Equipment to Placement Machine



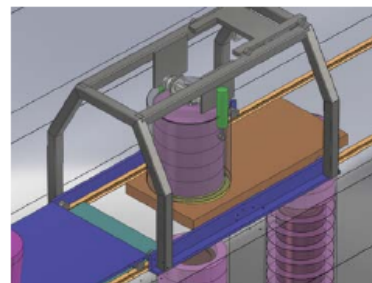
Phase 20
Fill Inner and Outer Gaps with
Bentonite Pellets



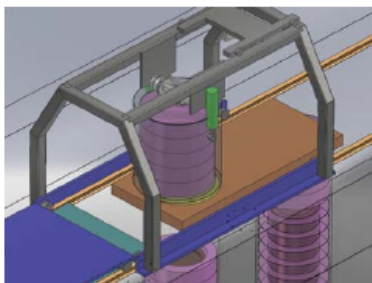
Phase 21
Move Trolley with Bentonite Pellet Blowing
Equipment to Storage



Phase 22
Move Trolley with Bentonite Disk Placement
Shield and Disk to Placement Machine

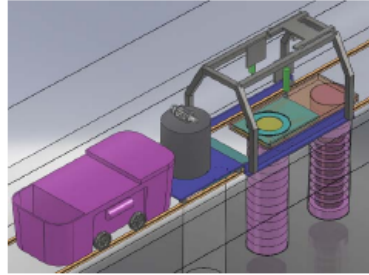


Phase 23
Lift Bentonite Disk Placement Shield onto
Shielding Barrier using Placement Machine

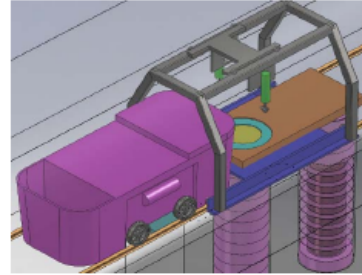


Phase 24
Lower 5 disks using Integral
Winch in Disk Placement Shield

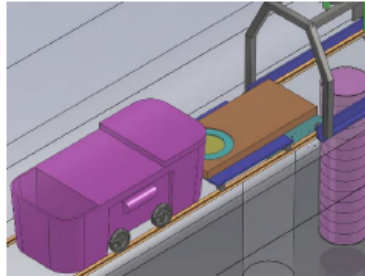
Figure 4-22: Container Placement – Sequence of Operations (continued)



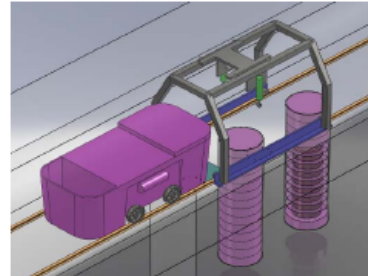
Phase 25
Move Trolley with Bentonite Disk
Placement Shield to Storage



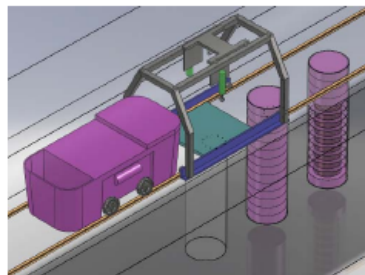
Phase 26
Lift Shielding Barrier with Placement
Machine and place onto Trolley



Phase 27
Move Trolley with Shielding
Barrier to Storage



Phase 28
Raise Placement Machine legs
and Lower onto Trolley



Phase 29
Move Trolley with Placement Machine to
the next Borehole and position

Figure 4-22: Container Placement – Sequence of Operations (concluded)

4.11 Extended Monitoring

Upon completion of all used fuel container placement activities all placement rooms will be sealed and closed, but the access tunnels and shafts will remain open. The facility will be placed in an extended care and maintenance program during which monitoring of the repository and surrounding geosphere will continue to confirm the performance of the repository system. The extended monitoring period could have a duration of several decades.

4.12 Decommissioning

Once the extended monitoring period has been completed, the facility will formally enter a decommissioning phase where the underground facilities will be prepared for backfilling and then backfilled and sealed from the surface. Subsequently, the surface facilities will be decommissioned and the site will be returned to a green-field condition. Further details of the decommissioning phase are discussed below.

4.12.1 Sealing of Underground Horizontal Openings

The sealing of underground horizontal openings consists of closing off access drifts and ancillary facilities. Such activities will commence with the inspection and preparation of exposed rock surfaces by removing loose rock before backfilling and sealing. This will be followed by removal of any remaining equipment. The central access drifts will then be backfilled, with sealing bulkheads installed at strategic locations.

The underground openings will be sealed using materials and methods similar to those used for backfilling the placement rooms. Clay-based fill will be complemented by strategically placed composite seals consisting of a concrete bulkhead and a clay component that may incorporate highly-compacted bentonite blocks to provide a barrier to groundwater movement.

The sequence for the closure of tunnels will see first the sealing of cross-cuts and perimeter tunnels in a retreating manner from the ventilation shaft to the service shaft while maintaining open a central access tunnel. Bulkheads will be installed near access drift intersections and also near intersections with significant zones (as appropriate). The purpose of the bulkheads is to provide mechanical restraint against the forces exerted by swelling clay seals and other repository sealing systems. The bulkheads will further act to keep the sealing materials isolated in their intended positions.

4.12.2 Sealing of Shafts

Sealing of the shafts is the last step in the decommissioning of the underground repository. This activity starts when the sealing of underground tunnels and ancillary areas is complete. At that time, the following activities will take place:

- Removal of shaft services including compressed air lines, water lines, power supply, lighting and communication cables;
- Removal of instruments and sealing from any impacted geological investigation boreholes;
- Removal of furnishings including all of the shaft guides and sets, steel support brackets, brattice and lower crash beam assemblies from bottom to top while backfilling; and

- Reaming of the shafts (as required) to remove the concrete linings and any degraded wall rock.

It is assumed that approximately 0.5 m of rock will be removed from the shaft walls to expose the sound rock. After this operation, each shaft will be re-equipped with services and staging, and backfilling will be initiated with sealing bulkheads installed at strategic locations. The proposed design for a shaft seal system is described in Table 4-7. The final design for the shaft seals will depend on the geological conditions of the site.

Table 4-7: Proposed Sealing System for Shafts

Depth from Surface	Material
0 – 20 m	Low-heat high-performance concrete– concrete cap at surface
20 – 150 m	70/30 bentonite/sand shaft seal compacted in-situ
150 – 170 m	Low-heat high-performance concrete for concrete bulkhead keyed into rock / overburden to a distance of 0.5 times the original radius of the shaft
170 – 330 m	70/30 bentonite / sand shaft seal compacted in-situ
330 – 380 m	Asphalt or highly-compacted bentonite seal
380 – 480 m	70/30 bentonite / sand shaft seal compacted in-situ
480 – 500 m	Concrete monolith – Low-heat high-performance concrete

4.12.3 Decommissioning of Monitoring Wells and Sealing of Geological Boreholes

The purpose of removing monitoring wells and then sealing the geological borehole is to inhibit groundwater movement and contaminant transport. A combination of cement-based materials and clay-based materials with low permeability and a high swelling potential will be installed will be used as required to isolate fractured and highly permeable zones and prevent the geological boreholes from becoming preferential transport paths.

A minimized administration area will be maintained during the end of decommissioning to support the post-decommissioning monitoring systems. If at that time it is felt that permanent facilities are no longer required, the monitoring systems could be supported by small enclosures for the electrical equipment, and all other remaining facilities could be removed and the site essentially fully returned to greenfield conditions.

The facility's environmental monitoring carried out during the operational and extended monitoring periods as well as throughout the decommissioning stage may be continued following decommissioning and closure. The scope and duration of such tasks will be decided at the appropriate time by both regulatory entities and society at large.

4.13 References for Chapter 4

- Baumgartner, P. 2006. Generic Thermal-Mechanical-Hydraulic (THM) Data for Sealing Materials – Volume 1: Soil-water Relationships. Ontario Power Generation Report 06819-REP-01300-10122-R00. Toronto, Canada.
- Kwong, G. 2011. Status of Corrosion Studies for Copper Used Fuel Containers under Low Salinity Conditions. Nuclear Waste Management Organization Report NWMO TR-2011-14. Toronto, Canada.
- Maak, P., P. Gierszewski and M. Saiedfar. 2001. Early Failure Probability of Used-Fuel Containers in a Deep Geological Repository. Ontario Power Generation Report 06819-REP-01300-10022-R00, Toronto, Canada.
- McMurry, J., D.A. Dixon, J.D. Garroni, B.M. Ikeda, S. Stroes-Gascoyne, P. Baumgartner and T.W. Melnyk. 2003. Evolution of a Canadian Deep Geologic Repository: Base Scenario. Ontario Power Generation Report 06819-REP-01200-10092-R00. Toronto, Canada.
- NEA. 2012. The Post-Closure Radiological Safety Case for a Spent Fuel Repository in Sweden. An International Peer Review of the SKB License-Application Study of March 2011 (Final report). Nuclear Energy Agency Report NEA/RWM/PEER(2012)2. Paris, France.
- Pitkänen, Jorma. 2010. Inspection of Bottom and Lid Welds for Disposal Canisters. Posiva Report 2010-04. Posiva Oy Olkiluoto, Finland.
- Sandlin, S. 2010a. X-Ray Inspection Setups for the Disposal Canister Welds. Posiva Oy Report 2009-98. Olkiluoto, Finland.
- Sandlin, S. 2010b. High-Energy Radiography for Inspection of the Lid Weld in Disposal Canisters. Posiva Oy Report 2009-82. Olkiluoto, Finland.
- Sandlin, S. 2010c. Defect Detectability in the Disposal Canister Lid-Weld using the 9 MeV Linear Accelerator. Posiva Oy Report 2009-84. Olkiluoto, Finland.
- SKB. 2007. RD&D Programme 2007. Programme for Research, Development and Demonstration of Methods for the Management and Disposal of Nuclear Waste. Swedish Nuclear Fuel and Waste Management Company Report SKB TR-07-12. Stockholm, Sweden.
- SKB. 2008. Inspection of Copper Canister for Spent Nuclear Fuel by means of Ultrasound. FSW Monitoring with Emission, Copper Characterization and Ultrasonic Imaging. Swedish Nuclear Fuel and Waste Management Company Report SKB TR-08-12. Stockholm, Sweden.
- SNC-Lavalin. 2011a. APM Conceptual Design and Cost Estimate Update. Deep Geological Repository Design Report Crystalline Rock Environment Copper Used Fuel Container. SNC-Lavalin Nuclear Report APM-REP-00440-0001. Toronto, Canada.

SNC-Lavalin. 2011b. APM Conceptual Design and Cost Estimate Update. Transportation Design Report. SNC-Lavalin Nuclear Report APM-REP-00440-0005. Toronto, Canada.

Villagran, J. 2012. Used Fuel Container Retrieval from a Deep Geological Repository in Crystalline Rock. Vertical Borehole Configuration. Nuclear Waste Management Organization Report NWMO TR-2012-03. Toronto, Canada.

Wersin, P., L.H. Johnson and I.G. McKinley. 2007. Performance of the bentonite barrier at temperatures beyond 100 °C: A critical review. *Physics and Chemistry of the Earth* 32, p. 780-788.

5. LONG-TERM EVOLUTION OF THE MULTIPLE BARRIER SYSTEM

Chapters 2, 3, and 4 of this report describe aspects of the hypothetical site, the used fuel and the repository design concept to support the presentation of an illustrative postclosure safety assessment. This chapter considers how the main components of the system will interact with each other and with the environment in the long term, consistent with CNSC Guide G-320 (CNSC 2006).

As noted in Chapter 1, a Geosynthesis will be required as part of a safety case for a repository at a selected site. The Geosynthesis provides a description of the site's past geologic evolution, its current state and potential future evolution as influenced by repository construction and external perturbations (i.e., glaciations and earthquakes). In this respect, the Geosynthesis provides evidence to support an understanding of the natural geologic barriers and, in particular, their function and long-term integrity at timeframes relevant to demonstrating repository safety. In the absence of a Geosynthesis, a number of assumptions have been made in this report to illustrate the safety assessment approach and methodology. The evolution of certain site parameters and conditions are presented simply herein to allow illustration of the type of considerations that would be given to specific aspects of the site.

The description in this report is consistent with the expectations of CNSC Guide G-320, which acknowledges that:

“Early in the licensing lifecycle, it may be necessary to rely on design specifications, waste acceptance criteria, generic or default data, and assumptions to describe the waste management system in sufficient detail that its performance can be predicted. At later stages in the facility's development, as-built information and operational data should be used to refine the model of the system for assessment purposes. As with the site model, the model of the waste management system should evolve to become more realistic, and less conservative, based on real data.”

Table 5-1 presents general information for the key repository components, many of which were described in Chapters 2, 3, and 4. The evolution of these components are discussed in separate sections of this chapter.

The NWMO continues technical work in a number of areas that are summarized in the NWMO's research, development and demonstration program as detailed in McKelvie et al. (2011) and Villagran et al. (2011). The technical program's objectives include increasing knowledge and reducing uncertainties associated with components described in this chapter.

Table 5-1: General Parameters

PROPERTY	REFERENCE VALUE
Used Fuel	
Waste form	Used CANDU fuel bundles
Bundle	37-element standard length (e.g., Bruce, Darlington)
Initial mass U	19.25 kg/bundle
Initial mass Zircaloy	2.2 kg/bundle
Average burnup	220 MWh/kgU
Average bundle power rating	455 kW/bundle
Minimum fuel age at placement	30 years (out of reactor)
Container	
Design	Copper outer vessel, with steel load-bearing inner vessel, bundles held in steel sleeves
Outer shell material	Oxygen-free, phosphorus-doped high-purity copper
Inner shell material	Carbon steel
Container fill gas	Inert gas installed at atmospheric pressure
Container capacity	360 bundles
Container dimensions	1.25 m outer diameter x 3.84 m long
Outer shell thickness	25 mm
Container mass	26.7 Mg loaded
Thermal output	1270 W at 30 years, 220 MWh/kgU, 360 bundles
Maximum temperature (outer surface)	100°C
Buffer/Backfill	
Buffer thickness	1.35 m ID with 1.87 m OD annular ring around container
Buffer composition	100% bentonite clay, MX-80 or equivalent
Buffer density	1.6 Mg/m ³ dry density (compacted 100% bentonite)
Backfill thickness (placement room)	See detailed room dimensions
Dense backfill composition	5% bentonite, 25% lake clay, 70% granite aggregate, 2.1 Mg/m ³ dry density
Light backfill composition	50:50 bentonite clay, granite sand, 1.2 Mg/m ³ dry density
Concrete	low-heat high-performance concrete
Repository	
Depth	500 m
Footprint	~6 km ²
General design	In-floor placement, single row of containers along room centre
Excavation method	Controlled drill-and-blast, with drilling of the placement boreholes
Total number of bundles	4.6 million
Total number containers	12,800
Operation phase	38 years
Extended monitoring phase	Up to 70 years (following container placement)

PROPERTY	REFERENCE VALUE
Geosphere	
Predominant rock type	Granite
Rock structure at depth	Intact granitic rock mass
Geothermal gradient	0.012 K/m
Hydraulic conductivity	Varies spatially (4.1×10^{-11} m/s at repository horizon)
Porosity	Varies spatially (0.003 at repository horizon)
Total Dissolved Solids	11,300 mg/L at repository horizon
Surface/Biosphere	
Land surface temperature	+5°C annual average (present)
Air surface temperature	+5°C annual average (present)
Ecosystem	Temperate boreal (present)

5.1 Conceptual Model for the Repository Environment

5.1.1 Repository-induced Disturbances

Disturbances to the geosphere as a result of construction and operation of a repository include those induced by excavation (damage to surrounding host rock and development of unsaturated conditions within the host rock) and due to placement of the waste, including temperature, changes to near-field chemistry and potential gas generation. These processes are summarized in Table 5-2.

Table 5-2: Processes with a Potential Influence on the Near-field Geosphere

PROCESS	POTENTIAL INFLUENCE
RADIATION	
None	<ul style="list-style-type: none"> None
THERMAL	
Heat transport from vault	<ul style="list-style-type: none"> Increased porewater pressure in rock around repository Altered hydraulic conductivity around repository
HYDRAULIC & PNEUMATIC	
Excavation-related drawdown along shaft and access tunnels	<ul style="list-style-type: none"> Temporary desaturated, oxygenated zone around vault
Groundwater flow	<ul style="list-style-type: none"> Saturation of repository Mass transfer of aqueous chemical species at repository interface

PROCESS	POTENTIAL INFLUENCE
MECHANICAL	
Excavation of shaft and rooms	<ul style="list-style-type: none"> • Formation of higher permeability excavation damage zone in shaft and rooms
Thermal stresses	<ul style="list-style-type: none"> • Microcracking
CHEMICAL	
Reactions with redox-sensitive minerals	<ul style="list-style-type: none"> • Maintenance of redox conditions at repository depth
Reactions with repository porewater	<ul style="list-style-type: none"> • Precipitation of secondary minerals near interface
BIOLOGICAL	
Microbial activity	<ul style="list-style-type: none"> • Maintenance of redox conditions at repository depth

Notes: Processes listed are those that are most likely to occur with a notable effect on the near-field geosphere, over a time scale of one million years. Other processes are described in the main text.

5.1.1.1 Excavation Damage Zone

The zone of rock immediately surrounding the placement rooms, tunnels, shafts and other underground openings that are mechanically disturbed during excavation is referred to as the excavation damaged zone (EDZ). This zone is characterized by irreversible structural changes in the rock, such as the formation of microcracks. The extent and properties of these zones depend on factors such as the nature of the host rock, including the rock stress regime, the excavation method, and the location and effectiveness of seals and grouts around the rooms and tunnels. Although it is not a physically separate entity from the host rock, the EDZ could comprise a layer of rock whose hydromechanical properties, particularly permeability, are significantly different from those of the surrounding host rock.

In tunnels constructed using drill-and-blast techniques in crystalline rock, the explosive charge density has been shown to influence the extent and severity of damage in the near-field. Damage is often more prevalent in the floor of such excavations because higher explosive charge densities are typically used in lifter holes in the floor. There is evidence to suggest that connected permeability associated with blast-induced damage may not be continuous across blast rounds in environments with high strength to stress ratio (Simmons, 1992). This is supported by recent in-situ work performed by Posiva (Posiva, 2010) which suggests that the EDZ is not continuous along the tunnel. The EDZ extends outwards from the tunnel wall for distances between 10 and 20 centimeters (Posiva, 2010). In contrast, stress-induced damage in rock environments with low strength to stress ratio may create a continuous zone of connected permeability along the axis of drill-and-blast tunnels. Other processes, such as thermal loading, can intensify the existing EDZ by creating new damage, especially around the in-floor deposition holes.

Perturbations to the geosphere, such as glaciation and earthquakes (see Section 5.5) are not expected to have any major structural effects on the long-term behaviour of the EDZ due the confining pressure of the backfill materials.

5.1.1.2 Repository Saturation

During the construction and operational phases, groundwater inflows into the excavations will be managed through pumping. At a depth of 500 m below the surface, the hydrostatic pressure within a water-saturated rock mass is about 5 MPa. A sharply defined hydraulic gradient would exist between the geosphere at repository depth and the excavated openings (rooms, cross-cuts and drifts), which would be at atmospheric pressure. This difference would tend to draw groundwater through the rock into the open spaces of the repository. The movement of fluids would occur slowly through the low permeability rock, but faster through any transmissive fractures. Groundwater seeping into the repository from the surrounding rock will be pumped away to maintain dry conditions within excavated openings, and may also result in drawdown of the groundwater level above the repository. Evaporation would tend to keep the rock surfaces in the excavated openings dry, and may induce partial desaturation of the rock immediately adjacent to the openings (i.e., within the excavation damaged zone and host rock near the repository). Any dewatering during construction of the repository will be of relatively short duration and will result in groundwater flow(s) toward the repository until pumping activities cease following repository closure. In the postclosure phase, water will flow towards the repository and the near-field will resaturate. Eventually, the flow will stabilize following saturation and will be broadly consistent with the original flow field.

The process of saturation may require long periods of time, as ingress of water may be restricted because of low host rock permeabilities and the use of grouting and effective seals. Furthermore, the rate of resaturation will likely vary at different locations within the repository. In partially-saturated rock, high near-field porewater pressures, as a result of repository heating, could change the flow field and affect resaturation time. McMurry et al. (2004) described a “pre-saturated period”, which covers the time period from when the containers are first placed in a repository until their exterior (copper) surface comes in contact with fully saturated sealing materials. In fractured crystalline rock, it is likely that this pre-saturated period would last from 100 to 1000 years.

Unsaturated conditions, and the time elapsed before resaturation is attained in different areas of the repository, will be affected by the local temperature, chemistry, stress states (including buffer swelling) and groundwater flow rates. Nearby sections of rock (and the buffer and backfill) may never return to their original moisture contents because of hysteresis. The bentonite buffer and backfill will uptake water during repository saturation, resulting in swelling of these materials. Swelling in response to the addition of water is a natural property of bentonite, resulting in the development of its barrier properties (low hydraulic conductivity and high swelling pressure) and self-sealing capabilities.

At the time that the placement rooms are backfilled and sealed, they would contain partially saturated (moistened) buffer and backfill (Table 4-4). Voids (porosity) in the sealing materials would contain trapped air. Heat from the container would cause the nearby bentonite to dry out, and condensation of the water vapour would occur in cooler portions of the sealing materials. The relative humidity of the trapped air in the sealing materials near a container is of interest because corrosion of copper and iron in air is observed to be slow or nonexistent at relative humidities of less than about 60%. Corrosion of steel under the same conditions produces hydrated iron oxides (“rust”).

5.1.2 Changes due to Presence of Waste Placed in the Repository

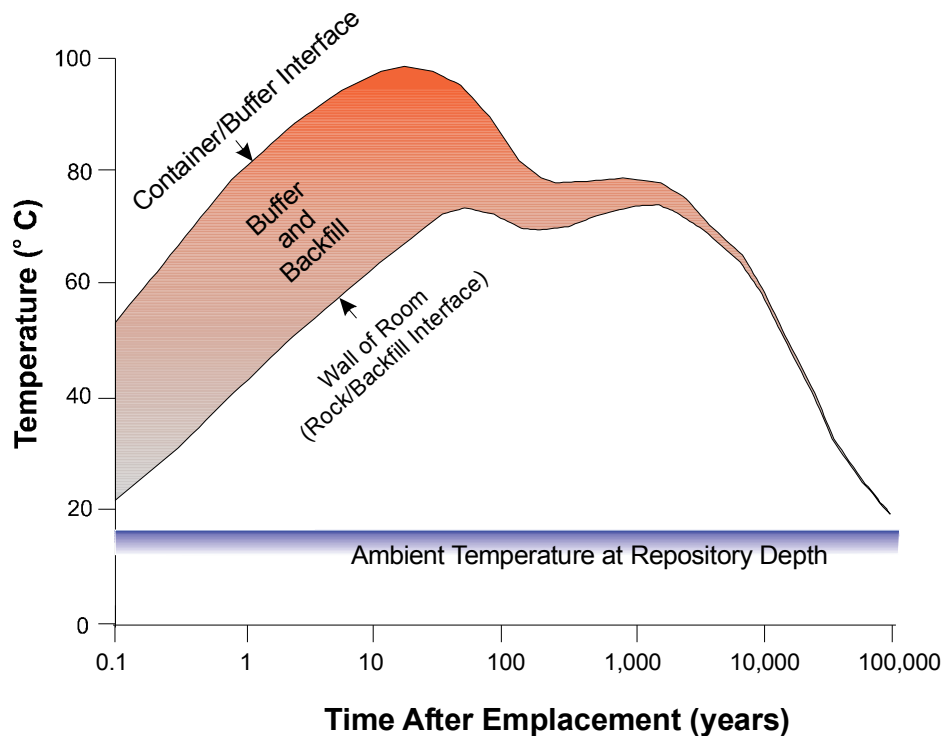
5.1.2.1 Temperature

Among the first changes to occur in a repository after container placement is an increase in temperature of the sealing materials around the containers. The exact distribution and time dependence of temperatures in a repository depends on design details and site-specific conditions.

The main results of the illustrative thermal profiles within the region closest to a container installed in a granitic medium using the in-floor borehole geometry are shown schematically in Figure 5-1 using an example of thermal profiles in a sealed placement room at two points: (a) at the exterior surface of a container, where temperatures of the adjacent buffer would be highest at any given time, and (b) at the interface between backfill and the rock wall at the outer perimeter of the room. In a placement room, the region between these two locations would be occupied by buffer (in borehole) and backfill materials (in placement rooms) that experience an intermediate range of temperature variations, as suggested by the shaded area in the figure.

Key points to note in Figure 5-1 are:

- The temperature of sealing materials adjacent to the surface of the container increases rapidly at first, within days or weeks of placement. Farther from the container, the walls of the placement borehole exhibit a similar temperature response.
- The maximum temperatures of the sealing materials occur within the first 30 years and remains below 100°C which meets the thermal requirements of the buffer. The time scale for this peak is related to the overlapping of the thermal plumes from containers in adjacent placement rooms (as well as the decreasing container thermal power).
- Within the first few hundred years, the localized effects of the multiple heat sources (containers) average out, so that temperature gradients within the repository are no longer sharply defined by component or location.
- After several thousand years, the thermal evolution is marked by a slow, steady cooling. Temperatures return to near-ambient conditions within about 100,000 years.



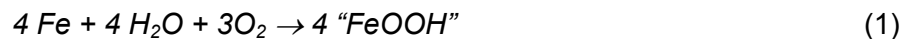
Note: Figure from McMurry et al. (2003).

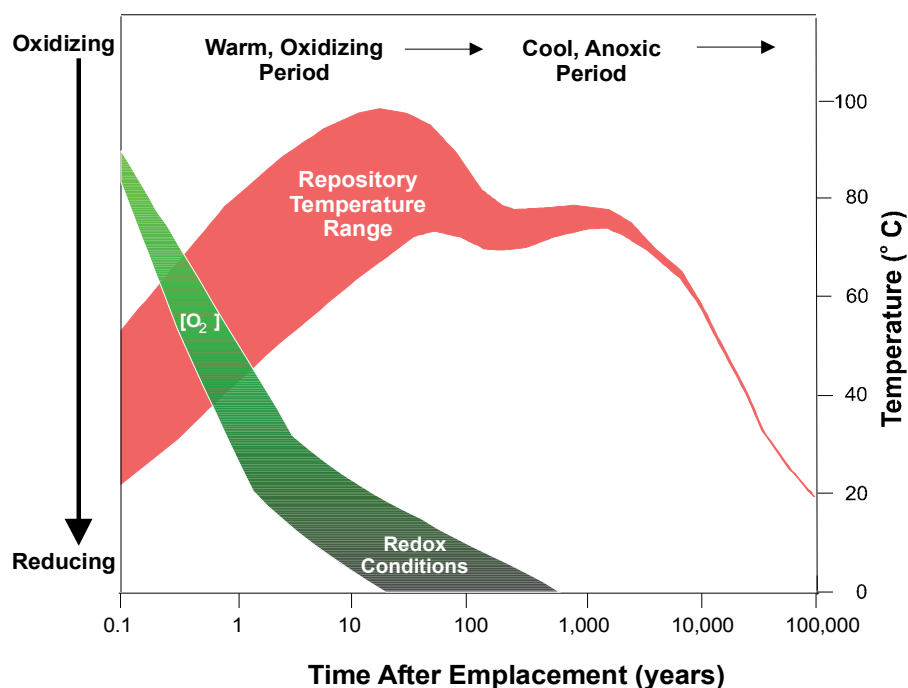
Figure 5-1: Illustrative Example of the Range of Temperature Variation over Time in a Placement Room

5.1.2.2 Near-Field Chemistry

During repository excavation and operations, oxidizing conditions would develop in the porewaters of the adjacent rock due to exposure to the air in the repository. The presence of open rooms at depth would create relatively high inward hydraulic gradients in the immediate vicinity of the repository. The temporary influence of such gradients on the low permeability rock mass enclosing the repository is likely to be negligible.

Redox conditions within the near-field will evolve from an initial oxidizing phase to an anaerobic state (Figure 5-2). The deep groundwater will be reducing (anaerobic), but can initially become oxygenated due to dissolution of O_2 from the repository and air-filled pores of the sealing material. Dissolved oxygen is consumed by a number of reactions, including the electrochemical reduction of O_2 on the surface of the containers (Reaction 1), as well as by reactions with microbes and with redox-sensitive materials throughout the backfill (McMurry et al. 2003).





Note: Figure from McMurry et al. (2003).

Figure 5-2: Evolution of the Repository Environment from an Initial Warm, Oxidizing Period to a Prolonged Cool, Anoxic Phase

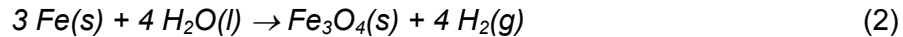
In a saturated repository, most of the repository-related changes in groundwater chemistry would occur at or near the interface between the geosphere and the sealing materials (McMurry et al. 2003). The diffusion of porewater components, or the mixing of fluids at the repository-geosphere interface, is likely to result in the precipitation of secondary phases such as calcite and gypsum at the interface or in nearby fractures in the geosphere. A broader effect would be due to heat from the repository, which would raise the temperature of water in the geosphere. This could result in a slightly greater dissolution rate for feldspars, which are generally the most abundant minerals in plutonic rocks, and for other minerals as well. Later, as the waters cool, the precipitation of secondary phases, such as amorphous silica and calcite, would occur. The extent and significance of the precipitation would depend on site-specific characteristics, such as the distribution and dimensions of the fractures. In the long term, the geosphere, as a whole, would act as a strong buffer in response to chemical and thermal perturbations from a repository. As the pore fluids in the repository evolved to compositions more similar to the surrounding groundwater, and as temperatures in the geosphere gradually returned to ambient levels, the chemical conditions in the geosphere would be diminishingly affected by the presence of a repository.

5.1.2.3 Gas Generation

The main gas phase present initially in the repository would be a relatively small amount of air trapped in the pore spaces of the sealing materials upon closure of the repository. The oxygen (20% of the air) would be consumed relatively quickly. The remainder of the air, mostly

nitrogen, would be compressed as hydrostatic and swelling pressures developed in the sealing materials, and eventually it would dissolve into the porewater and diffuse away.

Gas may also be generated within the repository, e.g., by corrosion of metals such as steel. Gas production is of interest in a repository because at gas pressures high enough to overcome the sealing properties of saturated bentonite, the potential would exist for the formation of cracks through the buffer as the gas escaped (Horseman et al. 1999). These microfractures would be expected to reseal. Under anaerobic conditions, the corrosion of iron (Fe) in steel leads to the formation of iron oxides (e.g., magnetite) and hydrogen gas, as in the following reaction:



For a repository with intact containers, the only steel available for reaction is material from repository construction and operations, such as rock bolts, that remain in the placement rooms after closure. Little hydrogen would be produced by corrosion of these metals. A quantitative discussion of the effects of gas generation appears in Section 7.10.4.

5.2 Used Fuel

A detailed description of the used fuel waste form when placed in the repository is provided in Chapter 3. The used fuel assemblies remain isolated and dry within the container. Nevertheless, their chemical and physical conditions are likely to change over time as a result of various intrinsic processes as outlined in Table 5-3. The main long-term process is radioactive decay (as long as there is no container failure).

Table 5-3: Processes with a Potential Influence on the Evolution of Used Fuel Bundles

PROCESS	POTENTIAL INFLUENCE
RADIATION Radioactive decay	<ul style="list-style-type: none"> • Production of heat, radiation and helium • Decay of radionuclides
THERMAL Heat transfer from fuel to container	<ul style="list-style-type: none"> • Change in fuel temperature
HYDRAULIC & PNEUMATIC None	<ul style="list-style-type: none"> • None
MECHANICAL None	<ul style="list-style-type: none"> • None
CHEMICAL None	<ul style="list-style-type: none"> • None
BIOLOGICAL None	<ul style="list-style-type: none"> • None

Notes: Processes listed are those that are most likely to occur with a notable effect on the used fuel bundles, over a time scale of one million years. Other processes that are expected to have less effect are described in the main text.

5.2.1 Radioactive Decay

When the used fuel is first removed from the reactor it is highly radioactive. This initial activity decreases rapidly over the first year and more slowly thereafter as shown in Figure 5-3.

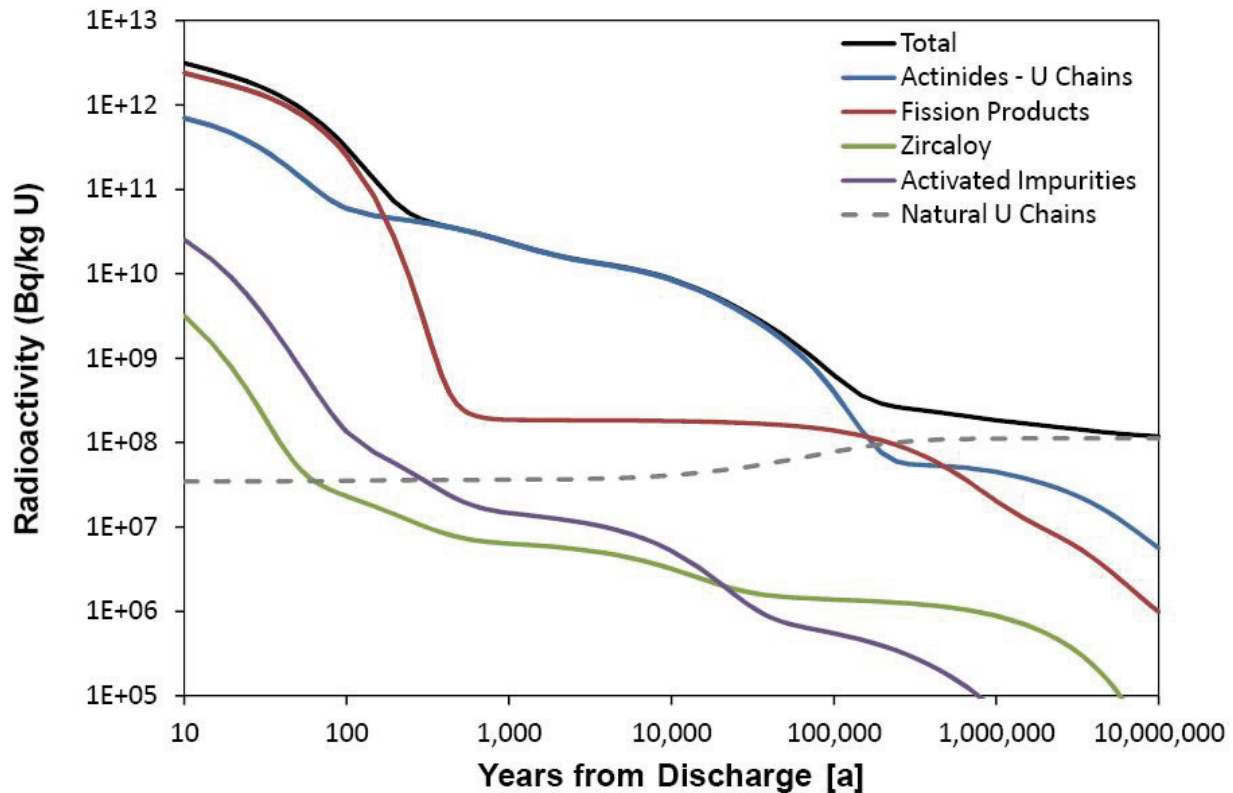
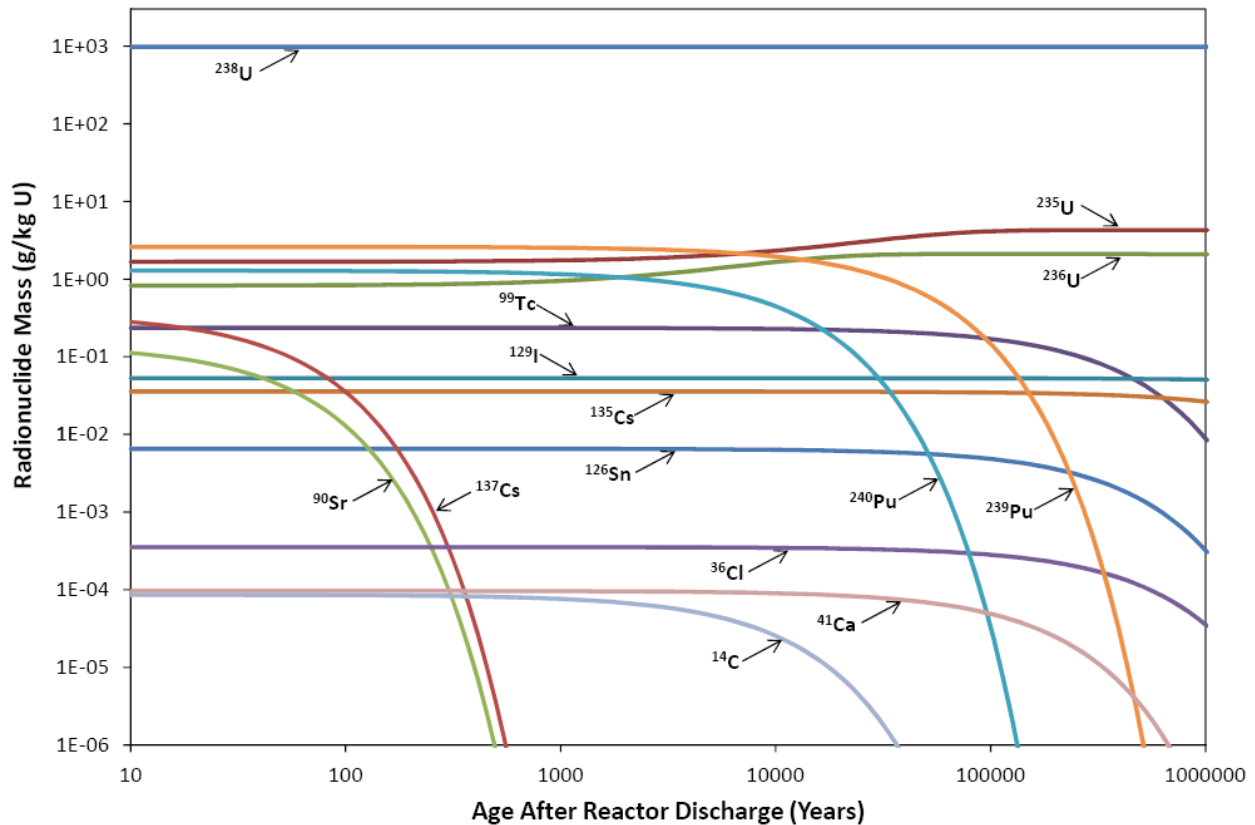


Figure 5-3: Radioactivity of Used CANDU Fuel with a Burnup of 220 MWh/kgU

During the first year out of the reactor, the overall radioactivity decreases to about 1% of its initial value, and within 100 years it decreases to about 0.01% of its initial value. For about 500 years, radioactive decay would be dominated by numerous short-lived fission products, most of which are gamma emitters. Thereafter, the decay process would be dominated by long-lived actinides, including uranium, many of which decay by emission of alpha particles. After about a million years, the total radioactivity in fuel would have declined to levels that are close to that in an equivalent amount of natural uranium.

Radioactive decay would gradually change the radionuclide composition of the used fuel. The radionuclide inventory, radiation output and heat output can be calculated as a function of time, as illustrated in Figure 5-4 for the radionuclide inventory. The greatest change in the composition of the used fuel is a pronounced decrease in fission products after about 500 years. Nevertheless, over a million-year timeframe all of the changes resulting from radioactive decay would represent only a modest rearrangement of the composition of the fuel, of which about 98% would persist as uranium and oxygen.



Note: Figure is based on data taken from Tait et al. (2000).

Figure 5-4: Amounts of Key Long-Lived Radionuclides in Used Fuel (220 MWh/kg U burnup)

5.2.2 Changes in Temperature

In-reactor fission and the subsequent decay processes are accompanied by alpha, beta and gamma radiation which is largely absorbed in the fuel itself, causing it to heat up. Immediately after being removed from a power reactor, a reference used fuel bundle would give off about 27,000 watts of heat. The amount of heat rapidly decreases. After 10 years, the thermal output has decreased to 5.4 watts and after 30 years the same bundle would produce only about 3.5 watts of heat (providing an approximate 10,000 times reduction after 30 years). Figure 5-5 illustrates the time dependence of thermal power for a container with 360 fuel bundles with an average burnup of 220 MWh/kg U. Within several thousand years after placement, the heat output of the entire container would be approximately that of a single 60-watt light bulb.

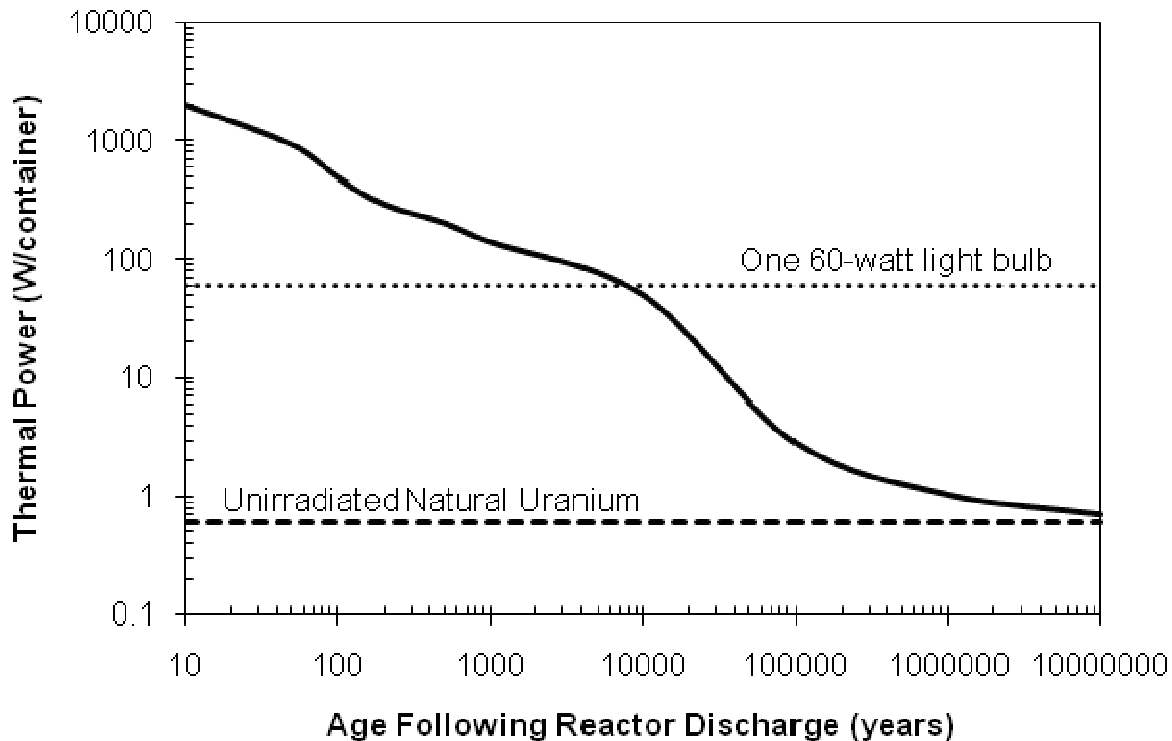


Figure 5-5: Heat Output of a Used Fuel Container with Time

The maximum temperature of the container outer surface is constrained by the design requirement that the temperature of the buffer surrounding the container will not exceed 100°C after placement. This is a conservative requirement common to container design specification in Canada, Sweden and Finland, and allows adverse processes such as thermally-induced alteration of the buffer to be excluded. The temperature of the used fuel bundles inside the container is determined largely by the internal container design which transfers heat from the bundles to the container surface.

The used fuel temperature inside the current reference container, loaded with 30-year-cooled used CANDU fuel, would not exceed 200°C. Temperature measurements of used fuel inside concrete storage containers suggest that, more likely, the interior temperature would be less than about 150°C. The maximum temperature of the used fuel bundles would be attained within about 30 years after placement in the repository and then would decrease correspondingly with the outer container surface temperature (McMurry et al. 2003).

5.2.3 Changes in the UO₂

In the dry and sealed environment inside the containers, there are few processes that would significantly alter the condition of the used fuel assemblies. Over long times, however, some changes are likely to develop by ongoing radioactive decay.

5.2.3.1 Radionuclide Diffusion

The crystalline structure of the UO₂ would experience radiation damage due to alpha-recoil during storage and after placement in a repository, and temperatures would not be high enough to ensure annealing of the damage. Radiation damage has the potential to increase the rate at which gaseous species diffuse through the UO₂; however, theoretical and experimental assessments (Ferry et al. 2008) indicate that this effect is small and there is little redistribution of radionuclides under repository conditions.

5.2.3.2 Changes in the Oxidation State of Fuel

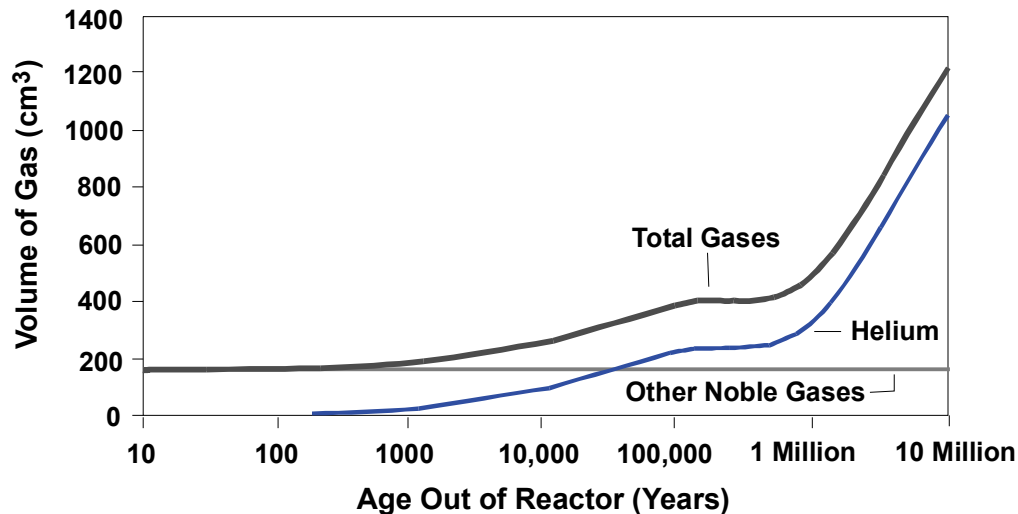
In some cases, radioactive decay results in the formation of an element with a higher oxidation valence than that of the parent radionuclide. In principle this could modify the oxygen potential and oxidation state of the UO₂ matrix, in turn affecting diffusion coefficients for radionuclides. Thermal diffusion coefficients of radionuclides are small at repository temperatures, but these values increase substantially with respect to an increase in the oxygen / metal (O/M) ratio of the fuel. However, any changes in CANDU fuel are expected to be quite small, from O/M ~ 2.001 to 2.010 or less, and would not produce a significant thermal diffusion effect.

The oxidation state of the fuel potentially could also be changed by the reaction of UO₂ and Zr to produce ZrO₂, which is more stable thermodynamically than UO₂. Where the cladding and UO₂ are in direct contact, the Zr eventually would reduce UO₂ to U by solid-state diffusion of oxygen atoms. (One purpose of the CANLUB coating in fuel elements is to inhibit this reaction on the interior surface at reactor temperatures.) This process is unlikely to be significant for used fuel due to the small amount of Zr present (10% of UO₂) and very slow solid-state diffusion rates at repository temperatures (McMurry et al. 2003).

5.2.3.3 Build Up of He Gas

Alpha decay results in the formation of helium (He) atoms in the used fuel. Because helium is stable (non-radioactive) and unreactive with other elements, the total amount of helium gas in the fuel elements would increase over time. Figure 5-6 compares the effective volume of helium gas that would be produced in a CANDU fuel element with the volume of fission gases present in the same element, assuming that none of the gases are retained in the UO₂ matrix. The fission gases formed during irradiation in the nuclear reactor, and their amount (except for radioactive decay) would be constant over time. In contrast, after about 30,000 years, the amount of helium would be equal to that of the fission gases, so that the total amount of gas present would be double that of the initial conditions. After about one million years, the rate at which helium was being produced in the fuel would slow to a value corresponding to the decay of natural uranium and its progeny, but the total amount of helium within the fuel element would continue to increase.

Under repository temperatures, He release from the UO_2 grains to the grain boundaries should be relatively low, so that helium would accumulate within the grains. For low burnup fuel (like CANDU fuel), the quantity of He produced is not sufficient to induce micro-cracking of grains (Ferry et al. 2008), which is the first step before any significant He release to grain boundaries occurs. Thus, the microstructure of CANDU fuel should not significantly evolve with He accumulation, and build up of He gas within the void volume of the fuel element should not occur (see also Section 5.2.4.1).



Note: Figure from McMurry et al. (2003).

Figure 5-6: Equivalent Volume of Gas at Normal Temperature and Pressure Produced in a CANDU Fuel Element (220 MWh/kgU burnup)

5.2.3.4 Alpha Radiation Damage

During radioactive decay, the crystalline matrix of the used fuel would experience localized damage to the crystal lattice from the emission of alpha particles, which travel only short distances from the nucleus but have high energy and a relatively large mass. The implications for radionuclide diffusion have been discussed above.

Natural analogue evidence suggests that alpha irradiation damage would not cause used fuel to crumble, even after extremely long times. At Oklo in western Africa, uraninite (UO_2) ore deposits underwent spontaneous nuclear fission reactions more than two billion years ago. Although affected by brecciation during fission and by subsequent hydrothermal alteration in some cases, the uraninite is still granular and massive (Jensen and Ewing 2001).

5.2.4 Changes in the Zircaloy Cladding

A summary of relevant work associated with changes in the zircaloy cladding is presented in McMurry et al. (2003) and also included in this section. As described below, some of the changes could potentially lead to cracking or rupture of the cladding. However, even if it

occurred, the cracking or rupture of the cladding inside a sealed container would have few consequences. Helium from alpha decay and fission gases would, for example, merely be released into the larger volume of the container interior, and the fuel pellets would be exposed to the inert gas atmosphere inside the container. Although cracked, the cladding itself would continue to provide physical support to most of the used fuel pellets in the fuel element. In the case of a defective container, intact cladding would provide a barrier to water contacting the fuel or to radionuclide release.

5.2.4.1 Zircaloy Creep and Rupture

The most significant physical process potentially affecting the cladding over time is likely to be long-term creep of the Zircaloy, as caused by stresses created by pressure build up inside the sealed fuel elements due to the decay-related production of helium gas. The mechanisms and extent of creep processes in Zircaloy are uncertain. Most creep data for cladding are from high stress, short-term experiments (McMurry et al. 2003).

Conservative calculations, assuming the He gas migrates to the fuel-cladding gap, suggest that given sufficient time, the gas pressure inside the sealed fuel element would increase to the point that the Zircaloy cladding would rupture. However, as indicated in Section 5.2.3.3, it is unlikely that the He would escape from the fuel grains and increase the pressure within the cladding. Hence, He generation should not lead to rupture of the Zircaloy cladding on relevant time scales.

5.2.4.2 Uniform Corrosion (Oxidation) of Cladding

The corrosion properties of Zircaloy cladding have been determined from almost 50 years of experience with reactor operation, pool storage, and dry storage of used fuel. When Zircaloy is exposed to air, a thin passive zirconium oxide film forms rapidly on its surface which then inhibits further corrosion. Experiments were conducted that examined the condition of used CANDU fuel under dry storage conditions over several decades. It was found that the average outer and inner surface zirconium oxide thickness, after 19 years of dry air storage at seasonally varying temperatures, was about 6 μm , slightly more than an average pre-storage oxide layer thickness of about 4 μm . Therefore, most of the uniform corrosion of the Zircaloy would have occurred prior to placement (McMurry et al. 2003). Shoesmith and Zagidulin (2010) also indicate that passive corrosion rates of Zircaloy would be very low.

For the repository, the containers would be sealed in an inert gas. In the absence of oxygen, further growth of a uniform oxidation film on the cladding cannot occur.

5.2.4.3 Hydrogen Absorption and Zircaloy Embrittlement

As-fabricated Zircaloy cladding has a residual hydrogen concentration of about 25 $\mu\text{g}\cdot\text{g}^{-1}$. After use in a CANDU reactor, the cladding also contains up to about 100 $\mu\text{g}\cdot\text{g}^{-1}$ of deuterium, absorbed in-reactor from the heavy water coolant, in addition to trace amounts of tritium. The hydrogen precipitates as zirconium hydrides in the Zircaloy after the fuel is removed from the reactor and cools. The hydrides result in a less ductile (more brittle) Zircaloy that is more susceptible to fracturing (McMurry et al. 2003).

In intact used fuel containers that had been dried and backfilled with an inert gas prior to sealing, little or no hydrogen would be available for reaction with the cladding after placement. Small amounts of H₂O may be present as residual humidity or as liquid water (e.g., in defected fuel elements). Hydrogen would be released from this water via radiolysis or as the water was consumed by corrosion of the steel interior of the container, which could be absorbed by the Zircaloy and also increase the amount of hydrides present.

5.2.4.4 Delayed Hydride Cracking

The main factors required for delayed hydride cracking are sufficient tensile stress, a defect site to concentrate the stress, and sufficient hydrogen in the metal. Even where hydrogen is distributed in relatively low concentrations in Zircaloy, under certain conditions of stress and temperature the hydrogen can diffuse through the metal to form locally high hydrogen concentrations that lead to the precipitation of zirconium hydrides. These hydrides are brittle and tend to crack.

Detailed examination of used CANDU fuel stored in dry air at 150°C for 15 years indicates that highly stressed areas in the cladding must be present for delayed hydride cracking to occur. Generally the most stressed areas in cladding are the heat-affected zones at and near welds. The timing and extent of delayed hydride cracking in a repository would be controlled by diffusion of hydrogen to the crack tip. At low (container interior) temperatures and under simple self-support loads, it is difficult to predict failure by hydride cracking using data from conventional short-term mechanical tests. The susceptibility of cladding to delayed hydride cracking is, however, unlikely to be significant (Freire-Canosa 2011).

5.2.4.5 Stress Corrosion Cracking

Stress corrosion cracking of zirconium metal occurs in oxidizing environments, in strongly oxidizing neutral saline solutions, and in the presence of some metals and gases such as cesium and iodine. Little work has been directed towards the study of stress corrosion cracking of Zircaloy under conditions such as would occur in a deep geological repository. However, the dry environment inside an unbreached container would not contain sufficient quantities of strongly oxidizing agents (such as nitric acid or hydrogen peroxide) or of iodine gas from fuel elements to induce stress corrosion cracking (McMurry et al. 2003). Moreover, CANLUB inhibits the diffusion of iodine into the Zircaloy. In addition, in CANDU fuel almost all of the iodine in the fuel gap is present as cesium iodide (CsI) and so is unable to form the zirconium iodides that are thought to be the chemical precursors of stress corrosion cracking (OPG 2002).

5.2.4.6 Pellet Swelling and Cladding “Unzipping”

Cladding “unzipping” is driven by the expansion of a fuel pellet (pellet swelling) in proximity to a defect in the cladding, causing a strain in the cladding that extends the size of the defect. If the two processes (i.e., swelling and rupture) perpetuate each other, the deformation would propagate in increments over time (“unzipping”). One example of this phenomenon occurs when water enters a fuel element through a pinhole defect and reacts with the fuel, transforming the UO₂ into the less-dense phase U₃O₈. The additional stress exerted on the defect site by the expansion in the volume of the pellet then leads to further cracking of the cladding. More water is then able to enter the fuel element, which in turn leads to more alteration, more swelling, and

further deformation of the cladding. In intact containers, there would be no source of water to initiate pellet swelling, so unzipping by this process can be disregarded.

5.2.5 Other Processes

Several other processes have been described (McMurry et al. 2003) and are expected to have minimal or no effects on the evolution of the used fuel, as indicated below.

5.2.5.1 Criticality

Criticality is not an issue for several reasons, the most important of which is that CANDU fuel cannot become critical under any circumstances without the presence of heavy water, regardless of the density or age of the fuel. Ordinary water is insufficient to induce criticality. Moreover, water would have no access to the used fuel in intact containers and so it could not act as a moderator (McMurry et al. 2003).

5.2.5.2 Hydraulic Processes

As long as the containers remain intact, there are no hydraulic processes affecting the used fuel assemblies.

5.2.5.3 Mechanical Stresses

As long as the fuel bundles are supported by baskets in intact containers, they are not subjected to significant load-bearing stresses. If tremors associated with earthquakes caused the fuel bundles to vibrate sufficiently, presumably some of the fuel pellets or the cladding could be damaged. The damaged material would remain in an intact container, and the overall evolution of the used fuel bundles would not be significantly changed.

5.2.5.4 Biological Processes

No changes arising from biological processes are expected because the combination of high temperatures, significant radiation fields, and the absence of water and organic carbon would exclude any biological reactions inside a container.

5.2.6 Confidence and Uncertainties

At the time of placement in a deep geological repository, the physical properties of the used fuel and the inventory of radionuclides would be well characterized. Radionuclide decay constants are well defined, and so the changes in the inventory and the related changes in decay heat over time can be estimated with a high degree of confidence.

The rates of several processes, such as the diffusion of helium in UO_2 and of hydrogen in Zircaloy, are influenced by temperature. These rates would be low since the temperature inside the container would be at most several tens of degrees hotter than the exterior container surface, which would be kept to less than 100°C by design, and drop to ambient host rock temperatures on a 100,000 year timeframe.

In the dry and closed-system environment provided by an intact and load-bearing container, the physical condition of the fuel is not expected to change significantly over long periods of time. The only significant factor would be container failure, which is discussed later.

5.3 Evolution of a Used Fuel Container

As described in Chapter 1, the design of the reference container is consistent with lifetimes in excess of 100,000 years. To achieve such lifetimes, a container must be able to withstand the expected geological evolution from hot, dry and aerobic, to cool, water saturated anaerobic conditions. Within this context, specific effects have been examined as they pertain to the evolution of the used fuel container in a deep geological repository; these are summarized in Section 5.3.1, below. In addition, and in keeping with the safety arguments described in Chapter 1, specific conditions that pertain to a defective container are described in Section 5.3.2, below.

5.3.1 Evolution of Intact Containers

As described in Section 4.2, the reference container design for a deep geological repository in crystalline rock consists of a copper outer vessel that encloses a steel inner vessel. Upon placement in the repository, the sole function of the copper outer vessel is to protect the inner steel vessel and container contents from corrosion, as the copper outer vessel is not designed to be load-bearing. When hydrostatic and swelling pressures are applied to the container, the copper shell would compress onto the steel inner vessel, transferring the external load to the steel inner vessel (Poon et al. 2001), which is designed to withstand an external isotropic pressure of 45 MPa at 50°C . This value includes the hydrostatic load exerted at repository depth plus a 3,000 m glacier above the repository, and the swelling pressure exerted by the buffer material. Thus, in the analysis of intact containers, many of the specific effects of placement of the containers within the repository are limited to processes that affect the outer copper shell and inner steel vessel. The main processes experienced by the container over time are listed in Table 5-4 and discussed in the succeeding sections.

Table 5-4: Processes with a Potential Influence on the Evolution of Containers

PROCESS	POTENTIAL INFLUENCE
RADIATION None	<ul style="list-style-type: none"> • None
THERMAL Heat transfer from fuel to container	<ul style="list-style-type: none"> • Change in container temperature
HYDRAULIC & PNEUMATIC Saturation of repository	<ul style="list-style-type: none"> • Hydrostatic and swelling pressure applied to container • Initiation of aqueous corrosion on container surface
MECHANICAL Hydrostatic and swelling pressure	<ul style="list-style-type: none"> • Stresses on container
Glacial loading	<ul style="list-style-type: none"> • Stresses on container
Creep	<ul style="list-style-type: none"> • Deformation of copper shell onto steel inner vessel
CHEMICAL Reactions with oxygen in sealing materials or sulphides in water	<ul style="list-style-type: none"> • Thin layer of corrosion products on container surface • Corrosion of container
BIOLOGICAL Aerobic microbial activity in vault	<ul style="list-style-type: none"> • Consumption of oxygen • Production of sulphide

Notes: Processes listed are those that are most likely to occur with a notable effect on the containers, over a time scale of one million years. Other processes are described in the main text.

5.3.1.1 Irradiation of Container Materials

McMurry et al. (2003) summarizes the considerations for the irradiation of container materials. The radioactivity inside the container is at its maximum value when the fuel is first loaded. The radiation field around the container is dominated by the gamma emission from short-lived fission products, which decay almost completely within the first 500 years after placement (see Figure 5-3). Thereafter, the residual radiation field would be very low because most of the remaining radioactivity would be from the alpha emission of long-lived actinides. Alpha particles do not penetrate beyond the fuel cladding.

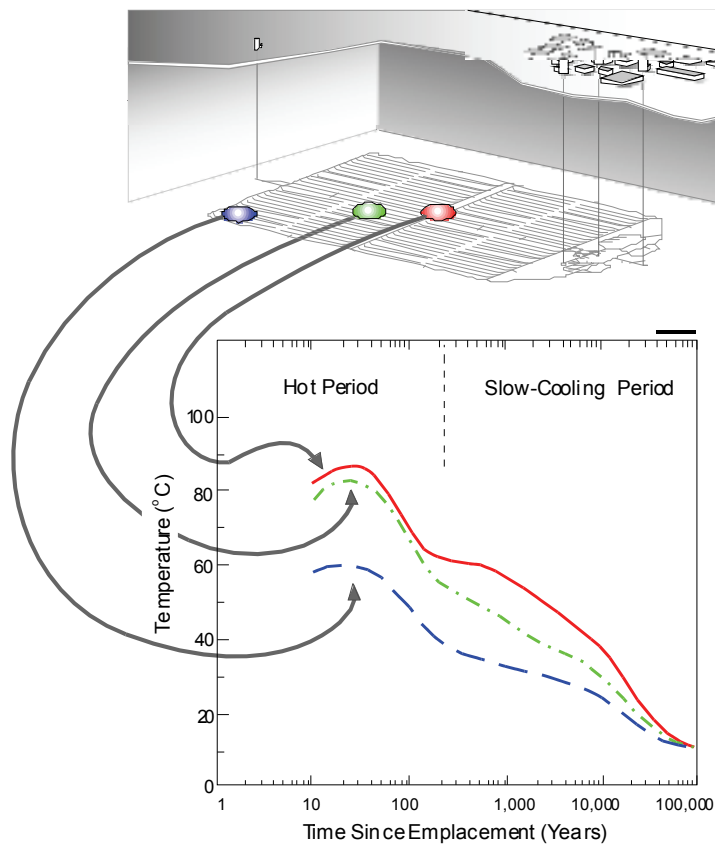
High levels of neutron radiation, as found in nuclear reactors, can lead to hardening and embrittlement of reactor parts. The neutron flux inside a reactor is on the order of $4 \times 10^{13} \text{ n}\cdot\text{cm}^{-2}\cdot\text{s}^{-1}$ (neutron per centimeter squared, per second). In comparison, the neutron flux from used fuel is much smaller ($\sim 10^2 - 10^3 \text{ n}\cdot\text{cm}^{-2}\cdot\text{s}^{-1}$ initially in a container of used CANDU fuel) and is mainly lower-energy thermal neutrons. Over a million-year timeframe, the total neutron fluence experienced would be less than $10^{15} \text{ n}\cdot\text{cm}^{-2}$ (based on Tait et al. 2000), whereas a neutron fluence greater than $10^{22} \text{ n}\cdot\text{cm}^{-2}$ would be required to produce measurable displacement effects in metal. Defect formation from thermal neutrons would require neutron fluences of $10^{19} - 10^{21} \text{ n}\cdot\text{cm}^{-2}$ in copper and iron at 70 - 80°C to result in significant hardening. Consequently, it is unlikely that the container metals would be significantly affected by radiation over a million year exposure to used fuel (McMurry et al. 2003).

Radiation would be more likely to have a small indirect influence on container properties, in terms of changes to the chemical environment that would result from the decomposition (radiolysis) of air and water in the vicinity of the container.

5.3.1.2 Changes in Container Temperature

The exterior surface temperature of the container after placement is constrained to a maximum value of 100°C for the reference in-floor borehole placement concept. The purpose of this design constraint is to minimize the effect of elevated temperatures on the physical properties of the buffer sealing material surrounding the container. Only a fraction of the containers in a repository (those with the youngest fuel and / or the highest burnup values) would approach this maximum temperature. In the case of containers that otherwise are identical, those near the edges of a repository would have lower maximum temperatures than those in the centre of a repository because they would be less affected by heat from adjacent containers as illustrated in Figure 5-7.

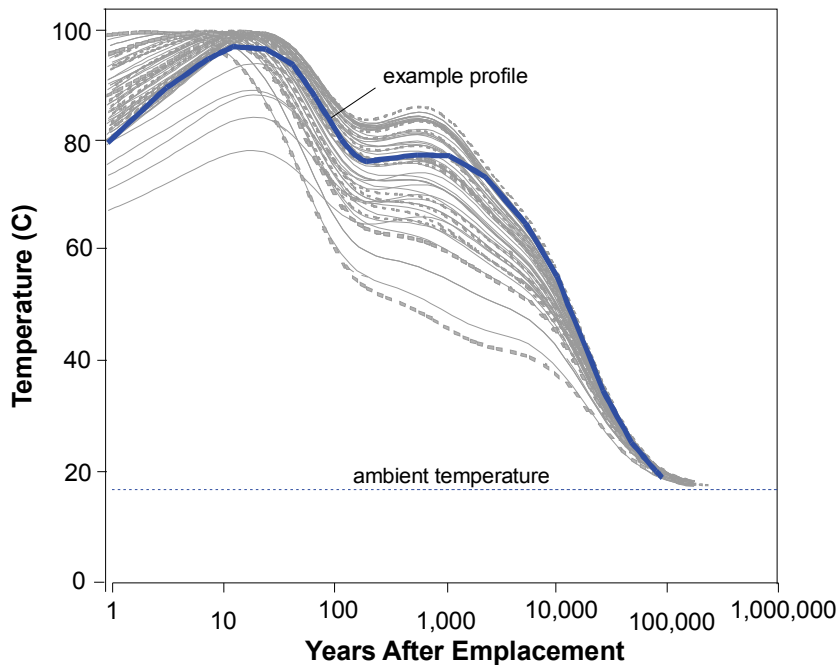
The temperature of the used fuel container changes over time due to the decay of the radionuclides inside the container. The extent of heating and cooling and the rate at which container temperatures change is influenced by many factors, such as the quantity of used fuel in the container, the burnup of the used fuel, the age of the used fuel at the time of placement, the dimensions and geometry of the container, the heat-transfer properties of the geosphere and of the sealing materials, the distribution of ambient temperatures at the site, the selected depth of repository, the selected waste placement method, and the design features of the repository layout (i.e., spacing between containers within a placement room, the spacing between placement rooms, and the plan area and shape of the repository). A difference in any of these factors would affect the thermal profile of a container.



Notes: Figure is from McMurry et al. (2003). Although otherwise identical, containers near the repository margin would remain cooler than those near the centre.

Figure 5-7: Illustrative Container Cooling Profiles at Three Generalized Locations within a Repository

This point is illustrated by a study by Baumgartner and Ates (2002) which calculated more than 70 different container thermal profiles, in each case assuming that the containers were placed in a hypothetical square repository containing 3.6 million used fuel bundles at a repository depth of 1,000 m. The study considered 14 different combinations of container geometries and quantities of used fuel per container, two different burnup values of used fuel, and two different waste placement methods. The resulting container surface temperature profiles are plotted in Figure 5-8.



Note: Figure from McMurry et al. (2003).

Figure 5-8: Illustrative Variation in Container Surface Temperature over Time for Various Container Designs and Fuel Loading Characteristics

Although the thermal profiles are represented by a wide distribution of curves, they share several key features:

- (1) The maximum container surface temperature does not exceed 100°C. This constraint is met for the conceptual repository in this study with axial container spacing of 4.2 m and room centre-to-centre spacing of 40 m.
- (2) The maximum container surface temperature is reached relatively soon after placement (i.e., within 30 years). In general, the greater the heat flux for the container, the sooner the peak temperature is attained.
- (3) There is a subsequent plateau or slow decline in the container temperature. The specific shape of this region is influenced by repository design and site conditions.
- (4) The containers cool to near-ambient conditions after approximately 100,000 years.

Within the container, transport of heat would take place by conduction through the metals, as well as by thermal radiation and convection through gas-filled spaces. Potential gaps affecting heat transfer inside the container include spaces between the fuel bundles and the steel baskets, between the steel baskets and the steel inner vessel, and between the steel and copper vessels. On the outside of the container, there may also be gaps in the contact between the copper vessel and the adjacent sealing materials. The temperature profile within the current reference container would depend on the details of the container design and placement, especially the nature of the steel-copper gap. Simple estimates indicate that the temperature

difference across the copper shell and steel inner vessel is unlikely to be more than about 30°C because of the relatively high thermal conductivity of these materials.

5.3.1.3 Changes to Mechanical Integrity

Containers would experience a range of stress conditions over time. The structural design of the container is determined largely by the requirement to provide adequate mechanical strength throughout its design life.

5.3.1.3.1 Early Conditions

As soon as the steel lid is bolted onto the steel vessel, heat from the used fuel bundles would increase the pressure of the inert gas inside the vessel. For example, at a temperature of 120°C inside the container, the internal gas pressure would increase by about 40%. This internal pressure would have a negligible effect on container stresses and would decrease with time as the container cooled.

Another early heat-related stress effect would be the differential expansion of the metals in the container. The coefficient of thermal expansion of steel is about 3.7×10^{-6} mm/mm/°C at 100°C, whereas that of copper is about 5.4×10^{-6} mm/mm/°C. Over a period of hours to days after the used fuel bundles are loaded, the temperature increase would result in a slight differential thermal expansion of the two container materials, causing the small gap between the outer and inner vessels to increase slightly (by less than a tenth of a millimetre). This effect would not be significant.

After the containers are loaded and sealed, they would be transferred from the fuel loading and container assembly area to a placement room in the repository. Depending on the facility design, the transportation and placement process would involve multiple stages of handling of the containers, possibly including several rotations from vertical to horizontal orientations during transfer from the surface facilities to a final position in a placement room. This handling would impose various short-term loads on the container that would be within its design basis.

5.3.1.3.2 Effects of Hydrostatic and Buffer Swelling Pressures

After placement, the external load on the containers initially would consist of little more than the weight of the overlying sealing materials. The load would gradually increase during saturation of the repository. The swelling of the bentonite in the sealing materials is likely to occur unevenly on a local scale because the swelling would be controlled by the supply of water from the rock, by the shape of the room, and by the pathway of water along interfaces. The heterogeneous development of swelling pressures would result initially in non-uniform external loads on the containers, an effect that is expected to diminish as full saturation is achieved (McMurry et al. 2003).

By the time a repository is fully saturated, the hydrostatic pressure would have increased to about 5 MPa at the repository depth of 500 m. Buffer swelling pressures would contribute up to another 5 to 10 MPa to the load on the containers, depending on groundwater salinity and buffer density. Under these loading conditions the copper shell would be expected to compress onto the steel load-bearing inner vessel. The resulting load is within the container design basis.

5.3.1.3.3 Effects of Glacial Loading

Additional compressive stresses would be applied to the container by glaciation. It is unlikely that an ice sheet would develop over the repository until at least several tens of thousands of years had elapsed. By this time, the buffer saturation-related pressure loads would be fully applied. The increased stresses associated with glacial loading are likely to recur several times over a million-year timeframe because of successive glaciation events (Figure 5-9).

The container design is based on an increase in hydrostatic pressure of 30 MPa from glacial loading, a value that corresponds to the maximum loading from a 3000-metre thick ice sheet above the repository location. The container thus is designed to withstand an external isotropic pressure of 45 MPa (30 MPa due to glaciation and up to 15 MPa due to the pre-glaciation hydrostatic and swelling pressures). Recent studies have indicated that a glacial loading estimate of 30 MPa is likely to be conservative, i.e., the additional hydrostatic pressure at repository depth is likely to be considerably less than this (Walsh and Avis 2010).

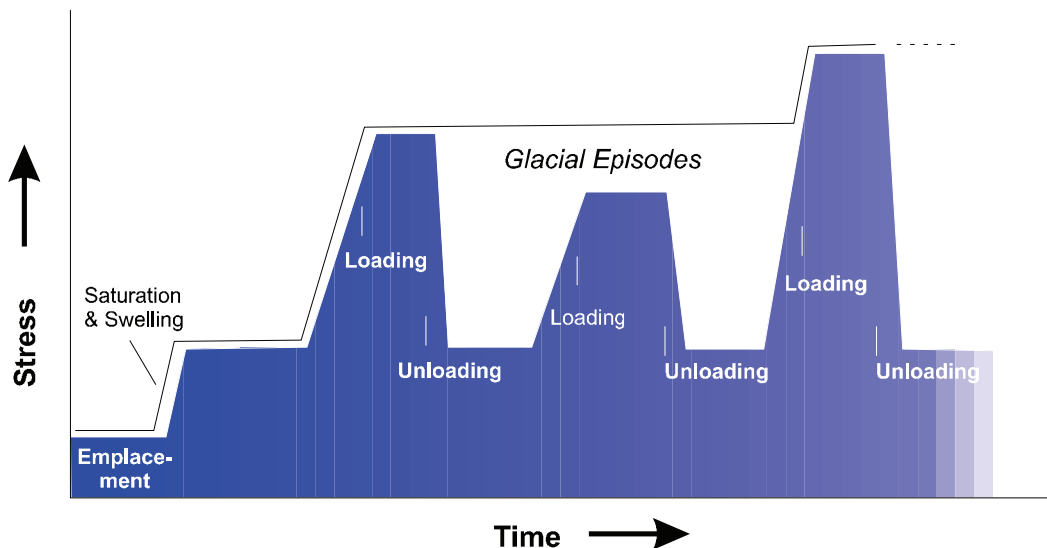


Figure 5-9: Schematic Representation of the Loading History in a Repository

5.3.1.3.4 Effect of Seismic Stresses

The Canadian Shield is characterized in general by low levels of seismic activity as it is in the center of a stable craton (Atkinson and Martens 2007). Large earthquakes would therefore be very unlikely, although an increase in the number and intensity of earthquakes is likely in response to the reduced pressure as ice sheets retreat.

Earthquakes in general are less destructive at depth than at the surface, diminishing the impact of any seismic activity on a deep geological repository, and post-glacial faulting is more likely to reactivate an existing zone of weakness in the rock than it is to develop new fractures (McMurry et al. 2003). In addition, an analysis conducted for an in-floor placement design by the Swedish repository program (Raiko et al. 2010) concluded that there would be no significant

effect on containers even if an earthquake resulted in shearing over a distance of 0.05 m in the rock directly across the container location.

The present hypothetical repository site is assumed to be a low seismicity area, consistent with the general Canadian Shield. The repository is placed away from the large fractures, and containers are only placed in boreholes without significant local fractures. Therefore, normal small earthquakes have no significant effect on the site, repository or containers, while large earthquakes are considered through the selection of high-permeabilities for the existing fractures. Other effects of a very large earthquake are considered within the Disruptive Scenarios discussion later.

5.3.1.3.5 Effect of Creep

McMurry et al. (2003) summarizes the potential effects of creep on the copper container. Creep is the slow deformation of a material under an applied stress that results in a permanent change in shape. The process of creep in copper is governed by properties of the metal (e.g., grain size, impurities at grain boundaries, crystallographic structure), temperature, stress level, and time. To maintain the mechanical integrity of the copper shell, the container is designed so that the total of the elastic, plastic, and creep strains developed in the metal does not exceed its creep-rupture strain over the design lifetime. A number of research and development studies have been carried out in the Canadian, Swedish, and Finnish nuclear fuel waste management programs to assess the creep lifetime of dual-vessel containers that have a copper outer shell. These studies have included the development of copper materials with improved creep ductility and container designs that limit the amount of creep deformation. The upper bound of the creep rates for a copper vessel in a deep geological repository have been estimated to be in the range of 3×10^{-13} to $1 \times 10^{-10} \text{ s}^{-1}$.

During the saturation period, when hydrostatic and swelling pressures begin to apply stress to the container, the copper shell would have a surface temperature of about 100°C at most. The copper would compress onto the steel vessel, closing the small assembly gap (1 mm) that was initially present between the two parts of the container. At the expected temperature and pressure, the main process by which this deformation takes place is likely to be creep. Plastic yielding, which occurs when the yield stress limit of a solid is exceeded, would be the other plausible mechanism by which the copper would deform onto the steel vessel. However, non-linear finite element analyses of container behaviour under these conditions have indicated that the creep-relaxation process would tend to relieve stress on a microscopic scale. This suggests that the maximum stresses that develop in the copper shell during deformation would be limited to values that are below the yield stress limit of the copper, preventing plastic yielding from taking place.

In certain areas (e.g., around the lid), some gap is likely to remain between the copper and steel, and localized creep of copper would be likely to continue. First-order analyses have suggested that the additional creep strain developed in these areas would be negligible because of the low stresses and low temperatures at long times (Saiedfar and Maak 2002).

Under isotropic loading, independent creep of the copper would cease after the copper compresses against the steel vessel. If any further creep of copper were to occur, it would be in response to deformation of the steel vessel. However, the thick-walled steel vessel would be designed to remain load-bearing over the design lifetime for a container (Werme 1998 and Saiedfar and Maak 2002). For example the maximum stresses developed in the reference steel

vessel are only about 30% of its yield strength under saturation-related pressures, and approaches the yield strength under peak design-basis glaciation pressures. The creep rate of steel under the anticipated loading conditions (20% of its ultimate tensile strength under saturation-related pressures) and temperature (20% of melting temperature) is insignificant. The exact rate is uncertain, but it is expected that it would take at least 100,000 years for any appreciable amount of creep deformation to develop in the steel vessel (Dutton 2006).

5.3.1.4 Effect of Chemical Processes Inside the Container

The containers remain intact throughout the timeframe of the study. Chemical changes over time involving those processes that affect the interior of the container (a closed system) may therefore be considered separately from those that affect its exterior surface (which is part of an open system).

At the time of packaging, the container interior is dry, as are the used fuel assemblies. Most water vapour is eliminated from the container interior during packaging operations because the air inside the container is replaced by an inert gas before the container is sealed. The small amount of residual air and water vapour would provide some oxygen to react with the metals in the container interior (Section 5.2.4.3), and the irradiation of any air present would produce small quantities of nitrogen oxides by radiolysis. For the anticipated “dry” conditions inside the container, aggressive corrosive agents such as nitric acid would not form (McMurry et al. 2003).

The zirconium alloy in the fuel bundles would already have a surface film of ZrO_2 that formed at high temperatures in a reactor. This resistant ZrO_2 surface layer on the cladding would inhibit any further reaction with the small amount of air initially available inside the container. In contrast, the more porous iron oxide layer on steel would slow but not prevent further reaction. Thermodynamic arguments predict that reaction between the iron and oxygen would occur even at a very low oxygen partial pressure. The steel inner vessel and the steel baskets holding the fuel bundles would tend to react rapidly with any available oxygen, forming iron oxides/hydroxides as corrosion products. Corrosion of the steel would effectively remove any gaseous oxygen from the interior of the container, so that conditions in the interior would become anoxic. An upper bound on the amount of corrosion from residual air can be obtained by assuming that the container is filled with air instead of with an inert gas. For a container design as indicated in Table 5-1, the total internal void volume is about 1.58 m^3 . The total consumption of oxygen from air trapped in this space would result in 0.01 mm of corrosion of the steel basket walls. This indicates that there would be more than enough iron present to consume any oxygen (McMurry et al. 2003).

Fuel elements with defective cladding would release some fission gases to the container interior, particularly if the cladding fails after the container is sealed. Iodine, which assists stress corrosion cracking of metals under some conditions, is the most noteworthy of these gases. The partial pressure and total quantities of any released gases would be small, (e.g., $<10^{-40}$ MPa for oxygen and $<10^{-17}$ MPa for iodine), and the CANLUB coating within the fuel element would tend to absorb any gaseous iodine. Most of the other released gases would be adsorbed onto the internal surfaces of the steel structure, or they would be distributed among the exposed iron, zirconium and copper surfaces, not resulting in any significant changes to the interior of the container (McMurry et al. 2003).

In summary, the scarcity of oxygen and water inside the sealed containers would greatly limit the chemical changes that would take place there. Water radiolysis, accompanied by reactions

with the metal interior of the container, would quickly consume the small amount of gaseous oxygen that would be present. The interior of the container thereafter would have a dry, reducing chemical environment that would persist as long as the container remains intact.

5.3.1.5 Effect of Chemical Processes Outside the Container

This section summarizes the current understanding of the corrosion behaviour of copper used fuel containers in a deep geological repository. This understanding has been developed on the basis of an extensive experimental program carried out in Canada and elsewhere over the past 30 years and on the results of mechanistically based mathematical modelling of various corrosion processes.

The corrosion behaviour of copper depends on the nature of the environmental conditions. For this discussion, the following attributes of the container and reference repository design are important:

- The container corrosion barrier is manufactured from an oxygen-free grade of copper;
- The containers are surrounded by a buffer material comprising highly compacted bentonite (HCB) with a dry density of at least 1.6 Mg/m^3 ;
- The groundwater is a Ca-Na-based chloride solution, with smaller amounts of sulphate and low levels of carbonate;
- The available O_2 is limited to that trapped initially in the pores of the buffer and backfill materials, the groundwater itself being O_2 -free;
- The container comprises a thick inner steel vessel resulting in a maximum surface absorbed dose rate of $<1 \text{ Gy}\cdot\text{h}^{-1}$;
- The maximum container surface temperature is 100°C (this is related more to the stability of the bentonite buffer in the reference design than the corrosion behaviour of the container);
- There is a period of unsaturated conditions immediately following container placement and prior to saturation of the repository;
- There is no sulphide (HS^-) present in the groundwater;
- The container is subject to external loading from a combination of the hydrostatic load and bentonite swelling pressure; and
- The container is placed in the deposition borehole soon after loading and sealing of the container.

Experimental research has focussed on uniform corrosion, SCC and MIC. Corrosion modelling has evaluated uniform and pitting corrosion, SCC, and MIC based on anticipated repository environments and their evolution with time. A list of studies conducted in the Canadian copper corrosion program is tabulated in Kwong (2011).

Overall, these studies conclude that a copper-shelled used fuel container in a deep geological repository will be primarily subject to general corrosion. The degree of localized attack (pitting), MIC and SCC will be negligible and can be controlled using sound engineering design and practice. All forms of corrosion will be stifled as the repository environment becomes anoxic. The various corrosion mechanisms are discussed in more detail in the following sections.

The important characteristics of the corrosion of copper containers in a deep geological repository are:

- The corrosion behaviour changes with time, largely as a result of the evolution of the repository environment (King and Shoesmith 2010). This environment evolves from an initial period of warm, aerobic conditions to an indefinite period of cool, anoxic conditions. From a corrosion perspective, this environmental evolution means that localized corrosion processes are limited to the early period, with corrosion becoming more uniform in nature as time progresses.
- The nature of the environment at the container surface determines the corrosion behaviour. The surface environment can be different from that in the host rock as a result of the chemical conditioning of the groundwater by the bentonite clay and the slow mass transport of reactants to, and of corrosion products away, from the container surface due to the presence of the bentonite (McMurry et al. 2003).
- In general, groundwater chloride promotes the uniform dissolution of copper and suppresses localized corrosion and SCC (King et al. 2010, 2011a).
- The highly compacted bentonite clay buffer around the container also suppresses microbial activity.

5.3.1.5.1 Uniform Corrosion

The uniform corrosion of copper in the environment expected in a deep geological repository has been extensively studied and the corrosion mechanism is well understood and summarized in Kwong (2011). Figure 5-10 illustrates the mechanism developed to describe the uniform corrosion of copper in compacted bentonite saturated with an oxygen (O₂)-containing chloride (Cl⁻) porewaters. The mechanism couples the interfacial electrochemical reactions that occur on the container surface to various processes occurring at or within the bentonite. These processes include: the diffusive mass-transport of species to and from the corroding interface (denoted by the wavy arrows in Figure 5-10); the adsorption and desorption of Cu(II) on the clay; redox reactions involving dissolved O₂, Fe(II), and Cu(I) and Cu(II) species; the dissolution and precipitation of various solid mineral phases and corrosion products; the partitioning of O₂ between the gaseous and aqueous phases, and, in a simplistic manner, the microbial consumption of dissolved O₂. This reaction scheme applies equally to both the buffer and backfill materials, as well as the host rock and further details are included in this section.

Copper can react in dry air as shown in Reaction 3. The rate of copper oxidation in dry air at temperatures below 150°C is of the order of nm/a, and, therefore, effectively negligible.

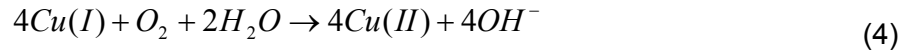


The corrosion behaviour of copper in O₂-containing Cl⁻ solution has been well studied. A detailed reaction mechanism exists that accounts for the various electrochemical, chemical, redox, adsorption/desorption, precipitation/dissolution, and mass transport processes involved in the corrosion process in compacted bentonite. The behaviour of copper over a range of chloride concentrations has also been experimentally evaluated. Kinetic rate constants, equilibrium constants and other thermodynamic parameters required for modelling are available, as summarized in Kwong (2011).

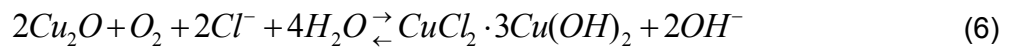
Copper will corrode in solutions containing O₂ and Cl⁻ and under atmospheric conditions providing the relative humidity is above that required to form a thin surface water film (approximately 50 to 70% Relative Humidity (RH)). The rate of corrosion will depend on the

presence of atmospheric contaminants, such as SO₂, NO₂, and CO₂. The ion-containing water film acts as an electrolyte to support electrochemical reactions and the dissolved impurities will further enhance the corrosion process. For instance, the SO₂ forms H⁺ and HSO₃⁻; the latter species can be oxidised to sulphate by oxidants in the air and NO₂ can be absorbed in the water film as HNO₃, which dissociates to H⁺ and NO₃⁻.

Copper dissolves in Cl⁻-containing solutions as the cuprous (Cu(I)) complex ion CuCl₂⁻. The anodic dissolution is coupled to the cathodic reduction of an oxidant, either dissolved O₂ or Cu²⁺. Cupric species are produced by homogeneous oxidation of Cu(I) by O₂ (Reaction 4).



Both Cu(I) and Cu(II) can precipitate as Cu₂O and CuCl₂·3Cu(OH)₂, respectively (Reactions 5 and 6). Such a duplex corrosion product layer would comprise an inner layer of Cu₂O and an outer layer of basic Cu(II) salts such as CuCl₂·3Cu(OH)₂ or Cu₂CO₃(OH)₂, depending on the specific composition of the porewater.



The precipitated surface film blocks surface electrochemical reactions and does not sustain the permanent separation of anodic and cathodic reactions that would be required for localized corrosion to occur. As the repository environment becomes anaerobic, the CuCl₂·3Cu(OH)₂ layer dissolves with further corrosion supported by the cathodic reduction of Cu(II).

In the absence of oxygen, corrosion would require a reaction with water to produce hydrogen gas (H₂):



or



Known thermodynamic relationships (Pourbaix 1974) indicate that the equilibrium shown in Reaction 7 is very strongly biased towards the reactants: metallic copper and water. Accordingly, upon formation of a very small amount of Cu₂O (i.e. a single layer), only a very small amount of hydrogen, with a partial pressure on the order of 10⁻¹⁴ atm, is necessary to suppress the corrosion (i.e. forward) reaction the unfavourable in the forward direction. In addition, the corrosion product in Reaction 8 has not been shown to be stable. Therefore, Reactions 7 and 8 are considered very improbable in water. Under anaerobic conditions, copper corrosion accompanied by the evolution of H₂ does occur in the presence of sulphide (Reaction 9).



Sulphide, in the presence of which copper corrosion is supported by the evolution of H_2 , is not widely found in deep groundwaters in crystalline rock on the Canadian Shield (McMurry 2004, McMurry et al. 2003). In Sweden and Finland, however, deep groundwaters do contain small amounts of HS^- (typically ~ 1 mg/L, King et al. 2010, 2011a), resulting in corrosion rates of the order of nm/year due to the slow transport of sulphide to the container surface through the compacted bentonite buffer (SKB 2011).

Researchers from the Royal Institute of Technology (Sweden) have published experimental results that they claim indicate that copper can corrode in pure, oxygen-free water. Their research claims that hydrogen ions are reduced in the anaerobic corrosion process to form hydrogen atoms (Szakalos et al. 2007, Hultquist et al., 2009, 2011). An expert review panel (Swedish National Council 2010) subsequently concluded that it was necessary to demonstrate that the proposed corrosion product was thermodynamically stable before it could be justifiably claimed that copper could corrode in oxygen and sulphide-free water. An SKB review also concluded that there were possible errors in the original experiments (SKB 2010).

Subsequent work commissioned by the Swedish Radiation Safety Authority (SSM) has found extremely small quantities of hydrogen in similar experiments, but the tests were not definitive (SSM 2011a). Further studies are underway in Sweden, as well as by NWMO. In addition, careful analysis of the thermodynamics of the reactions between copper, pure water, and sulfide (SSM 2011b) has indicated that copper-water interactions as described by (7) and (8) are theoretically possible, but would only produce very small quantities of hydrogen, and that reactions with sulphide species are much more important (SSM 2011b).

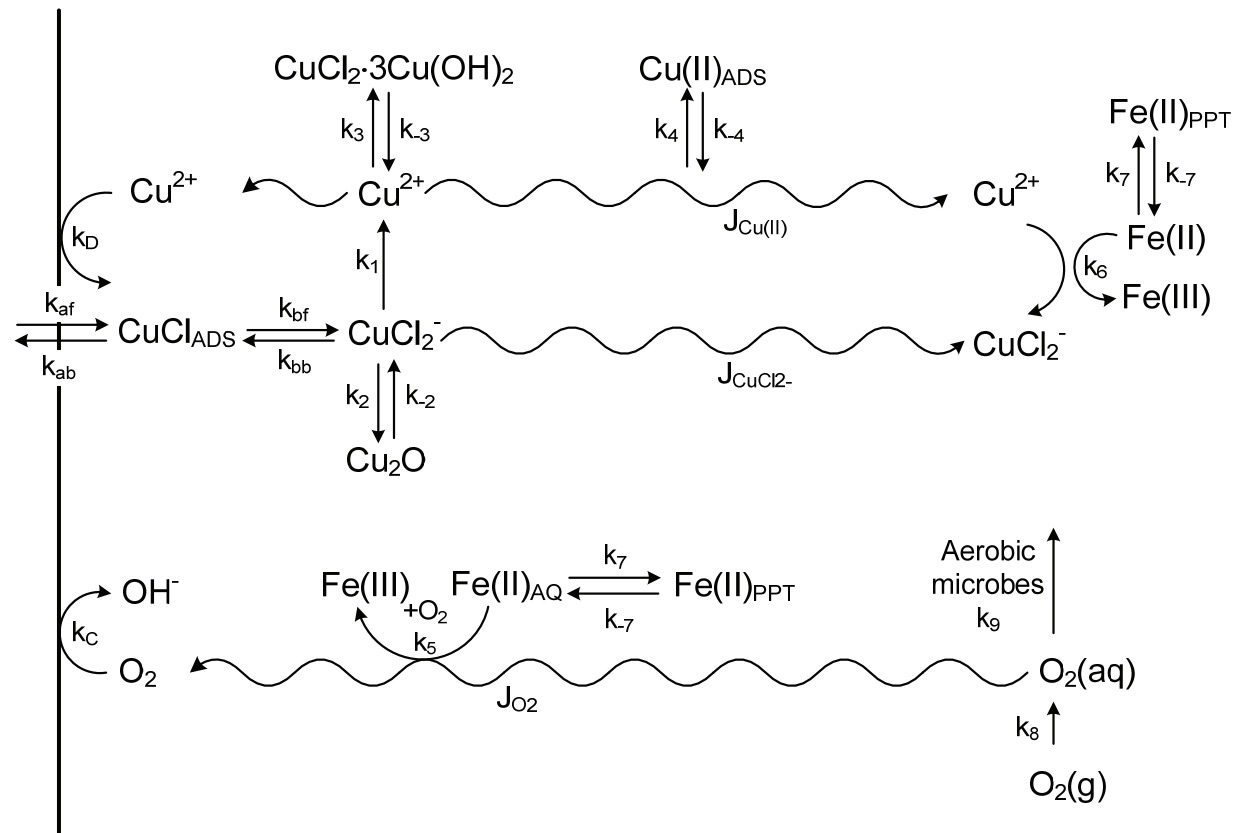
Regardless, the hydrogen produced from a copper-water interaction would be self limiting, and not a significant corrosion mechanism within a repository. Assuming the corrosion mechanism via reaction (8) occurs, then at temperatures of $73^\circ C$ and $45^\circ C$, hydrogen partial pressures of ~ 1 mbar (Szakalos et al. 2007) and 0.5 mbar (Hultquist et al. 2009), respectively, would suppress the corrosion reaction. This hydrogen could be present either from the copper-water reaction, if it occurs, or more likely from reactions with trace levels of sulphides or from native hydrogen levels (SKB 2010). For example, measurements at depth within crystalline formations have demonstrated hydrogen concentrations between 2 and $1600 \mu mol/L$, equivalent to partial pressures of 2.6 to 2000 mbar (Sherwood Lollar 2011).

The rate controlling process for the uniform corrosion of copper changes as the environmental conditions evolve. Under aerobic conditions, there is evidence that the transport of dissolved Cu away from the corroding interface is rate controlling (King et al. 2010, 2011a) (i.e., the corrosion reaction is anodically transport limited). As the repository environment becomes anoxic, the corrosion rate must eventually become cathodically transport limited as a result of the slow diffusion of oxidant to the container surface. In the presence of sulphide, if such species were to be found in Canadian groundwaters, the corrosion rate is limited by the rate of transport of HS^- to the container surface (Chen et al. 2011, King et al. 2011b).

Overall, the uniform corrosion behaviour of copper in conditions expected for a deep geological repository in crystalline rock is well understood. Both the mechanism of copper corrosion in oxygen-containing chloride (< 2 mol/L) and kinetic and thermodynamic parameters required for modelling are available.

In addition to the extensive experimental studies on which the mechanism in Figure 5-10 is based, a detailed reactive-transport model has been developed to predict the long-term uniform corrosion behaviour of copper containers in the repository. The model, referred to as the Copper Corrosion Model for Uniform Corrosion (CCM-UC), is based on the mechanism in Figure 5-10 and couples the corrosion behaviour of the container to the various processes occurring in the near- and far-fields of the repository, specifically the evolution of the environmental conditions. The corrosion behaviour is modelled using electrochemical mixed-potential principles. As a result, the model not only predicts the time-dependent corrosion rate (as a corrosion current density), but also the time-dependent corrosion potential (E_{CORR}). As discussed below, E_{CORR} is a useful parameter for assessing the probability of localized corrosion and stress corrosion cracking, as well as providing information about uniform corrosion.

Various methods have been developed to predict the rate or extent of the uniform corrosion of copper containers. Because uniform corrosion is limited by the availability of oxidant, the rate of corrosion is of less importance than the extent of corrosion. The maximum depth of corrosion can be assessed based on mass-balance principles (SKB 2011) or using the detailed mechanistically based CCM-UC model (King et al. 2008). The total amount of O_2 trapped in the repository at the time of closure, expressed per unit area of the container surface, is of the order of 1-10 $\text{mol}_{\text{O}_2}\cdot\text{m}^{-2}$. The exact amount depends on the volume and porosity of buffer and backfill materials and, crucially, the initial degree of saturation (since the majority of the trapped O_2 is present as gaseous O_2 in the air-filled pores of the buffer and backfill). If all of this oxygen is consumed by corrosion of the container, King et al. (2010) estimate that the maximum wall penetration for a copper container in a deep geological repository would be 0.17 mm. In reality, some of the O_2 will be consumed by aerobic microbial activity in the backfill material and the oxidation of ferrous species, so that the actual depth of uniform corrosion will be lower. Depending upon the relative rates of the different microbial and redox reactions, the model predictions suggest that more than 50% of the trapped O_2 could be consumed by processes other than corrosion. A consequence of the limited availability of oxidant is that once all of the O_2 (or the Cu^{2+} produced by the oxidation of CuCl_2^- by O_2) has been consumed, corrosion of the container ceases.



Notes: From King and Kolář (2000) and King et al. (2008, 2010, 2011a). The k 's denote rate constants for the various interfacial electrochemical and homogeneous reactions and the J 's denote diffusive fluxes.

Figure 5-10: Reaction Scheme for the Uniform Corrosion of Copper in Compacted Bentonite Saturated with O₂-containing Chloride Solution

5.3.1.5.2 Localized Corrosion

Kwong (2011) identifies that studies designed to specifically examine the surface profile of copper corroded in groundwater-saturated, compacted buffer materials have been completed. Results showed that the copper will only undergo a form of surface roughening as a result of the non-permanent separation of anodic and cathodic processes. Evaluations of the distribution of precipitated corrosion products and surface morphology on the coupon surface (i.e., distribution of peaks and valleys on the surface) indicated an “under-deposit” corrosion. A mechanism to account for the observed surface profile, which involved the periodic separation of anodic and cathodic processes through the formation of temporary occluded cells has since been proposed (King and Kolář 2000).

Experiments were carried out to assess the possibility of localized corrosion of copper for the situation in which there are differences in the flux of O₂ to different parts of the container surface, for example, in the case where bentonite blocks of different density might be used around the container. In this situation, the (semi-) permanent spatial separation of anodic and cathodic processes is possible. It was shown that the localized corrosion rates would decrease with decreasing oxygen concentration and decreasing container surface temperature. The corroded copper surface showed only general corrosion with minor surface roughening and no distinct pitting. It was concluded that the rate and extent of localized corrosion in a deep geological repository would be very small since there will only be a limited supply of oxygen. It was expected that the corrosion products on the container surface would further limit the rate and extent of localized corrosion.

The long-term localized corrosion behaviour of copper has also been extensively studied in the Swedish / Finnish nuclear waste management programs. They predicted the depth of localised corrosion based on pitting factors and an analysis of empirical pitting data from archaeological artifacts subject to long-term burial in natural environments. Extreme-value statistics developed by OPG for the Canadian program have also been applied to estimate the maximum pit depth on a container as a function of exposure time in the repository. A pit propagation model was developed for reducing conditions assuming the pit growth was limited by the transport of HS⁻ to the copper surface.

Based on these various measurements and models, it was generally agreed that a copper container in a deep geological repository will not undergo classical pitting corrosion, but only a surface roughening or under-deposit corrosion. Corrosion occurs under deposits on the surface, with the resultant temporary spatial separation of the anodic and cathodic sites accounting for the roughened surface. Surface roughening, or under-deposit corrosion, may add a maximum of 0.1 mm to the depth of general corrosion.

5.3.1.5.3 Stress Corrosion Cracking

This section summarizes the considerations for stress corrosion cracking (SCC) of the copper shell that are explored in Kwong (2011). The occurrence of SCC requires a susceptible metal to be exposed to sufficient tensile stress and an active SCC agent. Copper is known to be susceptible to SCC in environments containing ammonia, nitrite ions, acetate, or, possibly, high concentrations of sulphide. Studies focussed on SCC have concluded that the SCC of copper requires the prior formation of a thin oxide or tarnish film. When this film does not form, SCC is not observed.

While SCC agents are not normally found in natural groundwater, they could be introduced by either mining activities or microbial activity. Numerous tests have, therefore, been performed to assess the SCC behaviour of copper in nitrite-, ammonia- and acetate-containing environments. Results indicate that copper SCC susceptibility would decrease with decreasing concentrations of the SCC agents. These studies also suggest a threshold concentration level for each agent below which SCC would not occur. Also observed in these studies is the inhibiting effect of chloride on copper SCC in nitrite, ammonia and acetate environments, the SCC susceptibility decreasing with increasing chloride concentration. The ability of chloride to inhibit SCC also appears to be enhanced by elevated temperatures, as exhibited in tests conducted at 100 to 130°C (in nitrite only and nitrite/chloride solutions). This effect can be attributed to the ability of chloride ions to promote general dissolution of copper, which results in more uniform corrosion at the expense of the formation of the required thin oxide film.

Surface defects on the used fuel container surface can act as stress concentrators (notch-like defects) or stress intensifiers (crack-like defects) and may increase the probability of crack initiation or growth, respectively. A literature review and engineering analyses were performed to assess the effect of surface discontinuities on the initiation and propagation of localized corrosion and SCC of copper welds. The findings indicate no evidence that weld discontinuities would adversely affect the localized corrosion and SCC behaviour of copper containers. The predicted service life of the containers is not affected by the presence of the surface discontinuities.

A number of mechanisms have been proposed for the SCC of copper, including film-rupture/anodic dissolution, tarnish rupture, film-induced cleavage, and surface mobility mechanisms. Taking into account the pre-requisites for crack initiation and crack growth, a conceptual SCC model was defined for copper containers in a repository based on predicting whether the necessary environmental conditions will exist or co-exist. The model is mechanistically based and defines various absolute and conditional criteria for SCC. This model also addresses each of the environmental parameters that control the initiation and growth of SCC.

Research results have suggested SCC under aerobic conditions in a deep geological repository is unlikely as the pre-requisite conditions of corrosion potential, interfacial pH, and concentration of SCC agent do not exist simultaneously at the container surface. According to mechanistic arguments, there is also no evidence to indicate that SCC of copper is possible under anaerobic conditions at the sulphide levels expected at the container surface. Based on the nature of the repository environment, SCC does not appear to be a threat to the integrity of a copper used fuel container.

Despite the low risk of SCC on copper, suitable engineering procedures can be effectively applied to further minimize the probability of SCC. For instance; (i) the level of airborne ammonia and nitrite formed during blasting operations can be controlled to below the threshold concentration in order to preclude the possibility of cracking; (ii) the residual tensile stress following container shell and bottom manufacturing can be thermally relieved; and (iii) the residual stress on the final closure weld can be controlled and/or reduced using a suitable welding technique. It is nevertheless good engineering practice to perform a post-weld stress relief of the final closure weld, regardless of the apparent SCC susceptibility of the material. The introduction of a surface compressive stress has proven to be an effective way of preventing the initiation of SCC on various industrial structures. Ambient temperature

techniques, such as laser peening and low plasticity burnishing have been developed in the Yucca Mountain Project for this purpose (DOE 2008).

5.3.1.5.4 Microbiologically Influenced Corrosion

The microbiologically-influenced corrosion (MIC) program is summarized in Kwong (2011). Similar to other engineering materials, copper is susceptible to this type of corrosion. Microbial metabolic by-products may affect the SCC behaviour of copper as microbial activity may form SCC agents, namely ammonia, nitrite, and acetate ions. Ammonia and nitrite are produced (and also consumed) by different types of microbe as part of the nitrogen cycle. Acetate is produced by the fermentation of organic molecules. Another species often considered is HS^- produced by the reduction of sulphate by sulphate-reducing bacteria. This last reaction occurs under anaerobic conditions and requires the presence of simple organic molecules or H_2 as electron acceptors. Without the formation of biofilms on the container surface, the only form of MIC possible is that due to the diffusion of remotely-produced metabolic by-products through the bentonite to the container surface. Sulphide ions produced at a location away from the container surface must diffuse through the bentonite sealing materials to have any effect on container corrosion. The corrosion rate is, therefore, limited by the rate of diffusion of sulphide (HS^-) to the container surface, a continued supply of which is required to sustain MIC.

The Canadian microbial experimental program has demonstrated that a water activity of ≤ 0.96 in a bentonite buffer can effectively suppress the microbial activity, which can be achieved by a minimum bentonite dry density of 1.6 Mg/m^3 or a minimum pore-water salinity of 60 g NaCl/L . It has also been shown that microbial activity would be suppressed in a bentonite buffer system with swelling pressure of $\geq 2 \text{ MPa}$.

A reactive-transport corrosion model to predict the extent of MIC of copper containers has also been developed in the Canadian corrosion program. This model indicates that microbial activity in the repository will not result in shorter container lifetimes. The amount of sulphide ions provided by the microbial reduction of sulphate that reach the container surface is predicted to be insignificant over a million year timeframe. The amount of nitrite and acetate ions, both of which are associated with SCC of copper, are similarly insignificant. Although a higher maximum concentration of ammonia (another known SCC agent) of $\sim 10^{-6} \text{ mol.dm}^{-3}$ is predicted at the container surface, cracking is unlikely because of the relatively low concentration and because ammonia is only formed after all oxidants in the repository have been consumed.

Based on the assumption that sulphate-reducing bacteria activity would occur in the host rock near the borehole and would, conservatively, produce a continuous concentration of 3 ppm of hydrogen sulphide, the corrosion rate was estimated at 1 nm per year and the corrosion allowance for MIC was estimated to be 1 mm after 1 million years.

5.3.1.6 Summary

Research work over the past 20 years has established a good understanding of the long-term performance of copper used fuel containers in a deep geological repository in a low salinity crystalline rock environment.

In the low salinity environments anticipated in crystalline rock groundwater (i.e., $< 2 \text{ mol/L}$), copper will begin to corrode under early atmospheric conditions provided the relative humidity is above $\sim 50 - 70\%$. The rate and mechanism of corrosion will be affected by the presence of

atmospheric contaminants such as SO₂ and NO₂. Over time, as the repository environment evolves, the copper container will experience an initial aerobic period of uniform corrosion and some form of surface roughening, before establishing a long-term condition of thermodynamic stability. Uniform corrosion is associated with active copper dissolution in the presence of chloride, which causes the copper container to corrode uniformly, thereby avoiding localized corrosion. Stress corrosion cracking on the copper container is unlikely owing to the lack of the pre-requisite conditions for SCC; namely, the required threshold concentration of SCC agents, a suitable interfacial pH, and the required corrosion potential on the copper surface. Microbiologically influenced corrosion of copper will be controlled by the use of compacted bentonite around the copper container to suppress microbial activity in the near field and to limit the migration of any corrosive agents produced by microbial activity in the far field.

Although there have been claims that water acts as an oxidant for copper, the available evidence is not compelling and attempts to reproduce the observations have not been successful. At the current time, therefore, there is no evidence that water oxidises copper. It is expected that corrosion of a copper container in a deep geological repository would cease in the absence of oxygen and sulphide.

The knowledge gained over the past 20 years from studies on the corrosion of copper has allowed improved and more realistic predictions to be made for the lifetime of a copper container in a deep geological repository. Under low salinity groundwater conditions, a realistic estimate of the total extent of copper corrosion from all processes is a loss of wall thickness of about 1.27 mm (i.e., 0.17 mm (uniform corrosion) + 0.1 mm (under-deposit corrosion) + 1 mm (MIC) in 1 million years).

Therefore, the lifetime of a copper used fuel container is expected to exceed 1 million years in a deep geological repository in crystalline rock. This finding is consistent with the predicted container lifetime for the Swedish deep geological repository in crystalline rock.

5.3.2 Evolution of a “Breached Used Fuel Container”

Containers for a repository would be manufactured according to a process that includes careful design, fabrication, closure welding, and a series of inspections to avoid significant defects.

McMurry et al. (2004) summarizes a study of failure statistics for a variety of pressure vessels and nuclear components, which estimated that the probability of early failure of a used fuel container due to undetected manufacturing and installation defects is on the order of 1 defect per 5000 containers. In a repository with 12,800 containers, three would therefore be statistically likely to have an undetected through-wall defect. More recent SKB (2011) analysis of sample welded containers with a similar design but 50-mm thick copper shell, states that the likelihood of an undetected copper weld defect longer than 20 mm is negligible, and the likelihood of a 10-20 mm defect is one per 1000 containers. As a result, they do not expect any initial through-defects within their 6000 container repository. However, in the present study, it is assumed that three containers are placed within initial through defects.

The defect size would be constrained to some extent by the fact that it must be large enough to penetrate a sheet of copper that is about 25 mm thick but small enough that it escapes detection. For example, the area exposed by a defect was assumed to be 5 mm² in early SKB models, and 0.07 to 7 mm² in AECL models associated with the Second Case Study. In the current study, the size of the assumed initial defect is approximately 3 mm².

A discussion of the processes considered for a container defect was included in McMurry et al. (2004) and is also presented in this section.

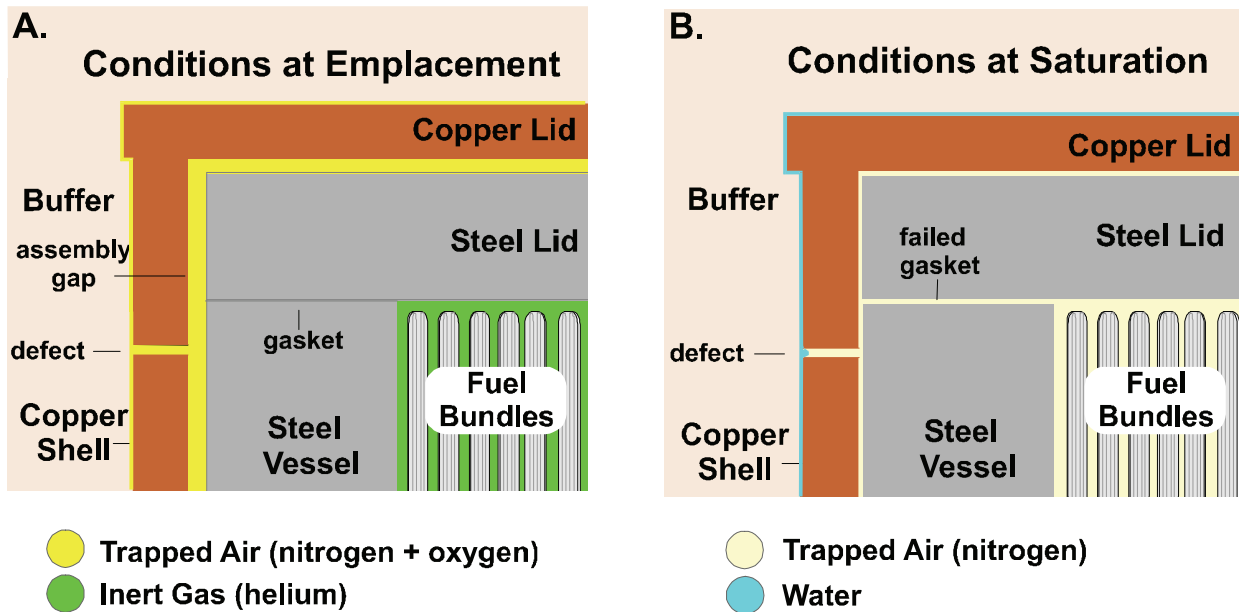
5.3.2.1 Description of Repository Conditions Prior to Saturation for a “Breached Container”

As described in McMurry et al. (2004), the pre-saturated period covers the time from when the containers are first placed in a repository until the time their exterior (copper) surface is in contact with fully saturated sealing materials (i.e., the time at which the buffer is saturated and is exerting a high swelling pressure on the container surface). In low permeability rock, it is likely that this pre-saturated period would last from 100 to 1000 years.

At the time that the placement rooms are backfilled and sealed, they would contain partially saturated (moistened) buffer and backfill (Table 4-4). Voids (porosity) in the sealing materials would contain trapped air. Heat from the container would cause the nearby bentonite to dry out. Condensation of the water vapour would occur in cooler portions of the sealing materials.

The relative humidity of the trapped air in the sealing materials near a container is of interest because corrosion of copper and iron in air is observed to be slow or nonexistent at relative humidities less than about 60%. Above this value, copper is subject to aerobic uniform corrosion. Corrosion of steel under the same conditions produces hydrated iron oxides (“rust”).

In a defective container, air would initially be present in the narrow assembly gap between the copper and steel vessel (Figure 5-11). The void space in the interior of the steel vessel would be filled with an inert gas (helium), held in place by a gasket seal beneath the bolted-on lid of the steel vessel. By the end of the pre-saturated period, the gas in the interior of the steel vessel would consist mainly of a mixture of oxygen-depleted air (largely N₂) and helium (Figure 5-11).



Note: Figure from McMurry et al. (2004).

Figure 5-11: Early Evolution of Conditions in a Container with a Small Defect in Copper Shell

At saturation, the hydrostatic pressure in the water-filled pores of the sealing materials would be 5 MPa; however, it is likely that the air pressure inside a defective container at this point would be less. This is because the internal free volume (void space) of a container is approximately 1.58 m³. Filling this volume to 5 MPa would require 75 m³ of air at 0.1 MPa (i.e., atmospheric pressure); however, this volume is a significant fraction of all of the air that was originally trapped in the room. Given other constraining factors, such as the low permeability of saturated buffer, it is likely that a pressure differential will develop between the interior and exterior of the defective container. As a result, water vapour or liquid would be drawn from the wet buffer into the container interior via the defect in the copper shell.

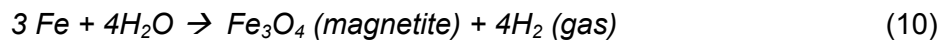
5.3.2.2 Description of Post-Saturation Processes for a “Breached Container”

The description of post-saturation processes begins when the clay buffer surrounding the defective container is saturated, and liquid water is able to enter the defect in the container (Figure 5-11). Approximately 100 to 1000 years will have passed after placement of the container in the repository. The assembly gap between the copper and steel vessels (about 1 mm in the reference design) will be almost completely squeezed closed except near the corner of the copper lid and shell. The temperature of the container at this time would be likely in the range of 60 to 90°C (McMurry et al. 2004).

5.3.2.3 Anaerobic Corrosion of the Steel Vessel

By the time that the repository is saturated, virtually all of the free oxygen in the sealing materials would have been consumed, and anaerobic conditions would prevail. A thin layer of corrosion products (mostly iron oxides or hydroxides from aerobic corrosion of the steel vessel) would be sandwiched between the copper and steel of the defective container. Compared to the metals, the corrosion products would be more porous and less dense. Gases would preferentially diffuse through them, and liquid water would be able to permeate them. Porewater (and possibly buffer material) would move from the buffer through the defect in the copper shell, and come into contact with the outside surface of the inner steel vessel. The copper itself would be chemically resistant under anaerobic conditions and would not be significantly affected by contact with water. In contrast, the steel vessel would undergo anaerobic corrosion as long as it was in contact with water; although the corrosion rate would be slower than under oxygenated conditions, and would also likely be reduced as corrosion products were generated.

Where water is in contact with the steel, a reaction will occur forming an iron corrosion product and, in the absence of oxygen, hydrogen.



An amorphous or poorly crystalline solid would be likely to form first, which would gradually transform into a more crystalline phase, (likely magnetite as per (10)) under repository conditions.

Initially, iron corrosion products would form only on the outside surface of the steel. After water leaked into the interior of the steel vessel, most likely via an undetected defect in the copper shell and the failed gasket, anaerobic corrosion would also occur on the inside steel surfaces. Literature values for the anaerobic corrosion rate of steel vary over a wide range, between 0.1 and 50 $\mu\text{m/a}$. The corrosion rate in a defective container likely would be at the lower end of the range, given that the water would be chemically buffered by clay and given that the water would be supplied at a limited rate to the steel; this same limitation would likely mitigate any radiolysis reactions that could potentially impact corrosion. Among other factors, the water ingress would be restricted by the low permeability of the clay around the container, by the small aperture of the defect in the copper shell, by slow passage through the porous corrosion products in the narrow copper-steel gap, and possibly by blockage of the opening by the build up of a hydrogen gas backpressure from the corrosion reaction inside the container. For a steel corrosion rate of 0.1 $\mu\text{m/a}$, the corresponding H_2 production rate would be about 0.1 to 1 mol/a (equivalent to 0.05 to 0.5 L/a at 5 MPa) depending on what fraction of the inner vessel surface was corroding.

5.3.2.4 Galvanic Corrosion

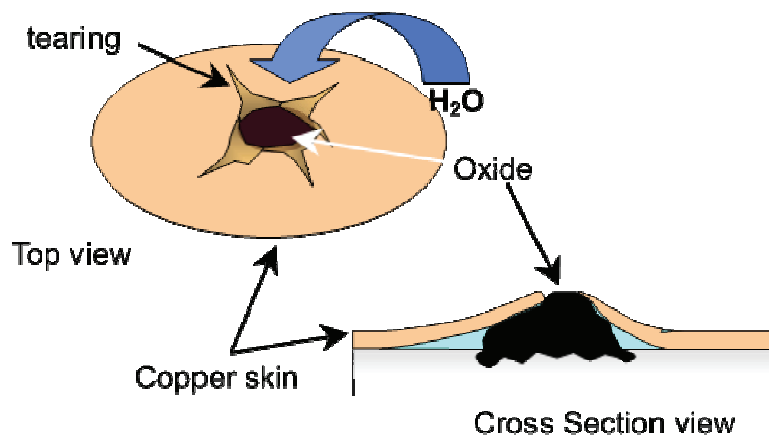
Although the design of the UFC makes it inevitable that the copper shell and inner steel container will be in physical contact, galvanic corrosion will not occur as long as the copper shell is intact. While this condition persists, corrosion reactions and rates will be defined by the outer copper shell, and there will be no effect of the physical contact on the electrochemical properties. However, for a "breached container", in principle, it is possible that galvanic corrosion issues may exist, where one metal performs/catalyzes the cathodic electrochemical reactions, while the other metal performs/catalyzes anodic reactions. In the case of steel (iron)

coupled to copper, oxidation of iron at the container breach would be enhanced if the very large intact copper surface could sufficiently support reduction reactions: either oxygen reduction during the aerobic period or hydrogen reduction during the long anaerobic period. Experiments conducted by Smart et al. have examined both conditions and measured galvanic currents as expected: with the copper behaving as a cathode and the iron behaving as an anode (Smart et al. 2004, 2005). In aerated conditions, galvanic corrosion rates of iron (coupled to copper) are as high as 100 $\mu\text{m/a}$. Other research has revealed that copper-steel couples in aerated seawater can cause an enhancement in corrosion of steel (Chen et al. 2007). However, the actual depth of corrosion from this process would be significantly limited by the repository oxygen volume, as described in Section 5.3.1.5. When their system was deaerated, galvanic currents measured by Smart et al. were much lower: typically 0.1 $\mu\text{m/a}$ at 30°C and 1 $\mu\text{m/a}$ at 50°C (Smart 2005). These values are no different from those measured on iron in deaerated groundwater that is not coupled to copper; in effect, the copper couple does not alter the corrosion properties of iron in this medium. The interpretation of this result is that the couple between iron and copper does not sufficiently polarize the copper negatively to support enhanced water reduction (King et al. 2010). Accordingly, the copper shell would be largely inactive to the iron corrosion process, as well as having the additional benefit of protecting the remainder of the steel container from corrosion processes.

5.3.2.5 Plastic Deformation and Rupture of the Copper Shell

Although experimental evidence has demonstrated that expansion of corrosion products leading to rupture of the copper shell is a very unlikely scenario (Smart et al. 2003, 2006), the scenario has been developed to assess the consequences of radionuclide release and transport.

Iron corrosion products are less dense than the metal itself, in addition to containing additional chemical species (i.e. oxygen/oxide, hydrogen/hydroxide). Thus, the volume of Fe_3O_4 formed by Reaction (10) is about twice the volume of the Fe metal consumed in its formation (McMurry et al. 2004). As a result of this volume change, the formation of corrosion products in a confined space has the potential to exert a compressive stress on the adjacent solids. These stresses would have little preliminary effect on the steel vessel, due to its thick walls (100 mm) and high mechanical strength. However, the copper shell and the surrounding clay buffer would be prone to deform more easily. For example, at 20°C the yield stress of copper is 63 MPa and its rupture stress is approximately 200 MPa, compared to a compressive strength in excess of 400 MPa for most iron oxides. The build up of corrosion products could eventually cause the copper shell to bulge outwards in places, probably near the defect itself, where the water supply for corrosion would be greatest and the copper would be already weakened (Figure 5-12).



Note: Figure from McMurry et al. (2004).

Figure 5-12: Possible Damage by Iron Oxide Expansion

Depending on whether the bulging occurs by creep deformation or plastic yielding, the copper shell would tear should its elongation exceed about 10% or 40%, respectively. If the steel corrodes at rates on the order of $0.1 \mu\text{m/a}$, for example, creep is more likely to be the dominant process due to the relatively low temperature ($< 1/3$ melting temperature) and the implied low copper strain rate (about $10^{-12}/\text{s}$).

For a 25-mm thick copper shell and a corrosion rate of $0.1 \mu\text{m/a}$ for the steel vessel, and assuming the above conditions, the iron corrosion product build up could push out the copper shell and lead to localized rupture of the copper in approximately 20,000 years, depending in part on the volume expansion from steel to corrosion product and depending on the shape of the bulge. For example, if the steel corrodes at a rate of about $1 \mu\text{m/a}$, the copper would rupture in a shorter time. The main effect of this localized rupture would be to allow more water to enter the container, leading to more extensive corrosion and further rupture.

In the discussion above, from McMurry et al. (2004), liquid water would have continuous access to the steel in at least one location (i.e., the defect site). However, McMurry et al. also describe other analyses, involving a defective container, in which it has been postulated that the iron corrosion reactions would produce hydrogen at a rate exceeding the ability of the gas to diffuse into the buffer. In this model, enough hydrogen gas would accumulate in and around the container that the pressure build-up would block liquid water from moving into the container through the defect. Then, only water vapour could diffuse through the opening to sustain the steel corrosion. In these analyses, the “bubble” of hydrogen gas blanketing the steel vessel would slow the rate of steel corrosion and expansion of corrosion product thereby delaying rupture of the copper shell for time scales of the order of 200,000 years. The hydrogen blanketing scenario is plausible, but the long time delay requires that there be complete blanketing of the steel, which depends on the interrelation of geometry and process rates (e.g., corrosion, gas transport, mechanical effects). In addition, this description leaves some ambiguity regarding the rate of corrosion at relative humidities approaching 100%, which may be similar to corrosion rates in liquid systems.

The bulging and rupture of the copper shell at the defect site would allow more water to enter the container. Eventually, water also would begin to seep between the steel vessel and the steel lid. The growth of iron corrosion products in this location would tend to pry the lid away from the vessel, increasing the size of the opening through which water could gain access to the interior of the steel vessel and to the used fuel bundles.

While the above description illustrates a potential catastrophic failure of the container at a rupture site, experimental evidence has been generated that shows such stresses will not be produced by iron corrosion products (Smart et al. 2003, 2006). During analysis of stresses produced during anaerobic corrosion, no detectable expansion was observed over a two year period for bentonite-equilibrated groundwaters under compressive loads (Smart 2006). In addition, the anaerobic corrosion products are easily deformable, and are incapable of producing expansion under simulated repository conditions. Only for aerobic conditions, and low applied loads were expansions measureable due to corrosion products. As a result, it is unlikely that the plastic deformation/rupture described above would occur; instead, the rupture would persist only at the initial defect site.

5.3.2.6 Plastic Deformation of the Steel Vessel

The container design for normal loading conditions (i.e., prior to glaciation) would have a significant margin of mechanical strength. For example, the reference container design with 100 mm of steel can meet the reference maximum 15 MPa external pressure with a safety factor of about three. At an anaerobic corrosion rate of 0.1 to 1 $\mu\text{m/a}$ (including corrosion of inner as well as outer surfaces of the steel vessel), it would take 10,000 to 100,000 years before even a 20 mm thickness of steel would be consumed.

Another factor to consider is the additional stress from glacial loading conditions, which would be expected to first occur in about 60,000 years (see Section 5.5.2.2). At the full design-basis glaciation load, there may be little margin for thinning of the steel vessel walls. If significant corrosion had occurred already, collapse or brittle fracture of the steel vessel would be likely in response to the glacial loading stresses. It is also plausible that the glaciation load would be less than the design basis. For example, if the ice thickness is less than the design-basis maximum, if the load transmitted to depth is less than the hydrostatic loading equivalent to the ice thickness, or if the container was full of water (which would provide hydrostatic balancing of the glacial load). In such cases, the container would be more likely to tolerate further corrosion before plastic deformation and buckling. Regardless of the specific timing and processes the key point is that at some point the steel vessel in a defective container would become sufficiently weakened by corrosion that it would cease to be load-bearing, and it would collapse by buckling inwards.

The stresses causing the steel vessel to collapse would produce a corresponding deformation of the copper shell around it. During this movement, the strain limit for copper would be exceeded in portions of the copper shell, and the copper would crack, but in a general sense the copper metal would continue to conform to the shape of the steel vessel. Similarly, as the copper and steel compressed inwards, the surrounding buffer would expand around the new configuration of deformed metal.

Even after the defective container collapsed, the overall change in its volume would not be substantial compared to the volume that was originally occupied by the container. Initially (at

the time of placement), the open or void space in a container, into which the collapse would occur, would be roughly 1.58 m^3 , which is about 30% of the container's total volume. Moreover, it is likely that much of this initially open volume would have become filled with iron corrosion products, further restricting the amount of collapse.

After the defective container buckled and the buffer around it expanded to conform to the change in shape, the copper shell would remain essentially unchanged in appearance for the remainder of the million-year timeframe. Complete corrosion of the copper is estimated to take several million years or longer, as indicated by sheets of natural copper that have persisted in sedimentary rocks for more than a hundred million years. In contrast to the copper, anaerobic corrosion of the steel vessel would continue in-situ until all of the steel was consumed (McMurry et al. 2004).

5.3.2.7 Corrosion and Deformation of Zircaloy Cladding

The first barrier against radionuclide release from used fuel bundles upon exposure to water through a breached container is the intact Zircaloy fuel sheath (cladding). At the time of placement in a repository, virtually all of the used fuel elements would have intact Zircaloy cladding. A few of the cladding sheaths would have become defective during their use in a reactor (estimates of this number range from approximately 1 per 10,000 to 1 per 100,000 fuel elements). While some others may have developed defects during post-reactor storage, during transportation, or during packaging into containers, the vast majority of the fuel elements would still have intact cladding. In a defective container, one of the most significant changes in the used fuel bundles over time would be mechanical failure of the cladding, mainly in association with corrosion of the steel vessel. In addition, the cladding would be subjected to hydrogen embrittlement, corrosion, and creep, as summarized in McMurry et al. (2004) and described below.

Over time, hydrogen gas would be produced inside a defective container by two separate processes - the anaerobic corrosion of steel and the radiolysis of water. Hydrogen-induced cracking is a potential failure mechanism for Zircaloy cladding. Studies of the durability of used fuel bundles in existing dry or moist air storage facilities have found no evidence of cladding failures over several decades. Given that significant partial pressures of hydrogen gas would not develop in a container until saturation of the repository had occurred, lifetimes of at least a hundred years would be feasible for Zircaloy cladding in a defective container, with a reasonable expectation that cladding lifetimes could exceed thousands of years.

On observable time scales, the uniform corrosion of Zircaloy cladding is negligible, likely between 1 and 5 nm / a, and with an upper limit of 20 nm / a, even in contact with water, due largely to the corrosion resistance of a passive oxide film on the Zircaloy surface (Shoesmith and Zagidulin 2010). In a defective container, pitting and crevice corrosion of cladding would be inhibited by the rapid consumption of oxidizing agents (residual oxygen and radiolysis products) by the iron and copper container materials. In addition, iodine-induced stress corrosion cracking would be inhibited because most of the iodine in the fuel gap in CANDU fuel exists as cesium iodide, preventing it from forming the zirconium iodides that are thought to be the chemical precursors to stress corrosion cracking in Zircaloy. Using the above values, a general corrosion lifetime for a 0.5 mm cladding could be calculated to exceed 25,000 years presuming the highest corrosion rate of 20 nm / a, and with a more realistic expectation above 100,000 years for the expected corrosion rates at or below 5 nm/a.

Ultimately, any used fuel bundles that otherwise remained unruptured would be likely to fail during the corrosion-induced collapse of the steel vessel. As discussed previously, the timing of this event is uncertain, but a reasonable estimate would be within 10,000 to 100,000 years after placement. With the load-bearing capability of the steel vessel removed, the full hydrostatic plus swelling pressure would be applied directly to the fuel bundles, which would be unable to support the high stresses. After the cladding is breached, the used fuel pellets in the damaged fuel elements would be exposed to water almost immediately.

5.3.2.8 Dissolution of Used Fuel Matrix

After the cladding is breached and the fuel pellets exposed to water, the next barrier against radionuclide release is the UO_2 fuel matrix, which contains most of the radionuclides and has a very low solubility. Dissolution of the UO_2 matrix of the used fuel would progress according to two general methods: oxidative dissolution (i.e., corrosion) and chemical dissolution. Radiolysis of water in contact with the fuel pellets would produce oxidizing conditions at or near the used fuel surface, contributing initially to oxidative dissolution of the UO_2 . To the extent that water is able to contact the fuel while radiation fields are high, this process would tend to promote the dissolution of the used fuel at a higher rate than would be expected solely on the basis of the chemical solubility of UO_2 in the near-field porewater. The production rate of oxidants by radiolysis would decrease with time as the strength of the radiation field decreases (Garisto et al. 2012).

At the fuel-water interface, the alpha dose rate exceeds the gamma and beta dose rates for most of the fuel history (Figure 5-13) and is the main contributor to radiolysis, producing molecular oxidants such as H_2O_2 . Other potential sources of oxidants, such as any O_2 trapped inside the container when it was sealed, would already have been consumed by Fe and Cu corrosion processes before the fuel cladding was breached because these corrosion reactions are much faster than the reaction with UO_2 . In principle, the radiolytically produced oxidants also would be consumed by reaction with container materials rather than by reaction with used fuel; however, for alpha radiolysis, the oxidants would only be produced within 20 μm of the fuel-water interface and they would have difficulty diffusing through openings in the cladding to react with container materials (McMurry et al. 2004).

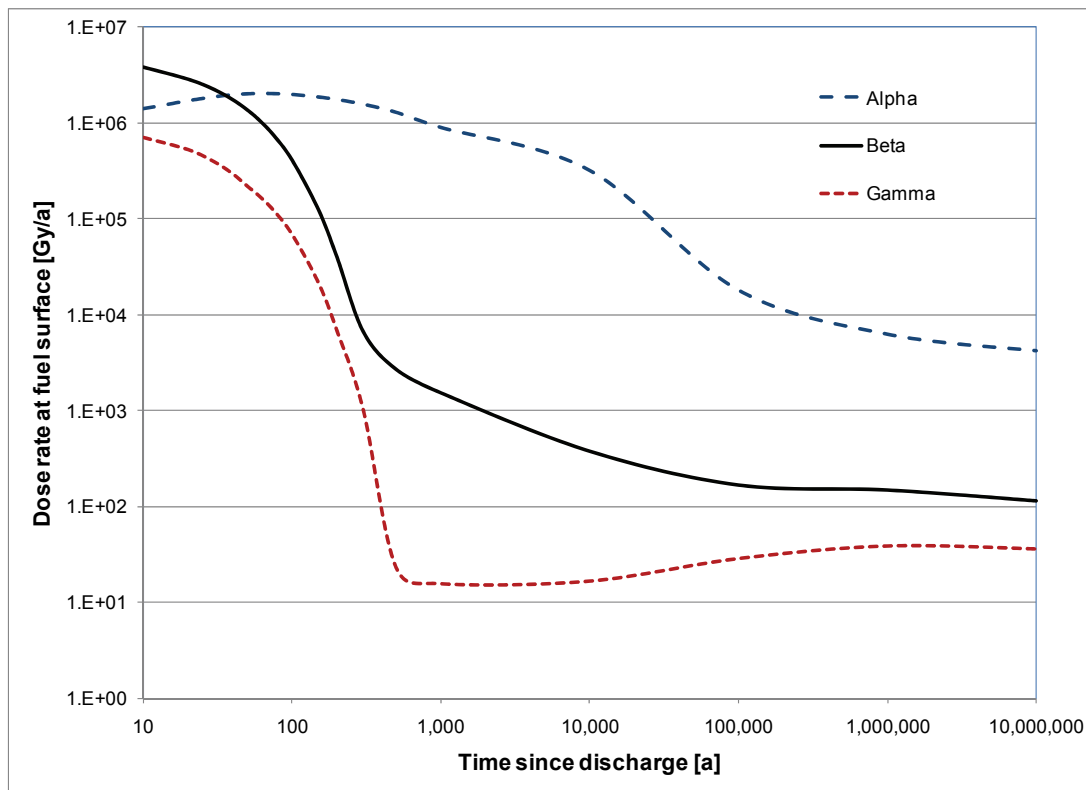


Figure 5-13: Radiation Dose Rate in Water at the Fuel Surface (220 MWh/kgU Burnup)

Oxidative dissolution of the fuel continues as long as the alpha radiation field is sufficiently high. After the alpha radiation field has decreased substantially, chemical dissolution of the fuel, which proceeds according to the reaction,



would dominate. Based on the data used in this study (Garisto et al. 2012, Appendix E), this occurs after about 10 million years if the potentially beneficial effects of H_2 are ignored (see below).

Over time, it is also likely that the UO_2 dissolution rate would be affected by the build up of hydrogen gas inside the steel vessel. In UO_2 and used fuel dissolution experiments the dissolution rate dropped by several orders of magnitude in the presence of even modest pressures of hydrogen gas (Shoesmith 2008). A number of mechanisms have been either demonstrated or proposed to explain these effects, all of which involved the activation of hydrogen to produce the strongly reducing H^\cdot radical which scavenges radiolytic oxidants and suppresses fuel oxidation and corrosion (Shoesmith 2008).

5.3.2.9 Radionuclide Release from the Fuel Pellets

McMurry et al. (2004) identifies that extensive studies of the interactions between used fuel and groundwater have established that radionuclide release from the used fuel occurs by two main processes. Initially, there would be a comparatively rapid release of a small fraction (typically a few percent) of the inventory of a selected group of radionuclides, that are either very soluble (such as ^{137}Cs , ^{129}I , ^{14}C and ^{36}Cl) or gaseous (such as Xe), and that are residing in the fuel sheath gap or at grain boundaries which are quickly accessed by water. This release process is referred to as “instant-release”. The second and slower release process comprises release of radionuclides from the UO_2 fuel matrix as the matrix itself corrodes or dissolves (called “congruent dissolution”).

The instant-release fractions for various important radionuclides in used CANDU fuel are given in Garisto et al. (2012). Note that the use of the term “instant release” with reference to the gap and grain boundary inventories is a simplification. In reality, it would take a finite time for water to penetrate into the grain boundaries and for the radionuclides located there to diffuse out. Compared to the much longer time required for dissolution of the UO_2 matrix itself, grain boundary releases are so much faster that they can be considered “instantaneous”. Therefore, in conceptual models of radionuclide release, both locations - the gap and grain boundary inventories - are considered to contribute to the instant-release fraction.

Table 5-5: Typical Instant-release Fractions for Selected Radionuclides

Radionuclide	Instant-Release Fraction (% of Inventory)
Cs	4
I	4
C	3
Cl	5
Tc	1
Actinides (Pu, Am, etc.)	0

Note: From Garisto et al. (2012).

Ferry et al. (2008) have shown that the instant release fractions do not change with time due to, for example, athermal diffusion of radionuclides induced by alpha-particle recoil displacements.

In addition to the bulk of the radionuclides in the used fuel pellets, there would be a small quantity of radionuclides present in the irradiated Zircaloy cladding from neutron activation. These radionuclides are generally distributed uniformly through the cladding and would only be released as the cladding itself dissolves. Zircaloy is corrosion-resistant in water due to the stability of its oxide coating, as described in Section 5.3.2.5. The strong adherence of the ZrO_2 corrosion layer to the metal surface suggests that radionuclides would be incorporated into the ZrO_2 as it forms and would only be released to solution when the oxide itself dissolves. Given

the low solubility of ZrO_2 , the rate of dissolution of the oxide and hence the release rate of the nuclides in the Zircaloy can be described using a solubility-limited dissolution model in which the rate of dissolution of the ZrO_2 is determined by the rate of diffusion of Zr away from the cladding (McMurry et al. 2004).

5.3.2.10 Fate of Released Radionuclides

As radionuclides are released to solution, some would become oversaturated and secondary radionuclide-bearing phases would precipitate (e.g., ThO_2) on the fuel surface or on other surfaces nearby, such as provided by the metal corrosion products. Besides the low overall amount of such nuclides in a container, it is expected that their concentration in a precipitate would be diluted by the co-precipitation of other elements. Precipitation of a large mass of fissile nuclides in particular would be hindered by the intergrowth of such mixed-isotope precipitates along with iron corrosion products or buffer clays.

The radionuclides that remained in solution as aqueous species, and solids suspended in colloidal form, would diffuse through the various metal corrosion products inside the container. The corrosion products would also provide a surface for sorption of many of the radionuclides. In some cases the sorption would be irreversible because the radionuclides would be incorporated into the crystal lattice of the corrosion product if it undergoes a transformation to a more stable solid phase.

Dissolved radionuclides would diffuse by a tortuous path through what was left of the steel container, through the cracks in the copper shell, through the low-permeability sealing materials, and finally through the rock around the repository. Migration of radionuclides away from the repository and their transport rate through the geosphere as a whole would be controlled by the local hydrogeological conditions. Radionuclides in colloid form or sorbed to colloids would be filtered by the buffer and not reach the geosphere.

5.3.3 Confidence and Uncertainties

Extensive corrosion experiments have been carried out over the past 30 years to improve the confidence for predicting the corrosion behaviour and lifetime of copper used fuel containers in a deep geological repository in crystalline rock.

Container Corrosion: Because of the extensive experimental database on the corrosion of copper, the level of mechanistic understanding that has been developed over the past 30 years, and the existence of natural and archaeological analogues (discussed in Chapter 9), there is a significant confidence in the prediction of the long-term corrosion behaviour of copper containers. Both the predictive models for corrosion processes that are expected to occur, such as uniform corrosion and localized surface roughening, and the reasoned arguments against those that are not thought to be possible, such as stress corrosion cracking, are robust.

The evidence from natural and man-made analogues builds confidence in the conclusions drawn from experimental and modelling studies. The existence of native metallic copper deposits indicates that, under certain environmental conditions, metallic copper is stable over geological time scales. The fact that the majority of copper deposits in the Earth's crust are in the form of sulphide minerals is also evidence of the potential role of HS^- species in the corrosion of copper containers. Although it is not a pre-requisite that the groundwater at

repository depth be free of sulphide, as the programs in Sweden and Finland ably demonstrate, there are clear advantages to selecting a site with no or low sulphide groundwater levels, as appears to be the case in crystalline rock over large parts of Canada. Man-made analogues, such as Bronze Age artifacts or more-recent anthropogenic objects (discussed in Chapter 9), also provide useful supporting evidence that copper corrodes slowly, even in near-surface aerobic environments.

Confidence in long-term predictions is also supported by the robustness of those predictions and on the underlying information on which they are based. This confidence can stem from achieving the same result from different modelling approaches. For example, the conclusion that the maximum depth of uniform corrosion is of the order of a few hundred micrometres is predicted by both simple mass-balance models (SKB 2011) and from detailed mechanistically based reactive-transport modelling (King et al. 2008). These detailed reactive-transport models have been validated against experimental data and evidence from archaeological analogues (King et al. 2001).

Confidence also results from having a sound mechanistic understanding of corrosion processes. For example, the proposed mechanism to explain observations discussed in Section 5.3.1.5.2 is strong evidence that under repository conditions the localized corrosion of copper containers will take the form of surface roughening rather than pitting. This understanding is equally important for processes that are not considered likely to occur, such as stress corrosion cracking. The fault-tree approach for stress corrosion cracking provides multiple lines of argument against this behaviour and it is not considered feasible that all of the pre-requisite conditions for cracking would exist in the repository at the same time. There are also multiple lines of argument for why microbiologically induced corrosion will have a minimal impact on the container (King 2009). Nevertheless, since the possibility of remote microbial activity cannot be excluded a corrosion allowance is made for this in lifetime assessments.

The multi-barrier repository system represents a robust system that is capable of withstanding upset or unexpected conditions whilst still maintaining a high degree of containment. For example, the predicted container lifetimes are insensitive to the groundwater salinity and, in fact, higher Cl⁻ concentrations promote uniform rather than localized corrosion (King et al. 2010, 2011a). Information from site investigations in crystalline rock in Canada suggest that there is little or no sulphide in deep groundwaters (McMurry 2004, McMurry et al. 2003). Experience from the Swedish and Finnish programs demonstrates that the combination of a copper container and highly compacted bentonite buffer provides long-term containment even if sulphide were to be present. Similarly, there is no evidence that O₂-containing water could reach repository depth, for example during future glaciation events. Even if oxidizing water did reach the repository, the slow transport of that O₂ through the compacted bentonite would result in low corrosion rates. For example, the steady-state transport of dissolved O₂ from an air-saturated saline solution across 25 cm of highly compacted bentonite is equivalent to a corrosion rate of only 0.014 μm·a⁻¹. Therefore, a copper container could withstand many thousands of years of such conditions without sustaining excessive damage.

To some degree, the robustness of the container lifetime is due to the combination of the copper container and the highly compacted bentonite buffer. Any process that leads to a loss of the bentonite properties, therefore, could potentially impact the container performance. Erosion of the bentonite, for example, could result in a decrease in bentonite density. In turn, the rate of transport of reactants to, and of corrosion products away from, the container would increase, as

would the possibility of microbial activity. Even if the bentonite properties were degraded, it is not certain that the container would necessarily corrode at a significantly higher rate, although further analyses would be required.

Copper Creep: Creep tests and modelling studies indicate that the copper creep deformation would stop once it has collapsed onto the inner steel vessel since the estimated creep deformation is extremely small. This also means that the amount of creep deformation of the copper vessel would depend on the gap width between the copper vessel and steel vessel.

Container Temperature: The copper container has been prescribed with a maximum design surface temperature of 100°C to meet the maximum buffer temperature requirements. The container surface temperature is affected by the container power, placement method, chemical composition, water content and thickness of sealing materials, distance between containers, distance between the placement rooms and tunnels, etc. For the reference copper container design (i.e., based on in-floor placement), thermal analyses have been performed to determine thermally acceptable layouts of a repository located at a depth of 500 m and a depth at 1000 m in crystalline rock using various computer codes such as CODE_BRIGHT and FLAC (Guo 2007, 2009a). Various heated field experiments have been conducted and modelled (e.g., the full-scale Canister Retrieval Test at the Äspö Hard Rock Laboratory in Sweden, Guo 2009b). The findings indicate that thermal responses were successfully modelled. There is good confidence that the evolution of temperatures of the container surface and surrounding bentonite buffer materials can be well estimated by existing computer models.

Container Structural Integrity: To maintain long-term structural integrity during its design life, the repository container is designed to withstand an external isotropic pressure of 15 MPa during the pre-glaciation period, which accounts for the hydrostatic pressure up to 1,000 m depth together with 5 MPa bentonite swelling pressure. The copper container is also designed to withstand an external isotropic pressure load of 45 MPa during the glaciation period, which represents the sum of the pre-glaciation pressure load of 15 MPa and a postulated glacial pressure load of 30 MPa (corresponding to a 3000 m thick ice sheet) with full load applied as hydrostatic head (i.e., no load carried by the rock matrix). These are conservative assumptions. While glaciation would be a significant load, the earliest site coverage due to an ice sheet would be thousands of years in the future, probably at least another 60,000 years.

The copper container would be subjected to uneven bentonite swelling loads during the transient period before the completion of full water saturation and also, possibly, after saturation (though to a reduced extent) because of density differences that do not entirely homogenise because of internal friction. It is expected that the uneven swelling pressure loads would not cause container failure, based on the results of analyses for similar SKB and Posiva containers (Werme 1998 and Raiko 2005). This will be verified by further engineering analyses.

Overall, there is high confidence in the structural integrity of the steel container for at least 100,000 years, and probably for as long as the copper shell maintains its integrity.

5.4 Evolution of Buffer, Backfill and Seals

Each borehole in the floor along the placement room centerline has a used fuel container surrounded by highly-compacted bentonite buffer disks, rings and gap-fill pellets. The placement room above the boreholes is filled with backfill materials such as a bentonite / sand mixture and other sealing materials. Bentonite and sand are durable natural materials that are expected to maintain their properties over the long term. Bentonite is a type of clay that swells on contact with water, providing a natural self-sealing ability.

The safety strategy acknowledges that properties of the engineered barriers will allow safety functions to be fulfilled. This includes the design characteristics of surrounding the container by a layer (approximately 30 cm) of dense bentonite-based clay that inhibits groundwater movement, has self-sealing capability, inhibits microbial activity near the container, and retards contaminant transport.

The main processes with potential influence on the evolution of the sealing systems are listed in Table 5-6 and discussed in the succeeding sections.

5.4.1 Changes during Saturation and Development of Swelling Pressure

As soon as sealing materials are installed, the water seeping into the repository would begin to wet them, and the bentonite in the buffer would expand. Once sufficient expansion has occurred to bring them into contact with its surroundings (backfill, rock and container) the buffer and to a lesser extent the backfill materials, would restrict water movement along these interfaces. Moreover, the swelling pressure generated by the sealing materials later would provide mechanical resistance to the local effects of large-scale flexing and crustal rebound processes associated with glacial loading, reducing the potential for or at least the severity of damage to the rock surrounding the backfilled openings of the repository. The swelling capacity of the bentonite decreases at high salinity, but the reference dense highly compacted bentonite is not sensitive to salinities expected at Canadian Shield sites at 500 m depth, around 10 g/L assumed at the present hypothetical site (Figure 5-14).

Table 5-6: Processes with a Potential Influence on the Evolution of Buffer/Backfill/Seals

PROCESS	POTENTIAL INFLUENCE
RADIATION	
None	<ul style="list-style-type: none"> • None
THERMAL	
Heat transport from container	<ul style="list-style-type: none"> • Change in temperature of sealing materials and rock • Redistribution of moisture prior to saturation • Temperature increases across gap or interface
HYDRAULIC & PNEUMATIC	
Saturation of repository	<ul style="list-style-type: none"> • Expansion of bentonite to close gaps • Chemical reactions between water and sealing materials • Development of swelling and hydrostatic pressure • Changes in thermal conductivity of buffer
Groundwater flow	<ul style="list-style-type: none"> • Rate of water supply for saturation • Erosion/piping under excessive amounts of inflow in the preclosure period
MECHANICAL	
Swelling pressure	<ul style="list-style-type: none"> • Density redistribution in clay-based sealing materials • Sealing of cracks and gaps in clay • Stresses in concrete/bulkhead
Thermal strains in concrete	<ul style="list-style-type: none"> • Fracturing in concrete; increased permeability
CHEMICAL	
Diffusion of chemical species	<ul style="list-style-type: none"> • Changes in porewater composition/salinity
Ion exchange in clays	<ul style="list-style-type: none"> • Changes in porewater composition • Change in hydraulic conductivity and swelling pressure of clay-based seals
Reactions with redox-sensitive minerals	<ul style="list-style-type: none"> • Consumption of oxygen in repository
Increase in salinity	<ul style="list-style-type: none"> • Changes in hydraulic conductivity and swelling pressure of clay-based seals
BIOLOGICAL	
Aerobic microbial activity in backfill	<ul style="list-style-type: none"> • Consumption of oxygen in repository
Anaerobic microbial activity in backfill	<ul style="list-style-type: none"> • Generation of sulphide which is a potential corrosion risk to copper container

Notes: Information in Table from McMurry et al. (2003).

Processes listed are those that are most likely to occur with a notable effect on the buffer/backfill/seals, over a time scale of one million years. Other processes are described in the main text.

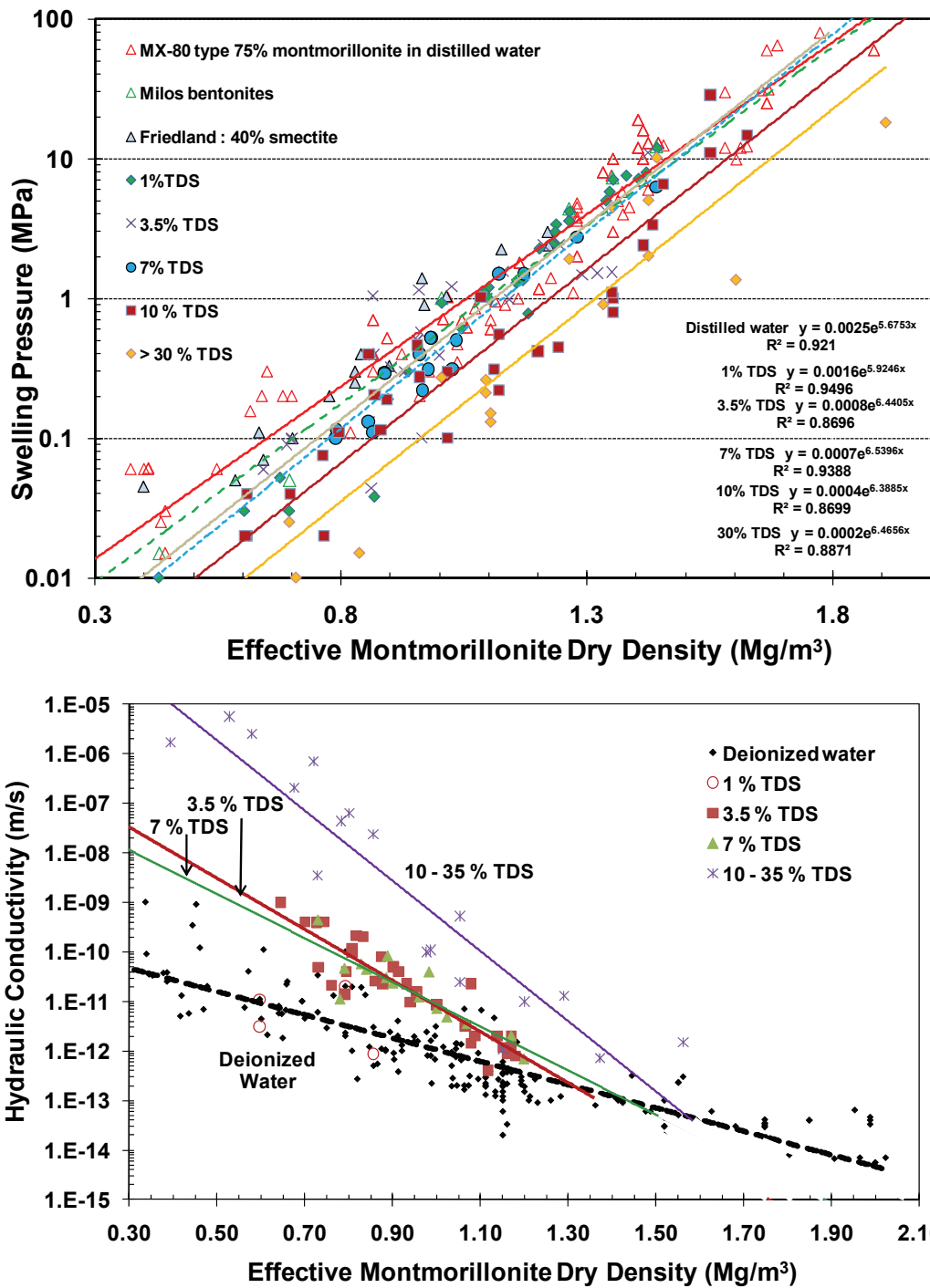


Figure 5-14: Hydraulic Conductivity and Swelling Pressure Variation with Porewater Salinity and Effective Montmorillonite Dry Density

The “effective montmorillonite dry density” is a parameter that allows a comparison of the behaviour of different types and densities of clay-based materials (Man and Martino 2009, Dixon et al. 2011a) (see Table 4-4).

Initially air would be present in the pores of the sealing materials, but it would be displaced or compressed by water as saturation proceeds. Gases that are trapped in small, isolated pore spaces of the sealing materials are likely to remain relatively immobile in occluded pockets. In contrast, the air in larger pores generally would be displaced along interconnected pore spaces towards regions of higher porosity or elevation (buoyancy). In the period prior to completion of placement room closure air can move either passively out of the system as water moves in, or if trapped as occluded, pressurised pockets may forcefully vent into still open areas (Dixon et al. 2011b). This process may affect backfilling operations and so its potential to occur needs to be assessed as part of operational planning. Eventually, once the placement room is closed the trapped air is expected to eventually dissolve into the water under hydrostatic pressures.

As the buffer in this region takes up water and swells, the shrinkage cracks generated as the result of earlier, temperature-gradient induced drying are expected to self-seal. Ultimately, the porewater pressure in the sealing materials would reach hydrostatic pressure, and saturation would be complete (McMurry et al. 2003).

The timing and rate of saturation of a repository depends on a number of site-specific conditions, although some generalized estimates are possible. For example, the amount of groundwater that would be required to saturate a backfilled and sealed placement room can be estimated based on the placement geometry and using other parameter values as needed from Table 5-1 and Table 4-4. At the time of placement room closure, the open pore spaces in the sealing materials would have a total volume of approximately 3 cubic metres per metre length of the placement room tunnel. The air in this volume would have to be displaced by groundwater to saturate the sealing materials. In low permeability rock with low porosity (approximately 0.3%, or 3 L of pore space per m³ of granite), this means that the water present in a volume of about 1200 m³ of granite must move into the repository excavations to saturate each metre-long section of tunnel. This would be equivalent to extracting all of the pore fluid from the rock for a distance of approximately 20 metres radially from the excavation walls.

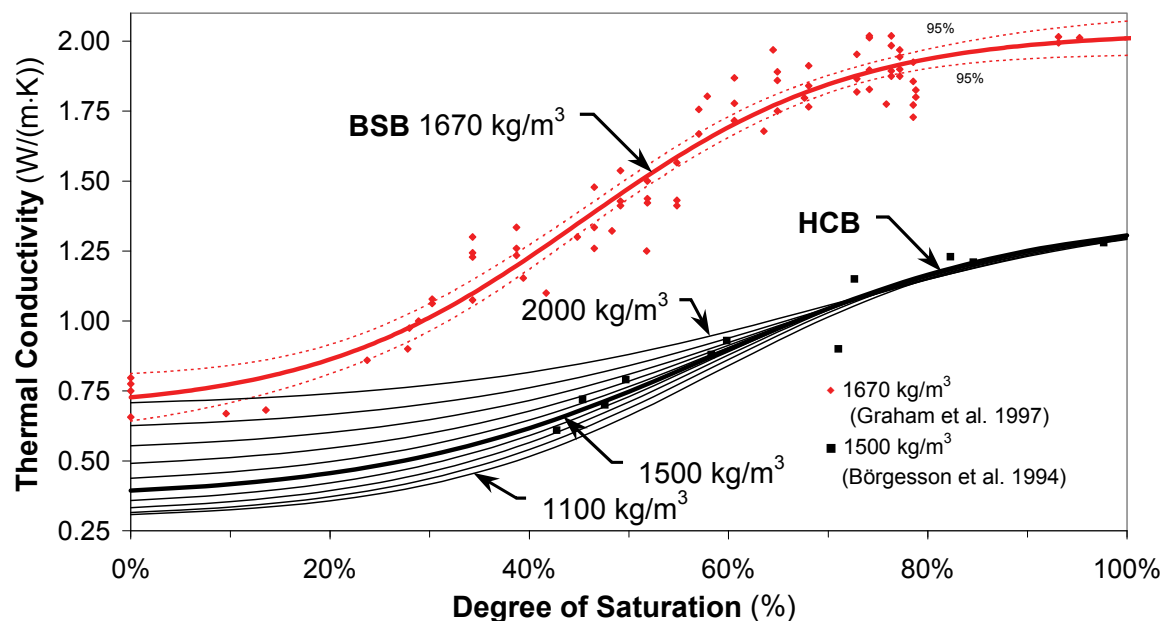
The amount of time required to achieve saturation can be estimated by treating the placement room as an empty, cylindrical tunnel into which groundwater is seeping without restriction (Freeze and Cherry 1979, p. 490). If it is assumed that the tunnel has a radius of 2.75 m and is located 500 metres underground (so the hydraulic head is approximately 5 MPa) in homogeneous rock having a hydraulic conductivity of 10⁻¹² m/s, it would take roughly 200 years for 3 m³ of groundwater to seep into a metre-long section of the room. A range in hydraulic conductivity from 10⁻¹¹ m/s (moderately fractured rock mass) to 10⁻¹⁴ m/s (very tight rock mass) results in a range of saturation times from 20 to 20,000 years (McMurry et al. 2003).

In practice, there would not be unrestricted seepage into such an excavation, for the room would be filled with low permeability sealing materials and the thermal gradient would counter the resaturation process. The repository saturation process can be assessed with numerical models capable of handling coupled thermal-hydraulic processes (e.g., CODE_BRIGHT, Guo 2009a, 2009b).

5.4.2 Temperature Changes

The thermal conductivity of the various clay-based sealing system components changes with their degree of water saturation. Figure 5-15 illustrates this relationship for bentonite-only and bentonite-sand compositions. This figure illustrates the effects of sealing material composition and water content on its heat-transfer characteristics. Initially considered for use as the buffer material in the repository concept developed by AECL, a mixture of equal dry weight proportions of sand and bentonite was defined as the reference bentonite-sand buffer for use in filling the region between the container and the surrounding rock in the in-floor borehole. Subsequent review identified highly compacted bentonite-only clay as the preferred buffer material in crystalline rock settings. The bentonite-sand mixture is still relevant as it is similar in composition to the light backfill that is planned as a component of the room backfilling system.

From the plots provided in Figure 5-15, it can be seen that in the region nearest the containers, the thermal conductivity of the buffer decreases as heat from the containers drives moisture out. In contrast, buffer thermal conductivity will improve as it moves towards saturation. Desiccation-related shrinkage cracks in the buffer would further reduce thermal conductivity if they develop circumferentially around a container. Instead, radial desiccation cracking has been observed in the unsaturated buffer closest to the heater (container) of the Buffer/Container Experiment, which is a crack orientation that is unlikely to significantly affect heat transfer (McMurry et al. 2003). Good agreement is obtained in modelling of thermal profiles in field experiments like the SKB Container Retrieval Test when the thermal conductivity characteristics provided in Figure 5-15 were used (Guo 2009b).

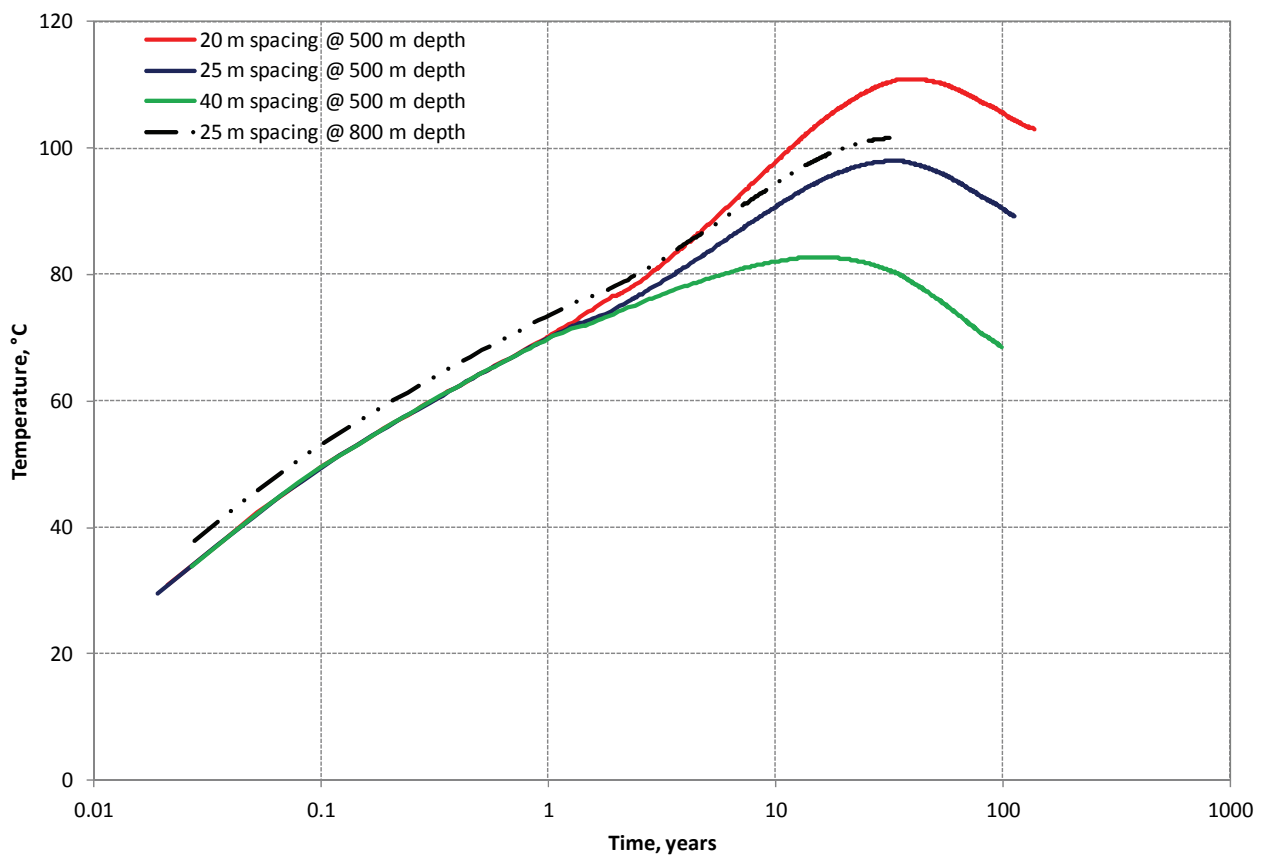


Notes: From Man and Martino (2009). Label units are dry densities.

Figure 5-15: Thermal Conductivity of 50:50 wt% Bentonite-Sand Buffer (BSB) and of Highly-Compacted Bentonite (HCB)

The maximum near-field temperatures are likely to be achieved within the first 30 years after closure as shown in Figure 5-16 for the reference case study (Carvalho and Steed 2012), so it is unlikely that the sealing system would be fully saturated with water at the time of maximum temperature. In fact, most of the pore spaces of the sealing materials closest to the container would likely be occupied by air. Heating during this time would result in expansion of the gas and a corresponding pressure increase. The compressibility of gas is large, and no significant changes in the mechanical conditions in the sealing materials will occur.

The main sealing material that would potentially be affected by thermal expansion is the concrete bulkheads (Figure 4-3), which could be affected by heat released during their curing process. These would be installed using low-heat concrete and in a manner that minimized thermal expansion and contraction during the concrete curing process.



Note: Figure is taken from Carvalho and Steed (2012).

Figure 5-16: Temperature versus Time for Three Placement Room Spacings for the In-Floor Borehole Placement Method in the Crystalline Geosphere

Later, as the temperature of the repository declines (Figure 5-1), thermal contraction of the concrete bulkhead is likely to cause some rejuvenation of cracks or the production of new

cracks at the rock-concrete interface. This process was observed in the concrete seal portion of the AECL URL Tunnel Sealing Experiment (Chandler et al. 2002). The concept of using a composite HCB-concrete structure in a repository anticipates that by the time temperatures decrease significantly in this region, the clay gasket that was installed as part of the composite seal should be fully saturated. The clay would expand (strain) providing a tight contact with the concrete and rock and if water flow is occurring from the backfilled tunnel past the concrete it is expected that some of the clay will move/intrude into the open interface and reduce mass-transport along this feature.

5.4.3 Chemical Changes

An important function of the buffer and backfill is to produce/maintain a chemical environment in the repository, which will inhibit corrosion of the containers and, in the case of a breach in a container, would tend to limit the solubility of the used fuel and the subsequent migration of radionuclides. Conversely, the composition of porewater in the repository will affect the mechanical and hydraulic properties of the buffer and backfill. The evolution of porewater chemistry in the sealing materials is a complex process that is influenced by many parameters, including the compositions and proportions of minerals in the buffer and backfill, the composition of the saturating groundwater, the temperature, the relative rates of diffusion and flow through the clay, the initial proportions of exchangeable cations in the clay minerals, and the composition of the water used during wetting and compaction of the sealing materials (McMurry et al. 2003).

5.4.4 Changes due to Biological Processes

Clay-based materials have been shown to contain indigenous aerobic and anaerobic microorganisms. Microorganisms could also enter the sealing materials during the operating phase of a repository from the air and from human activities in the short term and from the host rock in the long term. The current understanding of microbiology in the context of a repository for used nuclear fuel is summarized by Wolfaardt and Korber (2012).

Specific biogeochemical processes in the buffer, backfill and seals pertain to: i) consumption of oxygen and creation of an anaerobic environment; ii) gas production and consumption; and iii) microbiologically influenced corrosion (MIC). As the geosphere of a deep geological repository is nutrient-poor, microbial activity at depth is limited compared to the near-surface environment.

During the time that a repository is open, the Engineered Barrier System (EBS) and adjacent rock would be exposed to air. This would facilitate the growth of aerobic bacteria. After the repository is closed, the aerobic bacteria in this zone are expected to actively promote reducing conditions by consuming the remaining oxygen. Anaerobic bacteria, which were likely to have been the main forms of life in the deep subsurface environment prior to repository excavation, would eventually dominate again, and reducing groundwater conditions would be maintained far into the future. Upon establishment of anaerobic repository conditions, a variety of organisms with the capabilities to utilize alternate electron acceptors have the potential to become active. Anaerobic bacteria can both produce and consume gases, which have limited potential to impact both the physical and chemical aspects of the repository. Of particular interest, is the potential for microbial activity to cause microbiologically influenced corrosion, as discussed in

Section 5.3.1.5.4. As a result, a substantial amount of research has been conducted on ability of clay buffer to inhibit microbial activity (e.g., Stroes-Gascoyne 2010).

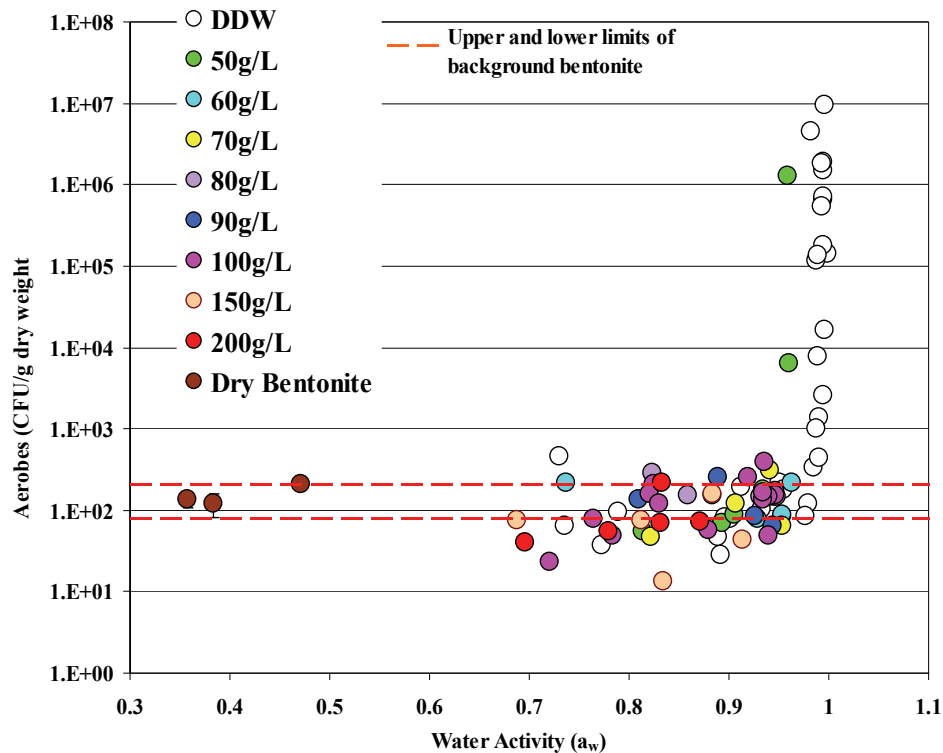
In the current Canadian EBS design, 100% highly-compacted bentonite buffer material surrounding the waste containers is proposed to prevent or minimize potential negative consequences of microbial activity, such as damage to the container or barrier integrity. Numerous studies have evaluated the survival and activity of microorganisms in clay-based sealing materials under relevant environmental conditions, as summarized in Wolfaardt and Korber (2012). The activity and abundance of microbes in a repository are affected by three main factors: the supply of usable nutrients and energy sources, the availability of water, and elevated temperatures (McMurry et al. 2003). Radiation fields are not expected to be significant due to the shielding provided by the thick-walled containers.

Sources of nutrients in the sealing materials would include organic matter associated with the clays, as well as nitrates and fuel oil from blasting residues, and hydrocarbons from diesel oils and exhaust gases, introduced during repository excavation and operation. As the organic matter in such clays has already persisted in the presence of indigenous microbial assemblages for thousands to millions of years, it is probably unrealistic to assume that all of the organic carbon would be accessible to microbes. It is likely, therefore, that “available” organic carbon would be the limiting nutrient for microbial activity in a repository.

The second factor that would have an important influence on microbes in clay-based sealing materials is the availability of water. Microbiologists generally use a thermodynamic parameter, water activity (a_w), to express water availability in a quantitative sense. This term corresponds to the ratio of a solution’s vapour pressure to that of pure water at a given temperature. The activity of porewater in sealing materials is affected in particular by the salinity of the water, as well as by the affinity of the clay for water. For example, while the water activity in pure water is 1, the water activity in a 2 mol/kg solution of CaCl_2 is about 0.85 within the compacted material (King and Stroes-Gascoyne 1997). Bacteria must expend extra effort to grow in a habitat with a low a_w because they must maintain a high internal solute concentration to retain water within their cells. Most bacteria flourish only at or above an a_w of approximately 0.98 (the a_w for seawater (see Figure 5-17)). In order for the 100% highly compacted bentonite to inhibit bacterial growth, it has been established that bentonite would need to meet one or both of the following criteria: i) a water activity of less than or equal to 0.96, resulting from a bentonite dry density of at least $1.6 \text{ Mg}\cdot\text{m}^{-3}$ or a porewater salinity greater than 60 g NaCl/L (Stroes-Gascoyne et al. 2006, 2007a, 2007b); or ii) a swelling pressure of at least 2 MPa (Pusch 1999). Swelling of clay is expected to restrict the mobility of microbes and of nutrients, causing starvation.

The third major factor affecting the viability of microbes in the sealing materials is temperature, which would range from ambient (10 - 20°C) to ~100°C adjacent to the container. Temperatures within this range would have some impact on the viability of most microbes indigenous to the sealing materials. The bacteria in dense buffer closest to the container would be subjected to the most intense heat and also the related buffer desiccation. Experiments assessing the effect of temperature suggest that microbes were not particularly sensitive to a temperature of 60°C and some culturability remained after exposure to 80°C at all dry buffer densities studied (0.8 to $2.0 \text{ g}/\text{cm}^3$), whereas at temperatures $\geq 121^\circ\text{C}$, culturability was reduced (Stroes-Gascoyne and Hamon 2010). Importantly, the effect of temperature on culturability in low dry density bentonite was reversible once the heat source was removed and re-saturation was allowed to occur,

highlighting the importance of maintaining high dry density to keep microbial activity to a minimum (Stroes-Gascoyne and Hamon 2010).



Notes: Stroes-Gascoyne and Hamon (2008). CFU – Colony Forming Units.

Figure 5-17: Effect of Water Activity on Aerobic Culturability in Compacted Bentonite

In summary, experimental evidence indicates that in a low-salinity repository environment, a highly compacted bentonite with a dry density of 1.6 g/cm³ will suppress microbial aerobic culturability below background levels (Stroes-Gascoyne et al., 2010b). In contrast, in a high-salinity repository environment, with porewater salinities ≥ 50 g/L, salinity will suppress microbial activity over a wider range of bentonite dry densities (~ 0.8 to 1.8 g/cm³) and a wide range of bentonite swelling pressures (Stroes-Gascoyne et al. 2010a and Stroes-Gascoyne et al. 2011). These studies also indicated that 100% highly compacted bentonite directly in contact with the used fuel containers will reduce microbial activity to insignificant levels.

Aerobic biodegradation of concrete is a well-known microbial process (McMurry et al. 2003, Humphreys et al., 2010). Initially, conditions in the vicinity of the concrete seals and floors in the deep geological repository may be moist and aerobic enough that any pyrite or other sulphide minerals present in the sealing materials (as part of the concrete aggregate or as minor components in buffer or backfill) could be converted to sulphuric acid by sulphate-producing bacteria. The extent of this corrosion would be minor, however, given the relatively short

duration of oxidizing conditions in the repository and the likely low abundances of sulphide accessory minerals in the sealing materials.

5.4.5 Radiation

Radiation would have little effect on the sealing materials, even near the container surfaces, because the thick-walled containers are largely self-shielding. It was estimated that for the reference container, the initial surface gamma dose rate would be approximately 0.05 Gy/h. Radiation may restrict biological processes in the immediate vicinity of the container, and it may result in minor chemical changes in gas and porewater composition due to radiolysis, but none of these effects are expected to be major (McMurry et al. 2003).

5.4.6 Sorption

Sorption is a general term for surface-related processes that involve the transfer of ions from a solution in which they have freedom of movement to a fixed position on a surface. In addition to ion exchange (Section 5.1), sorption includes surface complexation, in which ions form a strong chemical bond with a reactive surface group at the mineral surface without the displacement of any other ions, and surface precipitation, in which a chemical reaction occurs on the surface because conditions there differ from those in solution. An important function of the clay-based sealing materials is to provide a substrate for the sorption of contaminants if there is a breach of containment. The crystal structure of montmorillonite, which consists of sheet-like layers of molecules to which water and certain positively charged cations are attracted, would promote the sorption of many radionuclides and would retard the movement of anions through the clay by the process of anion exclusion (McMurry et al. 2003).

5.4.7 Vertical Movement of Containers

In the in-floor placement design, used fuel containers would rest on and be surrounded by highly-compacted bentonite buffer material. One of the design requirements of this buffer is to prevent containers from sinking further into the placement borehole, which would reduce the barrier separating used fuel from the geosphere.

One of the design requirements of the dense backfill in the placement rooms is to keep the highly-compacted bentonite surrounding the used fuel containers in place, preventing it from swelling upwards and reducing in density.

Both the bentonite buffer and the dense backfill consist of high-density blocks with different degrees of saturation; bentonite pellets fill all remaining spaces between the blocks and the rock surface. Upon closure, water is expected to enter the placement rooms and container boreholes, wetting, swelling and compressing the blocks and pellets. The rate of resaturation will depend on the rate and location of water inflow and the actual evolution of the saturation and homogenisation of the buffer and backfill. Variability in resaturation is expected to lead to an uneven distribution of swelling pressures within the boreholes and placement rooms. In addition, some upwards swelling is expected since the dense backfill has a lower swelling pressure than the bentonite buffer and a certain degree of compressibility.

Modelling uneven swelling of buffer and backfill materials within the placement rooms has been carried out by Börgesson and Hernelind (2009), including both finite element modelling and

analytical calculations. The conclusions were that swelling pressure of the buffer would be sufficient to meet design requirements under all possible permutations of resaturation.

Uneven resaturation was predicted to cause between 3.2 mm and 5.0 mm vertical displacement of containers (SKB 2011). Vertical displacement was very insensitive to consolidation or creep due to reduced buffer density: with densities as low as 1500 kg/m³ at saturation, containers were predicted to sink no more than 2.25 cm.

5.4.8 Erosion and Colloid Formation

Under conditions where buffer or backfill is exposed to advective groundwater, physical erosion of the sealing materials may occur, creating voids into which the sealing materials would expand under reduced swelling pressures, and the clay particles may be suspended in water as colloids. This would likely be a localized condition associated with the period of time prior to saturation of the repository, when hydraulic gradients are greatest. This would be minimized by avoiding placement of containers near water conducting fractures and the use of grout to seal fractures. After saturation, low groundwater gradients would be re-established.

Colloids are small solid particles between 1 nm and 1 µm in diameter that are suspended and dispersed in groundwater. Colloids also may form by microbial activity or as precipitates due to a change in porewater chemistry. Colloids are of interest in a repository primarily because they have the potential to sorb radionuclides if containers have failed, at which point the transport of the contaminant is controlled by the mobility of the colloid rather than by the chemical speciation of the radionuclide.

Destabilization of the engineered barriers due to influx of low salinity groundwater (e.g., water from melting of ice sheets) could occur. In this case, if freshwater contacts the bentonite around a container through a fracture, then the bentonite may expand into a gel in the low-salinity water and release material as colloids that could slowly diffuse away. Eventually, this could result in erosion of the buffer around the containers, and potentially allow the corrosion of the copper shell. For the current study, it is assumed that the repository is located at a site where glacier meltwater penetration is low, and therefore, the buffer erosion process has been neglected.

5.4.9 Confidence and Uncertainties

The engineered sealing system components would be installed subject to design, manufacturing, and construction specifications, and so their properties initially would be known with a high degree of confidence. Nevertheless, there are uncertainties about the long-term behaviour of the materials and the processes that would affect them.

Temperature: There is good confidence in the results of thermal models over long timeframes. Temperatures in the near-field are generally well-predicted in modelling of in-situ tests. Uncertainties would tend to be localized, and due to spatial variability in properties or in local gap dimensions.

Saturation: Considerable confidence exists in the ability to describe repository performance in a saturated state, but there would exist a period of tens to hundreds of years in which saturation has not yet been achieved. It is during this pre-saturation stage of repository evolution that many of the interactions between repository components would occur. The saturation of a

repository involves coupling of thermal-hydraulic-mechanical processes. Current numerical models are able to broadly explain the evolution of saturation conditions from in-situ tests.

Swelling Pressures and Stresses: The swelling pressures generated by the buffer would depend on the buffer composition, buffer density, and groundwater conditions. The swelling characteristics of a wide range of bentonite based sealing materials have been determined through testing but would need to be confirmed for site-specific conditions. The manner in which stresses develop within a repository would also influence the swelling pressure. Strains within one component of the repository sealing system may affect the density and hence the swelling pressure development of another component. The development of thermal stresses in conjunction with the hydraulic and swelling stresses within a multi-component system is complex. Numerical models are presently weakest in explaining the evolution of the stress field in the near-field.

Evolution of Material Properties: A few of the sealing materials, such as the light backfill, are not yet well-defined or well-characterized with respect to their performance under repository conditions. Further studies on the long-term evolution of the seal materials under interaction with adjacent materials and groundwater are warranted.

Mineralogical Stability of Montmorillonite: Under the expected repository conditions (temperatures less than 100°C, moderate pH levels, low potassium concentrations in groundwater), it is very unlikely that substantial conversion of montmorillonite to illite would occur over a million-year timeframe. Uncertainties remain about the kinetics of the process under certain adverse conditions.

Microbial Processes: Although viable microbes would inhabit at least some portions of a deep geological repository, there are a number of uncertainties associated with the extent of changes that would result from their presence. Experimental data indicate it is unlikely that bacteria would become active or able to recolonise saturated, highly compacted buffer material that contains a large proportion of bentonite; however, the factors that control this effect (e.g., water activity, space restrictions due to swelling, and material property differences at interfaces) are not clearly understood.

Redox Conditions: There is some uncertainty about when reducing conditions would be established in the sealing materials. McMurry et al. (2003) notes that estimates of the time required to reach anaerobic conditions have varied, depending on assumptions made in the calculations, from approximately ten years to several thousand years. Regardless of the amount of time required for oxygen in the repository to be consumed, the total amount of oxygen available for reaction is limited. There are no processes applicable to the expected evolution of the repository (including radiolysis), that are likely to introduce significant additional quantities of oxygen after closure.

Interactions Between Sealing System Components: The interfaces between materials might provide preferential pathways for the migration of water, contaminants, or microbes within a repository. Examples of such interfaces include; installation assembly gaps (e.g., between blocks of compacted buffer), shrinkage cracks during the desaturation phase, and the formation of an open space along the top of the room if there is insufficient backfill swelling.

5.5 Long-term Natural Evolution of the Geosphere

As noted in Chapter 1, the geosciences program for a future candidate site will be designed to support the safety case. As part of Geosynthesis activities, both regional and site-specific information from site characterization activities would be integrated to provide improved understanding of the natural processes that might affect the performance of a repository over one million years. These processes include climate change (specifically glaciations) and geologic processes such as glacial erosion, seismicity, fault rupture/reactivation and volcanism (Table 5-7). The probability and likely effects of each of these processes are described in the following sections, in support of two key geologic site attributes (see also Chapter 1):

- The depth of the host rock isolates the repository from surface disturbances and changes caused by human activities and natural events; and
- Current and future seismic activity at the repository site does not adversely impact the integrity of the repository during operation or in the very long term.

Table 5-7: Processes with a Potential Influence on the Geosphere

PROCESS	INFLUENCE
THERMAL	
Glaciation-related cooling	<ul style="list-style-type: none"> • Permafrost formation • Development of thick ice sheet
HYDRAULIC & PNEUMATIC	
Glaciation and permafrost formation	<ul style="list-style-type: none"> • Regional changes in groundwater flow pattern • Depth-related changes in groundwater composition
MECHANICAL	
Glacial loading and unloading	<ul style="list-style-type: none"> • Glacial erosion • Repository rock mass stability
CHEMICAL	
Glaciation-related changes in groundwater flow	<ul style="list-style-type: none"> • Depth-related changes in groundwater composition • Potential precipitation of secondary mineral phases due to depth-related changes in groundwater composition
BIOLOGICAL	
Glaciation-related changes in groundwater flow	<ul style="list-style-type: none"> • Potential changes in microbial activity due to depth-related changes in groundwater composition

Notes: Glaciation is the most significant process likely to disturb the geosphere at repository depths over a time scale of one million years. Other processes are described in the text.

5.5.1 Geological Disturbances

The following sections describe, in general terms, the probability and likely effects of seismicity, fault rupture/reactivation and volcanism on a repository located in a Canadian Shield setting.

5.5.1.1 Seismicity and Seismic Hazard Assessment

In general, the Canadian Shield is characterized by low levels of seismic activity as it is located within the center of the stable North America craton (Hayek et al. 2010). Large earthquakes are infrequent, with present day seismicity confined to pre-existing zones of weakness, such as ancient faults and fracture networks. An increase in the frequency of earthquakes is expected during a glacial cycle but the magnitude of these events is expected to remain low. This scenario is based on the lack of apparent evidence for post-glacial rupture within the Canadian Shield even though ice sheet loads act to increase vertical stresses. To further improve confidence in long-term stability regarding seismic hazards, there is a considerable body of evidence to show that earthquakes, in general, are less destructive at depth than at the surface, diminishing the impact of any seismic activity (including proximal events) on a deep geological repository (Bäckblom and Munier 2002, Atkinson and Kraeva 2011).

Although beyond the scope of the current study, it is noted that for an actual site (or sites) selected as potentially suitable to host a deep geological repository, a probabilistic seismic hazard assessment would be conducted for the area, following the guidance of the Senior Seismic Hazard Advisory Committee (SSHAC 1997). Seismic monitoring would also be conducted as part of site characterization activities to capture additional information on low-magnitude seismic events.

5.5.1.2 Fault Rupture and Reactivation

As previously mentioned, seismicity within a shield environment is expected to be confined to regions containing pre-existing features (e.g., faults, fractures) within the rock mass. Damage to intact rock is not expected to occur, because in-situ tectonic and glacially induced stresses are not considered sufficient to generate the forces required to create new ruptures within fresh rock (Lund 2006). There is, however, evidence from the Scandinavian Shield that the effects of glacial loading on the lithosphere can lead to fault reactivation. Examples of fault reactivation include the Pärvie fault, which displays offsets of up to 10 m over distances of 150 km (Kukkonen et al. 2010). Within the Canadian Shield, there is only one example of a modern earthquake being linked to surface rupture – the 1989 Ungava (Northern Quebec) earthquake that displayed up to 3 m of offset over 7 km (Adams 1989). There is currently no evidence for surface rupture within Ontario, and no structures can be conclusively linked to postglacial reactivation (Fenton 1994).

5.5.1.3 Volcanism

Volcanoes are primarily found at plate boundaries. Because the Canadian Shield is located several thousands of kilometers from the nearest plate boundary, the risk to a repository from a volcano is considered insignificant. Another mechanism that might create a volcano is a mantle plume, or “hot spot”. There is evidence for ancient hotspots and associated volcanism within the Canadian Shield; the last volcanic eruptions in the Canadian Shield occurred more than a billion years ago (Wheeler 1995). The closest active “hotspot” is located in the Snake River Plain and Yellowstone area of the western United States. If relative plate motions continue as they are today, some new volcanic activity may be initiated 20 million years in the future, when a portion of the Canadian Shield passes over this mantle plume (McMurry et al. 2003).

5.5.2 Climate Change (Glaciation)

The last 2 million years of Earth's history has been marked by a period of glaciation. Ice coverage was not continuous over the shield during this period, but was marked by many cycles of glacial ice sheet advance and retreat, separated by ice-free periods of warmer climate (interglacials), lasting from thousands to hundreds of thousands of years. Nine glacial cycles occurred over the past million years. During the last glaciation, starting approximately 120,000 years before present, more than 97 percent of Canada was covered by ice. The Laurentide Ice Sheet covered all of the Canadian Shield and much of the remainder of Canada. The final retreat of the ice sheet occurred between about 9,000 and 6,500 years ago. Discussion on the current understanding of glaciations, and the processes that cause glaciations, can be found in Peltier (2002).

If a reglaciation of the Canadian land mass should occur again in the future, such an event is most likely to begin approximately 60,000 years from present (Peltier 2011, Garisto et al. 2010). If at that time, the concentration of carbon dioxide and other greenhouse gases in the atmosphere were similar to present levels, it is unlikely that a renewed episode of glaciation could occur. Because our ability to predict the CO₂ level that will exist at a time so far into the future is difficult, we cannot discount the possibility of a renewed glacial event and, therefore, must take glacial processes into account when developing the safety case for a used fuel repository.

The numerous characteristics of the glaciation process that are relevant to the understanding of repository performance include: 1) erosion, related to ice sheet movement across the land surface and 2) mechanical properties, such as the time dependence of the thickness of glacial ice that could develop over the site and the normal stress regime associated with the weight of this load. Also relevant is the evolution of temperature at the base of the ice sheet. Periods of thickest ice cover are associated with the warmest basal temperatures, which is a consequence of the degree of thermal insulation provided by the thick ice and the continuing flow of heat from the Earth's interior into the base of the ice sheet. The subsurface thermal regime is also important to repository performance, in particular is the depth to which frozen ground (permafrost) may extend. This issue is important not only in the regions that are episodically ice-covered, but also in exterior regions where the influence of permafrost may be even more extreme. In regions within which the base of the ice sheet is temperate (i.e., having temperatures above the freezing point), meltwater is continually generated by the outflow of geothermal heat, and the rate of such generation is crucial to understanding the extent to which such meltwater may be forced to infiltrate into the subsurface and potentially impact deep groundwater systems.

The phenomena associated with glaciation potentially affecting a repository and/or the geologic setting at the repository site can be grouped into three broad categories: glacial erosion, glacial loading, and permafrost formation. These are discussed under the headings below.

5.5.2.1 Glacial Erosion

The primary process interpreted to result in erosion over the next million years is glacial activity. Glacial meltwater can erode sediment and rock by abrasion, quarrying, and mechanical erosion. Regardless of the mechanism, the rate of surface erosion can be limited by the ability of the meltwater to remove debris (e.g., due either to an insufficient hydraulic head gradient to carry

debris-laden subglacial water out of the basin, or the lack of adequate subglacial pathways for water). In terms of erosion at a local level, the basal sliding velocity is the primary factor controlling the rate of erosion. However, rapid basal sliding velocity does not necessarily correlate with rapid erosion at the base of the glacier, as the glacier may be decoupled from the bedrock surface by a thin layer of basal melt water.

A number of studies have produced estimates of the amount of erosion by the Laurentide Ice Sheet and Fennoscandian ice sheets. Geomorphic studies indicate many examples where the pre-glacial regoliths or river valleys have been preserved. Most work performed to-date to estimate glacial erosion suggests that total erosion during the Quaternary did not exceed 10 m to 40 m for both the Laurentide Ice Sheet and Fennoscandian ice sheets (Sugden 1976, Lidmar-Bergstrom 1997). Therefore, glacial erosion is not expected to affect a repository located at a depth of 500 m.

5.5.2.2 Glacial Loading

As indicated above, the onset of the next glacial event will likely occur approximately 60,000 years into the future, assuming that atmospheric CO₂ levels are reduced to approximately 280 ppm by volume (Peltier 2011). Climate modelling of the late Quaternary ice advances and retreats has predicted ice thicknesses of up to 4 km of ice over northern Canada (Peltier 2002). The last glacial episode had a duration of approximately 120,000 years, and involved multiple glacial advances and retreats, resulting in loading and unloading cycles on the underlying rock with each advance and retreat.

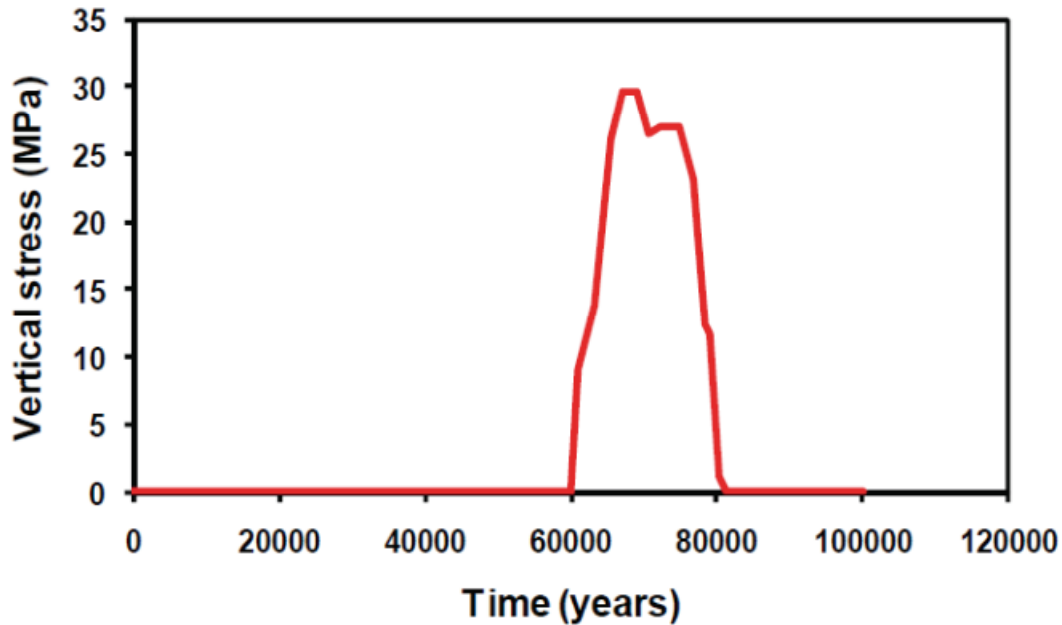
The weight of the thick ice sheet acts to depress the Earth's crust and removal of the ice load by melting leads to crustal rebound, a process known as isostasy, which continues today. Peltier (2011) has predicted that the maximum crustal depression from the equilibrium level occurred at the Last Glacial Maximum (LGM) and reached values in excess of 500 m. The present-day uplift rate is about 6 mm per year around Hudson Bay. Uplift rates are lower farther away from this region, and all of the rates are gradually diminishing with time.

The University of Toronto Glacial Systems Model (UofT GSM), which is a model of continental-scale glaciation events, was used by Peltier (2011) to develop a description of glaciation of the Canadian Shield as a means of assessing the impact that such an event would have on performance of the deep geological repository. A maximum glacial event time profile for ice loading was developed based on Peltier (2011), as shown in Figure 5-18, and indicates that the vertical stress reached a maximum value of approximately 30 MPa. In addition to changing the vertical stress at depth, glaciation can also cause the horizontal stress to increase due to both Poisson's effect and plate bending. The horizontal stress increase due to Poisson's effect is:

$$\Delta\sigma_h = \frac{\nu}{1-\nu}\Delta\sigma_v \quad (11)$$

where σ_h is the horizontal stress, σ_v is the vertical stress and ν is the poisson's ratio. The increase in the horizontal stress due to plate bending is also proportional to the increase in vertical stress, with the maximum increase assumed to be 2 MPa. Numerical analyses carried out by Lund et al. (2009) showed that shear stresses are relatively minor compared to the vertical and horizontal normal stresses.

Numerical modelling of the effects of stress changes associated with glacial advance and retreat (as described above) on a repository is beyond the scope of this study for a hypothetical site, but would be conducted in order to support a safety case for a candidate site.



Notes: Time from present is for first event.

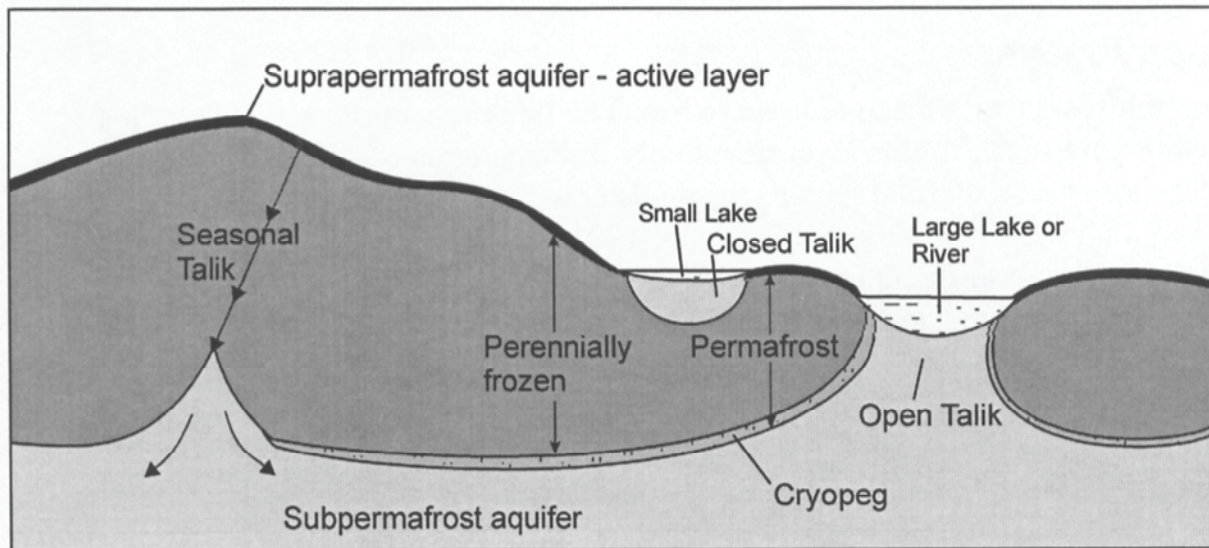
Figure 5-18: Simulated Evolution of Ice Sheet Load

5.5.2.3 Permafrost Formation (Changes in Groundwater Recharge)

Permafrost formation as a result of glaciation will impact the extent to which glacial meltwater will infiltrate into the subsurface. Future glacial conditions in the Canadian Shield would be preceded by an extended period with widespread formation of permafrost. In more southern Canadian locations, the permafrost would likely be discontinuous. Under permafrost conditions, groundwater would freeze in the subsurface, decreasing the connected porosity and permeability and thus significantly decreasing recharge and altering flow system hydraulic gradients for up to tens of thousands of years (Lemieux et al. 2008, Peltier 2002). Model-based analyses that employ 3-D thermo-mechanically coupled ice sheet models and constrained climate chronologies could be used to analyze and predict past and present subsurface temperature fields and, thus, permafrost depth at a specific site (e.g., Peltier 2011).

In regions of permafrost, taliks are regions of perennially unfrozen ground that exist within otherwise continuous permafrost environments (Peltier 2004). Figure 5-19 illustrates the different types of taliks that may form in permafrost environments. The formation of taliks is dependent on site-specific thermal, chemical, geological and hydrological conditions

(Peltier 2004). Heat emanating from the repository is unlikely to create a talik because periglacial conditions are not expected for several tens of thousands of years, after heat from the repository has already decreased.



Note: Figure is from Van Everdingen (1990).

Figure 5-19: Aquifers Commonly Found within Regions of Permafrost

Meltwater beneath glacial ice sheets can be pressurized, resulting in hydraulic heads far in excess of those found during interglacial periods. The two most important factors affecting the penetration of this pressurized water into the rock are permafrost depth and stress changes developed from the ice load. In a crystalline rock environment, changes in the stress field within the rocks may alter the hydraulic conductivity of the fracture network as a result of isostatic depression and forebulge development.

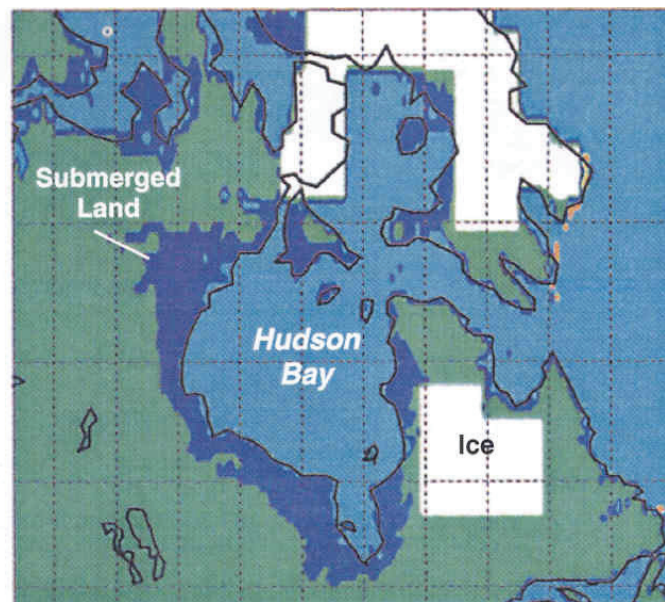
When permafrost exists under the ice sheet (cold-based conditions), groundwater recharge to depth is inhibited, despite the high hydraulic head imposed by the ice sheet. A warm-based ice sheet is one in which the free water at the base is at temperatures above the pressure freezing point beneath the ice (i.e., no permafrost), and enhanced recharge can occur. Subglacial groundwater flow patterns associated with warm-based conditions are likely to involve increased volumes of water and more rapid movement than pre-glacial or cold-based conditions, particularly in the shallow groundwater flow system.

Glaciation-related changes in groundwater chemistry are not expected to affect the redox or salinity conditions of groundwaters at repository depth in the Canadian Shield (Gascoyne 1999). Recent studies of the thermal and fluid history of calcite formation in the Lac du Bonnet batholith and in crystalline rocks of the Fennoscandian Shield (Gascoyne et al. 2003, Blyth et al. 2002) suggest that the downward percolation of geologically recent waters, such as young glacial meltwaters, is limited in scope, even at moderate depths. Paleohydrogeology and geochemical

modelling studies can be used to evaluate changes associated with previous glaciation events in the Canadian Shield at a specific site. For example, geochemical, mineralogical and isotopic data from the Lac du Bonnet batholith (Gascoyne 2000) indicate that only the upper, actively circulating groundwater system was affected by past glaciations, with deeper, denser, high salinity waters remaining largely stagnant.

During and after glacial retreat (melting), the weight of the ice would be removed, and the flow system would begin to return to pre-glacial conditions. Depending on site-specific properties, such as permeability, groundwater salinity and specific storage, the time required for the system to stabilize is likely to vary. Where glacial melting results in groundwater recharge, a hydraulic gradient promoting subsurface recharge would most likely develop either near the edge of the ice sheet (if there is a sharp change in topographic relief) or in the transition zone between the unmelted base of the glacier bed and the start of subglacial meltwater tunnels (McMurry et al. 2003).

The end of a glacial cycle would also increase the proportion of the Canadian Shield covered by surface waters. For example, it is likely that two factors - a regional isostatic depression of the Canadian Shield due to glacial loading, and a rise in global sea level due to melting of the ice sheet - would expand the size of Hudson Bay. Modelling by Peltier (2002), based on information from the last major glaciation, indicated that the combined effect of these two factors would extend the Hudson Bay shoreline by as much as a few hundred kilometres in some places (Figure 5-20); a condition that would persist for at least several thousand years while the crust rebounds. Furthermore, the end stages of continental-scale glaciation commonly are associated with the formation of large freshwater lakes, such as glacial Lake Agassiz in central Canada (Teller 1995).



8 KBP

Notes: Figure from Peltier (2002). Modelled time = 8,000 years before present.

Figure 5-20: Simulated Expansion of Hudson Bay Coastline during Glacial Melting

Detailed evaluations of the potential effects of glaciation on regional and site groundwater flows in crystalline environments are provided in Walsh and Avis (2010) and Normani (2009). To assess the depth of penetration of glacial waters into the deep groundwater system at the hypothetical crystalline site considered in this study, paleohydrogeological modelling was completed for the Laurentide glacial episode (120,000 to 10,000 years before present) and presented in detail in Chapter 2 (Section 2.3.5.3). The key insights from the illustrative modelling are summarized below.

A total of ten paleohydrogeologic simulations were performed to investigate the role of varying paleoclimate boundary conditions. Details of the paleoclimate modelling scenario can be found in Section 2.3.5.3. The performance measure of choice to compare the paleohydrogeologic simulations is the movement of a conservative unit tracer applied with a Cauchy boundary condition at the top surface of the model domain. This tracer represents the predicted migration of recharge waters into the groundwater system over the course of a 120,000 year simulation. The depth of the tracer is determined by the 5% isochlor, which is conservative in that it represents a pore fluid containing 5% recharge water. The 5% isochlor provides an indication of recharge water migration into the subsurface, which can be used to compare alternative paleohydrogeologic scenarios. The paleohydrogeologic simulations do not consider reactive transport; therefore, although the 5% isochlor provides an indication of the percentage meltwater, it does not take into account the consumption of oxygen. As discussed in Section 2.3.5.3, field evidence from crystalline environments investigated to-date suggests that all dissolved oxygen within recharging glacial meltwater is expected to be consumed within the shallow groundwater system. In addition to the tracer, Péclet numbers were estimated to assess changes in transport mechanisms during the paleohydrogeologic scenarios. The Péclet number is estimated by comparing rates of advection to diffusion.

The depth of penetration of the conservative tracer is shown as a cumulative density function plot in Figure 5-21. Given the conservatism chosen in defining the conceptual model of the geosphere, the CDF of the 5% isochlor will represent a lower bounds on the depth to which glacial meltwater will penetrate. The distribution and duration of permafrost at the site will play a strong role in governing the depth of meltwater penetration.

The impact of permafrost distribution and duration on recharge can be observed by comparing the 50th percentile tracer depths for fr-base-paleo and fr-base-paleo-nn2778. Scenario fr-base-paleo represents a cold-based glaciation with a more extensive permafrost extent, compared to the warm-based glaciation for fr-base-paleo-nn2778. The permafrost distributions and durations are shown in Section 2.2.2.3, Figures 2-6 and 2-7. Because the permafrost duration for a warm-based glacier is shorter than that of a cold-based glacier, recharging groundwater (fr-base-paleo-nn2778) is predicted to reach greater depths in a warm-based glacier scenario than for the cold-based glacier scenario (fr-base-paleo).

The fracture network hydraulic conductivity used for this case study is conservatively assumed to be uniform with depth. However, fracture zones encountered during site-characterization activities at a potential repository location will likely have hydraulic conductivities that decrease with depth, which is supported by statistical analyses of fracture permeability data undertaken by Normani et al. (2007). It is expected that including a depth-dependent fracture permeability distribution in the hydrogeological modelling will act to decrease the predicted the depth of penetration of glacial meltwater, and will more realistically represent the stability of the intermediate and deep groundwater systems.

Plots of Péclet number versus time are shown in Figure 5-22 for points bounding the repository, as well as at the repository centre. As illustrated by the plots, mass transport mechanisms within the repository during the 120,000 year paleohydrogeologic simulation will remain diffusive.

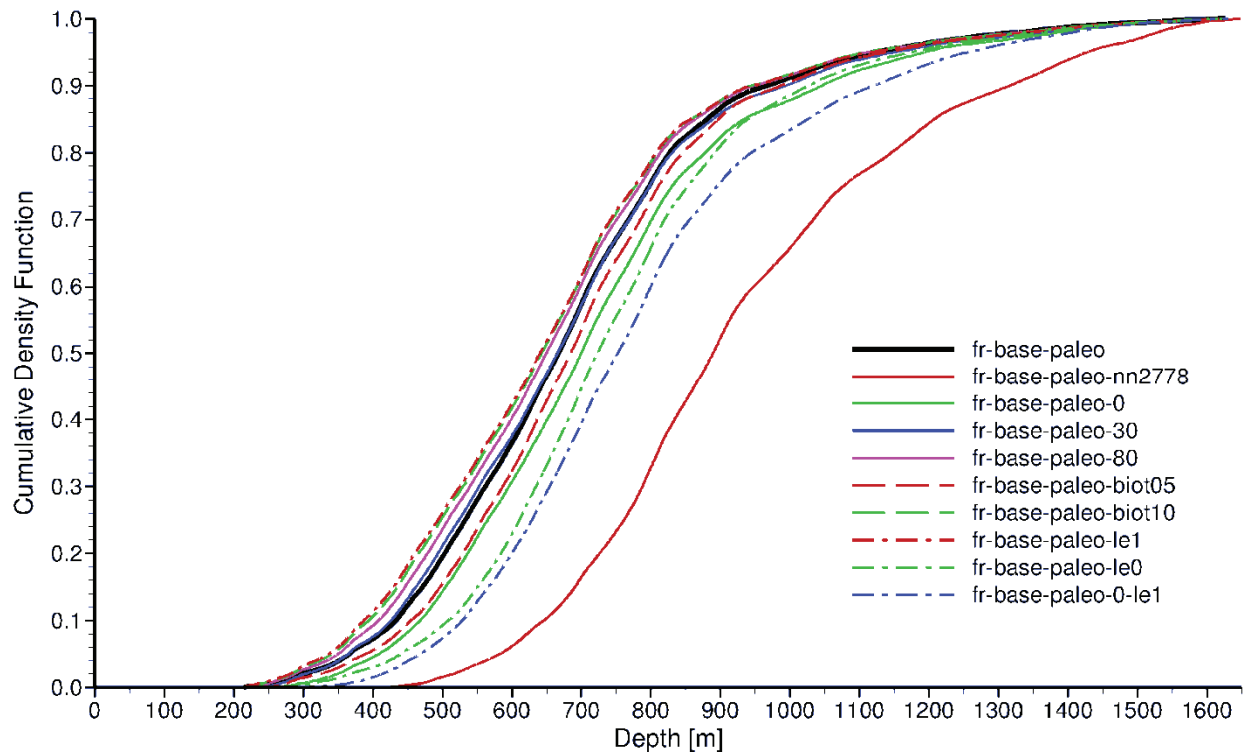


Figure 5-21: A Cumulative Density Function of 5% Isochlor Depth for Paleohydrogeologic Sensitivity Cases

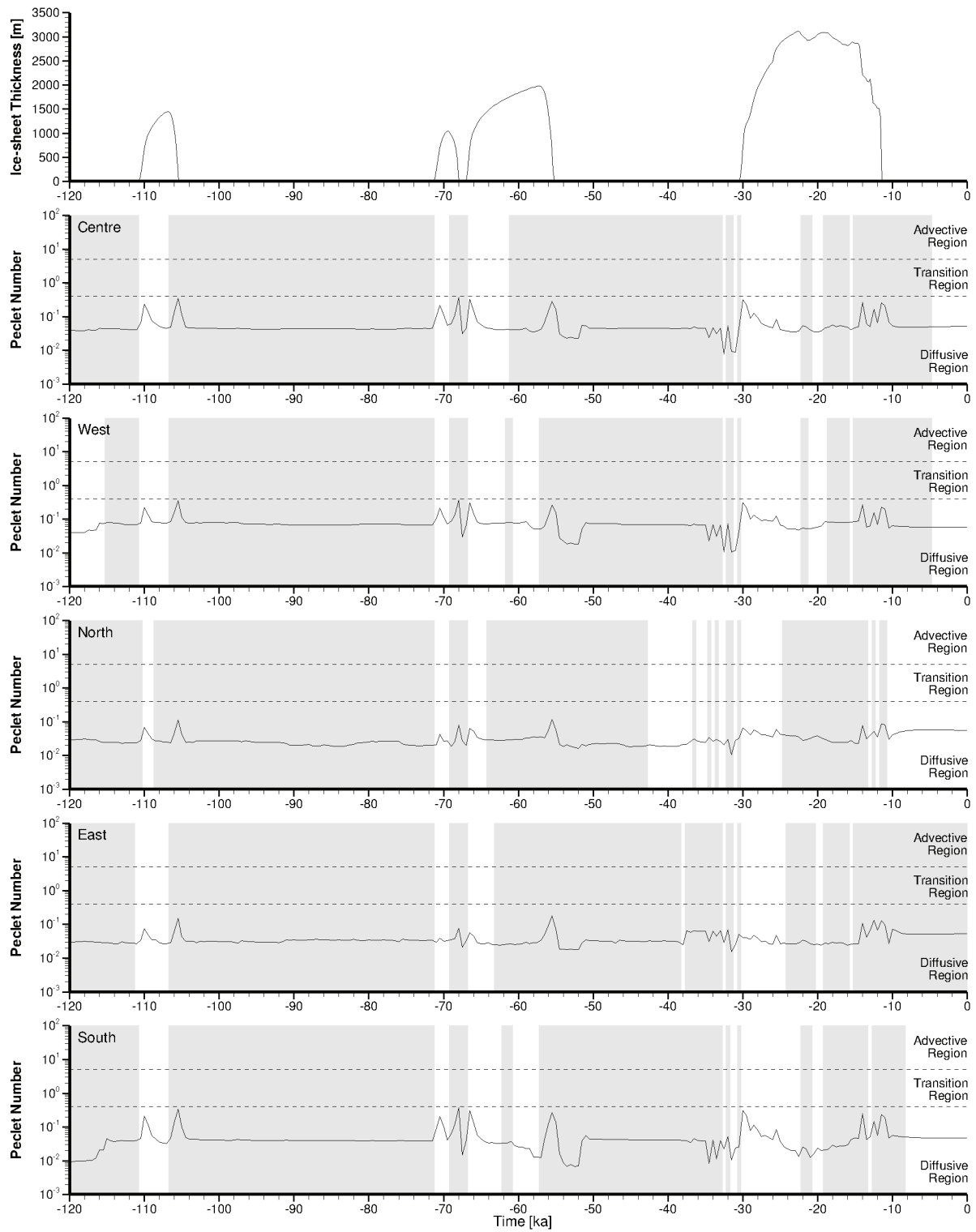


Figure 5-22: Péclet Number versus Time for the Reference Case Paleohydrogeological Scenario (fr-base-paleo)

5.5.3 Confidence and Uncertainties

As noted in Chapter 1, the geosciences program for a future candidate site will be designed to support the safety case. A site model and Geosynthesis will be developed in the phased site characterization work program. The work program will allow for the iterative development, testing and refinement of a site-specific model that will contribute to managing uncertainties in scientific understanding, data and models.

Temperature: The thermal conductivity of crystalline rock is primarily influenced by the rock composition and structure. Many of the uncertainties associated with estimates of heat transport in the geosphere would be resolved during site characterization activities. Temperature distributions in the geosphere would vary on a local scale as a result of details of repository design. Sensitivity analyses indicate that the overall magnitude and duration of temperature changes in the geosphere are broadly similar for a many different repository designs (e.g., Baumgartner and Ates 2002).

Fracture Development: The main uncertainties about future fracture development are those associated with site-specific variables such as regional stresses, rock strength, rock type, rock fabric (e.g., foliated or granitoid), and the rate at which groundwater saturates the repository and induces a swelling pressure in the buffer and backfill. Many of these uncertainties would be defined, or would become more closely bracketed by a range of values, during detailed site investigations.

A factor in repository siting is the geomechanical environment. The host rock would be demonstrably resilient to fracture development based on its history, and further the actual repository location would avoid fracture zones or faults where future fracture movement or development is more likely.

Groundwater Flow: The primary uncertainty in understanding the groundwater flow in crystalline rock is the location and characteristics of the fractures. The understanding and confidence in characterisation of the fracture network will depend on site-specific conditions. Evidence gathered during site characterisation activities would attempt to minimize uncertainties through a synthesis of geologic, structural geologic, hydrogeochemical and physical hydrogeology to assess long-term groundwater system evolution and stability. Such efforts would be aided through the application of numerical methods that provide a systematic framework to integrate independent data sets. Such techniques, as supported by field data, can provide a basis to gain insight into trends (i.e., time rate of change and magnitude) of groundwater system response to external events and constrain influence of fracture system uncertainty with regard to geosphere performance.

Glacial Processes: Peltier (2011) provides a review of what is currently known concerning the geologically recent history of long-term climate change, as background to the detailed analysis of the conditions that would be expected to develop at and below the surface of the Earth if the Canadian land mass were to be reglaciated. Results from an appropriately calibrated model of the most recent glaciation events that occurred in the Late Quaternary period of Earth history are used as a model of a future reglaciation event. The physical model employed for the purpose of this analysis is the University of Toronto Glacial Systems Model (UofT GSM).

The analyses that have been performed using the UofT GSM, for the purpose of contributing to the development of the required future glacial event predictions, are explicitly based upon the fact that it is impossible to provide a unique description of the detailed characteristics of such an event. The approach used is to apply Bayesian methods to examine the range of models that would be compatible with the constraints that can be brought to bear upon the detailed characteristics of the most recent North American glaciation event of the Late Quaternary ice-age. It is thereby shown that the spread of model characteristics is rather broad, sufficiently broad, it is believed, to encompass the characteristics of any similar event that could occur in the future (Peltier 2011).

Geochemistry: Uncertainties in the future evolution of groundwater compositions are coupled to uncertainties about the movement of groundwater. Similarly, impacts of glaciation at repository depth will be dependent on site-specific conditions, particularly with respect to the nature of the fracture network. The age, and potential influence of glaciation on most groundwaters cannot be determined directly, but is inferred from paleohydrogeological evidence such as fracture mineralization, fluid inclusion data, and stable isotope ratios in groundwaters and porewaters. Together with numerical tools, such as reactive transport modelling, this information can be used to illustrate the potential evolution of geochemical conditions at repository depths.

5.6 Summary

This discussion describes changes that would occur in the multi-barrier repository system during its lifetime. The discussion is based on reasonable expectations for conditions that are likely to be encountered in granitic rock of the Canadian Shield.

Confidence is provided by the fact that many properties of the repository components, and the processes that would affect them, are well-characterized. The system is based on durable materials and passive natural processes. Natural and archaeological analogues help to support the descriptions of system behaviour into the far future. Of the uncertainties that remain, some questions would be resolved during the site characterization. Other uncertainties about the future evolution of the system arise from the recognition that simplifying assumptions and simple models may not in all cases adequately represent the complexity or heterogeneity of an actual repository over long periods of time. These uncertainties would be addressed by further analyses, by additional experimental or field studies (including extended monitoring in the repository itself), and by using conservative or bounding assumptions in the safety assessment models.

5.7 References for Chapter 5

Adams, J. 1989. Postglacial faulting in eastern Canada: Nature, origin and seismic hazard implications. *Tectonophysics* 163, 323-331.

Atkinson, G.M. and S.N. Martens. 2007. Seismic hazard estimates for sites in the stable Canadian craton. *Canadian Journal of Civil Engineering* 34, 1299-1311.

Atkinson, G. and N. Kraeva. 2011. Polaris Underground Project at Sudbury Neutrino Observatory (P.U.P.S.). Nuclear Waste Management Organization Report TR-2009-02. Toronto, Canada.

Bäckblom, G. and R. Munier. 2002. Effects of earthquakes on the deep repository for spent fuel in Sweden based on case studies and preliminary model results. Swedish Nuclear Fuel and Waste Management Company Report TR-02- 24. Stockholm, Sweden.

Baumgartner, P. 2006. Generic Thermal-Mechanical-Hydraulic (THM) Data for Sealing Materials – Volume 1: Soil-water Relationships. Ontario Power Generation Report 06819-REP-01300-10122-R00. Toronto, Canada.

Baumgartner, P. and Y. Ates. 2002. Packaging Plant and Repository Factors Affecting the Selection of Preferred Used-fuel Container Geometries and Capacities. Ontario Power Generation Report 06819-REP-01200-10064-R01. Toronto, Canada.

Blyth, A.R., S.K. Frape, T. Ruskeeniemi, and R. Blomqvist. 2002. Long-term hydrogeological stability of crystalline bedrock in glaciated terrains: Evidence from the Palmottu natural analogue research site, Finland. Geological Society of America, Abstracts with Programs, 34(6), 498-499.

Börgesson L. and J. Hernelind. 2009. Mechanical Interaction Buffer/Backfill. Finite Element Calculations of the Upward Swelling of the Buffer against both Dry and Saturated Backfill. Swedish Nuclear Fuel and Waste Management Company Report R-09-42. Stockholm, Sweden.

Carvalho, J. L. and C. M. Steed. 2012. Thermo-Mechanical Analysis of a Single Level Repository for Used Nuclear Fuel. Nuclear Waste Management Report APM-REP-00440-0010. Toronto, Canada.

Chandler, N.A, A. Cournut, D.A. Dixon, C. Fairhurst, F. Hansen, M. Gray, K. Hara, Y. Ishijima, E. Kozak, J. Martino, K. Masumoto, G. McCrank, Y. Sugita, P. Thompson, J. Tillerson and B. Vignal. 2002. The Five-year Report of the Tunnel Sealing Experiment: An International Project of AECL, JNC, ANDRA and WIPP. Atomic Energy of Canada Limited Report AECL-12727. Pinawa, Canada.

Chen, J., Z. Qin and D.W. Shoesmith. 2011. Rate controlling reactions for copper corrosion in anaerobic aqueous sulphide solutions. Corrosion Engineering, Science and Technology 46, 138-141.

Chen, Y., X.H. Wang, J. Li, J.L. Lu, F.S. Wang. 2007. Polyaniline for corrosion prevention of mild steel coupled with copper. Electrochimica Acta 52, 5392-5399.

CNSC. 2006. Regulatory Guide G-320: Assessing the Long Term Safety of Radioactive Waste Management, Canadian Nuclear Safety Commission, Ottawa, Canada.

Dixon D., T. Sandén, E. Jonsson and J. Hansen. 2011a. Backfilling of Deposition Tunnels: Use of Bentonite Pellets. Swedish Nuclear Fuel and Waste Management Company Report SKB P-11-44. Stockholm, Sweden.

Dixon D., E. Jonsson, J. Hansen, M. Hedin and G. Ramqvist. 2011b. Effect of Localized Water Uptake on Backfill Hydration and Water Movement in a Backfilled Tunnel: Half-Scale

- Tests at Äspö Bentonite Laboratory. Swedish Nuclear Fuel and Waste Management Company Report SKB R-11-27. Stockholm, Sweden.
- DOE. 2008. Final Supplemental Environmental Impact Statement for a Geologic Repository for the Disposal of Spent Nuclear Fuel and High-Level Radioactive Waste at Yucca Mountain. Department of Energy Report DOE/EIS-0250F-S1. Nevada, USA.
- Dutton, D. 2006. Preliminary Evaluation of the Creep Behaviour of the Inner Steel Vessel of a Used-fuel Container. Ontario Power Generation Report 06819-REP-01300-10108-R00. Toronto, Canada.
- Fenton, C.H. 1994. Postglacial faulting in eastern Canada: an annotated bibliography, Geological Survey of Canada, Open File 2774, pp. 1–98. Ottawa, Canada.
- Ferry, C., J.-P. Piron, A. Poulesquen and C. Poinssot. 2008. Radionuclides release from the spent fuel under disposal conditions: Re-evaluation of the instant release fraction. Materials Research Society Symposium Proceedings 1107, 447-454.
- Freeze, R. A. and J.A. Cherry. 1979. Groundwater. Prentice Hall, Inc. Englewood Cliffs, N.J.
- Freire-Canosa, J. 2011. Used Fuel Integrity Program: Summary Report. Nuclear Waste Management Organization Report NWMO TR-2011-04. Toronto, Canada.
- Garisto, F., J. Avis., T. Chshyolkova, P. Gierszewski, M. Gobien, C. Kitson, T. Melnyk, J. Miller, R. Walsh and L. Wojciechowski. 2010. Glaciation Scenario: Safety Assessment for a Used Fuel Geological Repository. Nuclear Waste Management Organization Report NWMO TR-2010-10. Toronto, Canada.
- Garisto, F., M. Gobien, E. Kremer and C. Medri. 2012. Fourth Case Study: Reference Data and Codes. Nuclear Waste Management Organization Report NWMO TR-2012-08. Toronto, Canada.
- Gascoyne, M. 1999. Long-term maintenance of reducing conditions in a spent nuclear fuel repository: A re-examination of critical factors. Swedish Nuclear Fuel and Waste Management Company (SKB), Report R-99-41. Stockholm, Sweden.
- Gascoyne, M. 2000. Hydrogeochemistry of the Whiteshell Research Area. Ontario Power Generation, Nuclear Waste Management Report 06819-REP-01200-10033-R00. Toronto, Canada.
- Gascoyne, M., J. McMurry, and R.B. Ejeckam. 2003. Paleohydrogeologic interpretation of fracture infill mineralogy and flow system stability. In Proceedings, 4th Joint IAH-CNC/CGS Conference, Winnipeg, Canada, 2003 Sept. 29-Oct. 1.
- Guo, R. 2007. Numerical Modelling of a Deep Geological Repository using the In-floor Borehole Placement Method. Nuclear Waste Management Organization Technical Report NWMO TR-2007-14. Toronto, Canada.
- Guo, R. 2009a. Application of Numerical Modelling in Choosing Container Spacing, Placement–room Spacing and Placement-room Shape for a Deep Geological Repository

using the In-floor Borehole Placement Method. Nuclear Waste Management Organization Report NWMO TR-2009-28. Toronto, Canada.

- Guo, R. 2009b. Coupled Thermal-Hydraulic- Mechanical Modelling of the Canister Retrieval Test. Nuclear Waste Management Organization Report NWMO TR-2009-31. Toronto, Canada.
- Hayek, S.J., J.A. Drysdale, J. Adams, V. Peci, S. Halchuk and P. Street. 2010. Seismic Activity in the Northern Ontario Portion of the Canadian Shield: Annual Progress Report for the Period January 01 – December 31, 2010. Nuclear Waste Management Organization Report DGR-TR-2010-03. Toronto, Canada.
- Horseman, S.T., J.F. Harrington and P. Sellin. 1999. Gas migration in clay barriers. *Engineering Geology* 54, 139-149.
- Hultquist G, Szakálos P, Graham M J, Belonoshko A B, Sproule G I, Gråsjö L, Dorogokupets P, Danilov B, Aastrup T, Wikmark G, Chuah G-K, Eriksson J-C, Rosengren A, 2009. Water corrodes copper. *Catalysis Letters* 132, 311.
- Hultquist G, Graham M J, Szakálos P, Sproule G I, Rosengren, A. Gråsjö L, 2011. Hydrogen gas production during corrosion of copper by water. *Corrosion Science*. 310.
- Humphreys, P.N., J.M. West and R. Metcalfe. 2010. Microbial Effects on Repository Performance. Prepared by Quintessa Limited for the Nuclear Decommissioning Authority Report No. QRS-1378Q-1. Oxfordshire, United Kingdom.
- Jensen, K.A. and R.C. Ewing. 2001. The Okélobondo natural fission reactor, southeast Gabon: Geology, mineralogy, and retardation of nuclear-reaction products. *Geological Society of America Bulletin* 113, 32-62.
- King, F. and S. Stroes-Gascoyne. 1997. Predicting the effects of microbial activity on the corrosion of copper nuclear waste disposal containers. *In* *Microbial Degradation Processes in Radioactive Waste Repository and in Nuclear Fuel Storage Areas*. Kluwer Academic Publishers, Netherlands. 149-162.
- King, F. and M. Kolář. 2000. The Copper Container Corrosion Model Used in AECL's Second Case Study. Ontario Power Generation Report 06819-REP-01200-10041-R00. Toronto, Canada.
- King, F., L. Ahonen, C. Taxen, U. Vuorinen and L. Werme. 2001. Copper Corrosion under Expected Conditions in a Deep Geologic Repository. Swedish Nuclear Fuel and Waste Management Company Report SKB TR-01-23. Stockholm, Sweden.
- King, F., M. Kolář and P. Maak. 2008. Reactive-transport model for the prediction of the uniform corrosion behaviour of copper used fuel containers. *Journal of Nuclear Materials* 379, 133-141.
- King, F. 2009. Microbiologically influenced corrosion of nuclear waste container. *Corrosion* 65, 233-251.

- King, F. and D. Shoesmith. 2010. Nuclear waste canister materials, corrosion behaviour and long-term performance in geological repository systems. *In Geological Repository Systems for Safe Disposal of Spent Nuclear Fuel and Radioactive Waste*. Woodhead Publishing, Cambridge, United Kingdom.
- King, F., C. Lilja, K. Pedersen, P. Pitkänen and M. Vähänen. 2010. An Update of the State-of-the-art Report on the Corrosion of Copper under Expected Conditions in a Deep Geologic Repository. Swedish Nuclear Fuel and Waste Management Company Report SKB TR-10-67. Stockholm, Sweden.
- King, F., C. Lilja, K. Pedersen, P. Pitkänen and M. Vähänen. 2011a. An Update of the State-of-the-art Report on the Corrosion of Copper under Expected Conditions in a Deep Geologic Repository. Posiva Oy Report POSIVA 2011-01. Olkiluoto, Finland.
- King, F., M. Kolář, M. Vähänen and C. Lilja. 2011b. Modelling long term corrosion behaviour of copper canisters in KBS-3 repository. *Corrosion Engineering, Science and Technology* 46, 217-226.
- Kukkonen, I.T., O. Olesen, M.V.S. Ask and the PFDP Working Group. 2010. Postglacial faults in Fennoscandia: targets for scientific drilling. *Geologiska Föreningens i Stockholm Förhandlingar (GFF)* 132, 71–81.
- Kwong, G. 2011. Status of Corrosion Studies for Copper Used Fuel Containers Under Low Salinity Conditions. Nuclear Waste Management Organization Report NWMO TR-2011-14. Toronto, Canada.
- Lemieux, J.-M., E.A. Sudicky, W.R. Peltier and L. Tarasov. 2008. Dynamics of groundwater recharge and seepage over the Canadian landscape during the Wisconsinian glaciation. *Journal of Geophysical Research* 113, F01011.
- Lidmar-Bergström, K. 1997. A long-term perspective on glacial erosion. *Earth Surface Processes and Landforms* 22, 297-306.
- Lund B. 2006. Stress variations during a glacial cycle at 500 m depth in Forsmark and Oskarshamn: Earth model effects. Swedish Nuclear Fuel and Waste Management Company Report R-06- 95., Stockholm, Sweden.
- Lund, B., P. Schmidt and C. Hieronymus. 2009. Stress evolution and fault stability during the Weichselian glacial cycle. Swedish Nuclear Fuel and Waste Management Company Report TR-09-15. Stockholm, Sweden.
- Man, A. and J.B. Martino. 2009. Thermal, Hydraulic and Mechanical Properties of Sealing Materials. Nuclear Waste Management Organization Technical Report NWMO TR-2009-20. Toronto, Canada.
- McKelvie, J., K. Birch, J. Freire-Canosa, M. Garamszeghy, F. Garisto, P. Gierszewski, M. Gobien, S. Hirschorn, N. Hunt, M. Jensen, A. Khan, E. Kremer, G. Kwong, T. Lam, L. Lang, C. Medri, A. Murchison, S. Russell, U. Stahmer, E. Sykes, J. Villagran, A. Vorauer, T. Wanne and T. Yang. 2011. Technical Program for Long-Term

- Management of Canada's Used Nuclear Fuel – Annual Report 2010. Nuclear Waste Management Organization Report NWMO TR-2011-02. Toronto, Canada.
- McMurry, J., D.A. Dixon, J.D. Garroni, B.M. Ikeda, S. Stroes-Gascoyne, P. Baumgartner and T.W. Melnyk. 2003. Evolution of a Canadian Deep Geologic Repository: Base Scenario. Ontario Power Generation Report 06819-REP-01200-10092-R00. Toronto, Canada.
- McMurry, J., B.M. Ikeda, S. Stroes-Gascoyne, D.A. Dixon and J.D. Garroni. 2004. Evolution of a Canadian Deep Geologic Repository: Defective Container Scenario. Ontario Power Generation Report 06819-REP-01200-10127-R00. Toronto, Canada.
- Normani, S.D., Y.-J. Park, J.F. Sykes and E.A. Sudicky. 2007. Sub-Regional Modelling Case Study 2005-2006 Status Report. Nuclear Waste Management Organization Report NWMO TR-2007-07. Toronto, Canada.
- Normani, S.D. 2009. Paleoevolution of Pore Fluids in Glaciated Geologic Settings. Ph.D. Thesis, Department of Civil Engineering, University of Waterloo. Waterloo, Canada.
- OPG. 2002. Pickering Waste Management Facility Safety Report. Ontario Power Generation Report 92896-SR-01320-10002-R02. Toronto, Canada.
- Peltier, W.R. 2002. A Design Basis Glacier Scenario. Ontario Power Generation Report 06819-REP-01200-10069-R00. Toronto, Canada.
- Peltier, W.R. 2004. Permafrost Influences Upon the Subsurface. Ontario Power Generation Report 06819-REP-01200-10134-R00. Toronto, Canada.
- Peltier, W.R. 2011. Long-term Climate Change. Nuclear Waste Management Organization Report NWMO DGR-TR-2011-14 R000. Toronto, Canada.
- Poon, F., M. Saiedfar and P. Maak. 2001. Selection of a Primary Load-bearing Component Conceptual Design for Used-fuel Containers. Ontario Power Generation Report 06819-REP-01200-10051-R00. Toronto, Canada.
- Posiva. 2010. EDZ09 Project and related EDZ studies in ONKALO 2008-2010. Posiva Working Report 2010-27. Oikiluoto. Finland.
- Pourbaix, M. 1974. Atlas of Electrochemical Equilibria in Aqueous Solutions. 2nd English Edition. National Association of Corrosion Engineers (NACE). Houston, USA.
- Pusch, R. 1999. Mobility and Survival of Sulphate-reducing Bacteria in Compacted and Fully Water Saturated Bentonite – Microstructural Aspects. Swedish Nuclear Fuel and Waste Management Company Report SKB TR 99-30. Stockholm, Sweden.
- Raiko, H. 2005. Disposal Canister for Spent Nuclear Fuel – Design Report. Posiva Oy Report POSIVA 2004-06. Oikiluoto, Finland.

- Raiko H., R. Sandström, H. Rydén and M. Johansson. 2010. Design Analysis Report for the Canister. Swedish Nuclear Fuel and Waste Management Company Report SKB TR-10-28, Stockholm, Sweden.
- Saiedfar, M. and P. Maak. 2002. Preliminary Assessment of the Deformation and Stresses of Copper Used-fuel Containers in a Hypothetical Deep Geologic Repository. Ontario Power Generation Report, 06819-REP-01300-10049-R00. Toronto, Canada.
- SSHAC. 1997. Recommendations for Probabilistic Seismic Hazard Analysis. Guidance on Uncertainty and Use of Experts. Senior Seismic Hazard Advisory Committee, U.S. Nuclear Regulatory Commission, NUREG/CR-6372.
- Sherwood Lollar, B. 2011. State of Science Review: Far-field Microbiological Considerations Relevant to a Deep Geological Repository for Used Nuclear Fuel. Nuclear Waste Management Organization Report NWMO-TR-2011-09. Toronto, Canada.
- Shoesmith, D. 2008. The Role of Dissolved Hydrogen on the Corrosion/Dissolution of Spent Nuclear Fuel. Nuclear Waste Management Organization Report NWMO TR-2008-19. Toronto, Canada.
- Shoesmith, D. and D. Zagidulin. 2010. The Corrosion of Zirconium under Deep Geological Repository Conditions. Nuclear Waste Management Organization Report NWMO TR-2010-19. Toronto, Canada.
- Simmons, G. R. 1992. The Underground Research Laboratory Room 209 Excavation Response Test - A Summary report. Atomic Energy of Canada Limited. Report AECL-10564, COG-92-56. Chalk River, Canada.
- SKB. 2010. Critical Review of the Literature on the Corrosion of Copper by Water. Swedish Nuclear Fuel and Waste Management Company Report SKB TR-10-69. Stockholm, Sweden.
- SKB. 2011. Long-term Safety for the Final Repository for Spent Nuclear Fuel at Forsmark. Main Report of the SR-Site Project. Volume I. Swedish Nuclear Fuel and Waste Management Company Report SKB TR-11-01. Stockholm, Sweden.
- Smart N. R., Rance A. P., Fennell P., Werme L. 2003. Expansion due to anaerobic corrosion of steel and cast iron: experimental and natural analogue studies. In: Férom D, Macdonald D D (eds). Proceedings of the international Workshop Prediction of Long Term Corrosion Behaviour in Nuclear Waste Systems, November, Cadarache, France. London: Maney Pub. (European Federation of Corrosion Publications 36), paper 19, pp 280–294.
- Smart N. R., Fennell P. A., Rance A. P., Werme L. 2004. Galvanic corrosion of copper-cast iron couples in relation to the Swedish radioactive waste canister concept. In: Proceedings of the 2nd International Workshop on Prediction Of Long Term Corrosion Behaviour in Nuclear Waste Systems, Nice, France, September 2004. European Federation of Corrosion, pp 52–60.

- Smart N. R., Rance A. P., Fennell P. A. 2005. Galvanic corrosion of copper-cast iron couples. Swedish Nuclear Fuel and Waste Management Company Report SKB TR-05-06. Stockholm, Sweden.
- Smart N R, Rance A P, Fennell P A H, 2006. Expansion due to the anaerobic corrosion of iron. Swedish Nuclear Fuel and Waste Management Company Report SKB TR-06-41, Stockholm, Sweden.
- SSM . 2011a. Evolution of hydrogen by copper in ultrapure water without dissolved oxygen, Strål säkerhets myndigheten, Richard Becker, Hans-Peter Hermansson, SSM Rapport 2011:34, Stockholm, Sweden.
- SSM . 2011b. Is Copper Immune to Corrosion When in Contact With Water and Aqueous Solutions?, Strål säkerhets myndigheten, Digby D. Macdonald Samin Sharifi-Asl, SSM Rapport 2011:09, Stockholm, Sweden.
- Stroes-Gascoyne, S. 2010. Microbial occurrence in bentonite-based buffer, backfill and sealing materials from large-scale experiments at AECL's Underground Research Laboratory. Appl. Clay Sci. 47, 36-42.
- Stroes-Gascoyne, S., C.J. Hamon, C. Kohle and D.A. Dixon. 2006. The Effects of Dry Density and Porewater Salinity on the Physical and Microbiological Characteristics of Highly Compacted Bentonite. Ontario Power Generation Report 06819-REP-01200-10016 R00. Toronto, Canada.
- Stroes-Gascoyne, S., C.J. Hamon, D.A. Dixon and J.B. Martino 2007a. Microbial analysis of samples from the tunnel sealing experiments at AECL's Underground Research Laboratory. Phys. Chem. Earth 32, 219-231.
- Stroes-Gascoyne, S., P. Maak, C.J. Hamon, and C. Kohle. 2007b. Potential implications of microbes and salinity on the design of repository sealing system components. Nuclear Waste Management Organization report NWMO TR-2007-10. Toronto, Canada.
- Stroes-Gascoyne, S. and C.J. Hamon. 2008. The Effect of Intermediate Dry Densities (1.1-1.5 g/cm³) and Intermediate Porewater Salinities (60-90 g NaCl/L) on the Culturability of Heterotrophic Aerobic Bacteria in Compacted 100% Bentonite. Nuclear Waste Management Organization Technical Report NWMO TR-2008-11. Toronto, Canada.
- Stroes-Gascoyne, S. and C.J. Hamon. 2010. The Effects of Elevated Temperatures on the Viability and Culturability of Bacteria Indigenous to Wyoming MX-80 Bentonite. Nuclear Waste Management Organization Report NWMO TR-2010-08. Toronto, Canada.
- Stroes-Gascoyne, S., C.J. Hamon, D.A. Dixon and D.G. Priyanto. 2010a. The Effect of CaCl₂ Porewater Salinity (50-100 g/L) on the Culturability of Heterotrophic Aerobic Bacteria in Compacted 100% Bentonite with Dry Densities of 0.8 and 1.3 g/cm³. Nuclear Waste Management Organization Technical Report NWMO TR-2010-06. Toronto, Canada.

- Stroes-Gascoyne, S., C.J. Hamon, P. Maak and S. Russell. 2010b. The effects of the physical properties of highly compacted smectitic clay (bentonite) on the culturability of indigenous microorganisms. *Applied Clay Science*, 47, 155-162.
- Stroes-Gascoyne, S., C.J. Hamon and P. Maak. 2011. Limits to the Use of Highly Compacted Bentonite as a Deterrent for Microbiologically Influenced Corrosion in a Nuclear Fuel Waste Repository. *Physics and Chemistry of the Earth*, 36(17-18): 1630-1638.
- Sugden, D.E. 1976. A case against deep erosion of shields by ice sheets. *Geology* 4, 580-582.
- Swedish National Council. 2010. Nuclear Waste State-of-the-Art Report 2010 – Challenges for the Final Repository Programme. Swedish Government Official Reports SOU 2010:6. Stockholm, Sweden.
- Szakálos P., Hultquist G., Wikmark G. 2007. Corrosion of copper by water. *Electrochemical and Solid-State Letters*, 10, pp C63–C67.
- Tait, J.C., H. Roman and C.A. Morrison. 2000. Characteristics and Radionuclide Inventories of Used Fuel from OPG Nuclear Generating Stations. Ontario Power Generation Report 06819-REP-01200-10029-R00. Toronto, Canada.
- Teller, J.T. 1995. History and drainage of large ice-dammed lakes along the Laurentide ice sheet. *Quaternary International* 28, 83-92.
- Van Everdingen, R.O. 1990. Groundwater hydrology. In: Prowse, T.D. and C.S.L. Ommanney eds., 1991. Northern Hydrology, Canadian Perspectives. National Hydrology Research Institute, Environment Canada, NHRI Science Report No. 1, ISBN 0-662-17076-8. Saskatchewan, Canada.
- Villagran, J., M. Ben Belfadhel, K. Birch, J. Freire-Canosa, M. Garamszeghy, F. Garisto, P. Gierszewski, M. Gobien, S. Hirschorn, N. Hunt, A. Khan, E. Kremer, G. Kwong, T. Lam, P. Maak, J. McKelvie, C. Medri, A. Murchison, S. Russell, M. Sanchez-Rico Castejon, U. Stahmer, E. Sykes, A. Urrutia-Bustos, A. Vorauer, T. Wanne and T. Yang. 2011. RD&D Program 2011 – NWMO's Program for Research, Development and Demonstration for Long-Term Management of Used Nuclear Fuel. Nuclear Waste Management Organization Report NWMO TR-2011-01. Toronto, Canada.
- Walsh, R. and J. Avis. 2010. Glaciation Scenario: Groundwater and Radionuclide Transport Studies. Nuclear Waste Management Organization Report NWMO TR-2010-09. Toronto, Canada.
- Werme, L. 1998. Design Premises for Canister for Spent Nuclear Fuel. Swedish Nuclear Fuel Waste Management Company Report SKB TR-98-08. Stockholm, Sweden.
- Wheeler, R.L. 1995. Earthquakes and the cratonward limit of lapetan faulting in eastern North America. *Geology* 23, 105-108.

Wolfaardt, G. and D. Korber. 2012. Near-field Microbiological Considerations Relevant to a Deep Geological Repository for Used Nuclear Fuel. Nuclear Waste Management Organization Technical Report NWMO TR-2012-02. Toronto, Canada.

6. SCENARIO IDENTIFICATION AND DESCRIPTION

Postclosure safety is assessed through consideration of a set of potential future scenarios, where a scenario is a postulated or assumed set of conditions or events. The purpose of scenario identification is to develop a comprehensive range of possible future evolutions against which the performance of the system can be assessed.

Consistent with the specification of CNSC Guide G-320 (CNSC 2006), both Normal Evolution and Disruptive Event Scenarios are considered. The Normal Evolution Scenario represents the normal (or expected) evolution of the site and facility, while Disruptive Event Scenarios examine the effects of unlikely events that might lead to penetration of barriers and abnormal degradation and loss of containment.

Scenarios of interest are identified through consideration of the various Features, Events and Processes (FEPs) that could affect the repository system and its evolution (Figure 6-1). FEPs are categorised as either "external" or "internal", depending on whether they are outside or inside the spatial and temporal boundaries of the repository system. Repository and contaminant factors can be considered as "internal" factors, whereas the external factors originate outside these boundaries. Hence, the repository and contaminant factors will be referred to as Internal FEPs and the external factors will be referred to as External FEPs.

The External FEPs provide the system with boundary conditions and include influences originating outside the repository system that might cause change. Included in this group are decisions related to repository design, operation and closure since these are outside the temporal boundary of the postclosure behaviour of the repository system. If these External FEPs can significantly affect the evolution of the system and / or its safety functions of containment and isolation, they are considered scenario-generating FEPs (IAEA 2004) in the sense that whether or not they occur (or the extent to which they occur) could define a particular future scenario that should be considered.

The External FEPs are listed in Table 6-1. Those that are likely to affect the repository system and its evolution are discussed in Section 6.1. The effects of less likely External FEPs and certain Internal FEPs that might lead to abnormal degradation and loss of containment are discussed in Section 6.2.

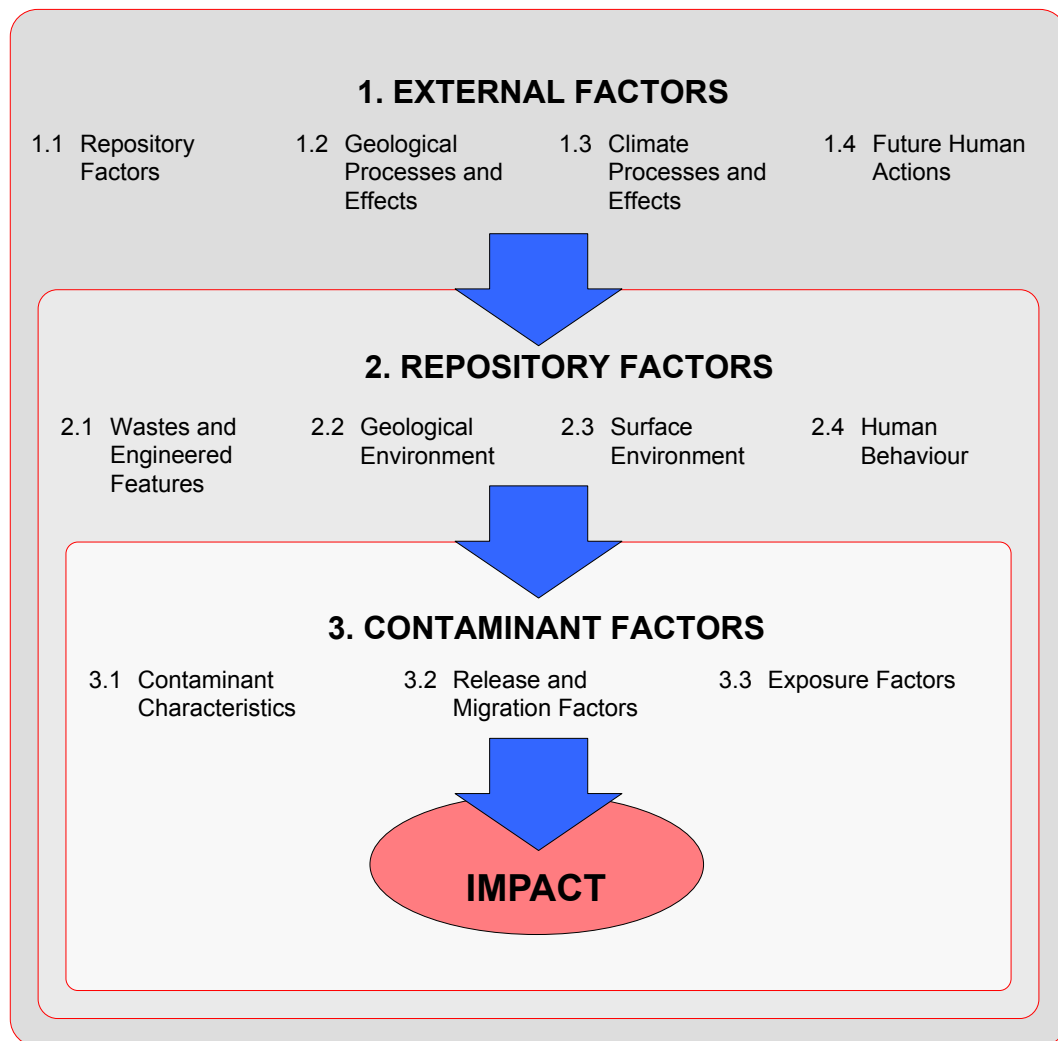


Figure 6-1: External, Repository and Contaminant Factors / FEPs

6.1 The Normal Evolution Scenario

The Normal Evolution Scenario is based on a reasonable extrapolation of present day site features and receptor¹ lifestyle. It includes the expected evolution of the site and repository.

6.1.1 External FEPs

The External FEPs have been reviewed to identify those that are likely to occur and could potentially affect the repository and therefore be included in the Normal Evolution Scenario.

¹ The receptor is a person (or persons) who may be exposed to contaminants potentially released from the repository.

The resulting list of included / excluded items is shown in Table 6-1 together with a brief justification for their inclusion / exclusion. Further details are provided in Garisto (2012).

Table 6-1 shows that the repository is largely unaffected by many External FEPs, primarily due to its depth and associated geological characteristics. The main External FEPs that are likely to have an impact are:

- Placement of some containers with undetected defects (FEP 1.1.03);
- Glaciation and its effects (FEPs 1.3.01, 1.3.02, 1.3.04, 1.3.05, 1.3.08, 1.3.09, 1.2.02 and 1.2.03);
- Earthquakes (FEP 1.2.03); and
- Human influence on global climate (FEP 1.4.01) delaying onset of the next glaciation.

The containers are robust and there are multiple inspection steps to ensure they are fabricated and placed correctly. However, with the large number of containers, it is possible that some containers could be placed in the repository with defects. Consequently, for the assessment of the Normal Evolution Scenario, it is assumed that some containers with undetected defects are present in the repository.

An important external influence is glaciation. Although glaciation is likely to cause major changes in the surface and near-surface environment, the repository itself is intentionally isolated by its depth from these changes. Geoscientific observations at some sites in the Canadian Shield indicate that conditions at 500 m depths have been isolated from surface changes through the past nine glacial cycles (i.e., for $>10^6$ years). For example, geochemical data from the Whiteshell Research Area in Manitoba indicate that: deep groundwaters are millions of years old (Gascoyne 2004); glacial meltwaters have not penetrated below about 350 m (Zhang and Frape 2002, Blyth et al. 2000); oxygenated waters have not penetrated below about 50 m (Gascoyne et al. 2004, McMurry and Ejeckam 2002, Spiessl et al. 2009); and, transport in the deep groundwater domain has been diffusion-dominated (Gascoyne 2000).

For the hypothetical repository site, the paleohydrogeologic simulations described in Chapter 2 suggest that glacial meltwaters may reach the repository level. Within the rock matrix at the repository horizon tracer meltwater concentrations ranged between 5% and 45% in the paleohydrogeologic simulations (see Section 2.3.5.3); although, significantly higher meltwater concentration occurred within the discrete higher permeability fracture zones. However, the glacial recharge penetrating below the shallow groundwater system (i.e., > 150 mBGS) is not expected to be oxygenated or influence redox conditions at the repository horizon (Section 2.3.5.3). These characteristics are used in the scenario identification.

Table 6-1: Status of External FEPs for the Normal Evolution of the Repository System

External FEP		Status*	Remark	
1.1	Repository Factors			
	1.1.01	Site Investigation	Included	The site is hypothetical. The topography and hydrological properties are based on a Regional Groundwater Flow Model relevant to Canadian Shield conditions and the fracture ² network is based on a statistical representation of Canadian Shield fracture patterns. It is assumed that there are no identified commercially viable mineral resources at the site. The site is described in Chapter 2.
	1.1.02	Excavation and Construction	Included	The repository is built consistent with the design basis as described in Chapter 4. Controlled drill and blast excavation is used, which reduces but does not avoid formation of an excavation damaged zone.
	1.1.03	Placement of Wastes and Backfill	Included	The in-floor container placement method is used. Rooms are backfilled as wastes are placed as described in Chapter 4. Due to the large number of containers, it is assumed that some containers are placed with defects that are not detected during the fabrication, inspection and placement processes.
	1.1.04	Closure and Repository Sealing	Included	The repository is closed and sealed as described in Chapter 4. This includes sealing of the fracture passing through the repository footprint and the shafts.
	1.1.05	Repository Records and Markers	Included	Repository records and markers (and passive societal memory) are assumed sufficient to ensure that inadvertent intrusion would not occur for at least a few hundred years.

²Fractures are defined here as significant permeable features of the geosphere that are explicitly included in groundwater modelling simulations. These fractures are represented in modelling simulations as equivalent porous media (see Chapter 7) with a thickness of 1m.

Used Fuel Repository Conceptual Design and Postclosure Safety Assessment in Crystalline Rock

Document Number: NWMO TR-2012-16

Revision: 000

Class: Public

Page: 241

External FEP		Status*	Remark	
	1.1.06	Waste Allocation	Included	The repository holds 4.6 million CANDU fuel bundles. There is no placement of other radioactive or chemically hazardous material at the site.
	1.1.07	Repository Design	Included	The repository design concept is described in Chapter 4.
	1.1.08	Quality Control	Included	Construction, operation, monitoring and closure of the repository are all undertaken under a project quality plan that ensures that the design and safety basis is met (see Chapter 10).
	1.1.09	Schedule and Planning	Included	The assumed schedule is 38 years operation, 70 years extended monitoring and 30 years for decommissioning and closure.
	1.1.10	Repository Administrative Control	Included	Administrative controls ensure proper operation and closure of the repository. Institutional controls (e.g., land use restrictions) will be implemented on closure to prevent inadvertent human intrusion.
	1.1.11	Monitoring	Excluded	The postclosure monitoring program will not compromise the safety of the repository.
	1.1.12	Accidents and Unplanned events	Excluded	Preclosure accidents or unplanned events that could impact the long-term safety of the repository will be mitigated before the repository is closed.
	1.1.13	Retrieval of Wastes	Excluded	The repository schedule includes an extended period of monitoring after rooms have been filled but before the access tunnels and shaft are sealed, which would facilitate retrieval if required. However, retrieval after closure is not expected and is not included in this safety assessment.
1.2	<i>Geological Processes and Effects</i>			
	1.2.01	Tectonic Movement and Orogeny	Excluded	The hypothetical site is in a tectonically stable region away from plate margins, with no tectonic activity over the time scale of interest (i.e., 1,000,000 years).

Used Fuel Repository Conceptual Design and Postclosure Safety Assessment in Crystalline Rock

Document Number: NWMO TR-2012-16

Revision: 000

Class: Public

Page: 242

External FEP		Status*	Remark
	1.2.02	Deformation (Elastic, Plastic or Brittle)	Included The Canadian Shield is one of the most tectonically stable regions on the planet. Over the next million years, the only significant deformation force is that due to ice sheet advance over the site. This could cause crustal depression of 500 m, but would occur on a continental scale. Ice sheet weight could cause local movement along existing fractures but would not lead to creation of new fractures.
	1.2.03	Seismicity (Earthquakes)	Included Earthquakes will occur over the time scale of interest; however, since the Shield is not a seismically active region, the likely magnitude, frequency and distance of earthquakes would limit their impact at the repository location. Larger earthquakes are more likely during retreat of ice sheets. These could reactivate existing faults. Earthquakes are in general less destructive at depth than at the surface, diminishing the impact of any seismic activity on a deep repository. The main concern would be shearing along a fracture plane intercepting the repository, providing either a groundwater pathway or damaging containers.
	1.2.04	Volcanic and Magmatic Activity	Excluded No volcanic or magmatic activity over the time scale of interest due to the site location.
	1.2.05	Metamorphism	Excluded No processes occur over the time scale of interest that will cause metamorphism.
	1.2.06	Hydrothermal Activity	Excluded The hypothetical repository is located on the Shield, which is geologically stable with a low geothermal flux. Hydrothermal processes therefore act too slowly to be of concern over the time scale of interest.
	1.2.07	Erosion and Sedimentation	Excluded The area is topographically relatively flat and the surface is primarily granite bedrock so there is limited potential for large-scale denudation. This is in part due to the ice sheet erosion that has already occurred over the past 1,000,000 years which has removed easily erodible material.
	1.2.08	Diagenesis	Excluded The site is granitic rock, not sedimentary rock.

Used Fuel Repository Conceptual Design and Postclosure Safety Assessment in Crystalline Rock

Document Number: NWMO TR-2012-16

Revision: 000

Class: Public

Page: 243

External FEP		Status*	Remark	
	1.2.09	Salt Diapirism and Dissolution	Excluded	No significant salt deposits are in the vicinity of the site because it is in the granitic rock of the Canadian Shield.
	1.2.10	Hydrological Response to Geological Changes	Included	A severe seismic event could potentially change fracture permeabilities or activate a fault and therefore change local hydrology. For this reason and others, fractures at the repository site are modelled with high permeabilities.
1.3	<i>Climate Processes and Effects</i>			
	1.3.01	Global Climate Change	Included	After a period of global warming, it is assumed that glacial / interglacial cycling will eventually resume since the solar insolation variation driving this cycling will continue.
	1.3.02	Local and Regional Climate Change	Included	In the near term, global warming is likely to cause temperature and precipitation changes, although the local / regional climate is likely to remain generally temperate due to its northerly latitude location. In the long term, it will respond to global climate change, and in particular will cool or warm with glacial cycles.
	1.3.03	Sea-level Change	Excluded	Changes in sea level do not affect the site due to its assumed mid-continental location.
	1.3.04	Periglacial Effects	Included	These will occur during colder climate states experienced during the glacial cycles that are likely to occur at the site over a one million year timeframe. In particular, this would include permafrost development.
	1.3.05	Local Glacial Effects	Included	Ice sheets will cause a range of local effects. These include change in rock stress (FEP 1.2.02), earthquake initiation (FEP 1.2.03), change in surface and near-surface hydrology (FEP 1.3.07), penetration of glacial waters to depth, changes in ecosystems (FEP 1.3.08) and human behaviour (FEP 1.3.09).

Used Fuel Repository Conceptual Design and Postclosure Safety Assessment in Crystalline Rock

Document Number: NWMO TR-2012-16

Revision: 000

Class: Public

Page: 244

External FEP		Status*	Remark	
	1.3.06	Warm Climate Effects (Tropical and Desert)	Excluded	Climate change is unlikely to result in development of tropical or hot desert conditions at the site due to its northerly latitude. An initial period of human-induced global warming is not expected to result in extreme temperature rise resulting in tropical or desert conditions in this region.
	1.3.07	Hydrological Response to Climate Change	Excluded	Surface and near-surface groundwater systems could be altered by large climactic change to wetter or drier conditions. Specifically, the water table on the Canadian Shield is generally within a few meters of the surface and is maintained by small influx of the total annual precipitation. The deep groundwater system at the site would not be significantly altered by climatic change to wetter or drier conditions (within expected variation, see FEP 1.3.06), due to its low-permeability and depth. Changes in hydrology due to glaciation are discussed separately under Periglacial Effects (1.3.04) and Local Glacial Effects (1.3.05).
	1.3.08	Ecological Response to Climate Changes	Included	Flora and fauna at the site change in response to glacial / interglacial cycling.
	1.3.09	Human Behavioural Response to Climate Change	Included	Human behaviour changes in response to glacial / interglacial cycling.
1.4	<i>Future Human Actions</i>			
	1.4.01	Human Influences on Climate	Included	Human actions are a possible cause of global climate change, which is included in expected evolution (see FEP 1.3.01, Global Climate Change).
	1.4.02	Deliberate Human Intrusion	Excluded	Deliberate human intrusion into the repository is not considered. It is assumed that any future society choosing to recover materials from the repository would have the technology to understand and manage the hazards.

Used Fuel Repository Conceptual Design and Postclosure Safety Assessment in Crystalline Rock

Document Number: NWMO TR-2012-16

Revision: 000

Class: Public

Page: 245

External FEP		Status*	Remark
1.4.03	Non-Intrusive Site Investigation	Excluded	Non-intrusive site investigations would not have any effect because of the repository depth.
1.4.04	Drilling Activities (Human Intrusion)	Excluded	Note that this FEP does not include drilling of shallow wells which are considered under FEP 1.4.07. The drilling of deep exploration boreholes that penetrate to the repository is excluded from the expected evolution due to the repository depth (around 500 m), the relatively small repository footprint (~6 km ²), and the assumed lack of commercially viable natural resources at the site.
1.4.05	Mining (Human Intrusion)	Excluded	It is assumed that no commercially viable mineral resources are present at the site.
1.4.06	Surface Environment, Human Activities	Excluded	Unlikely to have any direct impact on repository due to the repository depth.
1.4.07	Water Management (Wells, Reservoirs Dams)	Included	The drilling of shallow water wells in the area is considered once institutional controls are no longer effective (see FEP 1.1.10). Wells in the deeper groundwater zones are excluded since the groundwater in these zones is not potable. This is consistent with present-day practice for extraction from the shallow groundwater system in the Canadian Shield. Construction of dams and reservoirs is unlikely to have significant effects on the deep groundwater system due to the generally low topography around the site and the low permeability of the rock.
1.4.08	Social and Institutional Developments	Included	Institutional controls ensure appropriate use and control of the site in the near term, but it is assumed that this institutional control is eventually lost. Thereafter, the site is assumed to return to land use typical of the region and the site is occupied, including drilling of wells (see FEP 1.4.07).
1.4.09	Technological Developments	Excluded	It is assumed that the capabilities of future humans will largely resemble present-day capabilities. There is no credit taken for advances that might reduce the risk from the repository.

Used Fuel Repository Conceptual Design and Postclosure Safety Assessment in Crystalline Rock

Document Number: NWMO TR-2012-16

Revision: 000

Class: Public

Page: 246

External FEP		Status*	Remark	
	1.4.10	Remedial Actions	Excluded	Remedial actions are not expected following closure of the repository. If any were to occur, their effects would need to be assessed at the time to ensure that they would not detrimentally affect long-term safety.
	1.4.11	Explosions and Crashes	Excluded	Most surface explosions and crashes would have no direct impact on the repository due to its depth. Explosions large enough to affect repository depth would likely have larger direct consequences.
1.5	Other External Factors			
	1.5.01	Meteorite Impact	Excluded	Excluded due to low probability (due to relatively small repository footprint) and / or low consequence (due to depth of repository).
	1.5.02	Species Evolution	Excluded	No evolution of humans assumed, consistent with the International Commission on Radiological Protection's (ICRP) recommendation to apply the concept of (present-day) Reference Man to the management of long-lived solid radioactive waste (ICRP 2000). Similarly, no evolution of non-human biota assumed. General characteristics of biota are assumed to remain similar to current biota.
	1.5.03	Miscellaneous FEPs	Excluded	Consideration of unusual FEPs such as earth tides, reversal of earth's magnetic poles, polar wander, etc. are excluded because of their low probability or because they have no significant effect on the repository.

Note: * Status – *Included* means this factor is considered in the Normal Evolution Scenario. *Excluded* means this factor is not considered in the Normal Evolution Scenario.

6.1.2 Internal FEPs

Internal FEPs are important aids in defining the expected evolution of the repository. They assist in determining which features and processes are important to include in the conceptual model and related computer codes.

The significant FEPs are accounted for in the description of the Normal Evolution Scenario which appears in the following section.

The internal FEPs are reviewed in Garisto (2012).

Internal FEPs are not usually scenario generating; however, they are considered with respect to Disruptive Scenarios in Section 6.2.1.

6.1.3 Description of the Normal Evolution of the Repository System

From consideration of the External FEPs and the Internal FEPs, the following high-level narrative of the expected evolution of the repository system can be developed. This understanding is based on many years of study, including laboratory studies, underground research studies, and observations of analogous natural and long-lived human-made structures and materials. This narrative is used to guide both the subsequent development of the conceptual model for the safety assessment and the variations to this model considered in alternative calculation cases.

The narrative summarizes the main events in the evolution of the repository in broad terms, including the long-term changes in the geosphere and biosphere due to glaciation. It is based on the reference design concept where used fuel is placed in the repository in long-lived copper-and-steel containers. These containers are designed not to fail and will be carefully fabricated and inspected. Most of these containers do not fail in the relevant time scale; however, as noted earlier there could be some containers with undetected defects in the copper shell, potentially leading to early releases of radioactivity. Since defective containers behave differently than intact containers, they are described separately in the following sections.

Most of the processes identified are well understood as discussed in Chapter 5. Key points are that the geosphere isolates the repository from the surface, that the groundwater around the repository level remains within its natural chemistry range and low oxygen state, and (in the longer term) that the load-bearing capacity of the containers is sufficient to withstand the effects of glaciation and earthquakes at repository depth.

6.1.3.1 Events Occurring for Intact Containers

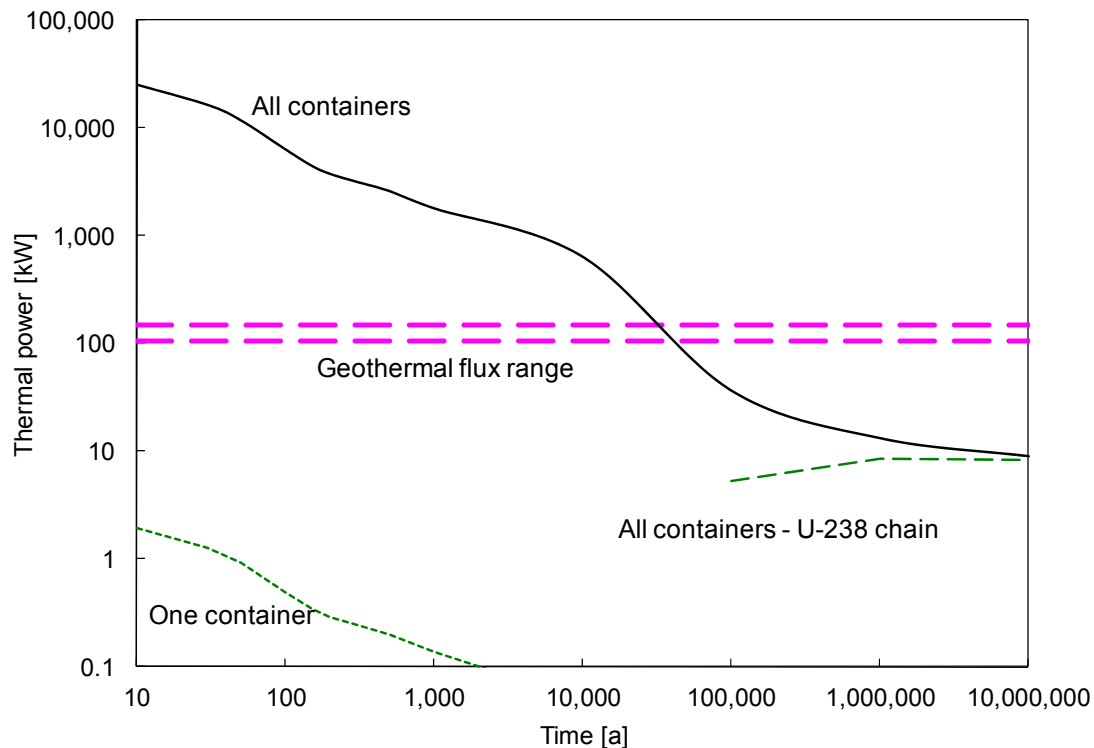
0-100 years

The repository is assumed to be open and actively monitored for a period of about 100 years. The 100 year period consists of the reference design assumption of 38 years of operation and up to 70 years of monitoring during which access tunnels are kept open. Decommissioning and closure will take a further 30 years. In the operation period, 12,778 containers (containing about 4.6 million used fuel bundles, or about 90,000 Mg of uranium) are placed in the repository with the placement rooms backfilled with clay-based sealing materials. The initial radioactivity in a

full repository (assuming 30 year old fuel on average) is about 10^{20} Bq and the initial thermal load is about 16 MW (Figure 6-2).

During the first 100 years after placement:

- Radioactivity drops by a factor of 10 and the thermal output drops by a factor of four. Radionuclides with short half-lives such as tritium (H-3) and Co-60 decay to negligible levels.
- Peak temperatures are reached within the repository (with values less than 100°C at the container outer surface).
- The copper container reacts with oxygen from the buffer to form a very thin corrosion layer;
- Thermal expansion and contraction of the rock and concrete combine to create near-field stresses within the low-permeability rock and the concrete bulkhead at the ends of the placement rooms, and a limited amount of microcracking occurs.
- In the rock around the repository, groundwater flow and heads are influenced by the presence of the open tunnels and the high-suction clay, which draw water towards the repository. This is countered by the container thermal power, which redistributes water away from the containers.
- Microbes in the buffer material near the containers die or become dormant because of heat, desiccation, lack of nutrients or space to be viable.



Notes: The power is similar to the natural geothermal flow (Perry et al. 2010) through the repository area after about 30,000 years. After about 1 million years, the residual power is due to radioactive decay of the decay products of uranium.

Figure 6-2: Total Thermal Power of the Repository (Average 220 MWh/kgU Burnup)

100-1,000 years

Shortly after the beginning of this time period, all access tunnels and shafts tunnels are backfilled and sealed, with particular attention paid to sealing the shafts and the fracture passing through the repository footprint. All intrusive monitoring systems and deep boreholes are removed or closed. For several hundred years thereafter, distinct physical and chemical differences (e.g., temperature, porewater composition) will exist between the various components of the repository, and between the repository and the geosphere. Many of the changes that occur within this timeframe are driven by these gradients. During this period:

- Radioactivity drops by a factor of 30. Most fission products decay to insignificant levels, including Sr-90 and Cs-137.
- Container thermal power drops to around 120 W per container. Residual heat comes from decay of the remaining actinides.
- The oxygen initially present in the sealing materials (as trapped air) is consumed.
- Groundwater from the geosphere enters the repository. As the clay layers become saturated, they start to swell and exert pressure on adjacent materials. The swelling process proceeds slowly and perhaps non-uniformly. Peak swelling loads are about 5 MPa. The swelling clay fills cracks and voids.
- Hydrostatic loads and some of the rock mechanical loads are transmitted through the clays onto the container. The copper shell is compressed onto the inner steel vessel, which is rigid and maintains its shape.
- By the end of this time, the repository is saturated and anaerobic, conditions typical of deep rock environments.
- Climate change may have occurred. Global warming with higher average temperatures could lead to more or less precipitation at the site. This would affect the surface waters (lakes and rivers) and shallow groundwaters, and also the local ecosystem around the site, but deep groundwaters are unaffected.

1,000-60,000 years

- The repository components gradually achieve equilibrium with the surrounding geosphere.
- Radionuclides like C-14 decay.
- Thermal power drops to 6 W per container. The temperatures in and around the repository return to approximately the ambient rock temperatures of around 15°C.
- Corrosion of the container has essentially stopped since the lack of oxygen prevents both uniform and localized corrosion.
- The main microbial activity occurring in the repository is due to anaerobic bacteria, including sulphate-reducing bacteria, located mainly at the interfaces with the rock and in the backfill. The buffer remains largely inhospitable because of the high clay density and pressure, which creates adverse conditions of small pore size and low water activity.
- Locally near concrete surfaces, a more alkaline porewater develops in the clay-based sealing materials, resulting in an altered layer of clay, several centimetres thick, with a reduced swelling capacity near the interface.
- Changes continue to occur in the surface environment. Climate change due to natural or human influences would likely occur. In particular, the climate might start to cool as part of a long-term glacial cycle with possible formation of permafrost and initiation of glaciation at the site.

60,000-1,000,000 years

- Over this timeframe, the perturbations to the system will be driven by external events. The most important events will be glaciation cycles, which are likely to occur over this time period. These are likely to repeat on a period of roughly every 120,000 years.
- The residual radioactivity is dominated by the decay of actinides. By the end of this period, all plutonium has decayed.
- The onset of a glacial cycle will start with a cooling period, with mean surface temperatures over the Canadian Shield dropping to about 0°C. Permafrost develops, disrupting groundwater flow down to a few hundred metres.
- Eventually, an ice sheet will form and extend across the site. The hydrological conditions at the edge of the glacier cause major perturbations to the near-surface groundwater flow system. The hydraulic heads at depth also change, but groundwater response is muted due to the low permeability of the deep rock.
- In some areas, glacially driven recharge may penetrate deeper, but reactions with minerals and microbes along the flow path of recharging meltwaters consume dissolved oxygen. Conditions at repository depth remain reducing.
- At its maximum development, the glacial ice sheet could be 2 to 3 kilometres thick above the repository, potentially increasing the hydrostatic pressure at repository depth by 20 to 30 MPa (possibly much less, depending on the rock properties and the nature of the ice sheet). This value is within the design tolerance of the containers.
- During glaciation, broad regions of the Canadian Shield flex vertically by as much as a kilometre in response to the weight of the ice sheets. During glacial retreat, earthquakes may occur. Existing fracture zones may be reactivated in these locations although there is little change in terms of new fracture development.
- The advancing and retreating ice sheets both erode and deposit rock and till. Since the site has already experienced multiple glaciations in the past one million years, the amount of additional bedrock erosion is expected to be meters to tens of meters.
- The chemistry of the porewater within the sealing materials slowly changes to resemble that of the groundwater.
- Along with the porewater chemistry change, the montmorillonite component of the bentonite has lost Na and gained Ca, Mg, and Fe but has still retained its swelling capacity. Due to the low temperatures and low concentration of K⁺ ions, very little of the montmorillonite has converted to illite.
- Microbial activity is limited in terms of mobility by the impermeable dense buffer around the containers on one side and the low permeability rock on the other, and it is limited metabolically by the low rate of anaerobic reactions at the ambient temperatures and by the requirement for nutrients to diffuse through the clay-based sealing materials.

Beyond 1,000,000 years

Virtually all the reactor-generated radioactivity has decayed, and most of the residual radioactivity in the used fuel comes from its natural uranium content. The amount of uranium in the repository is comparable to the large uranium ore bodies in north-central Canada. These natural deposits of uranium oxide have been stable for billions of years. Similarly, many ore deposits of metallic copper and sedimentary deposits of bentonite are known that range in age from millions to hundreds of millions of years. The ultimate fate of the repository and the materials it contains will be largely indistinguishable from these natural analogues.

6.1.3.2 Events Occurring for Defective Containers

The evolution of any defective containers will be different from that of intact containers. This evolution is summarized below (see McMurry et al. (2004) for a more detailed description).

Only the additional events that may occur in the evolution of these containers are summarized here, since most of the events occurring for the intact containers (e.g., radiation-related changes, thermal changes, etc.) also occur for defective containers. For this discussion, it is assumed that some containers are placed in the repository with small undetected defects that penetrate the copper shell. The inner steel container is therefore exposed to evolving conditions in the repository.

0-100 years

Over this period the repository is not fully saturated. Atmospheric corrosion of the steel next to the defect may occur but only to a very limited extent because the relative humidity near the copper container is low and oxygen is consumed by other processes.

100-1,000 years

- During this period the repository becomes saturated.
- As the repository saturates, water enters the defect and contacts the steel vessel. Anaerobic corrosion of the steel vessel begins, generating iron oxides and hydrogen gas. The most likely iron corrosion product is magnetite.
- A small amount of water leaks into the interior of the steel vessel through the bolted lid and the inside of the steel vessel also starts to corrode.

1,000-60,000 years

- Corrosion of the steel vessel continues and the hydrogen gas pressure increases near the defective container. The timing of events depends on the behaviour of the hydrogen.
- Iron corrosion products build up between the steel and copper vessels. These corrosion products occupy more volume than the iron metal from which they were formed.
- The build up of corrosion products causes local deformation of the copper shell and the initial defect enlarges.
- Rupture of the copper shell allows more water to contact the steel vessel, accelerating the rate of degradation of the container. Formation of iron oxides however also covers the surface and inhibits the reaction.
- Hydrogen gas generated by the steel corrosion forms a bubble or blanket that also inhibits water contact with the container. If hydrogen generation is fast enough, the gas will reach sufficient pressure to create a channel through the buffer and escape into the backfill and geosphere. The pathway through the buffer re-seals after the gas passes so the effectiveness of the buffer is not impaired.
- Water in the steel vessel contacts the fuel bundles. Local failure or corrosion of the Zircaloy cladding allows water to contact the used fuel in places. The more soluble radionuclides (typically a few percent) in the fuel / cladding gap and grain boundaries are released into the water inside the steel vessel.

- A small amount of the used fuel dissolves, releasing other radionuclides into the water. The presence of hydrogen gas from corrosion of the steel container sustains conditions that significantly decrease the rate of fuel dissolution (Shoesmith 2008).
- Most radionuclides have decayed, or are trapped within the used fuel. Dissolved radionuclides diffuse out of the container and into the buffer surrounding the container.

60,000-1,000,000 years

- The steel vessel continues to corrode until all of the steel is consumed.
- Corrosion of the copper vessel continues but only a small fraction of the copper corrodes over this time period.
- Hydrogen gas from the steel corrosion leaks away. Any initial hydrogen gas bubble dissolves or is consumed by microbes, allowing full saturation of the container.
- At some point, the steel vessel is sufficiently weakened by corrosion that it is no longer load bearing and collapses. Any remaining intact fuel bundles are damaged and exposed to water.
- Most of the UO₂ is fractured but intact. A small amount is dissolved; and
- Some radionuclides migrate out of the container, through the buffer and backfill materials, and into the nearby rock. Most radionuclides decay within or near the repository and surrounding rock. Slow migration of the more mobile, soluble and long-lived species (such as I-129) through the geosphere and eventually into the shallow groundwater system and the biosphere can occur.

6.2 Disruptive Event Scenarios

Disruptive Event Scenarios postulate the occurrence of unlikely events leading to possible penetration of barriers and abnormal loss of containment.

6.2.1 Identification of Disruptive Scenarios

A set of Disruptive Scenarios has been identified by evaluating the potential for the External FEPs (Table 6-1) to compromise the safety of the repository system. Specifically, the repository system safety attributes and features identified in Chapter 1 are checked to see if they could be significantly compromised by any of the External FEPs, with the results of this assessment summarized in Table 6-2.

As a further check, the potential for the Internal FEPs to compromise the long-term safety features is also considered, and summarized in Table 6-3. Note that the FEPs considered under the “Contaminant Factor” category are not capable on their own of modifying the repository system to an extent that results in a fundamentally different evolution to that considered in the Normal Evolution Scenario. These are therefore not scenario generating and their effects can be evaluated through different calculation cases for the Normal Evolution Scenario rather than through the development of Disruptive Event Scenarios.

The failure mechanisms identified in Table 6-2 and Table 6-3 can be grouped into seven Disruptive Scenarios as discussed below and summarized in Table 6-4. Since the long-term safety of the repository is based on the strength of the geosphere and engineered barriers (including the container and the shaft seals), the scenarios focus on events in which these can be bypassed.

Table 6-2: External FEPs Potentially Compromising Arguments Relating to the Long-Term Safety

Safety Feature	Potentially Compromised by	Consider as Failure Mechanism
1. The depth of the host rock formation should be sufficient for isolating the repository from surface disturbances and changes caused by human activities and natural events.	Near-surface design adopted (FEP 1.1.02).	No , only a deep design is being considered for the repository
	Meteorite impact (FEP 1.5.01).	No , due to low probability of meteor impact capable of compromising safety due to relatively small repository footprint (~6 km ²) and depth of repository (~500 m). See Garisto (2012) for further discussion of probabilities.
	Exploration borehole penetrates into repository providing enhanced permeability pathway to surface environment and potential for direct exposure to waste (FEP 1.4.04).	Yes , although the absence of economically exploitable resources, and the depth (~500 m) and relatively small repository footprint (~6 km ²) mean that the probability of such a borehole intruding into the repository would be very low during the period of greatest potential hazard.
	Mining and other underground activities resulting in excavation in the vicinity of the repository (FEP 1.4.05).	No , due to assumption of the absence of commercially viable mineral resources at or below repository level. Shallow quarrying or tunnelling activities are unlikely to affect the repository because of repository depth (~500 m). Also, most underground activities would likely be preceded by exploration boreholes, as addressed above.
	Deliberate human intrusion into repository (FEP 1.4.02).	No , exclude deliberate human intrusion since it is expected that the intruders would take appropriate precautions.

Used Fuel Repository Conceptual Design and Postclosure Safety Assessment in Crystalline Rock

Document Number: NWMO TR-2012-16

Revision: 000

Class: Public

Page: 254

Safety Feature	Potentially Compromised by	Consider as Failure Mechanism
	<p>Could discover resources that were not identified during site investigations (FEP 1.1.01) or exploit existing rocks that have become a commercially viable resource. These new resources are exploited by drilling or mining at or below repository level (FEP 1.4.04 and 1.4.05).</p>	<p>No, The lack of resources at the site is assumed to be consistent with regional information. Even if the existing rocks became commercially viable, the repository site is unlikely to become a mine site because similar rocks exist near the surface over a large lateral extent of the Canadian Shield.</p> <p>Also, deep mining activities would likely be preceded by an exploration borehole, which is considered under FEP 1.4.04.</p>
	<p>Repository, intersecting fractures and shafts not properly sealed at time of closure providing an enhanced permeability pathway to the surface environment (FEP 1.1.04).</p>	<p>Yes, although NWMO quality control and regulatory oversight will ensure that poor sealing is very unlikely.</p>
	<p>Site investigation / monitoring borehole not properly sealed at time of closure providing an enhanced permeability pathway to the surface environment (FEP 1.1.01 and 1.1.11).</p>	<p>Yes, although NWMO quality control and regulatory oversight will ensure that poor sealing is very unlikely.</p>
	<p>Poor construction techniques impact on the performance of the repository and shaft excavation disturbed zones providing an enhanced permeability pathway to the surface environment (FEP 1.1.02).</p>	<p>Yes, although NWMO quality control and regulatory oversight will ensure that poor sealing is very unlikely.</p>
	<p>Site investigations do not identify an existing permeable fracture that provides a connection between the repository horizon and shallow groundwater system (FEP 1.1.01).</p>	<p>Yes, a nearby fracture could be missed due to the limits of current technologies to identify all fractures in crystalline rock.</p> <p>Note that all known fractures are assumed open (transmissive) in the Normal Evolution Scenario.</p>

Used Fuel Repository Conceptual Design and Postclosure Safety Assessment in Crystalline Rock

Document Number: NWMO TR-2012-16

Revision: 000

Class: Public

Page: 255

Safety Feature	Potentially Compromised by	Consider as Failure Mechanism
	High magnitude seismic event results in reactivation of currently closed fractures and / or failure of shaft or fracture seals which provides an enhanced permeability pathway to higher horizons (FEP 1.2.03).	Yes , the assessment time scales are such that a significant event may occur even though the annual probability is low. Even then, the probability that the earthquake could actually reactivate a nearby fracture or fail the shaft or fracture seals is very small.
	Ice sheet erosion removes a significant thickness of rock above repository (FEP 1.2.07, 1.3.01, 1.3.02, 1.3.05).	No , Extrapolating the past rate of erosion implies that on the order of 30 m of granitic bedrock may be eroded over 1,000,000 years. This would not significantly reduce the geosphere barrier at the site given the depth of the repository (~500 m).
	Advance / retreat of ice sheets generate large hydraulic gradients which affect groundwater flow velocities in the deep groundwater zone (FEP 1.3.05).	Yes , The changing hydraulic head due to ice sheet advance and retreat over the repository site could affect groundwater flow at the repository level, although flow is likely to remain low in the deep rock due to its permeability.
	Other external geological processes disrupt the repository system, i.e., Tectonic Movement (FEP 1.2.01), Volcanic and Magmatic Activity (FEP 1.2.04), Metamorphism (FEP 1.2.05), Hydrothermal Activity (FEP 1.2.06), Diagenesis (FEP 1.2.08) and Salt Diapirism and Dissolution (FEP 1.2.09).	No , since precluded by site's location and assessment time scales.
2. The volume of available competent rock at repository depth should be sufficient to host the repository and provide sufficient distance from active geological features such as zones of deformation or faults and unfavourable heterogeneities.	Site investigations do not identify an existing permeable fracture that provides a connection between the repository horizon and shallow groundwater system (FEP 1.1.01).	Yes , a nearby fracture could be missed due to the limits of current technologies to identify all fractures in crystalline rock.
	High magnitude seismic event results in reactivation of currently closed fractures and / or failure of shaft or fracture seals which provides an enhanced permeability pathway to higher horizons (FEP 1.2.03).	Yes , the assessment time scales are such that a significant event may occur even though the annual probability is low. Even then, the probability that the earthquake could actually reactivate a nearby fracture or fail the shaft seals is very small.

Used Fuel Repository Conceptual Design and Postclosure Safety Assessment in Crystalline Rock

Document Number: NWMO TR-2012-16

Revision: 000

Class: Public

Page: 256

Safety Feature	Potentially Compromised by	Consider as Failure Mechanism
	Other external geological processes disrupt the repository system, i.e., Tectonic Movement (FEP 1.2.01), Volcanic and Magmatic Activity (FEP 1.2.04), Metamorphism (FEP 1.2.05), Hydrothermal Activity (FEP 1.2.06), Diagenesis (FEP 1.2.08) and Salt Diapirism and Dissolution (FEP 1.2.09).	No , since precluded by site's location and assessment time scales.
3. The hydrogeological regime within the host rock should exhibit low groundwater velocities.	High magnitude seismic event results in reactivation of undetected or unknown existing structural discontinuity and / or failure of shaft or fracture seals which provides an enhanced permeability pathway to higher horizons (FEP 1.2.03).	Yes , the assessment time scales are such that a significant event may occur even though the annual probability is low. Even then, the probability that the earthquake could actually reactivate a nearby fracture or fail the shaft seals is very small.
	Other external geological processes disrupt the repository system, i.e., Tectonic Movement (FEP 1.2.01), Volcanic and Magmatic Activity (FEP 1.2.04), Metamorphism (FEP 1.2.05), Hydrothermal Activity (FEP 1.2.06), Diagenesis (FEP 1.2.08) and Salt Diapirism and Dissolution (FEP 1.2.09).	No , since precluded by site's location and assessment time scales.

Used Fuel Repository Conceptual Design and Postclosure Safety Assessment in Crystalline Rock

Document Number: NWMO TR-2012-16

Revision: 000

Class: Public

Page: 257

Safety Feature	Potentially Compromised by	Consider as Failure Mechanism
4. The mineralogy of the rock, the geochemical composition of the groundwater and rock porewater should not adversely impact the expected performance of the repository multi-barrier system.	Infiltration of oxygenated glacial meltwater into the repository leads to oxidizing conditions in the repository, causing relatively rapid corrosion of copper containers, rapid corrosion of used fuel in any defective containers, and enhanced mobility of redox sensitive nuclides such as U and Tc.	No , glacial recharge penetrating below the shallow groundwater system (> 150 mBGS) is not expected to be oxygenated or influence redox conditions at the repository horizon (see Chapter 2). Repository and boreholes would be located to avoid or seal off permeable fractures.
5. The mineralogy of the host rock, the geochemical composition of the groundwater and rock porewater should be favourable to retarding radionuclide movement.	Infiltration of glacial meltwater (without oxygen) into the repository modifies the hydrogeochemical conditions in the repository, affecting, for example, the stability of the buffer and backfill materials (i.e., leads to erosion of these materials due to colloid formation) (FEP 1.3.05).	No , the paleohydrogeologic simulations described in Chapter 2 suggest that tracer meltwater concentrations at the repository horizon, excluding fracture zones, would be in the range 5% to 45%. Such a change in the composition of the porewater should not significantly affect the properties or stability of the engineered barrier system. Repository and boreholes would be located to avoid or seal off permeable fractures.
	Other external geological processes disrupt the repository system, i.e., Tectonic Movement (FEP 1.2.01), Volcanic and Magmatic Activity (FEP 1.2.04), Metamorphism (FEP 1.2.05), Hydrothermal Activity (FEP 1.2.06), Diagenesis (FEP 1.2.08) and Salt Diapirism and Dissolution (FEP 1.2.09).	No , since precluded by site's location and assessment time scales.
6. The host rock should be capable of withstanding mechanical and thermal stresses induced by the repository without significant structural deformation or fracturing that could compromise the containment and isolation functions of the repository.	Presence of repository weakens rock near repository, potentially making it susceptible to fracturing during earthquakes which could be caused by ice sheet loading/unloading (FEP 1.2.02).	Yes , although all known fractures are assumed open (transmissive) in the Normal Evolution Scenario, an unknown fault or fracture could be reactivated by seismic activity particularly if it has been weakened by presence of repository.

Used Fuel Repository Conceptual Design and Postclosure Safety Assessment in Crystalline Rock

Document Number: NWMO TR-2012-16

Revision: 000

Class: Public

Page: 258

Safety Feature	Potentially Compromised by	Consider as Failure Mechanism
<p>7. Current and future seismic activity at the repository site should not adversely impact the integrity of the repository during operation and in the very long term.</p>	<p>High magnitude seismic event results in reactivation of currently closed fractures and / or failure of shaft or fracture seals which provides an enhanced permeability pathway to higher horizons (FEP 1.2.03).</p>	<p>Yes, the assessment time scales are such that a significant event may occur even though the annual probability is low. Even then, the probability that the earthquake could actually reactivate a nearby fracture or fail the shaft seals is very small.</p>
	<p>Large seismic event results in shearing along an existing local fracture that passes through a borehole. The shearing load causes failure of the used fuel container in the borehole.</p>	<p>Yes, the assessment time scales are such that a significant seismic event may occur even though the annual probability is low. However, the probability that an earthquake would cause a container failure due to a shear load is likely small (SKB 2011).</p>
<p>8. The expected rates of land uplift, subsidence and erosion at the repository site should not adversely impact the containment and isolation of the repository.</p>	<p>Ice sheet erosion resulting from climate change removes a significant thickness of rock above the repository (FEP 1.2.07, 1.3.01, 1.3.02, 1.3.05).</p>	<p>No, see discussion of ice sheet erosion under Argument 1.</p>
	<p>Land uplift decreases depth of repository.</p>	<p>No, land uplift occurs on a continental scale so relative depth of repository does not change. Land uplift and large-scale erosion are also not significant factors in affecting repository depth on assessment time scale.</p>
<p>9. The repository should not be located within rock formations containing economically exploitable natural resources such as minerals and other valuable commodities as known today.</p>	<p>Mining and other underground activities resulting in excavation in the vicinity of the repository (FEP 1.4.05).</p>	<p>No, due to the assumption of the absence of commercially viable mineral resources at or below repository level. Other underground activities are unlikely to affect the repository (e.g., rock quarry) because of repository depth (~500 m). Also, such activities would likely be preceded by exploration boreholes, as addressed above.</p>
<p>10. The repository is not located within geological formations containing groundwater resources at repository depth</p>	<p>Deliberate human intrusion into repository (FEP 1.4.02).</p>	<p>No, exclude deliberate human intrusion since it is expected that the intruders would take appropriate precaution.</p>

Used Fuel Repository Conceptual Design and Postclosure Safety Assessment in Crystalline Rock

Document Number: NWMO TR-2012-16

Revision: 000

Class: Public

Page: 259

Safety Feature	Potentially Compromised by	Consider as Failure Mechanism
<p>that could be used for drinking, agriculture or industrial uses.</p>	<p>Could discover resources that were not identified during site investigations (FEP 1.1.01) or exploit existing rocks that have become a commercially viable resource. These new resources are exploited by drilling or mining at or below repository level (FEP 1.4.04 and 1.4.05).</p>	<p>No, The lack of resources at the site is assumed to be consistent with regional information. Even if the existing rocks became commercially viable, the repository site is unlikely to be the mine site because similar rocks exist near the surface over a large lateral extent of the Canadian Shield.</p> <p>Also, the impact of drilling is already considered under exploration borehole (FEP 1.4.04).</p>
<p>11. The used nuclear fuel is a durable uranium oxide (UO₂); it will dissolve very slowly under the chemical conditions within a failed container.</p> <p>12. Most of the initial radioactivity is held within the UO₂ grains, where it can only be released as the used fuel dissolves.</p>	<p>Infiltration of oxygenated glacial meltwater into the repository leads to oxidizing conditions in the repository, causing relatively rapid corrosion of the copper containers and, after container failure, relatively rapid fuel oxidation and contaminant releases from fuel. (FEP 1.3.05)</p>	<p>No, glacial recharge penetrating below the shallow groundwater system (> 150 mBGS) is not expected to be oxygenated or influence redox conditions at the repository horizon (see Chapter 2).</p>
<p>13. The used fuel container has a design life of at least 100,000 years under the geomechanical and chemical repository conditions expected to exist within the repository.</p>	<p>Poor manufacturing techniques or unanticipated material problems / interactions impact on the durability of the used fuel containers (FEP 1.1.03, 1.1.07) significantly reducing the expected lifetime of some containers.</p> <p>Used fuel containers fail due to increase in the isostatic load caused by a thick ice sheet passing over the repository site.</p>	<p>Yes, although application of NWMO's quality control will make it very likely that poorly manufactured containers would be discovered and not used.</p> <p>Yes, although the containers are designed to withstand the isostatic load from buffer swelling, hydrostatic load and a 3 km thick ice sheet over the repository site, the possibility that the design load of the container could be exceeded due to the passage of a thicker ice sheet needs to be considered.</p>

Used Fuel Repository Conceptual Design and Postclosure Safety Assessment in Crystalline Rock

Document Number: NWMO TR-2012-16

Revision: 000

Class: Public

Page: 260

Safety Feature	Potentially Compromised by	Consider as Failure Mechanism
	Infiltration of oxygenated glacial meltwater into the repository leads to oxidizing conditions in the repository, leading to relatively rapid corrosion of the copper containers (FEP 1.3.05).	No , glacial recharge penetrating below the shallow groundwater system (> 150 mBGS) is not expected to be oxygenated or influence redox conditions at the repository horizon (see Chapter 2).
14. The container is surrounded by a layer (approximately 30 cm) of dense bentonite-based clay that inhibits groundwater movement, has self-sealing capability, inhibits microbial activity near the container, and retards contaminant transport.	Bentonite buffer layer not properly installed and, therefore, the density of the buffer around the container is lower than design requirement.	Yes , although application of NWMO's quality control will ensure that poor sealing is very unlikely.
	Infiltration of glacial meltwater (without oxygen) into the repository modifies the hydrogeochemical conditions in the repository, affecting, for example, the stability of the buffer and backfill materials (i.e., leads to erosion of these materials due to colloid formation) (FEP 1.3.05).	No , the paleohydrogeologic simulations described in Chapter 2 suggest that tracer meltwater concentrations at the repository horizon, excluding fracture zones, would be in the range 5% to 45%. Such a change in the composition of the porewater should not significantly affect the properties or stability of bentonite clay.
15. Institutional Controls will limit the potential for human encounter with the repository in the near term after closure	Institutional controls on the development of the site are ineffective (FEP 1.4.08). This allows development of the site (1.4.06) and human intrusion into the repository to occur by drilling (FEP 1.4.04) and / or mining (FEP 1.4.05)	No , Measures are assumed to be taken in the near term to ensure that information regarding the purpose, location, design and contents of the repository is preserved so that future generations are made aware of the consequences of any actions they may choose to take. With these institutional measures as well as general societal memory, and with the absence of commercially viable natural resources at depth, inadvertent intrusion in the near term after closure is not considered. However, Human Intrusion is considered in the long term.

Table 6-3: Internal FEPs Potentially Compromising Arguments Relating to Long-Term Safety*

Safety Feature	Potentially Compromised By	Consider as Failure Mechanism
1. The depth of the host rock formation should be sufficient for isolating the repository from surface disturbances and changes caused by human activities and natural events..	No Internal FEP could result in a significant change in the depth of the repository. Note that FEP 2.3.12 relates to the erosion of surficial deposits and not bedrock.	No.
2. The volume of available competent rock at repository depth should be sufficient to host the repository and provide sufficient distance from active geological features such as zones of deformation or faults and unfavourable heterogeneities.	An undetected feature (e.g., a fracture) in the geosphere provides a relatively high permeability connection between the repository horizon and higher horizons (FEPs 2.2.04 and 2.2.12)	Yes , a nearby fracture could be missed due to the limits of current technologies to identify all fractures in crystalline rock.
3. The hydrogeological regime within the host rock should exhibit low groundwater velocities.	An undetected feature (e.g., a fracture) in the geosphere provides a relatively high permeability connection between the repository horizon and higher horizons (FEPs 2.2.04 and 2.2.12)	Yes , a nearby fracture could be missed due to the limits of current technologies to identify all fractures in crystalline rock.
4. The mineralogy of the rock, the geochemical composition of the groundwater and rock porewater at repository depth should not adversely impact the expected performance of the repository multi-barrier system. 5. The mineralogy of the host	Various repository FEPs (e.g., FEPs 2.1.04, 2.1.07 to 2.1.11), e.g., temperature rise in the repository, have the potential to modify the hydrological, mechanical and chemical conditions at repository depth, affecting seal properties and / or radionuclide movement.	No , the effects are likely to be localized to the immediate vicinity of the repository and these FEPs can be evaluated through considering different calculation cases for the Normal Evolution Scenario (e.g., no sorption and no solubility sensitivity cases) rather than through the development of alternative Disruptive Scenarios. For conservatism, concrete seals are assumed degraded from the time of repository closure.

Used Fuel Repository Conceptual Design and Postclosure Safety Assessment in Crystalline Rock

Document Number: NWMO TR-2012-16

Revision: 000

Class: Public

Page: 262

Safety Feature	Potentially Compromised By	Consider as Failure Mechanism
<p>rock, the geochemical composition of the groundwater and rock porewater should be favourable to retarding radionuclide movement.</p>	<p>Various repository FEPs (e.g., FEP 2.1.03, 2.1.04, 2.1.07, 2.1.09, 2.1.10) can influence the durability of the used fuel containers, potentially leading to container failures.</p>	<p>Yes, poor local conditions might cause a limited number of container failures. Note that the Normal Evolution Scenario already includes a number of containers with pre-existing defects (e.g., welding defects) which lead to early container failures.</p>
	<p>Various repository FEPs (e.g., FEPs 2.1.07 to 2.1.11) and geosphere FEPs (e.g., FEPs 2.2.05 to 2.2.10) can affect the rate at which contaminants are released from the repository and migrate through the shafts and geosphere.</p>	<p>No, the effects of these FEPs can be evaluated through considering different calculation cases for the Normal Evolution Scenario rather than through the development of alternative Disruptive Scenarios (e.g., no sorption and no solubility sensitivity cases). The possibility of repository and shaft excavation damage zones is considered in the Normal Evolution Scenario. Also, concrete seals are assumed degraded from the time of repository closure.</p>
	<p>Changes in porewater chemistry in repository due to, for example, presence of concrete adversely affects clay seals (FEP 2.1.05, 2.1.06).</p>	<p>No, use of low-temperature, low pH concrete in the repository minimizes interactions with clay seals. Also, the amount of concrete in the repository is small compared to the amount of clay sealing materials. Note that the Normal Evolution Scenario already includes a number of containers with pre-existing defects (e.g., welding defects) which lead to early container failures.</p>

Used Fuel Repository Conceptual Design and Postclosure Safety Assessment in Crystalline Rock

Document Number: NWMO TR-2012-16

Revision: 000

Class: Public

Page: 263

Safety Feature	Potentially Compromised By	Consider as Failure Mechanism
<p>6. The host rock should be capable of withstanding mechanical and thermal stresses induced by the repository without significant structural deformation or fracturing that could compromise the containment and isolation functions of the repository.</p>	<p>Mechanical and thermal stresses induced by presence of repository are underestimated and cause greater than expected fracturing within the repository and shaft excavation damage zones, providing an enhanced permeability pathway to the surface environment (e.g., FEPs 2.1.07, and 2.1.11).</p>	<p>Yes, although application of NWMO's quality control will ensure that stresses are not underestimated and engineering calculations include safety factors.</p>
<p>7. Current and future seismic activity at the repository site should not adversely impact the integrity of the repository during operation and in the very long term.</p>	<p>Relates to External FEPs only (see Table 6-2).</p>	
<p>8. The expected rates of land uplift, subsidence and erosion at the repository site should not adversely impact the containment and isolation of the repository.</p>	<p>Relates to External FEPs only (see Table 6-2).</p>	

Used Fuel Repository Conceptual Design and Postclosure Safety Assessment in Crystalline Rock

Document Number: NWMO TR-2012-16

Revision: 000

Class: Public

Page: 264

Safety Feature	Potentially Compromised By	Consider as Failure Mechanism
<p>9. The repository should not be located within rock formations containing economically exploitable natural resources such as minerals and other valuable commodities as known today.</p> <p>10. The repository is not located within geological formations containing groundwater resources at repository depth that could be used for drinking, agriculture or industrial uses.</p>	<p>Relates to External FEPs only (see Table 6-2).</p>	
<p>11. The used nuclear fuel is a durable uranium oxide (UO₂); it will dissolve very slowly under the chemical conditions within a failed container.</p> <p>12. Most of the initial radioactivity is held within the UO₂ grains, where it can only be released as the used fuel dissolves.</p>	<p>Various repository FEPs (e.g., FEPs 2.1.08 to 2.1.11 and 2.1.13) can affect the rate at which contaminants are released from the used fuel.</p>	<p>No, geological, hydrogeological, and geochemical evidence indicates that the geosphere at a Canadian Shield site will be robust to uncertainties in repository or geosphere FEPs. Furthermore, these FEPs can be evaluated through considering different calculation cases for the Normal Evolution Scenario rather than through the development of alternative Disruptive Scenarios.</p>
	<p>Release due to criticality accident.</p>	<p>No, the fuel is natural uranium. The fissile content of the used fuel is too low.</p>

Safety Feature	Potentially Compromised By	Consider as Failure Mechanism
<p>13. The used fuel container has a design life of at least 100,000 years under the geomechanical and chemical repository conditions expected to exist within the repository.</p>	<p>Containers are not fabricated to specifications and so are placed in the repository with defects (FEP 2.1.03).</p>	<p>Yes, although the fabrication method is designed to be robust, and there would be multiple methods of inspection, there is statistically some probability of initial defects not being detected such that a few containers are placed with initial defects. Defects in the steel vessel, for example, could lead to container collapse.</p> <p>The Normal Evolution Scenario assumes some containers with undetected defects are present in the repository at the time of closure, leading to early container failures.</p>
	<p>Various repository FEPs (e.g., FEPs 2.1.04, 2.1.07 to 2.1.11) can influence the durability of the used fuel containers, potentially leading to container failures.</p>	<p>Yes, although evidence suggests that the copper container would be thermodynamically stable under the reducing conditions expected in the repository, poor local conditions might cause a limited number of container failures.</p> <p>The Normal Evolution Scenario assumes some containers with undetected defects are present in the repository at the time of closure, leading to early container failures.</p>

Safety Feature	Potentially Compromised By	Consider as Failure Mechanism
<p>14. The container is surrounded by a layer (approximately 30 cm) of dense bentonite-based clay that inhibits groundwater movement, has self-sealing capability, inhibits microbial activity near the container, and retards contaminant transport.</p>	<p>Various repository FEPs (e.g., FEPs 2.1.04, 2.1.07 to 2.1.11) can influence the durability of the used fuel containers, potentially leading to container failures.</p>	<p>Yes, although evidence suggests that the copper container would be thermodynamically stable under the reducing conditions expected in the repository, poor local conditions might cause a limited number of container failures.</p> <p>Note that the Normal Evolution Scenario already includes a number of containers with pre-existing defects (e.g., welding defects) which lead to early container failures.</p>
	<p>Various repository FEPs (e.g., FEPs 2.1.05 to 2.1.11) have the potential to modify the hydrological, mechanical and chemical conditions at the repository depth, affecting properties of clay-based materials.</p>	<p>No, the effects are likely to be localized to the immediate vicinity of the repository and these FEPs can be evaluated through considering different calculation cases for the Normal Evolution Scenario (i.e., no sorption and no solubility sensitivity cases) rather than through the development of alternative Disruptive Scenarios.</p>
<p>15. Institutional Controls will limit the potential for human encounter with the repository in the near term after closure</p>	<p>Affected by External FEPs relating to Future Human Actions (see Table 6-2) rather than the Internal FEPs relating to human behaviour that responds to the Future Human Actions.</p>	

Note: * - the Internal FEPs are shown in Garisto (2012).

Table 6-4: Potential Failure Mechanisms and Associated Scenarios

Failure Mechanism	Associated Disruptive Scenario
Exploration borehole penetrates into the repository providing an enhanced permeability pathway to the surface environment and potential for direct exposure to waste	Human Intrusion
Poor construction techniques lead to a large excavation damage zone around shaft or fracture seals, which provides an enhanced permeability pathway to the surface environment	Shaft Seal Failure and Fracture Seal Failure
Repository and shafts are not properly sealed at the time of closure, providing an enhanced permeability pathway to the surface environment	Shaft Seal Failure and Fracture Seal Failure
Long-term performance of shaft or fracture seals and excavation damage zone deviates from that expected, due to some unexpected internal processes, resulting in an enhanced permeability pathway to the surface environment	Shaft Seal Failure and Fracture Seal Failure
Site investigation / monitoring borehole is poorly sealed at time of closure providing an enhanced permeability pathway to the surface environment	Poorly Sealed Borehole
Long-term performance of site investigation / monitoring borehole seal deviates from that expected, due to some unexpected internal processes, resulting in an enhanced permeability pathway to the surface environment	Poorly Sealed Borehole
Site investigations do not identify a relatively high permeability fracture that provides a connection between the repository horizon and higher horizons	Undetected Fault
Seismic event results in reactivation of an existing fracture and / or failure of shaft or fracture seals that provides an enhanced permeability pathway to higher horizons	Undetected Fault, Shaft Seal Failure and Fracture Seal Failure
Seismic event results in shearing along an existing local fracture passing through a borehole, resulting in failure of some container(s) due to the shear load.	Container Failure
Manufacturing defect in steel vessel or unexpected high local loads lead to mechanical failure of some containers.	Container Failure
Unexpected corrosion of copper container due to, for example, initial defects in copper, higher microbial corrosion caused by incorrect placement of a low density buffer around container, or unanticipated interaction of copper container with groundwater in the repository.	Container Failure
Passage of thicker than expected ice sheet over repository site causes isostatic load on all containers to exceed design load of containers, resulting in failure of all containers.	All Containers Fail

The repository siting process will ensure that there are no known commercially viable natural resources at or below repository depth. Also, the repository panels have a small footprint (~6 km²) and the repository is at a depth of around 500 m. These factors limit the range of human activities that could directly affect the closed repository to a borehole unintentionally drilled into the repository as part of a future geological exploration program³. Even this situation has a low probability of occurrence. Nevertheless, once controls on the use of the site are no longer effective, the possibility of inadvertent human intrusion by this method cannot be ruled out over long time scales⁴. Such a borehole could provide an enhanced permeability pathway to the surface environment and potential for direct exposure to waste. This scenario is referred to as the **Human Intrusion Scenario**.

A second scenario by which the geosphere barrier can be bypassed is via the shafts (main, service and ventilation shafts). These are ~8 m diameter holes that penetrate the geosphere, but are placed away from the waste panels and carefully sealed in the design. The **Shaft Seal Failure Scenario** considers the possibility that the shaft seals are not fabricated or installed appropriately, or that the long-term performance of the shaft seals and shaft / repository Excavation Damage Zones (EDZs) is poor due to unexpected physical, chemical and / or biological processes, or the shaft seals are damaged by a seismic event. While these situations could result in an enhanced permeability pathway to the surface, they are very unlikely due to quality control measures that will be applied during shaft seal closure and due to multiple durable material layers in the shaft.

A third scenario in which the geosphere barrier can be bypassed is via failure of the seals that isolate the repository from the fracture passing through the repository footprint. In the Normal Evolution Scenario this fracture is the main conduit for contaminated groundwater from the repository to the surface. The **Fracture Seal Failure Scenario** considers the possibility that the fracture seals are not fabricated or installed appropriately, or that the long-term performance of the fracture seals and / or repository EDZ is poor due to unexpected processes or that the seals are damaged by seismic activity. While these failures could result in an enhanced permeability pathway to the surface, they are unlikely due to quality control measures that will be applied during seal placement and due to the multiple durable materials used for the fracture seals.

In both the Shaft Seal and Fracture Seal Failure Scenarios, it is assumed that the other repository engineered barriers (i.e., the tunnel and room seals, and the backfill and buffer), are not degraded relative to their design properties except for the concrete component of the seals, for which degraded properties are used throughout the simulations, as in the Normal Evolution Scenario. As a worst case, failure of the other seals in the repository is considered. This case is even more unlikely due to the large spatial separation between the various seals.

Another way in which the geosphere barrier can be bypassed is through the site characterization / monitoring boreholes. These boreholes are located in the vicinity of the repository down to and below repository depth. These boreholes will be appropriately sealed on

³ The assessment excludes deliberate human intrusion since it is expected that the intruders would take appropriate precaution.

⁴ The repository might appear as an anomaly in any surface / air-borne survey of the area, and this could encourage drilling at the site. However, the assumed absence of interesting minerals or geologic features in the area would argue against deliberate surveys of the area. Furthermore, a cautious approach to drilling might be used if such unexpected anomalies were identified that would minimize the consequences of any intrusion into the repository.

completion of site investigation / monitoring activities so they will have no effect on repository performance. However, if a deep borehole were not properly sealed or were to extensively degrade, then it could provide a small but relatively permeable pathway for the migration of contaminants from the repository horizon. The scenario is termed the **Poorly Sealed Borehole Scenario**. Like the Shaft Seal Failure Scenario, such a situation is very unlikely due to the adoption of good engineering practice and quality control.

The fracture zone network at the hypothetical site is based on a geostatistical model that represents a Canadian Shield location consistent with surface lineaments (Chapter 2). At a real site in crystalline rock, there could be some uncertainty in the fracture network, and in the properties of the fractures. Site characterization may not identify all existing significant fractures at the site, and therefore a scenario is defined to investigate the safety implications of a hypothetical transmissive fault that is either undetected or formed by the displacement of an unknown existing discontinuity. The hypothetical fault is assumed to be in close proximity to the repository and to extend from below the repository level to the shallow groundwater system. This scenario is termed the **Undetected Fault Scenario**.

While the copper used fuel containers have a design requirement for a minimum functional life of not less than 100,000 years, they are expected to last much longer based on thermodynamic, experimental and natural analogue evidence that copper is stable for very long periods under deep geological repository conditions. Nevertheless, there are several mechanisms by which the containers could fail some time after they are installed in the repository. These container failures would be more severe than the small defects considered in the Normal Evolution Scenario (which could be due to, for example, undetected welding defects.) Failure mechanisms include the following:

1. The container has a manufacturing defect in the steel vessel that weakens it sufficiently that the container fails under the isostatic load imposed by a passing ice sheet. The probability of such an event depends on the quality assurance procedures in place, the thickness of the ice sheet and the swelling pressure of the buffer (which contributes to the isostatic load).
2. A container could be damaged by a sufficiently large shear load. A large seismic event that causes the rock to slip along a local fracture intersecting a borehole could produce such a shear load (SKB 2011). The probability of such an event depends on the likelihood of an earthquake of a sufficient magnitude to produce slip along a minor fracture, the likelihood that a borehole is intersected by a local fracture (or conversely, the likelihood that unsuitable boreholes can be avoided) and, finally, how the shear load is transmitted through the buffer material, which depends on the buffer thickness and density. Based on the analysis in SKB (2011), the probability of a single container failure in their repository due to shear load would be less than 0.2 over the one-million year assessment period.
3. After the repository attains reducing conditions, the copper containers should be immune to further corrosion. However, if the buffer is not installed correctly, then the buffer density could be sufficiently low to permit growth of microbes near the copper surface and to allow transport of nutrients from groundwater to the microbes. Under such conditions microbial corrosion could damage the copper container sufficiently over the time frame of interest that the steel vessel would be exposed to water, leading to weakening of the steel vessel due to corrosion and / or seepage of water into the container.

The specific failure mode is not defined here, but the consequences are evaluated in the **Container Failure Scenario**. The key characteristics of this scenario are that only a few containers are affected, that the container damage is significant, but also that the failure occurs at least 10,000 years and possibly 60,000 years after closure.

The containers are designed to withstand an isostatic load of 45 MPa. With this design, the containers could withstand the sum of the hydraulic load due to a 3 km ice sheet (maximum load of 35 MPa for a 500 m deep repository, if the ice sheet is warm-based and the water table reaches the surface of the ice sheet) and a buffer swelling pressure of about 6 MPa. However, the design load of the container could be exceeded if, for example, the ice sheet thickness is greater than 3.5 km. Such an event could lead to multiple container failures and a significant increase in the contaminant releases from the repository and calculated impacts.

Consequently, an **All Containers Fail Scenario** is considered in which all the containers in the repository fail at 60,000 years, the time of the assumed first passage of an ice sheet over the site (Loutre and Berger 2000). Note that the probability of such a scenario is likely low since the maximum ice sheet thickness at the repository site during the last glacial cycle was less than 3 km and it is not likely that the water table would reach the surface of such a thick ice sheet, given the low atmospheric temperatures needed to promote formation of thick ice sheets (Garisto et al. 2010).

Other potential Disruptive Scenarios were considered but ruled out on various grounds as discussed further in the FEPs report (Garisto 2012). No volcanic activity is anticipated in the area over the next one million years. The probability of being hit by a large meteor capable of damaging the repository is remote and the consequences of the impact itself would likely be more significant than those from the repository. Seismic activity is possible, and likely earthquakes are included in the Normal Evolution Scenario. Such seismic activity will not cause rockfall because the repository is backfilled. Large earthquakes are unlikely since the Canadian Shield in general, and the assumed site in particular, is a low-seismicity area. The main effects on the repository are represented by the Shaft Seal Failure, the Fracture Seal, the Undetected Fault and the Container Failure Scenarios, so there is no need to consider an additional earthquake scenario. Glaciation, which could affect the repository system, is considered within the Normal Evolution Scenario.

Further confidence that an appropriate set of Disruptive Scenarios has been identified can be obtained by comparing the scenarios considered in the postclosure safety assessments of other deep repositories. A review of the scenarios considered in assessments of deep repositories in other countries was undertaken. The results, summarized in Table 6-5, show that most assessments have identified a limited number of additional scenarios that consider the degradation / failure of engineered and natural barriers by natural processes (e.g., earthquakes, climate change) and human actions (e.g., drilling, poor quality control). Although there are some scenarios identified that are not considered in the current study, these are either not relevant to a Canadian Shield site (e.g., volcanic activity, sea-level rise, mining of resources) or have been included in the Normal Evolution Scenario (e.g., climate change, container failure).

Table 6-5: Additional Scenarios Considered in Other Safety Assessments

Assessment	Reference	Additional Scenarios Considered
SR-Site (Sweden)	SKB (2011)	<ul style="list-style-type: none"> • Canister failure due to corrosion or shear load • Disrupted buffer (due to erosion, advection) • Extended greenhouse effects • Exploratory drilling • Rock facility (e.g., quarry) • Poorly sealed repository
Olkiluoto (Finland)	POSIVA (2010)	<ul style="list-style-type: none"> • Defective canister (early and delayed penetration) • Earthquake/rock shear • Disrupted buffer • Release affected by gas • Exploratory drilling
Dossier Argile (France)	ANDRA (2005)	<ul style="list-style-type: none"> • Seal failure and defective plug • Defective waste and spent fuel containers • Borehole penetrating repository • Functioning of repository greatly degraded
H12 (Japan) ¹	JNC (2000)	<ul style="list-style-type: none"> • Climate and sea-level change • Exploitation drilling (water well) • Engineering defects, including poorly sealed repository
Opalinus (Switzerland)	NAGRA (2002)	<ul style="list-style-type: none"> • Gas pathways • Exploratory drilling • Poorly sealed repository
GPA (UK)	NIREX (2003)	<ul style="list-style-type: none"> • Exploratory drilling
WIPP (USA)	DOE (2004)	<ul style="list-style-type: none"> • Mining • Exploratory drilling
Yucca Mountain (USA) ²	DOE (2002)	<ul style="list-style-type: none"> • Exploratory drilling • Seismicity • Volcanic event
SAFIR 2 (Belgium)	ONDRAF/NIRAS (2001)	<ul style="list-style-type: none"> • Exploratory drilling • Greenhouse effect • Poor sealing of repository • Fault activation • Severe glacial period • Failure of engineered barriers • Gas-driven transport

Notes

¹ Isolation Failure Scenarios that involve penetration of the repository (including magma intrusion, human intrusion and meteorite impact) were also considered but screened out on the grounds that they are extremely unlikely to occur. Some 'what if' calculations were carried out instead.

² The term 'scenario' is used in a way that differs from the other assessments reviewed. Three Thermal Load Scenarios are discussed that are design variants, while two No-action Scenarios refer to futures in which the Yucca Mountain facility does not go ahead.

6.2.2 Description of Disruptive Event Scenarios

The identified Disruptive Event Scenarios are described below. These scenarios are evaluated separately rather than in combination since they have low probability and independent causes, and so the likelihood of simultaneous occurrence is even lower.

6.2.2.1 Inadvertent Human Intrusion Scenario

The Inadvertent Human Intrusion Scenario considers the impact of human intrusion sometime in the future. In this scenario, an exploration borehole is drilled through the geosphere and into the repository with the drill bit intersecting a used fuel container.

It is assumed that the drill crew is unaware of the facility (i.e., the intrusion occurs after institutional controls are no longer effective and societal memory of the site is lost). The investigators will most likely collect samples or conduct measurements at the repository level, due to the unusual nature of the materials. This would identify significant residual radioactivity (e.g., gamma logging is a standard borehole measurement) and the investigators would likely take precautions to prevent further exposure including appropriate management of any surface-released materials and sealing of the borehole. Therefore, under normal drilling, there would be little impact after the initial drill crew exposure.

Nevertheless, the Inadvertent Human Intrusion Scenario assumes:

- It is not recognized that the drill has intercepted a waste repository so no safety restrictions are applied; and
- The borehole and drill site are not managed and closed to current standards, and material from the borehole is released onto the surface around the drill site.

Contaminants can be released and humans and biota exposed via:

- Retrieval and examination of drill core contaminated with waste; and
- Uncontrolled dispersal of contaminated drill core debris on the site.

This could result in the exposure of the drill crew or other people at the time of intrusion, and people who might occupy the site subsequent to the intrusion event.

If the borehole is not properly sealed, it could provide an enhanced permeability pathway to the surface environment or even be used as a well by a future site resident. The impact of this open borehole on the future residents of the site is examined as part of the Inadvertent Human Intrusion Scenario.

6.2.2.2 Shaft Seal Failure Scenario

The shafts represent a potentially important pathway for contaminant release and therefore the repository design includes specific measures to provide good shaft seals, taking into account the characteristics of the geosphere. The Shaft Seal Failure Scenario considers the consequences of rapid and extensive shaft seal degradation. This scenario, like the other Disruptive Event Scenarios, is a bounding scenario designed to investigate the robustness of the repository system.

A variant case of the Shaft Seal Failure Scenario is also identified in which both the shaft seals and the repository engineered barriers degrade rapidly and extensively.

The exposure pathways are the same as those considered in the Normal Evolution Scenario.

6.2.2.3 Fracture Seal Failure Scenario

The fracture passing through the repository footprint represents a potentially important pathway for contaminant release and therefore the repository design includes specific measures to provide good fracture seals, taking into account the characteristics of the geosphere. The Fracture Seal Failure Scenario considers the consequences of rapid and extensive fracture seal degradation. This scenario, like the other Disruptive Event Scenarios, is a bounding scenario designed to investigate the robustness of the repository system.

A variant case of the Fracture Seal Failure Scenario is also identified in which both the fracture seals and the repository tunnel and room seals degrade rapidly and extensively.

The exposure pathways are the same as those considered in the Normal Evolution Scenario.

6.2.2.4 Poorly Sealed Borehole Scenario

Multiple deep site investigation / monitoring boreholes will be drilled in the vicinity of the repository during the site investigation phase. The Poorly Sealed Borehole Scenario considers the consequences of one of the boreholes not being properly sealed or having a seal that extensively degrades. The poorly sealed borehole provides an enhanced permeability connection between the level of the repository, the overlying groundwater zones and the biosphere, thereby bypassing some of the natural geological barriers to contaminant migration from the repository. The exposure pathways are the same as those considered in the Normal Evolution Scenario.

6.2.2.5 Undetected Fault Scenario

The Undetected Fault Scenario considers the impact of an undetected or new transmissive fault extending from around the repository level into the shallow groundwater system in close proximity to the repository. Such a fault could provide an enhanced permeability pathway that bypasses the deep groundwater system.

The exposure pathways are the same as those considered in the Normal Evolution Scenario.

6.2.2.6 All Containers Fail Scenario

The long-lived used fuel containers are an important feature of the multi-barrier repository concept in this conceptual design. The copper containers are expected to last for a long time because copper is stable under anticipated conditions in a deep geological repository; however, the All Containers Fail Scenario considers the unlikely and hypothetical case in which all the containers simultaneously fail (i.e., water enters all containers and contacts the fuel) at 60,000 years. This timeframe corresponds to the approximate time scale for glacial cycles to resume and an ice sheet to first cover the site (Loutre and Berger 2000, Garisto et al. 2010), which could be assumed to cause multiple container failures if the isostatic load on the containers is higher than expected.

A variant case in which all containers are assumed to fail at 10,000 years is also investigated to determine the sensitivity to the assumed failure time.

The exposure pathways are the same as those considered in the Normal Evolution Scenario.

6.2.2.7 Container Failure

The Container Failure Scenario considers the impact of container failure due several possible mechanisms.

- 1) A large seismic event (earthquake) in the vicinity of the repository that causes slip along a local fracture that intersects a container borehole. The rock slip along the fracture is assumed to be so large that it causes complete failure of the container. The shear is also assumed to significantly increase the transmissivity of the fracture. Although the shear movement should not affect the buffer properties, the amount of buffer between the container and the shearing fracture would likely be reduced.
- 2) A defect in the container steel vessel weakens it sufficiently that the isostatic load from an expected ice sheet causes the container to collapse.
- 3) Corrosion of the container due to unexpected chemical conditions in the borehole due to unexpected chemical interactions with the groundwater or installation of a defective (i.e., low density) buffer which allows formation of biofilms on the copper surface.

The exposure pathways are the same as those considered in the Normal Evolution Scenario.

6.3 References for Chapter 6

- ANDRA. 2005. Dossier 2005 Argile Tome Evaluation de Sûreté du Stockage Géologique. Paris, France.
- Blyth, A., S. Frape, R. Blomqvist and P. Nissinen. 2000. Assessing the past thermal and chemical history of fluids in crystalline rock by combining fluid inclusion and isotope investigations of fracture calcite. *Applied Geochemistry* **13**, 1417-1437.
- CNSC. 2006. Regulatory Guide G-320: Assessing the Long Term Safety of Radioactive Waste Management. Canadian Nuclear Safety Commission. Ottawa, Canada.
- DOE. 2002. Final Environmental Impact Statement for a Geologic Repository for the Disposal of Spent Nuclear Fuel and High-level Radioactive Waste at Yucca Mountain, Nye County, Nevada. United States Department of Energy, Office of Civilian Radioactive Waste Management, DOE/EIS-0250. Nevada, USA.
- DOE. 2004. 2004 WIPP Compliance Recertification Application (CRA) - Main Volume. US Department of Energy Report DOE/WIPP 04-3231. Available at: http://www.wipp.energy.gov/library/CRA/CRA_Index.htm. Accessed January 2011.
- Garisto, F. 2012. Fourth Case Study: Features, Events and Processes. Nuclear Waste Management Organization Report NWMO TR-2012-14. Toronto, Canada.
- Garisto, F., J. Avis., T. Chshyolkova, P. Gierszewski, M. Gobien, C. Kitson, T. Melnyk, J. Miller, R. Walsh and L. Wojciechowski. 2010. Glaciation scenario: Safety assessment for a

used fuel geological repository. Nuclear Waste Management Organization Technical Report NWMO TR-2010-10. Toronto, Canada.

Gascoyne, M. 2000. Hydrogeochemistry of the Whiteshell Research Area. Ontario Power Generation Report 06819-REP-01200-10033-R00. Toronto, Canada.

Gascoyne, M. 2004. Hydrogeochemistry, groundwater ages and sources of salts in a granitic batholith on the Canadian Shield, southeastern Manitoba. *Applied Geochemistry* 19, 519-560.

Gascoyne, M., J. McMurry and R. Ejeckam. 2004. Paleohydrogeological Case Study of the Whiteshell Research Area. Ontario Power Generation Report 06819-REP-01200-10121-R00. Toronto, Ontario.

IAEA. 2004. Improvement of Safety Assessment Methodologies for Near Surface Disposal Facilities. Volume I: Review and Enhancement of Safety Assessment Approaches and Tools. International Atomic Energy Agency IAEA-ISAM-1. Vienna, Austria.

JNC. 2000. H12: Project to Establish the Scientific and Technical Basis for HLW in Japan. Japan Nuclear Cycle Development Institute Report JNC TN1410 2000-004. Tokai, Japan.

Loutre, M.F. and A. Berger. 2000. Future climate changes: Are we entering an exceptionally long interglacial? *Climate Change* 46, 61-90.

McMurry, J. and R.B. Ejeckam. 2002. Paleohydrogeological Study of Fracture Mineralogy in the Whiteshell Research Area. Ontario Power Generation Report 06819-REP-01200-10082-R00. Toronto, Canada.

McMurry, J., B.M. Ikeda, S. Stroes-Gascoyne, D.A. Dixon and J.D. Garroni. 2004. Evolution of a Canadian Deep Geologic Repository: Defective Container Scenario. Ontario Power Generation Report 06819-REP-01200-10127-R00. Toronto, Canada.

NAGRA. 2002. Project Opalinus Clay: Safety Report, Demonstration of the Disposal Feasibility for Spent Fuel, Vitrified HLW and Long-lived ILW. Nagra Technical Report 02-05. Wetingen, Switzerland.

NIREX. 2003. Generic Repository Studies: Generic Post-closure Performance Assessment. Nirex Report N/080. Harwell, United Kingdom.

ONDRAF/NIRAS. 2001. SAFIR 2: Safety Assessment and Feasibility Interim Report 2. ONDRAF/NIRAS Report NIROND 2001-06E. Brussels, Belgium.

Perry, C., C. Rosieanu, J.-C. Mareschal and C. Jaupart. 2010. Thermal Regime of the Lithosphere in the Canadian Shield, *Canadian Journal of Earth Sciences* 47, 389-408.

POSIVA. 2010. Interim Summary Report of the Safety Case 2009. Posiva Report 2010-02. Olkiluoto, Finland.

Shoesmith, D. 2008. The Role of Dissolved Hydrogen on the Corrosion/Dissolution of Spent Nuclear Fuel. Nuclear Waste Management Organization Report NWMO TR-2008-19. Toronto, Canada.

SKB. 2011. Long-term Safety for the Final Repository for Spent Nuclear Fuel at Forsmark, Main Report of the SR-Site Project. Swedish Nuclear Fuel and Waste Management Report SKB TR-11-01. Stockholm, Sweden.

Spiessl, S.M., K.U. Mayer and K.T.B. MacQuarrie. 2009. Reactive Transport Modelling in Fractured Rock – Redox Stability Study. Nuclear Waste Management Organization Report NWMO TR-2009-04. Toronto, Canada.

Zhang, M. and S.K. Frape. 2002. Permafrost: Evolution of Shield Groundwater Compositions during Freezing. Ontario Power Generation Report 06819-REP-01200-10098-R00. Toronto, Canada.

7. POSTCLOSURE SAFETY ASSESSMENT

This chapter presents an illustrative postclosure safety assessment for a used fuel repository located in the crystalline rock of the Canadian Shield. This assessment supports the pre-project review as identified in Chapter 1.

The purpose of a postclosure safety assessment is to determine the potential effects of the repository on the health and safety of persons and the environment during the postclosure period. The assessment timeframe extends from closure until the time at which the maximum impact is predicted, with a one million year baseline adopted based on the time period needed for the radioactivity of the used fuel to decay to essentially the same level as that in an equivalent amount of natural uranium.

The postclosure safety assessment is conducted by applying computer models to a range of analysis cases. The analysis cases examine the Normal Evolution Scenario and some of the Disruptive Event Scenarios identified in Chapter 6, together with a series of sensitivity studies performed to examine the importance of various model features and assumptions.

The assessment is arranged as follows:

- Section 7.1 – Interim Acceptance Criteria: four sets of interim acceptance criteria are presented against which the radiological and non-radiological impacts on persons and the environment are assessed.
- Section 7.2 – Scope: provides a detailed description of the analysis cases together with the rationale for their selection. Included is a brief discussion of items excluded from the scope but which might otherwise be included in a licence submission.
- Section 7.3 – Conceptual Model: discusses the conceptualization of the repository evolution.
- Section 7.4 – Computer Code: introduces the main computer codes used.
- Section 7.5 – Analysis Methods and Key Assumptions: the computer code representations created for this study are described in detail. Some numerical data are presented to provide context.
- Section 7.6 – Results of Radionuclide and Chemical Toxicity Screening Analysis: discusses potentially significant radionuclides and chemical elements included in the study.
- Section 7.7 – Results of Detailed 3D Groundwater Flow and Transport Analysis: discusses 3D simulations of groundwater flow and radionuclide transport for I-129, Ca-41, Cl-36, Sn-126, Cs-134, U-234 and U-238.
- Section 7.8 – Results of System Model: discusses deterministic and probabilistic (i.e., Monte Carlo) simulations of radionuclide release, transport and impact for all radionuclides of potential interest identified in Section 7.6.
- Section 7.9 – Disruptive Event Scenarios: describes the analysis and presents results for those Disruptive Event Scenarios included in the scope of this study.
- Section 7.10 – The Effects of Glaciation on the Normal Evolution Scenario: uses analysis performed for a similar crystalline rock geosphere to draw conclusions on the likely effects of glaciation on the dose consequences for the Normal Evolution Scenario.
- Section 7.11 – Other Considerations: describes results for two complementary indicators for radiological safety, results for the radiological protection of the environment, and results for the protection of persons and the environment from hazardous substances (including results

for one complementary indicator). The anticipated effects of gas generation and migration are also addressed.

- Section 7.12 – Summary and Conclusions.

7.1 Interim Acceptance Criteria

This section presents interim acceptance criteria applicable to the postclosure safety assessment. These criteria are used to judge the acceptability of analysis results.

CNSC Guide G-320 (CNSC 2006) identifies the following categories of acceptance criteria:

1. Radiological protection of persons;
2. Protection of persons from hazardous substances;
3. Radiological protection of the environment; and
4. Protection of the environment from hazardous substances.

Interim acceptance criteria defined for each category are discussed in the following sections. These criteria are consistent with current Canadian and international practice; however, it is recognized that the criteria used in a licence application will need to be accepted by the CNSC at that time, and may be different from the specific values identified here.

7.1.1 Interim Acceptance Criteria for the Radiological Protection of Persons

The main objective of the postclosure safety assessment is to provide reasonable assurance that the regulatory radiological dose limit for public exposure (1 mSv/a) will not be exceeded. To account for the possibility of exposure to multiple sources, a dose constraint below the regulatory limit is adopted.

For the Normal Evolution Scenario, the interim dose acceptance criterion is:

- An annual individual effective dose rate of 0.3 mSv/a with the calculation performed to encompass the time of maximum predicted impact to the average adult member of the critical group.

The 0.3 mSv/a dose constraint is consistent with ICRP and International Atomic Energy Agency (IAEA) guidance (ICRP 2007, IAEA 2006) and is significantly less the average Canadian individual dose rate of 1.8 mSv/a received from background radiation (Grasty and LaMarre 2004).

Calculating the exposure of the average adult member of the critical group is consistent with ICRP recommendations which recognize that since contamination of the biosphere is chronic in nature, the annual dose averaged over the lifetime of the individuals in the critical group is a reasonable measure of the radiological impact. This is adequately represented by the annual dose to an adult (ICRP 2006).

For Disruptive Event Scenarios, the interim acceptance criteria are:

- An annual individual effective dose rate target of 1 mSv/a for credible chronic release scenarios¹ with the calculation performed for the average adult member of the critical group; and
- Acceptability of any scenario with the calculated annual individual effective dose rate for chronic releases exceeding 1 mSv/a to be examined on a case-by-case basis taking into account the likelihood and nature of the exposure, uncertainty in the assessment and conservatism in the dose criterion. Where the probability of exposure can be quantified without excessive uncertainty, a measure of risk will be calculated based on the probability of exposure and the consequent health effects. This is compared with a reference risk value of $10^{-5}/a$.

A dose rate of 1 mSv/a corresponds to the current radiological limit for exposure of the public. It is less than the average natural background dose rate for Canadians (i.e., 1.8 mSv/a).

The reference health risk value of $10^{-5}/a$ is consistent with IAEA (2006). Based on the ICRP value of 0.057 fatal cancers or heritable effects per Sv (ICRP, 2007), and assuming a likelihood of $< 10^{-2}/a$ for disruptive events since they are intended to be unlikely events, then a calculated disruptive event dose rate of 1 mSv/a corresponds to a serious health risk of $< 6 \times 10^{-7}/a$.

Regulatory document G-320 (CNSC 2006) recognizes that inadvertent human intrusion into a repository could result in doses greater than 1 mSv/a since human intrusion by definition bypasses the barriers. The risk from human intrusion is made low by the site selection criteria which require the facility to be located deep underground in an area known not to have economically exploitable natural resources or potable groundwater resources at repository depth. Institutional controls will also reduce risk in the short-term.

7.1.2 Interim Acceptance Criteria for the Protection of Persons from Hazardous Substances

For this category, the interim acceptance criteria are based on Canadian guideline values for concentrations in environmental media relevant to human health and environmental protection, supplemented as needed.

The values are shown in Table 7-1. The criteria are based on federal and provincial guideline concentrations for surface water, groundwater, soil and sediment, and in particular Canadian Council of the Environment (CCME 2007). In cases where federal guidelines do not currently exist, Ontario Ministry of the Environment guidelines (MoE 2011, MoEE 1994) have been adopted as interim acceptance criteria. Depending on the actual site location, the applicable provincial guidelines would be used.

Estimated environmental concentrations of contaminants are compared with the above interim acceptance criteria. Additive effects are not considered in this stage. If any concentrations exceed the criteria in the Normal Evolution Scenario, these contaminants are assessed further in a tiered approach with decreased conservatism in the models. If any concentrations exceed

¹ Chronic refers to a release that is sustained over many years.

these criteria for Disruptive Event Scenarios, acceptability is judged on a case-by-case basis taking into account the likelihood and nature of the exposure, uncertainty in the assessment and conservatism in the criteria.

Table 7-1: Interim Acceptance Criteria for the Protection of Persons and the Environment from Non-Radiological Impacts

Chemical Hazard Criteria				
Element	Groundwater [ug/L]	Surface Water* [ug/L]	Soil [ug/g]	Sediment [ug/g]
Ag	0.3	0.1	0.5	0.5
As	13	5	11	5.9
Cd	0.5	0.017	1	0.6
Ce	-	22	53	19000
Co	3.8	0.9	19	50
Cr	11	1	0.4	26
Cu	5	1	62	16
Eu	-	10.1	50	4700
Hg	0.1	0.004	0.16	0.17
I	-	100	4	-
La	-	10.1	50	4700
Nd	-	1.8	50	7500
P	-	4	-	-
Pb	1.9	1	45	31
Pr	-	9.1	50	5800
Te	-	20	250	-
U	8.9	5	1.9	-
Y	-	6.4	50	1400

Notes: '-' indicates that there are no defined criteria for that element in the given medium.

* Surface water values differ from groundwater values because the surface water values protect biota and humans, whereas groundwater values protect humans only (i.e., biota (other than microbes) do not live in groundwater).

7.1.3 Interim Acceptance Criteria for the Radiological Protection of the Environment

For radiological protection of the environment, the interim acceptance criteria are based on dose benchmarks developed for the assessment of priority substances in relation to discharges of radionuclides from nuclear facilities (EC/HC 2003).

No-Effect Concentrations are derived from Estimated No Effect Values (ENEVs) for the most limiting indicator species relevant to the Southern Canadian Deciduous Forest ecosystem, the Boreal Forest ecosystem and the Inland Tundra ecosystem. For every indicator species, the radionuclide concentration that corresponds to the ENEV is calculated for each medium (i.e., surface water, soil, and sediment) assuming zero radionuclide concentration in other media. The lowest concentration from all indicator species is then selected as the No-Effect Concentration for that radionuclide. The interim acceptance criteria are shown in Table 7-2.

If any radionuclide concentration exceeds the No-Effect Concentration in the Normal Evolution Scenario, an Ecological Risk Assessment will be carried out for that radionuclide, taking into account uncertainties and potential need for the effect of several radionuclides to be summed into account. If any concentration exceeds the No-Effect Concentration in Disruptive Event Scenarios, then acceptability will be judged on a case-by-case basis taking into account the likelihood and nature of the exposure, uncertainty in the assessment and conservatism in the dose criterion.

The ENEVs are based on the dose benchmarks from EC/HC (2003) or lower; and the transfer factors are based on literature review. The analysis is summarized in Garisto et al. (2008). It is recognized that there has been a substantive effort over the past few years to obtain new data in this area, and that the parameter values will need to be reconsidered as new information becomes available. Criteria will also need to be provided for other radionuclides of potential interest; however, the basic concept of comparing media concentrations with benchmark values remains a plausible approach for non-human biota. Note that the NWMO has an ongoing work program in which different methods, including the ERICA method (Brown et al. 2008), are being investigated for defining these criteria. When this work matures, the acceptance criteria will be updated.

Table 7-2: Interim Acceptance Criteria for the Radiological Protection of the Environment

Radionuclide	Media		
	Water (Bq/L)	Soil (Bq/kg)	Sediment (Bq/kg)
C-14	2.7×10^{-2}	2.4×10^2	2.8×10^5
Cl-36	2.8×10^0	3.8×10^{-1}	4.1×10^4
I-129	3.2×10^0	2.4×10^3	1.2×10^6
Cs-135	2.1×10^{-3}	8.5×10^0	3.5×10^5
Ra-226	5.9×10^{-4}	2.5×10^2	9.3×10^2
Np-237	5.8×10^{-2}	5.0×10^1	1.1×10^3
U-238	2.3×10^{-2}	4.2×10^1	1.1×10^4
Pb-210	4.3×10^0	3.7×10^3	6.3×10^3
Po-210	7.0×10^{-3}	3.0×10^1	5.6×10^3

7.1.4 Interim Acceptance Criteria for the Protection of the Environment from Hazardous Substances

For this category the criteria defined in Section 7.1.2 also apply because the values selected are the lowest values relevant to either human health or the environment.

7.2 Scope

This section presents the scope of the postclosure safety assessment.

The scope is developed for consistency with the objectives of the pre-project review. As such, analysis cases are limited to those needed to provide a demonstration of the overall approach and the main analysis needed to reach possible conclusions for the hypothetical site. Items excluded from the scope but which might be included in a licence submission as part of a more comprehensive assessment are discussed in Section 7.2.4.

The scope is defined taking into account the discussion of the Normal Evolution Scenario and the Disruptive Event Scenarios in Chapter 6 together with experience gained from previous postclosure studies performed for other hypothetical sites and conceptual designs.

Results for all scenarios and their associated sensitivity cases are measured against the interim acceptance criteria for the radiological protection of persons provided in Section 7.1.1.

Results for the Reference Case (see below) of the Normal Evolution Scenario and selected sensitivity cases are also measured against the criteria for the protection of persons from hazardous substances provided in Section 7.1.2, the criteria for the radiological protection of the environment provided in Section 7.1.3, and the criteria for the protection of the environment from hazardous substances provided in Section 7.1.4. Comparisons are also done for the Disruptive Event Scenario with the most significant consequences.

7.2.1 Analysis Cases for the Normal Evolution Scenario

The Normal Evolution Scenario is based on a reasonable extrapolation of the site and repository. It accounts for anticipated significant events, in particular glaciation.

Chapter 5 presents information describing why the used fuel containers are expected to remain intact over the time scale of interest. No releases are anticipated for very long times, during which radioactivity in the used fuel decays to levels similar to that of a natural uranium ore body.

However, with the large number of containers, it is possible that some containers could be placed with undetected defects. In particular, a simple estimate of the likelihood of undetected defects arising in the copper shell welding and inspection process (i.e., 1/5000, Maak et al. 2001), indicates that statistically there could be three containers with defects placed in the repository. While these statistics have been conservatively estimated, for the Normal Evolution Scenario it is assumed that three containers with undetected defects are present.

Recognizing that the geosphere characteristics at a candidate site and the design of the repository may be different from the assumed reference conditions, a number of sensitivity

cases are also examined to illustrate the function of the various engineered and natural barriers. Both deterministic and probabilistic simulations are performed.

In the deterministic simulations, parameters are varied about a Reference Case of the Normal Evolution Scenario, where the Reference Case has the following attributes:

- Geosphere properties as per Chapter 2;
- Used fuel inventories as per Chapter 3;
- Repository design as per Chapter 4;
- Three containers each with an undetected defect placed in the repository at the position with the shortest groundwater transport time to the surface;
- Defect radius = 1 mm, no evolution of the defect size with time;
- No other container failures occur;
- Groundwater fills the defective containers 100 years after the containers are placed in the repository;
- Constant temperate climate and steady-state groundwater flow;
- Self-sufficient farming family growing crops and raising livestock on the surface above the repository;
- Drinking and irrigation water for the family obtained from a 100 m deep well located along the main pathway for contaminants released from the defective containers;
- The well is pumping at a rate of 911 m³/a. This is sufficient for drinking water and irrigation of household crops; and
- Input parameters that are represented by probability distributions are set to either the most probable value (when there is one) or to the median value otherwise.

The sensitivity cases are shown in Table 7-3 and listed below. The table includes a description of the variation from the Reference Case assumptions together with a brief rationale for each case selection.

The sensitivity cases are:

- Fuel dissolution rate increased by a factor of 10;
- Instant release fractions set to 0.10 for all radionuclides;
- Container defect area increased by a factor of 10;
- No solubility limits in the container;
- No sorption in the near field;
- Fracture distance with respect to the defective containers increased and decreased;
- Geosphere hydraulic conductivity changed (increased and decreased) from the Reference Case value;
- No sorption in the geosphere;
- Hydraulic conductivity of the excavation damage zone and Thermal Damage Zone (TDZ) increased by a factor of 10; and
- Low sorption in the geosphere with coincident high solubility limits in the container.

For the probabilistic simulations, random sampling is used to simultaneously vary all input parameters for which probability distribution functions are available. In particular, the radionuclide release and transport parameters were varied within the fixed reference geosphere. This case is also described in Table 7-3.

An assessment based on the results of an existing study performed for a similar crystalline rock geosphere is used to discuss the anticipated effects of glaciation.

Results are developed for two complementary radiological indicators.

Results are developed for the non-radiological chemical hazard and a related complementary indicator.

Finally, the consequences of gas generation caused by decomposition of organics and by corrosion of steel in the defective containers and rock bolts are determined.

Table 7-3: Sensitivity Cases for the Normal Evolution Scenario

Uncertainty	Reference Case Assumption*	Sensitivity Case Assumption	Rationale
Fuel			
Dissolution Rate	Generated via a model that takes into account the effects of radiolysis and chemical dissolution. No credit for H ₂ gas effects on suppressing dissolution. With this model, ~22% of the fuel dissolves in the one million year timeframe of interest.	The dissolution rate is increased by a factor of 10. With this increase, all of the fuel dissolves in the one million year timeframe of interest.	The fuel is an important barrier to the release of radionuclides because most radionuclides are contained within the fuel matrix. As the fuel dissolves in the long term these radionuclides become available for transport. The factor of 10 increase roughly corresponds to the 95 th percentile value accounting for uncertainties.
Instant Release Fractions	Most radionuclides have no instant release. Instant release fractions for selected radionuclides are: C = 0.027 Ca = 0.00 Cl = 0.06 Cs = 0.04 I = 0.04 Np, Pu, Sn, Th, U = 0.00	Instant release fractions for all radionuclides are set to 0.10.	Some radionuclides in the used fuel are present initially in the fuel sheath gap and grain boundaries and are therefore available for release early after contact with water. This fraction of the inventory is referred to as the instant release fraction. Assigning an instant release fraction to all radionuclides (including actinides) ensures the results are bounding.
Container			
Defect Area	Defect Radius = 1.0 mm Defect Area = 3.14 mm ²	The defect area is increased by a factor of 10.	The container is an important barrier to the release of radionuclides. The size of the defect can influence the rate at which radionuclides escape the container and enter the buffer. Defects of greater size (~ 30 mm ²) are unlikely to be missed during inspection.

Uncertainty	Reference Case Assumption*	Sensitivity Case Assumption	Rationale
Solubility Limits	<p>Solubility limits are determined externally from thermodynamic data and specified as input.</p> <p>Solubility limits (mol/m³) for selected radionuclides are:</p> <p>C = 0.83 Np = 1.1x10⁻⁶ Pu = 9.1x10⁻⁵ Sn = 9.6x10⁻⁴ Th = 2.5x10⁻⁵ U = 3.5x10⁻⁶ Ca, Cl, Cs, I = no limit</p> <p>The solubility limits are increased in the Reference Case by a factor of ten above the values listed here to account for uncertainties in groundwater chemistry and thermodynamic data.</p>	Solubility limits for all radionuclides are set to 2000 mol/m ³ . This is equivalent to having no solubility limit.	<p>The concentration of dissolved radionuclides is one of the parameters that affect the rate of radionuclide release from the defective container. While some radionuclides are highly soluble (e.g., I and Cl), others (e.g., Pu and U) are not.</p> <p>Removal of all solubility limits provides information on the importance of this parameter to the overall dose consequence.</p>
Buffer, Backfill and Seals (i.e., the Near Field)			
Sorption in the Buffer, Backfill and Seals	<p>Use of linear equilibrium sorption model. Sorption coefficients from SKB SKB reviews have been adopted where based on similar materials and conditions.</p> <p>Some elements are non-sorbing (e.g., Cl and I) while others are highly sorbing in the reducing environment (e.g., Np, Pu, Th, and U).</p>	Sorption coefficients for all near field barrier components are set to zero. Sorption coefficients in the geosphere barrier are maintained at their Reference Case values.	<p>The clay-based seals have a high surface area and can effectively sorb radionuclides released into the groundwater from the containers, thereby retarding their transfer to the geosphere.</p> <p>Colloid transport within the dense clay seals is not expected, so it is not included in the Reference Case values. Sorption on iron oxides from the container is conservatively neglected.</p> <p>Disregarding sorption provides information on the importance of this process to the overall dose consequence.</p>

Uncertainty	Reference Case Assumption*	Sensitivity Case Assumption	Rationale
Geosphere			
Fracture Location	<p>A large water conducting fracture intersects the repository footprint. A minimum offset distance of 25 m is assumed, with the distance measured from the fracture to the nearest part of the repository.</p> <p>Because of the repository layout, the nearest container is 33 m away on one side of the fracture and 94 m away on the other.</p>	<p>Offset distances of 10 m, 50 m and 75 m are considered.</p> <p>These distances are measured from the fracture to the part of the repository containing the three defective containers.</p>	<p>The minimum thickness of rock between the repository boundary and a major water conducting feature is a key barrier.</p> <p>While a minimum distance of 50 m is currently considered as a target design criterion for repository construction, the Reference Case adopts a value of 25 m so as to provide a more conservative (i.e., larger) estimate of consequences.</p>
Geosphere Conductivity	<p>Reference Case hydraulic conductivity profile as defined in Chapter 2:</p> <p>Zone 1 (10 – 150 m) = 2×10^{-9} m/s</p> <p>Zone 2 (150 – 700 m) = 4×10^{-11} m/s</p> <p>Zone 3 (700 – 1500 m) = 1×10^{-11} m/s</p>	<p><i>Sensitivity 1:</i></p> <p>A factor of 10 increase relative to the Reference Case as per Sensitivity Case 1 in Chapter 2.</p> <p>Zone 1 (10 – 150 m) = 2×10^{-8} m/s</p> <p>Zone 2 (150 – 700 m) = 4×10^{-10} m/s</p> <p>Zone 3 (700 – 1500 m) = 1×10^{-10} m/s</p> <p><i>Sensitivity 2:</i></p> <p>A factor of 10 decrease in hydraulic conductivity as per Sensitivity Case 2 in Chapter 2.</p> <p>Zone 1 (10 – 150 m) = 2×10^{-10} m/s</p> <p>Zone 2 (150 – 700 m) = 4×10^{-12} m/s</p> <p>Zone 3 (700 – 1500 m) = 1×10^{-12} m/s</p>	<p>Geosphere hydraulic conductivity is an important parameter controlling groundwater flow and radionuclide transport in the crystalline rock mass.</p> <p>The sensitivity cases cover a range of conductivities. The three cases represent an increase of 10 times, a decrease of 10 times and a decrease of 100 times the conductivity in the Reference Case.</p> <p>The higher conductivity case corresponds to rock mass conditions under which advective transport could be important, and therefore tests potential limits for acceptability.</p>

Uncertainty	Reference Case Assumption*	Sensitivity Case Assumption	Rationale
		<p><i>Sensitivity 3:</i> A factor of 100 decrease in hydraulic conductivity as per Sensitivity Case 3 in Chapter 2.</p> <p>Zone 1 (10 – 150 m) = 2×10^{-11} m/s Zone 2 (150 – 700 m) = 4×10^{-13} m/s Zone 3 (700 – 1500 m) = 1×10^{-13} m/s</p>	
Sorption in the Geosphere	<p>Use of linear equilibrium sorption model. Granite sorption coefficients from the SKB review.</p> <p>Some elements are non-sorbing (e.g., Cl and I) while others are highly sorbing in the assumed reducing environment (e.g., Np, Pu, Th, and U).</p>	<p>The geosphere sorption coefficients for all elements are set to zero.</p> <p>All other near field sorption coefficients (i.e., buffer, backfill and seals) are maintained at their Reference Case values.</p>	<p>Radionuclides can be sorbed onto the surfaces of the host rock minerals, thereby retarding their transport to the surface.</p> <p>Setting the sorption coefficients to zero provides information on the relative importance of sorption in the geosphere. It also tests the importance of colloidal transport, if that were to capture radionuclides and make them unavailable for sorption.</p>
Hydraulic Conductivity of EDZ and TDZ	<p>The excavation damage zone and thermal damage zone regions are defined with higher hydraulic conductivity than the surrounding rock.</p> <p>Hydraulic Conductivity (K/K_{rock}) for selected areas are:</p> <p>TDZ (floor and borehole) = 10,000 Inner EDZ (room, drifts and shaft) = 100 Outer EDZ (room, drifts and shaft) = 10 Room Seal and Bulkhead EDZ = 100</p>	<p>All damage zone values increased by a factor of 10.</p>	<p>The thermal damage zone is a region of rock damaged by thermal stress caused by heating of the rock due to heat generation in the used fuel. The excavation damage zone is a region of rock damaged during the construction process.</p> <p>Both regions have higher hydraulic conductivity than the surrounding intact rock and could be a pathway for radionuclide transport.</p> <p>Increasing the hydraulic conductivity provides information on the importance of these damage zones to the transport and subsequent release of radionuclides to the surface.</p>

Uncertainty	Reference Case Assumption*	Sensitivity Case Assumption	Rationale
Low Sorption Geosphere with Coincident High Solubility Limits	Geosphere sorption is as described above in the "Sorption in the Geosphere" sensitivity case. Solubility limits are as described above in the Fuel "Solubility Limits" sensitivity case.	"Low" / "High" means the values are set to three sigma values in the conservative direction.	This case determines the effect of simultaneous pessimistic assumptions affecting the solubility and geosphere barrier.
Combined			
Simultaneous Variation of all Probabilistically Defined Parameters	Input parameters represented by probability distributions are set to either the most probable value (when there is one) or to the median value otherwise.	Monte Carlo analysis in which all input parameters represented by probability distributions are simultaneously varied. An important caveat is that these probabilistic simulations do not consider the effects of different groundwater flow fields or uncertainties in the fracture locations. Rather, these consider the effect of variation in radionuclide source term and transport parameters, within a defined geosphere.	Many of the modelling parameters are uncertain or have a natural degree of variability and as such are more generally characterized by a range or distribution of values. Varying all such parameters simultaneously provides information on the overall range or uncertainty in the results.

Note: * A detailed description of the input data is available in Garisto et al. (2012).

7.2.2 Analysis Cases for Disruptive Event Scenarios

Disruptive Event Scenarios postulate the occurrence of unlikely events leading to possible penetration of barriers and abnormal loss of containment.

Chapter 6 describes the set of Disruptive Event Scenarios applicable to the conceptual design and hypothetical geosphere in this pre-project review. These have been identified through consideration of the features, events and processes that are important to this repository system, and through consideration of the key barriers. The scenarios are:

- Inadvertent Human Intrusion;
- All Containers Fail. A base case with failure at 60,000 years is considered together with a sensitivity case with failure occurring at 10,000 years;
- Fracture Seal Failure and its variant case in which both the fracture seals and the repository tunnel and room seals degrade rapidly and extensively; and
- Shaft Seal Failure;
- Poorly Sealed Borehole;
- Undetected Fault; and
- Container Failure¹.

The first four scenarios are within the scope of this illustrative safety assessment. Table 7-4 summarizes each scenario and includes a description of the parameters changed from the Reference Case and the rationale for the scenario selection. It is recognized that for an actual site, the full set of scenarios would need to be evaluated.

The consequences of gas generation caused by decomposition of organics and by corrosion of steel in the defective containers and rock bolts are determined for the All Containers Fail scenario because in this event there is significant exposure of steel.

In addition, the effect of geosphere hydraulic conductivity is further examined by simulating the All Containers Fail at 10,000 Years scenario for the same three geosphere hydraulic conductivities considered in the Normal Evolution Scenario sensitivity studies.

¹ This considers delayed but substantive failure of a few containers due to unexpected in-situ conditions, and is different from the Normal Evolution Scenario which considers a small defect initially present in some containers.

Although a detailed analysis of the Container Failure Scenario is outside the scope of this pre-project review, the peak dose arising from this event is anticipated to be significantly less than that associated with the All Containers Fail Scenario due to the much smaller number of affected containers.

With respect to the Undetected Fault Scenario, it is anticipated that any large fractures intercepting the repository not identified during site characterization could be discovered during construction such that appropriate mitigating measures could be taken. These measures could include grouting, rejection of boreholes and possible rerouting of the repository layout to avoid large transmissive features. Small fractures may remain undetected; however, these are likely to affect only local containers.

All scenarios are analysed with deterministic methods only.

7.2.3 Analyses for Miscellaneous Modelling Parameters

Some additional cases were simulated in the course of the analysis to check various FRAC3DVS-OPG modelling parameters. These cases are discussed in Table 7-5 and listed below:

- Discrete Fracture Network (DFN) modelling compared with the Equivalent Porous Media (EPM) approach; and
- Increased spatial resolution and increased number of time steps to confirm model convergence.

As will be discussed in later sections, none of the modelling choices had any material effect on the results.

Table 7-4: Analysis Cases for Disruptive Event Scenarios

Disruptive Event	Reference Case Assumption*	Disruptive Case Assumption	Rationale
Inadvertent Human Intrusion	Not Applicable	The engineered and natural barriers are bypassed via the drilling of a borehole into the repository. The borehole intersects a used fuel container and used fuel material is brought to the surface. The variant case, in which the borehole thereafter remains open, is not considered.	Institutional controls and knowledge of the repository can be lost in the future. This scenario examines the potential consequences to the drill crew and a future resident on the site for a stylized intrusion event.
All Containers Fail	Three containers each with an undetected defect (radius = 1 mm) are placed in the repository at the location with the shortest groundwater transport time to the surface. Groundwater fills the defective containers 100 years after the containers are placed in the repository.	<i>Simulation 1</i> All containers fail 60,000 years after repository closure and no containers fail prior to this time. The radionuclide release model takes no credit for the presence of the container. As such, the release of radionuclides from the slowly dissolving fuel to the near field is limited only by the buffer properties. <i>Simulation 2</i> Identical to the above, except the time of container failure is 10,000 years.	The containers are anticipated to last for a period in excess of one million years, based on the copper container, sturdy mechanical design and favourable site attributes, including geochemical stability. This scenario considers common cause failure of all containers. The base case considers failure at 60,000 years. This corresponds to the likely timeframe for an ice sheet to cover the site, and it is possible that some unanticipated effect of the ice sheet might cause failure, such as beyond-design mechanical loading or unexpected changes in groundwater chemistry. An extreme case with failure at 10,000 years provides information on the sensitivity of results to the assumed failure time.
Fracture Seal Failure	Tunnel seals, consisting of highly compacted bentonite keyed into the EDZ and supported by a length of high performance concrete, are placed on each side of the fracture. The hydraulic conductivities of the compacted bentonite and intact host	<i>Simulation 1</i> The hydraulic conductivity of the highly compacted bentonite in the keyed-in areas of the fracture seal is set to that of the inner EDZ (i.e., 100 times that of the rock) from the time of repository closure.	This scenario examines the sensitivity of results to assumed degradation in seal performance. For conservatism, this degradation is assumed to occur at the time of repository closure.

Disruptive Event	Reference Case Assumption*	Disruptive Case Assumption	Rationale
	<p>rock are 1.3×10^{-13} m/s and 4×10^{-11} m/s respectively.</p> <p>Tunnel seals are also placed at multiple locations along the perimeter drift, the access drifts and panel cross cuts.</p> <p>A similar seal is placed at the entrance to each placement room.</p>	<p><i>Simulation 2</i></p> <p>The hydraulic conductivity of the highly compacted bentonite in the keyed-in areas of all tunnel, room and fracture seals is set to that of the inner EDZ (i.e., 100 times that of the rock) from the time of repository closure.</p>	
Shaft Seal Failure	<p>The shaft is filled with a combination of bentonite / sand (70:30), concrete and asphalt with the following hydraulic conductivities (m/s):</p> <p>Bentonite / Sand = 4.8×10^{-13}</p> <p>Concrete = 1.0×10^{-10}</p> <p>Asphalt = 1.0×10^{-12}</p>	<p>The hydraulic conductivity of all shaft seal materials is set to 4.8×10^{-8} m/s from the time of repository closure.</p> <p>An important caveat is that the locations of the defective containers and the well are the same as in the Reference Case. In future studies these locations may need to be moved to ensure the most conservative consequence is obtained.</p>	<p>This scenario examines the effects of significant degradation in shaft seal. For conservatism, this degradation is assumed to occur at the time of repository closure.</p> <p>An increase in hydraulic conductivity by a factor of 1000 is representative of a severely degraded shaft. Since it was determined that such an increase has no effect, a further increase by another factor of 100 was implemented.</p>
Geosphere			
All Containers Fail at 10,000 Years for Different Geosphere Hydraulic Conductivity	<p>Results are compared against the All Containers Fail at 10,000 Years simulation performed using the Reference Case geosphere. The Reference Case hydraulic conductivity profile as defined in Chapter 2 is:</p> <p>Zone 1 (10 – 150 m) = 2×10^{-9} m/s</p> <p>Zone 2 (150 – 700 m) = 4×10^{-11} m/s</p> <p>Zone 3 (700 – 1500 m) = 1×10^{-11} m/s</p>	<p><i>Sensitivity 1:</i></p> <p>A factor of 10 increase in hydraulic conductivity as compared to the Reference Case, as per Sensitivity Case 1 in Chapter 2.</p> <p>Zone 1 (10 – 150 m) = 2×10^{-8} m/s</p> <p>Zone 2 (150 – 700 m) = 4×10^{-10} m/s</p> <p>Zone 3 (700 – 1500 m) = 1×10^{-10} m/s</p>	<p>These cases examine the effect of geosphere hydraulic conductivity on a high dose consequence case.</p>

Disruptive Event	Reference Case Assumption*	Disruptive Case Assumption	Rationale
		<p><i>Sensitivity 2:</i> A factor of 10 decrease in hydraulic conductivity as per Sensitivity Case 2 in Chapter 2.</p> <p>Zone 1 (10 – 150 m) = 2×10^{-10} m/s Zone 2 (150 – 700 m) = 4×10^{-12} m/s Zone 3 (700 – 1500 m) = 1×10^{-12} m/s</p> <p><i>Sensitivity 3:</i> A factor of 100 decrease in hydraulic conductivity as per Sensitivity Case 3 in Chapter 2.</p> <p>Zone 1 (10 – 150 m) = 2×10^{-11} m/s Zone 2 (150 – 700 m) = 4×10^{-13} m/s Zone 3 (700 – 1500 m) = 1×10^{-13} m/s</p>	

Note: * A detailed description of the input data is available in Garisto et al. (2012).

Table 7-5: Modelling Parameter Cases

Modelling Parameter	Description	Modelling Case Assumption	Rationale
Discrete Fracture Network	Equivalent porous media used to represent fractures and surrounding rock mass in all FRAC3DVS-OPG simulations.	Discrete fracture network adopted.	Equivalent porous media calculations are generally more stable, but averages properties especially around fracture zones. The discrete fracture network approach allows direct incorporation of fractures without property scaling. This sensitivity case is intended to show the Reference Case approach (i.e., equivalent porous media) is conservative.
Spatial Resolution and Time Step Size	User determined in the Reference Case.	Spatial resolution in the FRAC3DVS-OPG model is increased by a factor of two. Time step control in the FRAC3DVS-OPG model is adjusted to change the number of time steps, with the changes resulting in a factor of 7 decrease in one simulation and a factor of 3 increase in another.	Increasing the spatial resolution and the number of time steps provides information on whether the model results are numerically converged.

7.2.4 Analysis Exclusions

As noted earlier in Section 7.2, the scope of the postclosure safety assessment is defined for consistency with the objectives of the pre-project review. As such, the analysis cases are limited to those needed to provide a demonstration of the overall approach and to those needed to reach preliminary conclusions for the hypothetical site.

This section lists scope items that do not appear in this report but which might otherwise be included in a postclosure safety assessment for a licence submission. These are:

- **Fracture Uncertainty.** In a crystalline rock site, there will be uncertainties regarding the location and nature of the fractures. For a real site, these uncertainties will need to be assessed, possibly through evaluation of alternative fracture networks and properties;
- **Variable Climate Analysis.** The effects of permafrost and glaciation are not explicitly determined in this assessment. Instead, a glaciation study previously performed for a less permeable crystalline rock geosphere is described and inferences are drawn about the likely impacts of glaciation on the study site;
- **Disruptive Event Scenarios.** A reduced number of Disruptive Event Scenarios is evaluated; however, the full list of scenarios anticipated for a licence submission is identified and the rationale for their selection provided;
- **Alternative Critical Groups.** Other potential critical groups may be considered for a candidate site depending on communities nearby that could be interested in potential impacts - for example, downstream communities and / or First Nation lifestyles.

7.3 Conceptual Model

This section describes the conceptual model associated with key processes occurring in the repository with defective containers present. The presence of defective containers leads to releases of contaminants that eventually enter the biosphere. These biosphere releases have potential impacts on humans and non-human biota living nearby.

The conceptual model describes the release, migration and fate of contaminants through the identification of key features, events and processes. The model is used to guide the development and application of the computer codes used in the postclosure safety assessment.

Figure 7-1 illustrates the general conceptual model. There are four main elements:

- The used fuel containers;
- The engineered barriers;
- The geosphere; and
- The biosphere.

Each of these is discussed below. The discussion is aligned with the Reference Case of the Normal Evolution Scenario which, as noted in Section 7.2.1, assumes a constant temperate climate.

For simplicity, the description of conceptual models are given in terms of radionuclides but the models also can be applied to simulate the behaviour of potentially chemical hazardous elements, except that for chemical elements there is no radioactive decay and in the biosphere there is no food chain and no dose rate calculations. Instead, protection of the environment is ascertained by comparison of calculated chemical element concentrations in various biosphere media to the criteria outlined in Table 7-1.

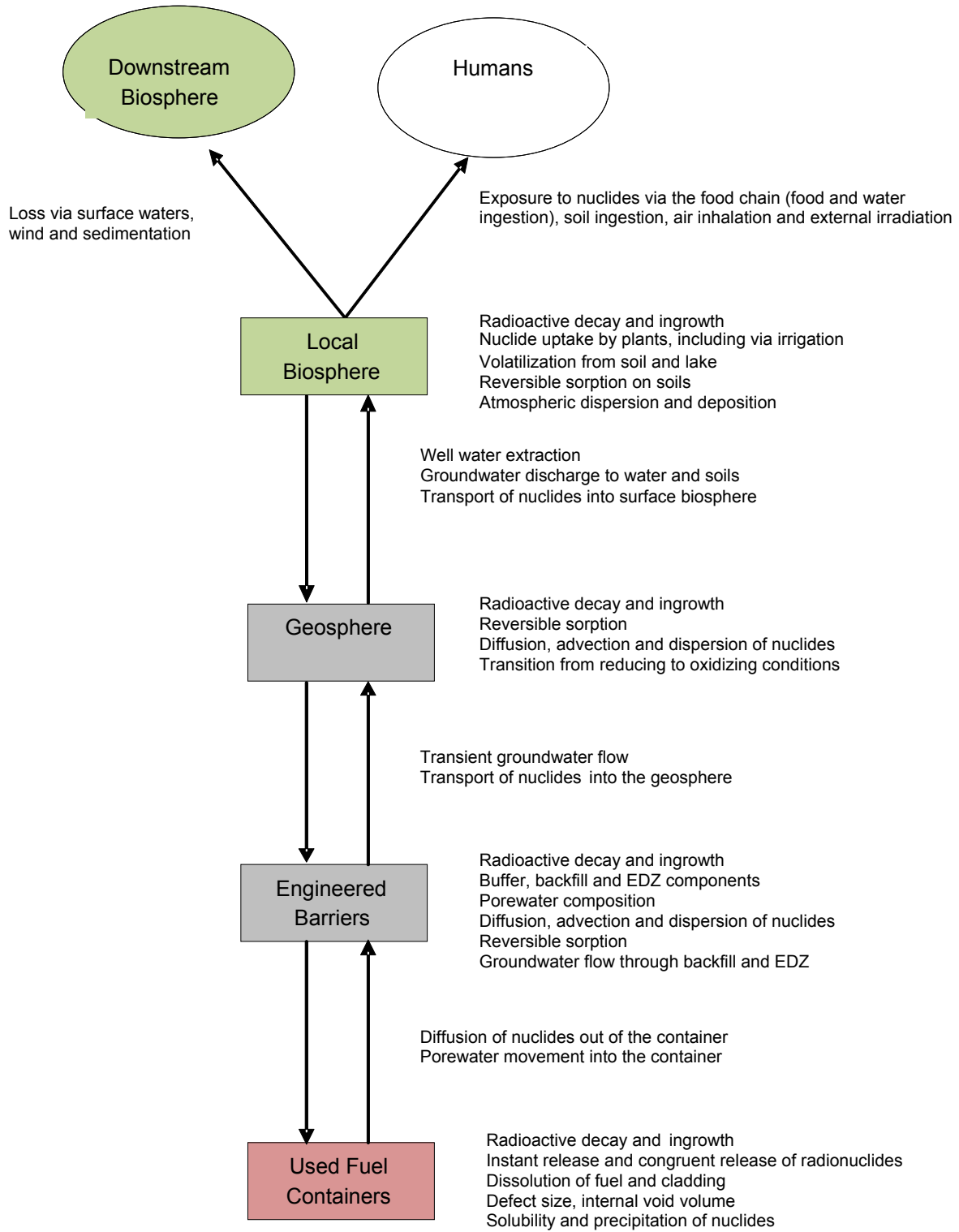


Figure 7-1: General Conceptual Model for Defective Containers

7.3.1 Used Fuel Containers

The principal fuel components and processes for the used fuel containers and waste form are shown in Figure 7-2.

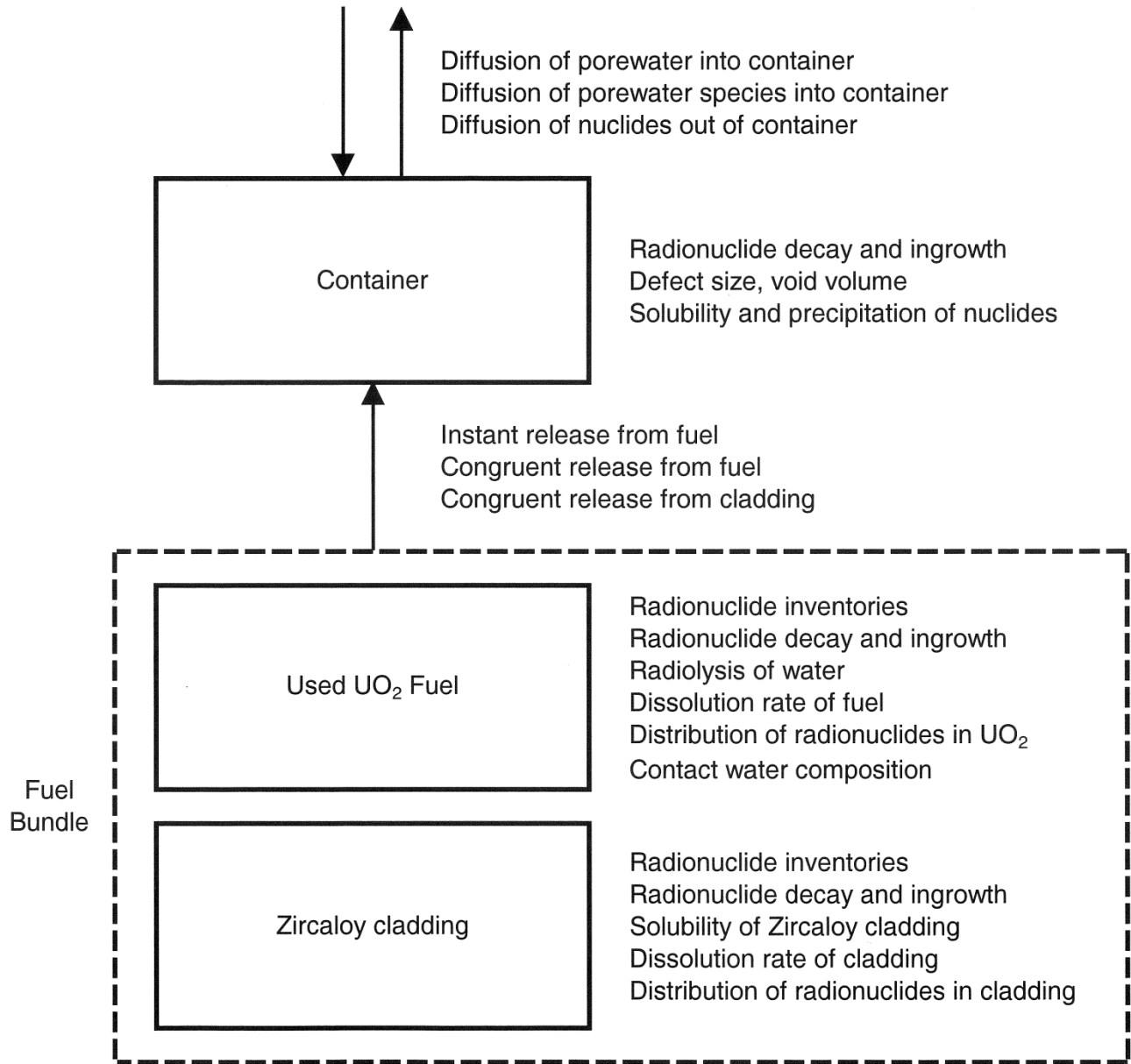


Figure 7-2: Conceptual Model for the Waste Form and Container

The container has a copper outer shell with a steel inner vessel for structural support.

The inner steel vessel is not specifically included in the conceptual model, except that it is assumed present to maintain the void volume inside the container. In practice, the steel components in any breached container would corrode, producing H₂ gas and iron oxides. Although H₂ could substantially reduce the dissolution rate of the UO₂ fuel, this effect is conservatively ignored. Similarly, formation of iron oxides would reduce the void volume of the container and provide a high surface area for adsorption of some of the radionuclides released from the fuel. These effects are also ignored.

The reference waste form is a standard CANDU 37-element fuel bundle with a burnup of 220 MWh/kgU and an average fuel power during operation of 455 kW as discussed in Chapter 3. The repository holds 4.6 million bundles.

After water enters the container, the Zircaloy cladding could prevent water from contacting the fuel for some time. However, the cladding is neglected in the fuel dissolution model and it is assumed that water contacts all the fuel as soon as the container fills with water.

The waste form has two distinct components: the UO₂ fuel and the Zircaloy cladding. Releases of radionuclides from these two waste forms are modelled separately.

Radionuclides within the UO₂ fuel are released by two mechanisms which operate on very different time scales (Grambow et al. 2010).

Instant Release from Fuel

Initially, there will be a comparatively rapid release of a small fraction (typically a few percent) of the inventory of a selected group of radionuclides that are either very soluble (such as C-14, Cl-35, Cs-137 and I-129) or gaseous (such as Xe), and that are residing in the fuel sheath gap or at grain boundaries which are quickly accessed by water (Garisto et al. 2012). This release process is referred to as "instant-release"; and is modelled assuming a certain fraction of the radionuclide inventory in the fuel is released at the time water contacts the fuel.

Ferry et al. (2008) have shown that the instant release fractions do not change with time due to, for example, athermal diffusion of radionuclides induced by alpha-particle recoil displacements.

The instant release fractions used in this assessment are given in Section 7.5.4.1.

Fuel Dissolution

The second and slower release process comprises release of radionuclides from the UO₂ fuel matrix as the matrix itself corrodes or dissolves (called "congruent dissolution").

At the fuel-water interface the alpha dose rate, which exceeds the gamma and beta dose rates for most of the fuel history (Figure 7-3), is the main contributor to radiolysis, producing molecular oxidants such as H₂O₂. Other potential sources of oxidants, such as any O₂ trapped in the porewater, will already have been consumed by corrosion processes (e.g., corrosion of the Cu shell) before the fuel cladding is breached because these corrosion reactions are relatively fast (King and Kolar 2006). In principle, the radiolytically produced oxidants will also be consumed by reaction with container materials rather than by reaction with used fuel; however, for alpha

radiolysis, the oxidants (e.g., H_2O_2) are only produced within 20 μm of the fuel-water interface (Garisto 1989), so they are much closer to the fuel than to the container and thus more likely to react with the fuel.

Radionuclide Releases from Zircaloy

All radionuclides trapped in the Zircaloy cladding, except for C-14, are assumed to be released congruently as the cladding dissolves. The cladding dissolution rate is calculated using a solubility-limited dissolution model, and dissolution continues until the cladding completely dissolves. For C-14, there is evidence that a fraction of the C-14 in the Zircaloy is released as soon as water contacts the cladding (Garisto et al. 2012).

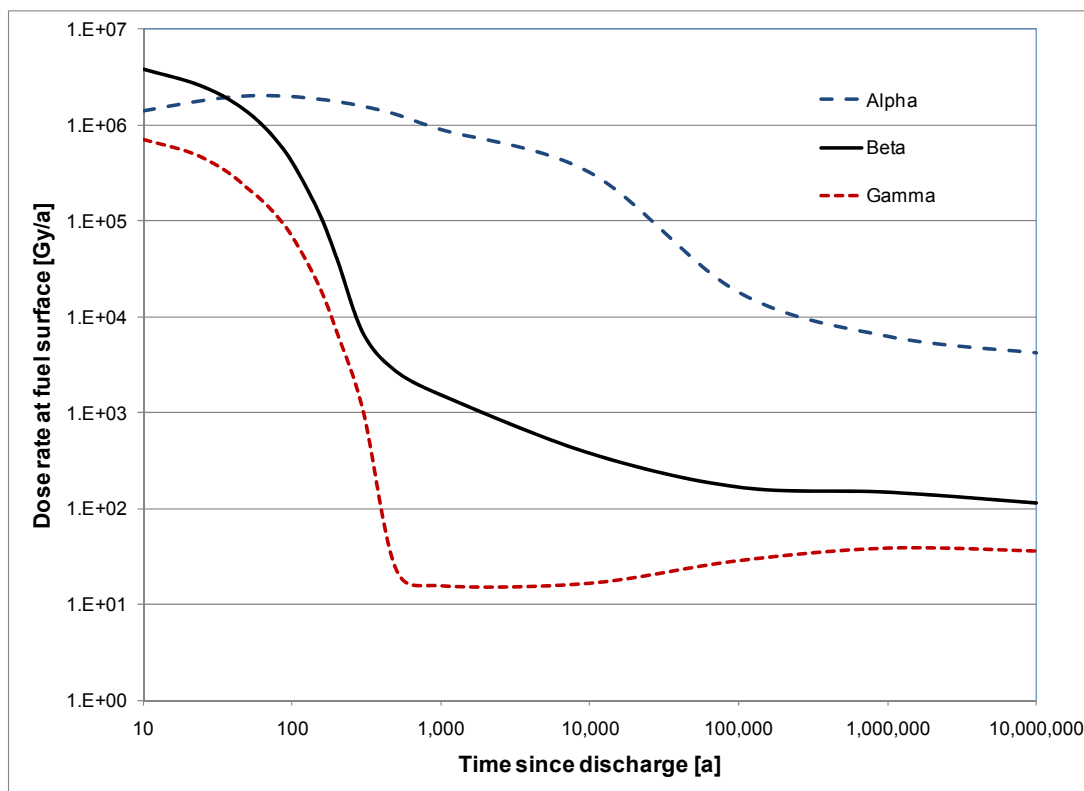


Figure 7-3: Radiation Dose Rate in Water at the Fuel Surface (220 MWh/kgU Burnup)

Oxidative dissolution of the fuel continues as long as the alpha radiation field is sufficiently high. Eventually, after about 10 million years (Garisto et al. 2012, Appendix E), chemical dissolution of the fuel dominates according to the reaction,



This is a very slow process, as illustrated by the presence of uranium ores that are millions or billions of years old.

The UO_2 dissolution rate would be affected by build up of hydrogen gas inside the steel vessel generated by anaerobic corrosion of the steel. Experimental evidence shows that the dissolution rate drops by several orders of magnitude in the presence of even modest pressures of hydrogen gas (Shoesmith 2008). This is likely due to the activation of hydrogen by various mechanisms to produce the strongly reducing H^\cdot radical, which in turn scavenges radiolytic oxidants and suppresses fuel corrosion (Shoesmith 2008 and references therein). While this hydrogen effect will suppress fuel dissolution, it is conservatively ignored in the current assessment.

The fuel dissolution rate in this assessment is given in Section 7.5.4.1.

7.3.2 Engineered Barriers

Chapter 4 provides a detailed description of the conceptual repository and engineered barriers assumed in this study.

The dense 100% bentonite layer that surrounds the container (a) prevents groundwater flow near the container; (b) mechanically supports the container; and (c) prevents microbial activity that could cause corrosion of the copper shell. The buffer has a sufficiently low hydraulic conductivity that transport through it is diffusion dominant (i.e., the advective velocity is negligible). In contrast, advection is possible in the backfill, which has a higher hydraulic conductivity.

The excavation damage zone (or EDZ) extends around the perimeter of the placement rooms and is modelled as a uniform porous medium. An area of higher hydraulic conductivity caused by thermal stress (referred to as the thermal damaged zone or TDZ) may develop around the borehole and along the floor in the space between boreholes.

The design includes seals at the end of each placement room, seals spaced throughout the access drifts and cross cuts, and seals around any transmissive fractures that may intersect the repository footprint. These seals are composed of concrete and clay bulkheads that interrupt the EDZ. These features are modelled as uniform porous media.

Groundwater contacting the fuel must pass through the buffer. Initially, the composition of this contact water is similar to the buffer porewater composition which depends strongly on the minor mineral components of the buffer (e.g., the calcite and gypsum contents (Muurinen and Lehikoinen 1999, Curti and Wersin 2002)). After some time, these minor mineral components are all dissolved and the contact water composition resembles the geosphere porewater composition.

This time evolution in contact water composition is not explicitly taken into account. Rather two contact water compositions are defined. The first composition is geosphere porewater equilibrated with buffer minerals and the second composition is geosphere porewater equilibrated with buffer minerals and the steel insert of the canister. These compositions are used for the calculation of radionuclide solubilities and the highest calculated solubility is used in the safety assessment calculations.

The composition of the groundwater and the diffusion and sorption coefficients for the buffer and backfill material assumed in this assessment are given in Section 7.5.

7.3.3 Geosphere

Chapter 2 provides a description of the hypothetical geosphere assumed in this study.

The principal components of the conceptual model are shown Figure 7-4. The geosphere has a defined fracture network surrounded by a rock mass. The fracture zones are conservatively assigned a uniform high hydraulic conductivity while the rock mass is assigned an effective hydraulic conductivity that decreases with depth.

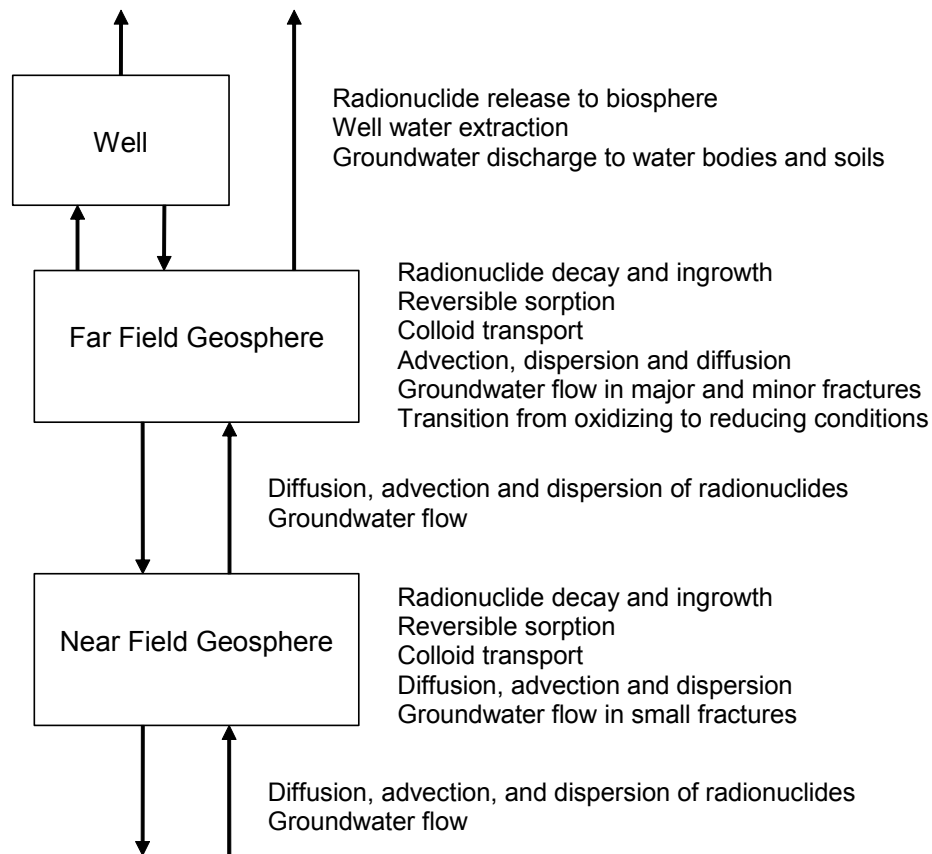


Figure 7-4: Conceptual Model for the Geosphere

The groundwater flow field is calculated assuming constant head boundary conditions at the surface, with the water table following the surface topography, and no-flow boundary conditions at the boundaries of the watershed. This is reasonable for this hypothetical site where there is limited topographic relief and conditions can be assumed relatively wet.

The hydrogeological model includes a 100 m deep well in a fracture zone, with the fracture able to supply water at the specified rate. The influence of the well on the overall groundwater flow field is small although the flow field near the well is affected by well drawdown. The groundwater at repository depth is only slightly saline (~11 g/L), so salinity is not an important factor in the hydrogeological modelling (i.e., the density of the groundwater is assumed to be uniform throughout the geosphere). This is supported by analysis considering the effects of salinity on the deep groundwater system presented in Chapter 2.

In the near-field geosphere (i.e., around the repository), chemically reducing conditions prevail. The temperature in the near field will initially be warmer than in the surrounding geosphere due to radioactive decay, with the maximum temperature reached within about 5,000 years (Guo 2009) and with ambient temperatures returning within about 100,000 years. Generally, the rock mass would be about 40°C for about a hundred metres around the repository for about 10,000 years. To account for uncertainties in chemical solubility at these higher temperatures, reference solubility values are increased by a factor of 10. For the contaminant transport times estimated in this study, however, the bulk of the transport occurs under close to ambient conditions. The temperature time dependence is therefore not considered further.

The physical properties of the rock are described in Chapter 2. The diffusion and sorption coefficients assumed for the rock at repository level are given in Section 7.5.

7.3.4 Biosphere

The main features of the biosphere model are illustrated in Figure 7-5.

The model includes only the local biosphere near the repository, since doses to the critical group living near the repository should be higher than for any individual living further away. Radionuclides are lost from the local biosphere by radioactive decay, by discharge from the local lake and river to downstream watershed locations, and by loss to the deep sediments at the bottom of the lake and river. For a few volatile nuclides, losses due to winds and atmospheric dispersion are also important.

The surface biosphere has the characteristics of the Canadian Shield region of central Canada. As noted earlier in Section 7.2.4, a constant temperate climate is assumed. While the properties of the biosphere could vary with time due to global warming in the near term, or due to other natural or human-induced changes, the assumption of a constant biosphere provides a convenient and clear measure of the potential impacts, which can be readily related to what is currently acceptable.

In the long term, it is assumed that glaciation will resume with consequent significant effects as a result of the glaciation itself and the related climate change. This is discussed in Section 7.10.

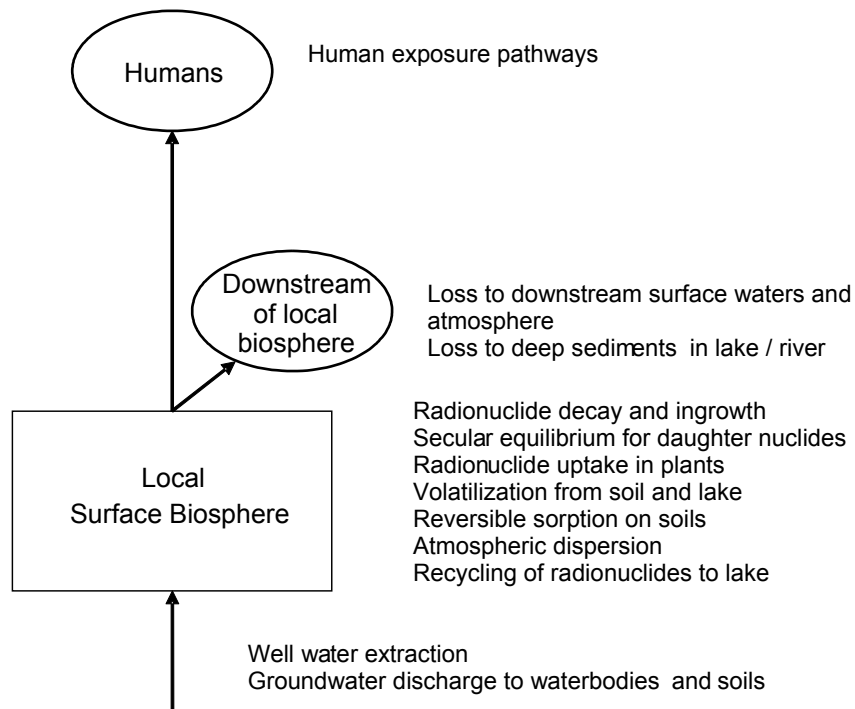


Figure 7-5: Conceptual Model for the Constant Biosphere

Following international practice, the site is assumed occupied by a group of people (i.e., the "critical group") that behaves in a plausible manner but with lifestyle characteristics that maximize their exposure to any radionuclides entering the biosphere. It is assumed that the members of the critical group spend all their lives in the local biosphere and obtain all their food, water, fuel and building materials from the local vicinity.

The characteristics of the critical group will change with climate; however, since a constant temperate climate is assumed a self-sufficient farmer is selected as the critical group. This group uses a well that intercepts the contaminant plume from the repository, and grows its own crops and raises animals. Their food includes plants grown in a garden, domesticated animals and fish. This lifestyle is more self-sufficient than current habits and will lead to higher estimates of impacts. Note that future safety assessments may consider additional lifestyles.

Plants growing near the repository can become contaminated directly by atmospheric deposition of radionuclides that reach the biosphere and become volatilized (e.g., I-129) or suspended due to aerosol formation (all nuclides). Plants can also become contaminated due to root absorption of groundwater discharge, irrigation with contaminated surface water (edible crops), and with radionuclides that are deposited to the soil from the atmosphere.

Radionuclides released from the repository reach the surface biosphere in several ways: via the well that intercepts the radionuclide plume; via groundwater discharge to surface water bodies; and via groundwater discharges to terrestrial areas. Given these radionuclide discharge rates, the biosphere model:

- describes the movement of radionuclides through soil, plants and animals, the water and sediment of a lake / river, and the atmosphere near the groundwater discharge locations;
- calculates the concentrations of radionuclides in water and air in the local habitat of the critical group;
- calculates radiological dose rates to an individual in the critical group caused by ingestion and inhalation of radionuclides and by external exposure to radiation from radionuclides in the environment (air immersion, water immersion, building materials and groundshine); and
- calculates radiological dose rates to non-human biota.

In the model, all radionuclide releases from the geosphere are assumed to enter the primary water body discharge point. In particular, radionuclides captured by the well or directly discharged into soils are not removed from the amount entering the water body. In effect, this assumes the holdup in these paths is relatively short, and the radionuclides eventually do transfer to the water body. This conservatively overestimates the amount of radionuclides in the biosphere, but simplifies the modelling because many processes that recycle radionuclides are accounted for implicitly, such as surface runoff into the water body.

A schematic representation of the environmental transfer model is shown in Figure 7-6. The dose model uses the concentration of radionuclides in the various biosphere compartments (water body, well, soil, plants, animals and air) to calculate the annual dose to a member of the critical group. The critical group is also exposed to sediments from the lake when these sediments are used for soil. In this case, the sediment exposure pathways are the same as those for the soil exposure pathways.

The internal exposure pathways considered are:

- soil-to-man;
- soil-to-plant-to-man;
- soil-to-plant-to-animal-to-man;
- soil-to-animal-to-man;

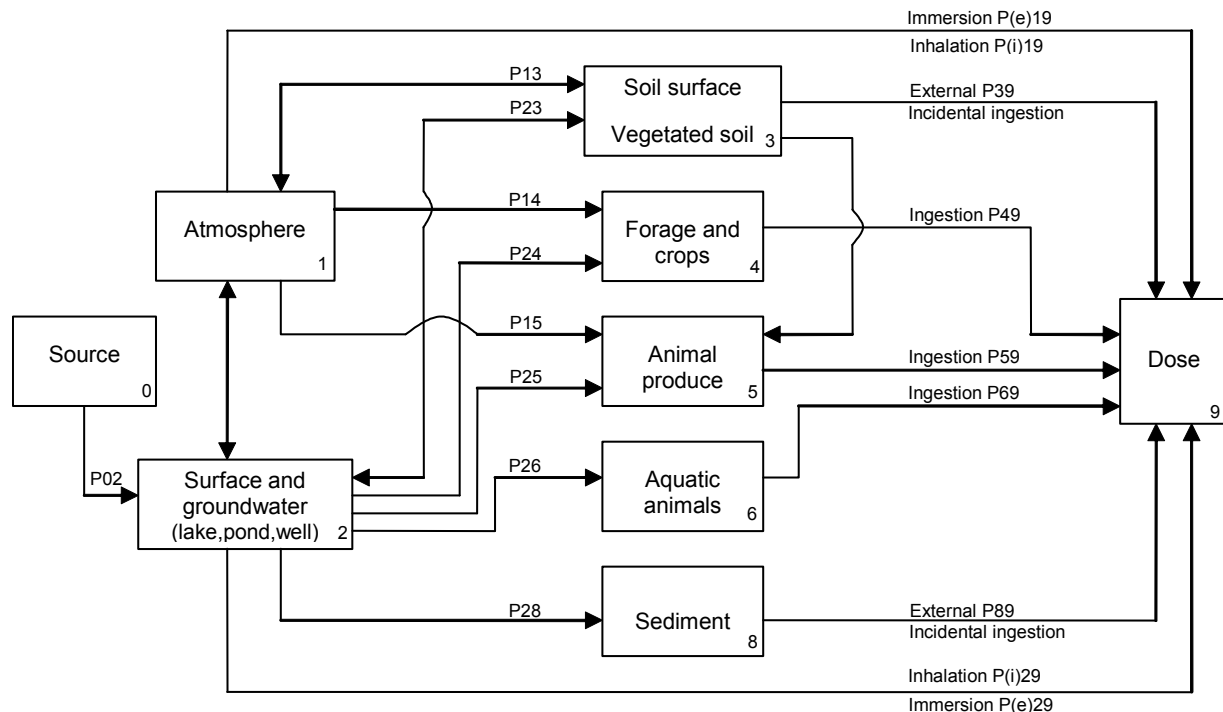
- air-to-man;
- air-to-plant-to-man;
- air-to-plant-to-animal-to-man;
- air-to-animal-to-man;

- water-to-man;
- water-to-plant-to-man;
- water-to-animal (including fish)-to-man; and
- water-to-plant-to-animal-to-man.

The external exposure pathways considered are:

- air immersion;
- water immersion (swimming or bathing);
- groundshine (exposure to radiation from contaminated soil); and
- building materials (exposure to radiation from building materials).

These exposure pathways are similar to those considered in the guidelines used to calculate derived release limits for normal operation of a nuclear facility (CSA 2008).



Notes: The nomenclature is from CSA (2008) and the P_{ij} represent transfer parameters from compartment i to compartment j . The biosphere model includes all these environmental transfers and exposure pathways. The building material exposure pathway is not shown here since it is not included in the CSA (2008) dose model.

Figure 7-6: Environmental Transfer Model Describing Critical Group Exposure Pathways

7.4 Computer Codes

The conceptual model is numerically represented in a suite of computer codes used in postclosure safety assessment modelling.

Figure 7-7 identifies the codes used and their interrelationship. Information from used fuel characteristics, engineering design and site characterization is used to develop a site-specific system description.

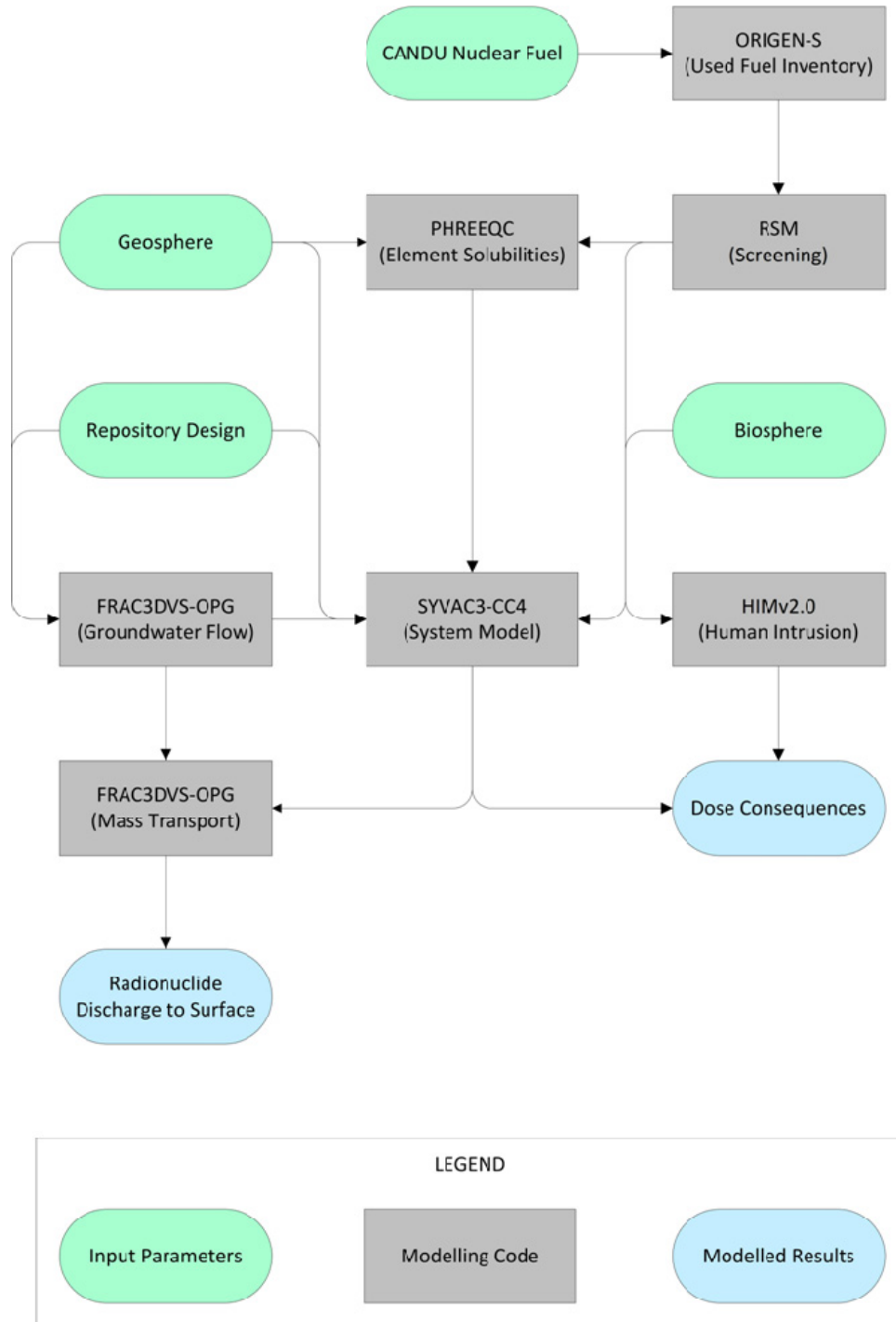


Figure 7-7: Main Computer Codes

ORIGEN-S is a CANDU-industry standard code used to calculate radionuclide inventories in the fuel and zircaloy cladding at the time of placement, based on a defined reactor exposure scenario (Hermann and Westfall 1995, Tait et al. 1995).

ORIGEN-S was used to derive the used fuel inventories used in this pre-project review (see Chapter 3).

PHREEQC is a widely used and tested open source computer program developed by the United States Geological Survey (Parkhurst and Appelo, 1999). PHREEQC is based on an ion-association aqueous model and is designed to perform a wide variety of low-temperature aqueous geochemical calculations.

In this assessment, PHREEQC Version 2.17 has been used for solubility and speciation calculations. The thermodynamic datasets used were the ThermoChimie v.7.b dataset and the ThermoChimie v.7.d dataset, as described in Garisto et al. (2012).

RSM (Radionuclide Screening Model) is a project-specific simple model of groundwater transport of radionuclides from container to humans via a well. Through a conservative choice of input parameters, a large input set of radionuclides can be screened so as to objectively identify which are worth analyzing using more detailed models. RSM incorporates data for all radionuclides with half-lives longer than 0.1 years as well as radionuclides with half-lives longer than one day if they have a parent with a half-life longer than 0.1 years.

Table 7-6 provides more information on RSM.

SYVAC3-CC4 is the reference system model for the assessment of radionuclide release, transport, decay, biosphere transfer and dose assessment. It has been developed for a deep geological repository concept based on used fuel placed in durable containers, surrounded by engineered barrier material and located deep underground. The code can perform both deterministic and probabilistic calculations.

Table 7-7 provides more information on SYVAC3-CC4.

FRAC3DVS-OPG is the reference groundwater flow and transport code. This is a commercially available 3D finite-element / finite-difference code (Therrien et al. 2010). FRAC3DVS-OPG supports both equivalent porous medium and dual porosity representations of the geologic media.

Table 7-8 provides more information on FRAC3DVS-OPG.

HIMv2.0 is a project-specific code that assesses the consequences of the Inadvertent Human Intrusion Scenario. The model considers a scenario in which a used fuel container is unknowingly intersected by a drilled borehole resulting in used fuel being brought directly to surface. Dose consequences are estimated for the drill crew and for a resident subsequently using the contaminated area.

Table 7-9 provides more information on HIMv2.0.

Table 7-6: RSM, Version RSM110

Parameter	Comments
Components:	
SYVAC3	Executive module, Version SV3.10.1
RSM	System model, Version RSM 1.1
Main Documents	<i>RSM Version 1.1 - Theory</i> (Goodwin et al. 2001)
	<i>RSM Version 1.1 Verification and Validation</i> (Garisto 2001)
Main Features	<ul style="list-style-type: none"> - Linear decay chains - Radionuclide release by instant release and by congruent dissolution - UO₂ dissolution calculated from user-supplied time-dependent data - Precipitation in container when user-supplied solubility limits exceeded - Durable containers, some fail with small defects - 1D buffer and backfill layer that surrounds the container and inhibits groundwater flow and radionuclide transport - Repository model based on one room containing failed container(s) - Linear sequence of 1D transport segments that connect the repository to a well. Transport segments are user-supplied; transport is solved considering diffusion, advection/dispersion and sorption - Dose impacts to a self-sufficient human household that uses well water, based on conservative model for drinking, immersion, inhalation and ground exposure. Effect of other ingestion pathways is included through a user-input multiplier - Ability to represent all input parameters with a probability density function (PDF) and to run Monte-Carlo type simulations - Time-independent material properties and biosphere characteristics - Database of all radionuclides with half-lives longer than 0.1 years as well as radionuclides with half-lives longer than one day if they have a parent with a half-life longer than 0.1 years

Table 7-7: SYVAC3-CC4, Version SCC4.09

Parameter	Comments
Components:	
SYVAC3	Executive module, Version SV3.12
CC4	System model, Version CC4.09
ML3	SYVAC3 math library, Version ML3.03
SLATEC	SLATEC Common Mathematical Library, Version 4.1
Main Documents	<i>SYVAC3-CC4 Theory Manual (NWMO 2012)</i>
	<i>SYVAC3-CC4 User Manual (Kitson et al. 2012)</i>
	<i>Summary of Verification and Validation Studies for SYVAC3-PR4 and its Submodels (Garisto and Gierszewski 2001)</i>
Main Features	<ul style="list-style-type: none"> - Linear decay chains - Radionuclide release by instant release and by congruent dissolution - UO₂ dissolution rate calculated using radiation dose-rate based model - Precipitation in container when user-supplied solubility limits exceeded - Durable container, but some fail due to small defects - Cylindrical buffer and backfill layer that surrounds the container and inhibits groundwater flow and radionuclide transport - Multiple sector repository connected to the geosphere at sector-specific nodes chosen considering the local groundwater flow - Geosphere network of 1D transport segments that connect the repository to various surface discharge locations, including a well - Transport considers diffusion, advection / dispersion and sorption - Biosphere model that calculates field soil concentrations, well water concentrations, and uses a surface water body as a final collection point - Dose impacts to a self-sufficient human household that uses water body or well water, locally grown crops and food animals, local building materials and heating fuel - Dose impacts to generic non-human biota - Flow-based models in repository and geosphere, concentration-based models in biosphere - Generally time-independent material properties and characteristics for the biosphere and geosphere model. Transitions from one geosphere (or biosphere) state to another at specific times can be accommodated - Ability to represent all input parameters with a probability density function and to run Monte-Carlo type simulations

Table 7-8: FRAC3DVS-OPG, Version 1.3

Parameter	Comments
Components:	
FRAC3DVS-OPG	Main code, Version 1.3
Main Documents	<i>A Three-dimensional Numerical Model Describing Subsurface Flow and Solute Transport</i> (Therrien et al. 2010)
Main Features	<ul style="list-style-type: none"> - Linear decay chains - 3 D groundwater flow and solute transport in saturated and unsaturated media - Variable density (salinity) fluid - 1D hydromechanical coupling - Equivalent porous medium or dual-continuum model; fractures may be represented as discrete 2D elements - Finite-element and finite-difference numerical solutions - Mixed element types suitable for simulating flow and transport in fractures (2D rectangular or triangular elements) and pumping/ injection wells, streams or tile drains (1D line elements) - External flow boundary conditions can include specified rainfall, hydraulic head and flux, infiltration and evapotranspiration, drains, wells, streams and seepage faces - External transport boundary conditions can include specified concentration and mass flux and the dissolution of immiscible substances - Options for adaptive time-stepping and sub-gridding

Table 7-9: HIMv2.0

Parameter	Comments
Components:	
AMBER	Executive Code, Version 5.5
HIMv2.0	Main Model Version
Main Documents	<i>Human Intrusion Model for the Fourth and Fifth Case Studies: HIMv2.0 (Medri 2012)</i>
Main Features	<ul style="list-style-type: none"> - Linear decay chains - Dose consequences by external, inhalation and ingestion pathways to drill crew and site resident - Surface contamination decreases with time due to radioactive decay and soil leaching - Time-independent material properties and biosphere characteristics - Includes data for potentially relevant radionuclides

7.5 Analysis Methods and Key Assumptions

This section describes the analysis approach and how the detailed models (FRAC3DVS-OPG and SYVAC3-CC4) are used in the analysis.

Data for selected parameters are also provided; however, a more detailed data description is available in Garisto et al. (2012).

7.5.1 Overall Approach

The general approach for conducting the postclosure safety assessment is as follows:

1) Radionuclide and Chemical Hazard Screening

Used nuclear fuel initially contains hundreds of radionuclides and chemically hazardous stable elements; however, most are short lived and / or present in very small amounts. Following placement in a deep geological repository only a small subset poses a potential risk to humans and the environment. The RSM code is used to identify this subset for more detailed assessment.

The methods used for performing the screening analysis are described in Section 7.5.2.

2) 3D Groundwater Flow and Radionuclide Transport Modelling

Detailed 3D steady-state hydrogeological modelling is performed with FRAC3DVS-OPG to determine the groundwater flow field near the repository.

Once the flow field is determined, detailed 3D diffusive and advective radionuclide transport modelling is performed to calculate radionuclide transport for I-129, C-14, Cl-36, Ca-41, Sn-126, Cs-135, U-234 and U-238. These radionuclides are typically the most important in terms of potential radiological impact or in representing a range of low-sorption to high-sorption species. Radionuclide releases from the defective containers are provided from the SYVAC3-CC4 container release model and imposed as a source term on the FRAC3DVS-OPG mass transport calculation.

Dose consequences cannot be determined because the FRAC3DVS-OPG code does not have biosphere and dose models. Transport results are therefore expressed in units of Bq/a for transport to the region of interest (e.g., to the well).

Due to the large size of the modelled environment, three different nested models are created. Figure 7-8 illustrates the spatial relationships. The models are:

- Sub-Regional Model - the model boundaries are located some distance (i.e., greater than five kilometres) from the repository to avoid boundary effects. Specific vertical boundary locations are selected based on topographical highs or lows that are likely zero-flow.

The model determines the groundwater flow field encompassing the repository and identifies the main surface discharge locations. It also determines the required domain and boundary conditions for the Site-Scale Model.

No repository features are incorporated at this scale of resolution.

This model is identical to the sub-regional model used for groundwater simulations in Chapter 2, except that a finer vertical discretization has been adopted in support of contaminant transport calculations.

- Site-Scale Model - the model domain includes the repository and the portion of the sub-regional flow system into which groundwater flow through the repository travels and discharges.

The model determines the most conservative source location (i.e., the container location with the most rapid groundwater transport to a conservatively located water-supply well). Reference Case and various sensitivity simulations are performed to determine radionuclide transport to the well and surface environment. The model supplies boundary conditions to the Repository-Scale Model.

A simplified representation of the repository and Engineered Barrier System (EBS) is included at this scale of resolution; however, individual containers are not modelled.

- Repository-Scale Model - the model domain is a small section of the repository surrounding the defective containers and the adjacent geosphere.

Reference Case and various sensitivity simulations are performed to corroborate results of the Site-Scale Model and to provide a more complete understanding of repository component functions.

The model incorporates a high level of detail and individual containers are represented at the source location.

The nested models are also used to obtain a description of the advective flow field for use in subsequent SYVAC3-CC4 system modelling. To provide data for confirming that the resulting SYVAC3-CC4 system model is appropriate for use, radionuclide transport calculations (taking into account both diffusion and advection) for I-129, C-14, Cl-36, Ca-41, Sn-126, Cs-135, U-234 and U-238 are performed with FRAC3DVS-OPG. Results are generated for transport out of a volume around the defective containers and for transport to the biosphere.

The methods used in this phase of the assessment are described in Section 7.5.3.

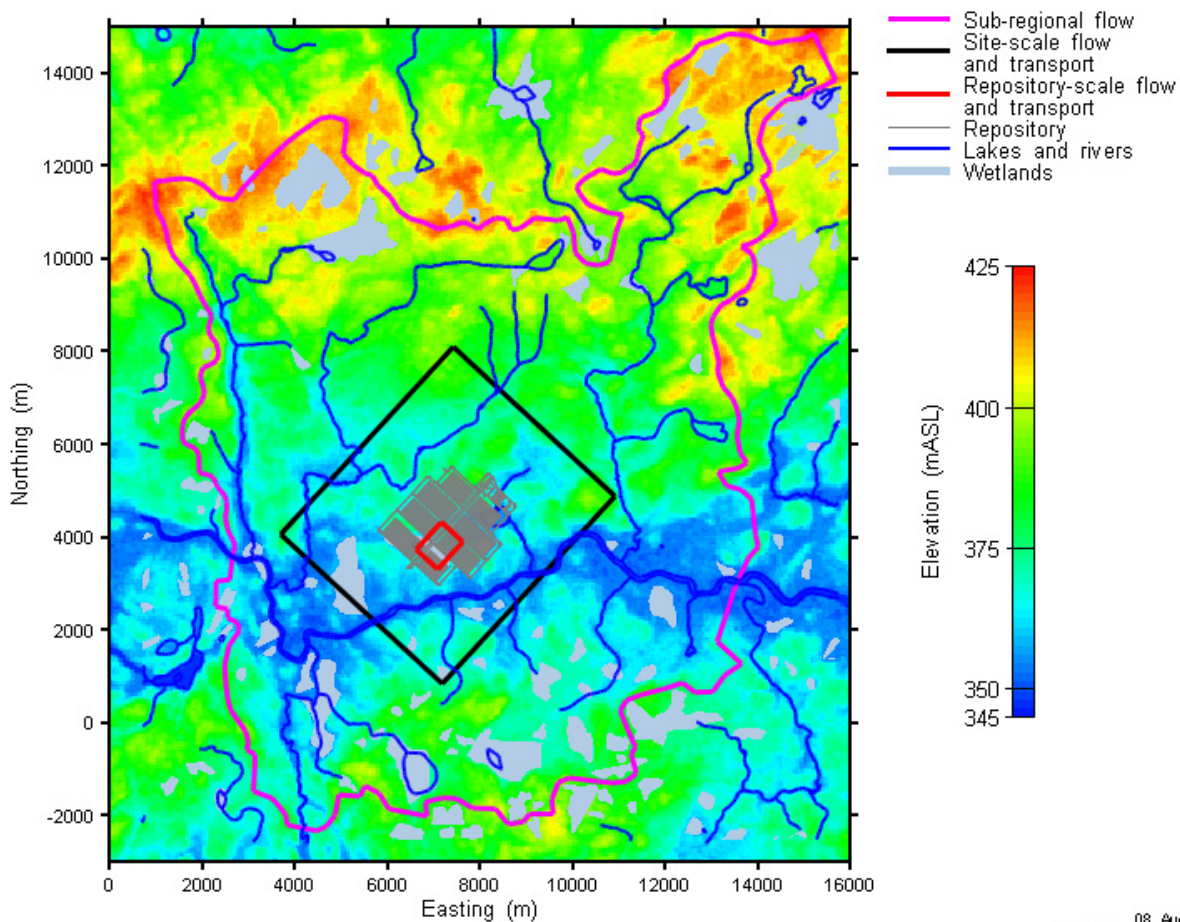


Figure 7-8: FRAC3DVS-OPG Model Domains and Basic Features at the Hypothetical Site

3) System Modelling

The 3D groundwater flow field generated with FRAC3DVS-OPG is used to guide development of the geosphere model in the SYVAC3-CC4 system model. The SYVAC3-CC4 geosphere transport network is calibrated to the groundwater results from FRAC3DVS-OPG.

The SYVAC3-CC4 geosphere model is then verified by comparing the radionuclide transport results through the geosphere with radionuclide transport results from FRAC3DVS-OPG. These calculations were performed for I-129, C-14, Cl-36, Ca-41, Sn-126, Cs-135, U-234 and U-238, as these represent the key radionuclides for groundwater transport, as well as provide a test of the two models for species that cover a range of sorptions as well as a simple decay chain.

All other aspects of the system model - used fuel, container, near-field and biosphere are defined by the scenario and by input data as previously described.

The dose consequences for the Reference Case and for various deterministic sensitivity cases are then determined for the full suite of radionuclides of interest.

The SYVAC3-CC4 system model is also used to carry out the probabilistic safety assessment, assuming a fixed geosphere. The radionuclide inventory, release and transport properties are varied about the Reference Case values, as are the characteristics of the biosphere and dose receptor.

The methods used in this phase of the assessment are described in Section 7.5.4.

7.5.2 Radionuclide and Chemical Toxicity Screening Model

This section provides information on how the radionuclide and chemical toxicity screening is performed. Section 7.5.1 describes how this fits into the overall assessment approach.

The screening uses the RSM model. RSM closely resembles the SYVAC3-CC4 system model used to perform the primary dose assessment; however, some simplifications are incorporated to ensure conservative results are obtained. The following discusses the RSM model in terms of its key features and whether they differ from those in the SYVAC3-CC4 model.

- Solubility limits, diffusion coefficients, sorption coefficients and decay constants are the same.
- The radionuclide source term is the same.
- The container release model is the same.
- The near field model (representing the engineered barriers) is represented by a simple one dimensional pathway consisting of a 30 cm thick bentonite buffer, which is thinner than the actual 36 cm buffer. The bentonite properties are identical to those in the SYVAC3-CC4 model.
- The geosphere model is similar in that it is based on a one dimensional diffusion-dispersion-advection transport model; however, unlike the detailed geosphere model in SYVAC3-CC4, only a single fast transport pathway is represented. This pathway is composed of three zones, these being a segment of the excavation damage zone (through which contaminants

move from the failure location to the end of the placement room), a segment of rock and a transmissive fracture that is connected to a well in the biosphere.

All defective containers share this same transport pathway.

The properties used to represent the three geosphere zones are shown in Table 7-10. These properties are selected to ensure a conservative representation of the transport time to the surface. For comparison, the transport time from the repository to the surface is 1.4×10^3 years in the RSM model and 3.2×10^4 for the fastest sector (Sector 8) in the Reference Case SYVAC3-CC4 model.

Table 7-10: Screening Model Geosphere Zone Properties

Geosphere Zone	Material Type	Length (m)	Velocity (m/a)	Porosity (-)	Tortuosity (-)
1	EDZ	28	1.5	0.003	0.09
2	Rock Mass	69	0.056	0.003	0.09
3	Fracture	415	2.4	0.1	0.03

- The biosphere model is greatly simplified. Both codes use the same critical group based on a self-sufficient farm family living on the site; however, SYVAC3-CC4 incorporates the biosphere model in Figure 7-6 with explicit modelling of various pathways while RSM has a more limited set of exposure pathways. RSM calculates doses from water ingestion, groundshine, air immersion and air inhalation. The plant ingestion dose rate is estimated from the drinking water dose rate using an ingestion multiplication factor.

The following assumptions are also incorporated in the biosphere model to ensure conservative results:

- The well demand is set to that corresponding to a single person, excluding irrigation. This ensures the minimum amount of dilution.
- The surface soil is a small irrigated garden large enough to support only a single person. This maximizes the soil concentration.
- Contaminant concentrations in surface water are set equal to those in the well. This maximizes the surface water concentrations.

Prior to running the model, a pre-screening is done. All radionuclides with half-lives longer than 0.1 years as well as radionuclides with half-lives longer than one day if they have a parent with a half-life longer than 0.1 years are included. This results in a total of 251 distinct radionuclides and 96 stable elements remaining in the used fuel and zirconium fuel sheath for further consideration.

The RSM model is then run for the suite of analysis cases shown in Table 7-11, with the cases selected for consistency with the cases described in Section 7.2 (i.e., the cases included in the postclosure safety assessment). The "3 Sigma" case in Table 7-11 captures a low probability scenario in which all parameters represented by probability distributions have simultaneous extreme values in the conservative direction. Because of its conservative nature, this case also

bounds several of the deterministic sensitivity cases in the postclosure safety assessment (i.e., Fuel Dissolution Rate Increased by a Factor of 10 and Container Defect Area Increased by a Factor of 10). All RSM cases are run for a 10 million year simulation time.

For the radiological dose assessment, the set of radionuclides that together contribute 0.1% or less of the total peak dose rate are screened out.

For the chemical hazard assessment, for all cases except the All Containers Fail scenario, all stable chemically hazardous elements whose peak groundwater, surface water or soil concentration exceed 10% of their associated interim acceptance criteria are screened in. For the All Containers Fail Disruptive Event Scenario, the screening threshold is set to 100%. This is done in recognition of the highly conservative nature of the screening model. Note that sediment concentrations are not evaluated because the screening model does not represent the surface water body in sufficient detail. Due to the conservative nature of the model, the water and soil concentrations are expected to represent a sufficient screening test.

Finally, the results of the screening are compared with previous Canadian and international case studies to verify that all important radionuclides and elements are included.

Table 7-11: Cases Considered for the Radionuclide and Chemically Hazardous Element Screening Assessment

Case	Description
Base Case	All parameter values identical to those in the Reference Case of the Normal Evolution Scenario.
3 Sigma	All parameter values set to their 3 sigma values in the conservative direction. This is bounding for several Normal Evolution Scenario sensitivity cases (e.g., Fuel Dissolution Rate Increased by a Factor of 10, Container Defect Area Increased by a Factor of 10).
No Sorption in the Geosphere	Geosphere sorption coefficients are set to zero with all other parameters maintained at their Base Case values.
No Sorption in the Buffer, Backfill and Seals	Near field (buffer + backfill) sorption coefficients are set to zero with all other parameters maintained at their Base Case values.
High Solubility	Solubility limits for all species set to to an arbitrarily high value of 2000 mol/m ³ with all other parameters maintained at their Base Case values.
High Instant Release Fraction	Instant release fractions for all elements set to 10% with all other parameters maintained at their Base Case values.
All Containers Fail	All containers fail 10,000 years after repository closure via a small penetrating hole (radius = 1 mm) with all other parameters maintained at their Base Case values. All containers are simultaneously assumed to be in the repository location that results in the shortest transport time to the surface.

7.5.3 Detailed Flow and Transport Models

This section provides detailed descriptions of the three nested models used in the FRAC3DVS-OPG groundwater and radionuclide transport calculations. Section 7.5.1 describes how this fits into the overall assessment approach.

All flow modelling is steady-state. This is consistent with the Reference Case assumption of constant climate. Small changes in climate may affect the shallow groundwater system, but would not affect the deep geosphere. The effects of large changes in climate associated with glaciation cycles are discussed separately in Section 7.10.

The flow modelling also assumes a freshwater fluid. This is a reasonable approximation because the groundwater composition assumed at 500 m depth is low salinity. The reference composition is shown in Table 7-12.

Data for effective diffusion coefficients, material porosities and tortuosities, and sorption coefficients are shown in Table 7-13 through Table 7-15. These data are described in Garisto et al. (2012).

Table 7-12: Deep Groundwater Composition

Groundwater	CR-10 EQ	CR-10 NF
pH	7.1	8.7
Environment	Reducing	Reducing
Eh (mV)	-194	-575
Density (g/mL)	1.006	1.006
Solutes (mg/L)		
Na	1,899	6,255
K	15	80
Ca	2,217	870
Mg	60	182
HCO ₃	50	4
SO ₄	1,243	4,314
Cl	6,099	6,059
Sr	25	25
F	2	2
Si	5	10
Fe	8	7
NO ₃	1	1
PO ₄	1	1
Total Dissolved Solids (mg/L)	11,625	17,810

Note: CR-10 EQ is equilibrated with minerals in the host rock (i.e., quartz, gypsum, calcite, magnetite and goethite), and CR-10 NF is CR-10 EQ equilibrated with both the carbon steel insert and bentonite.

Table 7-13: Data for Effective Diffusion Coefficients

¹Effective Diffusion Coefficients at 25°C (m²/a)				
Element	Free water	Buffer	Backfill	Rock
Ac	3.2x10 ⁻²	4.4x10 ⁻³	1.6x10 ⁻³	5.8x10 ⁻⁶
Aq	5.3x10 ⁻²	4.4x10 ⁻³	1.6x10 ⁻³	9.5x10 ⁻⁶
Am	3.2x10 ⁻²	4.4x10 ⁻³	1.6x10 ⁻³	5.8x10 ⁻⁶
As	6.7x10 ⁻²	4.4x10 ⁻³	1.6x10 ⁻³	1.2x10 ⁻⁵
Bi	6.7x10 ⁻²	4.4x10 ⁻³	1.6x10 ⁻³	1.2x10 ⁻⁵
C	3.8x10 ⁻²	4.4x10 ⁻³	1.6x10 ⁻³	6.8x10 ⁻⁶
Ca	2.5x10 ⁻²	4.4x10 ⁻³	1.6x10 ⁻³	4.5x10 ⁻⁶
Cd	2.3x10 ⁻²	4.4x10 ⁻³	1.6x10 ⁻³	4.1x10 ⁻⁶
Ce	6.7x10 ⁻²	4.4x10 ⁻³	1.6x10 ⁻³	1.2x10 ⁻⁵
Cl	6.3x10 ⁻²	3.5x10 ⁻⁴	1.3x10 ⁻⁴	1.1x10 ⁻⁵
Co	2.2x10 ⁻²	4.4x10 ⁻³	1.6x10 ⁻³	4.0x10 ⁻⁶
Cr	6.7x10 ⁻²	4.4x10 ⁻³	1.6x10 ⁻³	1.2x10 ⁻⁵
Cs	6.7x10 ⁻²	1.3x10 ⁻²	4.1x10 ⁻³	1.2x10 ⁻⁵
Eu	3.2x10 ⁻²	4.4x10 ⁻³	1.6x10 ⁻³	5.8x10 ⁻⁶
Hg	6.7x10 ⁻²	4.4x10 ⁻³	1.6x10 ⁻³	1.2x10 ⁻⁵
I	6.3x10 ⁻²	3.5x10 ⁻⁴	1.3x10 ⁻⁴	1.1x10 ⁻⁵
La	6.7x10 ⁻²	4.4x10 ⁻³	1.6x10 ⁻³	1.2x10 ⁻⁵
Nd	6.7x10 ⁻²	4.4x10 ⁻³	1.6x10 ⁻³	1.2x10 ⁻⁵
Ni	2.1x10 ⁻²	4.4x10 ⁻³	1.6x10 ⁻³	3.8x10 ⁻⁶
Np	3.2x10 ⁻²	4.4x10 ⁻³	1.6x10 ⁻³	5.8x10 ⁻⁶
P	6.7x10 ⁻²	4.4x10 ⁻³	1.6x10 ⁻³	1.2x10 ⁻⁵
Pa	3.2x10 ⁻²	4.4x10 ⁻³	1.6x10 ⁻³	5.8x10 ⁻⁶
Pb	6.7x10 ⁻²	4.4x10 ⁻³	1.6x10 ⁻³	1.2x10 ⁻⁵
Pd	3.2x10 ⁻²	4.4x10 ⁻³	1.6x10 ⁻³	5.8x10 ⁻⁶
Po	6.7x10 ⁻²	4.4x10 ⁻³	1.6x10 ⁻³	1.2x10 ⁻⁵
Pr	6.7x10 ⁻²	4.4x10 ⁻³	1.6x10 ⁻³	1.2x10 ⁻⁵
Pu	3.2x10 ⁻²	4.4x10 ⁻³	1.6x10 ⁻³	5.8x10 ⁻⁶
Ra	2.8x10 ⁻²	4.4x10 ⁻³	1.6x10 ⁻³	5.0x10 ⁻⁶
Rn	6.7x10 ⁻²	4.4x10 ⁻³	1.6x10 ⁻³	1.2x10 ⁻⁵
Sb	3.2x10 ⁻²	4.4x10 ⁻³	1.6x10 ⁻³	5.8x10 ⁻⁶
Se	3.2x10 ⁻²	4.4x10 ⁻³	1.6x10 ⁻³	5.8x10 ⁻⁶
Sn	6.7x10 ⁻²	4.4x10 ⁻³	1.6x10 ⁻³	1.2x10 ⁻⁵
Te	6.7x10 ⁻²	4.4x10 ⁻³	1.6x10 ⁻³	1.2x10 ⁻⁵
Th	3.2x10 ⁻²	4.4x10 ⁻³	1.6x10 ⁻³	5.8x10 ⁻⁶
U	3.2x10 ⁻²	4.4x10 ⁻³	1.6x10 ⁻³	5.8x10 ⁻⁶
Y	6.7x10 ⁻²	4.4x10 ⁻³	1.6x10 ⁻³	1.2x10 ⁻⁵

Notes: ¹ Reference Case values. Uncertainties in diffusion coefficients are provided in Garisto et al. (2012).

Table 7-14: Data for Sorption Coefficients (K_d)

¹ Sorption Coefficients (m^3/kg)			
Element	Buffer	Backfill	Rock/Fracture
Ac	61	19	3
Ag	0	0.0035	0.05
Am	61	19	13
As	0.3	0	0
Bi	35	2.5	0.001
C	0	0	0.001
Ca	0.0045	0.0015	9.8×10^{-5}
Cd	0.0045	0.0015	0.02
Ce	8	2.4	2
Cl	0	0	0
Co	0.0045	0.0015	0.02
Cr	0.0045	0.0015	2
Cs	0.093	0.036	0.042
Eu	8	2.5	2
Hg	0	0	0
I	0	0	0
La	8	2.4	2
Nd	8	2.4	2
Ni	0.3	0.091	0.01
Np	63	19	² 0.96
P	0	0	0
Pa	3	0.97	1
Pb	74	22	0.01
Pd	5	1.5	0.01
Po	0.06	0	0.1
Pr	8	2.4	2
Pu	63	19	5
Ra	0.0045	0	2.1
Rn	0	0	0
Sb	0.0045	0.0015	0
Se	0	7×10^{-5}	0.001
Sn	63	19	0.001
Tc	63	19	² 1
Te	0	7×10^{-5}	0
Th	63	19	1
U	63	19	² 6.3
Y	8	2.4	2

Notes: ¹ Reference Case values. Uncertainties in the K_d values are discussed in Garisto et al. (2012).

² The K_d values listed for Np and U are for reducing conditions. In oxidizing conditions, the sorption coefficients are significantly lower: Np = 0.018 and U = 0.0063 m^3/kg .

Table 7-15: Data for Material Porosity and Tortuosity

Material Properties at Saturation		
Material	Porosity	Tortuosity*
Buffer	0.43	0.03 to 0.49
Backfill	0.26	0.02 to 0.29
Rock	0.003	0.06

Notes: * Effective diffusion coefficients and porosity are measured directly for the buffer and the backfill. As a result the tortuosities are back-calculated and can vary with the element of interest. More detail is provided in Garisto et al. (2012).

7.5.3.1 Sub-Regional Model

Regional scale groundwater flow modelling of the Canadian Shield has indicated that flow patterns tend to be dominated by local topography rather than by large regional flows (Sykes et al. 2003). The flow model boundaries displayed in Figure 7-8 are therefore placed on topographical highs or lows that will likely form flow divides. They are also placed sufficiently far from the repository to avoid discharges from the repository approaching model boundaries.

Domain Discretization and Hydraulic Conductivity Profile

The repository is about 500 m below ground surface (mBGS). Since the surface elevation varies slightly across the repository, the horizontal depths are also defined in terms of an absolute measure of m above sea level (mASL). This hypothetical repository is assumed located at -135 mASL.

Horizontally, the domain is discretized in 50 m square elements, with 296 nodes in the X direction and 345 nodes in the Y direction, for a total of 101,480 elements in each model layer. The complete grid consists of 52 layers for a total of 5.18 million elements, of which 2.06 million are located outside the flow-domain and are set inactive. Although the repository footprint is shown in most plan-section figures in this section, there are no repository features or properties specified within the flow model grid. The repository representation in the figures is only provided to add context.

The bulk rock properties are described as a layered system with hydraulic conductivity decreasing with depth as discussed in Chapter 2. Hydraulic conductivities and model discretization are shown in Table 7-16. Reference Case values are used in all simulations except for sensitivity studies that examine the effect of different geosphere hydraulic conductivity.

Fracture hydraulic properties are constant with depth, with all fractures having a hydraulic conductivity of 1.0×10^{-6} m/s. Fracture zone thickness is set at 1 m with 10% porosity.

The fracture system is implemented using equivalent porous medium (EPM) elements with properties averaged in elements that are intersected by fractures or that share faces with

fractures mapped to element faces. Anisotropy in hydraulic conductivity within each EPM element is implemented to model vertical and horizontal fracture tendencies, while porosity is averaged to produce equivalent fracture element advective fluid velocities. Figure 7-9 illustrates fracture and rock mass hydraulic conductivity in an East-West vertical slice through the repository footprint.

A discrete fracture network flow model is also implemented as a sensitivity case. Fracture face mapping for this model is illustrated in Figure 7-10.

Table 7-16: Property Descriptors for Flow Model Layers

Depth (mBGS) or Elevation (mASL)	Thickness (m)	Hydraulic Conductivity (m/s)*				Model Layers
		Reference Case	Sensitivity 1	Sensitivity 2	Sensitivity 3	
Ground surface to 10 mBGS	10	1×10^{-8}	1×10^{-8}	1×10^{-8}	1×10^{-8}	2 layers at 5 m
10 mBGS to 150 mBGS (355 mASL to 215 mASL)	~140	2×10^{-9}	2×10^{-8}	2×10^{-10}	2×10^{-11}	12 layers, variable thickness (6 m to 20 m)
150 mBGS to 700 mBGS (215 mASL to -335 mASL)	550	4×10^{-11}	4×10^{-10}	4×10^{-12}	4×10^{-13}	13 layers, variable thickness (24 m to 50 m)
700 mBGS to 1500 mBGS (-335 mASL to -1135 mASL)	800	1×10^{-11}	1×10^{-10}	1×10^{-12}	1×10^{-13}	18 layers, variable thickness (50 to 60 m)

Notes: *Sensitivity 1, Sensitivity 2 and Sensitivity 3 are cases that examine the effect of changes in geosphere hydraulic conductivity. See Section 7.2.1 and Table 7-3 for a further explanation.

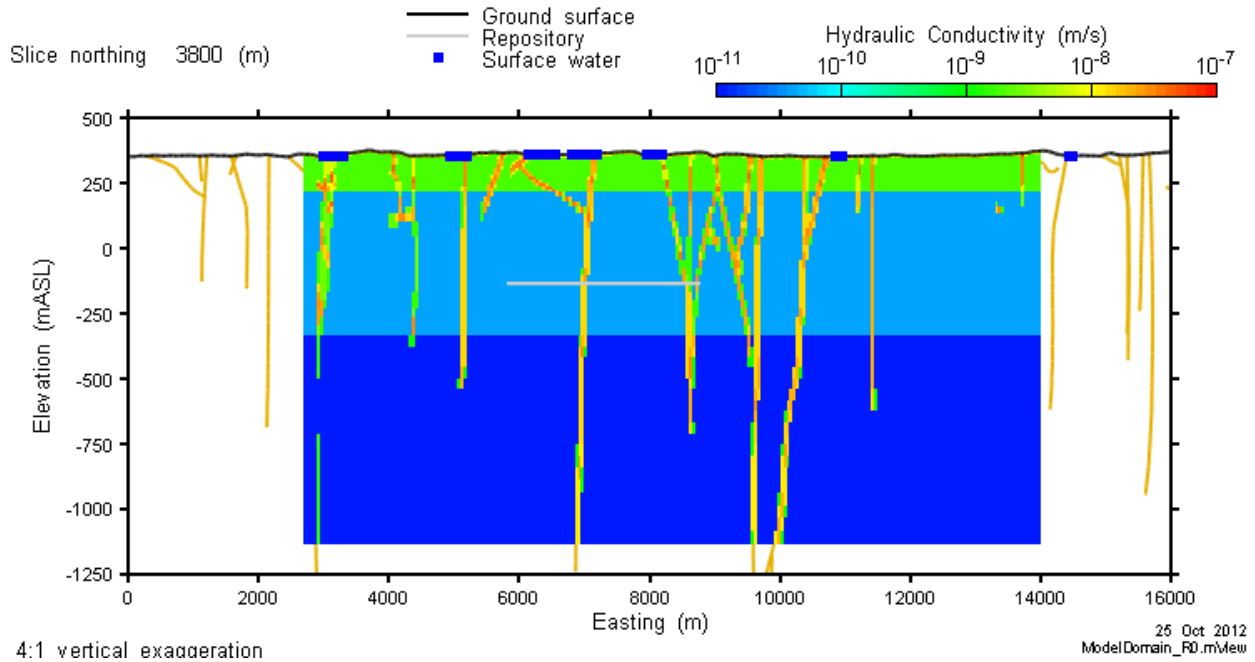


Figure 7-9: Sub-Regional Model: EPM Fracture Network and Vertical Hydraulic Conductivity Profile

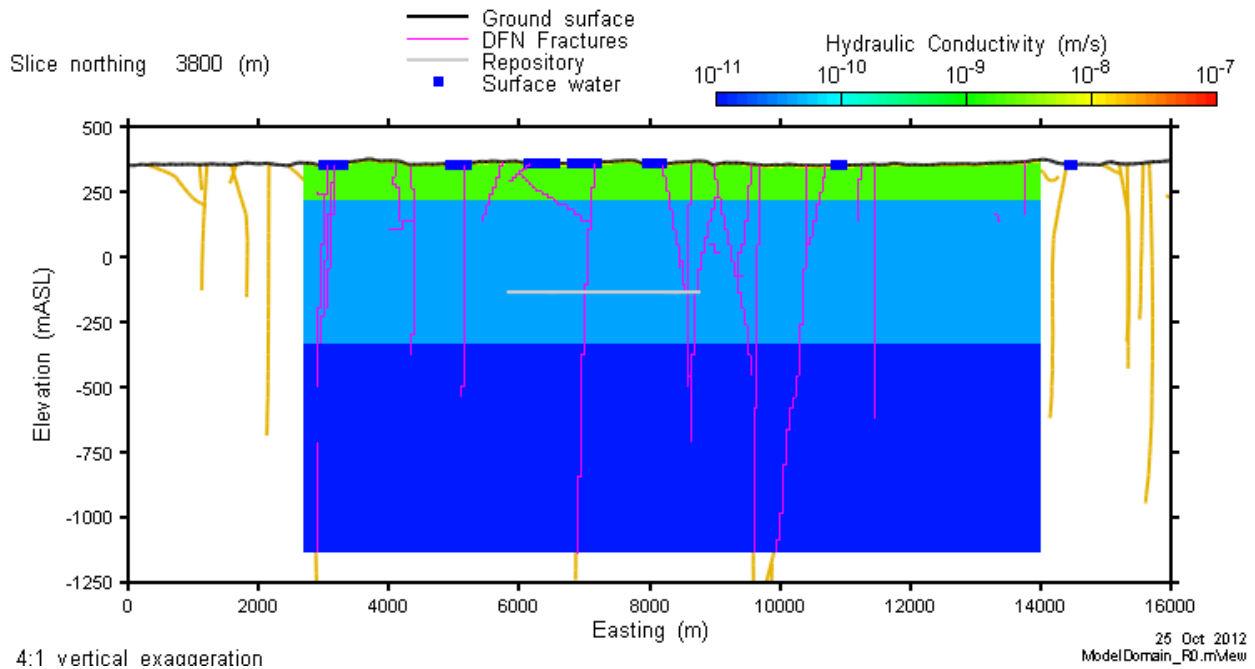


Figure 7-10: Sub-Regional Model: DFN Fracture Network and Vertical Hydraulic Conductivity Profile

Water Supply Well

The water supply well is located based on results from simulations performed using the Reference Case hydraulic conductivities.

Both particle tracking (based on the advective flow field) and transport calculations (including diffusion) indicate that transport from the repository to the deep fracture between the repository panels and then to surface is the fastest transport pathway. The well is therefore located within this fracture system at a depth of approximately 100 mBGS as shown in Figure 7-11. A number of different well locations within the fracture and other locations were assessed concurrently with the determination of the container location with the shortest transport time to the well (see Section 7.7.2.2). The combination of well and source location which yields the shortest transport times and maximum radionuclide mass flux to the well was selected.

The well is a 2D line element forming a segment, or edge, of a 3D element. Properties appropriate to a nominal 6" diameter well are assigned to the segment to specify the hydraulic conductivity of the well. The lowest node on the segment is defined as the withdrawal node from which water is abstracted.

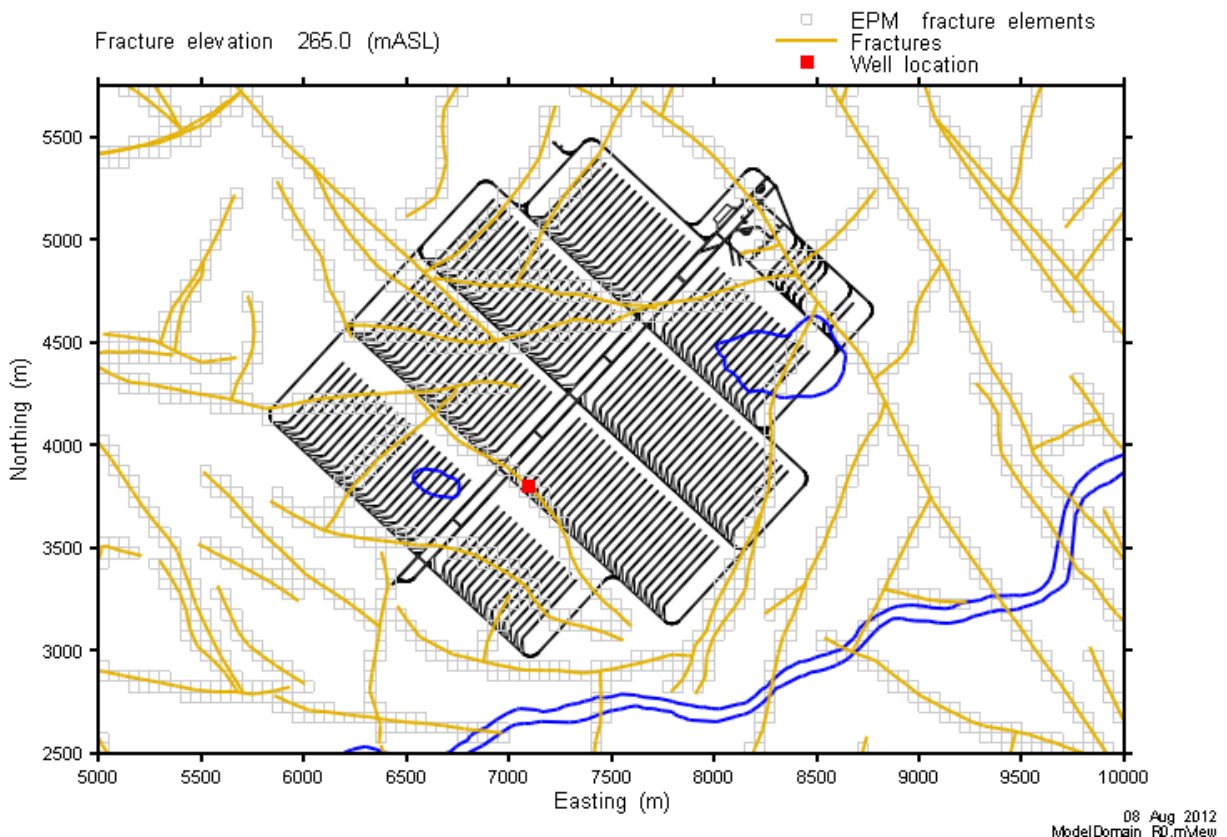


Figure 7-11: Sub-Regional Model: Well Location and Near-Surface Fracture System

Boundary Conditions

Zero-flow boundary conditions are specified on all external vertical faces and at the bottom of the model, which are located far from the repository and on topographic divides. Fixed head at elevation boundary conditions are specified for the top surface of the model, representing a water table close to surface and reflecting the generally low topographic relief. Steady-state hydrostatic conditions are adopted.

7.5.3.2 Site-Scale Model

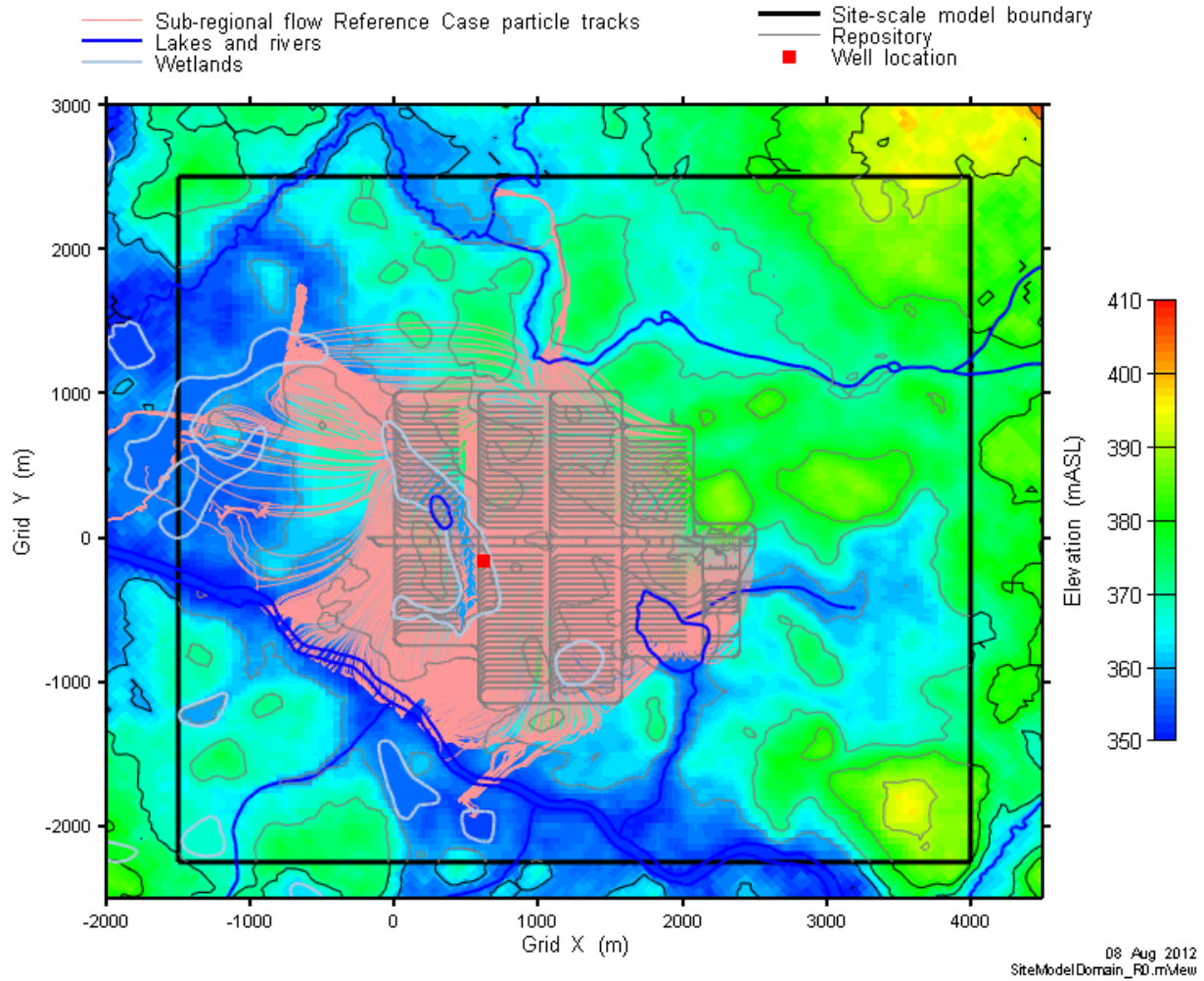
The Site-Scale Model is used to investigate the mass flows to the well and surface environment for I-129, C-14, Cl-36, Ca-41, Sn-126, Cs-135, U-234 and U-238 released from failed containers in the repository. The source containers are placed in the location with the shortest transport time and the maximum radionuclide flux to the well. The model supplies boundary conditions for use in the Repository-Scale Model, and examines sensitivity cases investigating the effect on transport of the EDZ hydraulic conductivity, shaft hydraulic conductivity, geosphere hydraulic conductivity, fracture location and fracture modelling.

There are minor simplifications in the implementation with respect to the reference data description provided in Garisto et al. (2012). In particular:

1. The inner and outer EDZ is specified only on the tops and bottoms of the access tunnels and placement rooms. As compensation for not including the side wall EDZ, the EDZ hydraulic conductivity is increased by a factor of two from the values given in Table 7-17.
2. No anisotropy is implemented in the tunnel and room EDZ or TDZ permeabilities.

The model domain is specified as the repository footprint together with approximately 1500 m of surrounding geosphere that encompasses the repository influenced flow domain. A new coordinate system is established, with the new system rotated 47.3 degrees counter-clockwise, so that the X axis follows the middle of Access Drift 2. This allows natural finite-difference discretization of the generally orthogonal repository features.

Figure 7-12 shows the coordinate system and model boundaries. It also shows the projected particle tracks that illustrate the potential transport pathways for contaminants released from the repository. This information shows that the model domain includes all major discharge points.



Notes: The particle tracks for assumed releases at repository level to surface discharge are shown.

Figure 7-12: Site-Scale Model: Coordinate System and Domain Boundary

Domain Discretization and Property Assignment

Unlike the Sub-Regional Model which is discretized with constant 50 m square elements, the Site-Scale Model uses variable element sizes in both the X and Y direction so as to incorporate repository related features with good geometric fidelity. The maximum element size is 50 x 50 m in the corners of the grid. The smallest dimension is 0.75 x 2.0 m, and is used to incorporate shaft excavation damage zone features. This results in grid layers containing 108,864 elements.

Figure 7-13 presents element areas on a plan section grid. Individual element edges are not shown due to the density of the elements.

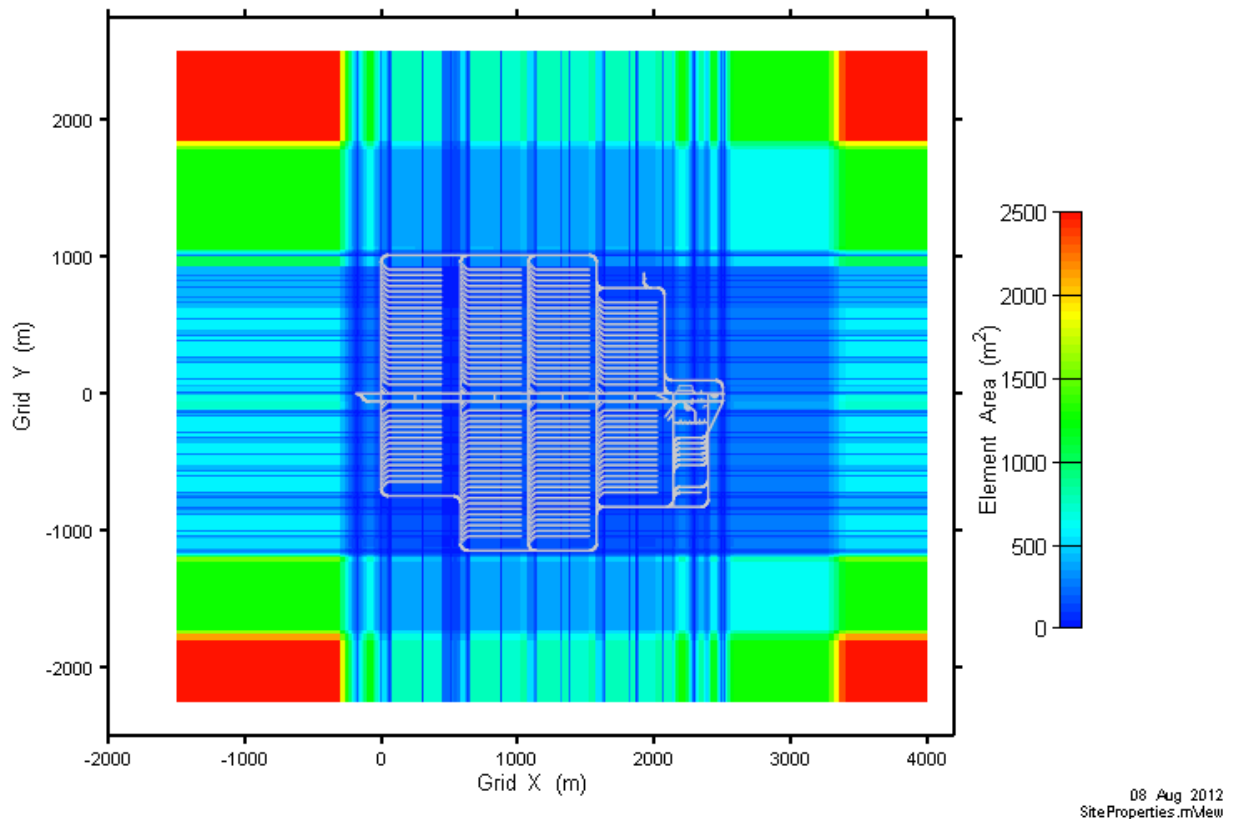


Figure 7-13: Site-Scale Model: Plan Section

Vertical discretization is driven by the requirement to incorporate geosphere and repository features as well as shaft sealing properties. Eighty-one layers are incorporated, yielding a total of 8.7 million elements. Figure 7-14 shows the vertical hydraulic conductivity profile of the Site-Scale Model, including the equivalent porous media fractures, repository and two main shaft elements.

In addition to geosphere properties described in Table 7-16, selected repository property groups are included as defined in Table 7-17. Not all sealing system components are included: the light backfill is not specified for rooms or seals.

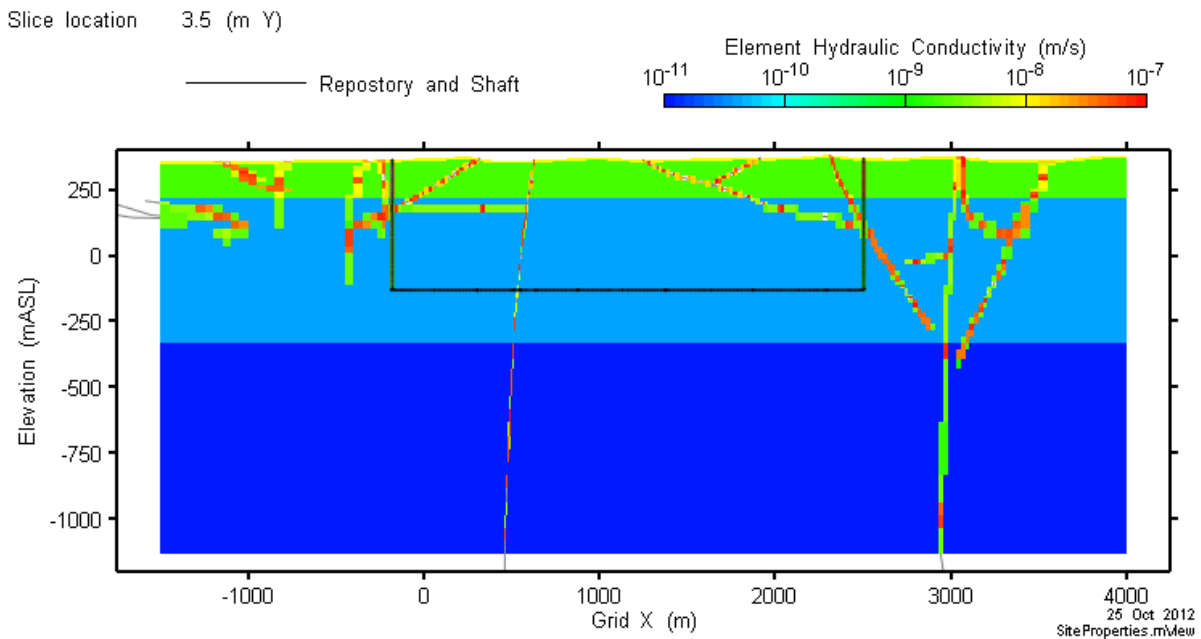


Figure 7-14: Site-Scale Model: Vertical Hydraulic Conductivity Profile

Table 7-17: Site-Scale Model: Flow Model Properties

Property Identifier	Description	Hydraulic Conductivity (m/s)	Porosity	Thickness (m)
INT_RIEDZ	Inner EDZ surrounding rooms and tunnels	4×10^{-9}	0.006	0.3
INT_ROEDZ	Outer EDZ surrounding rooms and tunnels	4×10^{-10}	0.003	1.0
INT_HDZ	Room TDZ	4×10^{-7}	0.006	0.7
INT_SOEDZ	Lower Shaft Outer EDZ	4×10^{-10}	0.003	4.75
INT_SIEDZ	Lower Shaft Inner EDZ	4×10^{-9} (xy) 4×10^{-8} (z)	0.006	4.75
SH_SOEDZ	Upper Shaft Outer EDZ	2×10^{-8}	0.003	4.75
SH_SIEDZ	Upper Shaft Inner EDZ	2×10^{-7} (xy) 2×10^{-6} (z)	0.006	4.75
Compacted Bentonite	Room Seal	1.3×10^{-13}	0.422	-
Dense Backfill Blocks	Tunnel and Drift Backfill	8.8×10^{-11}	0.195	-
Homogenized Backfill	Room Backfill	1.8×10^{-11}	0.264	
Concrete	Room Closure Bulkhead	1×10^{-10}	0.10	-
Bentonite Sand	Primary shaft seal	4.8×10^{-13}	0.411	-
Asphalt	Additional shaft seal	1×10^{-12}	0.02	-

Note: Data from Garisto et al. (2012)

Transport properties include dispersivity, diffusivity, and sorption. Longitudinal dispersivity is set at 20 m for intact rock, approximately 5% of the plume travel path length to discharge at the well, with transverse dispersivity specified as 2 m. EBS and EDZ dispersivities are set at 10 m and 1 m, reflecting shorter path lengths through these systems.

FRAC3DVS-OPG calculates an effective diffusion coefficient based on tortuosities, porosities, and free water diffusivity. Tortuosities were adjusted for each radionuclide and material type to yield correct D_e values. Sorption is also specified on a radionuclide and material type basis.

Figure 7-15 and Figure 7-16 illustrate property assignments on vertical cross-sections through a placement room seal and the main shaft.

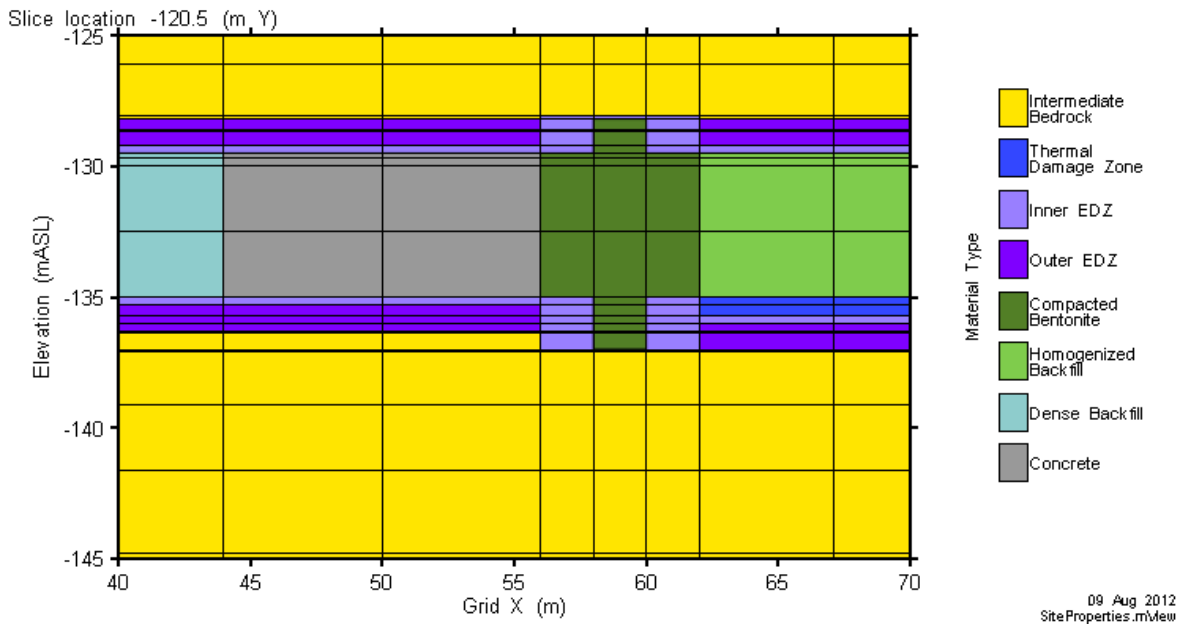


Figure 7-15: Site-Scale Model: Property Assignment on Vertical Cross-Section through Placement Room Seal

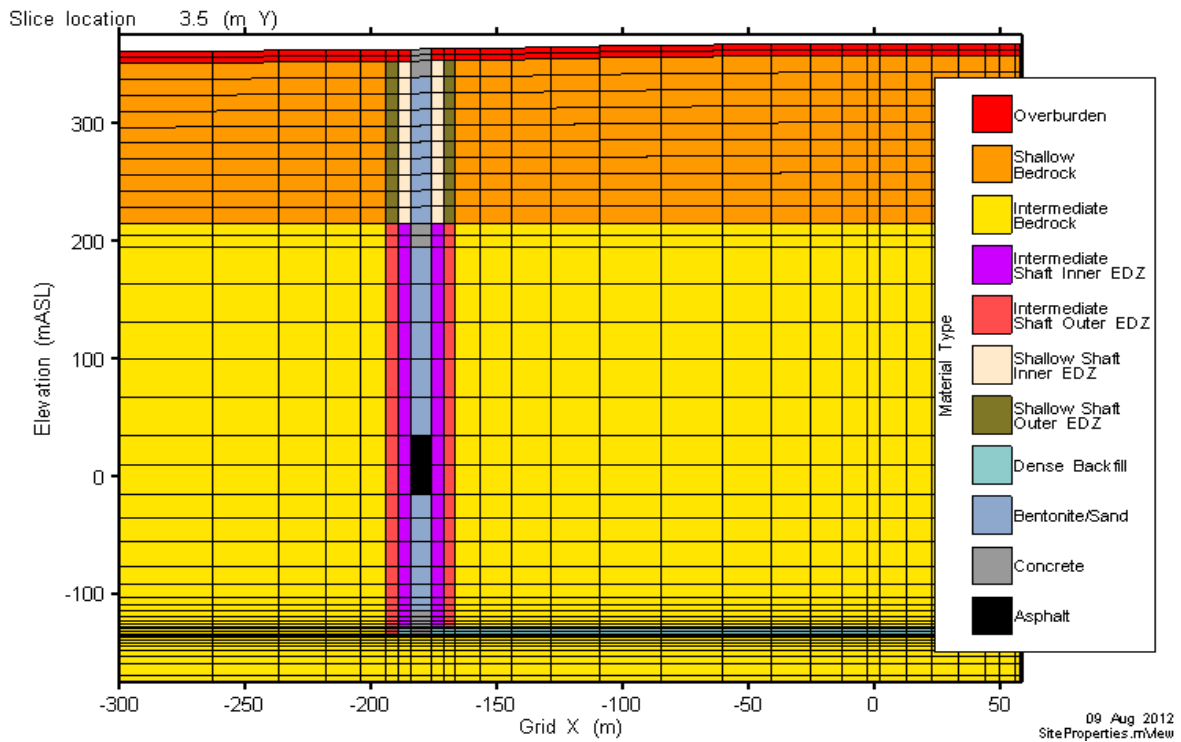


Figure 7-16: Site-Scale Model: Property Assignment on Vertical Cross-Section through Main Shaft

Property assignments on a plan section through placement rooms are shown in Figure 7-17. The curved entrances to the rooms are represented as right-angle intersections.

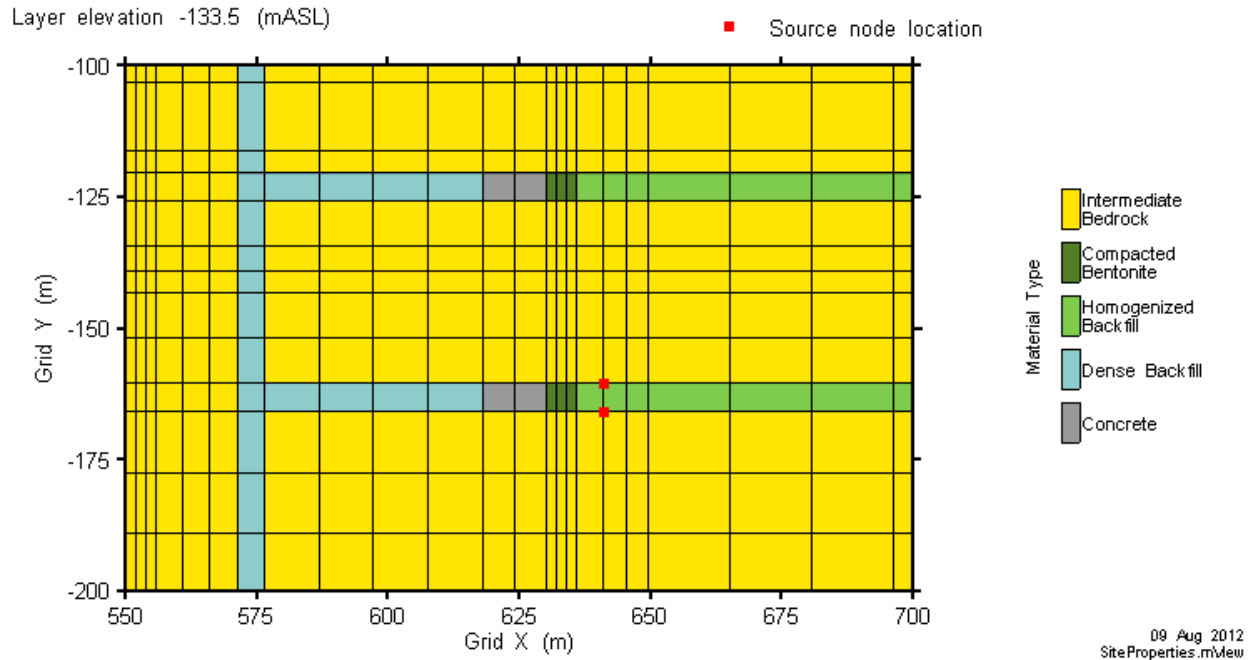


Figure 7-17: Site-Scale Model: Property Assignment on Plan View through Placement Rooms

Well Location and Hydraulic Head Boundary Conditions

The water-supply well is located on the element segment most closely corresponding to the Sub-Regional Model well segment. Head boundary conditions for the Site-Scale Model are extracted from the head field calculated with the Sub-Regional Model, with different boundary conditions applied for each well demand case.

Head values for the Reference Case along the vertical model boundaries are shown in Figure 7-18. Surface boundary conditions follow the surface topography and bottom boundary conditions (1500 mBGS) are set to zero flow; these are not illustrated in the figure.

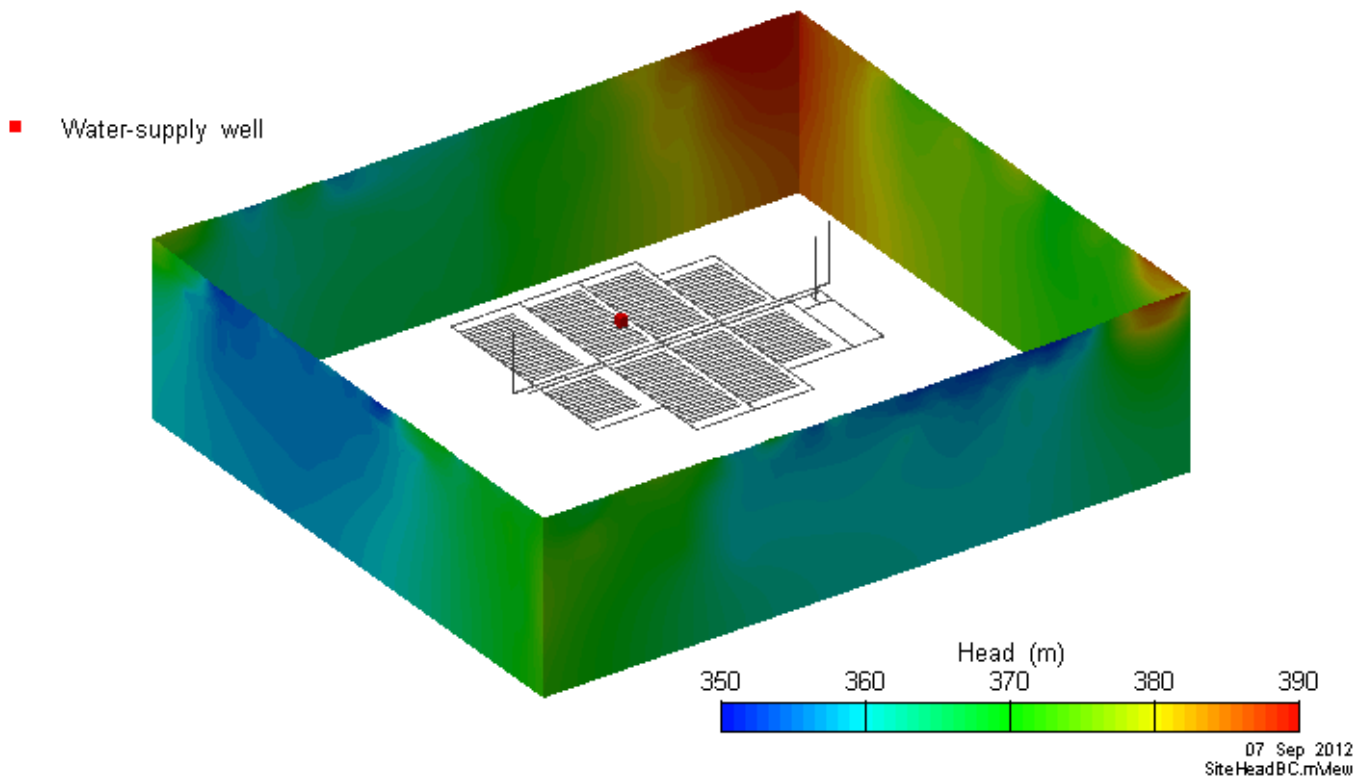


Figure 7-18: Site-Scale Model: 3D Visualization of Reference Case Head Boundary Conditions on Vertical Model Boundaries

7.5.3.3 Repository-Scale Model

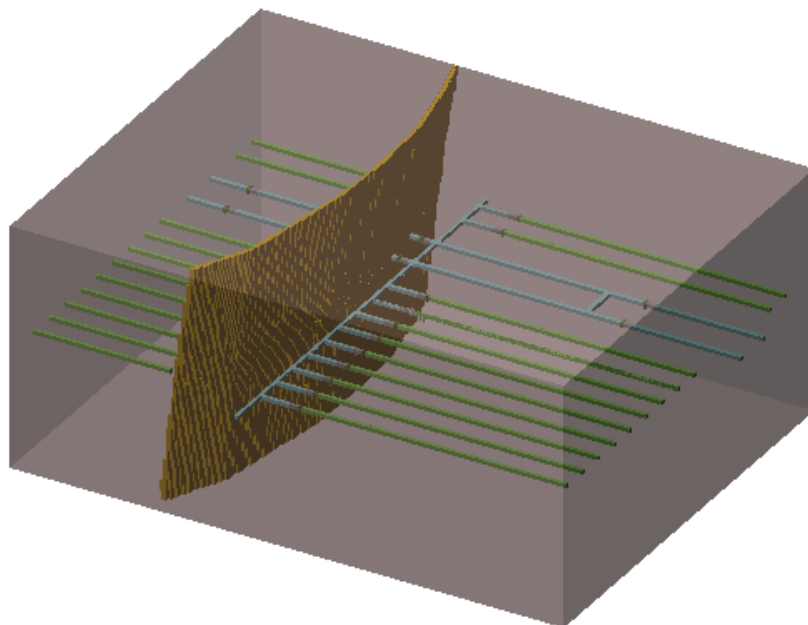
This model encompasses a small section of the repository surrounding the source location and the adjacent geosphere. The model incorporates significant detail and individual containers are represented. The model is used to corroborate results of the Site-Scale Model, to provide radionuclide transport results for comparison with results of the SYVAC3-CC4 system model, and to provide a more complete understanding of repository component functions.

Radionuclide transport calculations are performed for I-129, C-14, Cl-36, Ca-41, Sn-126, Cs-135, U-234 and U-238. These radionuclides are typically the most important in terms of potential radiological impact or in representing a range of low-sorption to high-sorption species.

Domain Discretization and Property Assignment

The model is discretized over a domain of approximately 800 m x 630 m x 350 m in the X, Y, and Z directions respectively. The domain incorporates a small number of placement rooms and a section of perimeter access tunnel near the well. The fracture connected to the well is shown within the domain, although the well is not. The model discretization is 285 nodes in the X direction, 376 nodes in the Y direction, and 91 node layers in the Z direction, for a total of 9.59 million elements.

The extent of the model is shown in Figure 7-19.



Note: The brown plane represents a fracture

Figure 7-19: Repository-Scale Model: 3D Visualization of Domain Elements

The model includes two material types in addition to those listed in Table 7-17. Gap Fill is used to seal the area between the compacted bentonite blocks and the room walls in the placement room seal while 70°C Compacted Bentonite surrounds the container (70°C refers to the temperature at which the hydraulic properties are calculated and reflects the thermal impact of the container on the near-field EBS). Material properties are given in Table 7-18.

Table 7-18: Repository-Scale Model: Flow Model Properties

Property Identifier	Description	Hydraulic Conductivity (m/s)	Porosity
70°C Compacted Bentonite	Around Container	3.4×10^{-13}	0.428
Gap Fill	Room Seal Component	3.7×10^{-13}	0.486

Note: Data from Garisto et al. (2012).

The placement rooms and engineered barrier system are discretized at differing levels of detail. The room containing the radionuclide source is discretized at the highest level of detail and contains representations of the first three containers in the room. The geometry includes a basic representation of the curved room ceiling, and includes light backfill (i.e., gap fill) surrounding the compacted bentonite blocks / bricks in the room seal. All other placement rooms are square, as shown in Figure 7-20. The figure shows fracture elements as translucent. The placement of the fracture seals in the main access drifts is also shown.

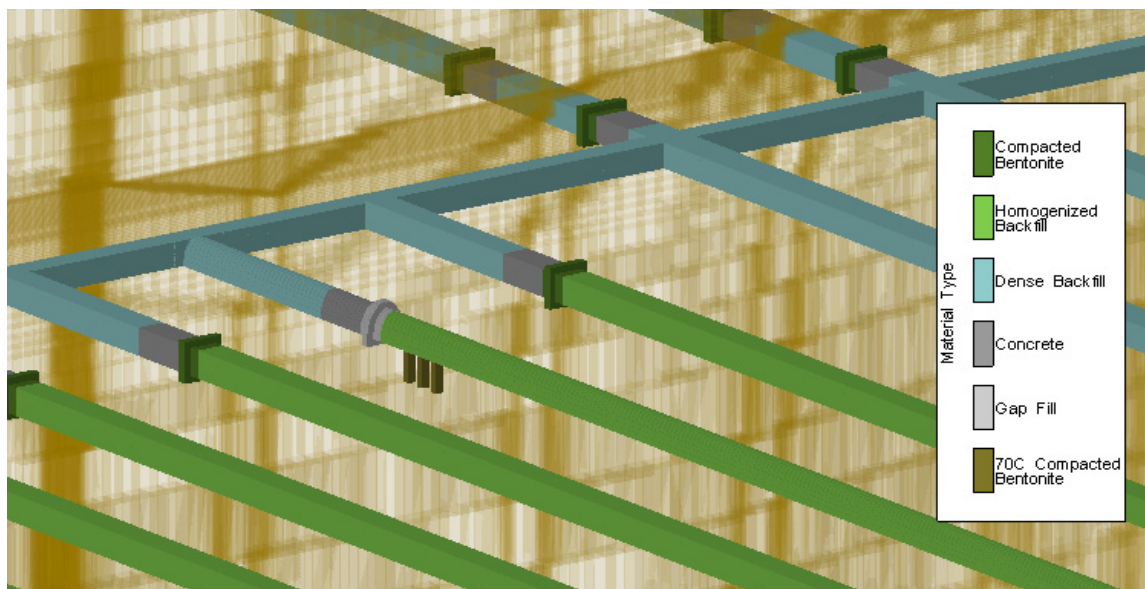


Figure 7-20: Repository-Scale Model: 3D View of Repository Room, Tunnel Seals and Three Assumed Defective Containers

The coordinate system is modified slightly from the Site-Scale Model, in that the X axis ($Y = 0$ m) is centred on the detailed placement room and the Y axis ($X = 0$ m) is shifted to the centre of the Panel C/D cross-cut tunnel, as shown in Figure 7-21.

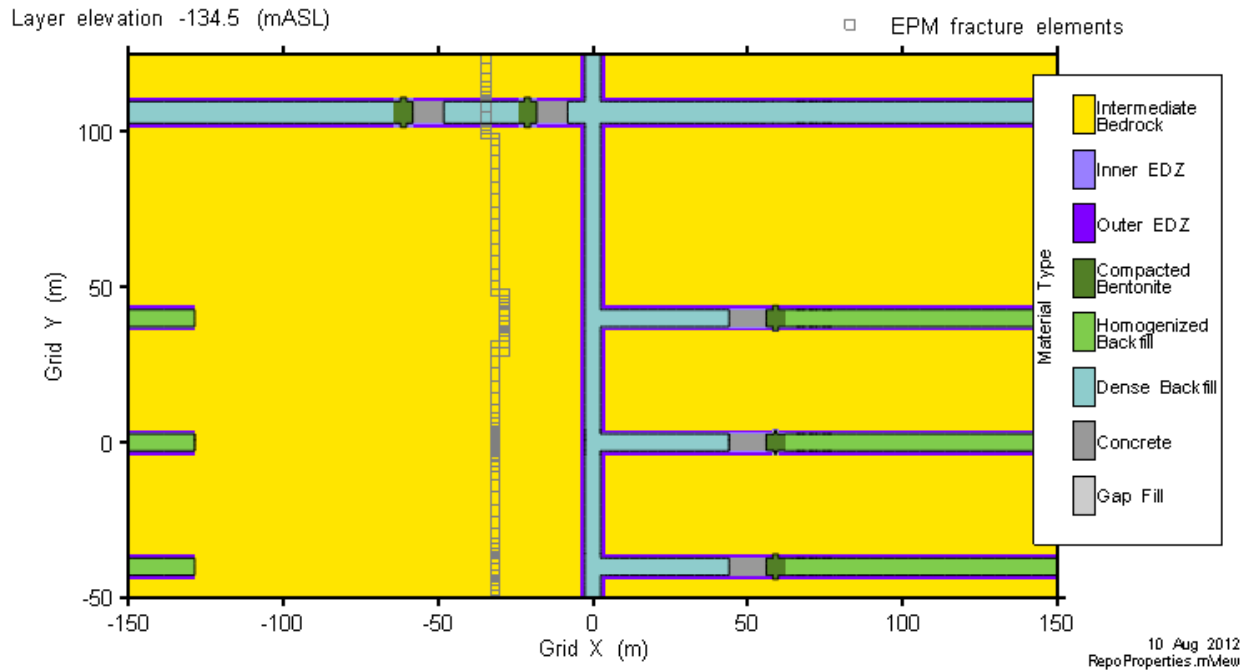


Figure 7-21: Repository-Scale Model: Plan View of Sealing Arrangement in Rooms and Tunnel

Figure 7-22 and Figure 7-23 show property assignments in vertical cross-sections along the placement room assumed to contain the containers with undetected defects and perpendicular through the room seal respectively.

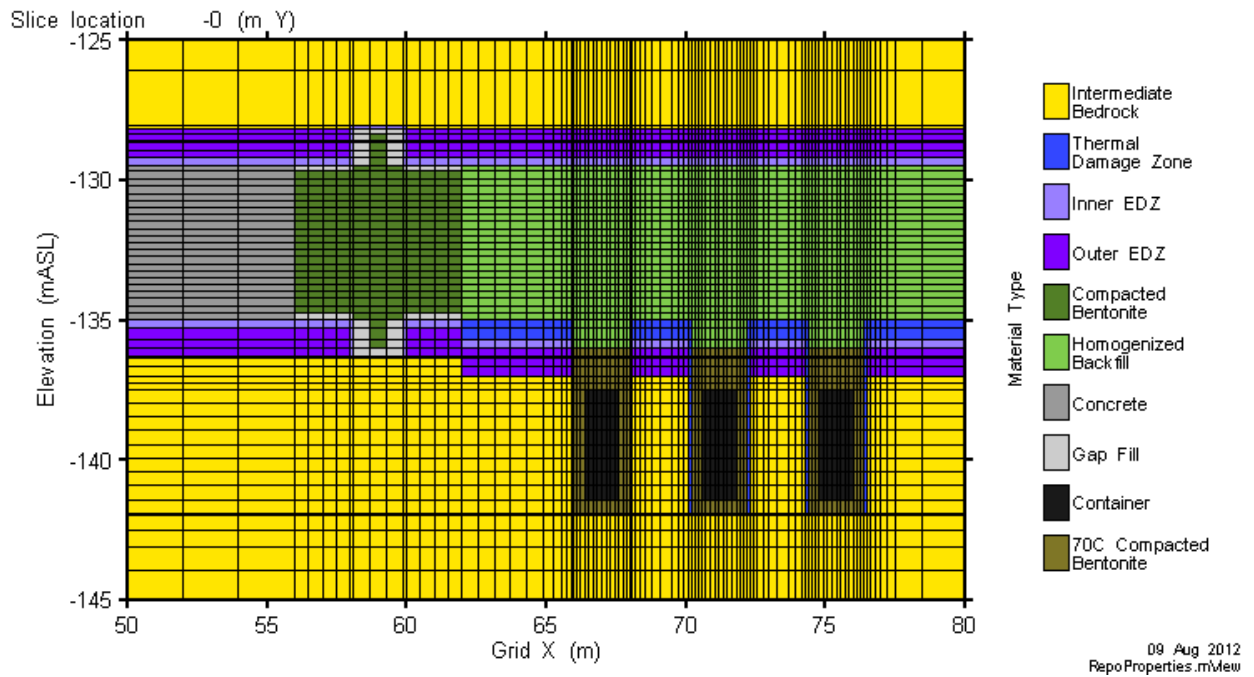


Figure 7-22: Repository-Scale Model: Vertical Slice along Placement Drift (Y = 0 m)

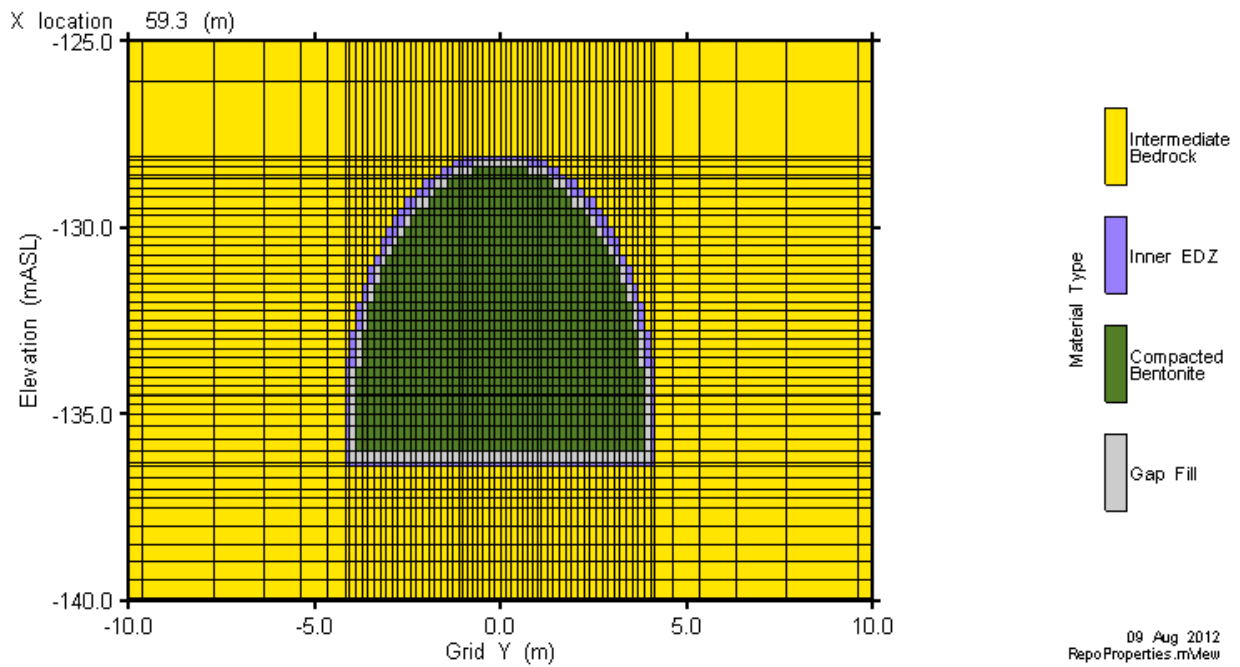


Figure 7-23: Repository-Scale Model: Vertical Slice through Placement Drift Room Seal (X = 60.5 m)

Figure 7-24 is a 3D cutaway showing the assignment of EBS and EDZ / TDZ materials. Source term nodes are also shown. Contaminants that escape the containers are applied over three nodes at the interface between the container and the surrounding buffer material, at the container-lid weld to represent a small hole. Note that only one source node is visible in the figure.

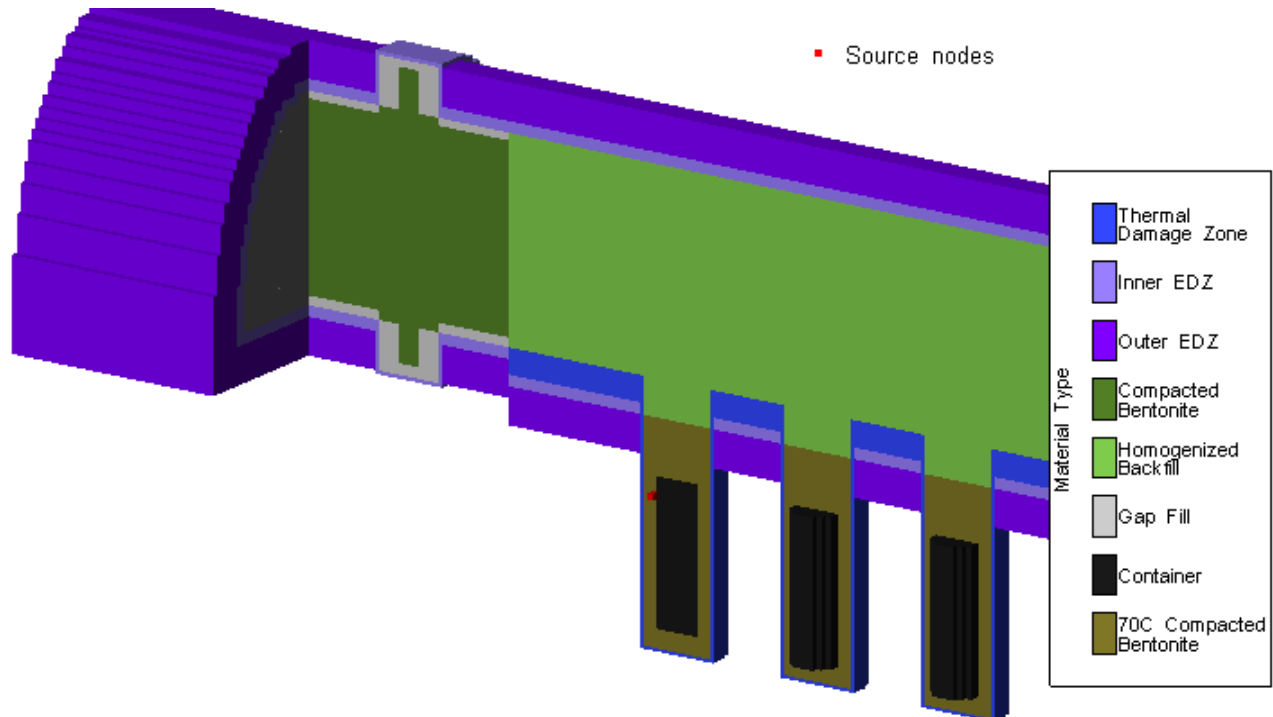


Figure 7-24: Repository-Scale Model: 3D View Showing Defective Container Source Nodes

Hydraulic Head Boundary Conditions

Head boundary conditions are extracted from the Site-Scale Model and values are specified for all external model nodes.

Boundary conditions for the Reference Case are shown in Figure 7-25.

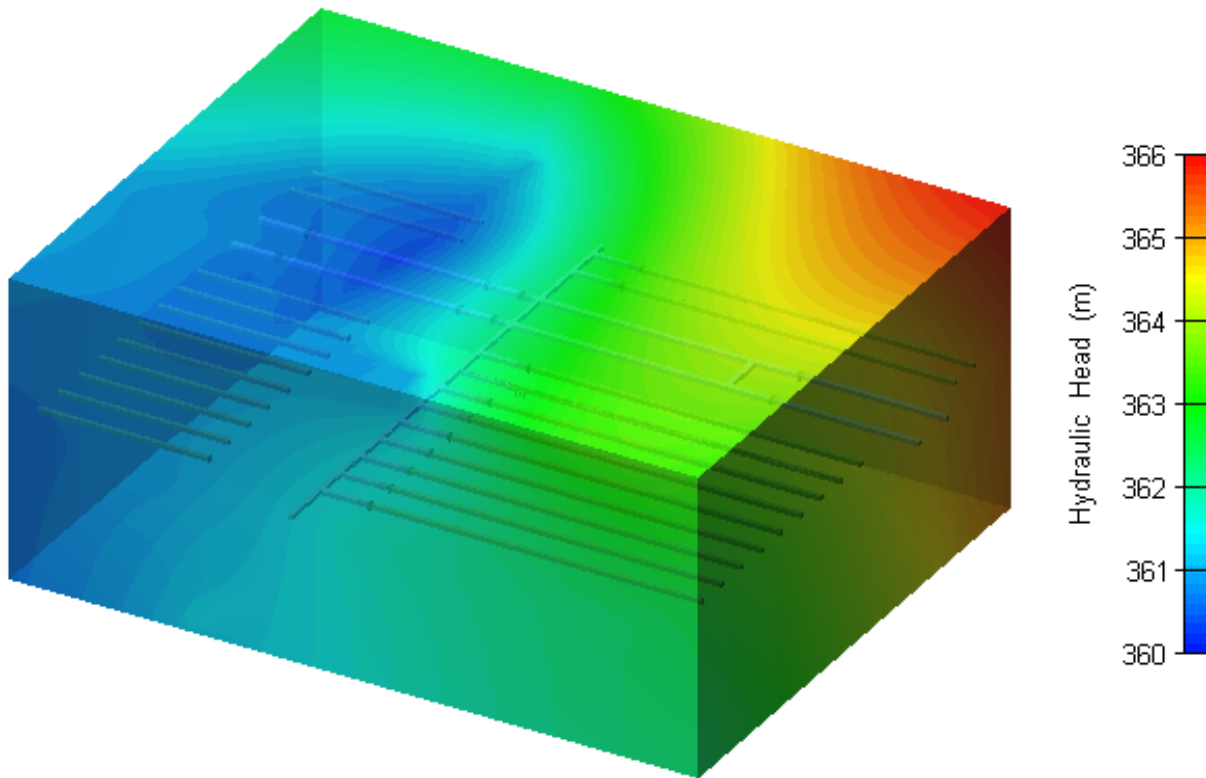


Figure 7-25: Repository-Scale Model: 3D View of Reference Case Head Boundary Conditions

Radionuclide Source Term

The FRAC3DVS-OPG code does not have a contaminant release model. Radionuclide release rates from the container¹ are therefore calculated with the SYVAC3-CC4 release model and imposed as a boundary condition at the source nodes, one of which is shown in Figure 7-24.

The radionuclide release rates used are shown in Figure 7-26.

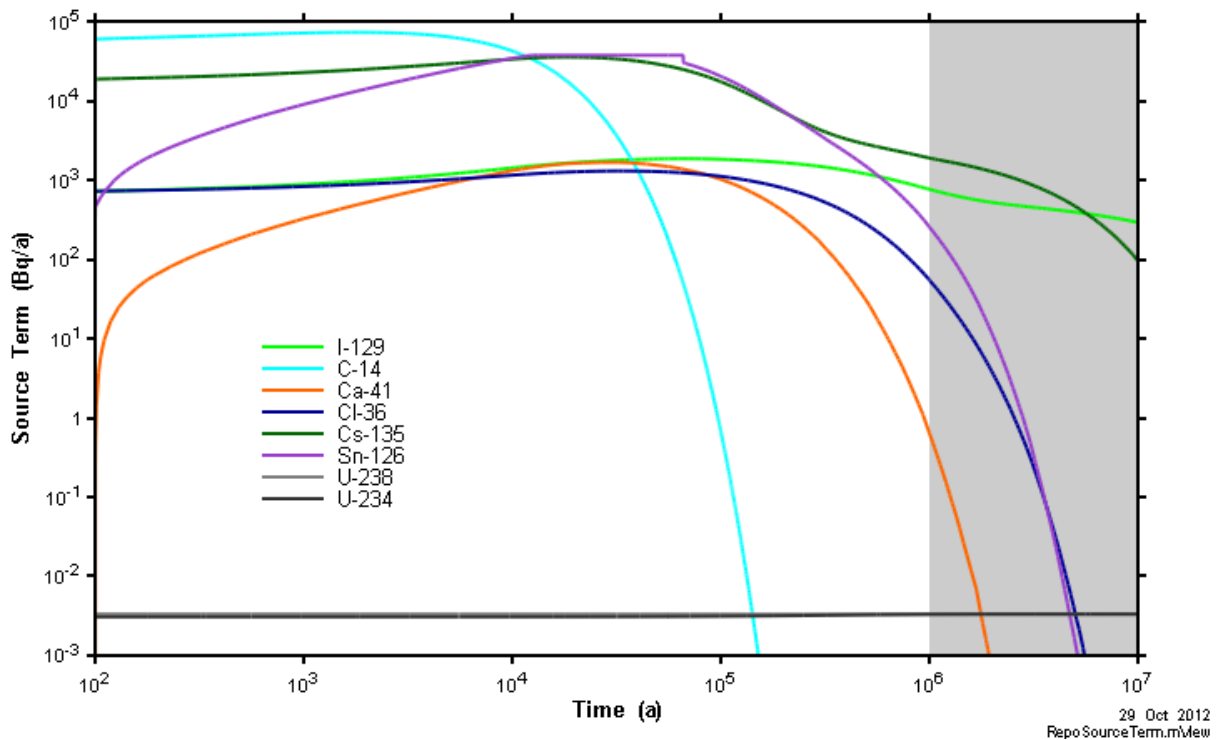


Figure 7-26: Radionuclide Release Rates from Three Defective Containers

7.5.4 System Model

The SYVAC3-CC4 system model combines an idealized geometric description of the repository and a simple geosphere transport model with more detailed representations of releases from the used fuel and radionuclide transport in the biosphere to compute the radiological consequences of releases to the environment.

¹ The Reference Case assumes three used fuel containers are placed in the repository with small undetected defects. Accordingly, mass transport simulations assume the release rate from the defective container is equivalent to the calculated release from three defective containers.

The description provided here applies to the situation in which the climate, biosphere and geosphere are constant throughout the simulation. The groundwater flow field is also constant.

7.5.4.1 Radionuclide Source Term

The reference waste form is a standard CANDU 37-element fuel bundle with a burnup of 220 MWh/kgU and an average fuel power during operation of 455 kW. Chapter 3 identifies the radionuclides of interest and their associated inventories.

Section 7.3.1 describes that radionuclides within the UO₂ fuel are released by two distinct mechanisms which operate on very different time scales. These mechanisms are referred to as “instant release” and “congruent dissolution”.

Table 7-19 shows the instant release fractions for selected radionuclides used in this study.

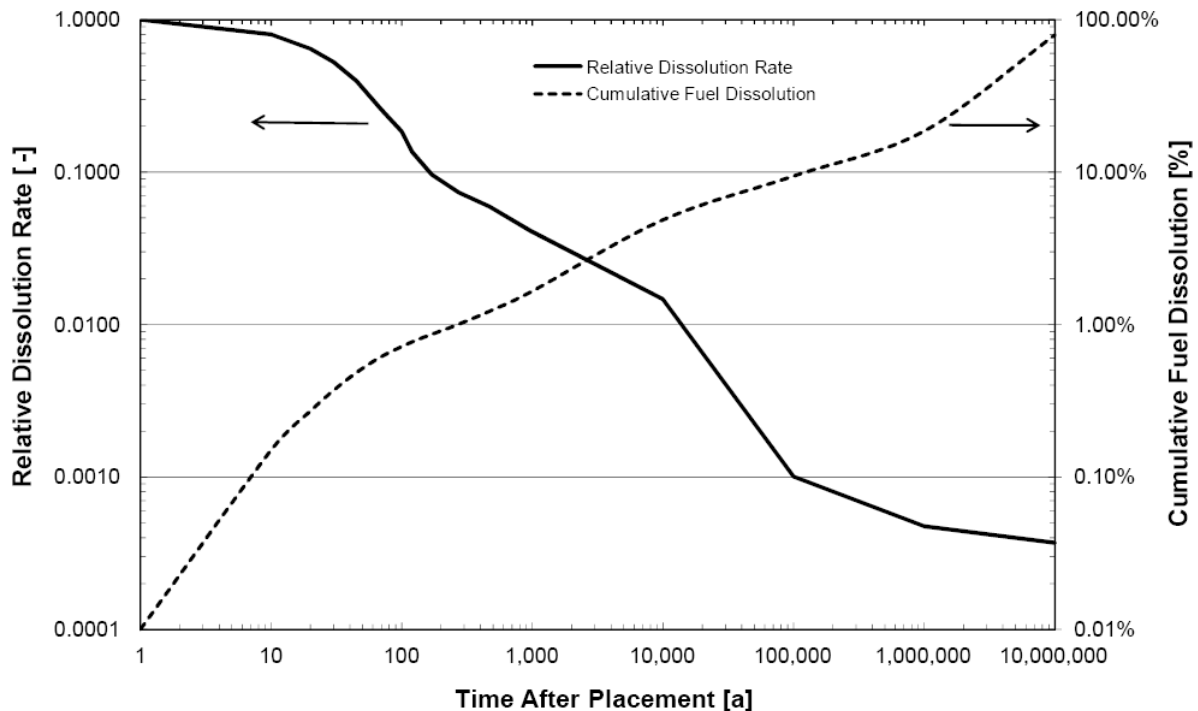
Table 7-19: Instant-release Fractions for Selected Radionuclides

Radionuclide	Instant-Release Fraction (% of Inventory)
C	2.7
Cl	6
Cs	4
I	4
Se	0.6
Sn	0
Am, Np, Pa, Pu, Th, U	0

Note: From Garisto et al. (2012).

Figure 7-27 presents fractional and cumulative information for congruent dissolution of the fuel.

The system model uses the instant release and congruent release together with solubility limits and information on the water volume inside the container to calculate radionuclide concentrations. Radionuclides thereafter escape the container and enter the surrounding low hydraulic conductivity buffer.



Notes: Relative Dissolution Rate is the ratio of the time-dependent fuel dissolution rate to the maximum fuel dissolution rate. The maximum dissolution rate is 3.12×10^{-3} [mol/m²/a] where the area is the surface area of the fuel in contact with water. A contact area of 1570 m² per container is used in this study which assumes the fuel is highly fragmented. The maximum dissolution rate is therefore 4.9 mol/a.

Figure 7-27: Fuel Dissolution Rate

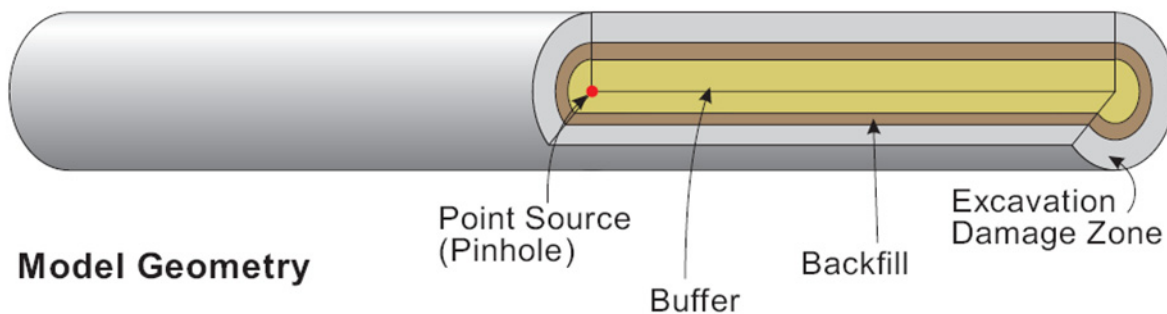
7.5.4.2 Repository Model

The repository model uses a series of concentric cylinders of varying thicknesses (as shown in Figure 7-28) to approximate radionuclide transport through the buffer, backfill and excavation damage zone. This simplification allows for the use of semi-analytical solutions which result in fast computation times suitable for use in probabilistic analyses.

Conceptually, the model is dimensioned to represent one in-floor borehole. Specifically, input data for the concentric rings are specified to represent only the buffer (36 cm radius) and borehole EDZ (a further 8 cm thickness). The length of the cylinder is 6.92 m which

corresponds to the depth of the borehole. Transport within the placement room is part of the geosphere related transport network.

The radionuclide release from the defect is represented by a source that lies along the axis of the nested cylinder. The container is not physically represented.



Note: the backfill thickness is 0 cm in the repository model used in this study.

Figure 7-28: SYVAC3-CC4 Repository Model

The repository model simulates the following processes:

- Container Failure – At a specified time some of the containers are assumed to fail. In the Normal Evolution Scenario failure occurs in the form of a small initial defect in the corrosion resistant copper shell allowing water to enter the container.
- Instant Release – A fraction of soluble fission products at the UO_2 fuel grain boundaries and cladding gap is instantaneously dissolved once the container is breached and water comes into contact with the fuel.
- Congruent Release – A slow long-term radionuclide release consistent with the long-term corrosion / dissolution of the ceramic fuel pellet and release of radionuclides trapped within the fuel matrix.
- Precipitation – The precipitation of elements whose concentration in the container exceeds the solubility of the element.
- Radioactive Decay and Ingrowth – Radioactive decay of radionuclides and progeny.
- Transport – The diffusive and advective transport of radionuclides through the engineered barrier system (including the defective container).

The failed container begins to fill with water as soon as the surrounding buffer is saturated. This buffer saturation is conservatively assumed to occur 100 years after the container is placed in

the repository, although it is likely to take much longer in low hydraulic conductivity rock. The time for the container to fill with water is further conservatively neglected so that a continuous water-filled pathway between the container interior and the surrounding buffer is assumed to exist immediately at 100 years. Note that some models indicate this pathway could take tens of thousands of years to establish due to formation of gas within the container (Bond et al. 1997).

In the deterministic analyses, the three failed containers are conservatively assumed to be in the repository location with the shortest groundwater transport time to surface. In the probabilistic analysis, since each container has only two states (i.e., intact or failed), the failure rate is described by a binomial distribution with the probability of failure being approximately 1 in 5000 containers. The location, time of failure, and number of failed containers are random variables.

The radius of the container defect for the Reference Case of the Normal Evolution Scenario is 1 mm. An upper limit of 2 mm is applied in the probabilistic analysis since defects of this size and larger will be readily detectable during the container inspection process prior to placement.

7.5.4.3 Geosphere Model

The geosphere is represented as a network of 1D transport segments. Each 1D segment represents a path in which transport is primarily in one direction, with relatively uniform material properties. This network is defined to approximate the stratigraphy and the hydrological and geochemical features of the geosphere zones located between the repository and the surface biosphere. Transport in each segment is characterized using the 1D advection-dispersion equation, for which robust semi-analytical solutions are available.

The starting point for generation of the SYVAC3-CC4 geosphere network is a detailed steady-state groundwater advective flow field for the site computed using FRAC3DVS-OPG. From this, a set of pathways is generated that map how a particle released at the repository moves with the advective flow field. Assembly of the transport network, including diffusion, then consists of the following steps:

- Sector Selection – The repository is divided into sectors. A sector is typically defined so that its properties are uniform. For example, it has the same waste form type and room length, and it connects to a portion of the groundwater flow field whose properties are approximately uniform for the entire sector. Different sectors typically have different properties, and often the properties of the surrounding geosphere are the delineating factor.
- Selection of Representative Pathways – A representative pathway for each sector is generally chosen to give the conservatively shortest travel time to the surface. In areas of low flow velocity, diffusion towards fractures may be the shortest travel path. Tracks may merge with tracks from other sectors along the pathway and may diverge as portions of the plume are captured by wells or terrestrial discharge areas.
- Selection of Nodes along Pathways – Nodes are generally selected at material property boundaries so that the resulting segments have constant properties. Additional nodes are selected to approximate curved transport paths.

- Addition of Well and Near-surface Nodes – Additional nodes are required for the well - for example, upper and lower reference nodes define the range of positions for the well and drawdown nodes, which give a better representation of the drawdown cone in the vicinity of the well. Also, near-surface nodes are added to define an overburden and a sediment node for each discharge location, and possibly terrestrial and wetland discharges associated with aquatic discharges.
- Property Assignment – Data needed include the Cartesian coordinates of all the nodes, hydraulic heads and temperatures at the nodes, and hydraulic and chemical properties of the different geosphere zones.
- Well Model – The effects of the well drawdown on adjacent node heads is accounted for via an analytical well model within the aquifer, and by a site-specific well-effects model outside the aquifer.

Sector Selection

Since all containers contain the same used fuel waste form and the placement room design is common across the repository, the main distinction between the sectors is the influence of the surrounding groundwater flow field.

For this study, a set of 7680 advective flow transport pathways is obtained from FRAC3DVS-OPG for the Reference Case of the Normal Evolution Scenario, with the pathways starting in the placement rooms at the repository horizon. FRAC3DVS-OPG identifies five discharge locations, hereafter referred to as “River”, “Lake”, “Central Wetland”, “West Wetland” and “East Wetland”.

The top panel of Figure 7-29 shows the origins of the pathways at the repository horizon. Note that some of the pathways that would otherwise go to the River, Central Wetland and East Wetland discharge areas are captured by the well, with the capture fraction depending on the well demand.

Some long-duration advective pathways travel through a deeper flow system and reach the edges of the model without discharging at surface, and these are shown as "stagnant" pathways in Figure 7-29. Also marked stagnant are pathways originating from an area near the northern edge of the repository. These stop due to numerical issues upon encountering a sub-horizontal fracture. Consistent with the head gradient from the point of stalling, these are assigned to the Central Wetland.

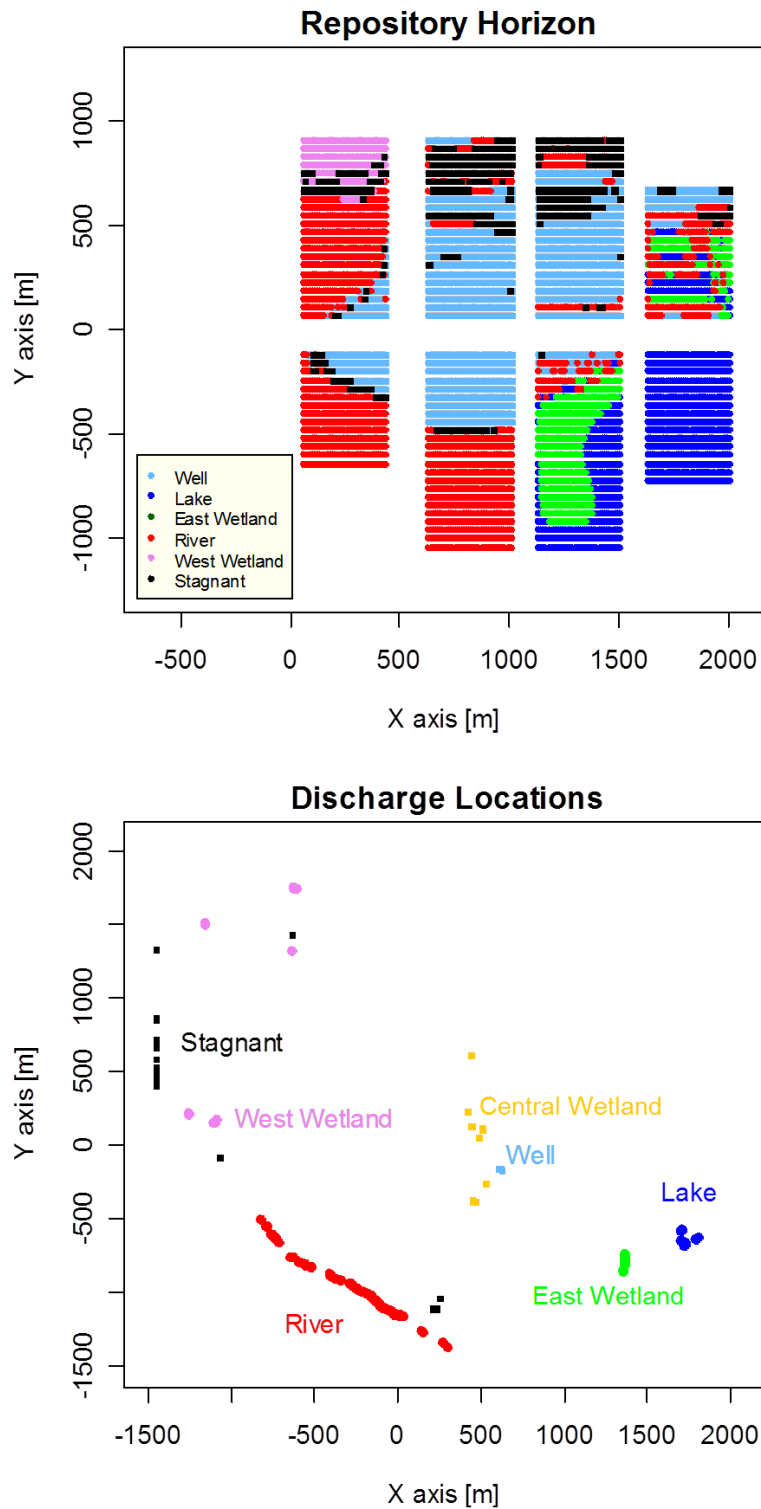
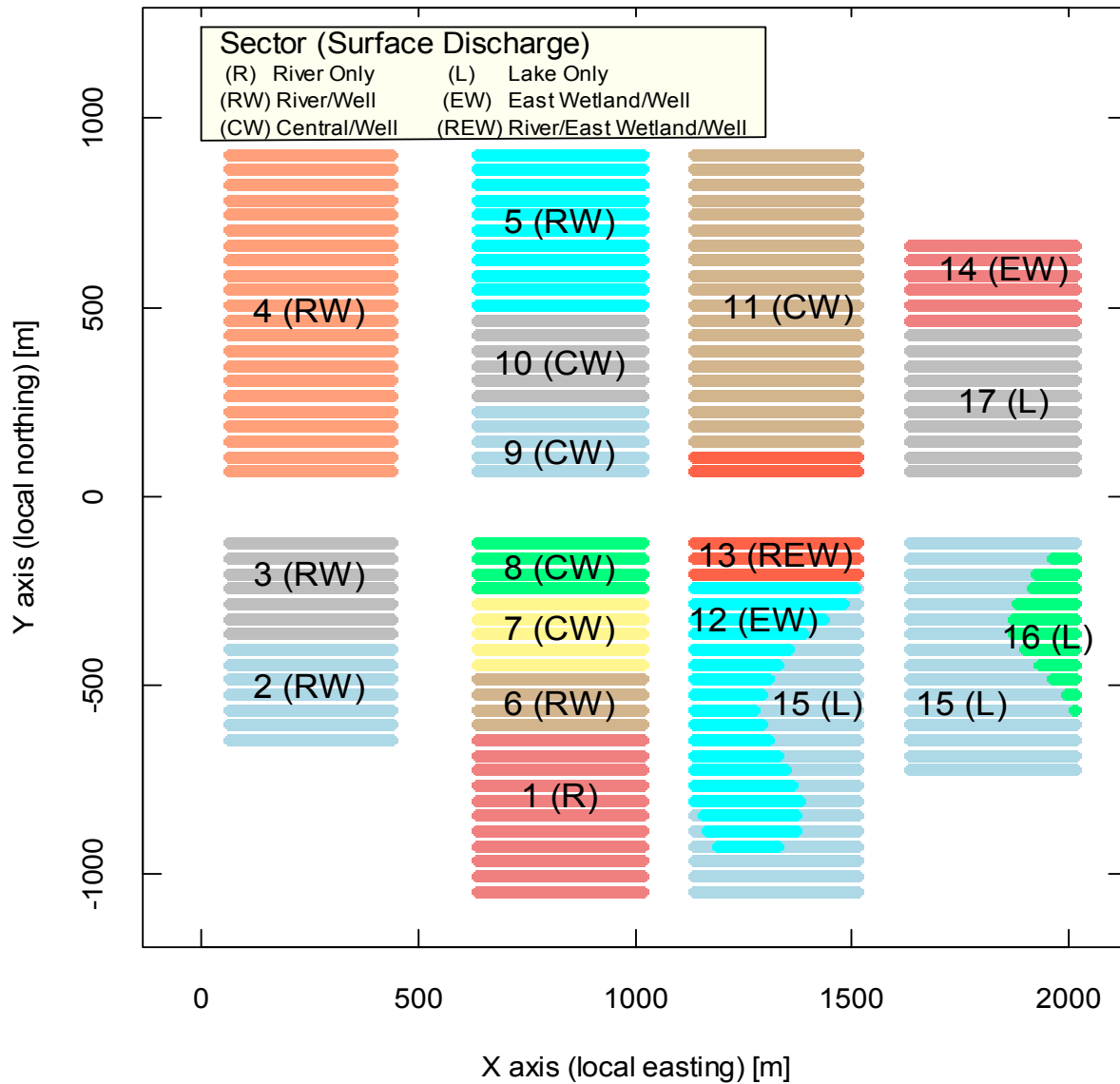


Figure 7-29: Origin and Discharge Locations of Advective Transport Pathways for a Well Demand of 911 m³/a

This consideration of the discharge patterns gives an initial division of the repository into several sectors, these being locations where the discharge is either to the Well, Lake, River, West Wetland, East Wetland or Central Wetland discharge location. Since a detailed analysis of the advective transport pathways shows there is a wide range of travel times and routes, the repository sectors are further combined or subdivided. For example, the number of pathways leading to the West Wetland is relatively small with travel times similar (or longer) to transport times for pathways originating from the neighbouring area leading to the River. To simplify the model, the pathways leading to the West Wetland have been combined with those leading to the River (a geographically close area) in Sector 4. Also, the multiple colors for the East-North corner of the repository (see the top panel of Figure 7-29) suggests a complicated groundwater flow field with multiple discharges for the $911\text{m}^3/\text{a}$ well case. The results of the detailed analysis of the transport pathways for that area indicate that the flow field there can be conservatively represented by three pathways with three discharge areas (Lake, East Wetland, and Well).

The final division resulted in 17 unique repository sectors arranged as shown in Figure 7-30. In this figure the sectors are numbered 1 through 17 with the surface discharge locations indicated by letter. For example the sector labelled 2 (RW) indicates Sector 2 has a groundwater flow path that discharges to the River with a portion of the ground water flow captured by the Well. Some sectors have no capture of the ground water flow by the well and hence a single letter is used.



Summarv v05a.r

Figure 7-30: Repository Sectors and Surface Discharge Locations

Over twelve thousand containers are distributed among the 17 sectors. The number of containers in each sector is obtained from the fraction of the 7680 pathways that have their origin in each sector. Table 7-20 shows the numbers of containers in each sector. Sector 13 has two discharge locations for the No Well case (East Wetland and River); hence, two travel times are shown.

Table 7-20: Container Distribution by Repository Sector

Repository Sector	Number of Containers	Well Demand = 0 m ³ /a		Well Demand = 911 m ³ /a*	
		Discharge Location	Travel Time (a)	Well Capture (%)	Travel Time to the Well (a)
1	878	River	8.88×10 ⁴	0	-
2	560	River	1.63×10 ⁵	0	-
3	560	River	5.29×10 ⁵	41	1.14×10 ⁵
4	1757	River	6.03×10 ⁵	10	1.76×10 ⁵
5	878	River	9.27×10 ⁵	43	1.03×10 ⁶
6	319	River	1.77×10 ⁵	2	3.30×10 ⁵
7	399	Central Wetland	4.88×10 ⁴	100	5.12×10 ⁴
8	319	Central Wetland	3.21×10 ⁴	100	2.24×10 ⁴
9	399	Central Wetland	1.92×10 ⁵	100	5.44×10 ⁴
10	479	Central Wetland	4.32×10 ⁵	94	3.95×10 ⁵
11	1597	Central Wetland	3.05×10 ⁵	53	3.05×10 ⁵
12	830	East Wetland	1.05×10 ⁵	0	-
13	399	East Wetland	1.42×10 ⁵	52	1.01×10 ⁵
		River	4.28×10 ⁵		
14	479	East Wetland	6.08×10 ⁵	46	5.96×10 ⁵
15	1922	Lake	1.22×10 ⁵	0	-
16	203	Lake	6.86×10 ⁴	0	-
17	800	Lake	2.34×10 ⁵	0	-

Note: * This is the Reference Case well demand.

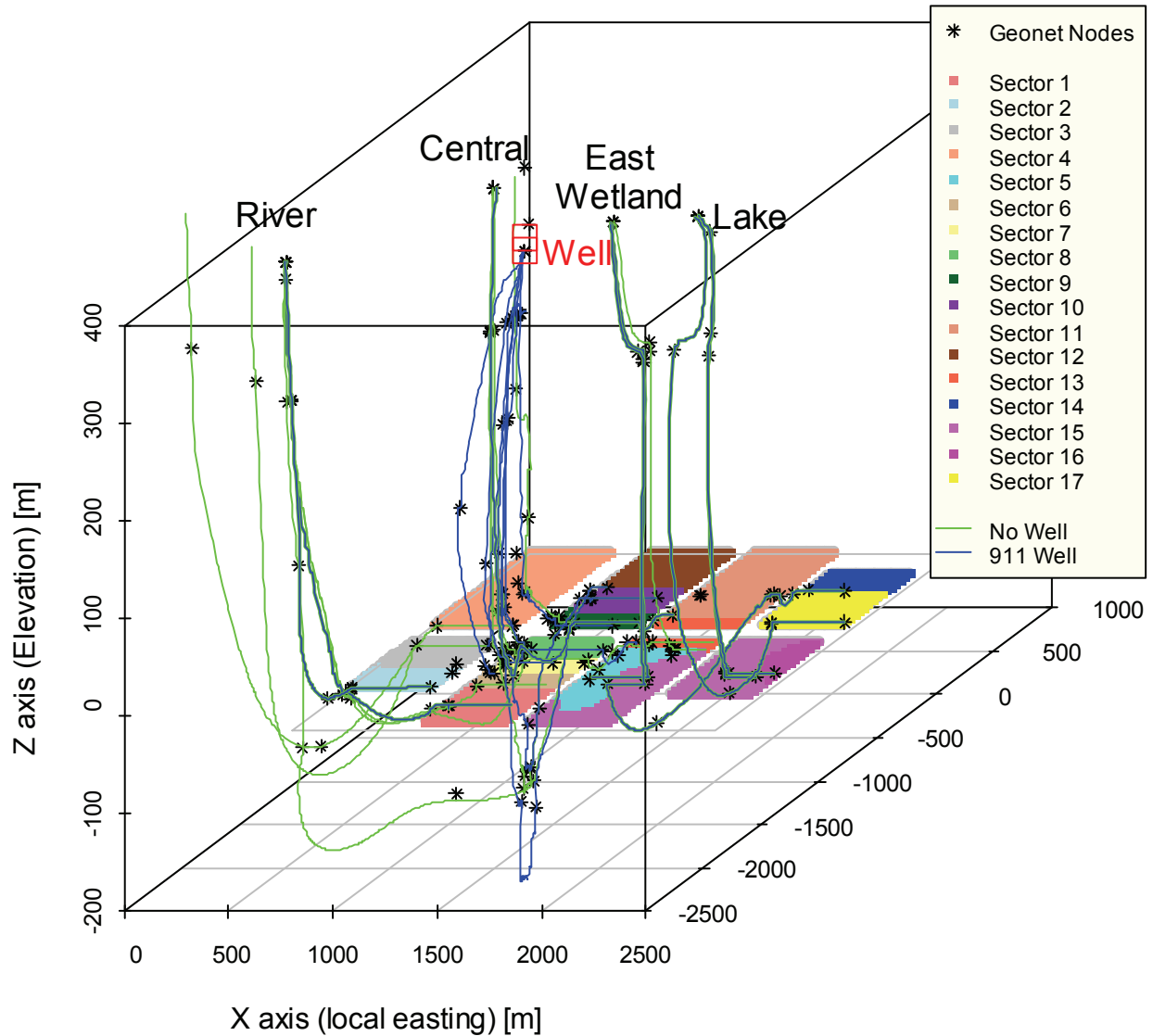
Selection of Representative Pathways

For each sector, a representative transport pathway is selected to approximate the transport segment leading to the discharge point at the surface. These pathways may converge and combine on the way to the surface, or conversely may diverge and lead to different discharge points, depending on conditions such as the well demand rate.

When choosing the representative pathway, the pathway from each sector with the shortest advective transport time is selected as a conservative approximation. Since these pathways are based on advective flow, radionuclides may move in different directions in regions where the transport is diffusion dominated. To account for this, in diffusion dominant regions the pathway is conservatively taken as the shortest distance to an area of advective flow that readily leads to the surface.

The minimum travel times and discharge locations for each sector are shown in Table 7-20.

Figure 7-31 shows a representation of the transport pathways for the case with a well demand of 911 m³/a (blue lines) and for the case with a well demand of 0 m³/a (green lines).



Notes: Green lines are the "No Well" case and blue lines are the "911 m³/a Well" case.

PartTracks_S1-17_v04a.r

Figure 7-31: Representative Transport Pathways for the Repository Sectors

Selection of Nodes along Pathways

The transport pathways in Figure 7-31 show convergence and curvature as they lead towards the discharge points. Nodes are defined at material property boundaries and at some intermediate points. Pathways are merged where appropriate, and divergence nodes are located where direction changes occur because of well operation.

Addition of Well, Overburden and Sediment, and Other Features

Four additional nodes are associated with the well. A well discharge node is located at the ground surface immediately above the well aquifer node (the resulting well depth is 100 m). A well capture algorithm determines how much of the contaminant plume is captured by the well.

Additional terrestrial discharge nodes are associated with the two aquatic discharges (Lake and River). Furthermore, each aquatic and terrestrial discharge has an overburden and sediment / soil node associated with it for a total of 12 additional nodes.

With these additional 16 nodes, the complete network consists of 190 nodes. The network and its connectivity are shown schematically in Figure 7-32. Radionuclides released from Sectors 15 to 17 (River group) are not captured by the well.

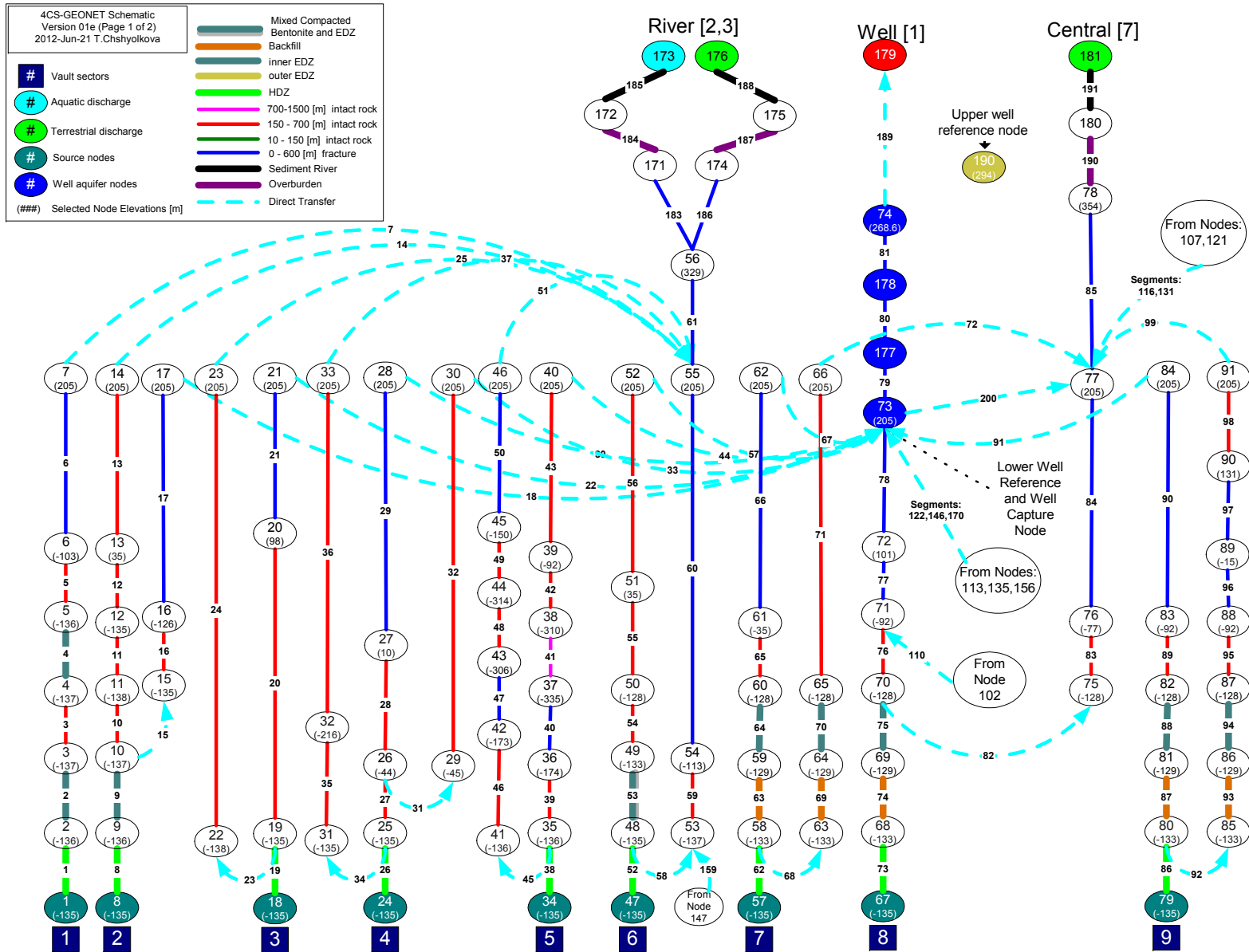
Used Fuel Repository Conceptual Design and Postclosure Safety Assessment in Crystalline Rock

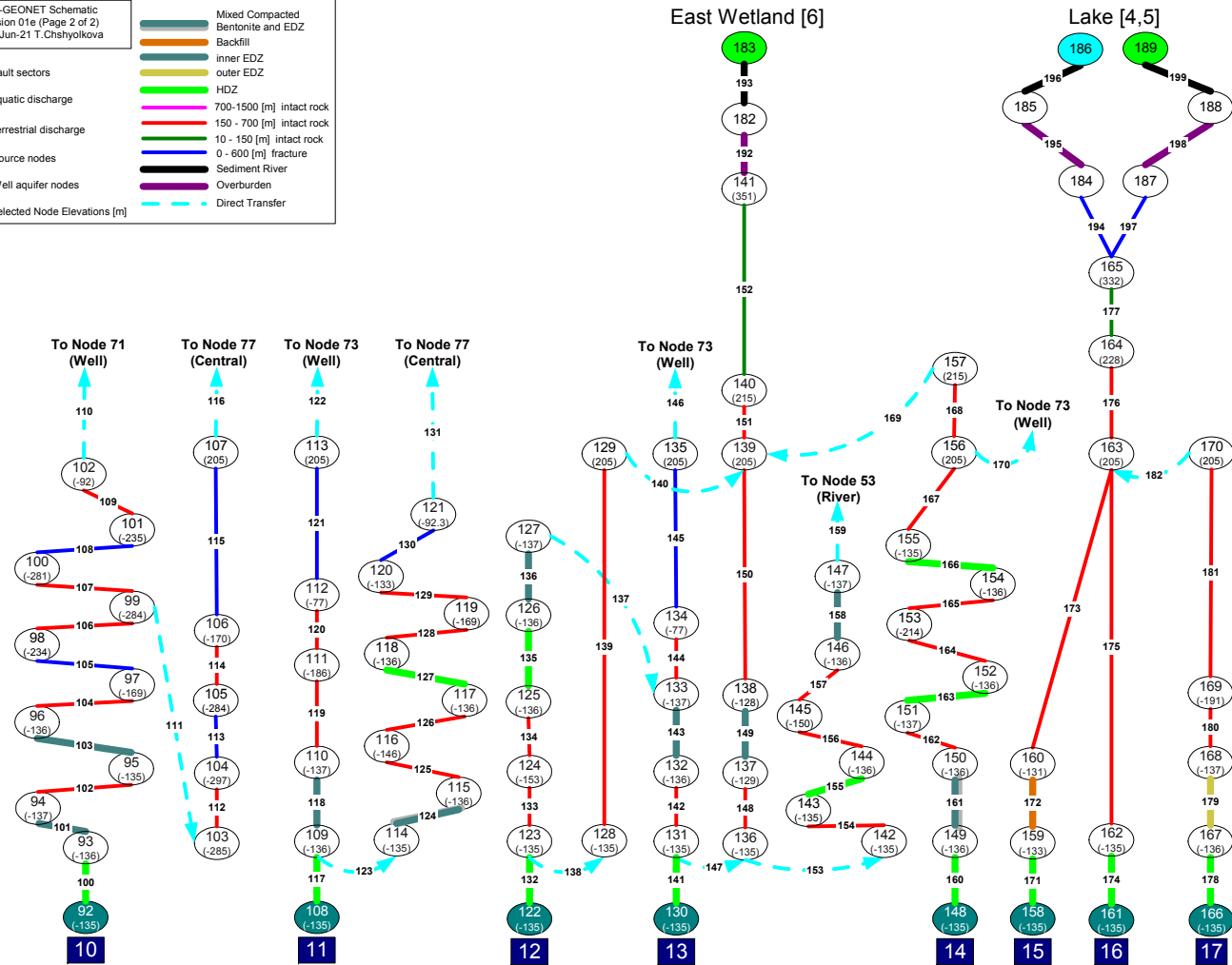
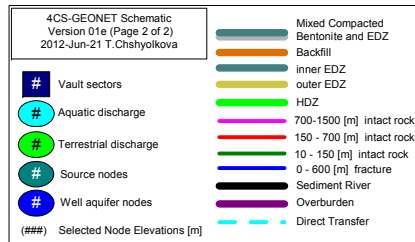
Document Number: NWMO TR-2012-16

Revision: 000

Class: Internal

Page: 352





Notes: Only nodes (ellipses) with a particular function are colour coded. The line segments, representing the 1D transport pathways, are colour coded (see legend) to indicate the geosphere zone through which they pass.

Figure 7-32: SYVAC3-CC4 Transport Network Showing Connectivity

Property Assignment

Once the network is defined, physical and chemical properties are assigned to the various rock, fracture, overburden, and sediment nodes and segments.

Values for the hydraulic heads at each node location are obtained from the FRAC3DVS-OPG results. Values for transport parameters such as porosity and permeability are supplied for each network segment. Advection is typically the dominant component of geosphere transport at shallow depths and in fractures; however, diffusion and dispersion processes are important in instances of very low advective flow (e.g., in the deep geosphere). The model accounts for both advective and diffusive transport processes.

Finally, retardation due to sorption is calculated using the sorption coefficient (K_d) assigned to each network segment.

Well Model

The well is located in a permeable zone capable of supplying sufficient water. This permeable zone is referred to as an "aquifer" although in the current study the actual location is a permeable subvertical fracture zone.

SYVAC3-CC4 uses an analytical solution to provide the hydraulic head drawdown at the nodes and the capture envelope for the groundwater flowing in the aquifer. The analytical solution is based on a constant head boundary condition at the discharge end of a non-leaky aquifer (where "non-leaky" means there is little inflow from the surrounding rock). The well model allows the assessment of well demands other than that in the Reference Case, which is useful in assessing alternative lifestyles or critical groups, and in probabilistic calculations.

The analytical well model is calibrated with the detailed FRAC3DVS-OPG groundwater flow field results. To approximate the FRAC3DVS-OPG groundwater velocities the thickness of the well aquifer is adjusted, as is the hydraulic conductivity of some segments.

In the detailed groundwater flow modelling, all transport pathways from repository Sectors 2 through 14 are captured by the well. In the absence of a well, these pathways lead to the River, Central Wetland, or East Wetland.

The effects of the well extend outside the well "aquifer". These cannot be calculated with the well model equations so the FRAC3DVS-OPG results for different well demands are used to derive empirical relationships that describe these effects. These include: drawdown at nodes outside the aquifer, plume fractionation towards the well at branching locations outside the well aquifer, and reduction factors for discharge areas due to capture of groundwater by the well.

The River, Central Wetland and East Wetland discharge areas are modified according to the portion of plume captured in the well aquifer. When the entire plume in the aquifer is captured by a well, these discharge areas are set to zero. The Lake discharge is unaffected by the well.

7.5.4.4 Biosphere Model

The biosphere model represents a hypothetical but plausible Canadian Shield site.

The topography of the watershed area near the repository is relatively flat as shown in Figure 7-8. The local biosphere is assumed to have the characteristics of the Shield region of central Canada and its properties are assumed constant during the simulation period. The normal present-day variation of climate and other biosphere parameters are included via use of probabilistically sampled parameter values.

Key elements of the model are discussed below. A detailed description of the input data used in the model is available in Garisto et al. (2012).

Surface Water Submodel

Radionuclides discharging from the geosphere enter one or more topological low points. It is conservatively assumed that radionuclides discharging to the well also simultaneously end up in the River, Lake, Central Wetland and East Wetland discharge areas. This allows local biosphere transfer processes such as runoff, recycling and atmospheric suspension and deposition to be treated very simply. The transport processes considered in the surface water submodel are:

- Discharge to River, Lake, Central Wetland or East Wetland – direct discharge from the geosphere into the river, lake, central wetland or east wetland area.
- Sedimentation – contamination of sediments by settling of particulates in the water.
- Biological Uptake – uptake of contaminants by plants and animals residing in the surface water bodies.
- Suspension and Volatilization – loss of contaminants from the surface water to the atmosphere.
- Outflow – flow of contaminated water further downstream. The impact of contaminant releases to the downstream environment is not assessed since they are bounded by the site impacts.
- Irrigation – well water or surface water can be used as the water source for irrigation of soil. In the current study well water is used for irrigation of gardens. The forage field is not irrigated.
- Domestic Use – human water use for drinking, cooking, bathing, laundry, and watering livestock.

Table 7-21 shows the surface water discharge areas. Since discharges are to low-lying areas, they may be covered in part by water. Table 7-21 also provides information on the relative proportions of the discharge covered by water.

Table 7-21: Surface Water Discharge Areas

Discharge Zone	Area of Discharge Zone [m ²]	Range of Discharge Zone Area* [m ²]	Aquatic Discharge Fraction	Terrestrial Discharge Fraction
River	7.9x10 ⁴	2.6x10 ⁴ - 1.6x10 ⁵	0.34	0.66
Lake	2.8x10 ⁴	1.1x10 ⁴ - 1.4x10 ⁵	0.75	0.25
East Wetland	2.2x10 ⁴	5.2x10 ³ - 7.8x10 ⁴	0.0	1.0
Central Wetland	2.9x10 ⁴	1.3x10 ⁴ - 6.0x10 ⁴	0.0	1.0

Notes: * Discharge area is described by a loguniform distribution. The range is determined through consideration of areas defined by particle track distributions and concentration profile. See Garisto et al. (2012) for further information

Soil Submodel

The soil submodel calculates the concentration of contaminants in the surface (rooting or cultivated) soil layer. This layer is assumed to be well-mixed due to, for example, plowing in an agricultural field or bioturbation. Two soil models are considered, one for upland soil and one for shallow soil. The upland soil model describes a typical soil layer, with the water table a reasonable distance below the surface soil layer. In the shallow soil model, the water table extends into the surface soil layer on a regular and extended basis (as in the case of marsh or swamp land). The distinction between these two soil types is important in determining how readily contaminated groundwater can reach the surface. In the upland soil model, it must be transported by processes such as capillary action while in the shallow soil model groundwater is directly discharged into the surface soil.

Areas of surface soils have specific designations including use as a vegetable garden, a forage field, and a woodlot. Some of the parameters describing the transport pathways in the soil model are dependent on the type of field (i.e., irrigation rate).

The transport processes considered in the soil submodel are:

- Irrigation – contaminated water from the well or surface water is added to the soil.
- Groundwater Discharge – direct discharge from a contaminated groundwater water source below the surface soil (shallow soil only).
- Capillary Rise – upwelling of contaminated groundwater from the water table (upland soil only).
- Leaching – contaminants in surface soil migrate to deeper soil layers as water percolates through the soil layer.
- Runoff – precipitation runoff from the watershed area entering the water body.
- Root Uptake – uptake of contaminants by plants and trees.
- Suspension and Volatilization – loss from the soil to the atmosphere due to soil resuspension (wind erosion) and volatilization.
- Deposition – deposition of contaminants from the atmosphere onto surface soils.

Some of the physical characteristics of the soil at the hypothetical site are described in Table 7-22 (Garisto et al. 2012). These reflect the values in CSA (2008) where available.

Table 7-22: Soil Properties

Parameter	Reference Case Value	Comment
Soil types	As per comment column	Distribution of soil types on Canadian Shield: 57% sand, 14% organic, 24% clay, and 5% loam. Soil properties (e.g., sorption coefficient) depend on soil type.
Active surface soil depth	0.2 m	This is the active or root zone layer for which radionuclide concentrations in the soil are determined.
Soil Depth to water table	1.5 m	Normal PDF, 1.5 m mean, 0.5 m standard deviation, and bounds of 0.01 to 2.5 m.
Minimum soil depth to water table for upland soil model	0.5 m	This is the minimum depth-to-water-table at which the upland soil model is used. For smaller depths, a shallow soil model is used that allows for flooding of the surface soil by contaminated groundwater.
Upland soil leach rate fraction	0.55	Fraction of net precipitation (precipitation + irrigation - evapotranspiration) that infiltrates into soil. The remainder runs off along the surface. Uniform PDF from 0.1 to 1.

Note: Data taken from Garisto et al. (2012).

Atmosphere Submodel

The atmosphere submodel calculates radionuclide concentrations in air due to the following transport processes:

- Suspension and Volatilization – contamination of the air from particulate or gaseous releases from surface water and soil.
- Dispersion – reduction in the concentration of contaminants in the air by having them disperse over a larger area.
- Fire – release of contamination into the air from fires assumed to occur on-site. This includes fuel fires used by the critical group as well as natural fires such as a forest fire.

A list of parameters important to the concentration of airborne contaminants is given in Table 7-23 (Garisto et al. 2012). When calculating the concentrations in the atmosphere, all contaminants are conservatively assumed to be located within a couple of meters above the land surface.

Table 7-23: Climate and Atmosphere Parameters

Parameter	Reference Case Value*	Comment
Annual total precipitation	0.76 m/a	Normal PDF, with a standard deviation of 0.12 m/a and bounds of 0.28 and 1.92 m/a.
Annual average runoff	0.31 m/a	This is the balance between total precipitation and evapotranspiration, and includes surface runoff as well as infiltration into the water table. Normal PDF with mean of 0.31 m/a, standard deviation of 0.08 m/a, and bounds of 0.01 and 0.71 m/a. Correlated to total precipitation with 0.80 correlation coefficient.
Average wind speed	2.36 m/s	Normal PDF with mean of 2.36 m/s (8.5 km/h), standard deviation of 0.64 m/s, and bounds of 0.44 and 6 m/s.
Dry deposition velocity	0.006 m/s	Lognormal PDF with geometric mean of 0.006 m/s and geometric standard deviation of 2.
Atmospheric dust load	$3.2 \times 10^{-8} \text{ kg}_{\text{drysoil}} / \text{m}^3_{\text{air}}$	Lognormal PDF with geometric mean calculated from suspended particulate matter concentrations in Ont, NB, Que and Sask during years 1996 to 2002. GSD of 1.7 with bounds of 7.0×10^{-9} and $7.5 \times 10^{-8} \text{ kg}_{\text{drysoil}} / \text{m}^3_{\text{air}}$.
Atmospheric aerosol load	$2.9 \times 10^{-10} \text{ m}^3_{\text{water}} / \text{m}^3_{\text{air}}$	Lognormal PDF with geometric mean of $2.9 \times 10^{-10} \text{ m}^3_{\text{water}} / \text{m}^3_{\text{air}}$, and geometric standard deviation of 1.41. Based on estimate for sea salt aerosol over oceans.
Washout Ratio	630 000	CSA (2008) washout ratio for deposition to plants for all elements other than noble gases and iodine. This value is conservative for iodine. CSA (2008) recommends 200 000 for elemental iodine and 8400 for organic iodine.

Note: * Data taken from Garisto et al. (2012).

Dose Calculations

The dose model uses the concentrations of radionuclides in the various biosphere compartments to calculate the annual dose to a member of the critical group.

To ensure that dose rates are not underestimated, conservative assumptions are made concerning the characteristics of the critical group. Specifically, it is assumed that the members of the critical group spend all their lives in the local biosphere and obtain all their food, water, fuel and building materials from the local biosphere. The water source for the critical group is a well that intercepts the radionuclide plume. The food includes plants grown in a garden, domesticated animals and fish. All plants and non-human biota used as food are subject to contamination from surface water, soil and air. This lifestyle is consistent with but more self-sufficient than current habits and leads to an overestimate of the impact. Because of these characteristics, the hypothetical member of the critical group is referred to as a Self-Sufficient Farmer. The Self-Sufficient Farmer has been found in previous studies to be a good indicator of risk for a range of plausible lifestyles (Garisto et al. 2005).

Some critical group lifestyle characteristics are shown in Table 7-24.

Table 7-24: Human Lifestyle Data

Parameter	Reference Case Value	Comment
People per household	3	Piece-wise uniform PDF from 1 to 12 people.
Domestic water demand per person	110 m ³ /a	Lognormal PDF with geometric mean 110 m ³ /a, geometric standard deviation of 2 and bounds of 40 and 240 m ³ /a.
Total energy needs per person	18744 kJ/d	Fixed value, set conservatively high at 90 th percentile value.
Man's air inhalation rate	8400 m ³ /a	95 th percentile
Man's water ingestion rate	840 L/a	90 th percentile
Man's meat ingestion rate*	103 g/d	Median intake for male adult. Defined as lognormal PDF with geometric mean equal to median and geometric standard deviation equal to 1.65. For a total energy intake of 18744kJ/d, this intake is prorated to 249 g/d.
Man's milk ingestion rate*	283 g/d	Median intake for male adult. Defined as lognormal PDF with geometric mean equal to median and geometric standard deviation equal to 1.35. For a total energy intake of 18744kJ/d, this intake is prorated to 685 g/d.
Man's plant ingestion rate*	796 g/d	Median intake for male adult. Defined as lognormal PDF with geometric mean equal to median and geometric standard deviation equal to 1.65. For a total energy intake of 18744 kJ/d, this intake is prorated to 1928 g/d.
Man's poultry ingestion rate*	53 g/d	Median intake for male adult. Defined as lognormal PDF with geometric mean equal to median and geometric standard deviation equal to 1.65. For a total energy intake of 18744 kJ/d, this intake is prorated to 128 g/d.
Man's fish ingestion rate*	7.9 g/d	Median intake for male adult. Defined as lognormal PDF with geometric mean equal to median and geometric standard deviation equal to 4.48. For a total energy intake of 18744 kJ/d, this intake is prorated to 19 g/d.
Soil ingestion rate	0.12 kg/a	95 th percentile of incidental soil ingestion rate.
Annual energy consumption per household	10 ⁵ MJ/a	Normal PDF with mean of 1.2x10 ⁵ MJ/a, standard deviation of 8x10 ³ MJ/a and bounds of 10 ⁵ MJ/ and 1.3x10 ⁵ MJ/a.
Building occupancy factor	0.8	Fixed value
Building air infiltration rate	0.35 /hr	Fixed value, minimum recommendation for tightly-sealed house.

Notes: Data taken from Garisto et al. (2012). * Based on a total energy intake of about 7750 kJ/d

7.6 Results of Radionuclide and Chemical Hazard Screening Analysis

This section presents the results of the RSM screening analysis performed to identify the potentially significant radionuclides and potentially significant chemically hazardous elements. The methodology used is described in Section 7.5.2.

Table 7-25 shows the list of radionuclides and hazardous elements that emerged from the screening assessment. Results are shown for each case simulated, with radionuclides listed in order of their dose contribution and hazardous elements listed in alphabetical order.

The results indicate the most important potentially significant radionuclides are I-129, C-14, Cl-36, Ca-41, Cs-135, and Sn-126. Actinides only appear in simulation cases with no sorption or no solubility limits. The parents and progeny of the screened in radionuclides are also included in the simulations to ensure that ingrowth is accounted for.

For the potentially significant chemically hazardous elements, the All Containers Fail case has the highest number of contributors (due to the conservative nature of this case) while elements associated with the other cases are Cd, Ag, Hg, Te and U. It should be noted that mass of some the chemical elements of interest (e.g., Pb, Te and Ag) increase with time due to radioactive decay of parent nuclides. Consequently, these parent nuclides are also included in the simulations of the potentially chemically hazardous elements carried out with system model.

Table 7-25: Summary of Screened in Radionuclides and Chemically Hazardous Elements for Each Case Considered

Case	Radionuclide	Chemically Hazardous Element
Median	Cl-36, C-14, I-129, Cs-135, Sn-126, Ca-41	Cd
3 Sigma	Cl-36, Sn-126, C-14, I-129, Cs-135, Sb-126, Ra-228, Ni-59, Ca-41, Np-237, Se-79	Ag, Cd, Hg, Te
No Sorption Geosphere	Po-210, Pb-210, Ra-226, Cl-36, C-14, I-129, Rn-222, Cs-135, Bi-210	Cd
No Sorption Near Field	Sn-126, Cl-36, C-14, I-129, Sb-126, Cs-135	Cd
High Solubility	Po-210, Pb-210, Rn-222, Cl-36, Th-230, Bi-210, C-14, I-129, U-234, Ra-226, U-238, Se-79, Ra-228, Cs-135, Np-237, U-236, Sn-126, Ra-224, Th-234, U-235, Pa-231, U-233	Cd, U
High IRF	Cl-36, C-14, I-129, Cs-135, Sn-126, Ca-41	Cd
All Containers Fail	Cl-36, I-129, C-14, Cs-135, Sn-126, Ca-41	Ag, Cd, Ce, Co, Cr, Eu, Hg, I, La, Nd, P, Pb, Pr, Te, Y

Table 7-26 shows the set of potentially significant radionuclides and Table 7-27 the set of potentially significant chemically hazardous elements. Items in red are items identified directly in the screening (i.e., Table 7-25) while items in black are added because of in-growth concerns. The one item in blue (As) was not screened in but has been added for historical reasons.

Table 7-26: List of Potentially Significant Radionuclides

Radionuclides	
Single	Cl-36, I-129, C-14, Cs-135, Ca-41, Ni-59, Se-79
Chain	
<i>Neptunium Series</i>	Am-241 → Np-237 = Pa-233 → U-233 → Th-229 = Ra-225 = Ac-225
<i>Uranium Series</i>	Pu-242 → U-238 = Th-234 → U-234 → Th-230 → Ra-226 = Rn-222 = Pb-210 = Bi-210 = Po-210
<i>Actinium Series</i>	Pu-239 → U-235 = Th-231 → Pa-231 = Ac-227 = Th-227 = Ra-223
<i>Thorium Series</i>	Pu-240 → U-236 → Th-232 = Ra-228 = Th-228 = Ra-224
<i>Misc</i>	Sn-126 → Sb-126

Table 7-27: List of Potentially Significant Chemically Hazardous Elements

Chemically Hazardous Elements	
Single	As, Ce, Cd, Co, Cr, Eu, Hg, I, La, Nd, P, Pr, Y
Chain	
<i>Uranium Series</i>	Pu-242 → U-238 = Th-234 → U-234 → Th-230 → Ra-226 = Rn-222 = Pb-210 = Bi-210 = Po-210 → Pb-ST
<i>Actinium Series</i>	Pu-239 → U-235 = Th-231 → Pa-231 = Ac-227 = Th-227 = Ra-223 → Pb-ST
<i>Thorium Series</i>	Pu-240 → U-236 → Th-232 = Ra-228 = Th-228 = Ra-224 → Pb-ST
<i>Misc</i>	Pd 107 → Ag, Sn-126 → Te

Note: '=' means the radionuclides are assumed to be in secular equilibrium with their parent

7.7 Results of Detailed 3D Groundwater Flow and Transport Analysis

This section presents results of the detailed FRAC3DVS-OPG groundwater flow and radionuclide transport analysis performed for the Reference Case of the Normal Evolution Scenario and for those sensitivity cases with the potential to affect the groundwater flow field. The sensitivity cases examined are:

- Geosphere hydraulic conductivity modified by factors of 10, 0.1 and 0.01 times the Reference Case values;
- Fracture offset with respect to the nearest part of the repository varied from the Reference Case value of 25 m to new values ranging between 10 m and 100 m;

- Hydraulic conductivity of the EDZ and TDZ increased by a factor of 10;
- Discrete fracture modelling (as opposed to equivalent porous media modelling); and
- Increased spatial resolution and increased number of time steps.

Analysis is also performed for the Fracture Seal Failure Disruptive Event Scenario and its variant case in which the fracture seals and all repository tunnel and room seals degrade. For ease of comparison, results for this scenario are considered together with the sensitivity cases listed above.

A further description of the cases is provided in Section 7.2.

A detailed description of the models used to generate the results is available in Section 7.5.2.

Radionuclide transport is determined for I-129, C-14, Cl-36, Ca-41, Sn-126, Cs-135, U-234 and U-238. These radionuclides are typically the most important either in terms of potential radiological impact or in representing a range of low-sorption to high-sorption species.

Figures in this section show advective¹ velocity vectors only in locations where velocities are greater than 10^{-4} m/a. Transport is diffusion-dominated at lower velocities. Figures are shown with shading at times greater than one million years to emphasize that results at these times are illustrative and included only to indicate peak impacts.

7.7.1 Sub-Regional Model

In the Sub-Regional Model, the lateral boundaries are placed on topographical highs or lows that are likely zero-flow at locations far removed from the repository (i.e., more than 5 km). The model is used to determine:

- the groundwater flow field in the vicinity of the repository;
- the main surface discharge locations; and
- domain and boundary conditions for the Site-Scale Model.

Sensitivity studies are conducted to determine the effect of differing geosphere hydraulic conductivity and the effect of discrete fracture modelling on the flow field.

Radionuclide transport calculations are not performed with this model.

There are no repository features incorporated at this scale of resolution. The repository representation in the figures is only provided to add context.

¹ Advective velocity is the Darcy velocity divided by the material porosity

7.7.1.1 Flow Results

7.7.1.1.1 Reference Case

Figure 7-33 shows groundwater velocity magnitudes and directions together with hydraulic heads. Advective velocities are the Darcy velocities divided by the material porosity.

Although the fracture system has a large effect on the head distribution and velocities, gradients across the repository footprint are relatively uniform in magnitude.

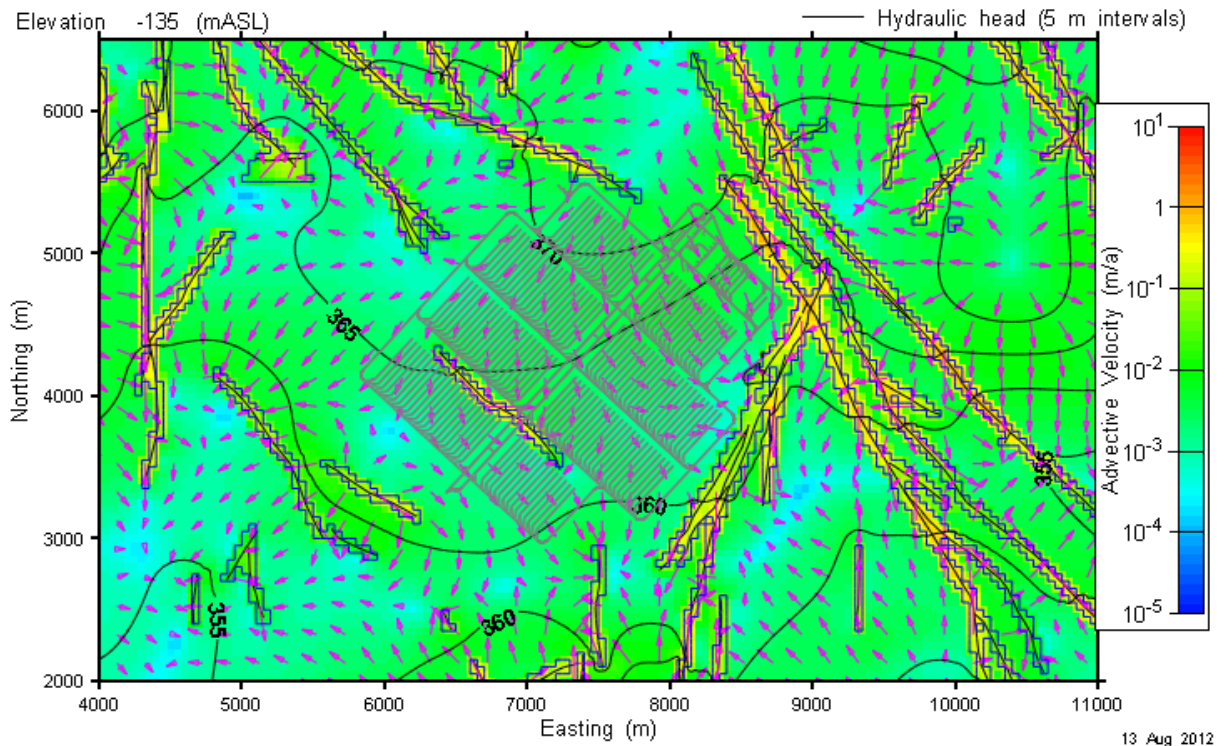


Figure 7-33: Sub-Regional Model - Reference Case Advective Velocity and Hydraulic Head at Repository Elevation

Figure 7-34 shows the direction of vertical flow within the same area as Figure 7-33. Flow is upward in the blue to magenta areas while flow is downward in the yellow to red areas. The upward flow induced by the well is evident; however, downward flow can also be seen within the same fracture. This behaviour is common in many fracture systems where the surface boundary conditions drive circulation flow.

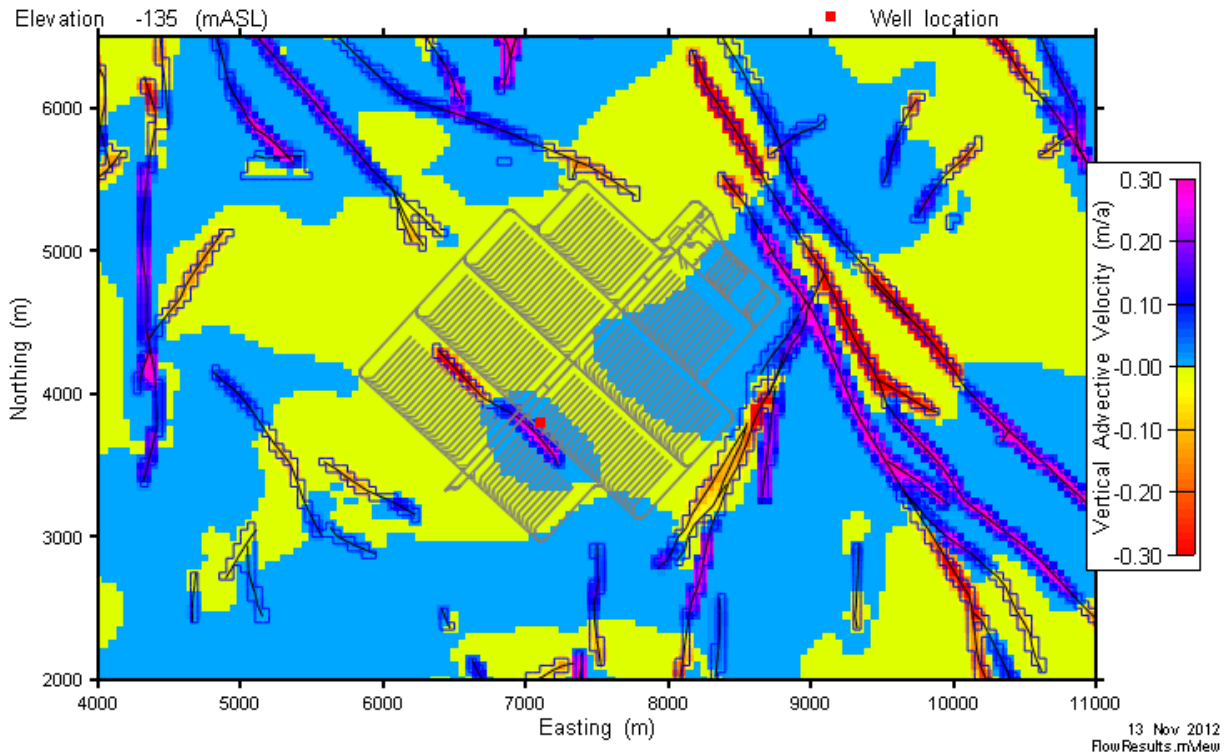


Figure 7-34: Sub-Regional Model - Reference Case Vertical Advective Velocity at Repository Elevation

Figure 7-35 shows the vertical flow and head distribution on a XZ section through the water supply well location at Northing 1200 m. The influence of the well is apparent with flow being collected by the connected fracture. The flow patterns are dominated by local topography.

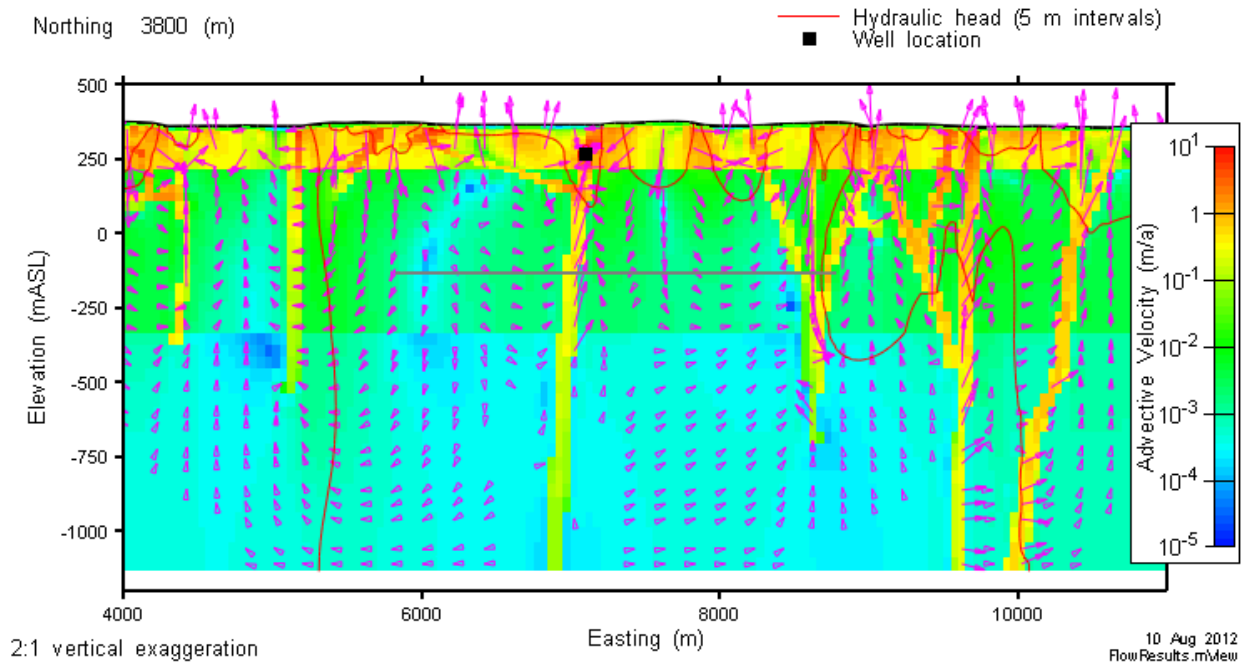


Figure 7-35: Sub-Regional Model - Reference Case Advective Velocity and Hydraulic Head on a Vertical Slice through the Well

7.7.1.1.2 Sensitivity to Changes in Geosphere Hydraulic Conductivity

Three sensitivity cases are defined in Section 7.2.1 to examine the effects of changes in geosphere hydraulic conductivity. Groundwater flow results for these cases are presented here.

Sensitivity 1

This corresponds to the Sensitivity Case 1 profile defined in Chapter 2. Hydraulic conductivities in the bedrock (in m/s) are 10 times greater than those in the Reference Case. Specifically:

- Zone 1 (10 – 150 m) is changed from 2×10^{-9} to 2×10^{-8}
- Zone 2 (150 – 700 m) is changed from 4×10^{-11} to 4×10^{-10}
- Zone 3 (700 – 1500 m) is changed from 1×10^{-11} to 1×10^{-10}

Results are shown in Figure 7-36 and Figure 7-37. Figure 7-36 shows the advective flow velocities and hydraulic heads at the repository elevation, while Figure 7-37 shows the same information but for a vertical slice through the well.

These figures can be compared with Figure 7-33 and Figure 7-35 for the Reference Case.

While flow velocities increase, no major changes in the flow directions are apparent.

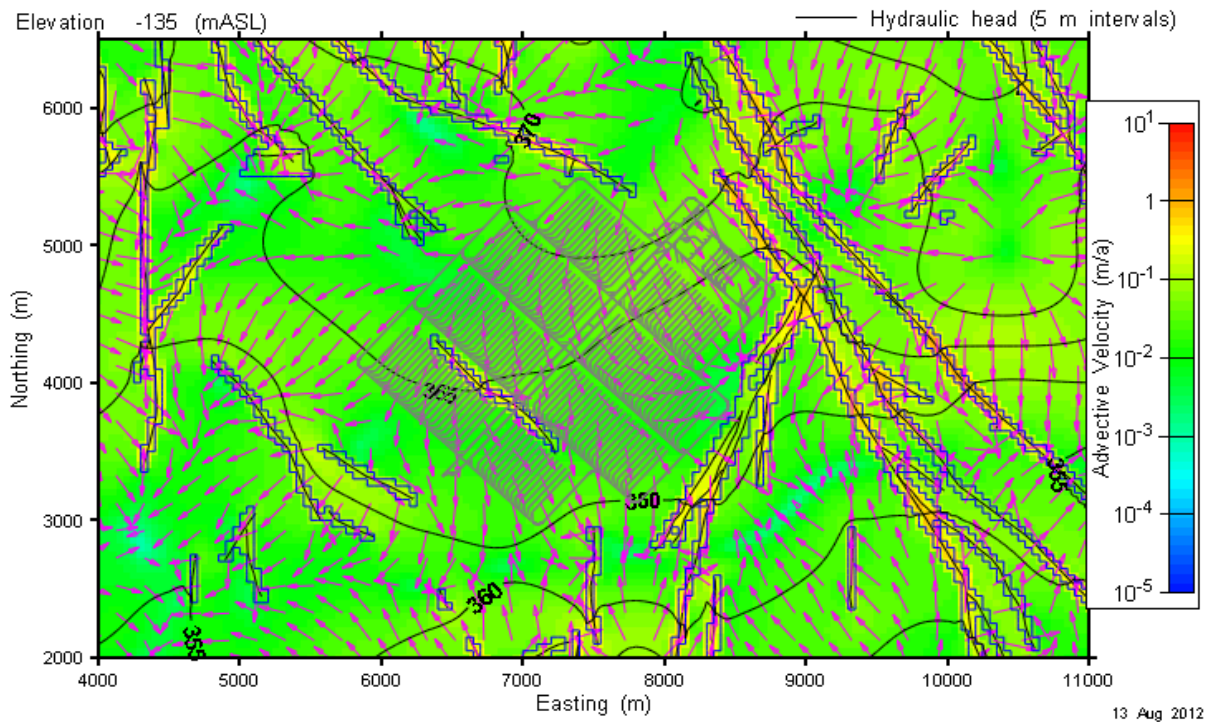


Figure 7-36: Sub-Regional Model - Hydraulic Conductivity Increase by a Factor of 10: Advective Velocity and Hydraulic Head at Repository Elevation

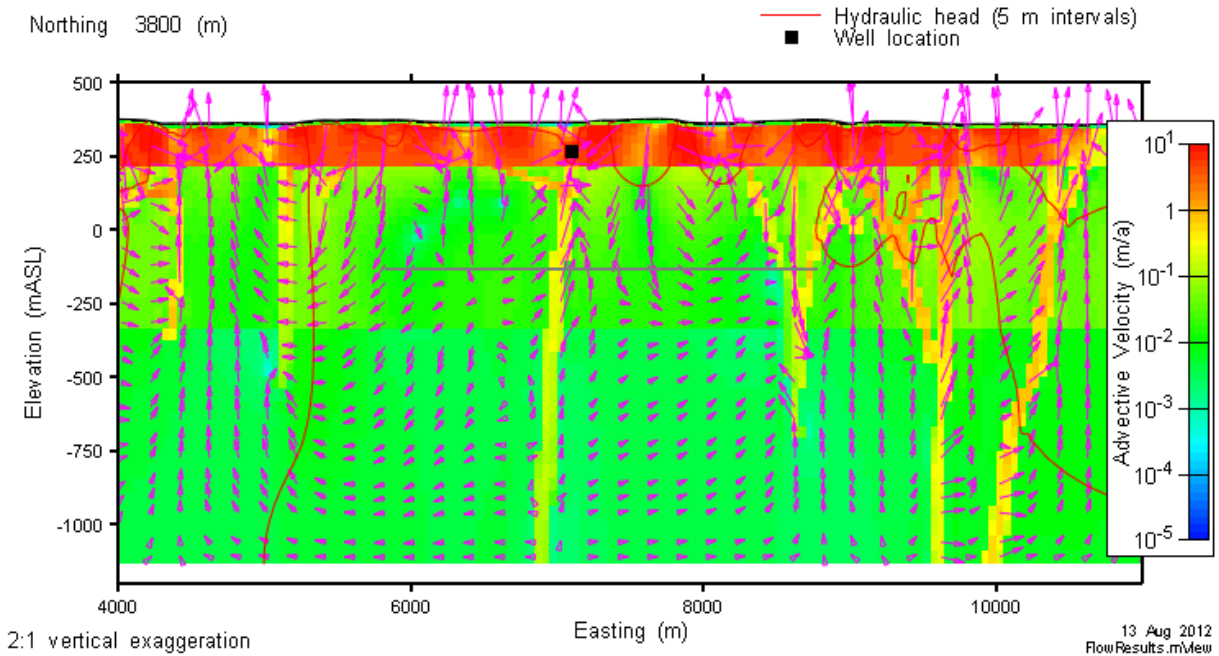


Figure 7-37: Sub-Regional Model - Hydraulic Conductivity Increase by a Factor of 10: Advective Velocity and Hydraulic Head on a Vertical Slice through the Well

Sensitivity 2

This corresponds to the Sensitivity Case 2 profile defined in Chapter 2. Hydraulic conductivities in the bedrock (in m/s) are 0.1 times those in the Reference Case. Specifically:

- Zone 1 (10 – 150 m) is changed from 2×10^{-9} to 2×10^{-10}
- Zone 2 (150 – 700 m) is changed from 4×10^{-11} to 4×10^{-12}
- Zone 3 (700 – 1500 m) is changed from 1×10^{-11} to 1×10^{-12}

Results are shown in Figure 7-38 and Figure 7-39. Figure 7-38 shows the advective flow velocities and hydraulic heads at the repository elevation, while Figure 7-39 shows the same information but for a vertical slice through the well.

These figures can be compared with Figure 7-33 and Figure 7-35 for the Reference Case, and with Figure 7-36 and Figure 7-37 for the Sensitivity 1 case. The comparison shows that as hydraulic conductivity decreases, the areas in which advective flow dominates decrease in size.

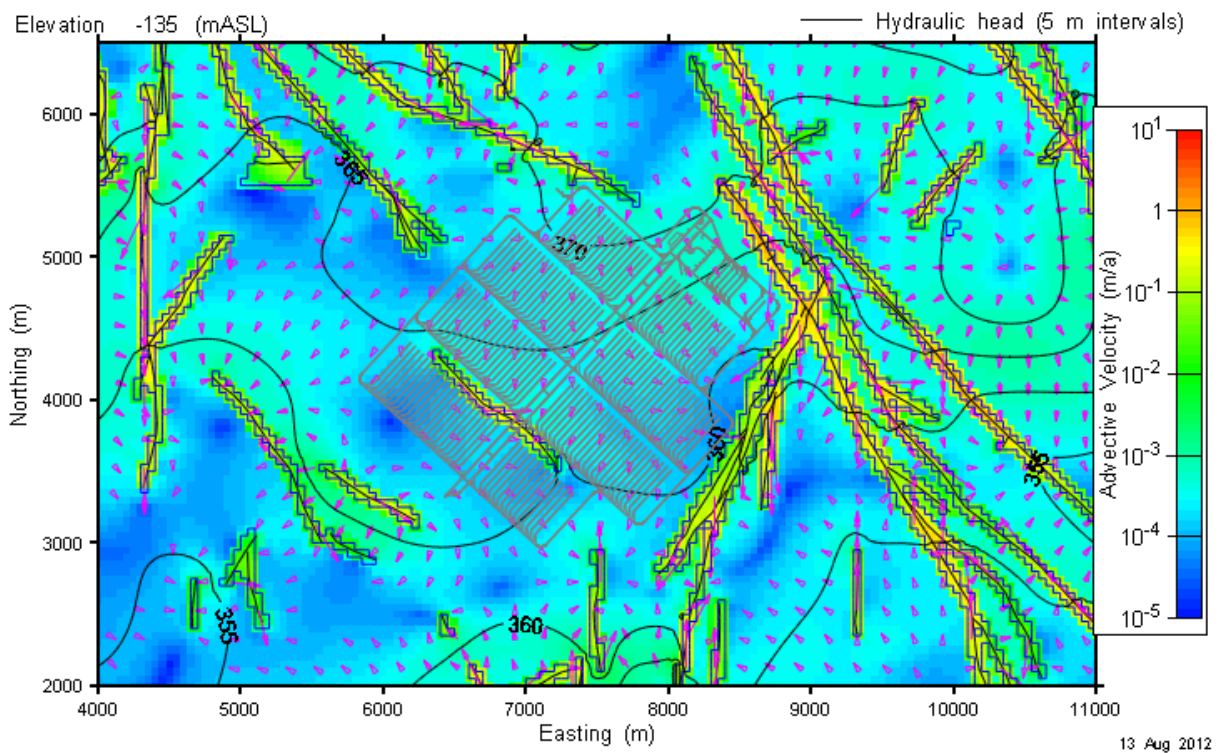


Figure 7-38: Sub-Regional Model - Hydraulic Conductivity Decrease by a Factor of 10: Advective Velocity and Hydraulic Head at Repository Elevation

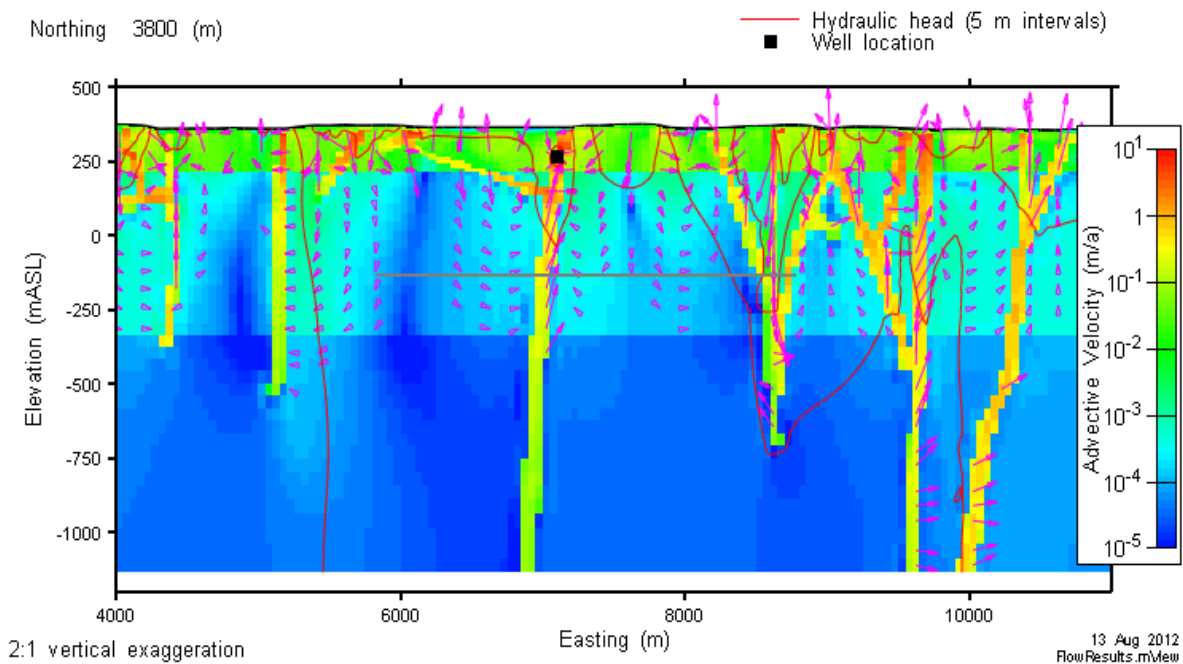


Figure 7-39: Sub-Regional Model - Hydraulic Conductivity Decrease by a Factor of 10: Advective Velocity and Hydraulic Head on a Vertical Slice through the Well

Sensitivity 3

This corresponds to the Sensitivity Case 3 profile defined in Chapter 2. Hydraulic conductivities in the bedrock (in m/s) are 0.01 times those in the Reference Case. Specifically:

- Zone 1 (10 – 150 m) is changed from 2×10^{-9} to 2×10^{-11}
- Zone 2 (150 – 700 m) is changed from 4×10^{-11} to 4×10^{-13}
- Zone 3 (700 – 1500 m) is changed from 1×10^{-11} to 1×10^{-13}

Results are shown in Figure 7-40 and Figure 7-41. Figure 7-40 shows the advective flow velocities and hydraulic heads at the repository elevation, while Figure 7-41 shows the same information but for a vertical slice through the well.

These figures can be compared with Figure 7-33 and Figure 7-35 for the Reference Case. The comparison shows that as the hydraulic conductivity is further decreased, the advective flow velocities decrease to below 10^{-4} m/a almost everywhere. This means the transport regime has moved from being advective dominant to diffusion dominant.

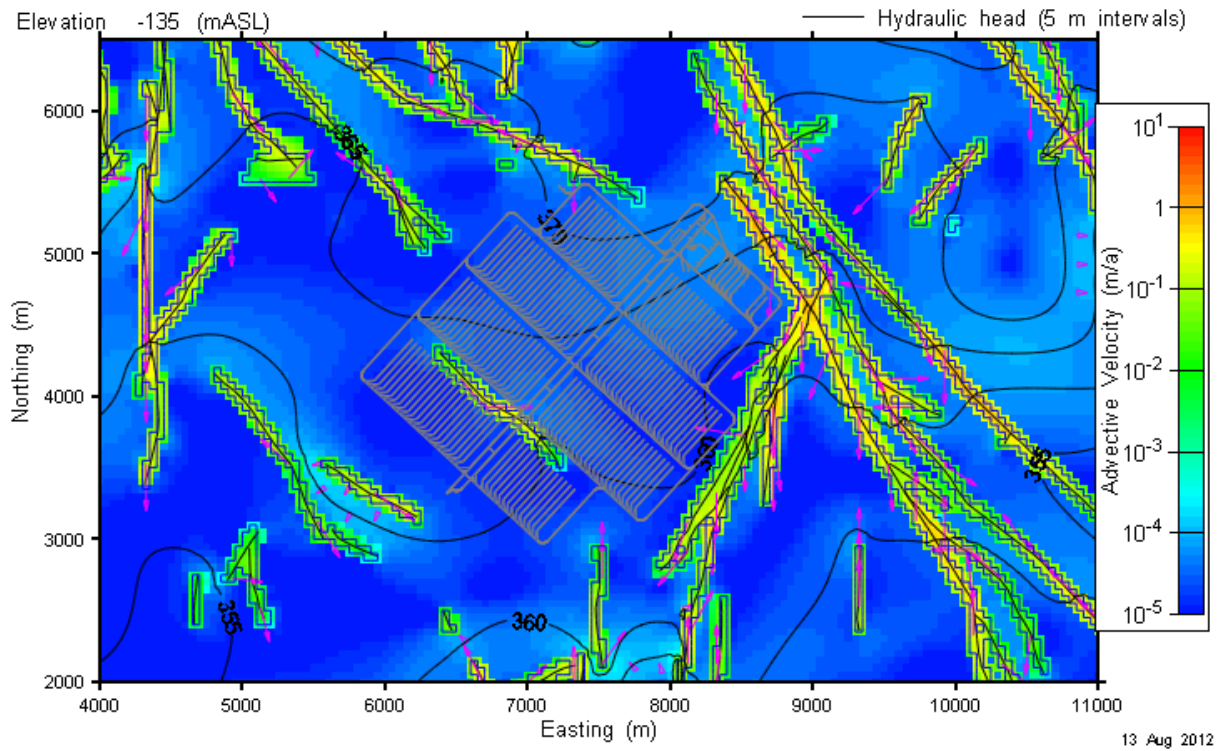


Figure 7-40: Sub-Regional Model - Hydraulic Conductivity Decrease by a Factor of 100: Advective Velocity and Hydraulic Head at Repository Elevation

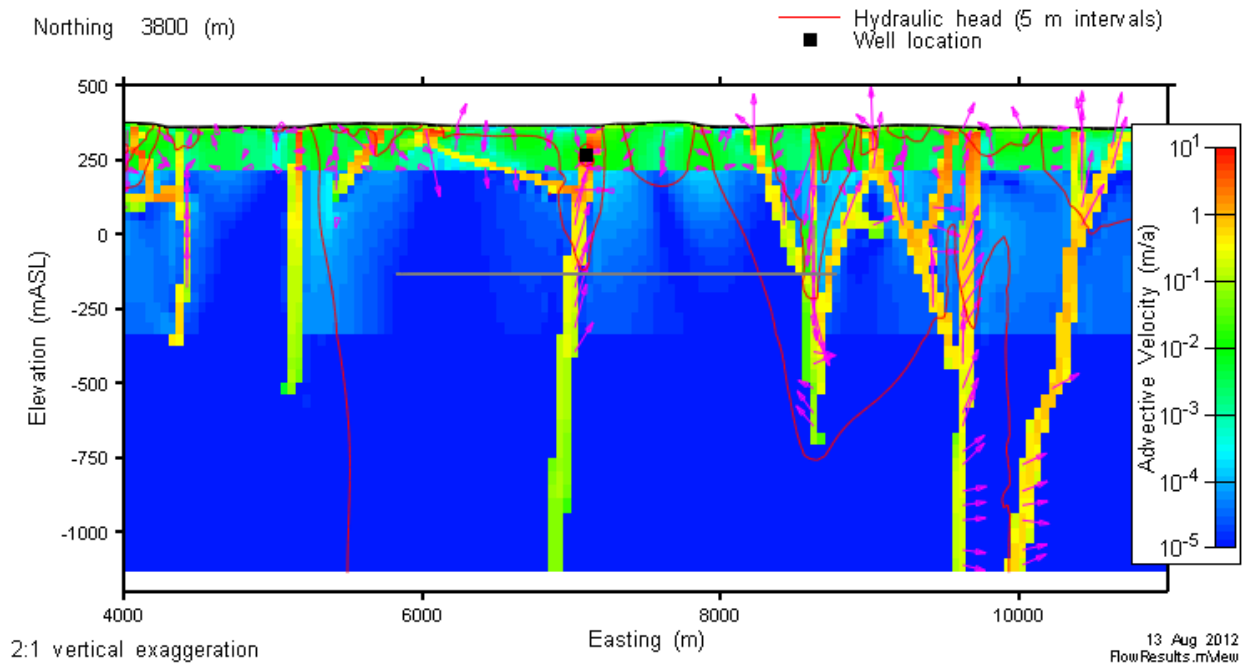


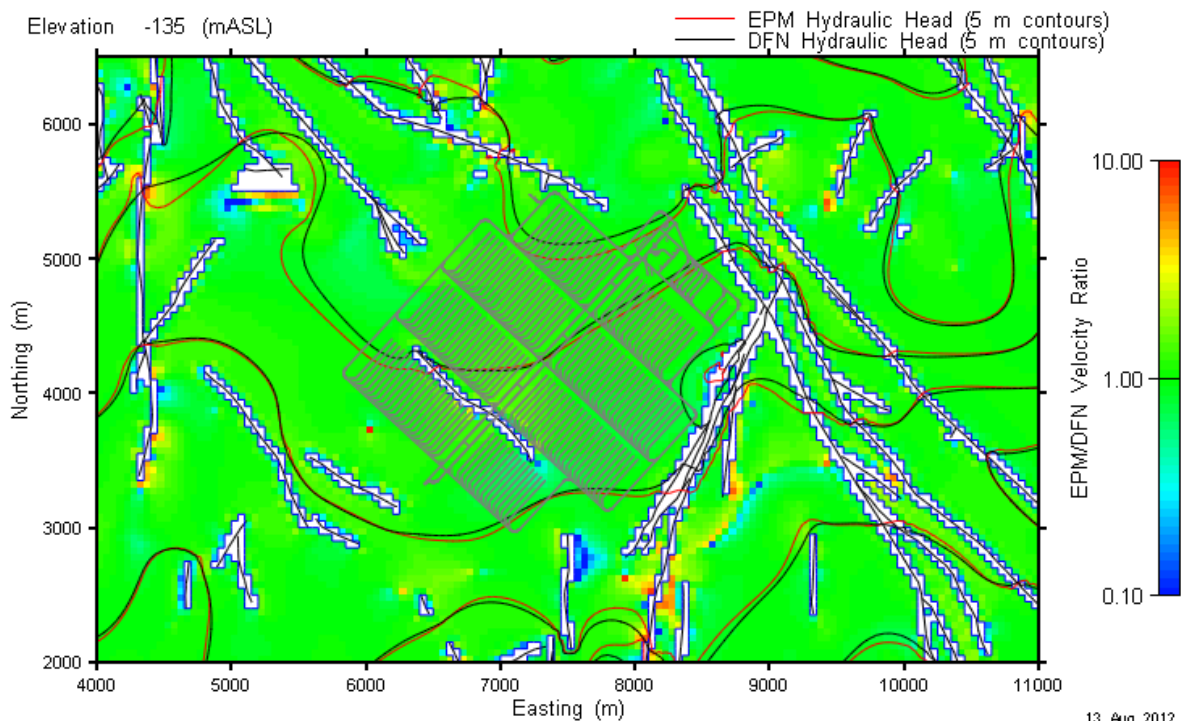
Figure 7-41: Sub-Regional Model - Hydraulic Conductivity Decrease by a Factor of 100: Advective Velocity and Hydraulic Head on a Vertical Slice through the Well

7.7.1.1.3 Sensitivity to Discrete Fracture Modelling

This section presents results for the sensitivity case in which a discrete fracture network is adopted in lieu of the equivalent porous media approach.

The discrete fracture network (DFN) model uses an alternative approach to implementing fractures within the full 3D model representing the intact bedrock. As for the EPM approach, the 3D model geometry is processed to determine which elements are intersected by the fracture system. Element faces that are closest to or intersected by the input fractures are specified as fracture faces. These are then specified as rectangular 2D planar elements with property assignments consistent with the fracture description. These 2D elements use the same nodal discretization as the 3D element model and are added to the 3D model during solution matrix assembly by FRAC3DVS. All other model features (boundary conditions, intact rock properties, source terms, etc) are identical to the EPM model.

Figure 7-42 compares heads and velocities in the rock mass with those of the Reference Case. The ratio of element velocities is plotted on the logarithmic colour scale. The results show that the heads and velocities for both approaches are very similar over most of the model domain, indicating that either approach is suitable for flow system calculations.



Note: The velocity ratio is calculated for three-dimensional elements only, which results in artificially high values for the EPM fracture elements. The colour has been set to white to avoid misinterpretation.

Figure 7-42: Sub-Regional Model - Discrete Fracture Network Sensitivity Case Comparison of Velocities and Hydraulic Heads in the Rock Mass at Repository Elevation

7.7.2 Site-Scale Model

The Site-Scale Model domain includes the repository and a portion of the sub-regional flow system into which groundwater flow travels and discharges. The model is used to determine:

- the container location with the shortest groundwater transport time to the well;
- advective transport pathways for use in creating the SYVAC3-CC4 geosphere network;
- Reference Case and sensitivity case radionuclide transport to the well and surface environment; and
- boundary conditions for the Repository-Scale Model.

A simplified representation of the repository and engineered barrier system is included at this scale of resolution; however, individual containers are not modelled.

The sensitivity simulations examine the effects of:

- geosphere hydraulic conductivity modified by factors of 10, 0.1 and 0.01 times the Reference Case values;
- hydraulic conductivity of the EDZ and TDZ increased by a factor of 10;
- discrete fracture modelling (as opposed to equivalent porous media modelling); and
- increased spatial resolution and increased number of time steps.

The Site-Scale model is also used in the assessment of the Shaft Seal Failure Disruptive Scenario and Fracture Seal Failure Disruptive Scenario.

7.7.2.1 Flow Results

7.7.2.1.1 Reference Case

Figure 7-43 compares hydraulic head results at the repository elevation with similar results from the Sub-Regional Model to verify correct implementation of the boundary conditions. The figure shows continuity of heads at the Site-Scale Model boundary and close correspondence of results within the model domain.

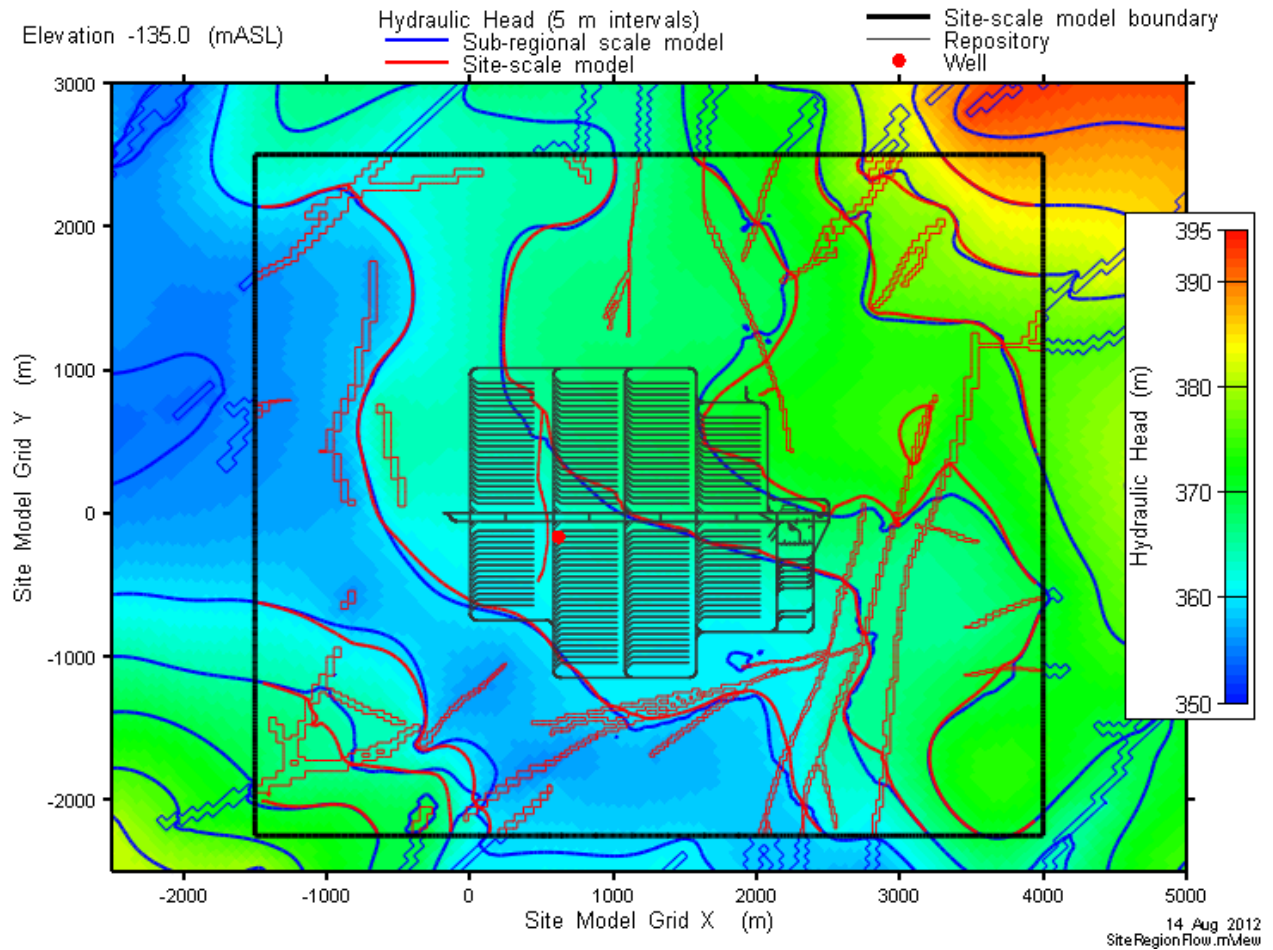


Figure 7-43: Site-Scale Model - Comparison of Hydraulic Heads With Sub-Regional Model at Repository Elevation (-135 mASL)

Figure 7-44 shows the effect of the repository features. The high hydraulic conductivity of the TDZ in the placement rooms causes changes in the Site-Scale head contours.

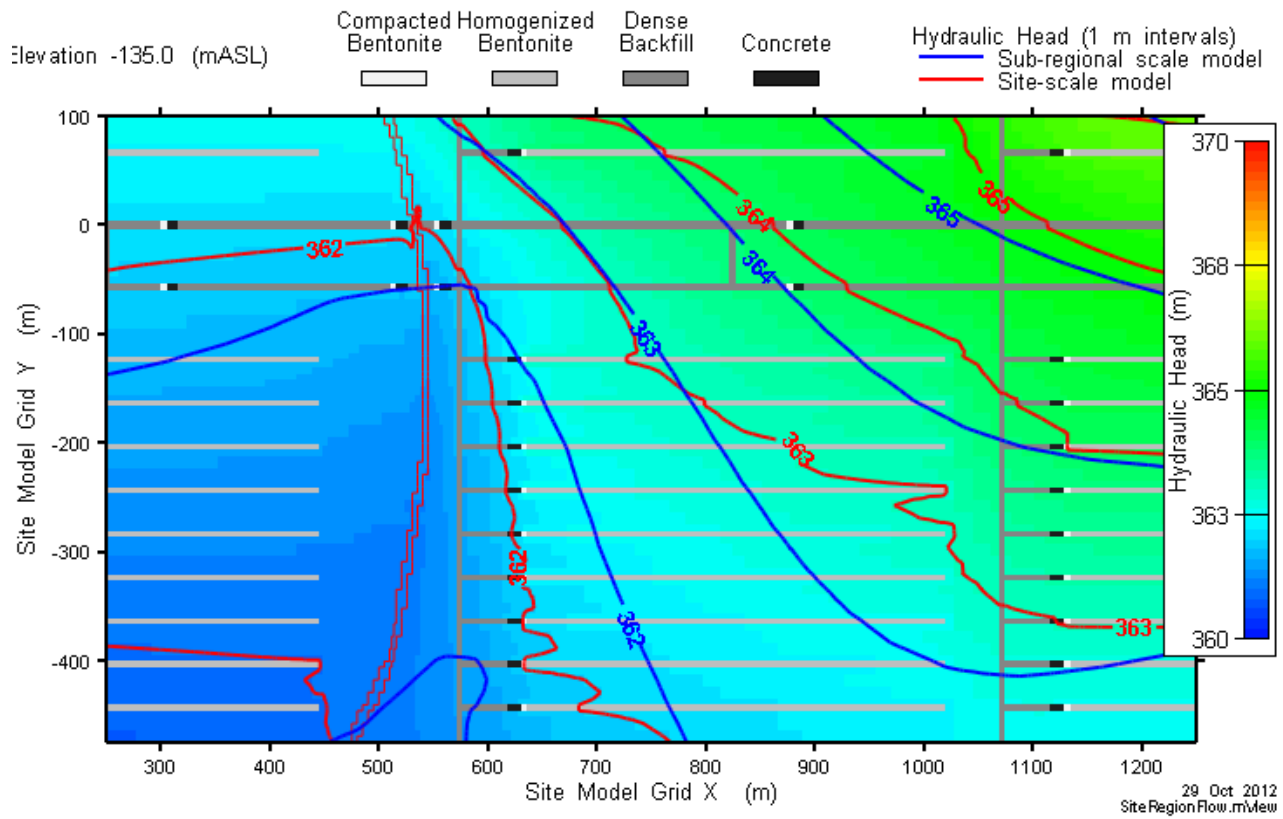


Figure 7-44: Site-Scale Model - Comparison of Hydraulic Heads With Sub-Regional Model Hydraulic Heads at Repository Elevation

Figure 7-45 shows the effect of the TDZ on the advective velocities. Relatively high velocities are present throughout the placement room TDZ. The effect of the seal in intercepting the TDZ (low velocity zone at X = 630) is also apparent.

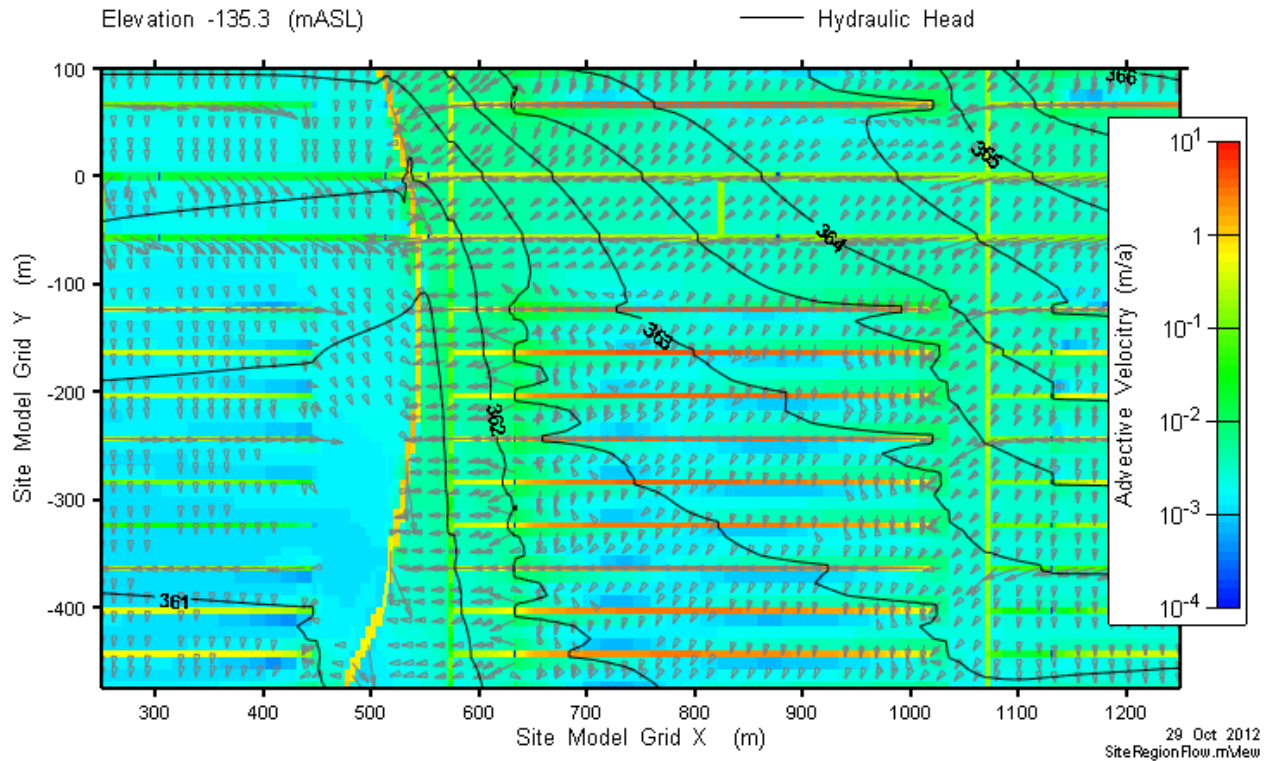


Figure 7-45: Site-Scale Model - Advective Velocities in TDZ Layer

Figure 7-46 is a visualization of the advective transport pathways, for pathways originating at the bottom of the repository within the centre of the placement rooms at the approximate location of every second container. The figure shows that the pathways generally travel directly to the well or to surface discharge locations near the lake, wetlands, or river. Some long duration pathways originating in the northern edges of the repository travel through a deeper system before reaching the edges of the model without discharging at surface. These are shown as “stagnant” pathways in the figures below.

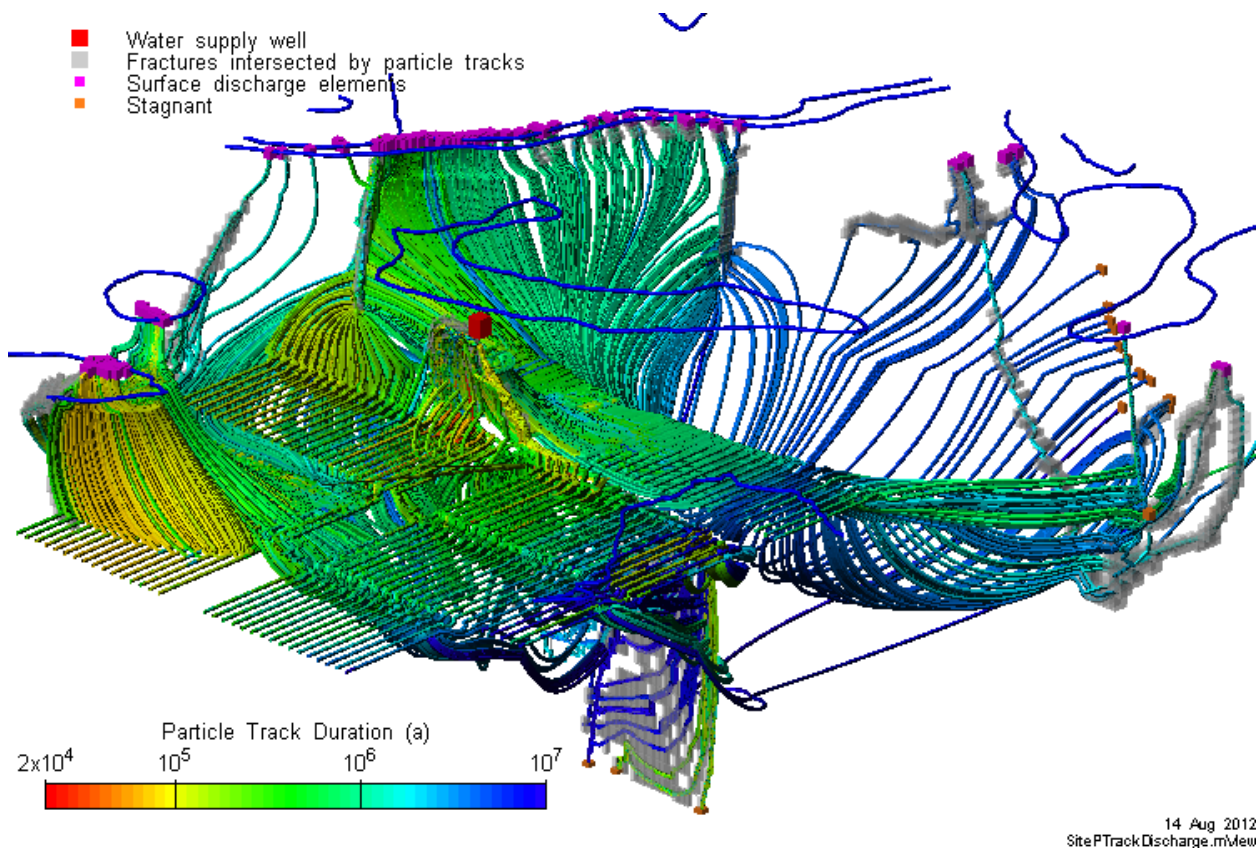
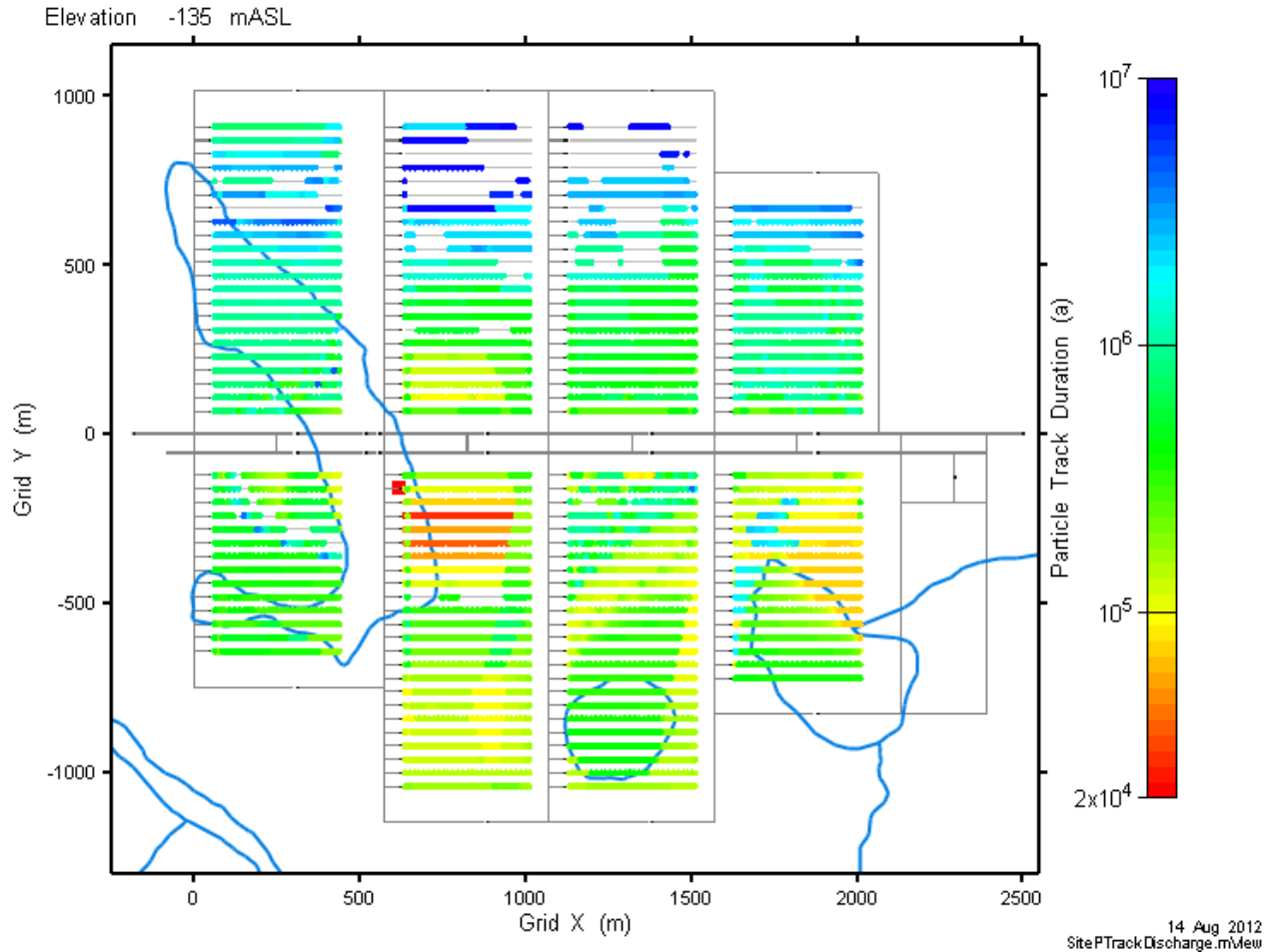


Figure 7-46: Site-Scale Model - Advective Transport Pathways

Figure 7-47 is a map of the advective travel times to the surface or to the water supply well.



Note: the well is the red square.

Figure 7-47: Site-Scale Model - Advective Transport Time to the Surface or Water Supply Well

Figure 7-48 shows the surface discharge points and indicates which repository locations map to which discharge location.

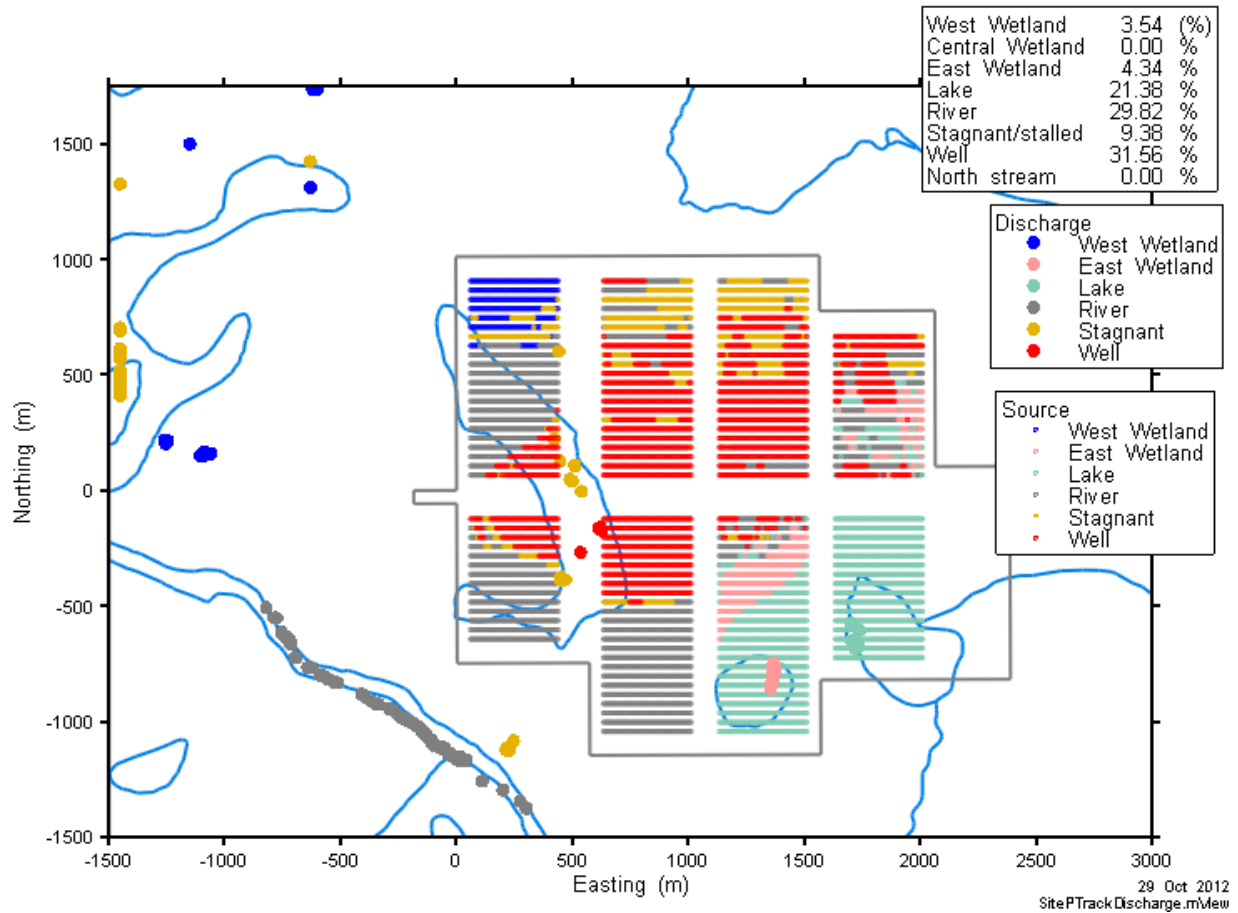


Figure 7-48: Site-Scale Model - Advective Transport Discharge Zones

Figure 7-49 shows the Mean Life Expectancy (MLE) taking both advective and diffusive processes into account. In this context, “Life Expectancy” is the time for a contaminant at any subsurface location to discharge to the biosphere. Since transport disperses the species through the geosphere, life expectancy is represented by a probability density function, obtained by solving for transport at each nodal upstream point. The mean life expectancy represents the average time for a contaminant any subsurface location to discharge to the biosphere.

The figure shows the majority of the repository is situated in rock in which the MLEs are 10^5 to 10^6 years, with longer MLEs evident along one boundary and shorter MLEs in areas adjacent to the fractures. This is consistent with the impact of the fracture and the well location intended to intercept the shortest duration transport path to the surface.

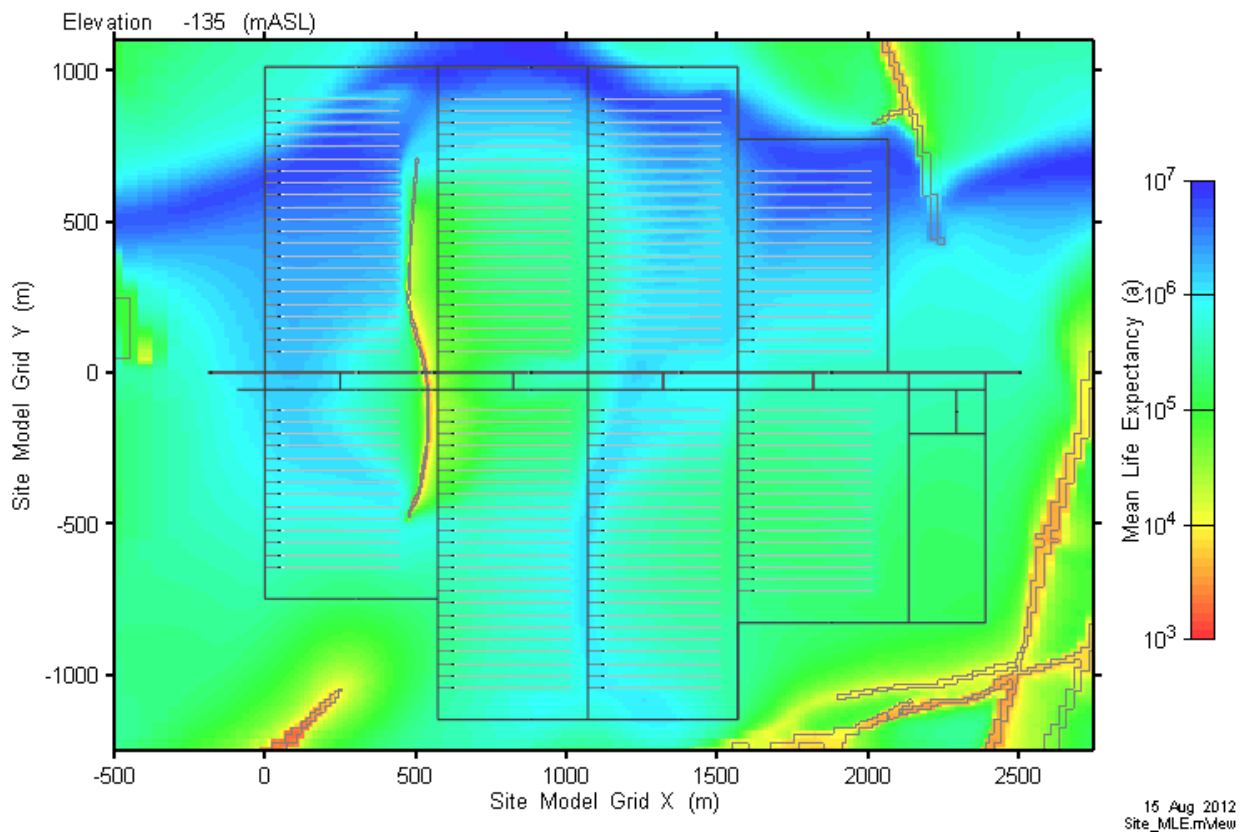


Figure 7-49: Site-Scale Model - Mean Life Expectancy

7.7.2.2 Radionuclide Transport Results

Radionuclide transport modelling is performed for I-129, C-14, Cl-36, Ca-41, Cs-135, Sn-126, U-234 and U-238. The model includes both advective and diffusive transport.

Radionuclide fluxes through a surface encompassing the defective containers determined from the Repository-Scale Model are applied as a boundary condition equally over two nodes located at the bottom of the placement room at the location of the defective containers. The defective containers are located in the room closest to the mid-repository fracture.

7.7.2.2.1 Location of the Well and Defective Containers

Seven potential well locations and nine potential contaminant source locations have been examined to identify the combination that yields the shortest travel time and maximum radionuclide mass flux to the well. This combination is of interest because it is the one most likely to yield the highest dose consequence.

The seven potential well locations are shown in Figure 7-50. With one exception, all potential locations intersect the fracture system at 100 mBGS. The exception was used to determine if the reference well demand (i.e., 911 m³/a) could be met by the intact rock; however, calculated heads showed that this is not possible. The selected well location is indicated in red.

Seven of the nine potential contaminant source locations are shown in Figure 7-51. Potential locations were selected based on transport pathways with the shortest duration to the surface, with additional locations added through an iterative process. The limiting combination was determined based on transport of I-129; however, some simulations were also performed for C-14 where the possibility of fast transport pathways existed. The two locations not shown are located near the edges of the repository and were placed to assess transport to adjacent fractures. These locations were not limiting and are not discussed further.

Figure 7-52 shows the I-129 transfer rates to the selected well location for each contaminant source location. Between Locations 1, 2, and 9 the variation is relatively small, indicating a general insensitivity of results to the source location, provided the source is located within the immediate vicinity of the well. Source "Location 9" is selected as the limiting location.

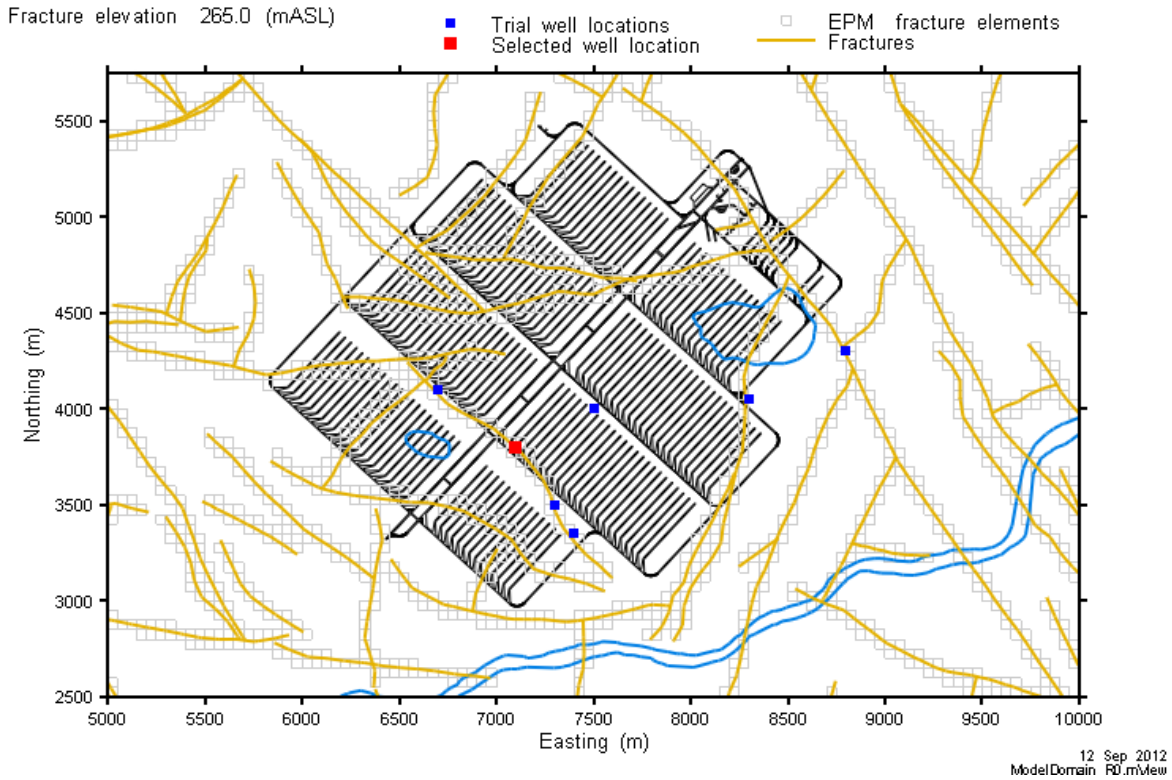


Figure 7-50: Site-Scale Model - Potential Well Locations

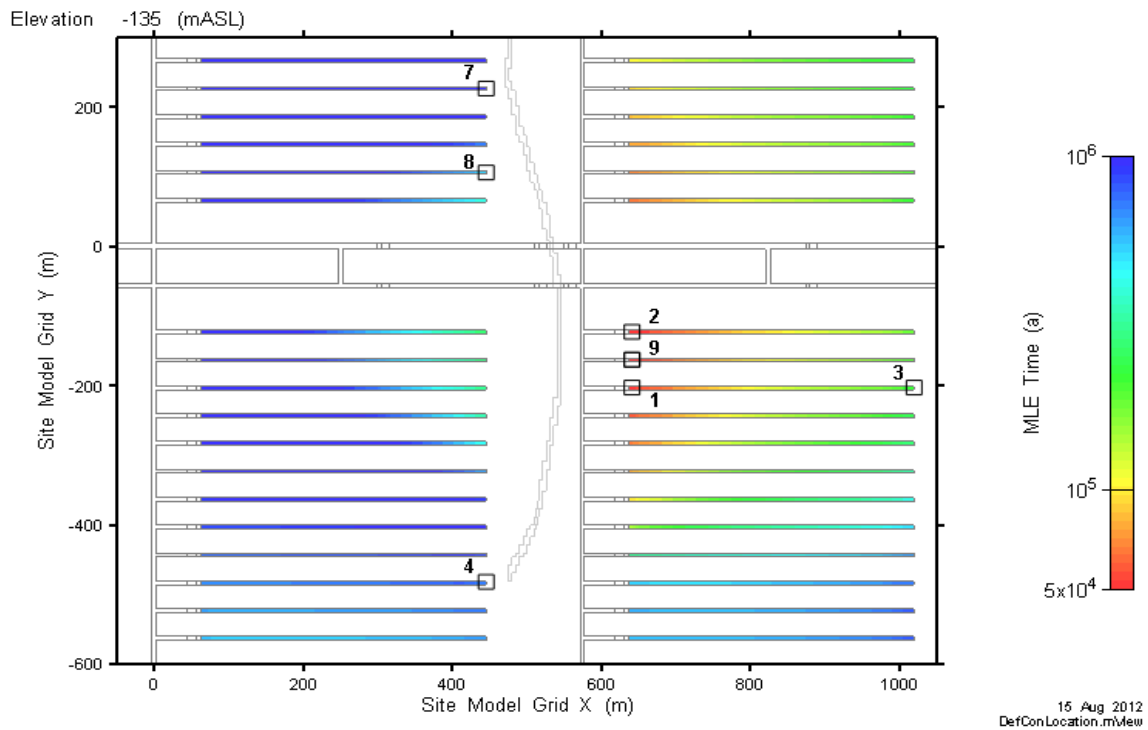


Figure 7-51: Site-Scale Model - Potential Contaminant Source Locations

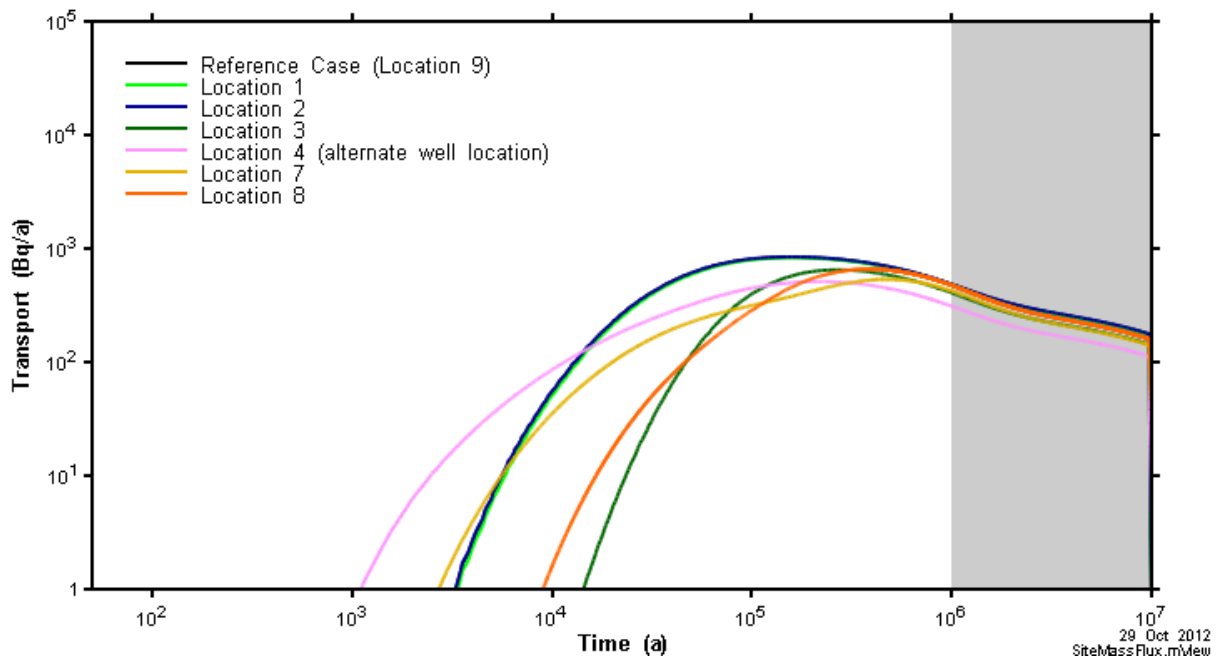


Figure 7-52: Site-Scale Model - Effect of Different Source Locations on I-129 Transport

7.7.2.2.2 Reference Case

Figure 7-53 through Figure 7-56 illustrate the time dependent behaviour of the I-129 plume along the repository and on a vertical slice through the placement room. By 10,000 years, the plume has encountered the fracture connected to the well which effectively bounds its lateral advance. In this context, “encounter” means the radionuclide concentration at the fracture location reaches 1 Bq/m^3 .

The contour plots are on a logarithmic scale. The outer concentration contour, 1 Bq/m^3 , corresponds to an effective I-129 drinking water dose of about $0.1 \mu\text{Sv/a}$ based on water consumption of $0.77 \text{ m}^3/\text{a}$ per person.

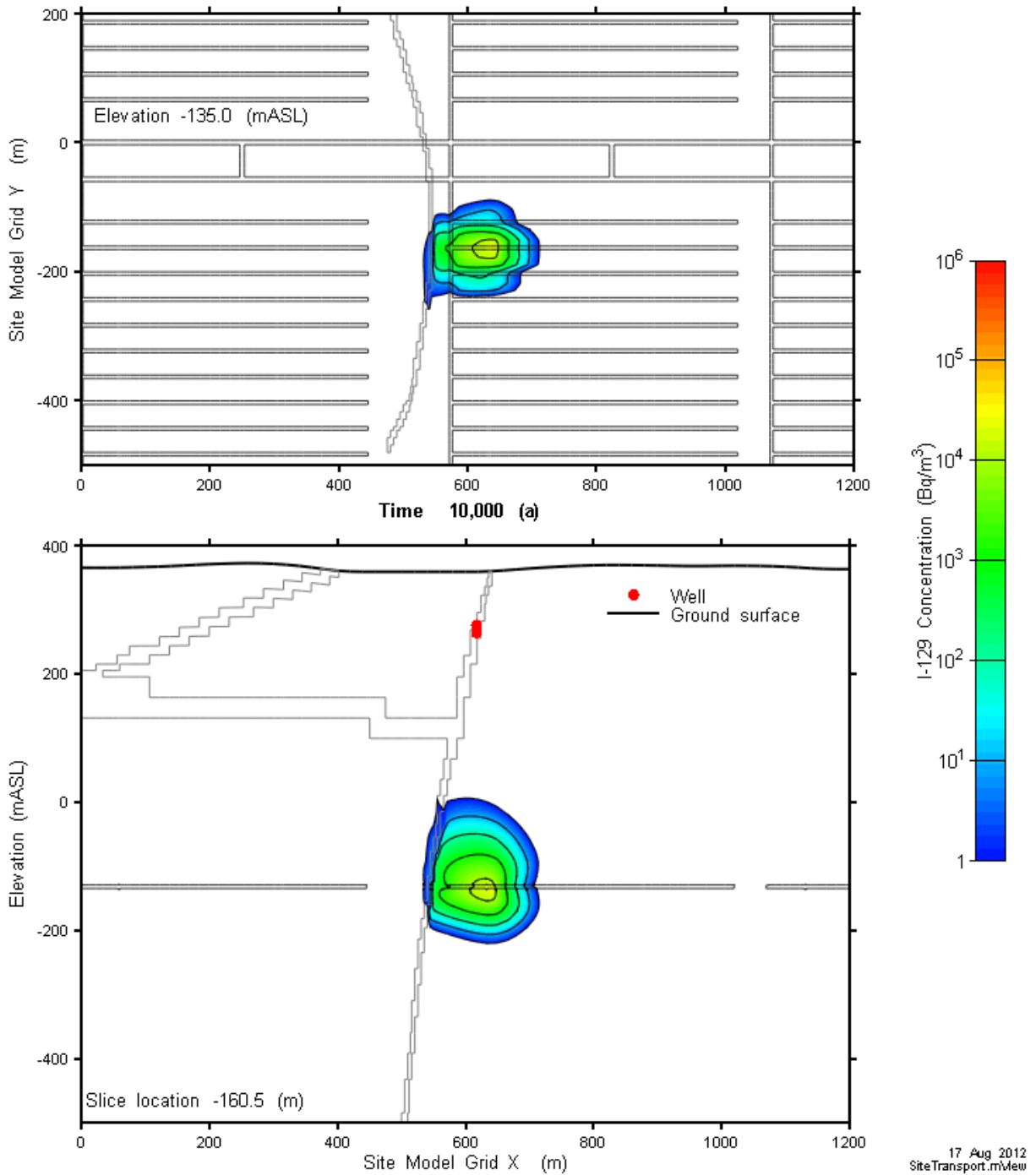


Figure 7-53: Site-Scale Model - Reference Case I-129 Concentration at 10,000 Years

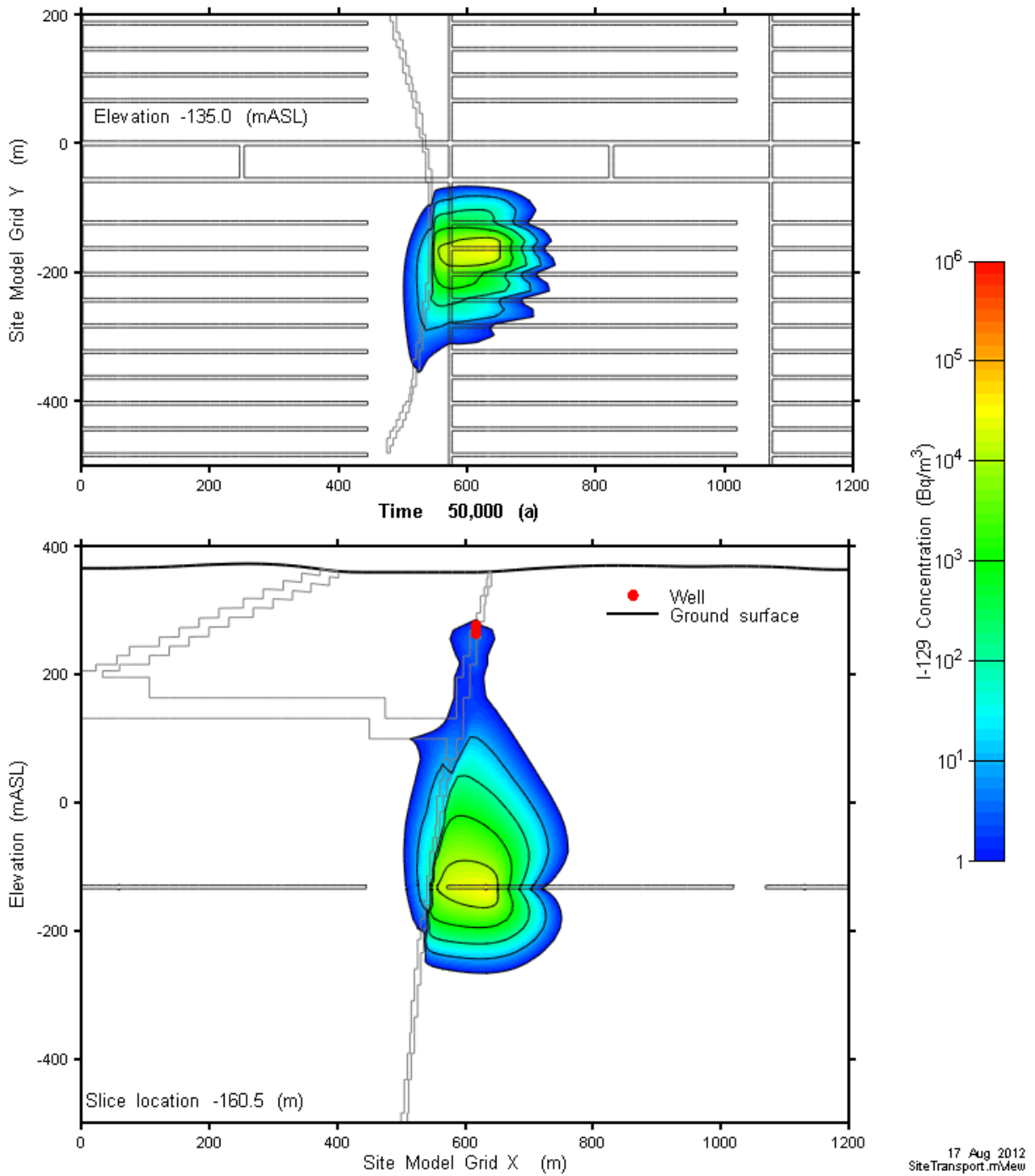


Figure 7-54: Site-Scale Model - Reference Case I-129 Concentration at 50,000 Years

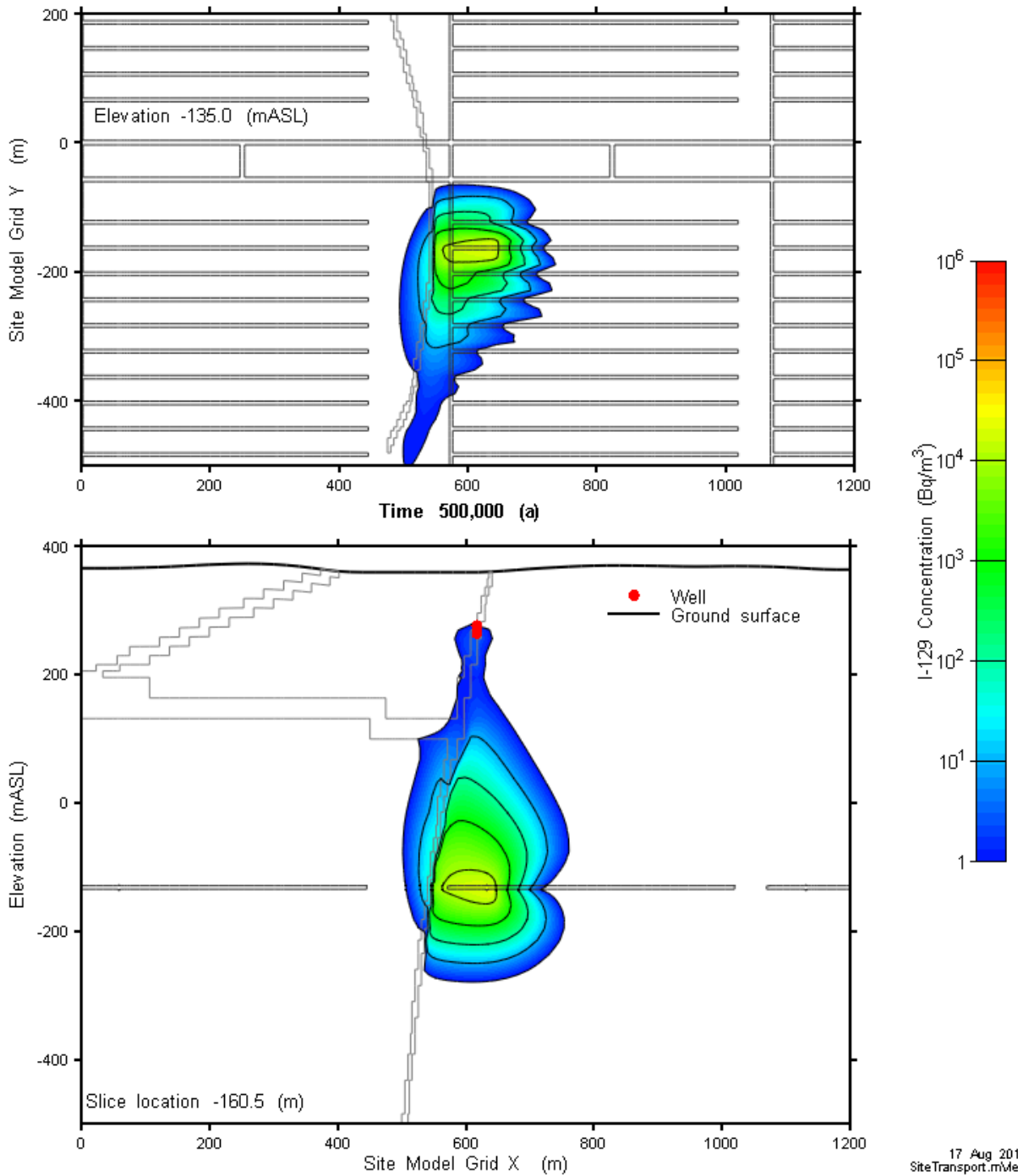


Figure 7-55: Site-Scale Model - Reference Case I-129 Concentration at 500,000 Years

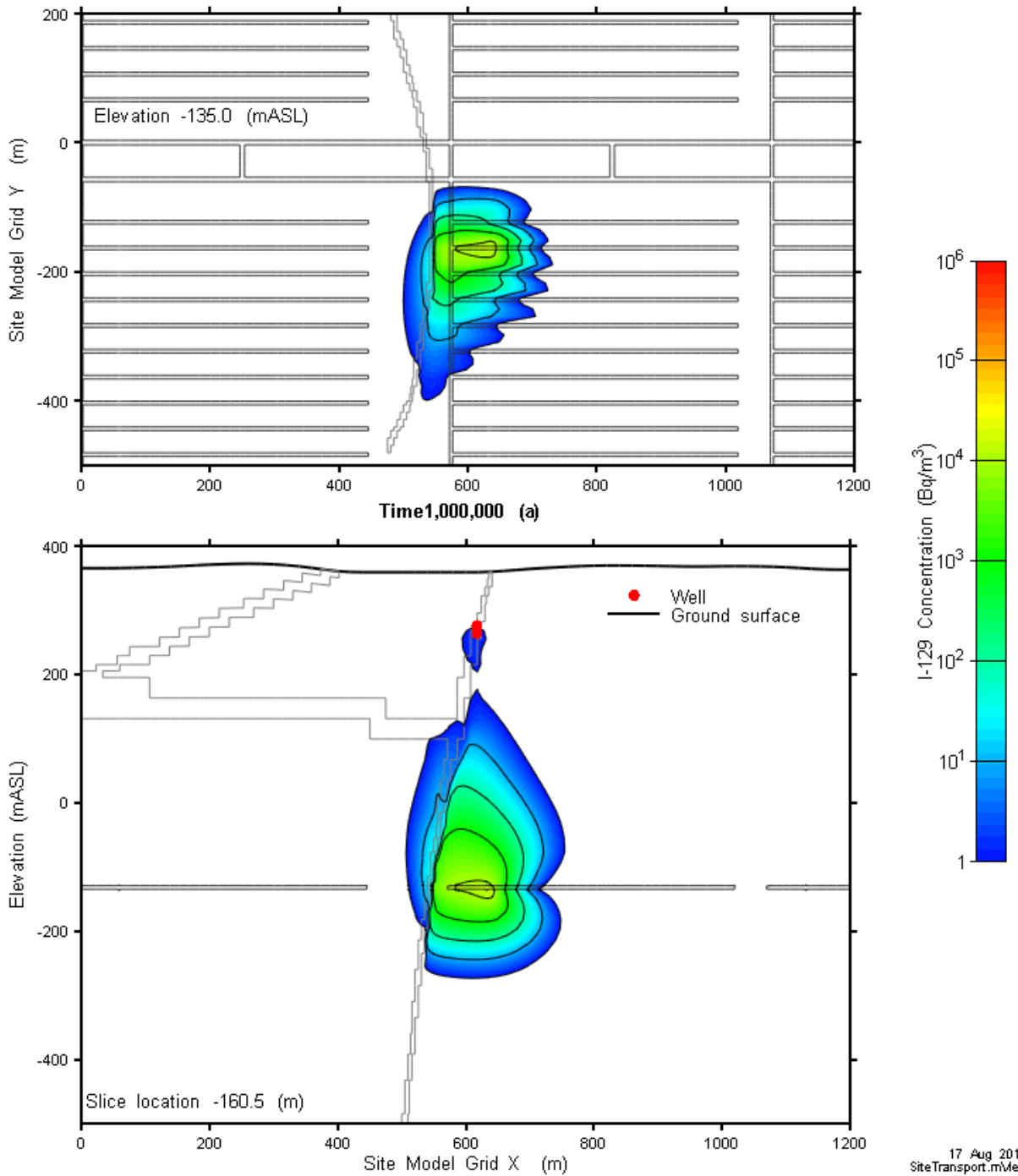


Figure 7-56: Site-Scale Model – Reference Case I-129 Concentration at 1 Million Years

In Figure 7-56, the discontinuity that develops directly below the well at about the 200 mASL depth is caused by the continuing evolution of the plume. This is illustrated in Figure 7-57 which highlights the structure of the plume at 1 million years, with isovolumes shown at concentrations of 1, 10, and 100 Bq/m³. The outermost isovolumes indicates the general structure of the flow-field. Flow above the repository horizon is upwards through the fracture towards the well (marked in red), while below the repository flow is towards the fractures connected to the river discharge zone. The core of the plume remains concentrated in the vicinity of the release. The discontinuity occurs because the 1 Bq/a concentration contour has evolved such that it no longer intersects the vertical slice used to generate Figure 7-56.

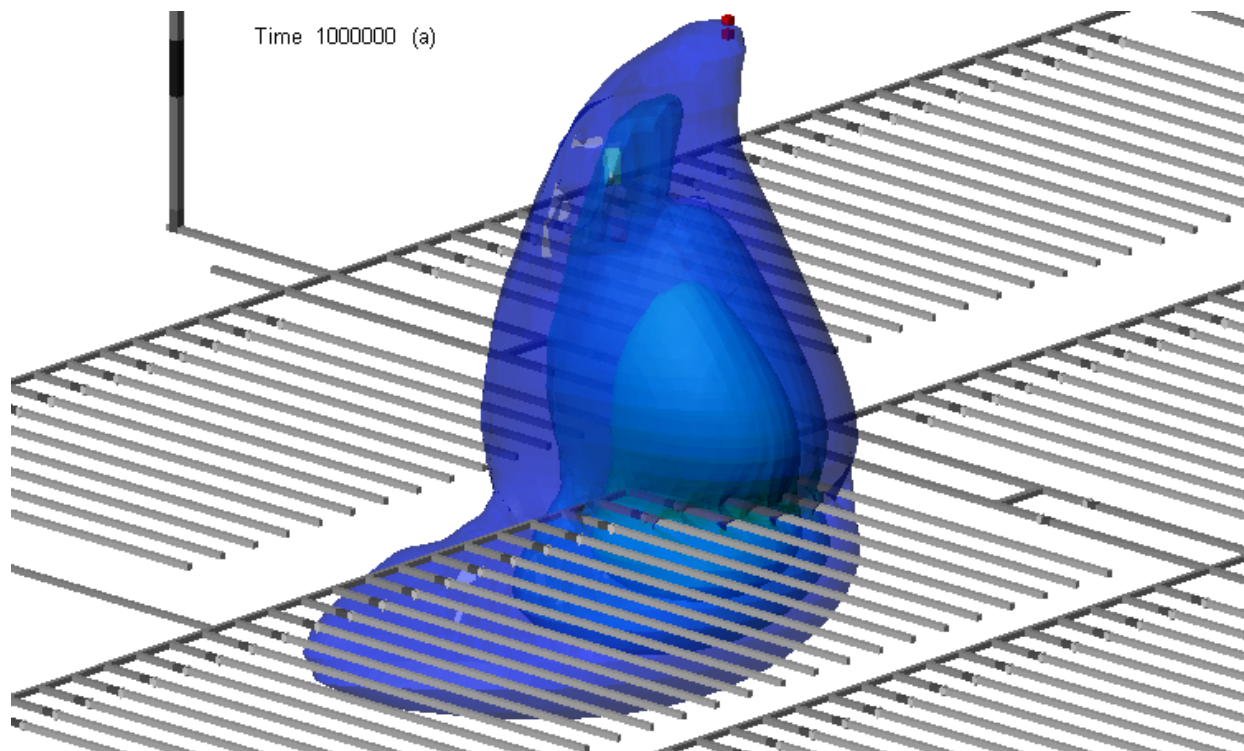


Figure 7-57: Site-Scale Model – Reference Case 3D View of I-129 Plume at 1 Million Years

Figure 7-58 presents radionuclide transport rates to the well for all simulated nuclides. These are useful metrics of overall transport and provide a means of comparing various cases. Sn-126, U-234 and U-238 do not reach the well due to retention and decay in the engineered barrier system and geosphere near the repository.

The time of peak concentration for I-129 at the well is about 103,000 years. The times of peak concentrations for the other radionuclides are as indicated on the figure.

The peak I-129 transport rate is 1675 Bq/a.

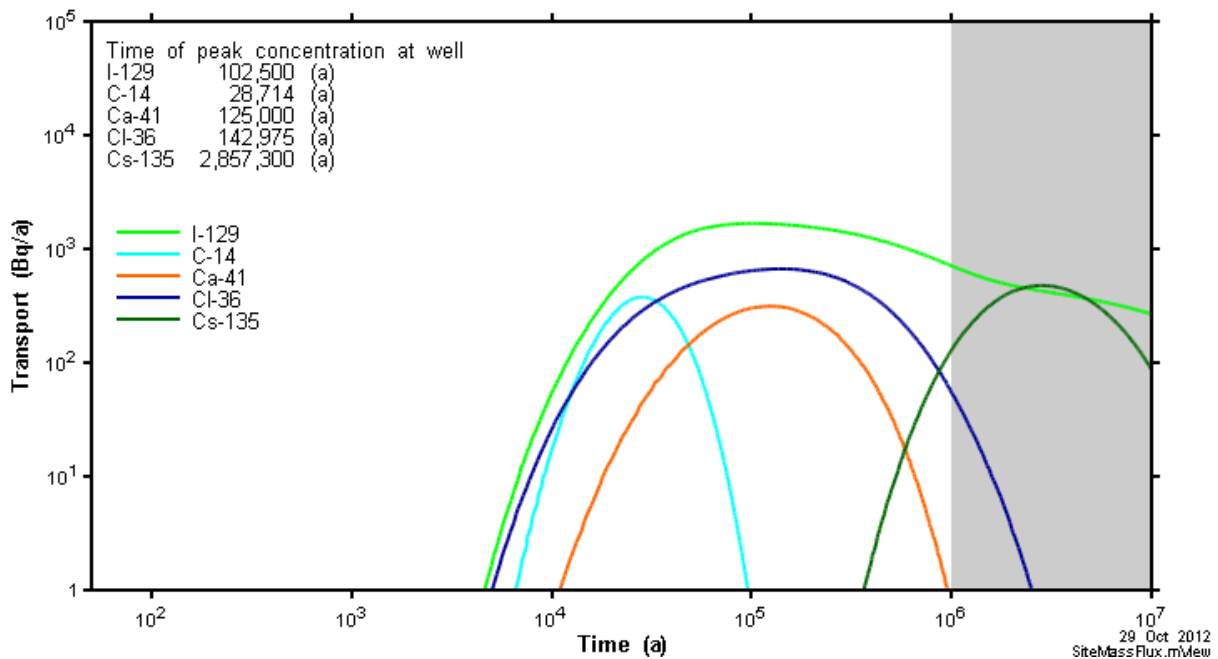


Figure 7-58: Site-Scale Model - Reference Case Radionuclide Transport to Well

7.7.2.2.3 Sensitivity to Changes in Geosphere Hydraulic Conductivity

Transport results for the three geosphere hydraulic conductivity sensitivity cases defined in Section 7.2.1 are presented here. Hydraulic conductivities for all cases are listed in Table 7-16.

Sensitivity 1

This corresponds to the Sensitivity Case 1 profile defined in Chapter 2. Hydraulic conductivities (m/s) in the bedrock are ten times greater than those in the Reference Case. Specifically:

- Zone 1 (10 – 150 m) = from 2×10^{-9} to 2×10^{-8}
- Zone 2 (150 – 700 m) = from 4×10^{-11} to 4×10^{-10}
- Zone 3 (700 – 1500 m) = from 1×10^{-11} to 1×10^{-10}

Figure 7-59 through Figure 7-64 show I-129 plume development over time. The plume reaches the fracture after 1000 a. At 50 ka, the plume is more dispersed in the horizontal plane as compared to the Reference Case, while its vertical structure (which is driven by the well and

flow through the fracture), is similar. The plume reaches an almost steady-state structure from this point until after 500,000 years when it responds to the reduction in source concentration.

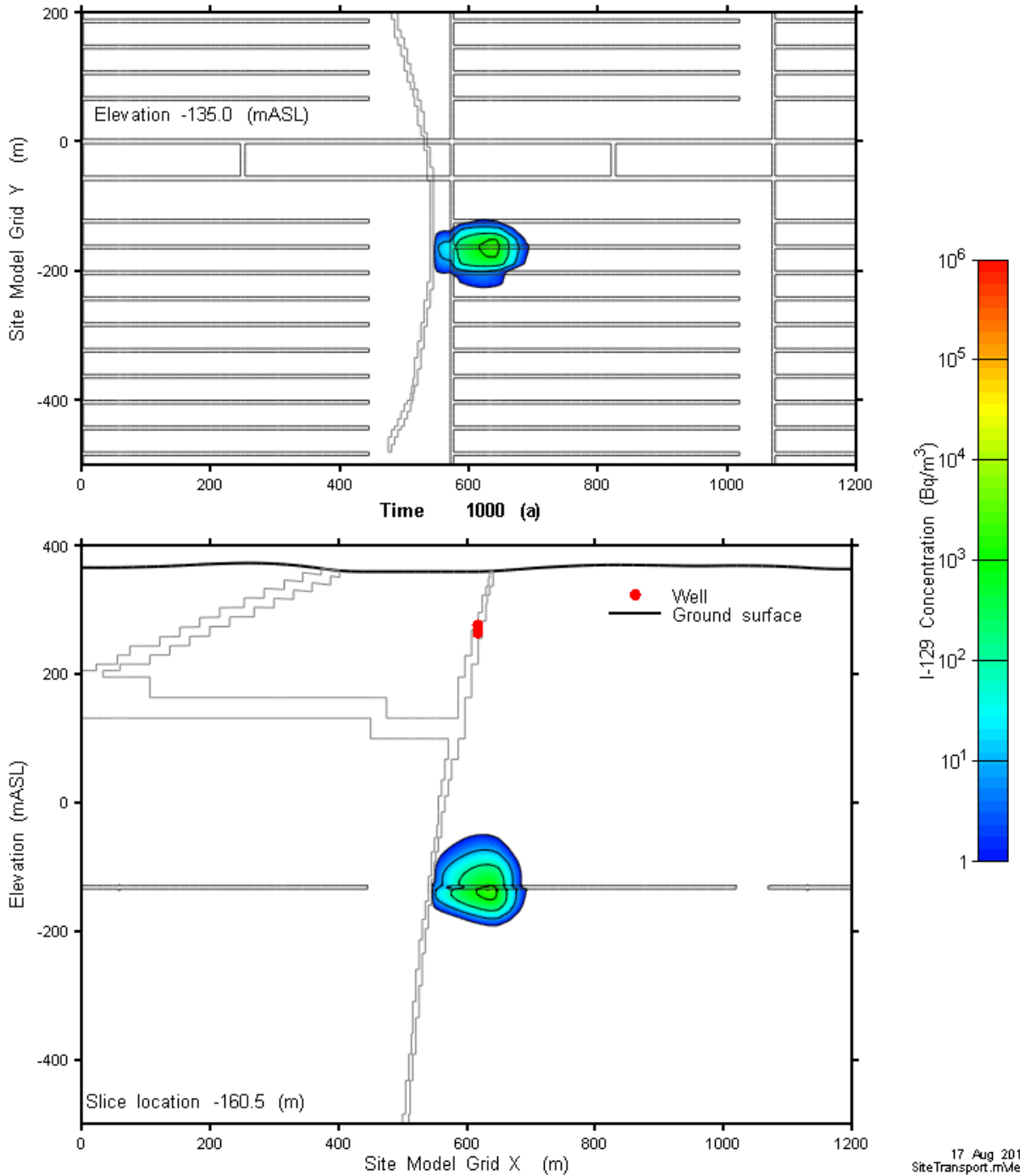


Figure 7-59: Site-Scale Model - Hydraulic Conductivity Increase by a Factor of 10: I-129 Concentration at 1 ka

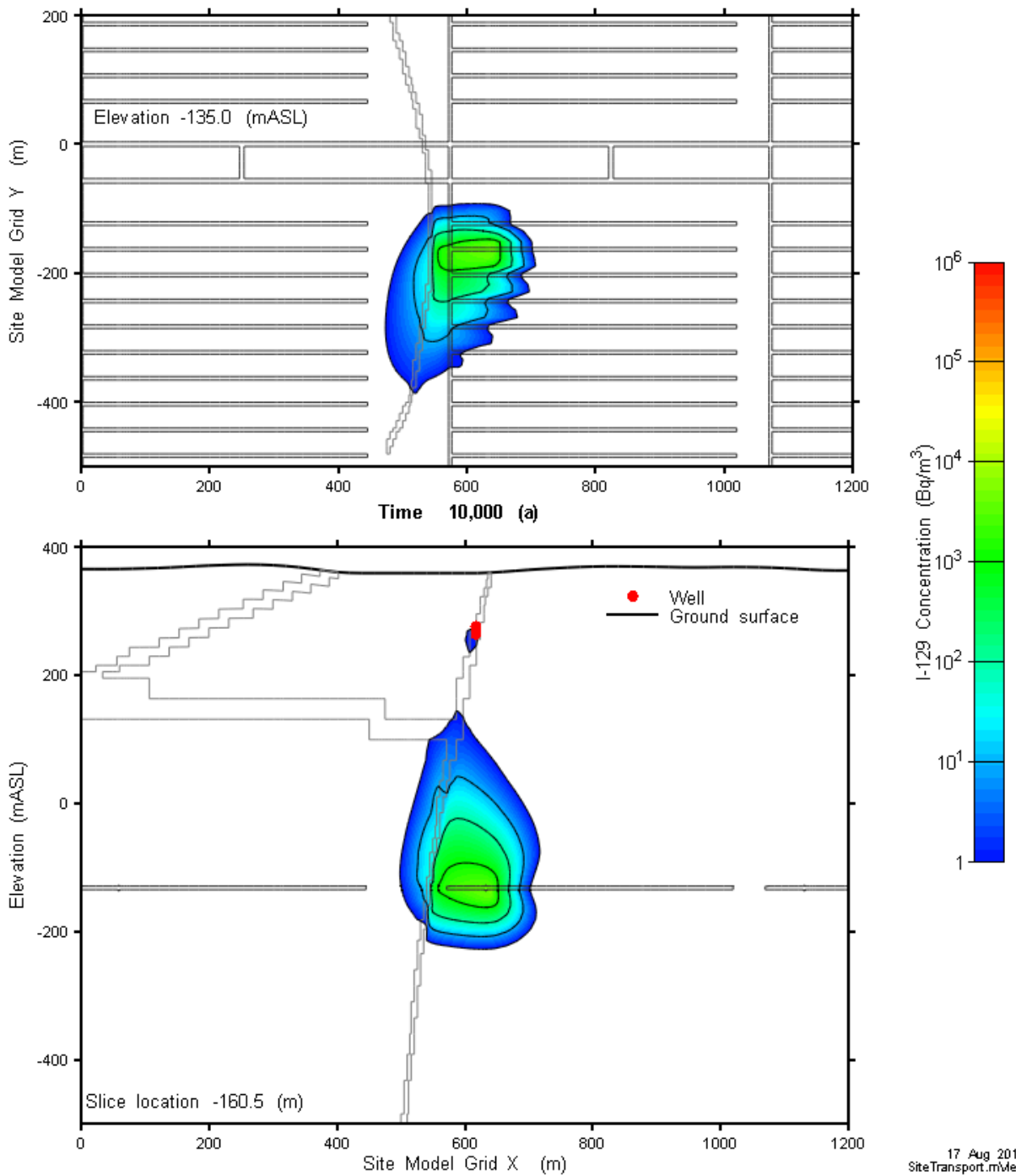


Figure 7-60: Site-Scale Model - Hydraulic Conductivity Increase by a Factor of 10: I-129 Concentration at 10 ka

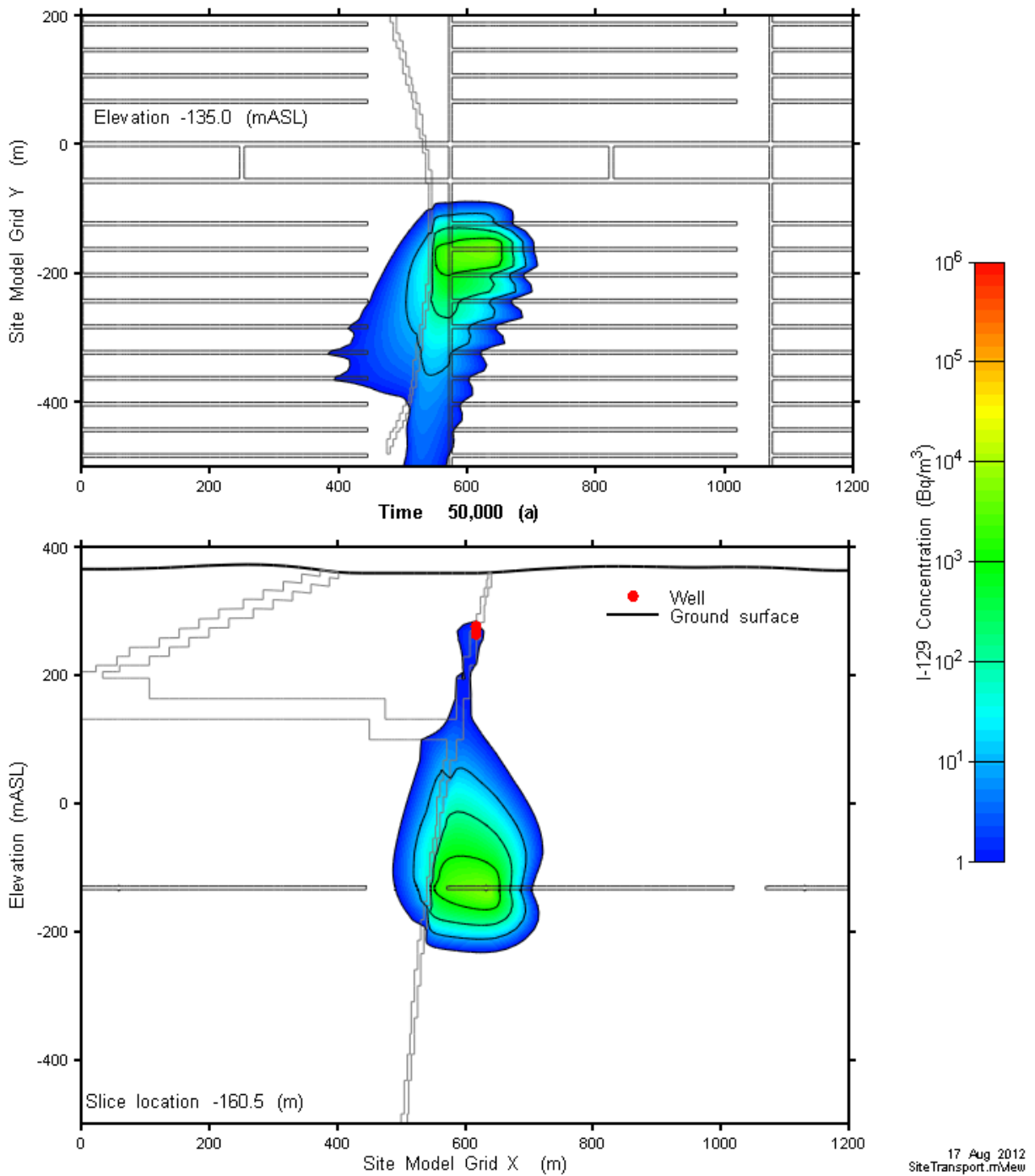


Figure 7-61: Site-Scale Model - Hydraulic Conductivity Increase by a Factor of 10: I-129 Concentration at 50 ka

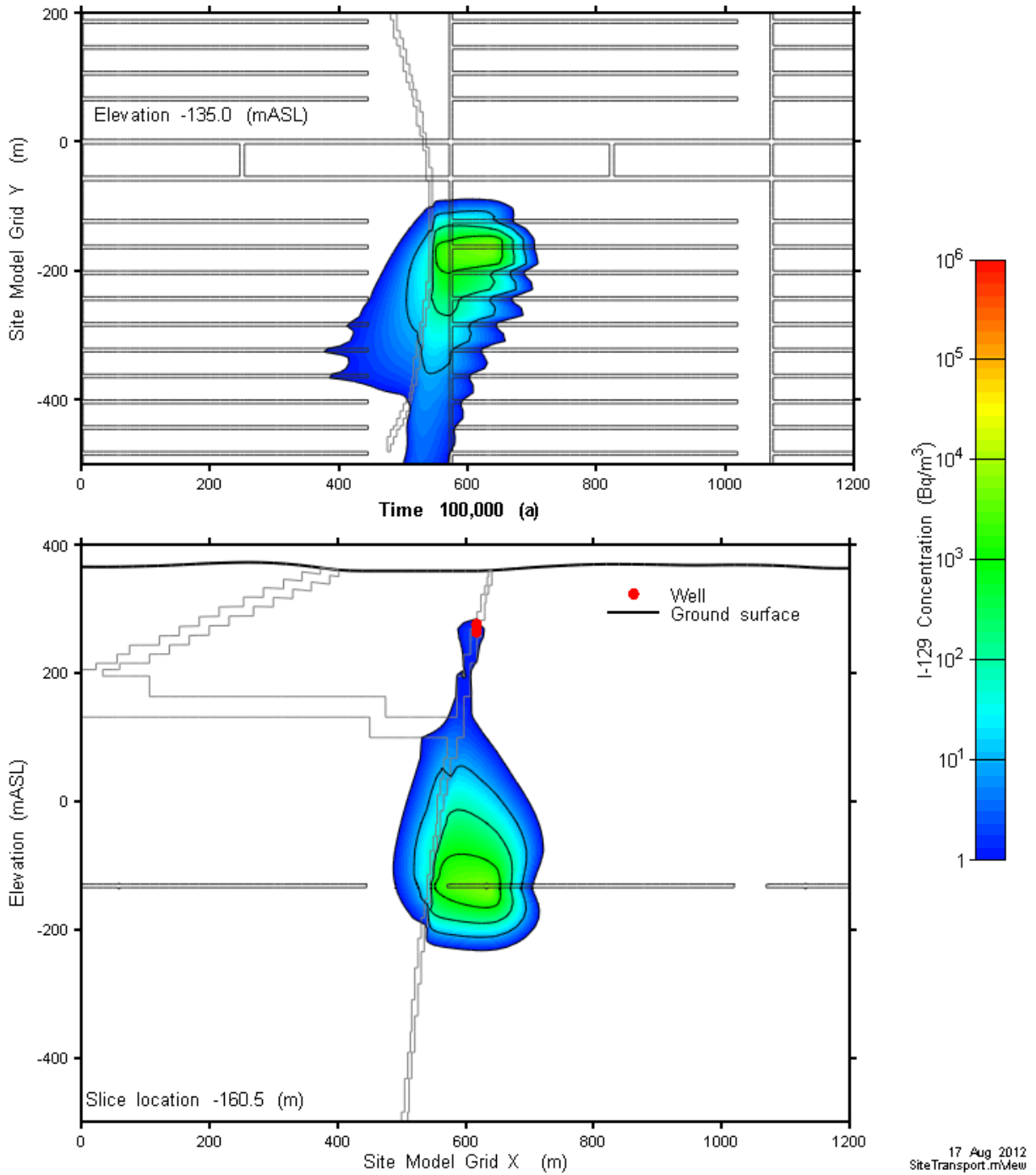


Figure 7-62: Site-Scale Model - Hydraulic Conductivity Increase by a Factor of 10: I-129 Concentration at 100 ka

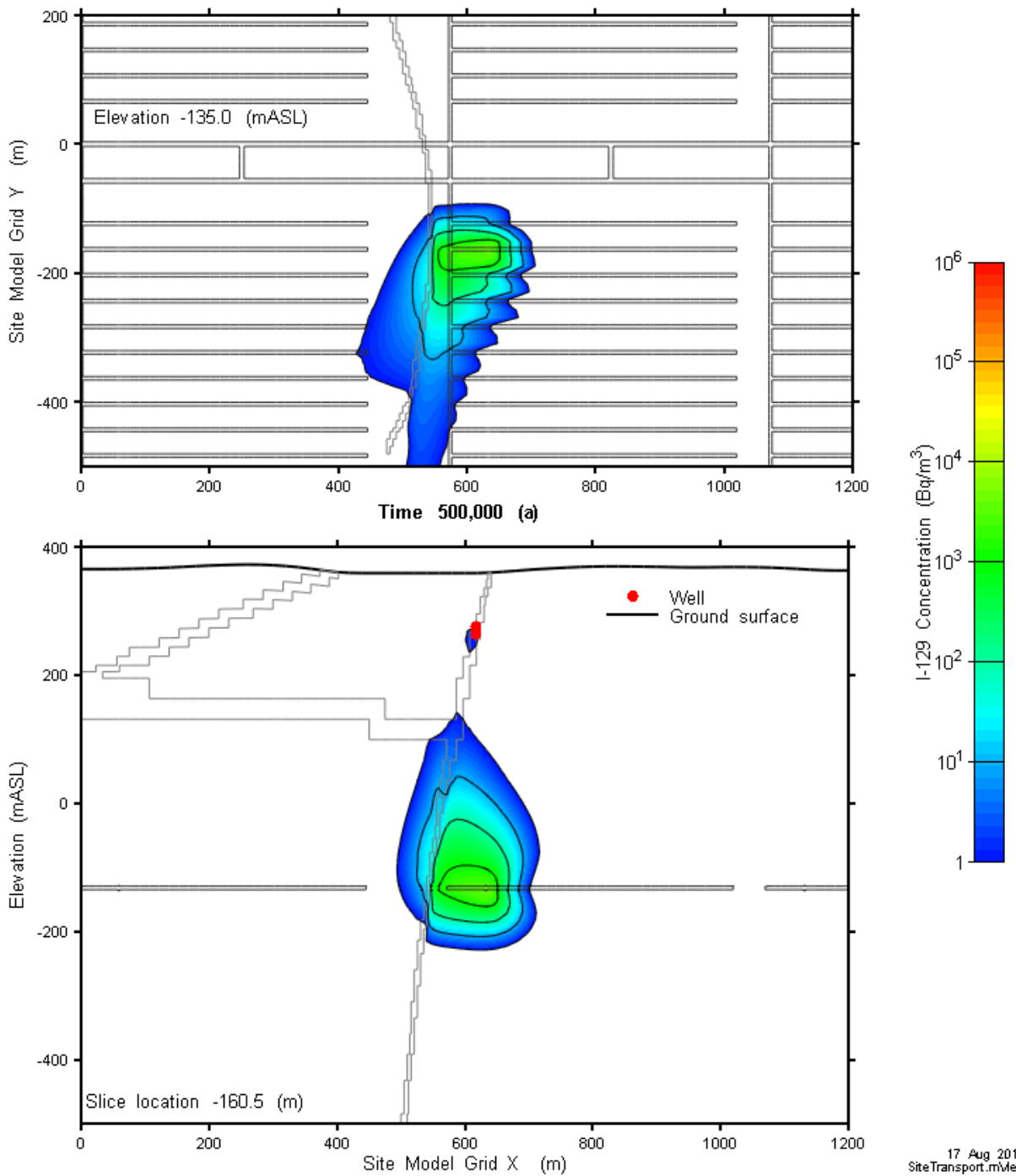


Figure 7-63: Site-Scale Model - Hydraulic Conductivity Increase by a Factor of 10: I-129 Concentration at 500 ka

The 'discontinuity' in the concentration contour shown in Figure 7-63 occurs for the same reason as discussed earlier for Figure 7-56.

Figure 7-64 shows the radionuclide transport rates to the well for all simulated nuclides. This can be compared with similar results for the Reference Case shown in Figure 7-58.

The results shown that I-129 transport rate reaches a peak value of 1083 Bq/a at 70,000 years. The rate is lower than in the Reference Case (1675 Bq/a) due to the greater extent of horizontal transport which moves some mass towards the river discharge rather than the well. The radionuclide arrival times are also earlier as would be expected in a higher hydraulic conductivity geosphere. These earlier times result in higher activity levels because of the shorter time period available for radioactive decay. This is illustrated by the C-14 transport curve which now reaches a peak value about ten times higher than that for I-129.

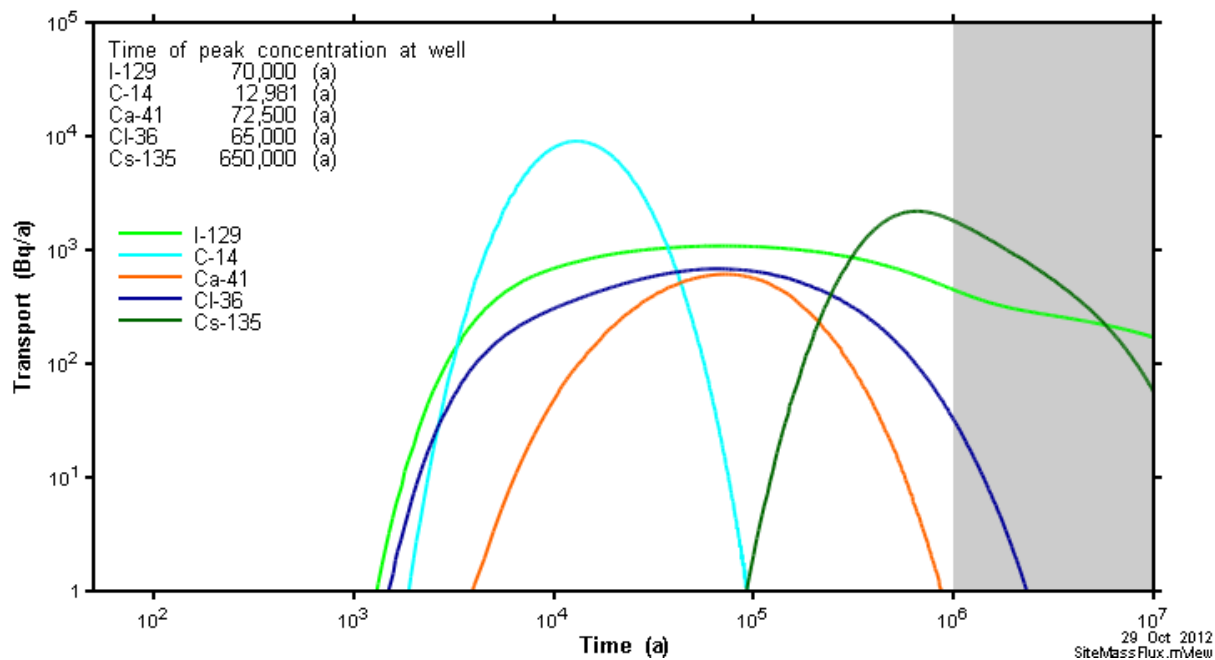


Figure 7-64: Site-Scale Model - Hydraulic Conductivity Increase by a Factor of 10: Radionuclide Transport to Well

Figure 7-65 and Figure 7-66 illustrate the behaviour of the C-14 plume at 10,000 years and 50,000 years. The plume extent decreases at longer times due to radioactive decay.

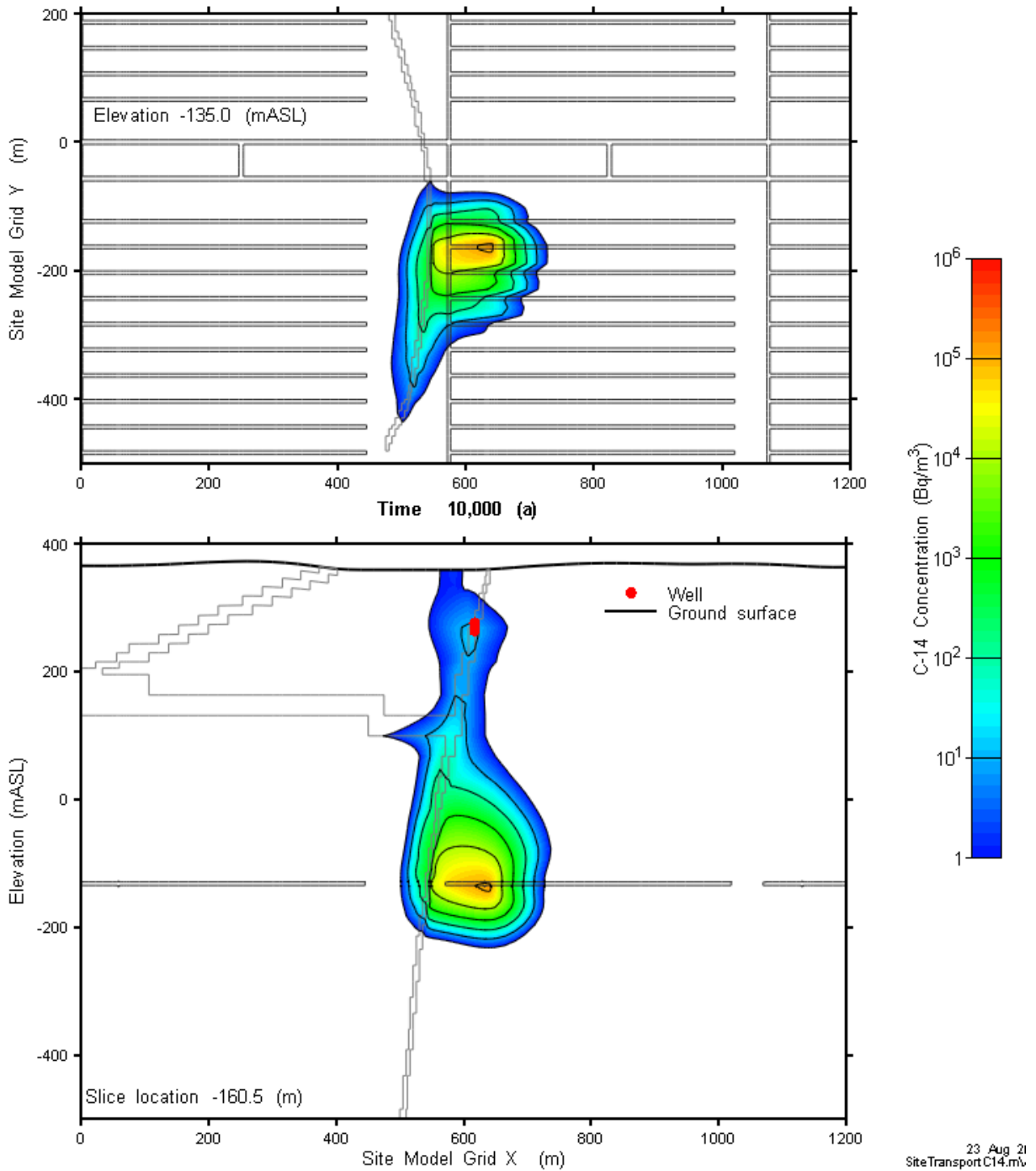


Figure 7-65: Site-Scale Model - Hydraulic Conductivity Increase by a Factor of 10: C-14 Concentration at 10 ka

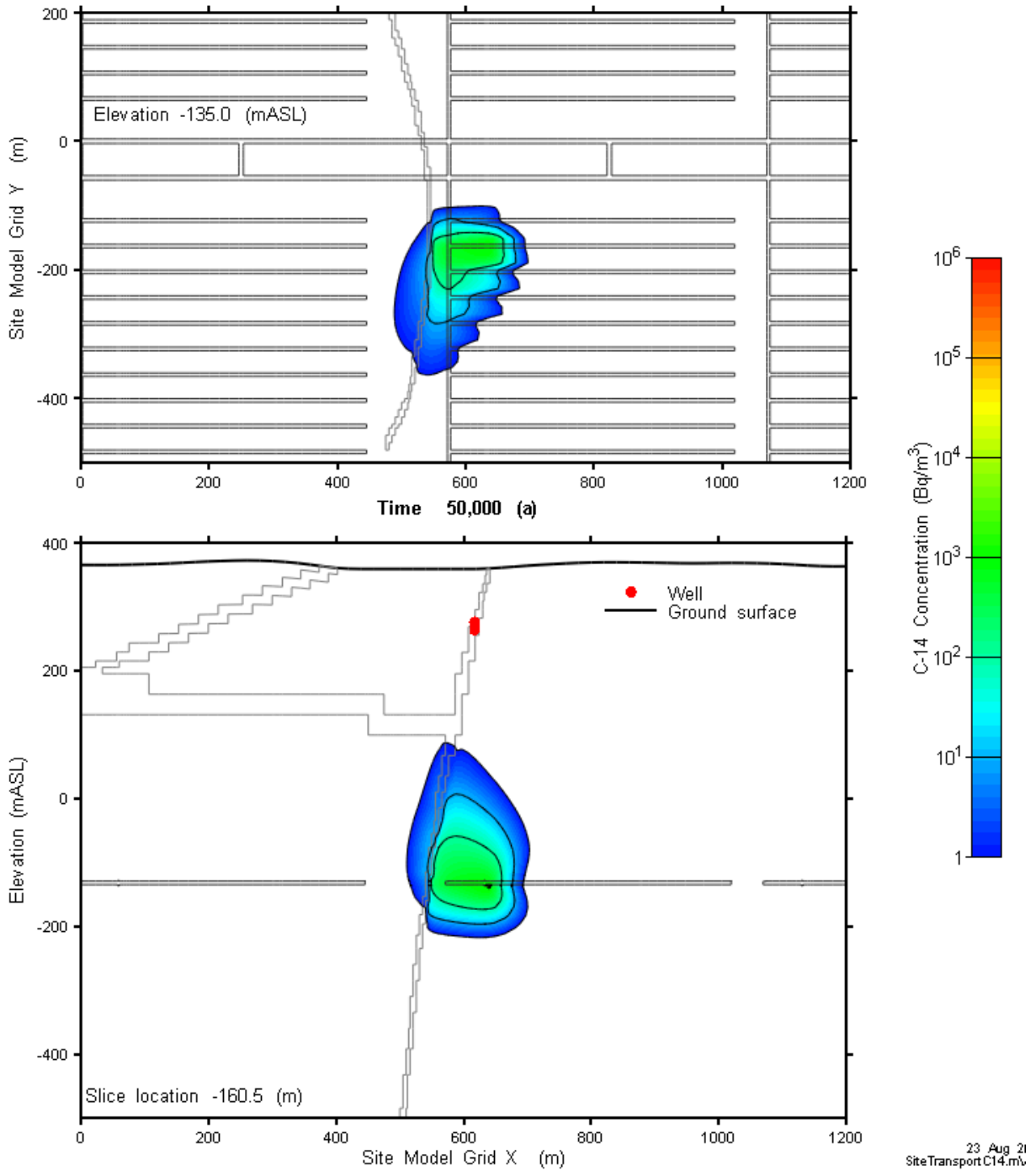


Figure 7-66: Site-Scale Model - Hydraulic Conductivity Increase by a Factor of 10: C-14 Concentration at 50 ka

Sensitivity 2

This corresponds to the Sensitivity Case 2 profile defined in Chapter 2. Hydraulic conductivities (m/s) in the bedrock are 10 times less than those in the Reference Case. Specifically:

- Zone 1 (10 – 150 m) = from 2×10^{-9} to 2×10^{-10}
- Zone 2 (150 – 700 m) = from 4×10^{-11} to 4×10^{-12}
- Zone 3 (700 – 1500 m) = from 1×10^{-11} to 1×10^{-12}

Figure 7-67 through Figure 7-70 show I-129 plume development over time. The plume extent is reduced as compared to the Reference Case and is of a marked diffusive character. Advective flow along the rooms and damaged zones is still apparent, indicated by the “dimples” in the plume at these locations.

The I-129 transport rate reaches a peak value of 1318 Bq/a at 375,000 years.

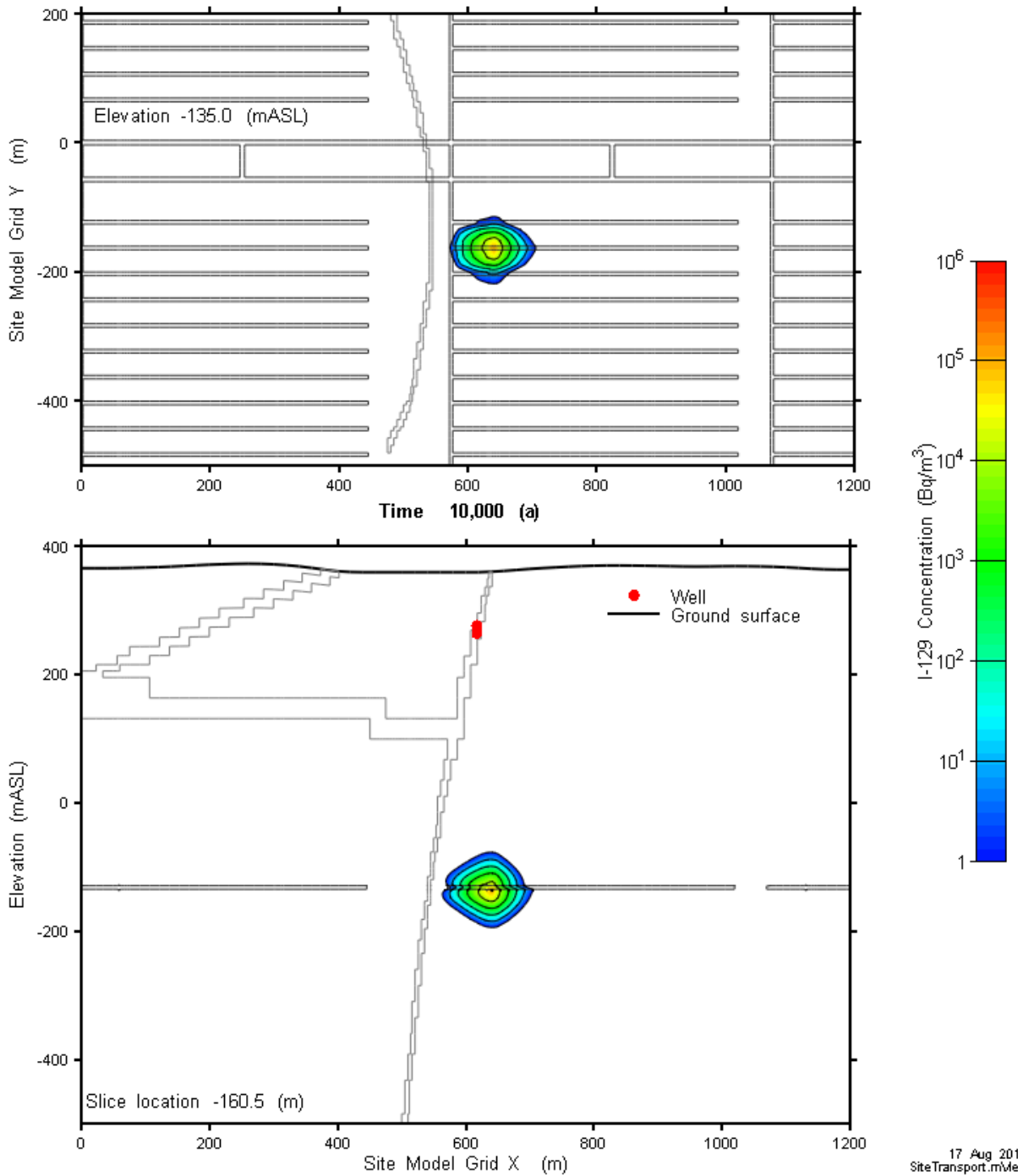


Figure 7-67: Site-Scale Model - Hydraulic Conductivity Decrease by a Factor of 10: I-129 Concentration at 10 ka

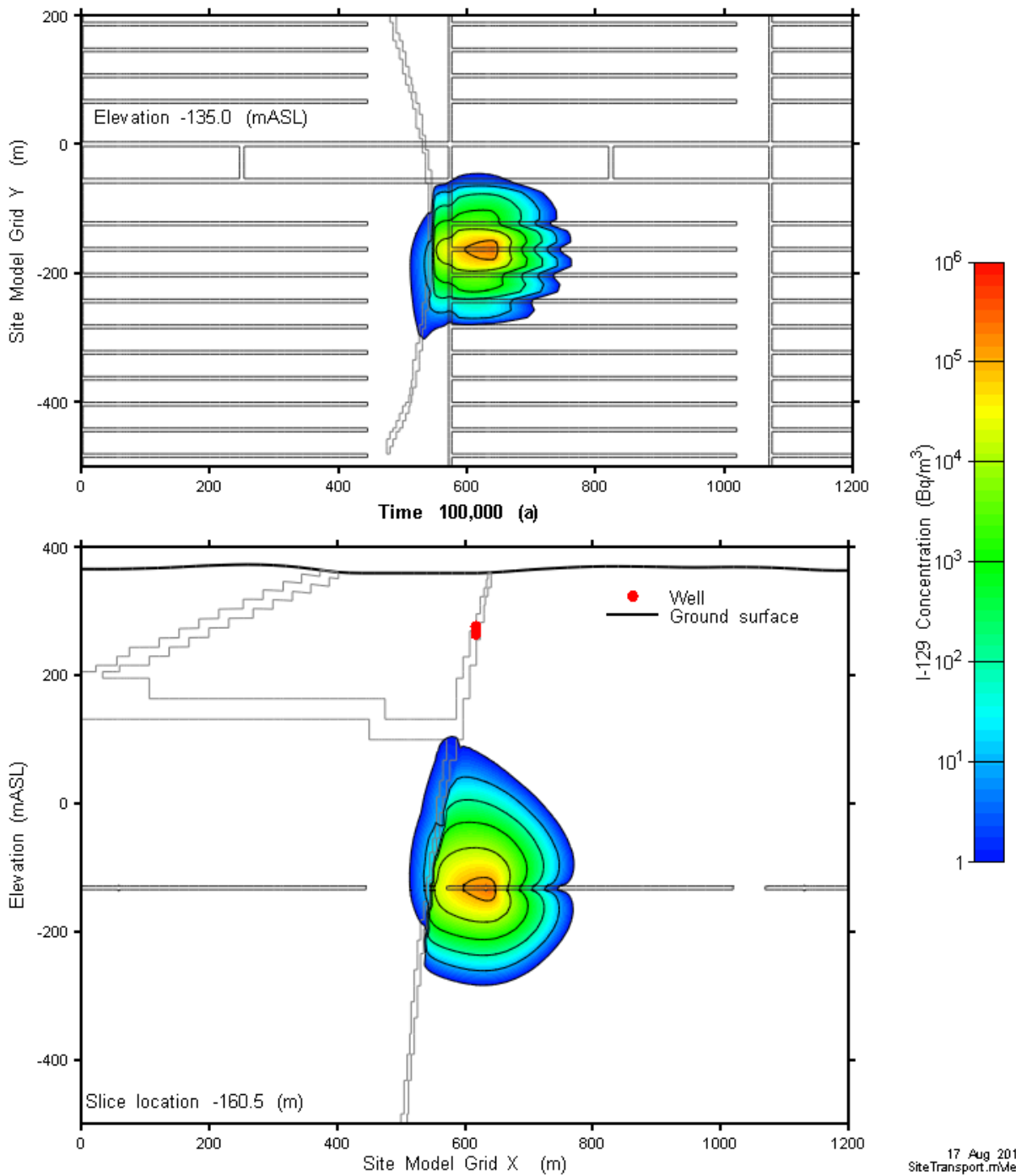


Figure 7-68: Site-Scale Model - Hydraulic Conductivity Decrease by a Factor of 10: I-129 Concentration at 100 ka

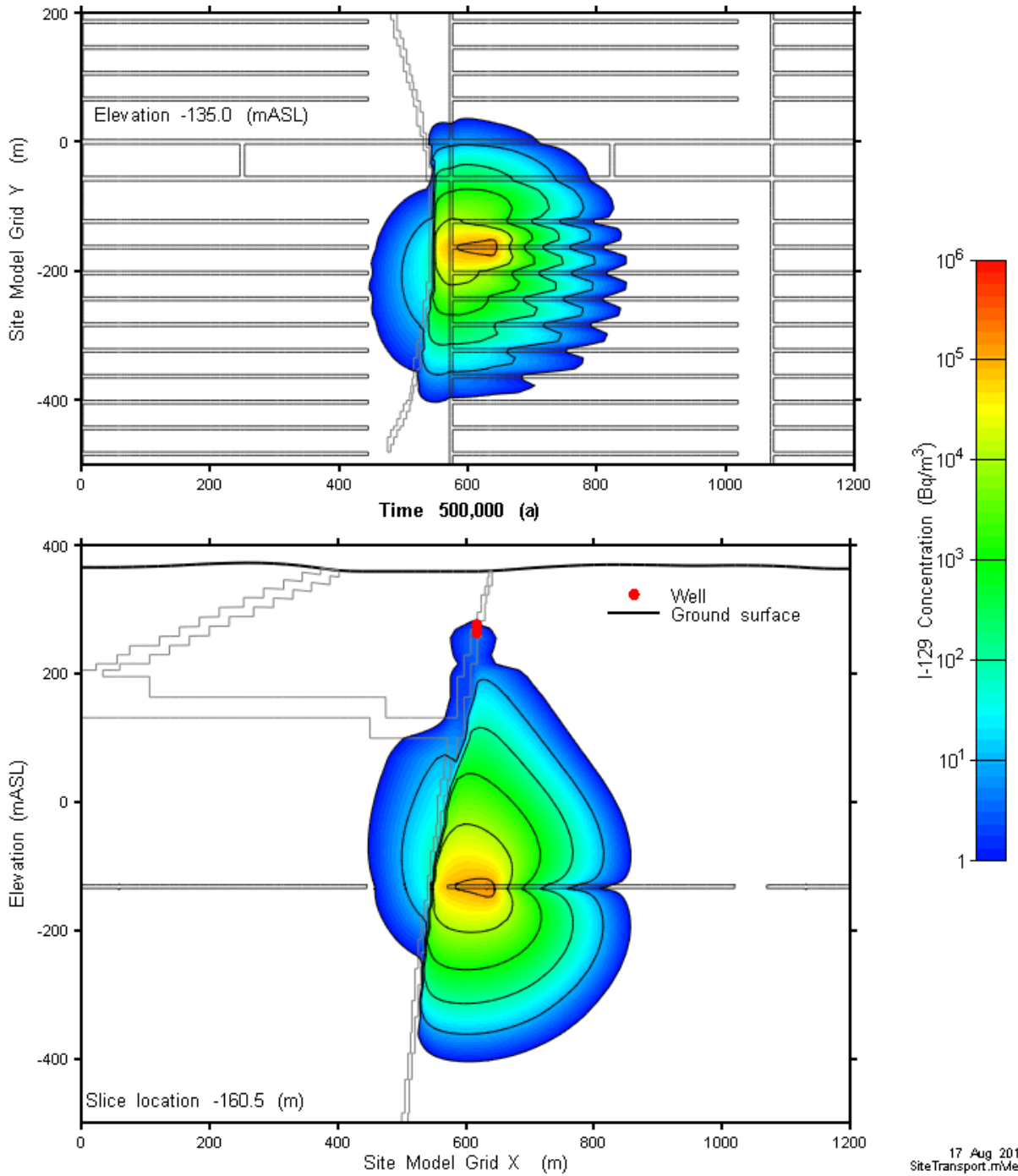


Figure 7-69: Site-Scale Model - Hydraulic Conductivity Decrease by a Factor of 10: I-129 Concentration at 500 ka

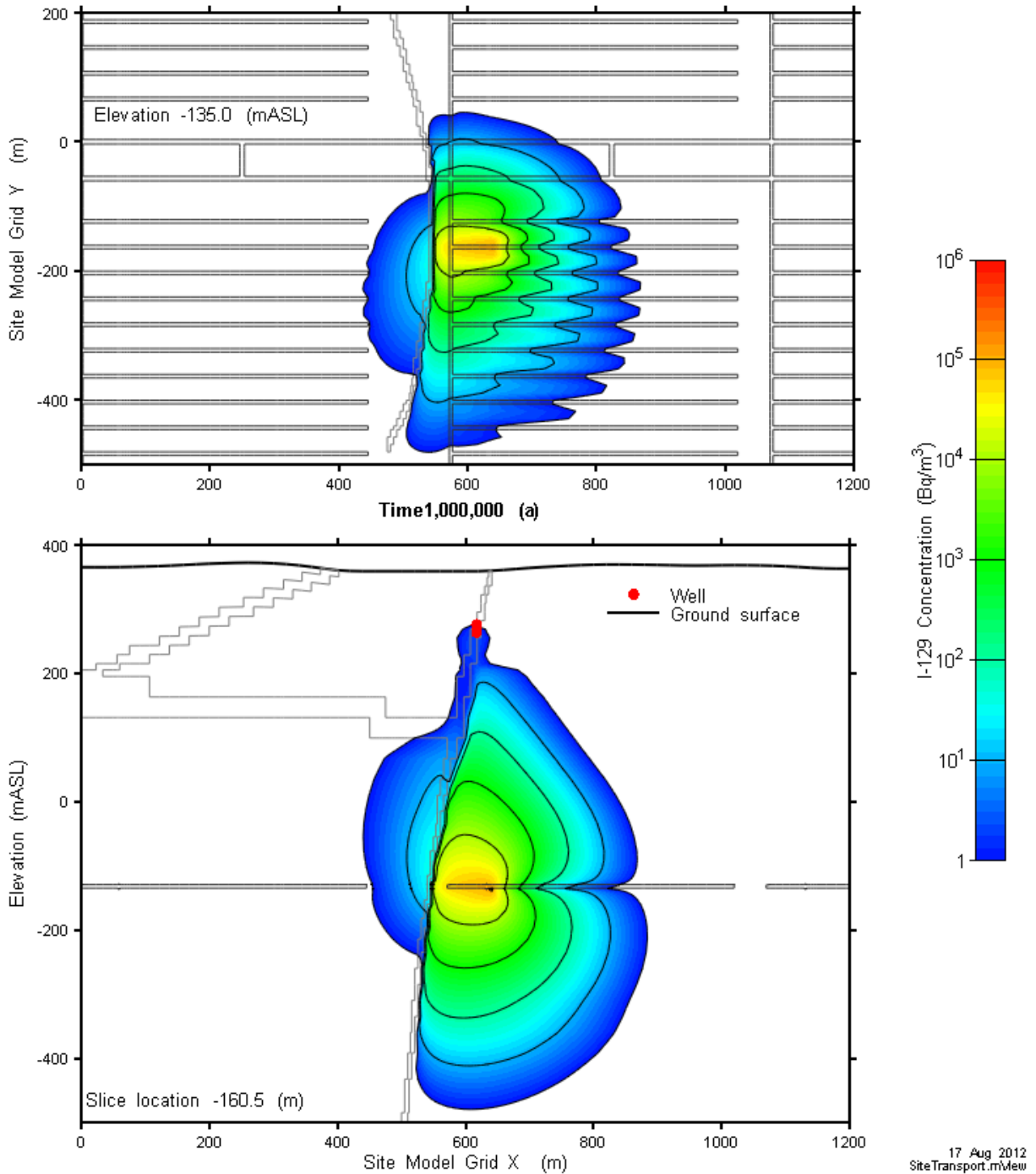


Figure 7-70: Site-Scale Model - Hydraulic Conductivity Decrease by a Factor of 10: I-129 Concentration at 1 Ma

Sensitivity 3

This corresponds to the Sensitivity Case 3 profile defined in Chapter 2. Hydraulic conductivities (m/s) in the bedrock are 100 times less than those in the Reference Case. Specifically:

- Zone 1 (10 – 150 m) = from 2×10^{-9} to 2×10^{-11}
- Zone 2 (150 – 700 m) = from 4×10^{-11} to 4×10^{-13}
- Zone 3 (700 – 1500 m) = from 1×10^{-11} to 1×10^{-13}

Figure 7-71 through Figure 7-74 show I-129 plume development over time. The plume extent shows more diffusive characteristics as compared to the Reference Case than does the previously discussed Sensitivity Case 2. Advective flow along the rooms and damaged zones is still apparent, indicated by the “dimples” in the plume at these locations.

I-129 transport rate reaches a peak value of 602 Bq/a at 1,151,000 years.

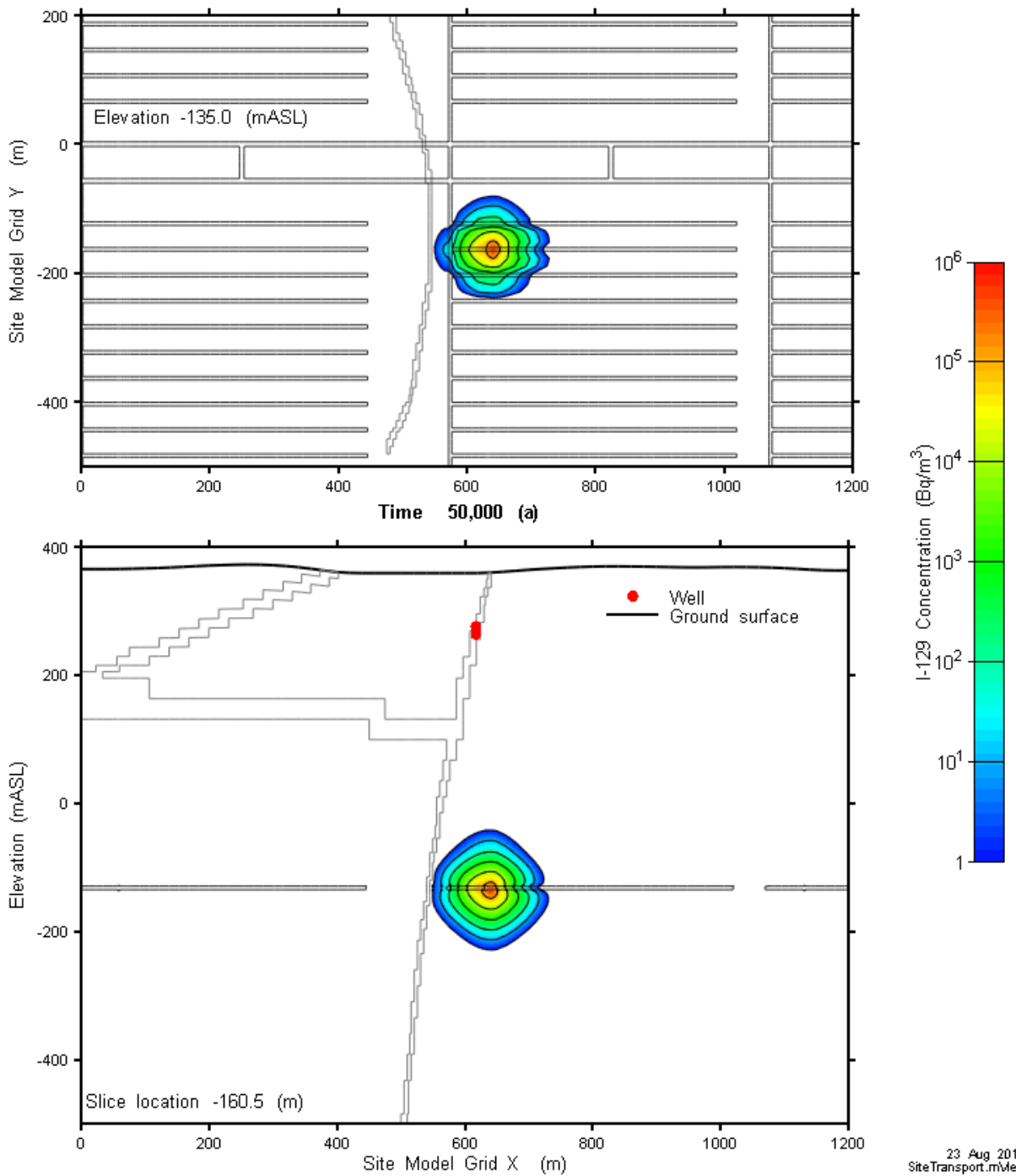


Figure 7-71: Site-Scale Model - Hydraulic Conductivity Decrease by a Factor of 100: I-129 Concentration at 50 ka

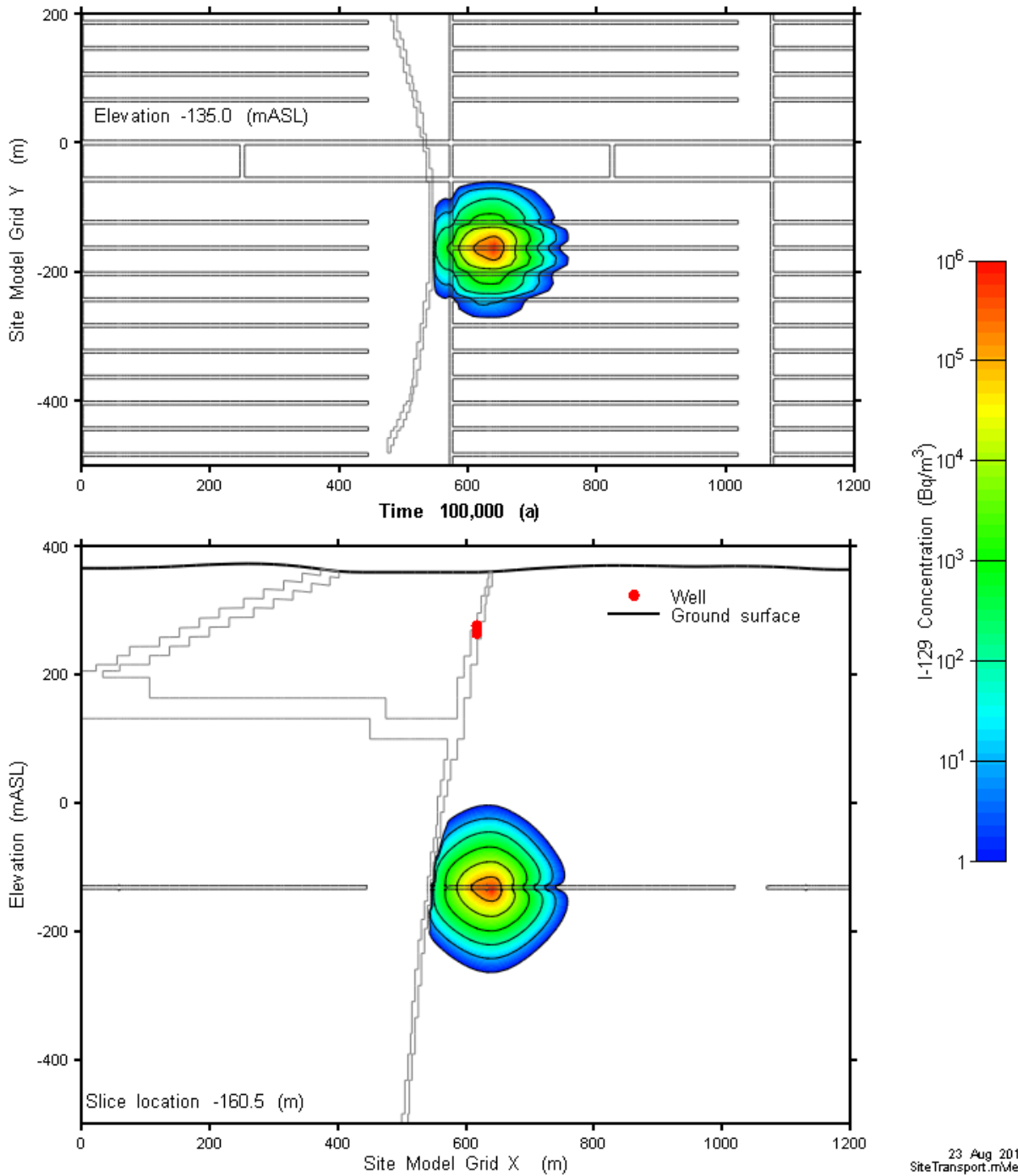


Figure 7-72: Site-Scale Model - Hydraulic Conductivity Decrease by a Factor of 100: I-129 Concentration at 100 ka

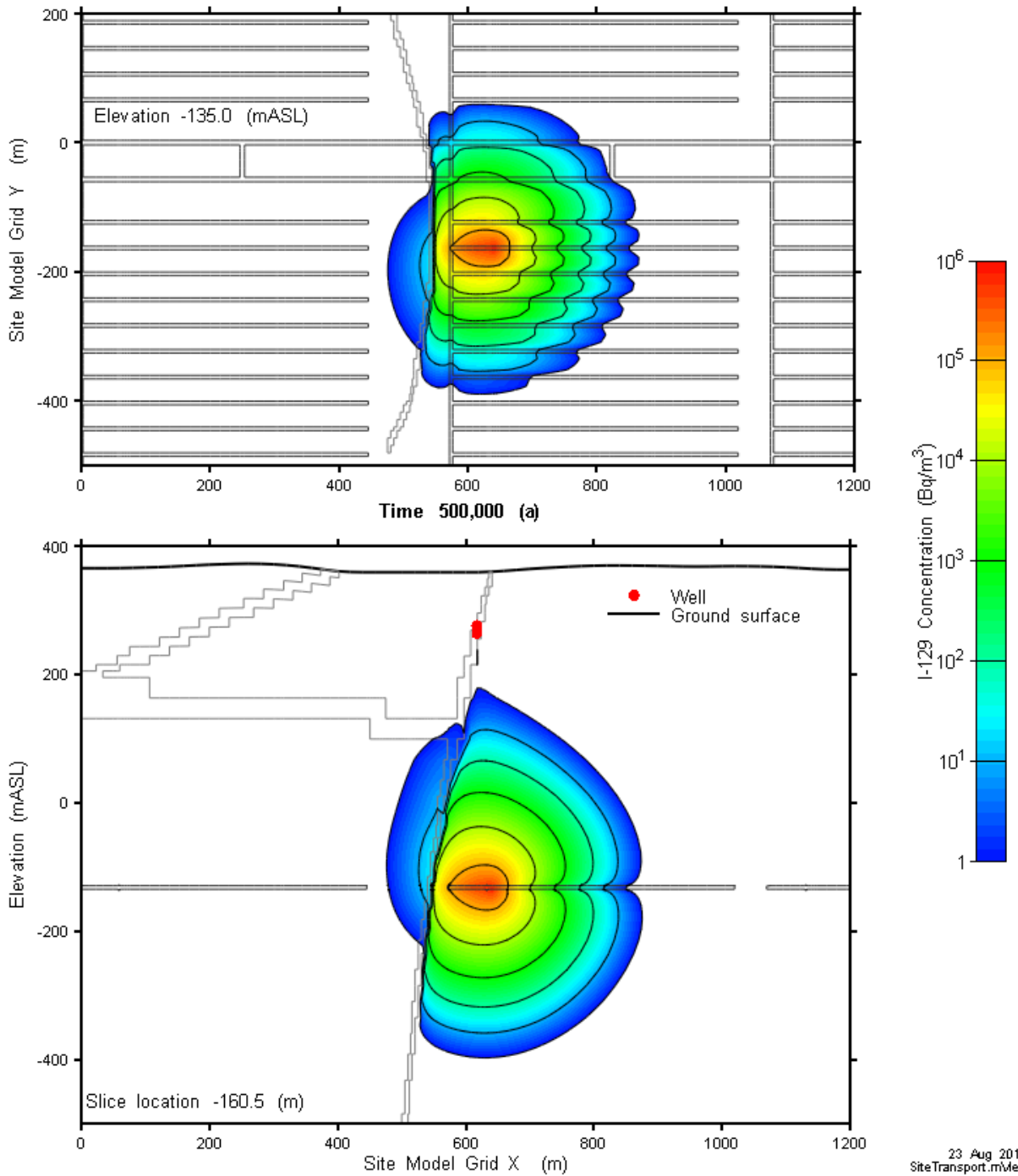


Figure 7-73: Site-Scale Model - Hydraulic Conductivity Decrease by a Factor of 100: I-129 Concentration at 500 ka

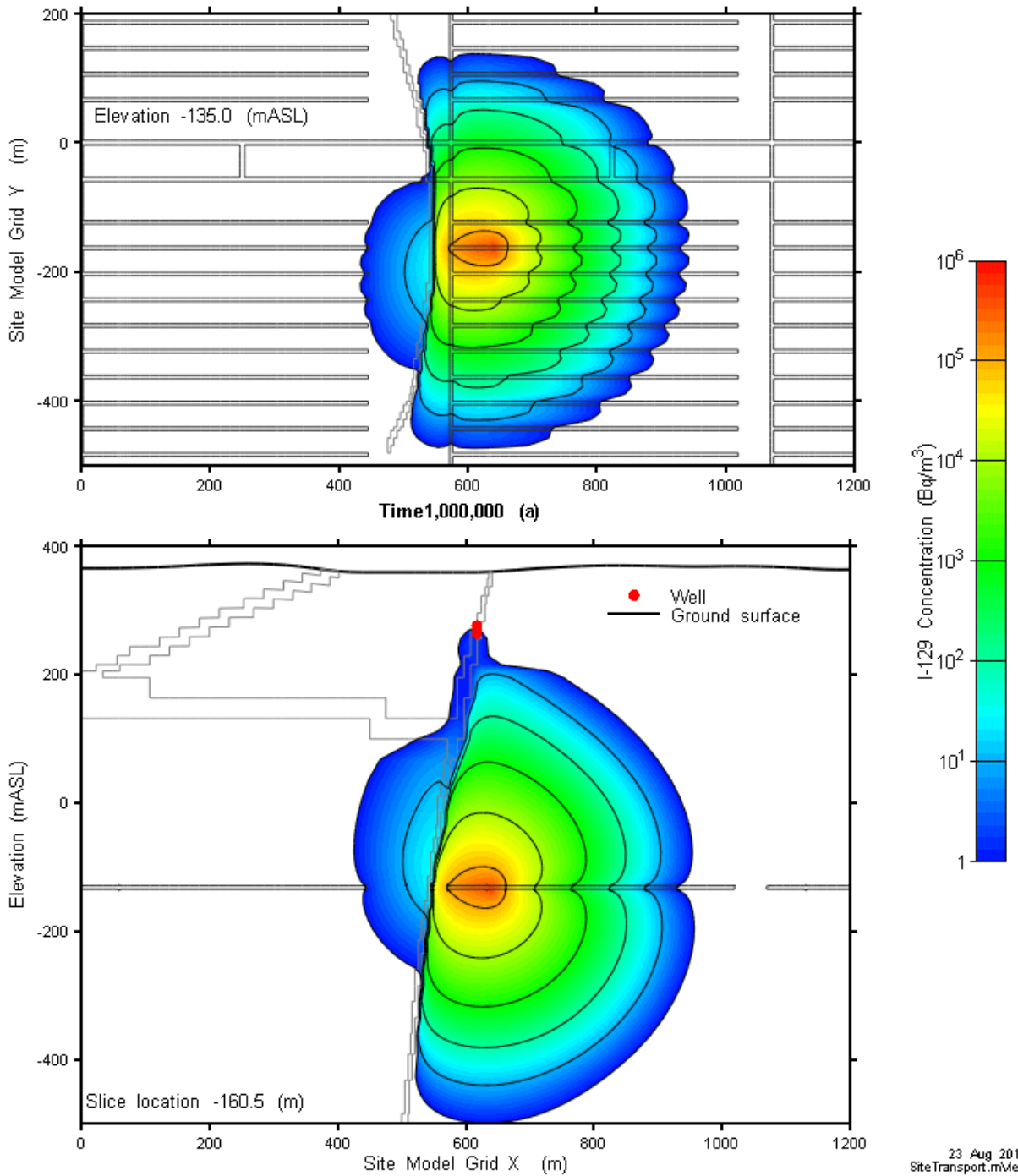


Figure 7-74: Site-Scale Model - Hydraulic Conductivity Decrease by a Factor of 100: I-129 Concentration at 1 Ma

Sensitivity Case Summary:

Figure 7-75 summarizes the results for I-129 transport to the well for the Reference Case and the three geosphere hydraulic conductivity sensitivity cases.

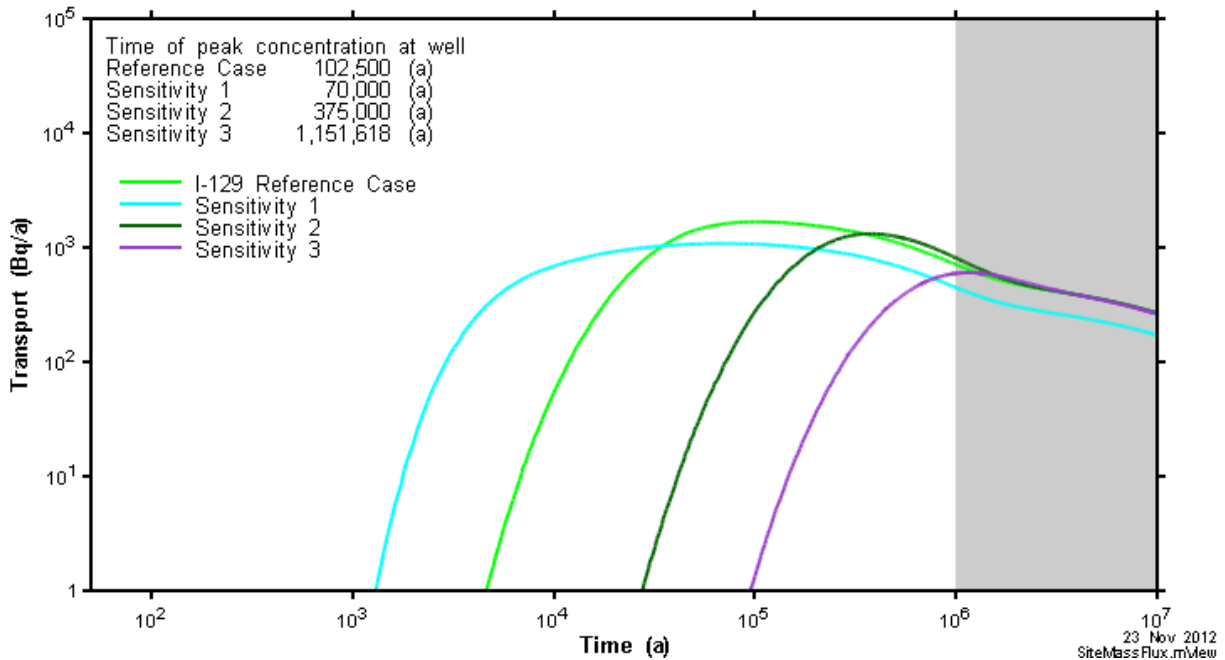


Figure 7-75: Site-Scale Model – Effect of Hydraulic Conductivity on I-129 Transport to the Well

7.7.2.2.4 Sensitivity to Fracture Location

This section examines the effect of varying the distance to the conductive fracture intersecting the repository footprint. In the Reference Case, the fracture is located 25 m from the access tunnel wall opposite the placement room containing the defective container. This is equivalent to a distance of 94 m from the nearest borehole on that side of the repository.

Three sensitivity cases are considered, these being the fracture at 10 m (i.e., 15 m closer to the access tunnel wall), the fracture at 50 m and the fracture at 75 m. The 50 m value is the target design criterion currently contemplated for repository construction.

Figure 7-76 and Figure 7-77 illustrate the locations of the Reference Case and sensitivity case fractures. The sensitivity cases are created by moving the fracture connected to the well horizontally closer / further from the portion of the repository containing the defective containers. Note that although the reference fracture location is physically closer to containers on the other side of the repository (as seen in Figure 7-51), Section 7.7.2.2.1 discusses that more conservative results are obtained for the well location as indicated, and therefore the fracture is

moved to reduce this distance. The well pumping node locations are also modified to ensure the well always intersects the fracture, as shown in Figure 7-77.

For modelling simplicity, the fracture seals were not relocated and only the fracture was moved. This had no effect on the results.

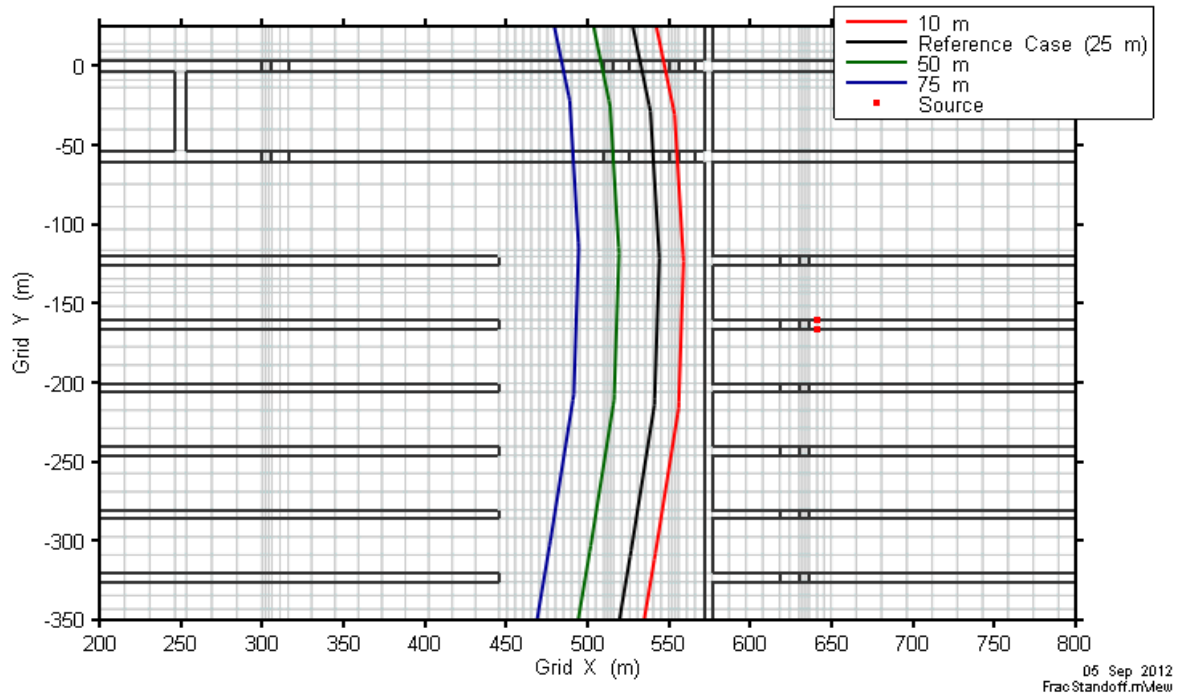


Figure 7-76: Site-Scale Model - Fracture Location Sensitivity Plan View

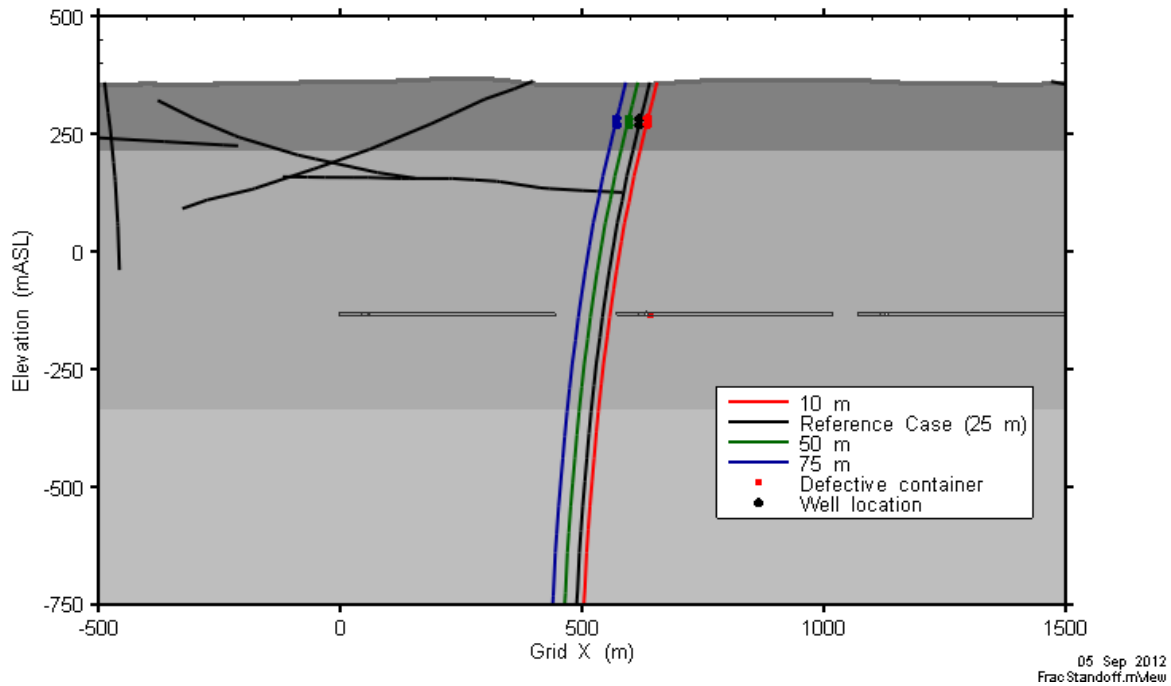


Figure 7-77: Site-Scale Model - Fracture Location Sensitivity Vertical Cross-Section View

Figure 7-78 presents the transport results for I-129. As the fracture is moved closer to the defective containers the peak transport rate increases and the time to reach the peak decreases. Conversely, as the fracture is shifted away from the source location travel times increase.

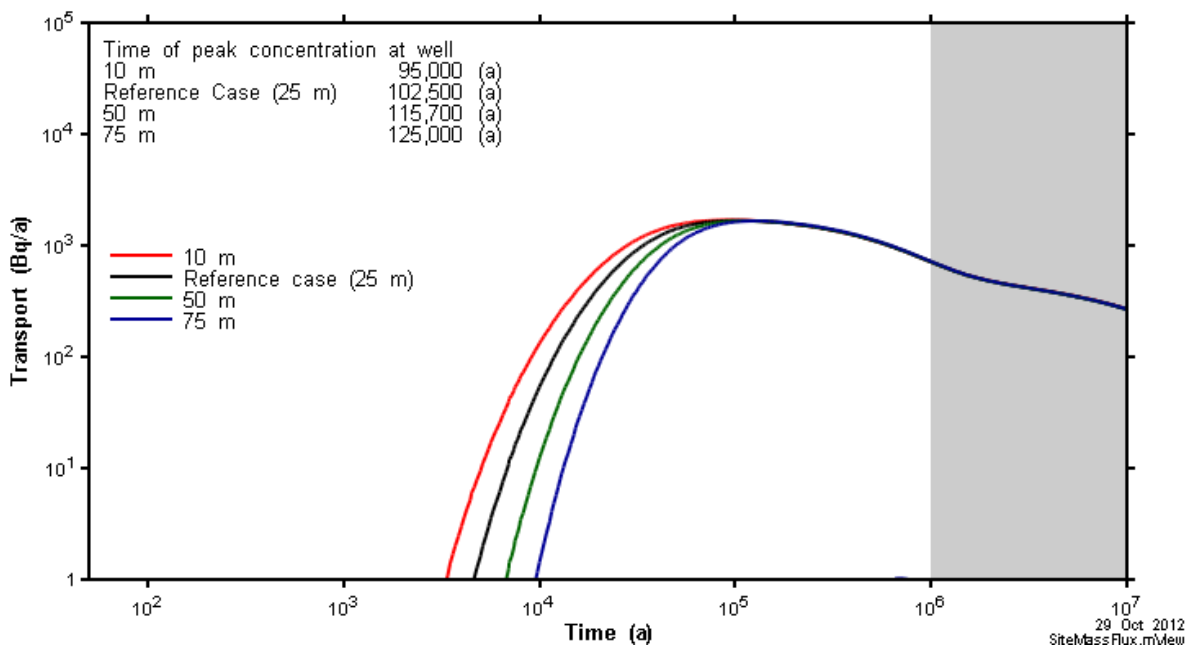


Figure 7-78: Site-Scale Model - Fracture Location Sensitivity I-129 Transport

Table 7-28 summarizes the I-129 transport metrics. Peak results are not overly sensitive to fracture location.

Table 7-28: Fracture Distance Sensitivity: Results for I-129 Transport

Sensitivity Case	Peak Transport Rate at Well (Bq/a)	Time of Peak (a)
10 m	1692	95,000
25 m*	1675	102,500
50 m	1662	115,700
75 m	1660	125,000

Note: * Reference Case

7.7.2.2.5 Sensitivity to Spatial Resolution and Time Step Size

This section examines the effect of increasing the spatial resolution and decreasing the time step size on the Reference Case results.

Spatial Resolution

To determine the effect of grid size a new version of the Sub-Regional Model was created using the same domain, parameter distributions and boundary conditions as in the Reference Case, but with discretization reduced from a nominal 50 m to 25 m, yielding about a factor of eight increase in the number of active nodes. Fracture properties on the refined grid were set to be consistent with the original grid, reflecting the 50 m EPM calculations.

Figure 7-79 displays head difference and head contours at the repository horizon. The results show very little difference in calculated heads as compared to the Reference Case, indicating that the original spatial discretization is adequate for flow calculations. The refined grid was also used to test the sensitivity of the flow model to the EPM approximation. In this case, new EPM hydraulic conductivity and porosity values were calculated for the 25 m discretization. The results, plotted as "Refined EPM" in the figure, are very similar to the 50 m EPM results, further indicating the suitability of the 50 m grid and EPM calculations.

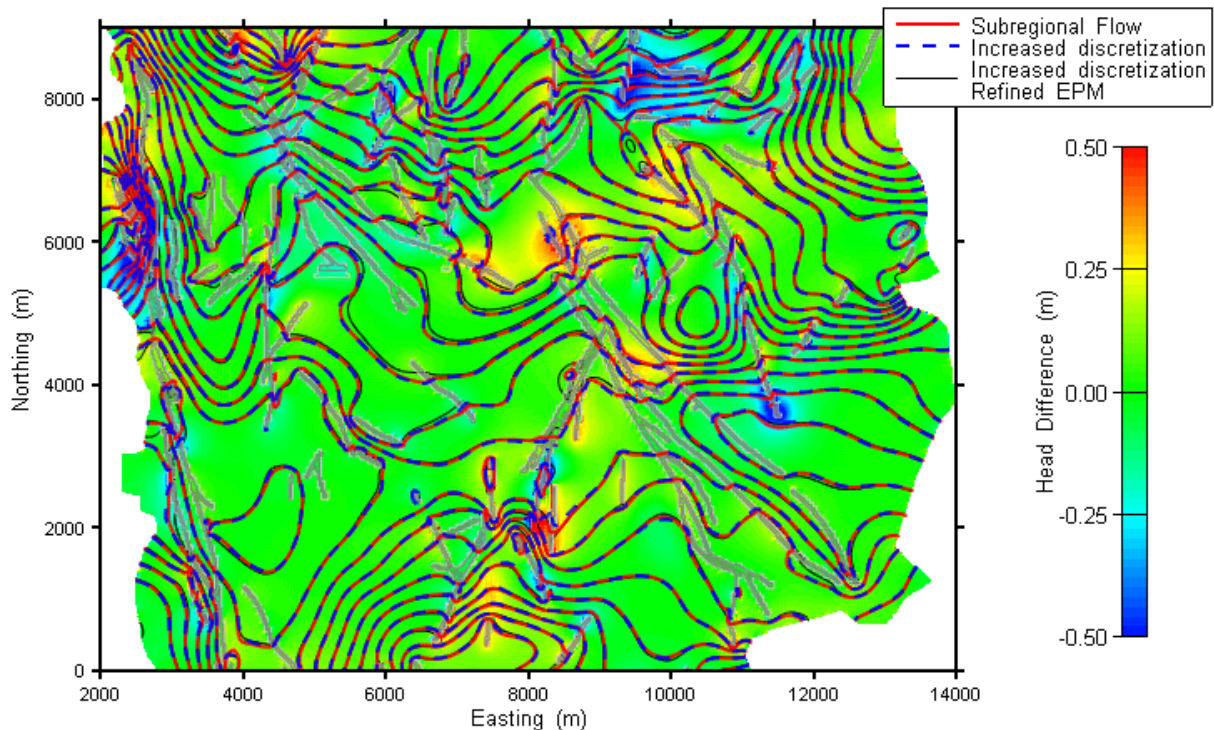


Figure 7-79: Sub-Regional Model - Spatial Convergence Sensitivity Comparison of Head Contours

A similar approach has been taken with the Site-Scale Model; however, in this case the grid is too large to increase discretization over the entire domain. Instead, discretization was doubled in a volume encompassing the source, the well, the fracture system and portions of the placement room. As for the Sub-Regional Model, two EPM simulations were performed, one matching the original model, and the other based on single elements of the refined grid.

Figure 7-80 compares results for the I-129 plume at 100,000 years. The figure shows only minor differences in concentration contours as compared to the Reference Case, with the largest variation occurring within the placement rooms, upgradient of the source term. The higher resolution grid slightly increases dispersive flux within the EBS.

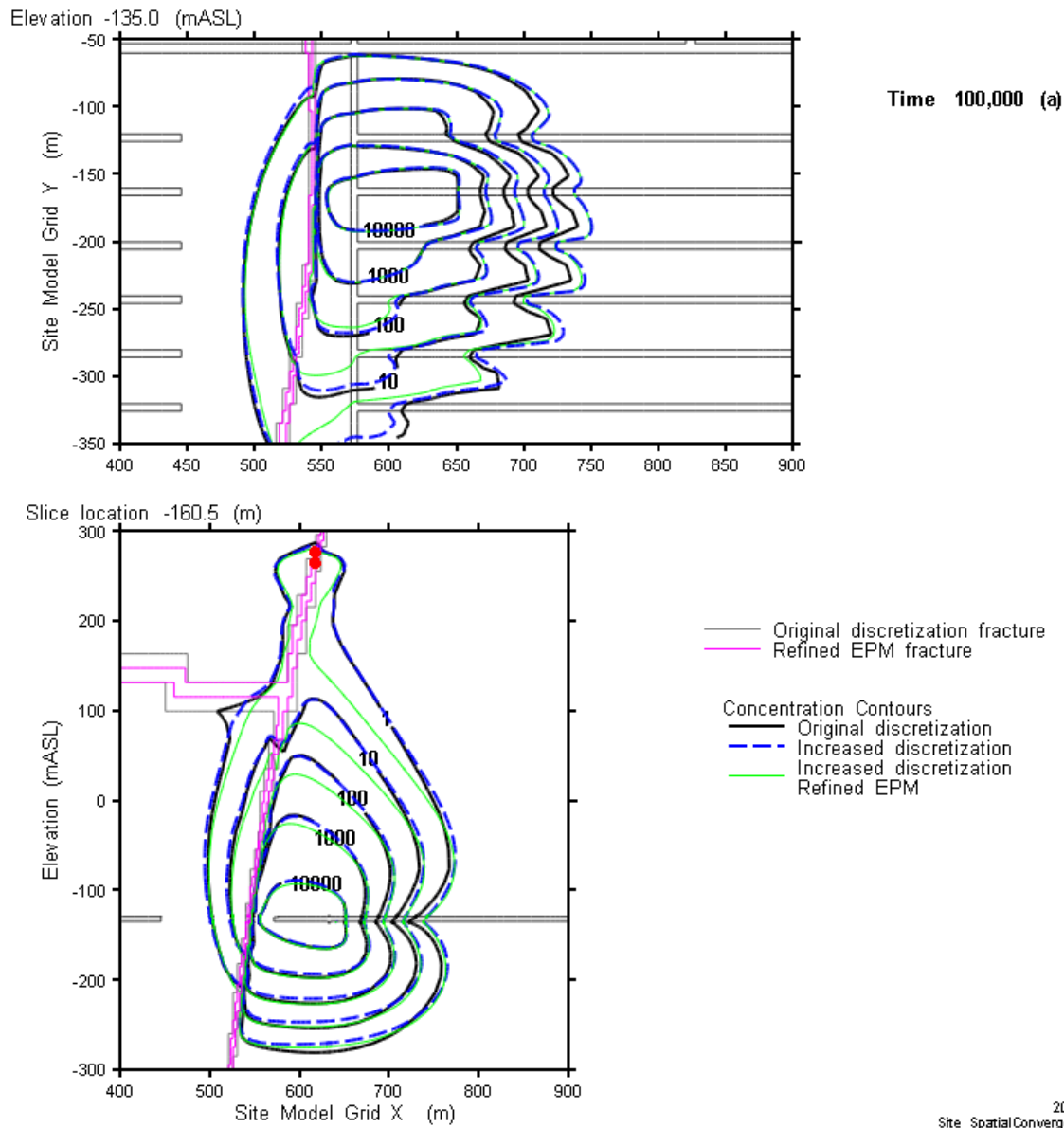


Figure 7-80: Site-Scale Model - Spatial Convergence Sensitivity I-129 Plume

Figure 7-81 compares results for I-129 transport to the well. While visually indistinguishable from the Reference Case result, the peak transport is about 5 % higher for the increased discretization. This is not significant in the context of the postclosure safety assessment and it is therefore concluded that the spatial discretization in the various models is appropriate.

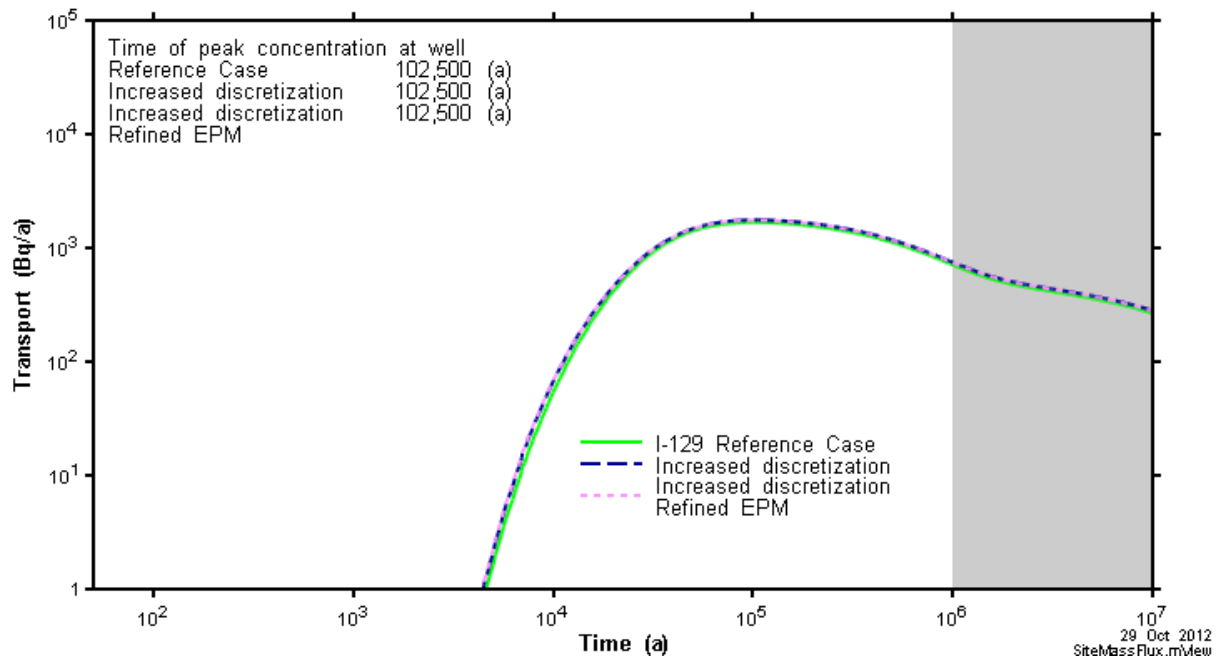


Figure 7-81: Site-Scale Model - Spatial Convergence Sensitivity I-129 Transport to the Well

Temporal Resolution

To determine the effect of time step size, control parameters were modified in the Reference Case Site-Scale Model. These changes resulted in a seven fold decrease in the number of time steps in one simulation and a threefold increase in another.

Results, illustrated in Figure 7-82, show essentially no sensitivity of peak I-129 transport to the well. It is therefore concluded that the temporal discretization in the various models is appropriate.

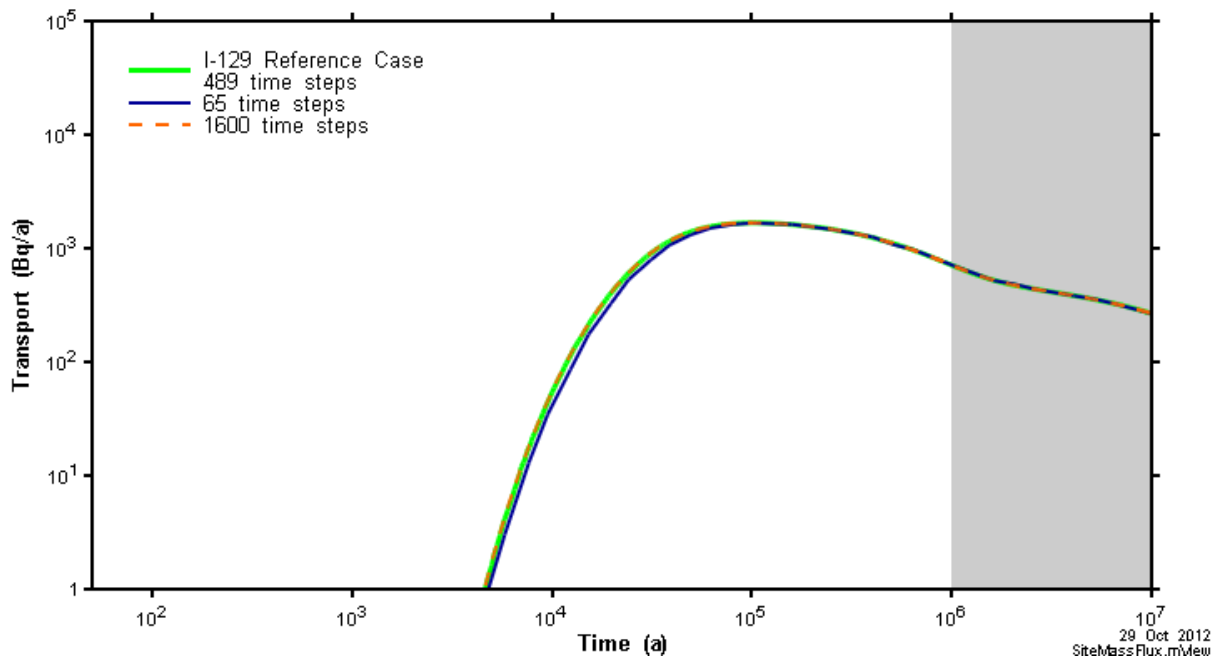


Figure 7-82: Site-Scale Model - Time Step Convergence Sensitivity - I-129 Transport to the Well

7.7.2.2.6 Other Sensitivity Cases

This section presents results for the sensitivity cases listed in Table 7-29.

Results for the Shaft Seal Failure, the Fracture Seal Failure and the Tunnel and Room Seal Failure Disruptive Event Scenarios are also presented here for ease of comparison.

Table 7-29: Site-Scale Transport Sensitivity Cases

Sensitivity Case	Description
EDZ High	All Reference Case EDZ and TDZ permeabilities increased by a factor of 10.
DFN	Discrete fracture network model in lieu of equivalent porous media.
Shaft Seal Failure*	The hydraulic conductivity of all shaft seal materials set to 4.8×10^{-8} m/s. The locations of the defective container and the well are the same as in the Reference Case.
Fracture Seal Failure* and Variant	The hydraulic conductivity of the highly compacted bentonite in the keyed-in area is set to that of the inner EDZ (i.e., 100 times that of the rock). This is a variant case of the Fracture Seal Failure Disruptive Event Scenario in which the hydraulic conductivity of the highly compacted bentonite in the keyed-in areas of all fracture, tunnel and room seals is set to that of the inner EDZ (i.e., 100 times that of the rock).

Note: * Disruptive Event Scenario

Figure 7-83 shows summary results for I-129 transport to the well for all cases. Included for comparison are results for the Reference Case and results for the geosphere sensitivity case in which hydraulic conductivity is increased by a factor of 10 (i.e., Sensitivity Case 1 in Section 7.7.2.2.3).

The results show that cases with higher geosphere and EDZ permeabilities lead to earlier arrival times at the well with slightly different peak transport rates. For the EDZ High case, the peak I-129 transport rate is 1681 Bq/a occurring at 87,500 year, as compared to Reference Case value of 1675 Bq/a occurring at 100,000 years. The increased geosphere hydraulic conductivity case has a lower peak transport rate, with the explanation for this given in Section 7.7.2.2.3.

Comparison of the DFN case with the subsequent EPM approximation indicates that for this assessment the EPM approach is bounding (i.e., EPM results show faster transport to the well and a higher peak transport rate).

The Shaft Failure Disruptive Event Scenario shows no perceptible difference from the Reference Case. This is primarily due to the lengthy distance between the defective containers and the shaft. In future studies, it may be necessary to reposition the locations of the well and the defective containers to ensure consequences are maximized for this event.

The Fracture Seal Failure Disruptive Event Scenario also shows no perceptible difference from the Reference Case. This is because the tunnel and room seals remain in place and because the hydraulic conductivity of the host rock supports advective flow without substantial transport within the repository. The buffer and backfill engineered barriers are assumed unaffected in this simulation.

The variant case of the Fracture Seal Failure Disruptive Event Scenario shows a small difference from the Reference Case with the arrival time at the well decreasing to 97.5 ka (from 103 ka) with the peak transport rate increasing to 1677 Bq/a (from 1675 Bq/a). The absence of sensitivity is due to the hydraulic conductivity of the host rock supporting advective flow outside the repository together with the continuing presence of the buffer and backfill.

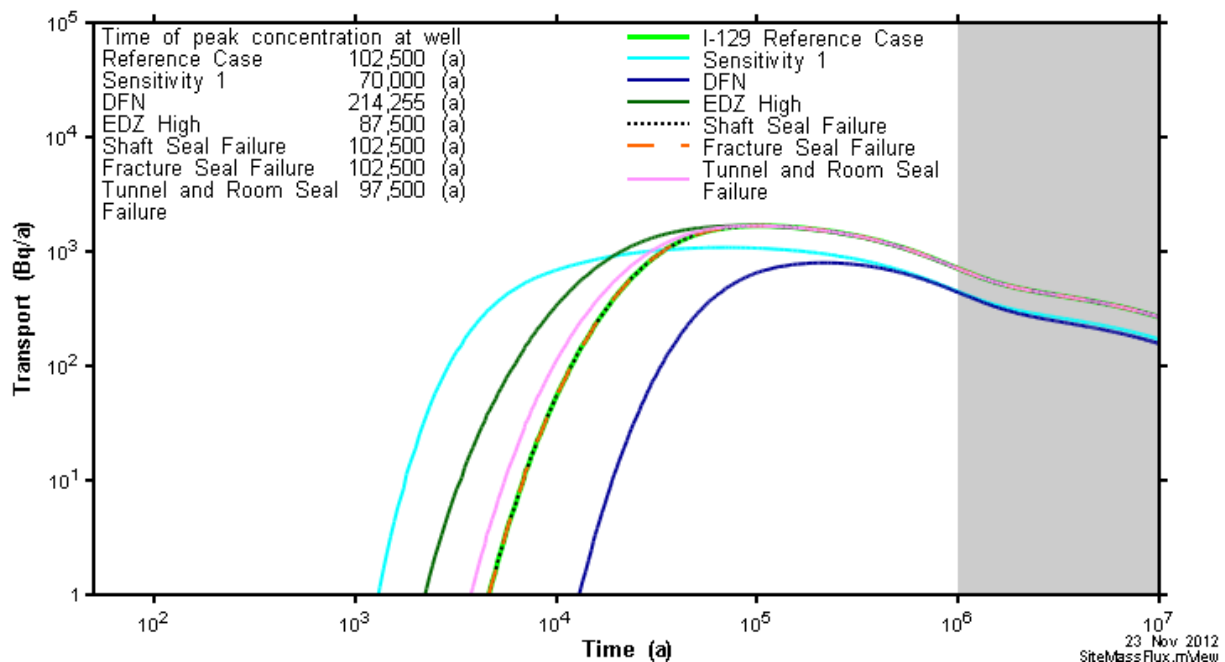


Figure 7-83: Site-Scale Model - I-129 Transport in Sensitivity Cases

7.7.2.2.7 Effect of Barriers on Radionuclide Transport

This section provides information on the effect of the various barriers on radionuclide transport for the Reference Case.

Figure 7-84 through Figure 7-86 show the transport rate for I-129 (a non-sorbing fission product), Ca-41 (an intermediate sorbing fission product) and U-238 (a highly sorbing actinide). Each figure shows:

- The release rate from the defective containers. As noted in Section 7.5.3.3, this is determined with the SYVAC3-CC4 release model and specified as input to the FRAC3DVS-OPG simulation. These release rates are the same as those shown in Figure 7-26.
- The release rate from the bentonite surrounding the defective containers. This corresponds to the transport through the pink-hued surface in Figure 7-92.
- The release rate from the repository. This corresponds to the pink hued surface in Figure 7-87. In this figure, the surface surrounding the three vertical containers has been expanded slightly over that shown in Figure 7-92 to incorporate the EDZ and TDZ.
- The release rate to the well and all surface locations.

The figures show the retarding effects of the various barriers on the transport of the different radionuclides.

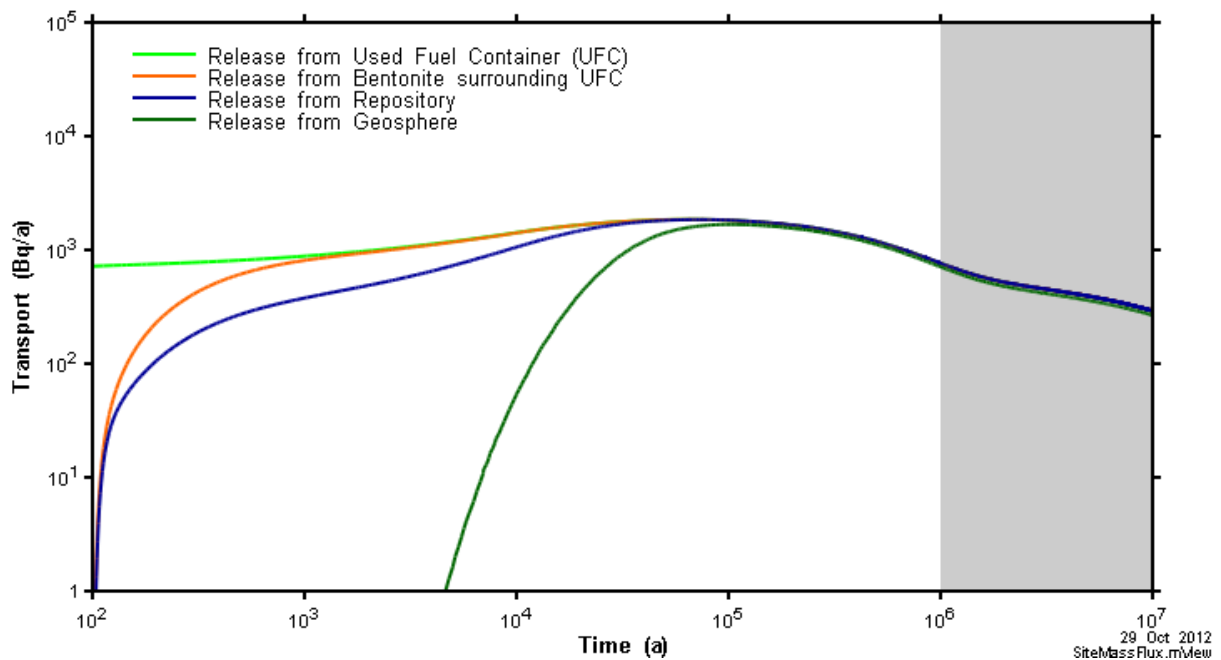


Figure 7-84: FRAC3DVS-OPG - I-129 Transport through Barriers

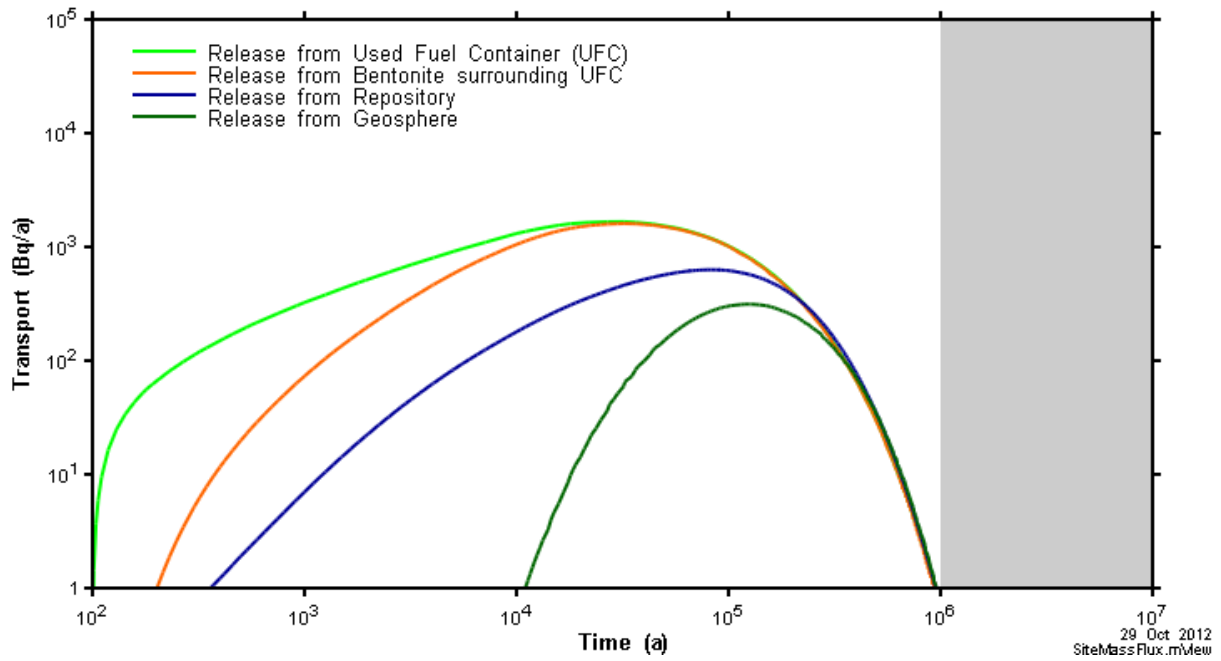
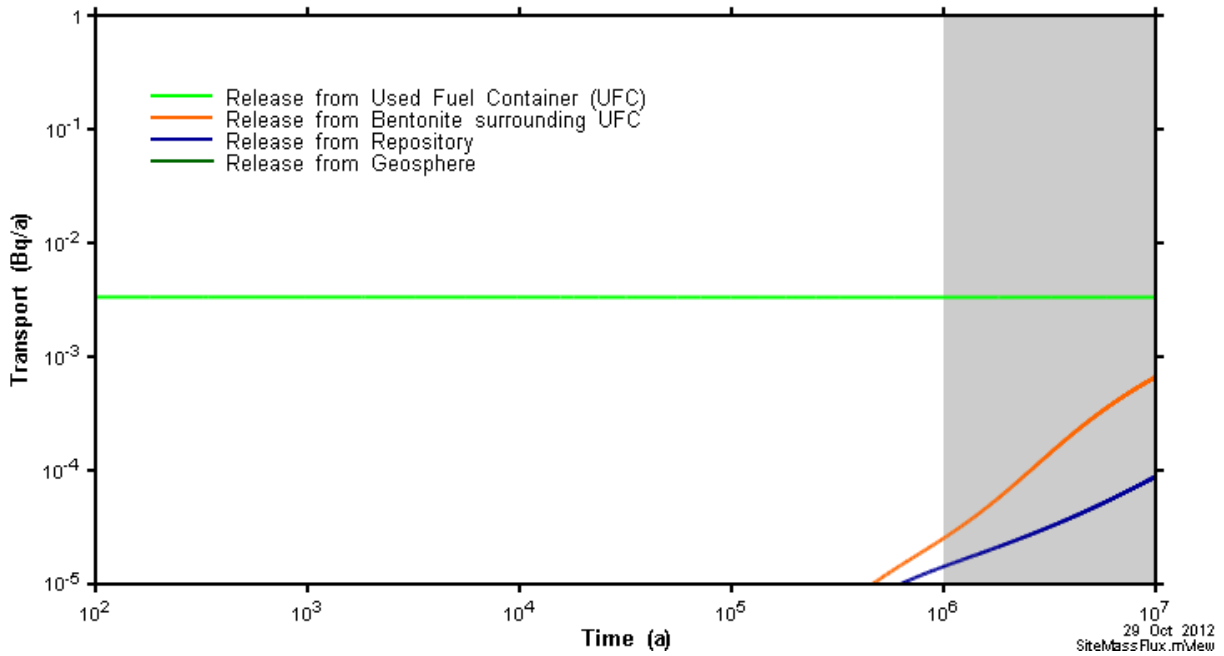
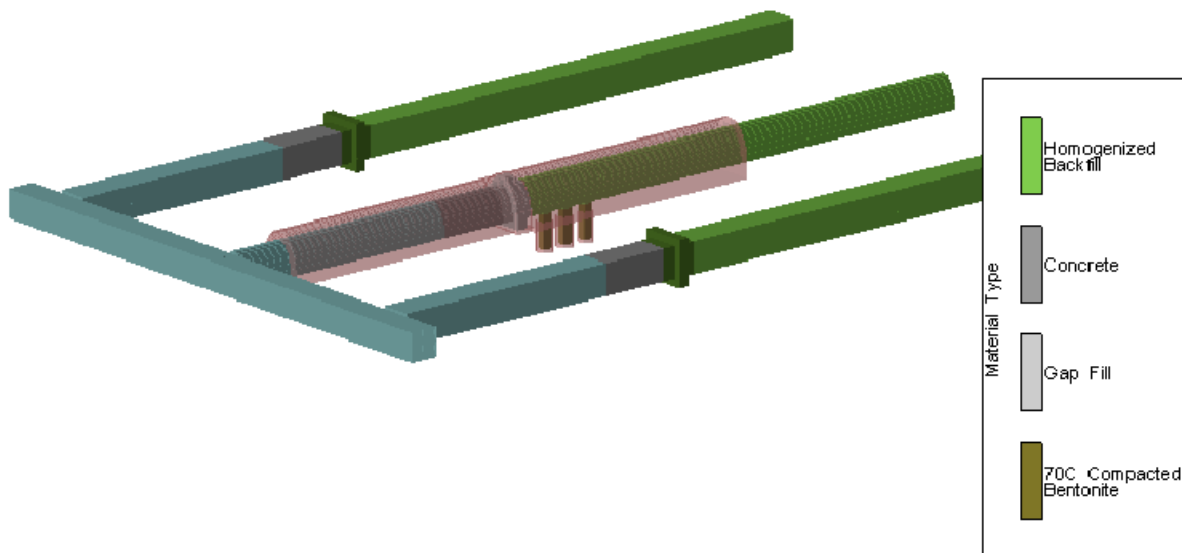


Figure 7-85: FRAC3DVS-OPG - Ca-41 Transport through Barriers



Note: Results indicated by the dark green line are off scale low by over 9 orders of magnitude.

Figure 7-86: FRAC3DVS-OPG - U-238 Transport through Barriers



Note: the pink hued surface is set at the boundary between the EDZ / TDZ and the intact rock

Figure 7-87: Transport Surface for the Repository Release

7.7.3 Repository-Scale Model

The Repository-Scale model represents a small section of the repository surrounding the defective containers and the adjacent geosphere. The model incorporates a high level of detail and individual containers are represented at the source location.

Reference Case simulations are performed to corroborate results of the Site-Scale Model and to provide a more complete understanding of repository component functions.

7.7.3.1 Flow Results

7.7.3.1.1 Reference Case

Figure 7-88 and Figure 7-89 show hydraulic head and advective velocities on a plan section through the placement room at the elevation of the TDZ. The effectiveness of the room seal in intercepting the groundwater flow in the TDZ is apparent at the X = 60 location.

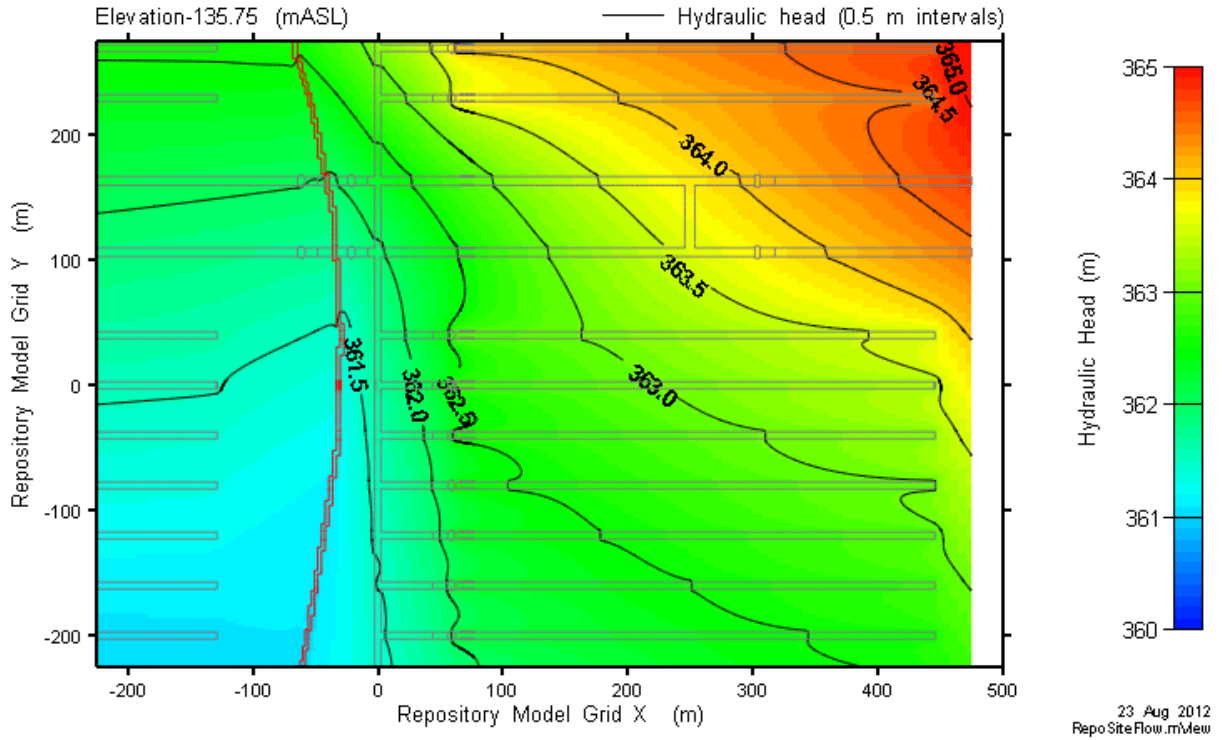


Figure 7-88: Repository-Scale Model - Head at TDZ Elevation

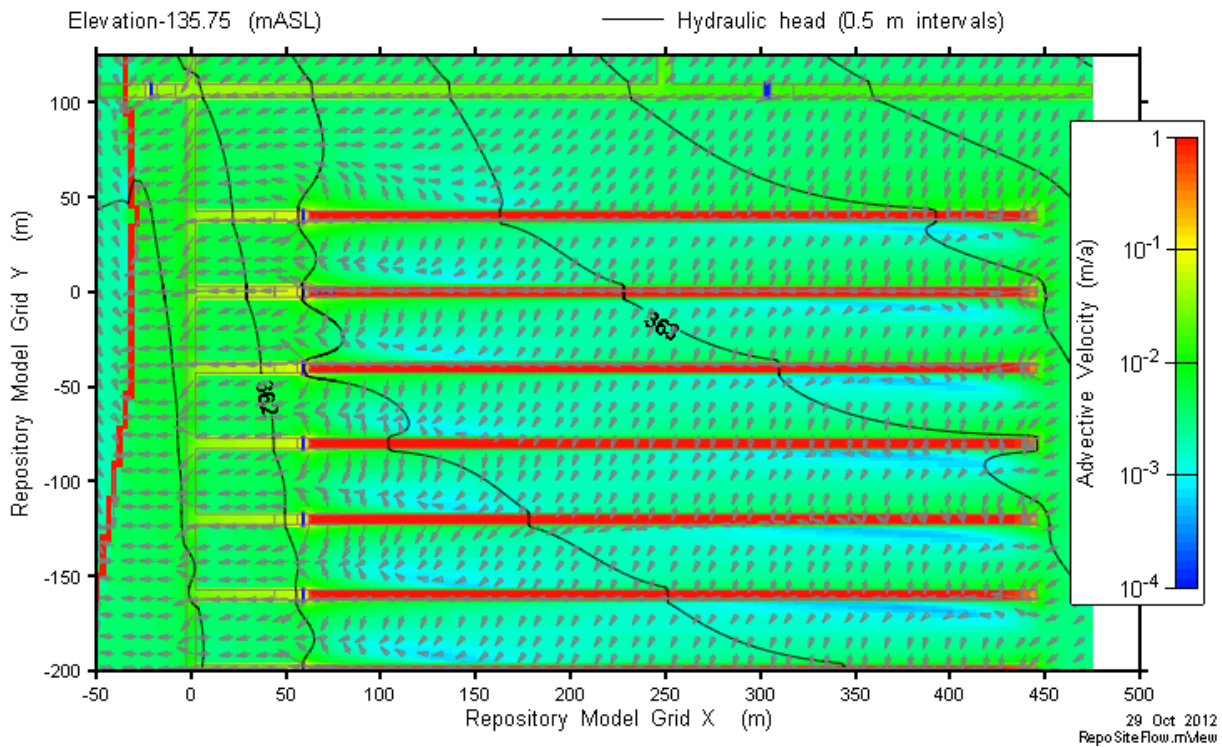


Figure 7-89: Repository-Scale Model - Advective Velocities in TDZ Layer

Figure 7-90 shows advective velocities in a 3D view through the EBS and EDZ / TDZ materials. The highest velocities are in the TDZ and in the thin section of inner EDZ around the seal EDZ intercept. The effectiveness of the room seal in reducing velocities throughout the main cross-sectional area of the room is apparent.

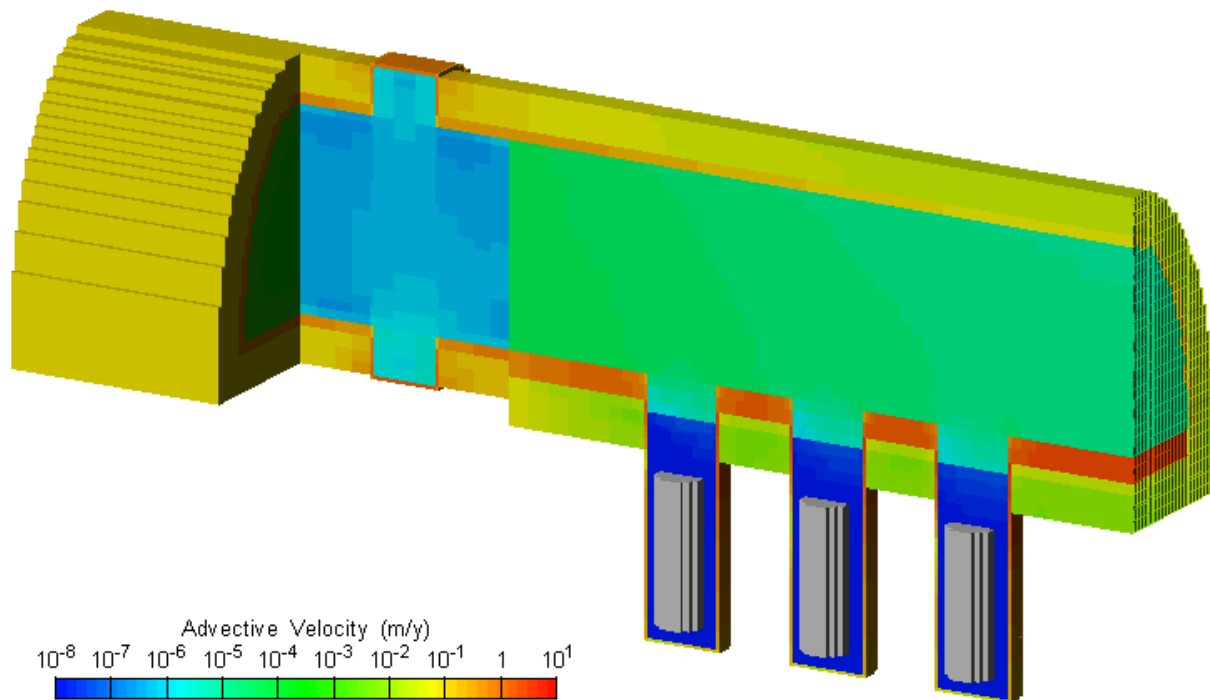


Figure 7-90: Repository-Scale Model - 3D View of Advective Velocity Magnitudes

Figure 7-91 is a visualization of the advective transport pathways. In this figure pathways originating in the middle of the TDZ, immediately above the containers are tracked until they leave the model domain. Particles are limited to those originating in the three rooms closest to the fracture. Some transport pathways initially travel through the room TDZ and EDZ and around the seal, while others directly enter the rock mass and start moving down through the intact rock towards the fracture.

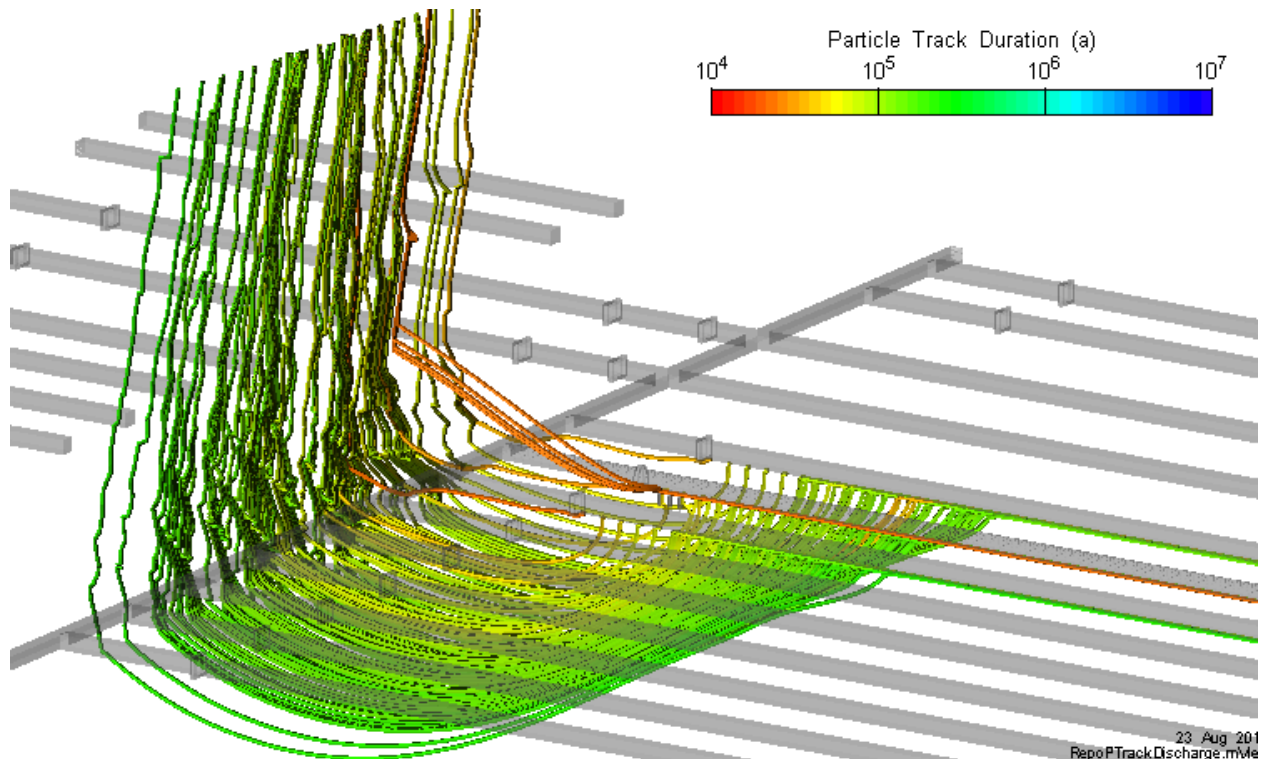


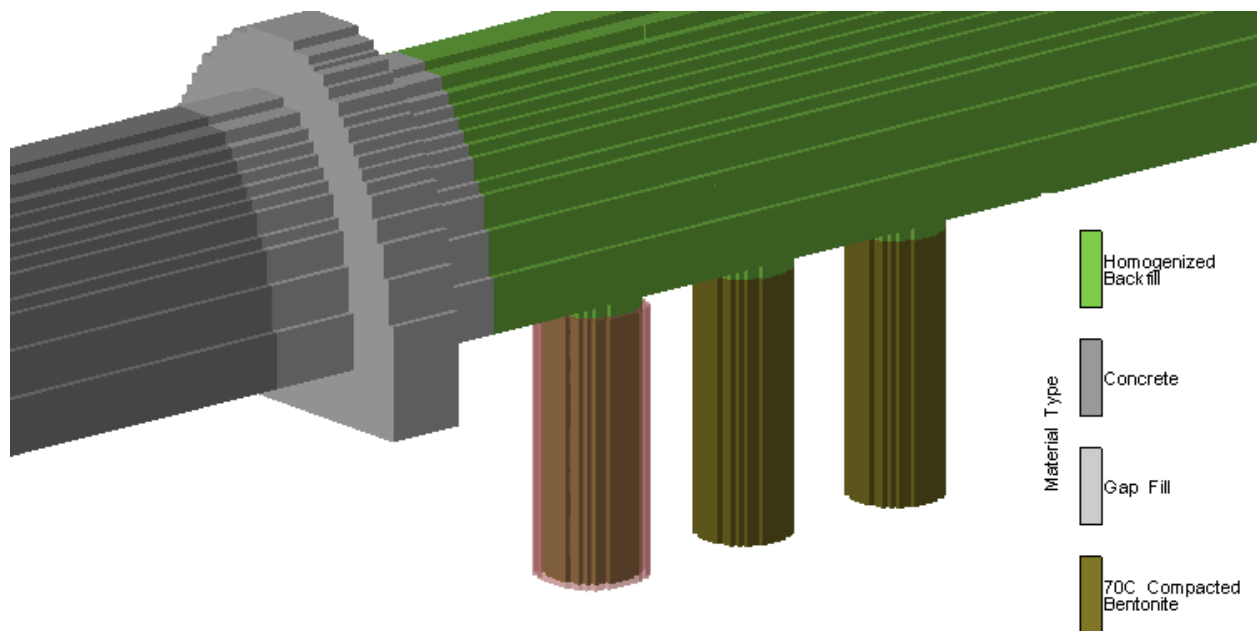
Figure 7-91: Repository-Scale Model - Advective Transport Pathways

7.7.3.2 Radionuclide Transport Results

Radionuclide transport modelling is performed for I-129, C-14, Cl-36, Ca-41, Cs-135, Sn-126, U-234 and U-238.

Although the source term is from three defective containers, the release is applied to a single container for modelling simplicity. The results are indistinguishable from adjacent container releases at significant distances from the source.

To provide data for later verification of the SYVAC3-CC4 model (Section 7.8.1), radionuclide transport from the used fuel container into the placement room and geosphere (i.e., out of the buffer) is computed over a volume surrounding the defective container as shown in Figure 7-92.



Note: Boundary volume shown as pink cylinder surrounding the container.

Figure 7-92: Repository-Scale Model - Boundary Volume for Calculation of Radionuclide Releases into the Geosphere

7.7.3.2.1 Reference Case

This section presents detailed results for I-129, U-238 and Cs-135, with summary results presented for the remaining radionuclides. The three selected radionuclides are representative of the behaviours for non-sorbing, highly sorbing and intermediate sorbing species.

Figure 7-93 through Figure 7-96 illustrate the time dependent behaviour of the I-129 plume along the repository level and on a vertical slice through the placement room. Contours of equivalent results from the Site-Scale Model are overlaid for comparison. The results show similar core concentration profiles with slightly lower I-129 concentrations at the plume margins, likely due to the more detailed discretization.

This comparison provides confidence in the Site-Scale results.

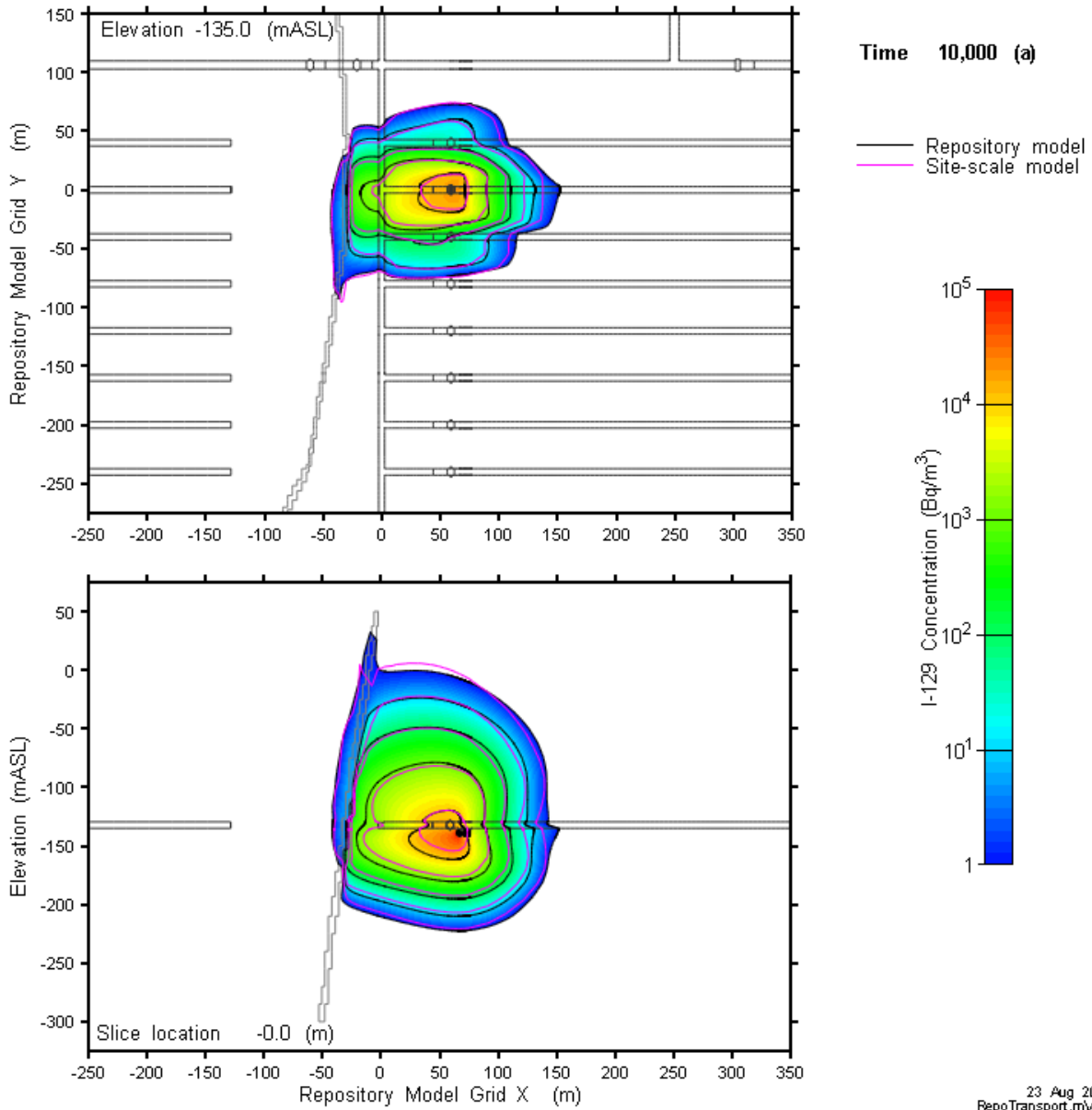


Figure 7-93: Repository-Scale Model - I-129 Concentration at 10 ka

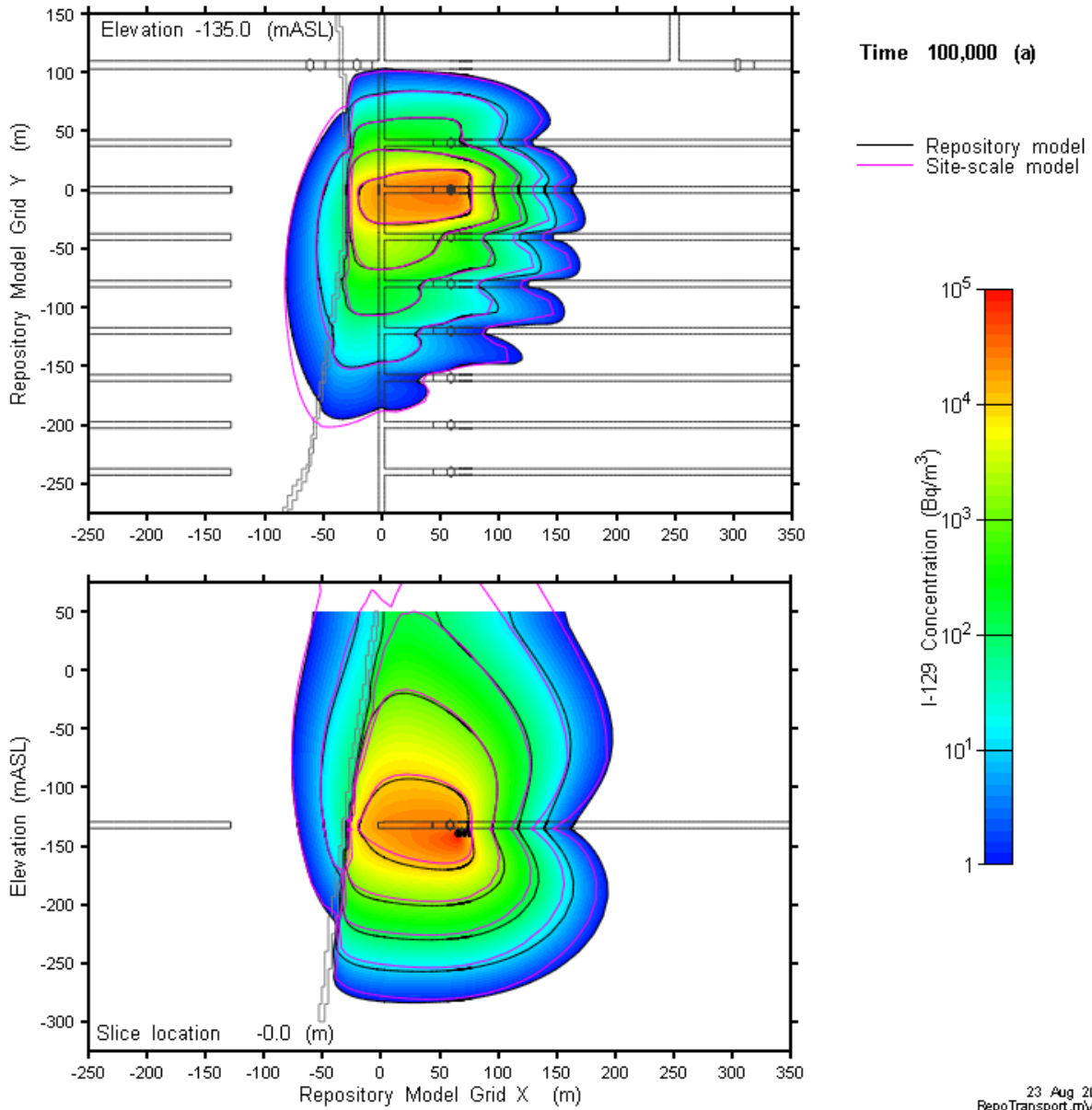


Figure 7-94: Repository-Scale Model - I-129 Concentration at 100 ka

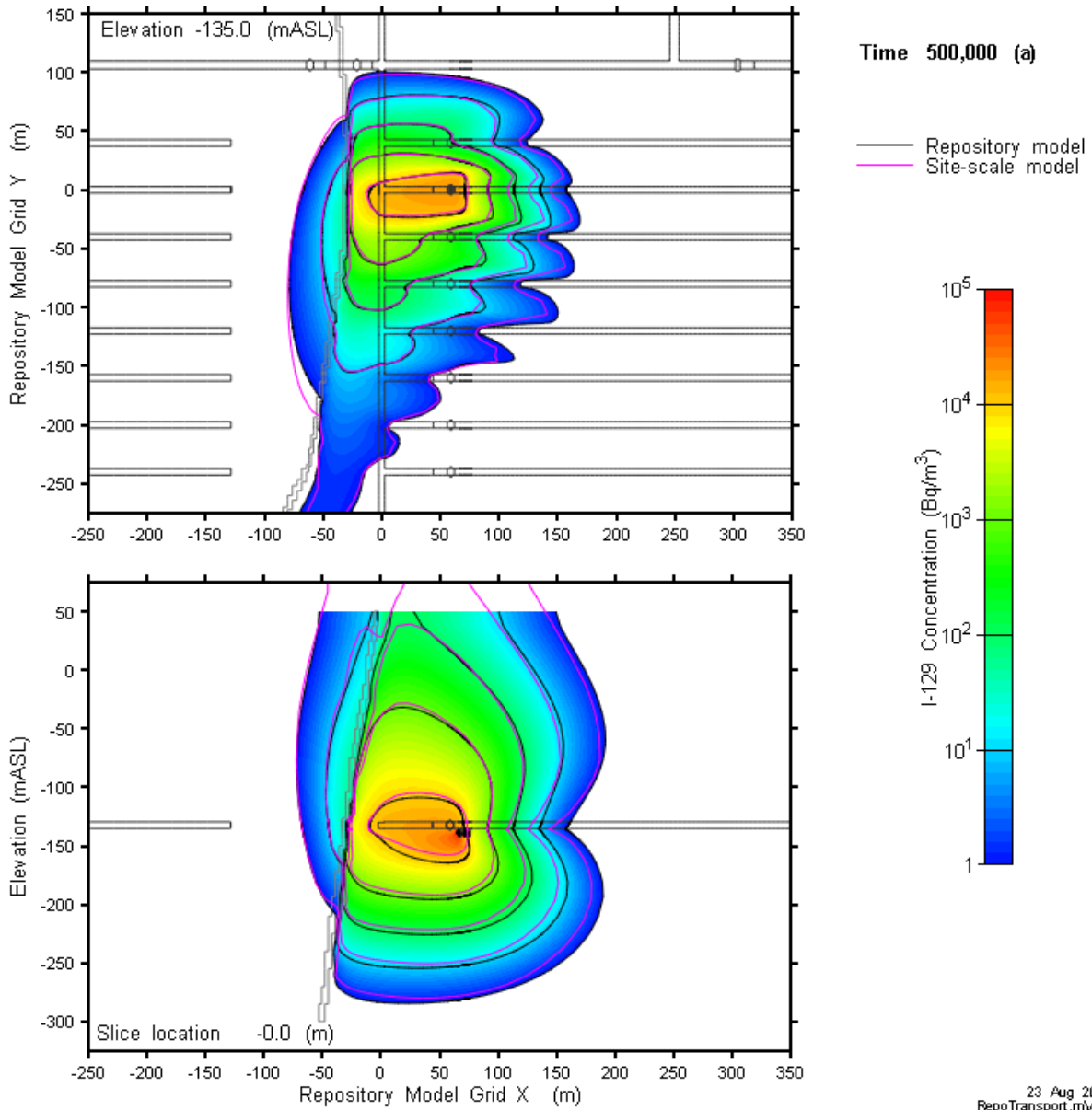


Figure 7-95: Repository-Scale Model - I-129 Concentration at 500 ka

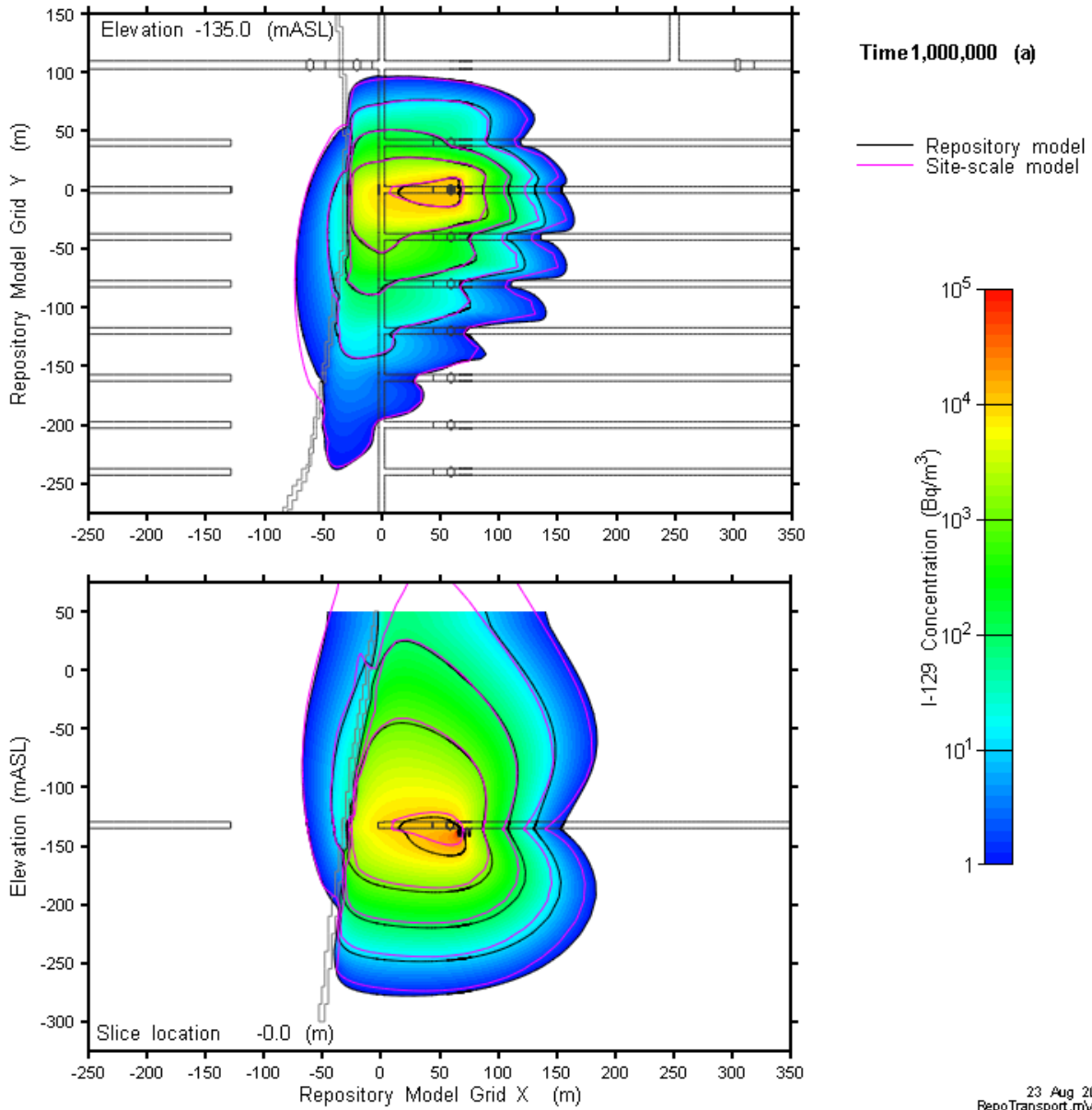


Figure 7-96: Repository-Scale Model - I-129 Concentration at 1 Ma

Unlike I-129, U-238 is strongly sorbed onto sealing materials and the host rock. Consequently, transport of U-238 is limited to a very small domain immediately surrounding the defective container. Figure 7-97 shows sectional views through the release plane and adjacent buffer at one million years.

The contour plots are on a logarithmic scale. The 0.001 Bq/m³ concentration contour corresponds to an effective U-238 drinking water dose of about 0.00003 µSv/a based on water consumption of 0.77 m³/a per person.

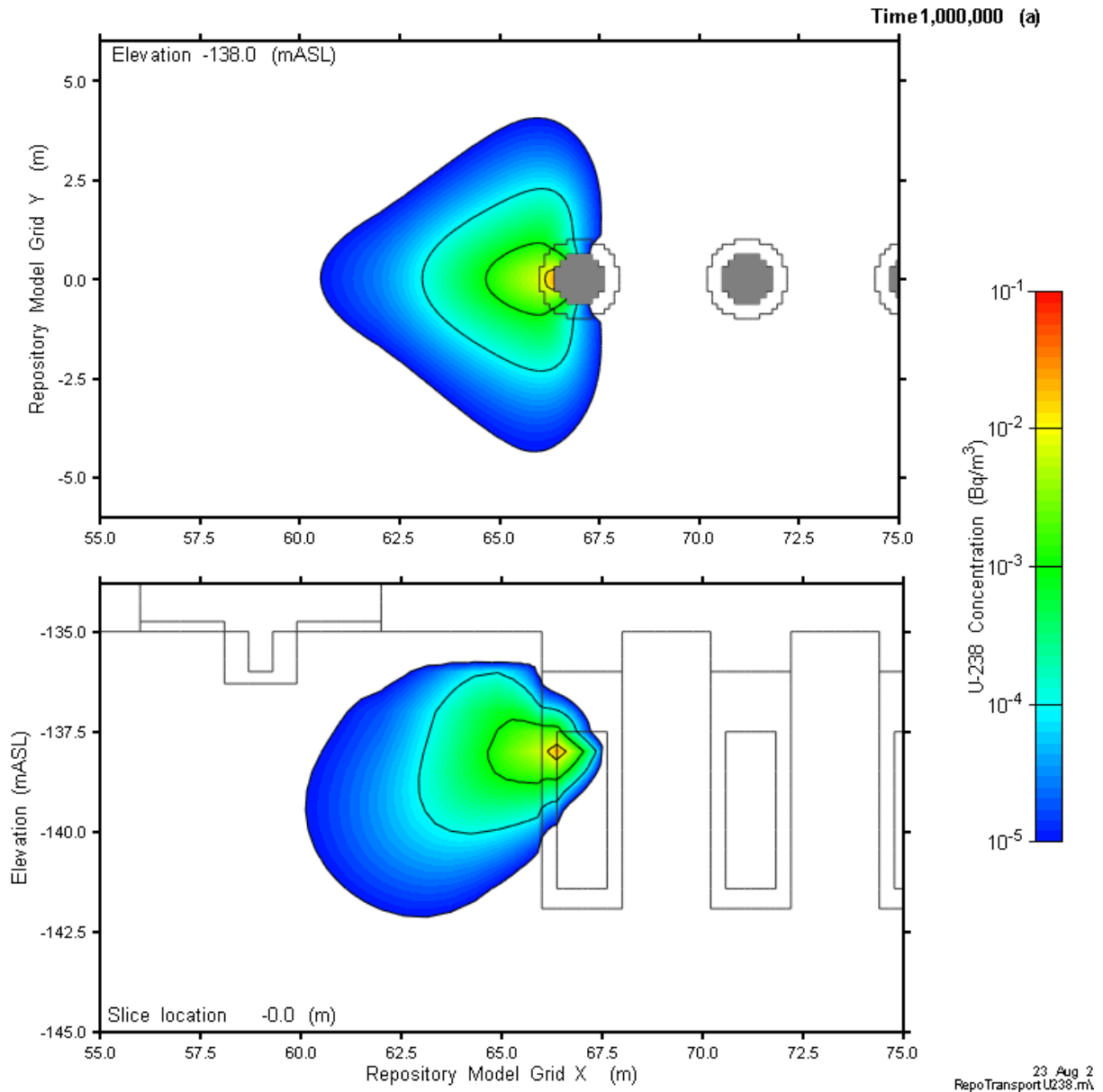


Figure 7-97: Repository-Scale Model - U-238 Concentration at 1 Ma

Figure 7-98 shows the Cs-135 plume at 100 ka. Cs-135 is less strongly sorbed than U-238 but is still subject to retardation. The results show transport is largely confined to the vicinity of placement room and that the room seal is effective in limiting transport towards the access tunnels.

The 100 Bq/m³ contour line corresponds to a Cs-135 drinking water dose of about 0.015 µSv/a based on water consumption of 0.77 m³/a per person.

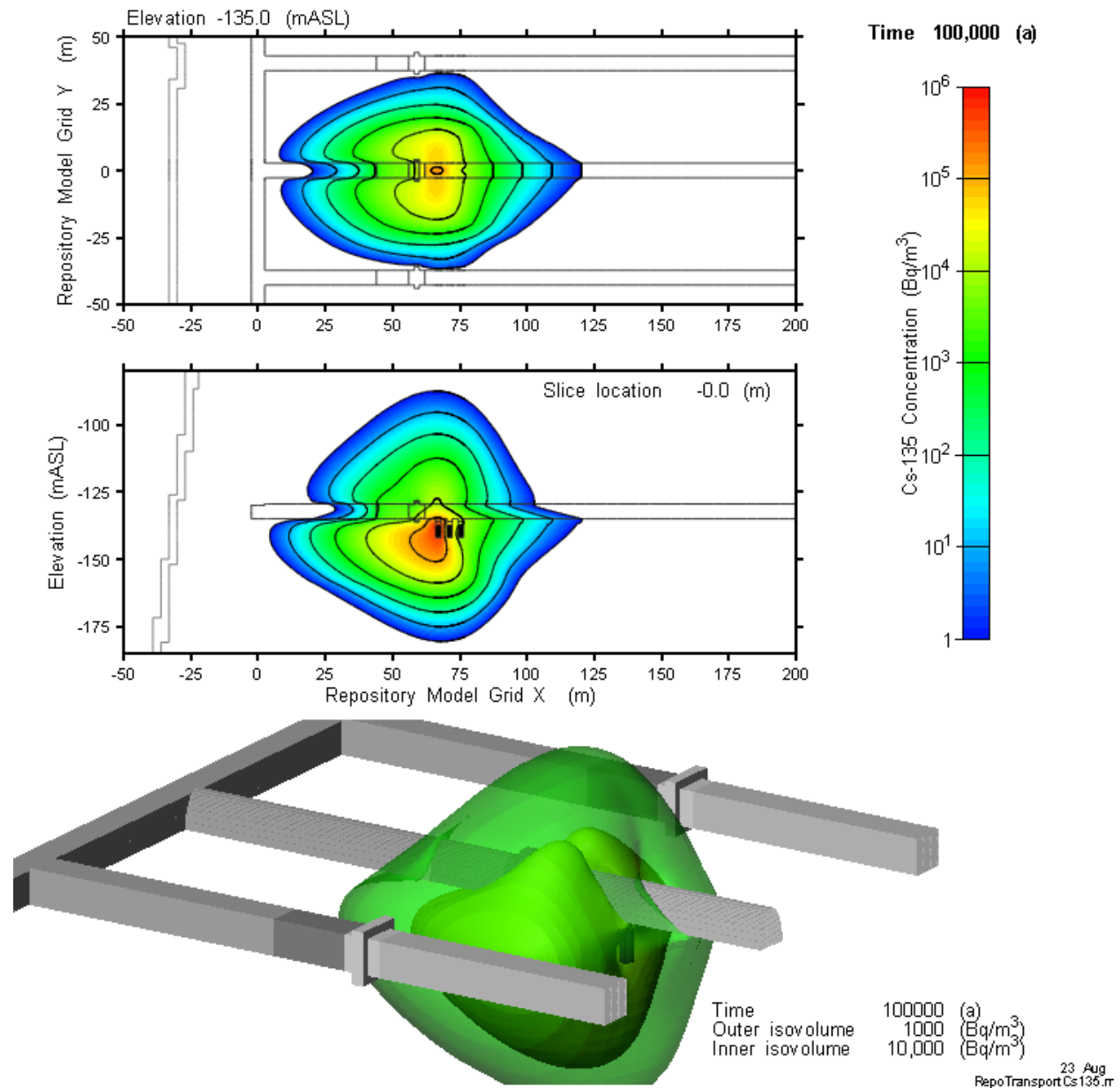


Figure 7-98: Repository-Scale Model – Cs-135 Concentration at 100 ka

Figure 7-99 and Figure 7-100 show summary results for all radionuclides considered. These figures show the transfer rates out of the boundary volume surrounding the defective container shown in Figure 7-92.

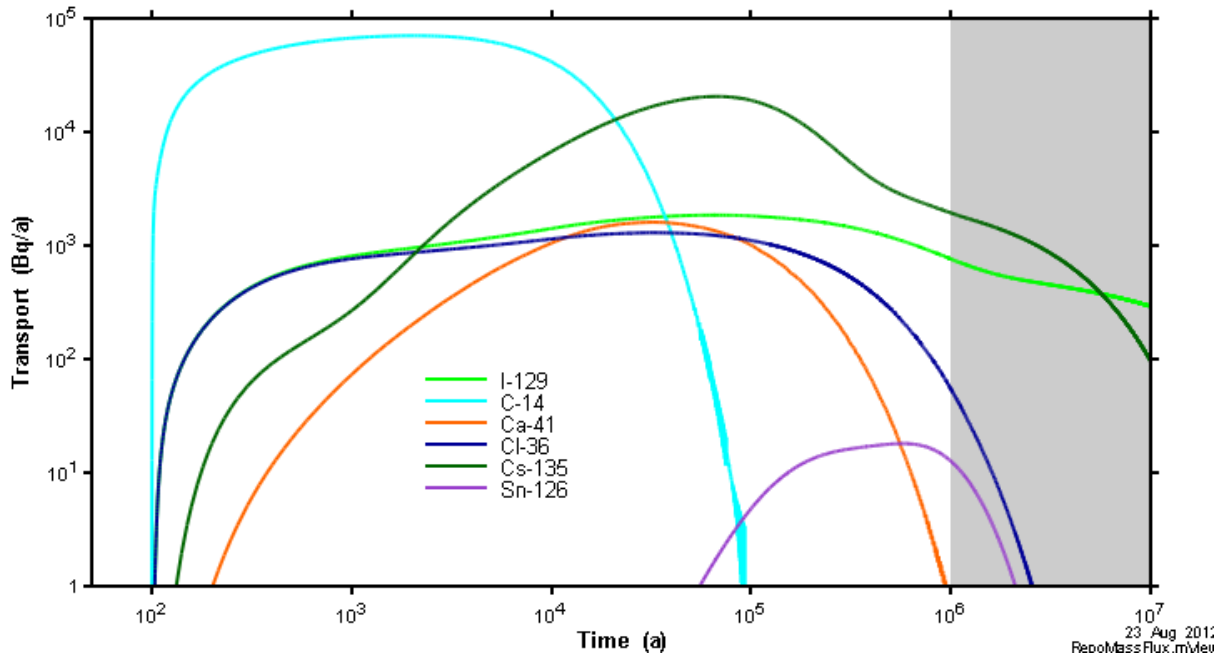


Figure 7-99: Repository-Scale Model - Transport Rates for I-129, C-14, Cl-36, Ca-41, Cs-135 and Sn-126

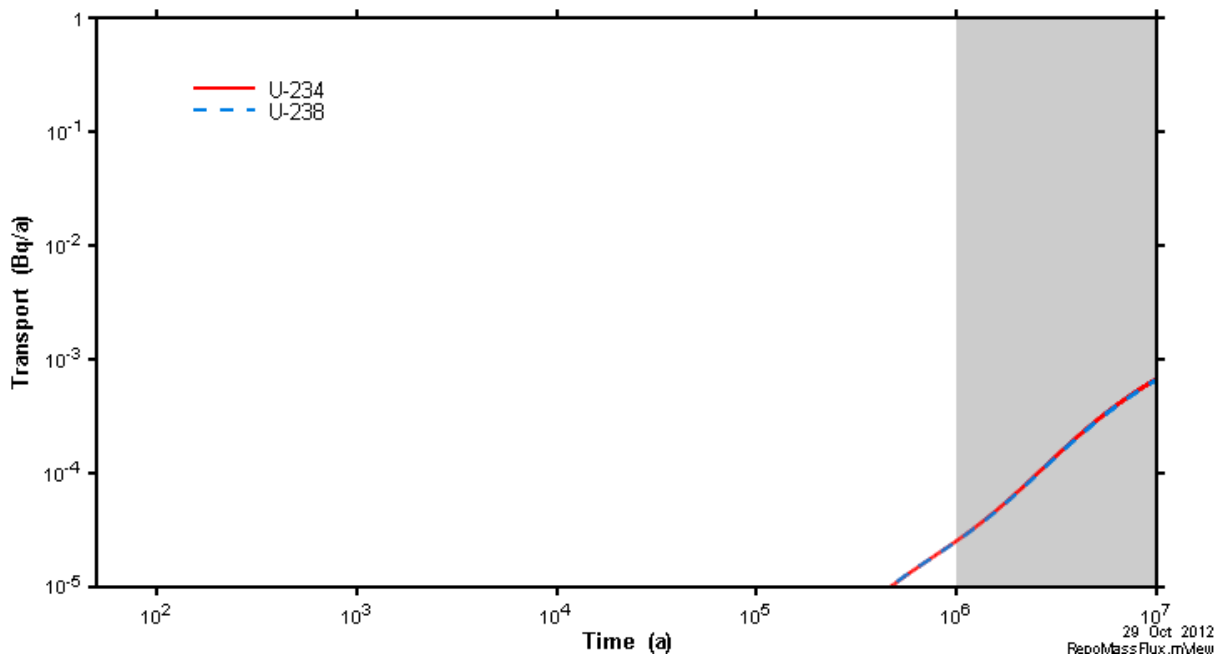


Figure 7-100: Repository-Scale Model - Transport Rates for U-234 and U-238

7.8 Results of System Modelling

The SYVAC3-CC4 system model combines an idealized geometric description of the repository and a simple geosphere transport model with representations of releases from the used fuel and container, and radionuclide transport in the biosphere to determine the radiological consequences of releases to the environment.

This section presents the results of deterministic and probabilistic analysis of the Reference Case and a set of related sensitivity cases.

The deterministic cases are:

- Fuel dissolution rate increased by a factor of 10;
- Instant release fractions set to 0.10 for all radionuclides;
- Container defect area increased by a factor of 10;
- No solubility limits in the container;
- No sorption in the near field;
- No sorption in the geosphere;
- Low sorption in the geosphere with coincident high solubility limits in the container; and
- Increased geosphere hydraulic conductivity.

For ease of presentation, the sensitivity cases are separated into those that represent a degraded physical barrier and those that represent a degraded chemical barrier.

Probabilistic simulations examine the effect of simultaneous variation of all probabilistically defined parameters.

Deterministic and probabilistic simulations are performed for complementary indicators.

A detailed description of these cases is provided in Section 7.2.1.

Figures in this section are shown with shading at times greater than one million years to emphasize that these results are illustrative and included only to indicate peak impacts. Shading for dose rates below 1 nSv/a indicate these values are negligible and are included to indicate trends.

7.8.1 Transport Model Verification

To provide confidence in the SYVAC3-CC4 model, transport results for I-129, C-14, Cl-36, Ca-41, Sn-126, Cs-135, U-234 and U-238 are compared with similar results obtained from the detailed FRAC3DVS-OPG 3D simulations.

Near-Field Transport Comparison

Transport from the container to the geosphere for the Reference Case is shown in Figure 7-101 and Figure 7-102. For FRAC3DVS-OPG the transport is across the surface of the pink hued cylinder in Figure 7-92 while for SYVAC3-CC4 the transport is across the outer surface of the grey cylinder in Figure 7-28. In both cases, the surface is the damage zone / rock boundary around a placement borehole.

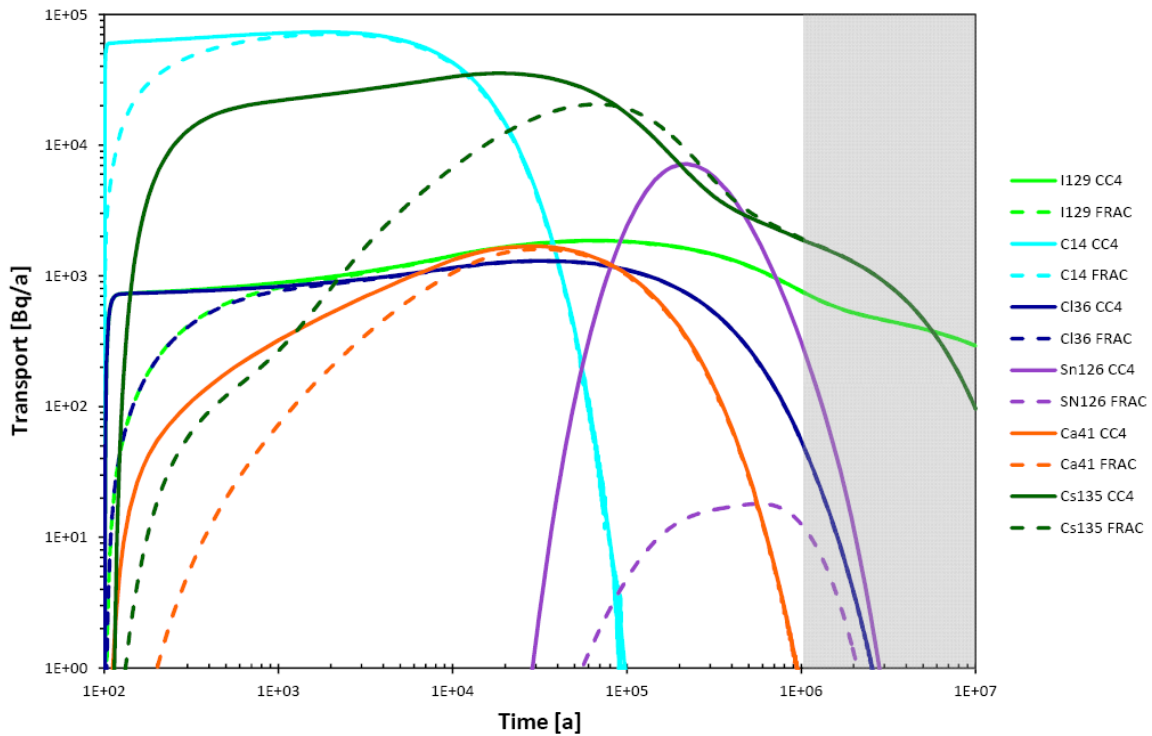
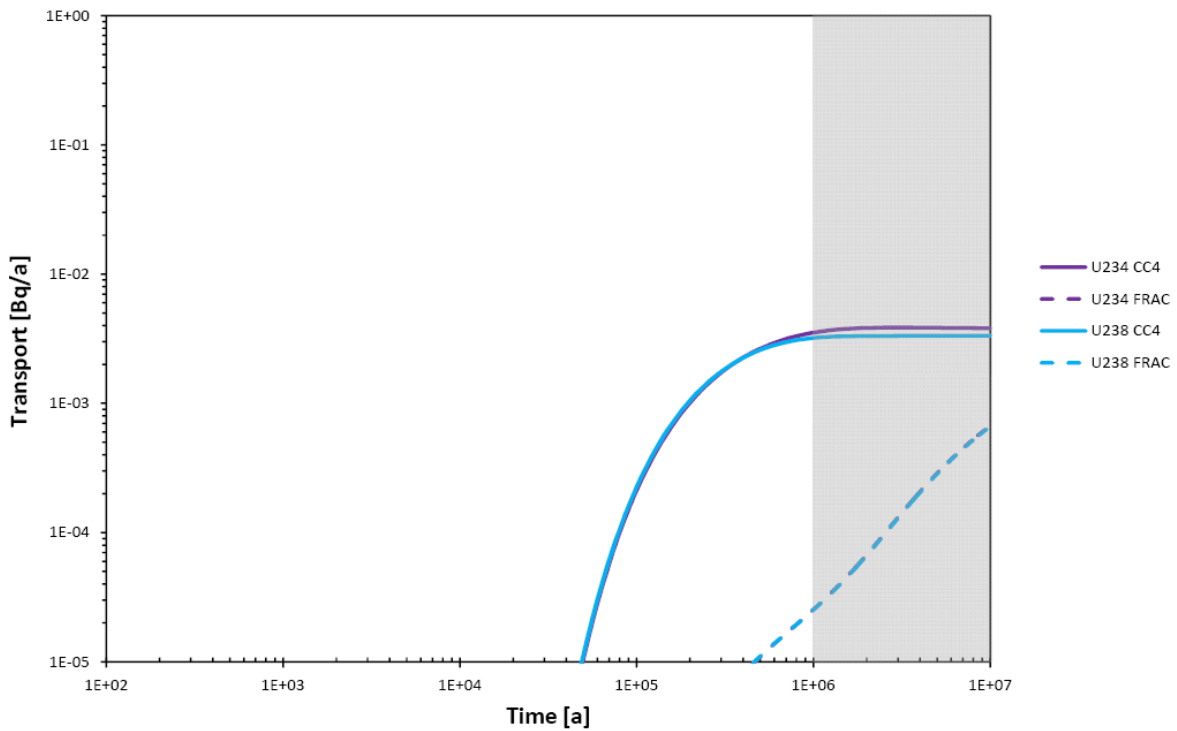


Figure 7-101: Comparison of SYVAC3-CC4 and FRAC3DVS-OPG Transport of I-129, C-14, Cl-36, Ca-41, Sn-126 and Cs-135 to the Geosphere



Note: FRAC3DVS-OPG-calculated transport of U-234 and U-238 overlap

Figure 7-102: Comparison of SYVAC3-CC4 and FRAC3DVS-OPG Transport of U-234 and U-238 to the Geosphere

Results for the peak values and their associated time occurrences are shown in Table 7-30. The agreement is very close for the non-sorbing radionuclides I-129 and Cl-36 and for the weakly sorbing radionuclides C-14 and Ca-41. The difference is conservative for the sorbing radionuclides, in the sense that higher peak values are calculated using SYVAC3-CC4.

The peak rates for U-234 and U-238 are not reached during the simulation period in either model.

The difference in results is mostly due to the larger amount of buffer in the FRAC3DVS-OPG model (i.e., the FRAC3DVS-OPG model is more geometrically accurate than the simplified SYVAC3-CC4 model). This affects sorbing radionuclides more than non-sorbing ones.

Table 7-30: Comparison of Peak Transport Rates to the Geosphere

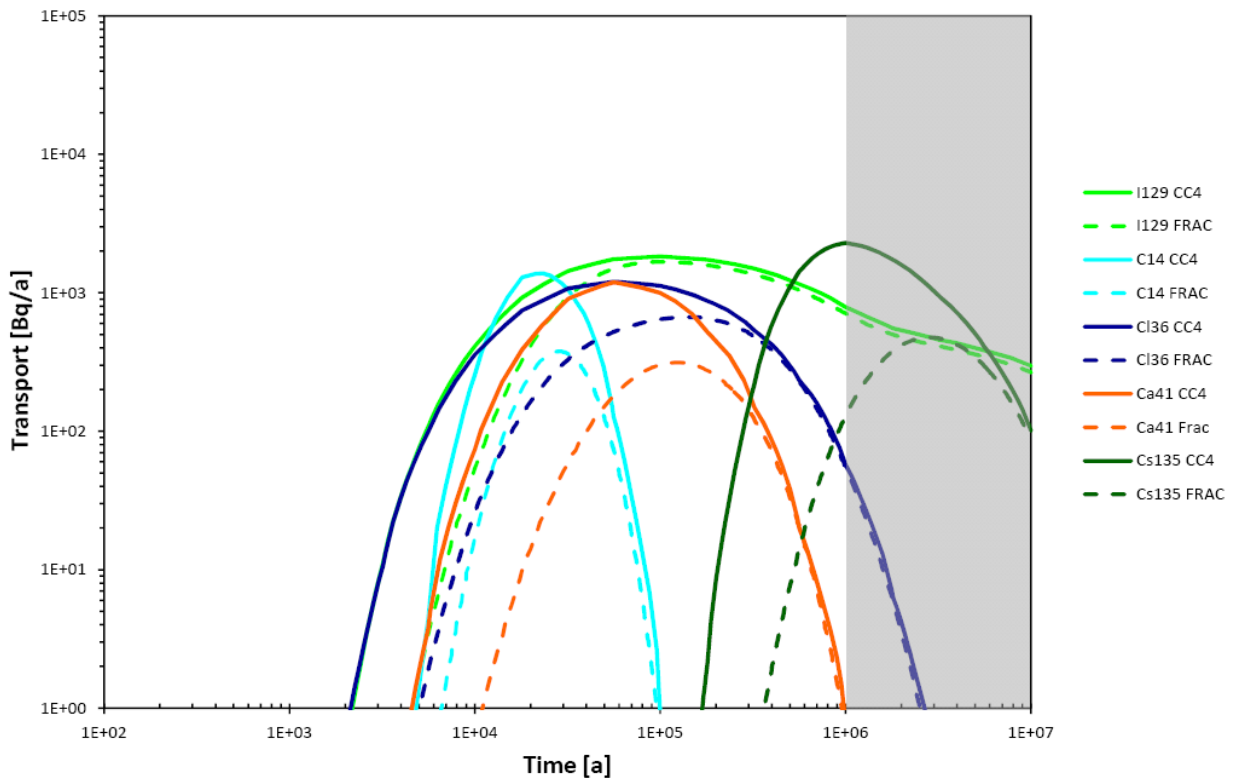
Nuclide	Peak Release Rate (Bq/a)			Time of Peak Release (a)		
	SYVAC3-CC4	FRAC3DVS-OPG	Ratio ¹	SYVAC3-CC4	FRAC3DVS-OPG	Ratio ¹
I-129	1.86x10 ³	1.85x10 ³	1.00	6.5x10 ⁴	6.5x10 ⁴	1.00
C-14	7.30x10 ⁴	7.04x10 ⁴	1.04	1.8x10 ³	2.1x10 ³	0.86
Ca-41	1.68x10 ³	1.60x10 ³	1.05	2.9x10 ⁴	3.2x10 ⁴	0.91
Cl-36	1.30x10 ³	1.30x10 ³	1.00	3.2x10 ⁴	3.2x10 ⁴	1.00
Cs-135	3.54x10 ⁴	2.05x10 ⁴	1.7	1.9x10 ⁴	6.8x10 ⁴	0.28
Sn-126	5.92x10 ³	1.80x10 ¹	330	2.3x10 ⁵	5.8x10 ⁵	0.40
U-234	-	-	-	>10 ⁷	>10 ⁷	N/A
U-238	-	-	-	>10 ⁷	>10 ⁷	N/A

Note: ¹ Ratio is the SYVAC3-CC4 value divided by the FRAC3DVS-OPG value.

Geosphere Transport Comparison

The transport from the geosphere to the surface for the Reference Case is shown in Figure 7-103 with Table 7-31 summarizing the peak values. The SYVAC3-CC4 results are conservative for all radionuclides shown (i.e., the peak values are greater than those from FRAC3DVS-OPG while the time of the peak is earlier).

For U-238 and U-234, the release rates are effectively zero in both models due to the highly sorbing nature of these radionuclides.



Note: Sn-126 results are off scale low

Figure 7-103: Comparison of SYVAC3-CC4 and FRAC3DVS-OPG Transport of I-129, C-14, Cl-36, Ca-41 and Cs-135 to the Surface

Table 7-31: Comparison of Peak Release Rates to the Surface

Nuclide	Peak Release Rate (Bq/a)			Time of Peak Release (a)		
	SYVAC3-CC4	FRAC3DVS-OPG	Ratio ¹	SYVAC3-CC4	FRAC3DVS-OPG	Ratio ¹
I-129	1.81x10 ³	1.67x10 ³	1.08	1.00x10 ⁵	1.02x10 ⁵	0.98
C-14	1.43x10 ³	3.77x10 ²	3.79	2.24x10 ⁴	2.92x10 ⁴	0.77
Ca-41	1.17x10 ³	3.13x10 ²	3.74	5.60x10 ⁴	1.25x10 ⁵	0.45
Cl-36	1.19x10 ³	6.67x10 ²	1.78	5.60x10 ⁴	1.43x10 ⁵	0.39
Cs-135	2.26x10 ³	4.76x10 ²	4.75	1.00x10 ⁶	2.86x10 ⁶	0.35

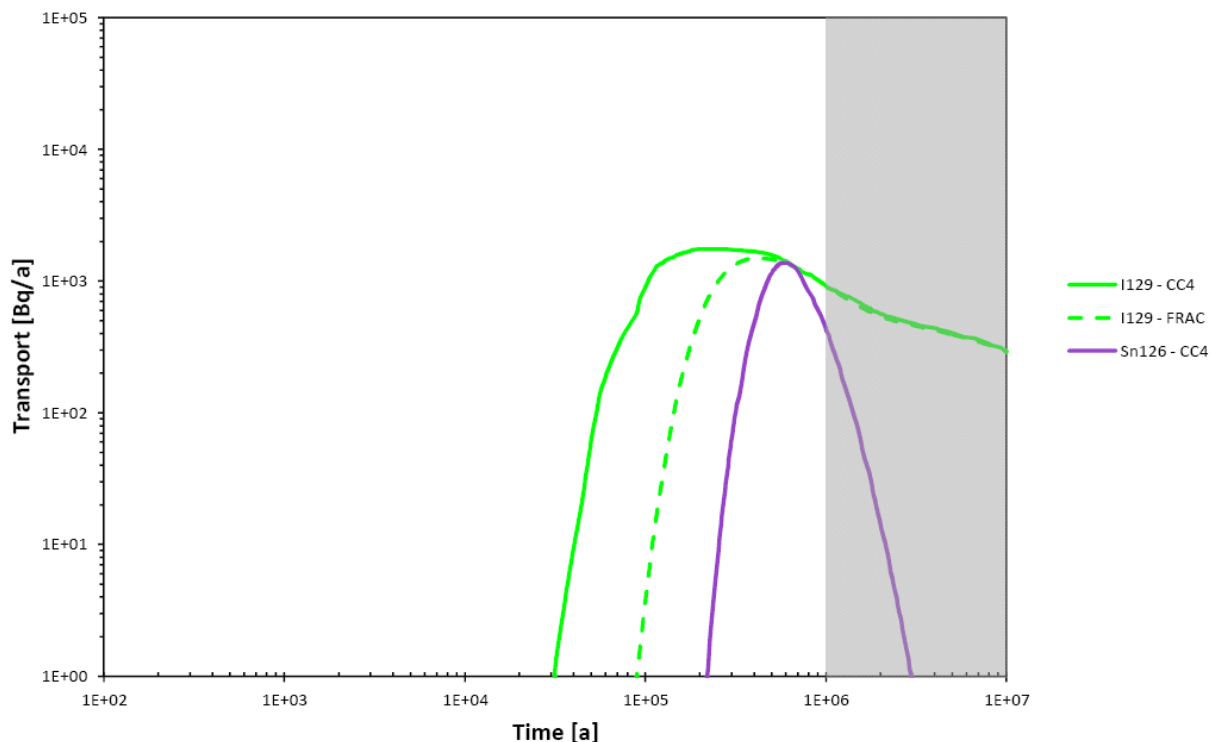
Note: ¹ Ratio is the SYVAC3-CC4 value divided by the FRAC3DVS-OPG value.

Transport from the geosphere to the surface for I-129 and Sn-126 is also shown in Figure 7-104 for the Reference Case but assuming the defective containers are located in a different sector of the repository (i.e., Sector 1, which discharges to the River). The I-129 results are again in good agreement; however, for Sn-126 the SYVAC3-CC4 result is much more conservative.

This is because the detailed FRAC3DVS-OPG model includes the capturing of a portion of the plume within the placement room backfill, whereas the simpler SYVAC3-CC4 model for Sector 1 does not include any backfill². The increased sorption in the FRAC3DVS-OPG model also leads to increased transport times so there is more time for Sn-126 ($t_{1/2} = 2.3 \times 10^5$ years) to decay.

The backfill pathway that is not represented in Sector 1 is included in Sectors 7, 8, 9 and 10 of the SYVAC3-CC4 model. This creates the potential for a large conservatism in some of the probabilistic simulations and in the All Containers Fail Disruptive Event Scenario. The conservatism occurs because a significant over estimate of the Sn-126 release rate to the surface arises when the defective containers are located in sectors without a backfill pathway. Further refinements to the SYVAC3-CC4 model could be made to improve agreement; however, this has not been done on the basis that the current model is conservative.

The above comparisons verify that the SYVAC3-CC4 near-field and far-field models provide a conservative representation of radionuclide transport for key radionuclides as compared to FRAC3DVS-OPG.



Note: the Sn-126 result from FRAC3DVS-OPG is off-scale low

Figure 7-104: Comparison of SYVAC3-CC4 and FRAC3DVS-OPG Transport of I-129 and Sn-126 to the Surface for Three Container Failures in Sector 1

² Particle track analysis of the geosphere indicate that contaminants leaving Sector 1 bypass the backfill and enter the host rock directly.

7.8.2 Deterministic Analysis

7.8.2.1 Reference Case

Figure 7-105 shows the total dose rate for the Reference Case. This is the sum of the individual contributions from all radionuclides of potential interest and their progeny.

The peak dose rate is 3.3×10^{-7} Sv/a occurring at 1.0×10^5 years. This is well below both the average natural background dose rate and the 3×10^{-4} Sv/a interim dose acceptance criterion established in Section 7.1 for the radiological protection of persons.

Figure 7-106 shows the individual contributions to the total dose rate from the most significant radionuclides. The figure shows that I-129 is the dominant dose rate contributor, followed by C-14 and Cs-135. This is because I-129 has a sizeable initial inventory, a non-zero instant release fraction, a very long half-life, is non-sorbing in the buffer, backfill and geosphere and has a radiological impact on humans.

Other fission products and actinides either decay away, or are released very slowly as the fuel dissolves and are thereafter sorbed in the engineered barriers and geosphere.

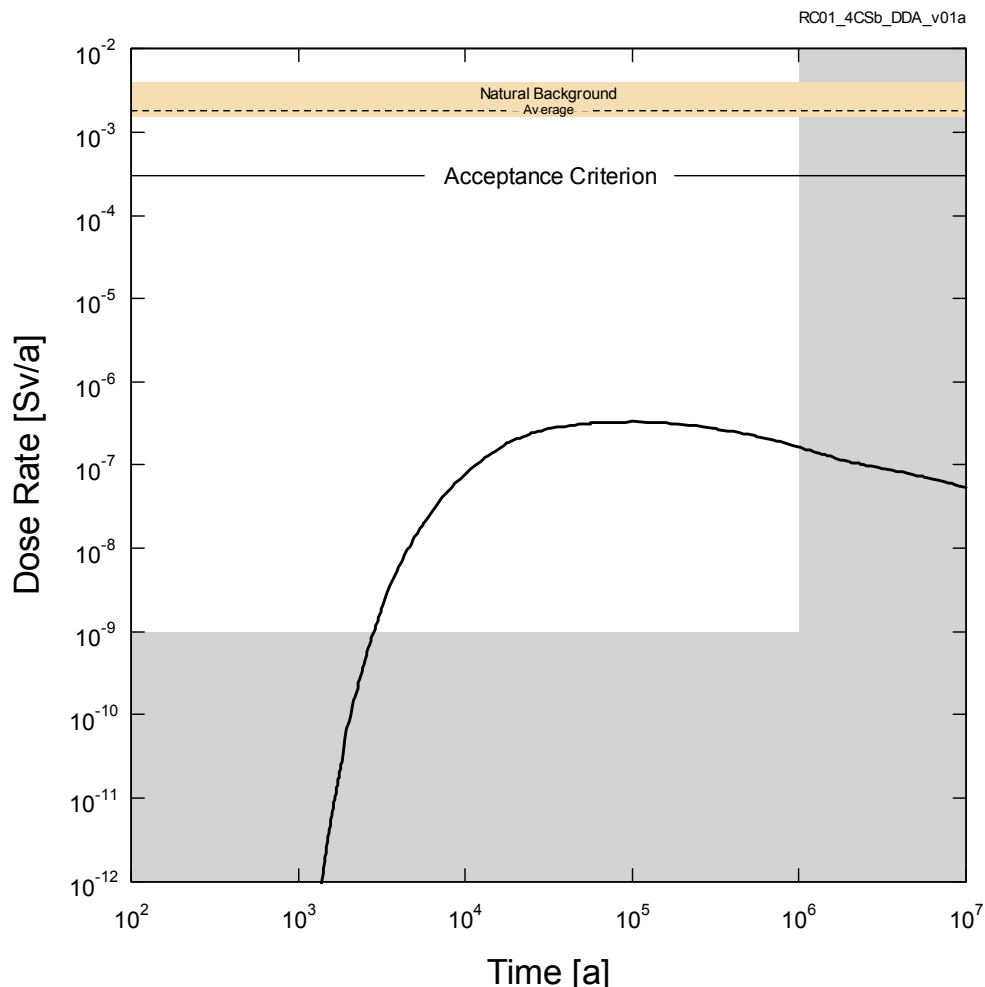


Figure 7-105: SYVAC3-CC4 – Reference Case Total Dose Rate

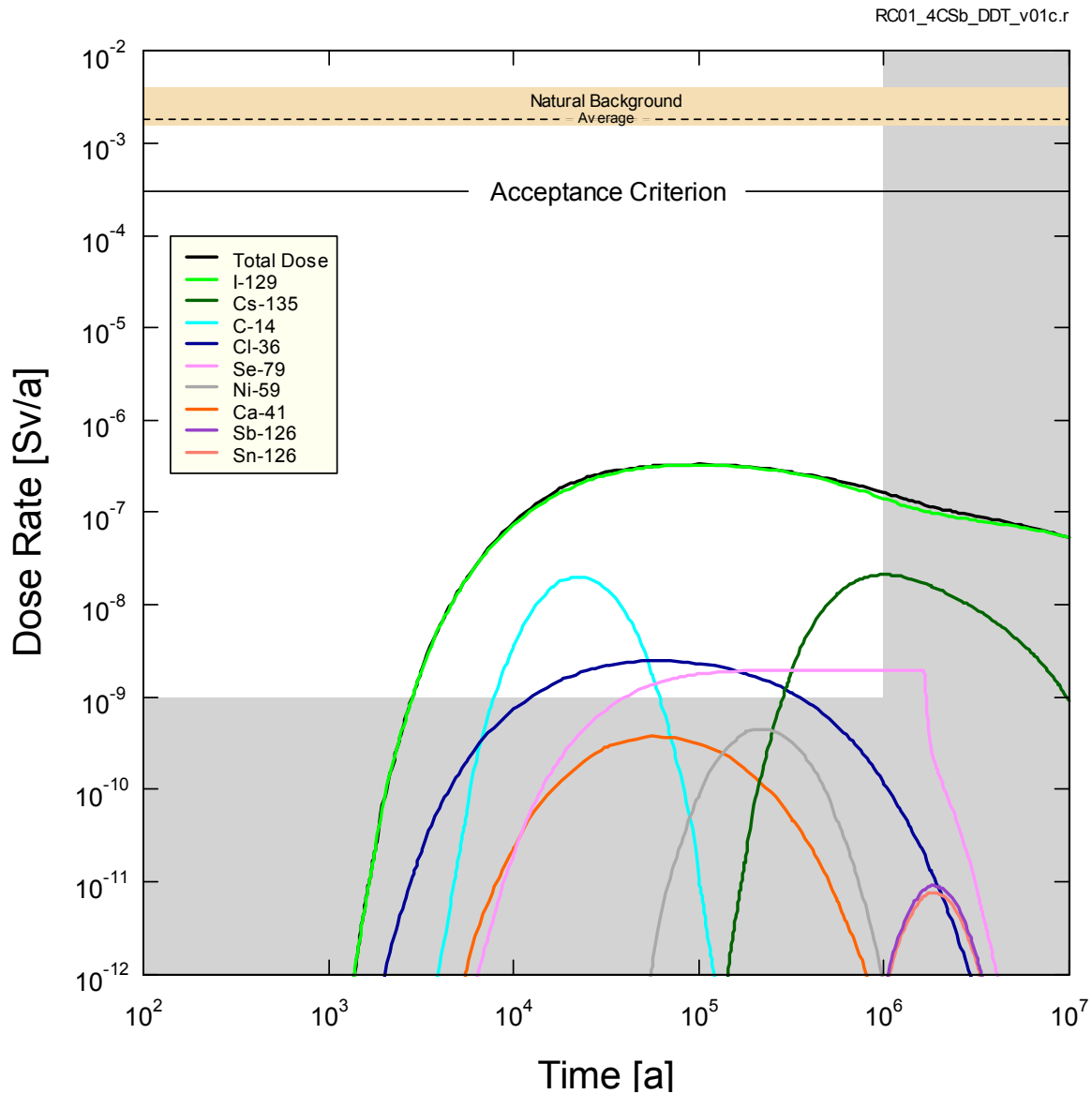


Figure 7-106: SYVAC3-CC4 – Reference Case Individual Radionuclide Dose Rates

Table 7-32 shows the dose pathways for each of the main contributors in Figure 7-106. These data are tabulated for times corresponding to the peak individual radionuclide contributions.

Table 7-32: Radionuclide Dose Pathways for the Reference Case

Element	Internal Dose [Sv/a]	Primary Pathway(s)	%	External Dose [Sv/a]	Primary Pathway(s)	%
I-129	3.3×10^{-7}	Water Ingestion	55	6.5×10^{-12}	Groundshine	72
		Food Ingestion	42		Water Immersion	26
Cs-135	2.1×10^{-8}	Food Ingestion	76	8.2×10^{-13}	Groundshine	96
		Water Ingestion	20			
C-14	2.0×10^{-8}	Inhalation	90	3.6×10^{-14}	Air Immersion	83
		Food Ingestion	7		Water Immersion	17
Cl-36	2.5×10^{-9}	Food Ingestion	52	3.7×10^{-13}	Water Immersion	92
		Water Ingestion	40			
Se-79	2.0×10^{-9}	Food Ingestion	75	3.7×10^{-15}	Groundshine	70
		Water Ingestion	23		Water Immersion	30
Ni-59	4.5×10^{-10}	Food Ingestion	98	4.1×10^{-20}	Wooden Building Materials	100

7.8.2.2 Sensitivity to a Degraded Physical Barrier

The following sensitivity cases investigate the effect of a degraded physical barrier on the Reference Case results:

- Fuel dissolution rate increased by a factor of 10;
- Container defect area increased by a factor of 10; and
- Instant release fractions set to 10%.

Figure 7-107 shows the individual contributions to the total dose rate from the most significant radionuclides for the sensitivity case with the fuel dissolution rate increased by a factor of 10. For this case, all fuel in the container dissolves within one million years whereas in the Reference Case only about 22% of the fuel dissolves (see Figure 7-27).

As in the Reference Case, I-129, C-14 and Cs-135 are the most significant dose contributors. The peak total dose rate occurs at 1.0×10^5 years and reaches a value of 2.4×10^{-6} Sv/a or about 7.3 times that of the Reference Case. The peak does not increase by 10 times because the instant release fraction for I-129 also affects its dose rate and this parameter is independent of the fuel dissolution rate. The decrease at longer times occurs because the UO_2 matrix is completely dissolved and the I-129 source term becomes zero.

Actinide dose rates are zero because they are strongly sorbed in the buffer and geosphere and do not reach the biosphere during the simulation time.

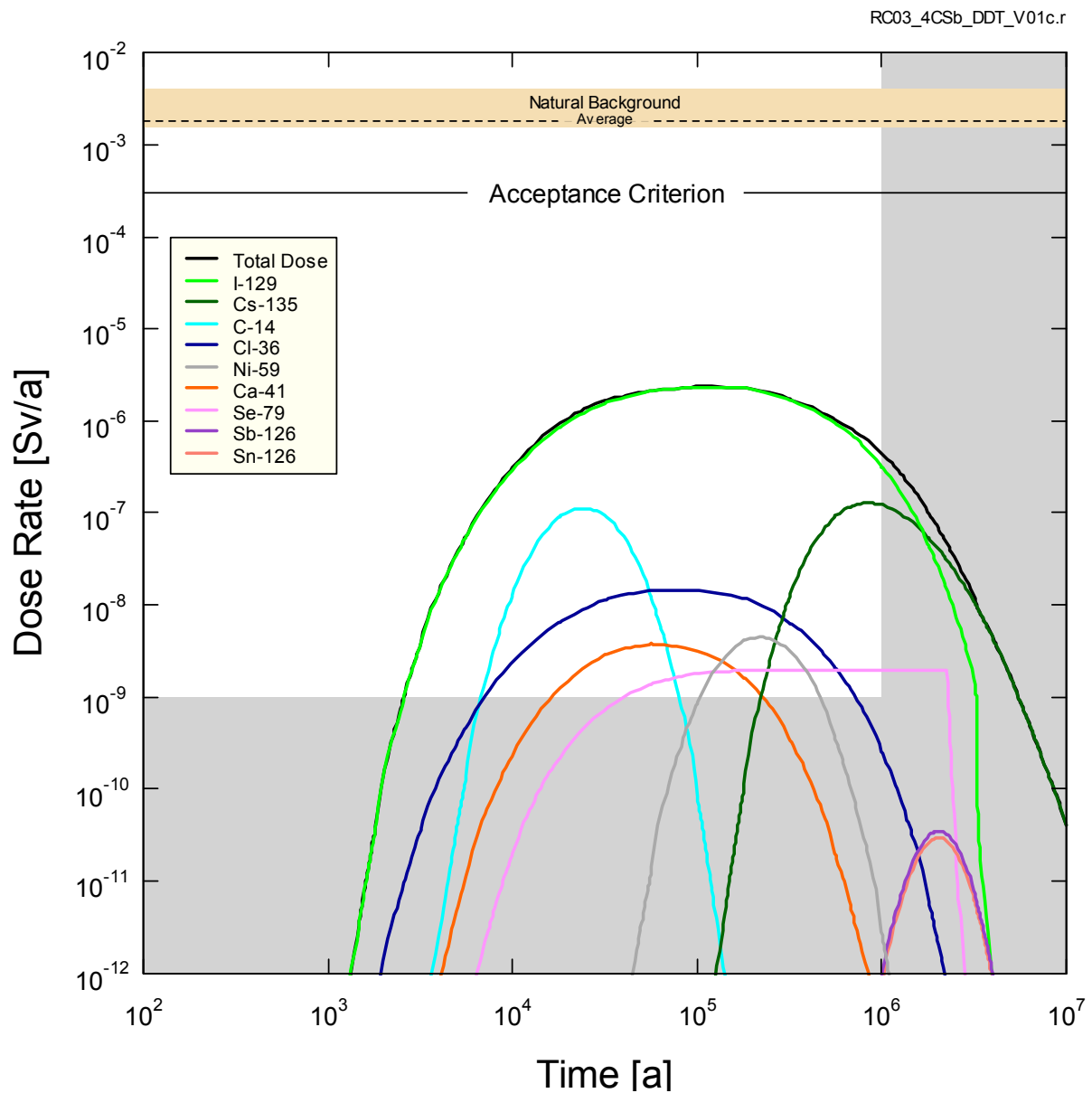


Figure 7-107: SYVAC3-CC4 - Sensitivity to a Factor of 10 Increase in Fuel Dissolution Rate

Figure 7-108 shows the individual contributions to the total dose rate from the most significant radionuclides for the sensitivity case with the defect area in the three defective containers increased by a factor of 10.

As in the Reference Case, I-129 is the main dose contributor. The peak total dose rate occurs at 4.51×10^4 years and reaches a value of 8.6×10^{-7} Sv/a or about 2.6 times that of the Reference Case. The I-129 peak is largely unaffected by the defect size because the release of I-129 is buffer-limited (proportional to the radius of the defect) rather than defect size-limited (proportional to the area of the defect). C-14 is defect size-limited and release of C-14 increases by a factor of 10 in this sensitivity case.

The actinide dose rates are zero because they are strongly sorbed in the buffer and geosphere and do not reach the biosphere during the simulation time.

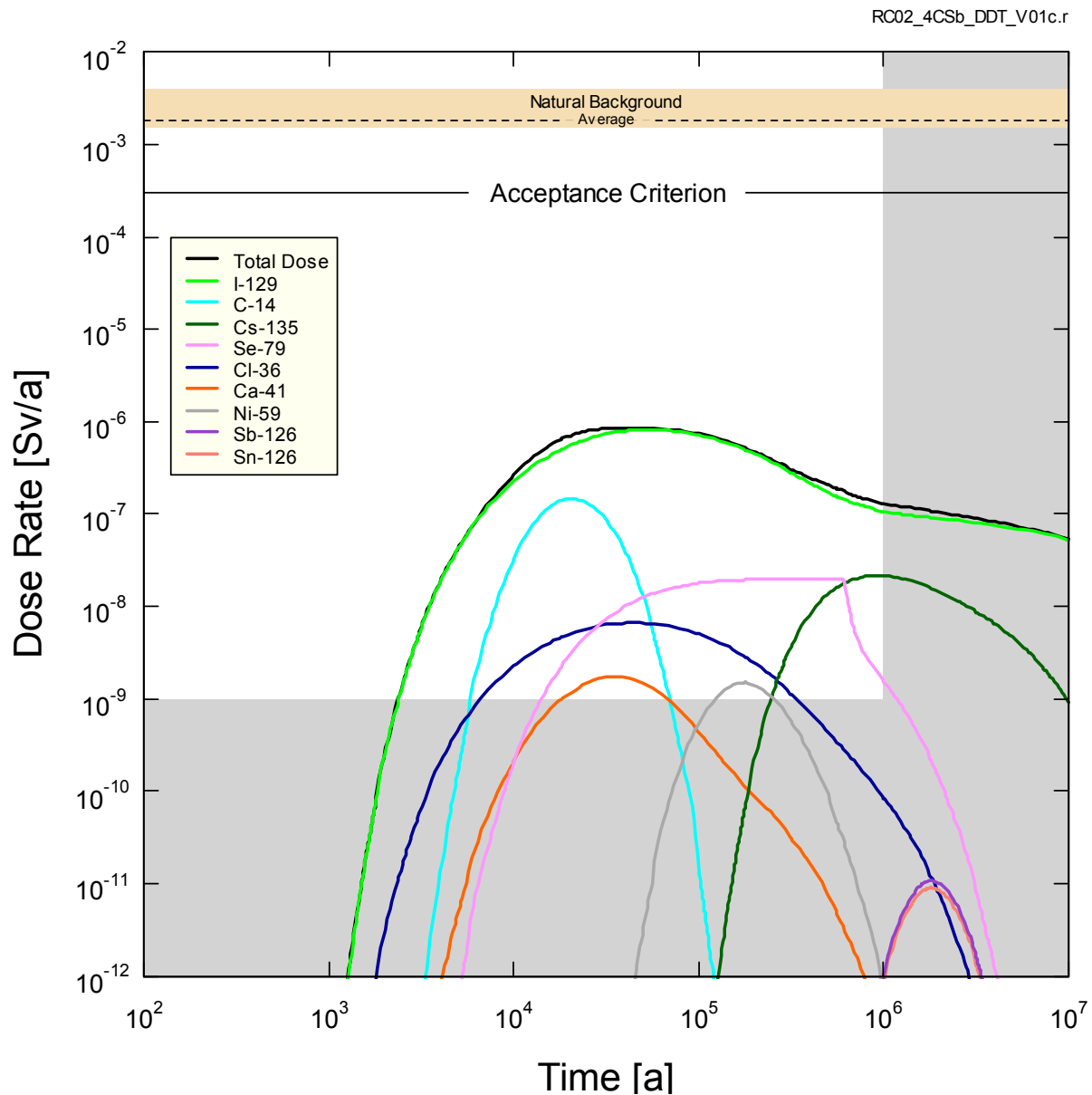


Figure 7-108: SYVAC3-CC4 - Sensitivity to a Factor of 10 Increase in Container Defect Area

Figure 7-109 shows the individual contributions to the total dose rate from the most significant radionuclides for the sensitivity case with the instant release fractions set to 10%.

As in the Reference Case, I-129 is the main dose contributor. The peak total dose rate occurs at 7.2×10^4 years and reaches a value of 4.8×10^{-7} Sv/a or about 1.5 times that of the Reference Case.

The actinide dose rates are zero because they are strongly sorbed in the buffer and geosphere and do not reach the biosphere during the simulation time.

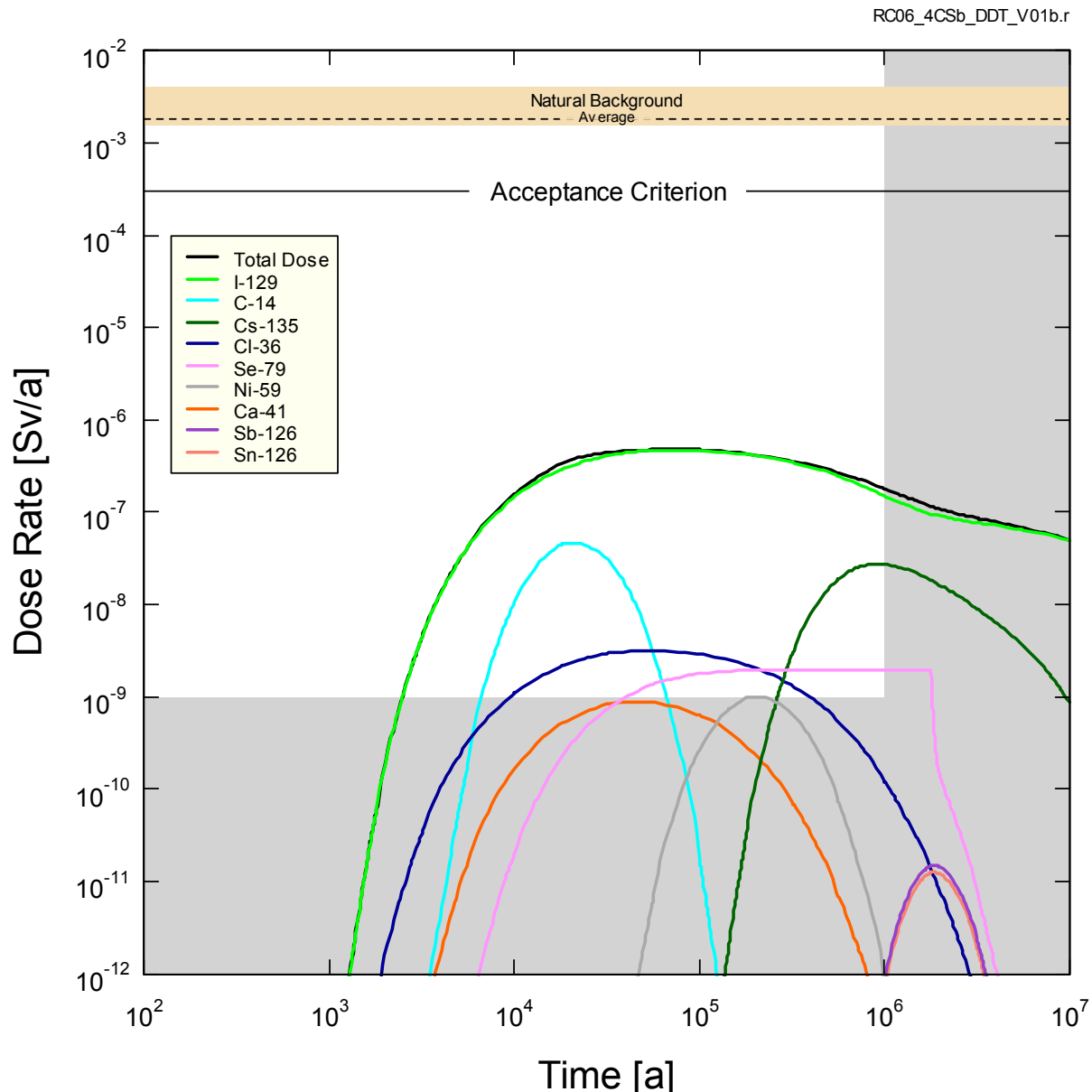


Figure 7-109: SYVAC3-CC4 - Sensitivity to All Instant Release Fractions Set to 10 Percent

Figure 7-110 summarizes the total dose rates for the Reference Case and all three degraded physical barrier cases. Table 7-33 provides results in numerical form. All results are below the interim dose acceptance criterion.

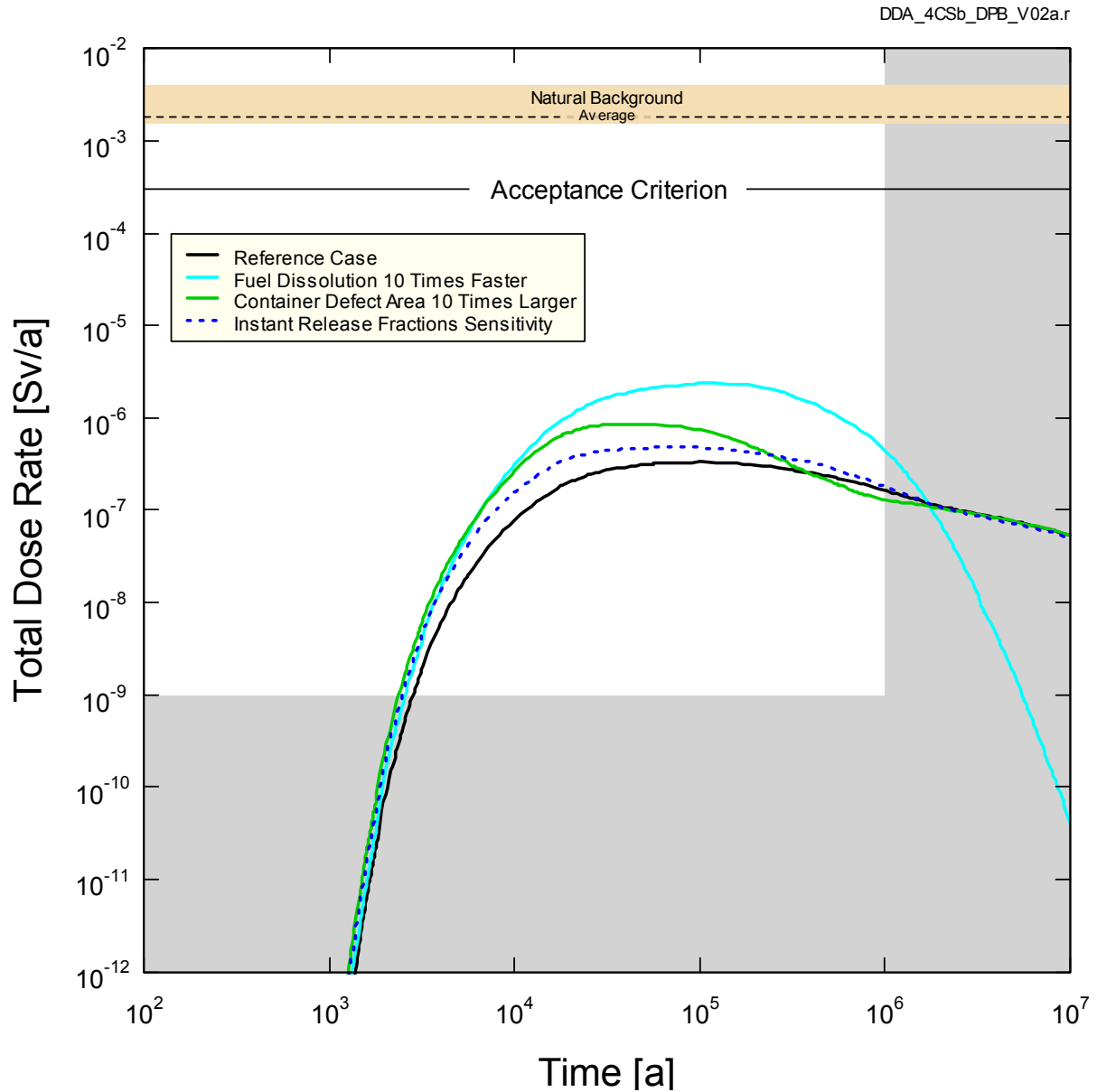


Figure 7-110: SYVAC3-CC4 - Result Summary for Defective Physical Barrier Sensitivity Cases

Table 7-33: Result Summary for Defective Physical Barrier Sensitivity Cases

Case	Peak Dose Rate (Sv/a)	Ratio to Reference Case	Time of Peak (a)
Reference Case	3.3×10^{-7}	-	1.00×10^5
Fuel Dissolution Rate 10 times Higher	2.4×10^{-6}	7.3	1.00×10^5
Container Defect Area 10 times Higher	8.6×10^{-7}	2.6	4.51×10^4
Instant Release Fraction Sensitivity	4.8×10^{-7}	1.5	7.20×10^4

7.8.2.3 Sensitivity to a Degraded Chemical Barrier

The following sensitivity cases investigate the effect of a degraded chemical barrier on the Reference Case results:

- No sorption in the geosphere;
- No solubility limits in the container;
- No sorption in the near field; and
- Low sorption in the geosphere with coincident high solubility limits in the container.

Figure 7-111 shows the individual contributions to the total dose rate from the most significant radionuclides (i.e., those accounting for 99% of the total dose) for the sensitivity case with no sorption in the geosphere.

The dominant dose contributor is Po-210; however, there are also contributions from other U-238 progeny. These rather short-lived radionuclides are important because, since there is no sorption in the geosphere, the long-lived U-238 is able to reach the surface biosphere, where it decays to form its progeny. The total dose rate reaches an approximately steady state value because the U-238 transport rate to the biosphere is approximately constant at long times.

The peak total dose rate occurs at 4.77×10^4 years and reaches a value of 6.8×10^{-5} Sv/a or 206 times higher than the Reference Case.

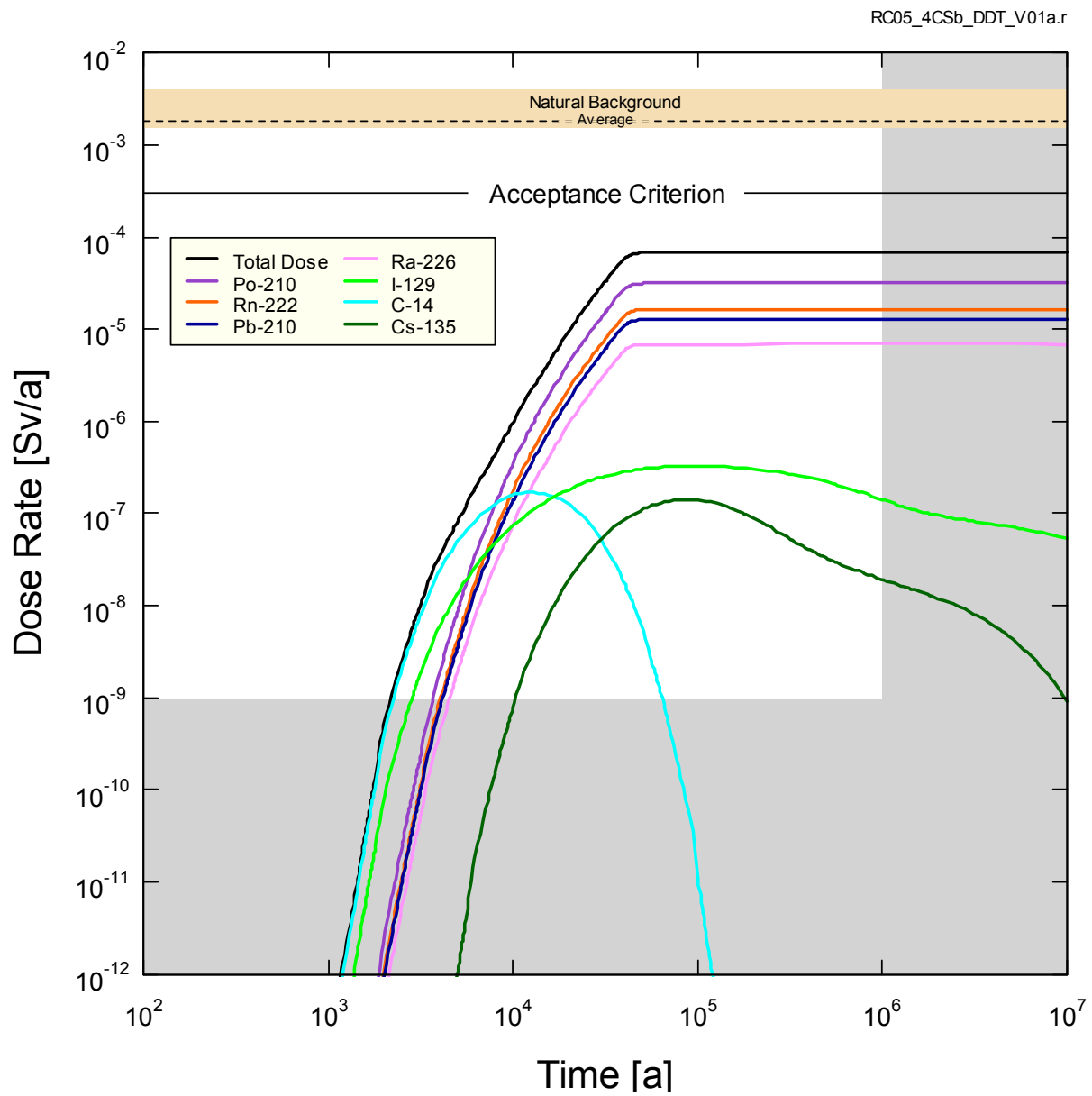


Figure 7-111: SYVAC3-CC4 – Sensitivity to No Sorption in the Geosphere

Figure 7-112 shows the individual contributions to the total dose rate for the most significant radionuclides for the sensitivity case with no radionuclide solubility limits.

As in the Reference Case, I-129 is the main dose contributor. The peak total dose rate occurs at the same time as in the Reference Case and reaches a value of 3.9×10^{-7} Sv/a or about 1.2 times that of the Reference Case. There is low sensitivity to solubility because I-129 is not solubility limited and because the actinides (which are solubility limited) continue to be strongly sorbed in the geosphere and do not reach the biosphere in the time period of interest. A comparison with Figure 7-106 shows there is a small additional contribution from Se-79.

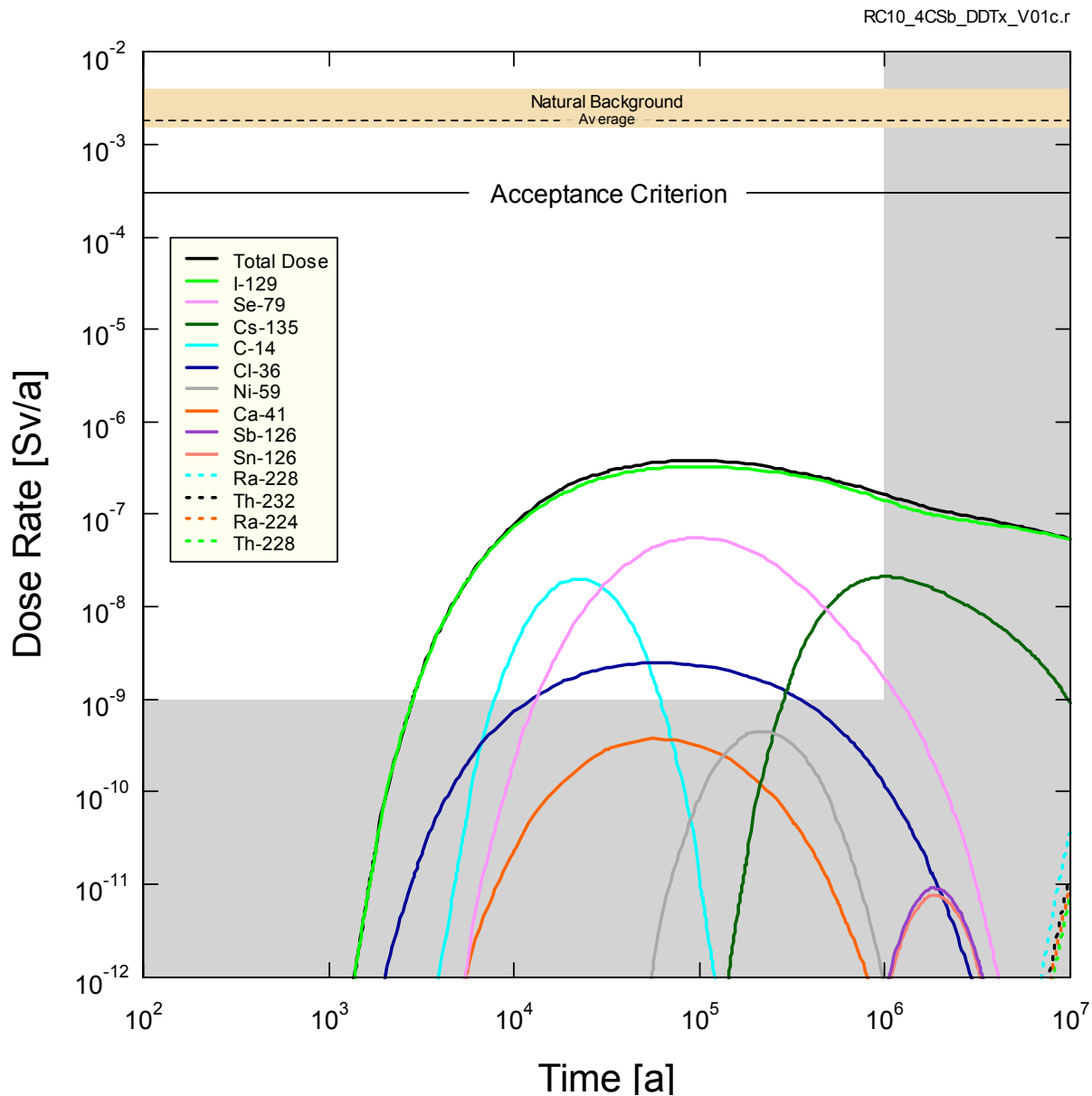


Figure 7-112: SYVAC3-CC4 – Sensitivity to No Solubility Limits

Figure 7-113 shows the individual contributions to the total dose rate for the most significant radionuclides for the sensitivity case with no sorption in the near field.

The peak total dose rate occurs at 8.36×10^4 years and reaches a value of 6.2×10^{-6} Sv/a or almost 19 times higher than the Reference Case. Unlike the Reference Case, the main dose contributors are Sn-126 and Sb-126. This occurs because Sn-126 and Sb-126 normally sorb in the near field materials and have little sorption in the far field.

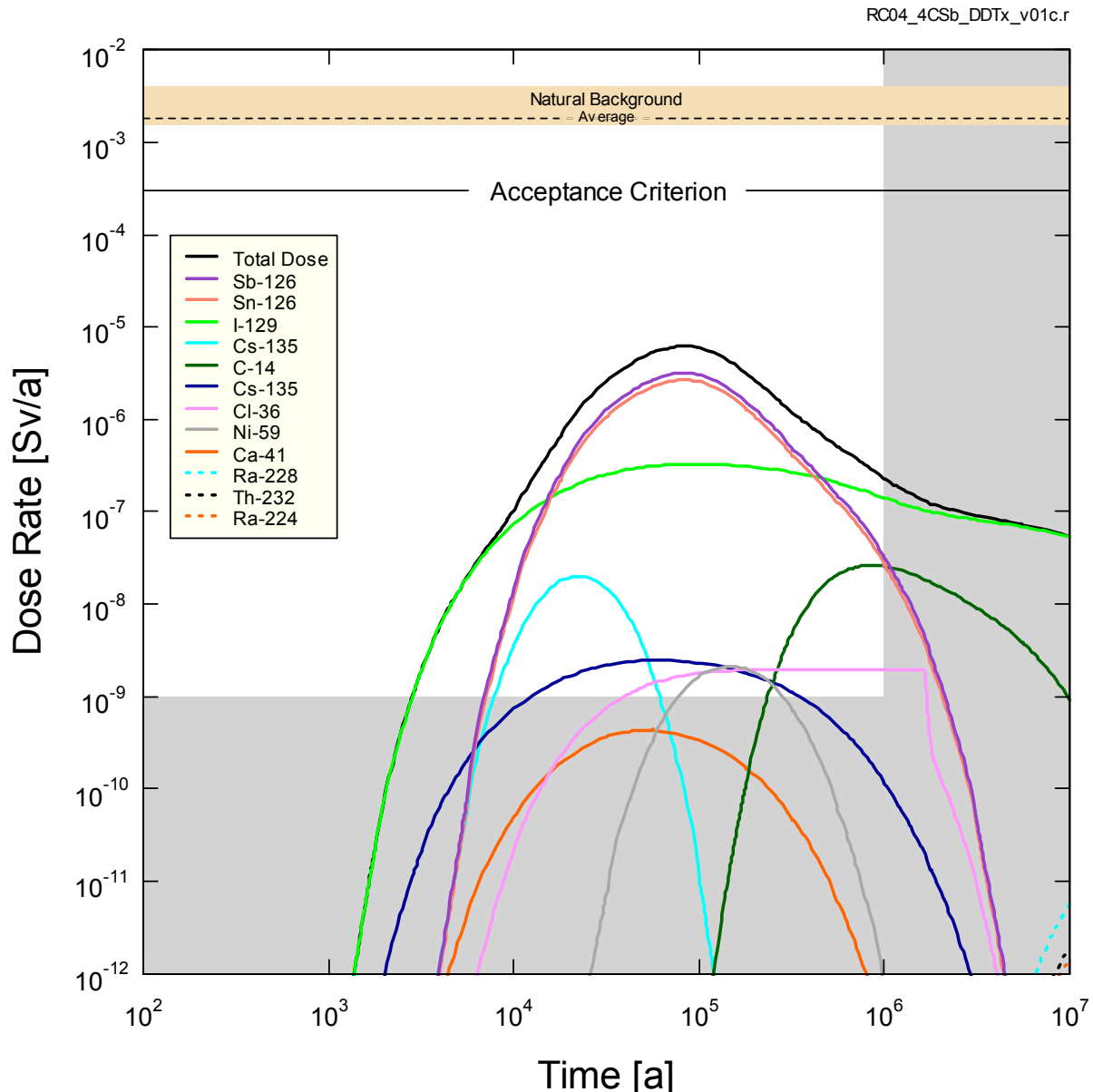


Figure 7-113: SYVAC3-CC4 – Sensitivity to No Sorption in the Near Field

Figure 7-114 shows the individual contributions to the total dose rate for the most significant radionuclides for the sensitivity case with low sorption in the geosphere and coincident high radionuclide solubility limits (where “low” / “high” means 1st quantile and 99th quantile of their sampling range).

As in the Reference Case, the highest dose contributor is I-129. The peak total dose rate occurs at the same time as in the Reference case (1×10^5 years) and reaches a value of 5.2×10^{-7} Sv/a or 1.6 times higher than the Reference Case. The change is largely due to Cs-135 which is less retarded and therefore less reduced by decay during transport. Actinides (which are solubility limited) continue to be sorbed in the buffer and geosphere.

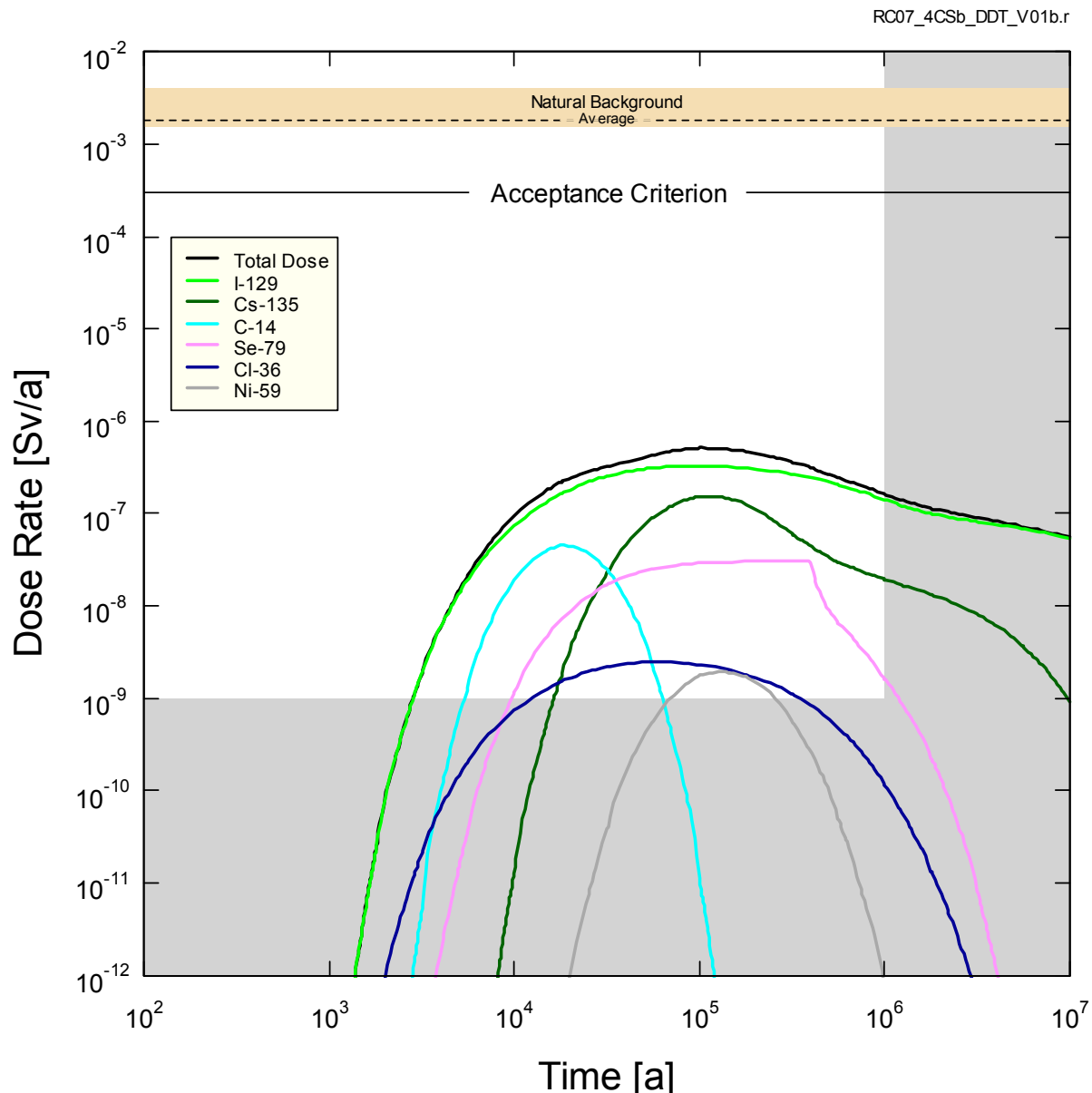


Figure 7-114: SYVAC3-CC4 – Sensitivity to Low Sorption in the Geosphere with Coincident High Solubility Limits

Figure 7-115 shows the total dose rates for the Reference Case and all four degraded chemical barrier cases. Table 7-34 provides the results in numerical form. All results are below the interim dose acceptance criterion.

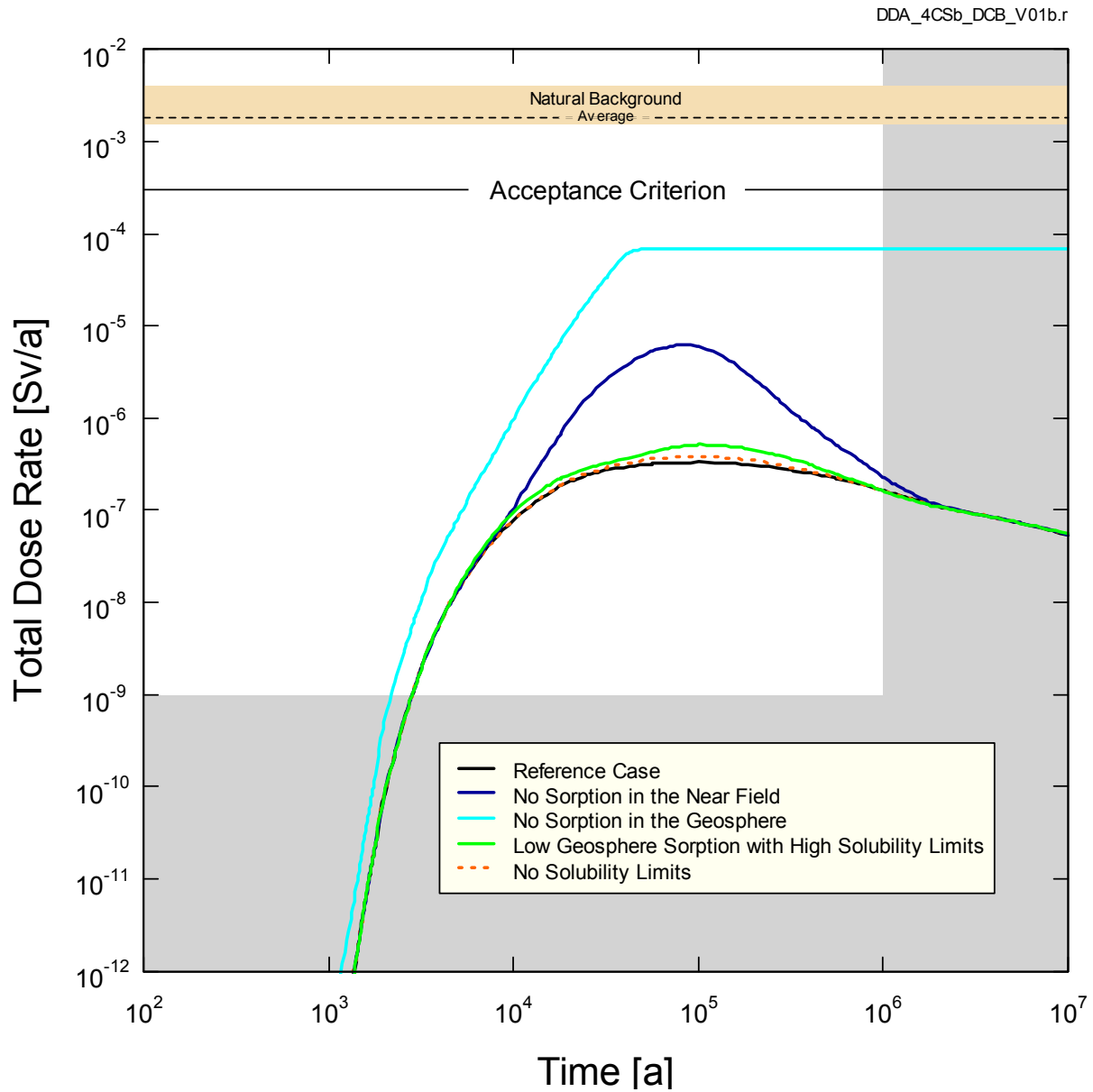


Figure 7-115: SYVAC3-CC4 - Summary for Defective Chemical Barrier Sensitivity Cases

Table 7-34: Result Summary for Defective Chemical Barrier Sensitivity Cases

Case	Peak Dose Rate (Sv/a)	Ratio to Reference Case	Time of Peak (a)
Reference Case	3.3×10^{-7}	-	1.00×10^5
No Sorption in the Geosphere	6.8×10^{-5}	206	4.77×10^4
No Solubility Limits	3.9×10^{-7}	1.2	1.00×10^5
No Sorption in the Near Field	6.2×10^{-6}	19	8.36×10^4
Low Sorption in the Geosphere With Coincident High Radionuclide Solubility Limits	5.2×10^{-7}	1.6	1.00×10^5

7.8.2.4 Sensitivity to a Higher Geosphere Hydraulic Conductivity

This section presents analyses performed for the sensitivity case with the highest geosphere hydraulic conductivity. This corresponds to the Sensitivity Case 1 profile defined in Chapter 2. In this case hydraulic conductivities (m/s) in the host rock are 10 times greater than those in the Reference Case. Specifically:

- Zone 1 (10 – 150 m) = changed from 2×10^{-9} to 2×10^{-8}
- Zone 2 (150 – 700 m) = changed from 4×10^{-11} to 4×10^{-10}
- Zone 3 (700 – 1500 m) = changed from 1×10^{-11} to 1×10^{-10}

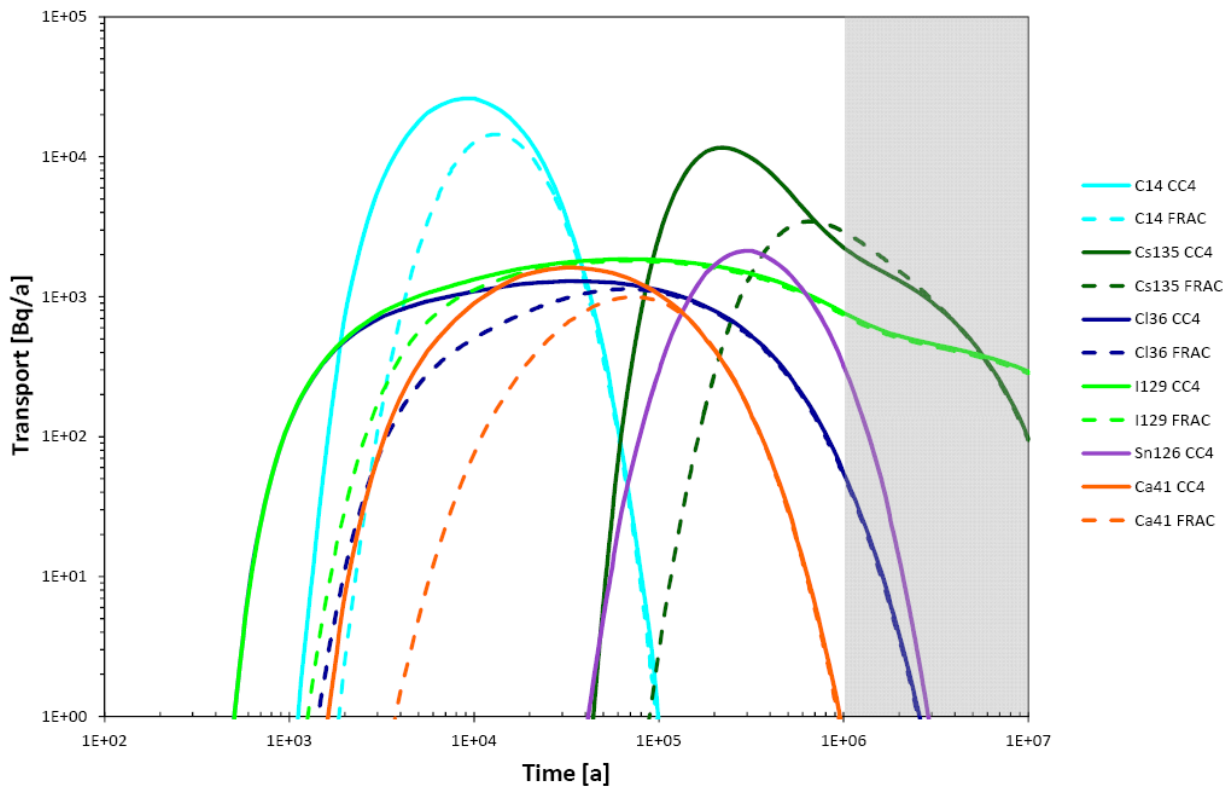
The standard approach for examining the effects of hydraulic conductivity variations is to use only the FRAC3DVS-OPG code. FRAC3DVS-OPG is required because the change affects the groundwater flow distribution and this is not computed by the SYVAC3-CC4 model. Once the new flow distribution is available, FRAC3DVS-OPG is used to perform radionuclide transport calculations for I-129. Experience typically shows I-129 to be the overwhelmingly dominant dose contributor and therefore estimates of the dose consequence can be obtained by scaling the I-129 release to the well. This experience is confirmed by the results presented in Section 7.8.2.1.

This approach has been followed for all three geosphere hydraulic conductivity sensitivity cases, with results of the FRAC3DVS-OPG groundwater flow and I-129 transport calculations presented in Section 7.7.1.1.2 and Section 7.7.2.2.3. The results show that the transport time to the surface for Sensitivity Case 1 is sufficiently short that non-sorbing radionuclides with intermediate half-lives may no longer decay away. Consequently, the use of the I-129 release as a surrogate for dose may not be valid and additional detailed analysis with SYVAC3-CC4 is necessary.

To perform the SYVAC3-CC4 analysis, the heads, x-y-z coordinates, non-aquifer drawdown, dispersion and hydraulic conductivity were changed for the nodes and segments leading from Sector 8 to the well in the input file. Groundwater flow simulations using FRAC3DVS-OPG showed that the increase in hydraulic conductivity caused an increase in the groundwater velocities; however, there were no substantial changes in the flow directions, so the same GEONET groundwater pathways to the surface could be used.

To confirm the validity of the new model, the same approach described in Section 7.8.1 for the Reference Case is followed. Figure 7-116 shows the resulting comparison between the FRAC3DVS-OPG and SYVAC3-CC4 computed releases to the biosphere for I-129, C-14, Cl-36 and Ca-41. C-14 is also now included in the comparison because, as will be shown below, this radionuclide makes a significant contribution to the dose consequence in this sensitivity case. The releases of U-238 and U-234 are off scale low and are therefore not shown.

The comparison shows the revised SYVAC3-CC4 system model is conservative in that it results in earlier releases than does the FRAC3DVS-OPG model with higher peak values.



Note: the Sn-126 value from FRACDVS-OPG is off-scale low

Figure 7-116: SYVAC3-CC4 - Comparison of C-14, Ca-41, Cl-36, Cs-135, I-129, Sn-126 Release Rates to the Surface for Geosphere Hydraulic Conductivity Increased by a Factor of 10

Figure 7-117 shows the total dose rate for this sensitivity case. The peak total dose rate occurs at 2.78×10^5 years and reaches a value of 8.6×10^{-7} Sv/a or about 2.6 times that of the Reference Case. This is well below both the average natural background dose rate and the 3×10^{-4} Sv/a interim dose acceptance criterion established in Section 7.1 for the radiological protection of persons.

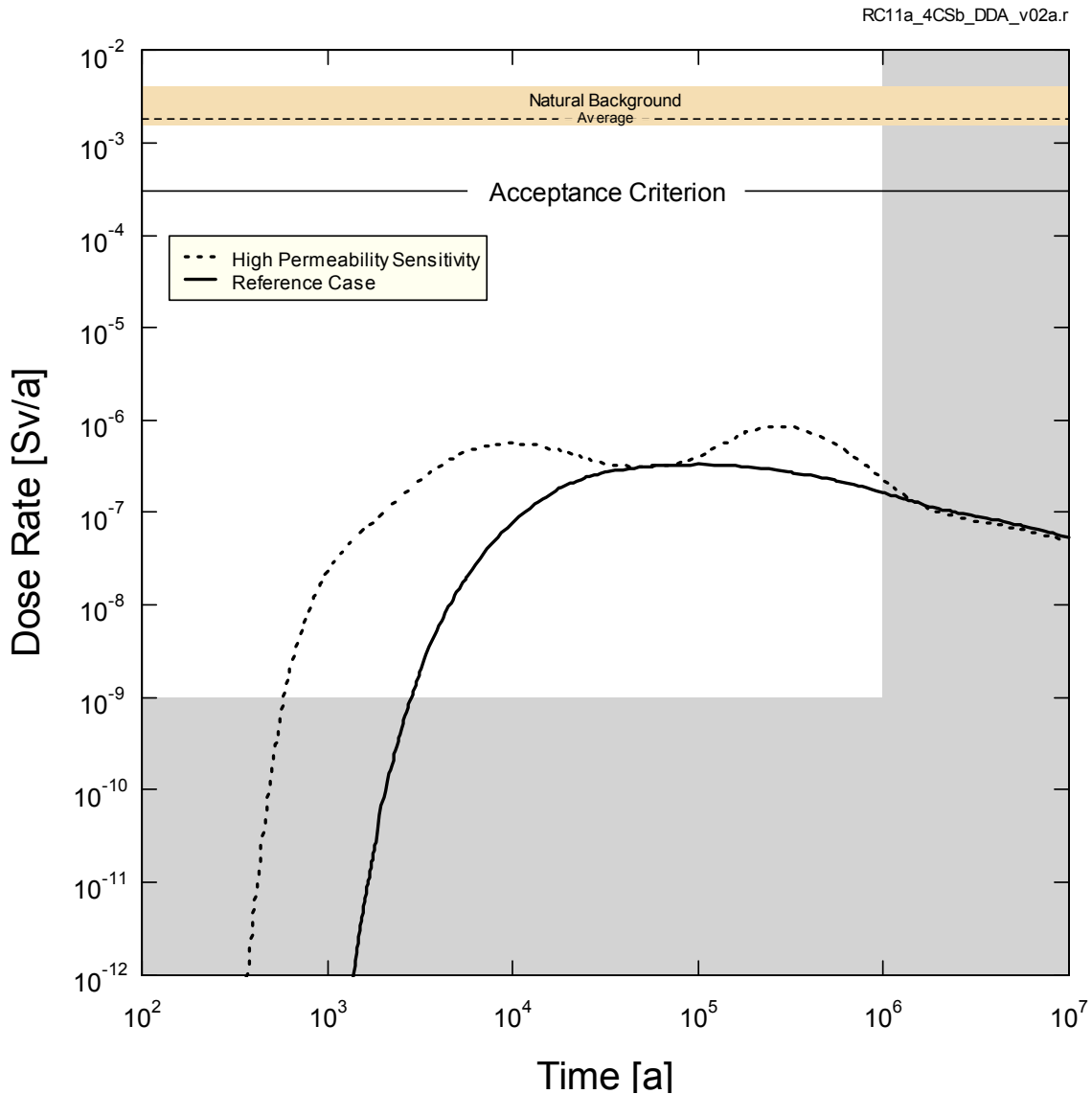


Figure 7-117: SYVAC3-CC4 - Total Dose Rate for Geosphere Hydraulic Conductivity Increased by a Factor of 10

Figure 7-118 shows the individual contributions to the total dose rate from the most significant radionuclides. C-14, I-129, and Sn-126 (in secular equilibrium with Sb-126) are the dominant dose contributors with peak dose rates of 3.5×10^{-7} Sv/a, 3.0×10^{-7} Sv/a, and 2.8×10^{-7} , respectively. Peak dose rates for these nuclides occur at 9.24×10^3 years, 6.16×10^4 years, and 3.20×10^5 years, respectively. Both C-14 and I-129 have a non-zero instant release fractions, are not solubility limited and do not sorb. Sn-126 is very strongly sorbed in the engineered barrier materials and very weakly sorbed in the host rock. Some of the actinide chains appear at later times.

All other fission products and actinides either decay away, or are released very slowly as the fuel dissolves and are thereafter sorbed in the engineered barriers and geosphere.

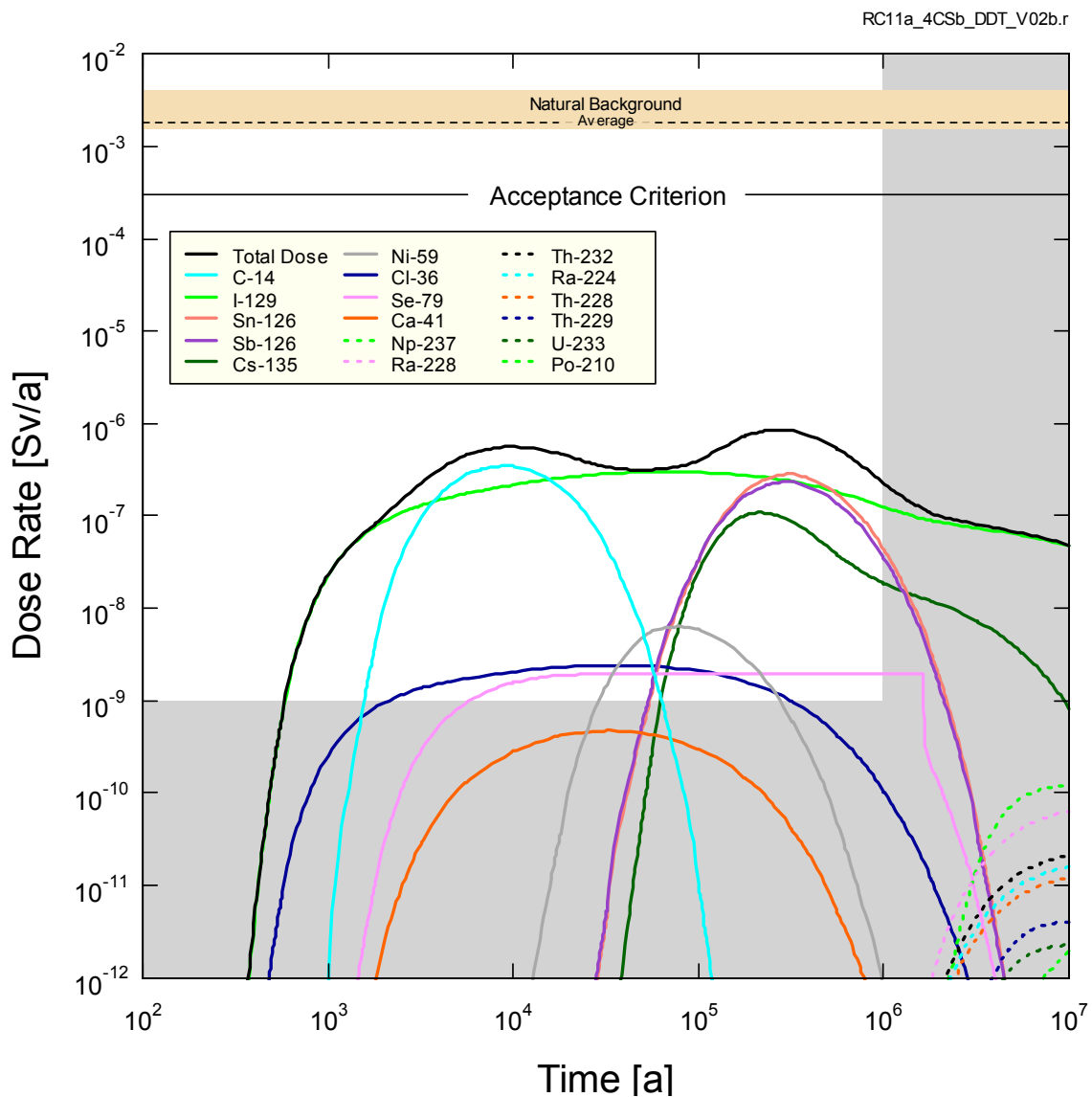


Figure 7-118: SYVAC3-CC4 - Radionuclide Dose Rates for Geosphere Hydraulic Conductivity Increased by a Factor of 10

7.8.3 Probabilistic Analysis

In the previous sections, deterministic analyses are performed for a Reference Case and a series of sensitivity studies that examine the effect of degraded physical and chemical barriers. The effect of a factor of 10 increase in geosphere hydraulic conductivity is also addressed.

Many of the modelling parameters are uncertain or have a natural degree of variability, and are therefore more generally characterized by a range or distribution of values. Simultaneous accounting of these uncertainties is achieved by using the SYVAC3-CC4 system model in probabilistic mode.

Probabilistic mode uses a Monte Carlo random sampling strategy that considers the full range of possible parameter values. The results presented here draw from 120,000 simulations in which parameter values are sampled randomly from their probability density functions. Each of these thousands of simulations produces a unique estimate of impact that is used to collectively generate a distribution that reflects the underlying uncertainty.

An important caveat is that these simulations do not consider the effects of different groundwater flow fields or uncertainties in the fracture locations. Rather, these consider the effect of variation in radionuclide source term and transport parameters within a defined geosphere.

A selection of biosphere parameters represented by probability distributions is provided in Table 7-21 through Table 7-24. A detailed description of the probability distributions for all parameters is provided in Garisto et al. (2012).

7.8.3.1 All Parameters Simultaneously Varied

This section reports on probabilistic simulations in which all parameters with probability distributions are simultaneously varied.

Number of Defective Containers

The number of defective containers is described by a binomial distribution that is characterised by the number of containers in the repository and the probability of container failure. Uncertainty in the container failure probability is accounted for by expressing the failure probability per container as a lognormal probability density function with a geometric mean of 2×10^{-4} , a geometric standard deviation of 2, and bounds of 10^{-4} and 10^{-3} . The best-estimate failure probability is 2×10^{-4} per container. The locations of defective containers are randomly assigned within the repository in each simulation.

Figure 7-119 shows the as-sampled distribution of container failures.

From Monte Carlo sampling of the probability distribution (see Section 7.2.1), the most probable number of defective containers, or *mode* of the distribution, is 2 (i.e., the peak in the profile), while the average or *mean* value is 3.5. The maximum number in any one simulation is 24, and in 8% of the simulations there is at least one defective container in Sector 8. Defective containers in Sector 8 produce the highest dose rates to the critical group.

There are 9602 simulations (about 8% of the total) with no defective containers.

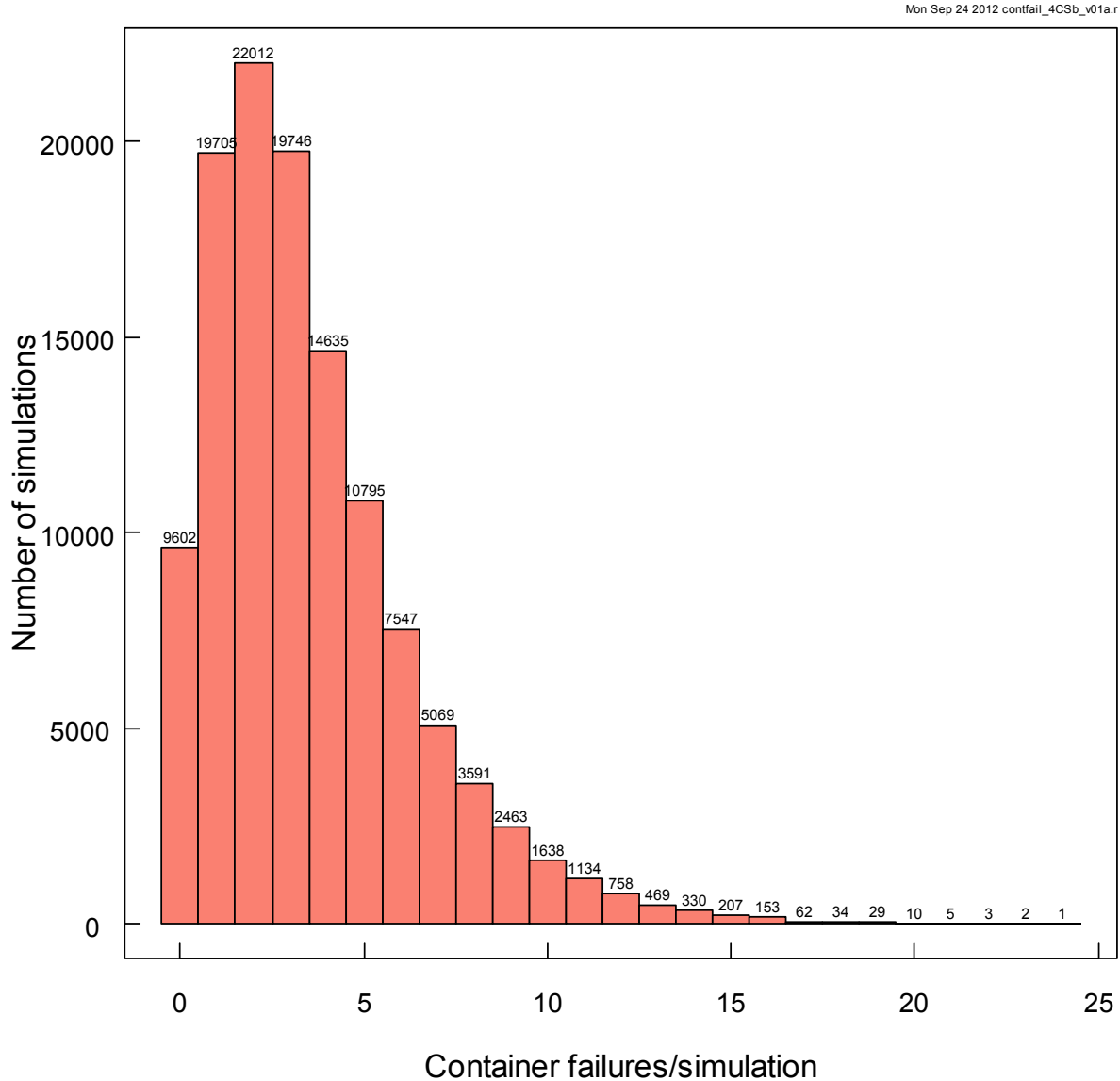


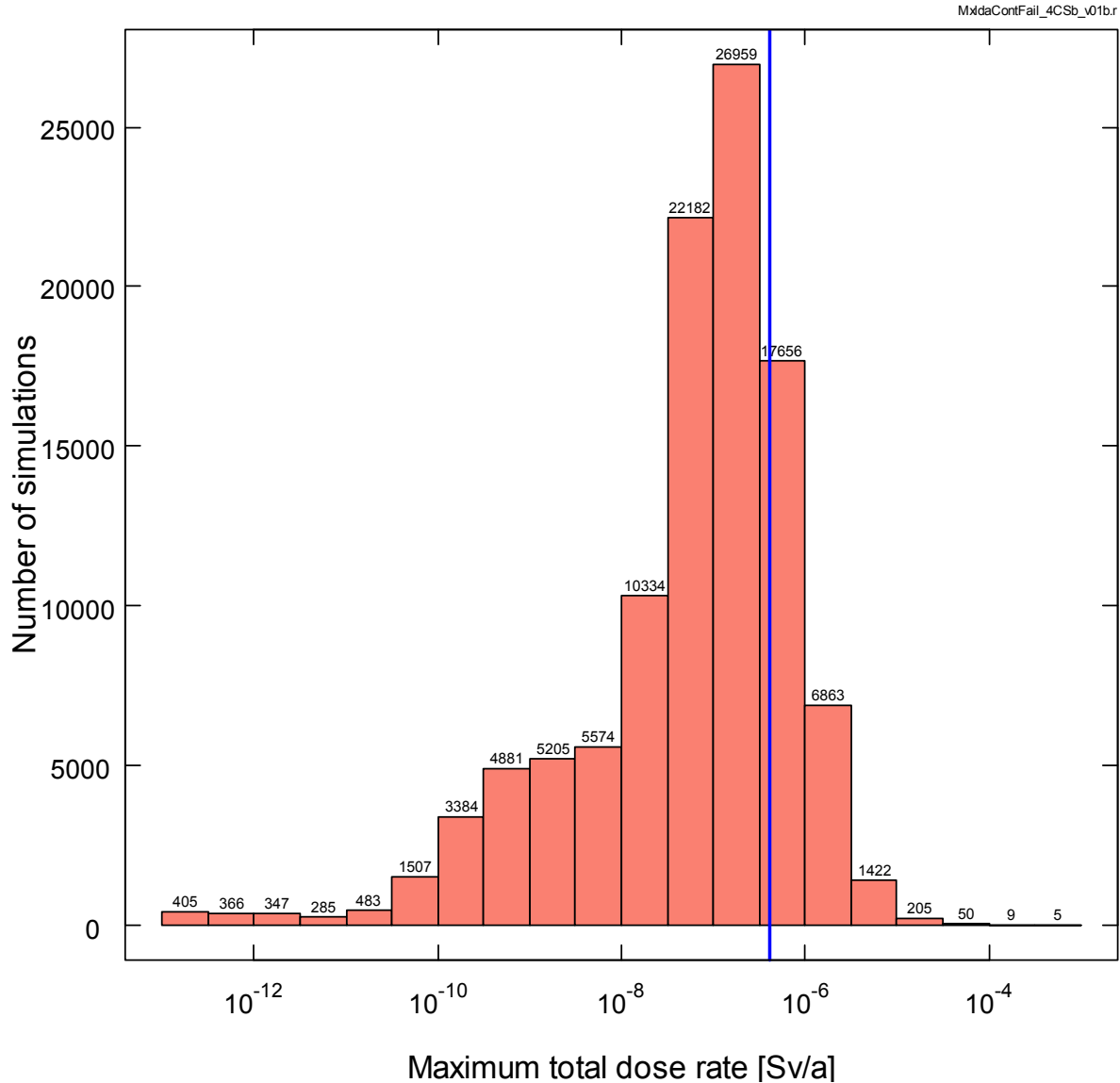
Figure 7-119: SYVAC3-CC4 - Distribution of Container Failures for 120,000 Simulations

Dose Rates

Figure 7-120 shows the distribution of the peak total dose rate to a member of the critical group for simulations with at least one defective container. The peak total dose rate is the maximum, at any time during a simulation, of the sum of the individual dose rates for all radionuclides. The

average dose rate, representing the arithmetic average of the peak total dose rates over all cases (including the cases with no defective containers) is also shown.

The most probable peak total dose rate is 7.4×10^{-8} Sv/a while the average dose rate is 3.7×10^{-7} Sv/a. The average dose rate is greater than the most probable value because of the non-Gaussian shape of the distribution. These values can be compared against the peak dose rate for the Reference Case of 3.3×10^{-7} Sv/a.



Note: The vertical blue line is the average peak total dose rate of 3.7×10^{-7} Sv/a.

Figure 7-120: SYVAC3-CC4 - Distribution of the Peak Dose Rate for Simulations with at Least One Defective Container

Statistical information concerning the distribution can be derived as summarized in Table 7-35. This table shows that the 95% confidence bound is symmetric around the average value. The median value and the average value differ by approximately a factor of five, indicating that the average peak total dose is influenced by a number of high consequence simulations (i.e., the distribution of results is somewhat skewed). The simulations causing the results to be skewed are discussed later in this section.

Table 7-35: Statistical Information Concerning the Distribution of the Peak Dose Rate

Statistic	Value	Bootstrap 95% Confidence Bounds ¹	
		Lower Bound	Upper Bound
Average (Sv/a)	3.7×10^{-7}	3.6×10^{-7}	4.0×10^{-7}
95 th Percentile (Sv/a)	1.3×10^{-6}	1.3×10^{-6}	1.4×10^{-6}
99 th Percentile (Sv/a)	3.9×10^{-6}	3.8×10^{-6}	4.0×10^{-6}
Probability the peak dose rate exceeds 3.0×10^{-4} Sv/a ²	0.004 %	0.0008%	0.008 %
Median (Sv/a)	7.4×10^{-8}	7.3×10^{-8}	7.5×10^{-8}

Notes:

¹ Based on 10,000 replicates of the dataset obtained using the bootstrap methodology. The confidence intervals are calculated using the bootstrap method (with replacement). Since the distribution of peak dose rates is skewed, the bootstrap BC_a methodology described by DiCiccio and Efron (1996) is used.

² Interim dose acceptance criterion.

The average and median peak dose rates for the individual radionuclides are shown in Table 7-36. As in the Reference Case, I-129 is the dominant dose contributor.

Table 7-36: Average and Median Peak Dose Rates for Individual Radionuclides

Radionuclide*	Average (Sv/a)	Median (Sv/a)
I-129	2.3×10^{-7}	6.0×10^{-8}
Sn-126	6.7×10^{-8}	1.8×10^{-10}
Sb-126	5.8×10^{-8}	5.4×10^{-12}
Cs-135	3.5×10^{-8}	2.7×10^{-11}
Cl-36	1.6×10^{-8}	3.5×10^{-10}
C-14	1.7×10^{-9}	6.1×10^{-17}
Se-79	1.6×10^{-9}	3.7×10^{-11}
Ca-41	2.1×10^{-10}	6.0×10^{-12}
Ni-59	1.6×10^{-10}	0.0
Th-229	4.7×10^{-12}	0.0
Ra-228	2.5×10^{-12}	0.0
Ra-225	1.9×10^{-12}	0.0
Ac-225	9.0×10^{-13}	0.0
Np-237	6.3×10^{-13}	0.0
Ra-224	4.7×10^{-13}	0.0
U-233	4.2×10^{-13}	0.0
Th-228	3.2×10^{-13}	0.0
Th-232	2.8×10^{-13}	0.0
Rn-222	2.0×10^{-13}	0.0
Po-210	1.6×10^{-13}	0.0
Ra-226	8.6×10^{-14}	0.0
Pb-210	2.0×10^{-14}	0.0
Ac227	1.9×10^{-14}	0.0
Th-230	1.3×10^{-14}	0.0
Pa-231	1.2×10^{-14}	0.0

Note: * A cutoff of 10^{-14} Sv/a is used.

Figure 7-121 shows the average dose rate as a function of time together with its 95% confidence intervals. The intervals are calculated using Chebychev's inequality (Guttman and Wilks 1965). Note that the Chebychev inequality gives upper bounds for the confidence intervals. The narrowness of the 95% confidence band indicates high statistical confidence.

The peak average dose occurs at 6.0×10^5 years.

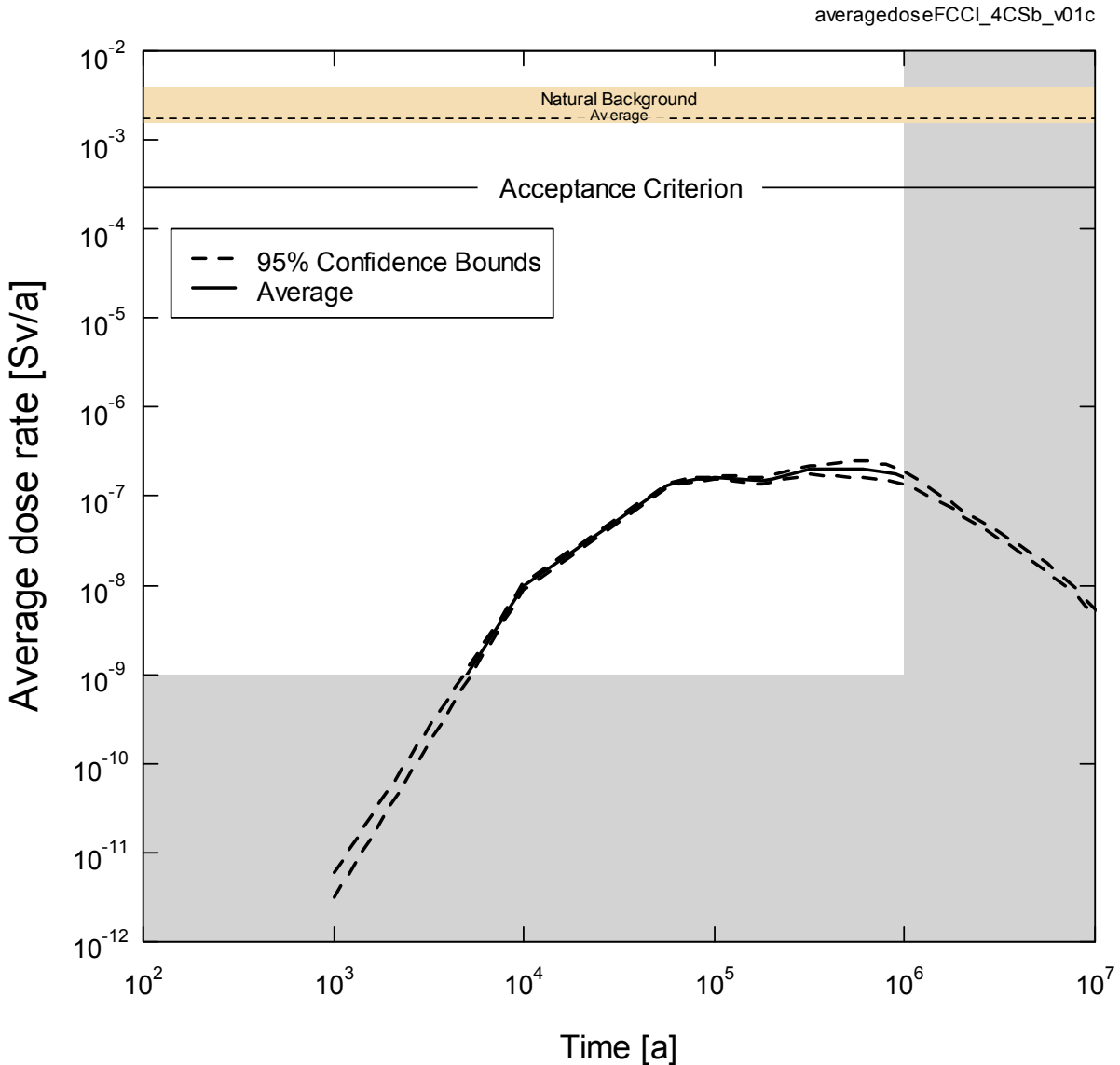


Figure 7-121: SYVAC3-CC4 - Average Dose Rate With 95% Confidence Bounds

Figure 7-122 shows the distribution of dose rates from all 120,000 simulations illustrating the 25, 50, 67, 90 and 99th percentile bands. These curves are all well below the interim dose acceptance criterion of 3.0×10^{-4} Sv/a established in Section 7.1.1 for the radiological protection of persons.

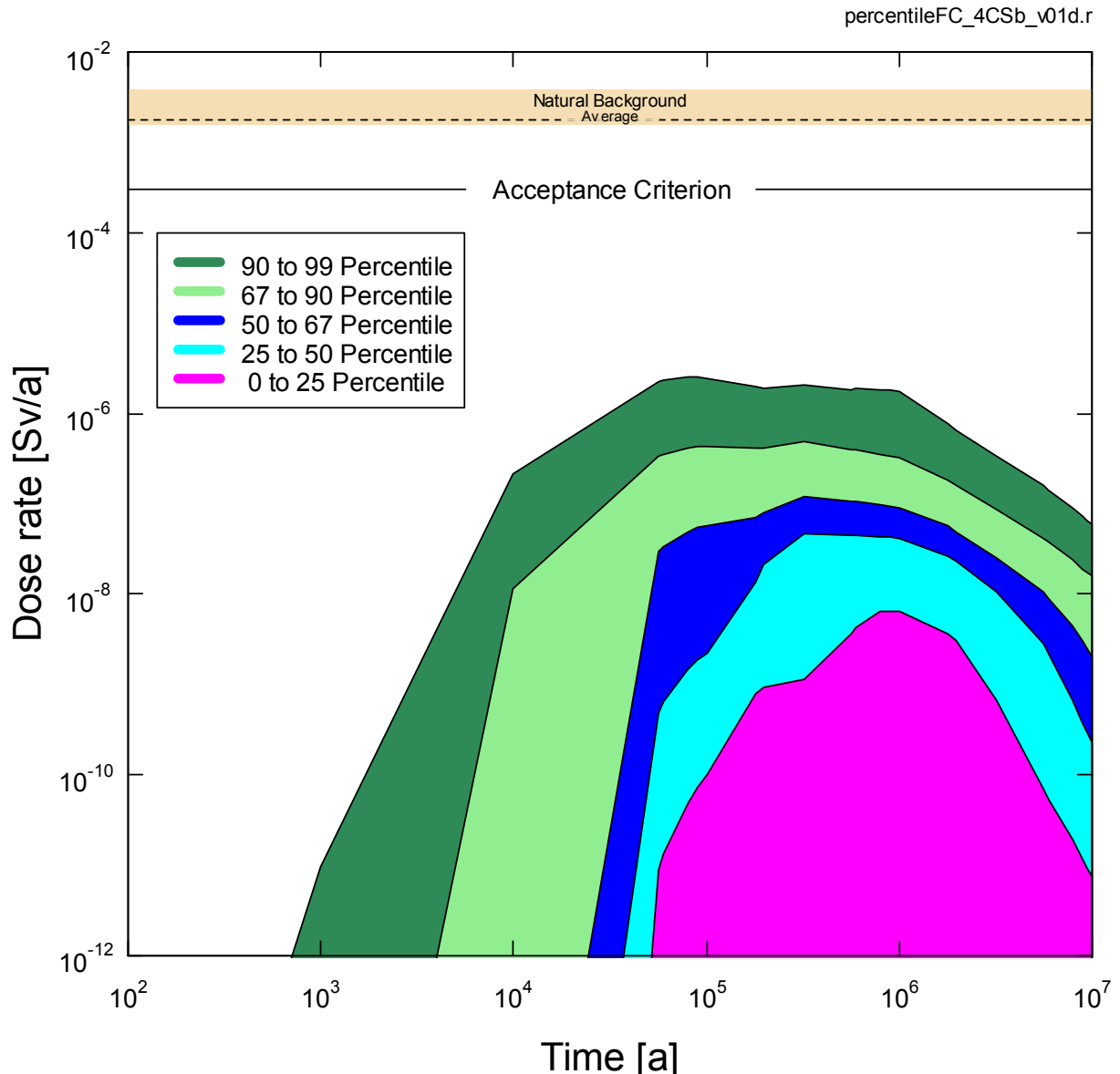


Figure 7-122: SYVAC3-CC4 - Dose Rate Percentile Bands

Maximum Value Simulations

Regulatory document G-320 (CNSC 2006) specifies that if the range of assessment results from probabilistic simulations indicates that acceptance criteria are exceeded, then it should be demonstrated that those results do not represent unreasonable risk to the environment or to the health and safety of persons, taking into account the conservatism built into the assessment and the likelihood of the circumstances leading to the results.

As per this guidance, all simulations were reviewed to identify runs that result in dose rates either very close to or above the interim dose acceptance criterion of 3.0×10^{-4} Sv/a. Six such cases were identified, with a maximum peak dose rate of 7.7×10^{-4} Sv/a, with Sn-126 and its progeny Sb-126 as the dominant dose contributors via external exposure by groundshine. Further examination of these cases indicated that two conditions are necessary to achieve these high values:

1. The failed containers must be located in a sector of the GEONET that does not include a backfill pathway; and
2. The soil K_d for Sn must be near the high end of its range. For the maximum dose case, the K_d for Sn in the soil is 2.4×10^4 L/kg, or about 3 sigma away from the geometric mean of 130 L/kg used in the Reference Case. The situation in the other five cases is similar.

Regarding the first point, Section 7.8.1 indicates that the SYVAC3-CC4 model is conservative with respect to the computation of Sn-126 that reaches the surface when the failed container(s) are located in model sectors that do not include a backfill pathway. Because of this, it is concluded that these six simulations do not represent unreasonable risk to the environment or to the health and safety of persons as they arise primarily as a consequence of modelling decisions. This aspect of the model may be further refined in subsequent work.

7.9 Disruptive Event Scenarios

Disruptive Event Scenarios postulate the occurrence of unlikely events leading to possible penetration of barriers and abnormal loss of containment. Chapter 6 describes how the Disruptive Event Scenarios are identified and concludes that the following are relevant to the hypothetical site and conceptual repository design:

- Inadvertent Human Intrusion;
- Shaft Seal Failure;
- Fracture Seal Failure;
- Poorly Sealed Borehole;
- Undetected Fault;
- All Containers Fail; and
- Container Failure.

As noted in Section 7.2, a limited scope of work has been adopted in this pre-project review to reflect the level of effort required to meet the study objectives. The Poorly Sealed Borehole Scenario, the Undetected Fault Scenario, the Container Failure Scenario and the variant case of the Human Intrusion Scenario in which the intrusion borehole is assumed to remain open are not within the scope of work.

The analysis results and dose consequences for the remaining Scenarios are discussed below.

7.9.1 Inadvertent Human Intrusion

The Inadvertent Human Intrusion Scenario considers the same evolution of the repository system as for the Normal Evolution Scenario with the only difference being the occurrence of human intrusion some time after institutional control of the site is no longer effective. In this scenario, an exploratory borehole is drilled through the geosphere and into the repository. The drill bit is assumed to intersect a used fuel container.

In an exploratory borehole, the investigators will most likely collect samples or conduct measurements at the repository level, which will readily identify any significant residual radioactivity (e.g., gamma logging is a standard borehole measurement). The investigators would then likely initiate appropriate precautions to prevent further exposure, including ensuring that any surface-released materials were appropriately disposed and that the borehole was sealed. Under normal drilling circumstances, there would be little impact.

Nevertheless, the Inadvertent Human Intrusion Scenario assumes:

- Interception of the repository is not recognized and therefore no safety restrictions are imposed; and
- The drill site is not managed according to current standards, and material from the borehole is released onto the surface.

As per Section 7.2.2, the scope of this pre-project review does not include the variant case in which the borehole is poorly sealed thereby resulting in a long-term pathway for contaminants to escape the repository. Such a case has been considered in SKB (2010a), and this work shows the consequences are orders of magnitude less than the SKB maximum dose rate for the human intrusion scenario.

7.9.1.1 Description

Figure 7-123 presents an event tree defining the possible outcomes associated with drilling in a repository location.

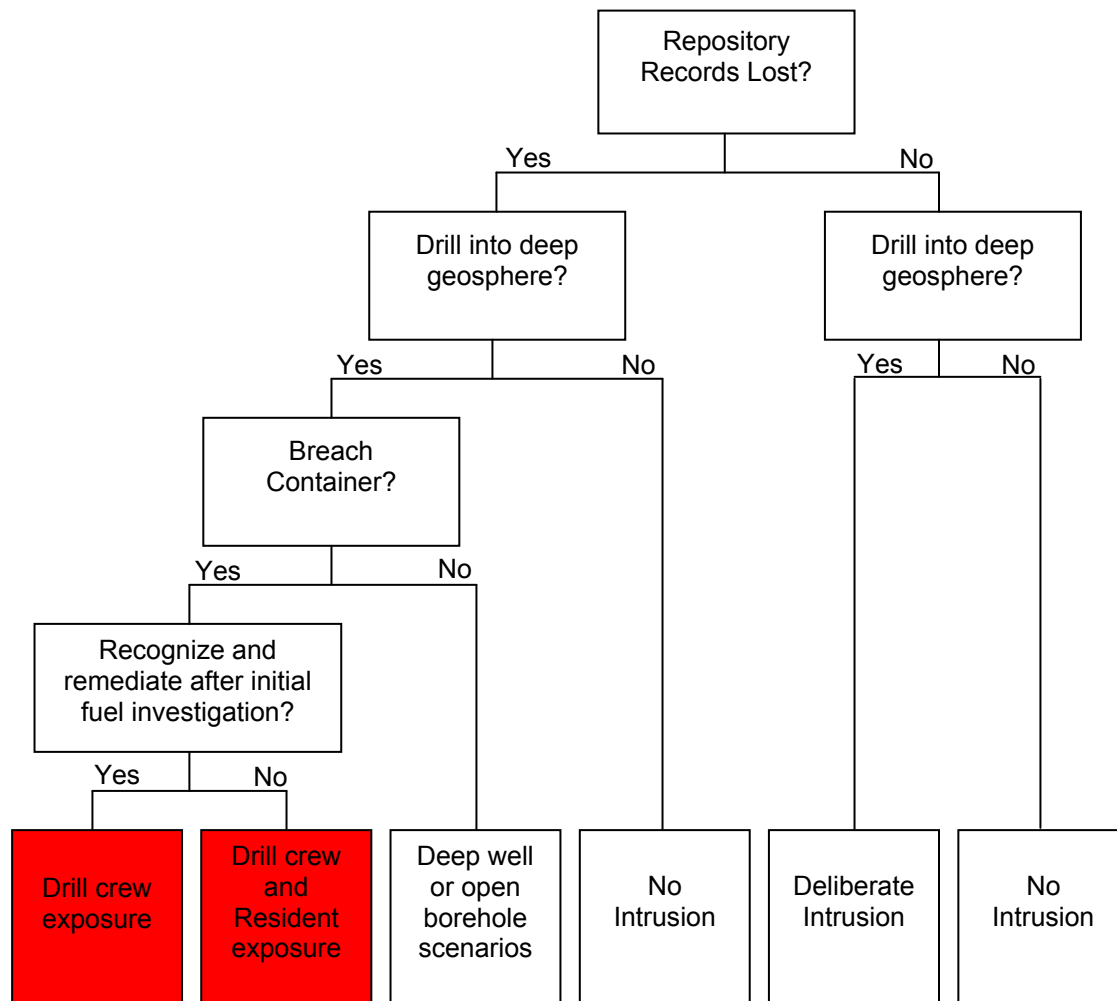


Figure 7-123: General Sequence of Events for Inadvertent Human Intrusion

Of interest to this discussion is the outcome in which:

- The repository records are lost;
- There is drilling into the deep geosphere; and
- The drilling breaches a used fuel container such that used fuel is inadvertently brought to the surface.

This then leads to potential exposure of the following two groups:

- The drill crew, exposed to contaminated drill slurry spread on the surface around the drill rig and to a core section containing used fuel; and
- A resident at the site, exposed by living nearby and growing food on soil contaminated by drill slurry³.

To provide context, Table 7-37 presents a summary of the exposure groups considered in recent national and international inadvertent human intrusion safety assessments.

Table 7-37: Human Intrusion Pathways Considered in Recent Safety Assessments

Assessment	Scenario / Exposure Cases Considered
Gierszewski et al. 2004 (Canada)	Drill crew Core examination technician Construction worker on contaminated soil from drilling slurry Resident on contaminated soil from drilling slurry *
SKB 2011 (Sweden)	Drill crew * Resident on contaminated soil from slurry growing a garden or exposed from irrigation and drinking from well using open borehole into waste
JNC 2000 (Japan)	Excavation workers (exposed externally to core sample and internally by inhalation)
DOE 2008 (USA)	Reasonable Maximally Exposed Individual (Resident) exposed as a result of direct pathway to the groundwater created by the borehole.
NAGRA 2002 (Switzerland)	Resident exposed as result of open borehole into waste creating pathway for waste to reach aquifer

Note: * Represents most limiting exposure case.

Intrusion Likelihood

Regulatory document G-320 (CNSC 2006) recognizes that inadvertent human intrusion events could result in dose results that exceed the regulatory limit and it states that reasonable efforts should be made to limit the probability of such high consequence scenarios. The following repository characteristics have been adopted to minimize the likelihood of this event:

- A deep location;
- Site selection based on an absence of groundwater resources at repository depth that could be used for drinking or agricultural purposes;
- Site selection based on an absence of economically exploitable natural resources; and
- The use of records and markers to preserve institutional memory to the extent practicable.

³ Note that this would not be allowed by current drilling standards, but is conservatively assumed here.

7.9.1.2 Model and Assumptions

Computer Code

The radiological consequences are determined using HIMv2.0 (Medri 2012), a human intrusion computer model developed using the AMBER v5.5 platform.

Screening calculations were initially done to identify the potentially radiologically significant radionuclides; consequently, 74 radionuclides are tracked in HIMv2.0. Short-lived radionuclides are included through the dose coefficients of their parents. Doses are obtained using inhalation, ingestion, groundshine and external dose coefficients.

A detailed description of the parameters and equations used in HIMv2.0 is available in Medri (2012).

Exposure Scenarios

The HIMv2.0 model determines the dose consequences to both exposure groups from the pathways illustrated in Figure 7-124. It models the acute dose to the drill crew at the time the material is brought to the surface and the annual chronic dose to residents who are assumed to live nearby and grow crops on the site after the intrusion has occurred.

In the Drill Crew exposure case, waste is brought to surface in the form of drill core and drill mud / slurry. Normal practice is for drill slurry to be contained at the site and ultimately be disposed of according to regulatory requirements. In this analysis, the drill slurry is conservatively assumed to be spilled around the drill rig without containment. The contaminated slurry would become mixed with surface material, as well as with subsequent drilled material. The waste is assumed to be uniformly mixed through a small near-surface volume of soil around the rig. The drill crew member handles the core sample containing used fuel for a short period of time, leading to an external exposure. This exposure is modelled using a point source approximation. The drill crew member is also exposed to the waste through groundshine, inhalation of contaminated dust and ingestion of contaminated soil from the mixed volume of near-surface material. The drill crew member is assumed not to wear a mask.

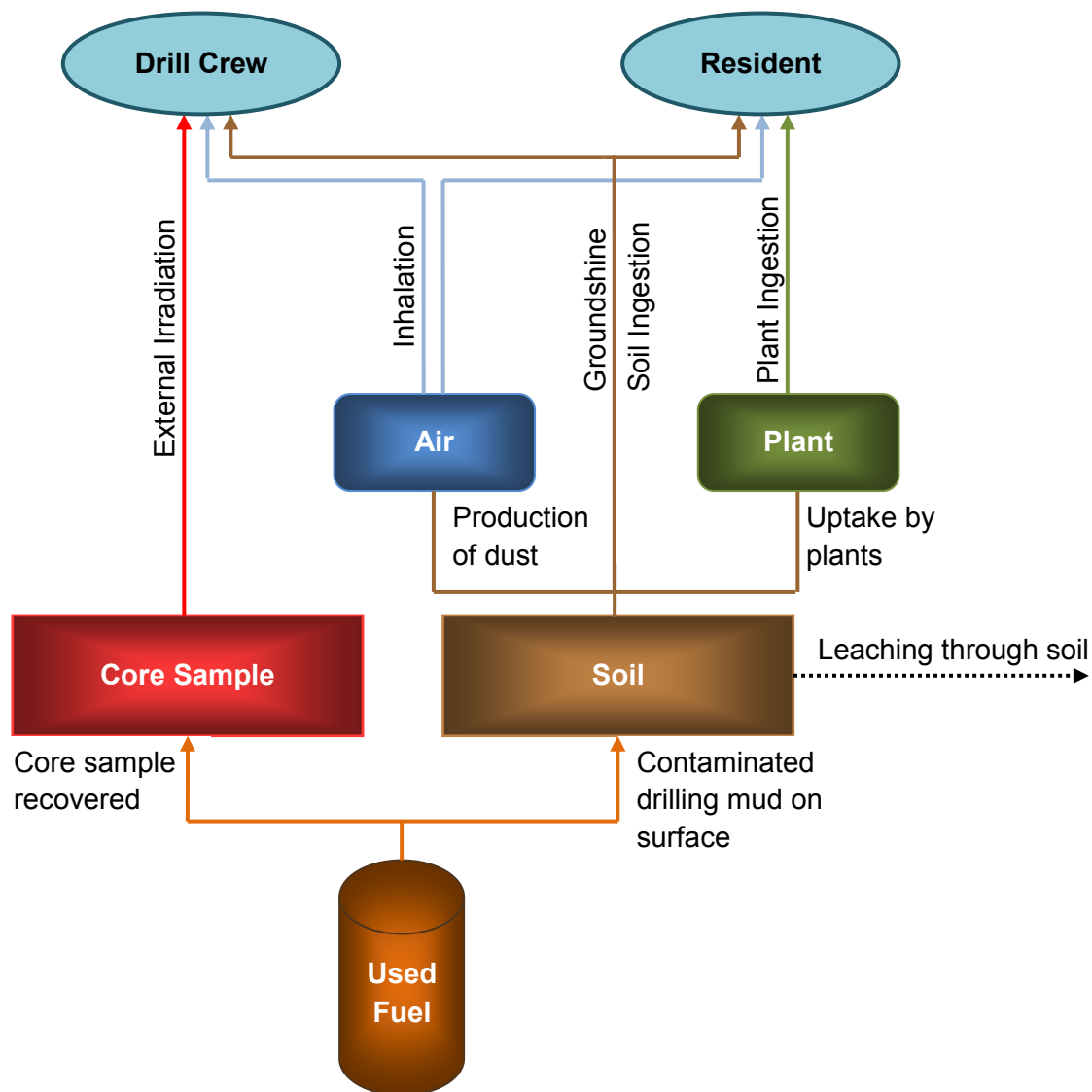


Figure 7-124: Inadvertent Human Intrusion - General Conceptual Model

In the Resident exposure case, the waste brought up with the drill slurry and deposited on the surface around the drill rig is assumed to remain in place without remediation. It remains on the surface, subject only to radioactive decay and leaching. Leaching is caused by precipitation that percolates downwards into the deeper soil. The resident lives around the contaminated site some time after the original intrusion, and grows some food on the contaminated soil. The resident is exposed to the contaminants through groundshine, dust inhalation and through ingestion of contaminated plants and soil. The area contaminated by drilling fluid would be small but have high contaminant concentrations, and therefore an allowance is made for the fraction of time that the resident is exposed to the contaminated site on an annual basis.

As a conservative estimate, the Resident case assumes that the exposure occurs in the first year after intrusion, before leaching has any significant effect on contaminant levels in the soil. The resident annual dose is also examined 100 years after intrusion, in which case the effect of leaching is included.

Key Assumptions and Parameters

Key assumptions are:

- Institutional control is maintained for a minimum of 300 years after closure, at which point intrusion becomes possible;
- Decay and ingrowth calculations start at the time of placement, at which point the used fuel is 30 years old;
- There is a minimum period of 70 years of extended monitoring and 25 years of decommissioning and closure following placement, which means the fuel is 425 years old (i.e., 30 + 70 + 25 + 300) at the earliest time of intrusion. This is conservative in that the fuel will likely be older at a real site; and
- The drill intercepts a container in the repository and brings used fuel debris to the surface, either mixed with the drill slurry or as a section of intact drill core.

Table 7-38 lists parameters common to the intrusion cases and Table 7-39 lists the main exposure specific parameters used in HIMv2.0. Source references for these values can be found in Medri (2012).

Table 7-38: Common Parameters for Human Intrusion Scenario

Parameter	Value
Fraction of used fuel per container that is damaged by borehole	0.04
Mass of used fuel in a container (kg)	8650
Net infiltration rate of water through soil (m/a)	0.325
Human air inhalation rate (m ³ /a)	8400
Soil type	Clay
Soil density (kg/m ³)	1400
Soil water content (m ³ /m ³)	0.3
Instant release fractions (selected radionuclides)	Table 7-19

Table 7-39: Exposure Specific Parameters for Human Intrusion Scenario

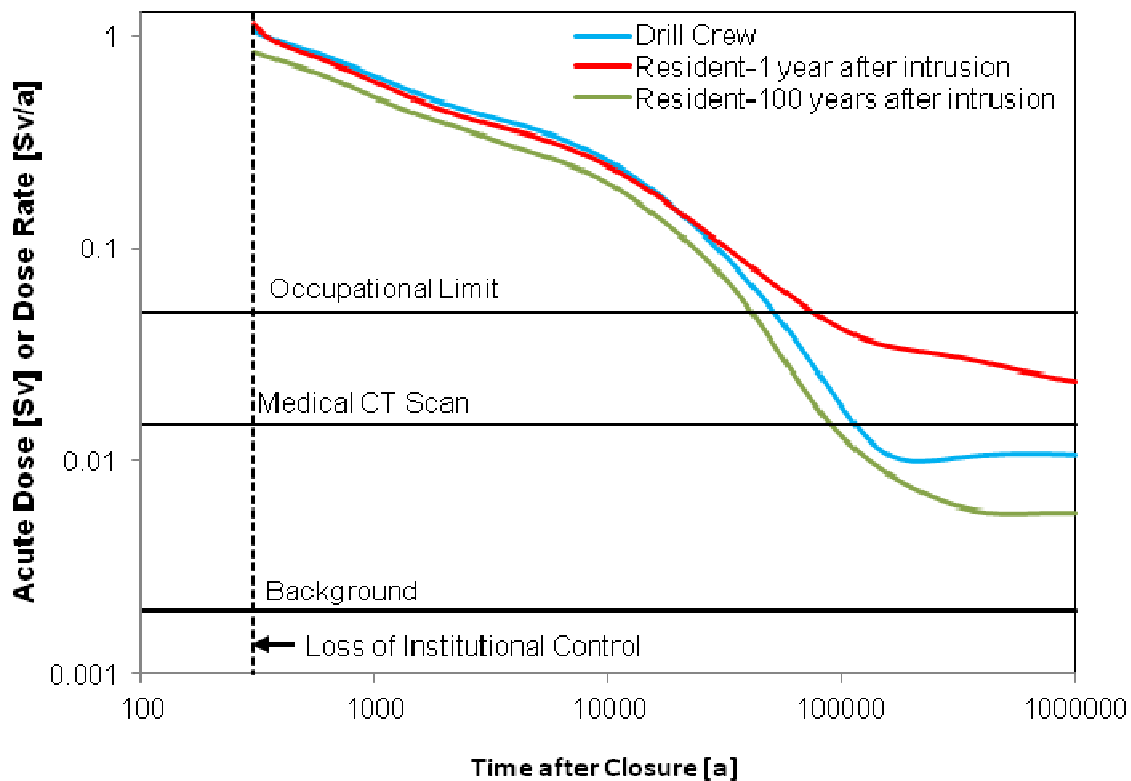
Parameter	Drill Crew	Resident
Slurry area (m ²)	30	80
Activity duration	168 hrs (14 days, 12 hr shifts) 1 hr (core handling)	10% of the time (year-round)
Dust loading in air (kg _{soil} /m ³)	1.0×10^{-7}	3.2×10^{-8}
Plant ingestion (kg/a)	-	291
Soil ingestion	4.62×10^{-3} kg	0.12 kg/a
Contaminated food fraction (%)	-	10
Thickness of contaminated soil (m)	0.2	0.2
Fraction of U intercepted brought to surface as core	0.4	-
Fraction of U intercepted brought to surface as slurry	0.3	0.3

7.9.1.3 Results

Dose Impact

Figure 7-125 shows the acute dose to the Drill Crew and chronic annual dose to the Resident as a function of time after closure. The red line is the dose received assuming the Resident moves onto the site 1 year after the intrusion while the green line is the dose received assuming the Resident moves onto the site 100 years after the intrusion.

The exposure scenarios are stylized. They include all credible exposure pathways such that the overall dose estimate is credible, but not necessarily accurate.



Note: The drill crew receives a one-time (acute) dose, while the resident receives a (chronic) dose rate.

Figure 7-125: Inadvertent Human Intrusion - Exposure as a Function of Intrusion Time

The results show:

- The maximum one-time dose to the Drill Crew is 1.06 Sv;
- The maximum annual chronic dose to the Resident in the first year after intrusion is 1.14 Sv;
- After 100 years of leaching, the maximum annual dose to the Resident decreases to 0.83 Sv; and
- Doses decrease as a function of the assumed time of intrusion due to radioactive decay.

Figure 7-126 and Figure 7-127 show the breakdown of exposure pathways for the Drill Crew and the Resident.

The dose for both groups tends to be dominated by Am-241 for the first 300 to 1000 years, by Pu-240 and Pu-239 from 10^3 to 10^5 years, and by the U-238 decay chain radionuclides for longer times. This is in contrast to the Normal Evolution Scenario in which actinides are slow to dissolve, sorb strongly in the repository and geosphere, and generally do not reach the surface.

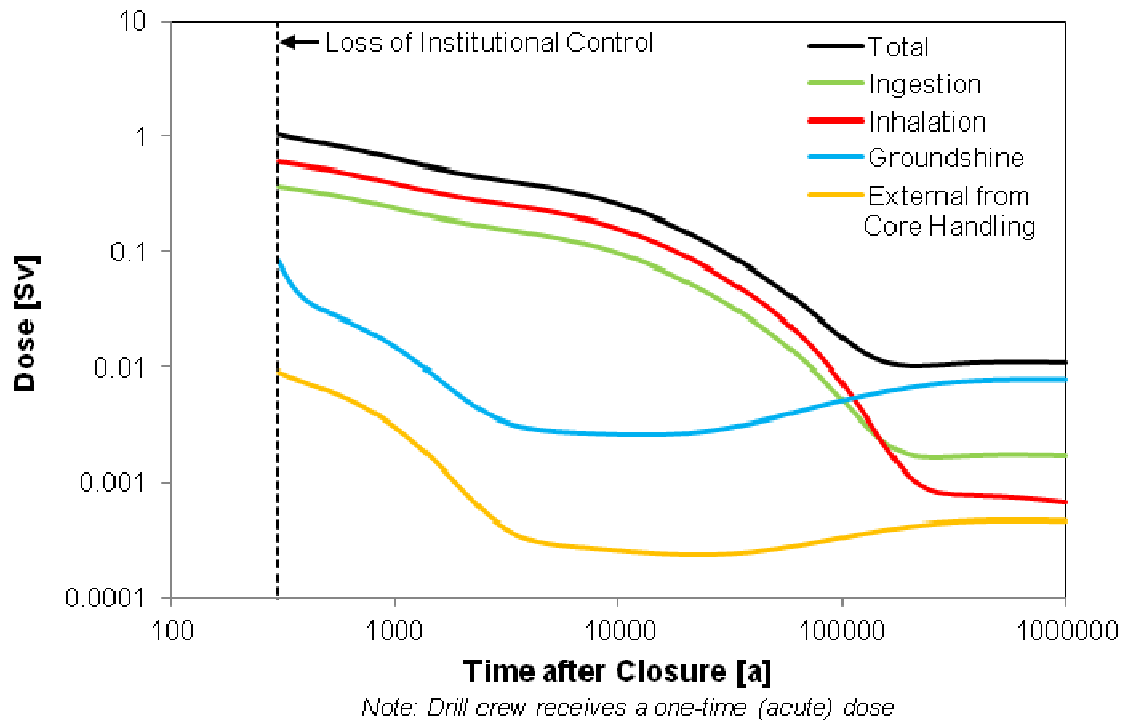


Figure 7-126: Inadvertent Human Intrusion - Exposure Pathway Doses for Drill Crew

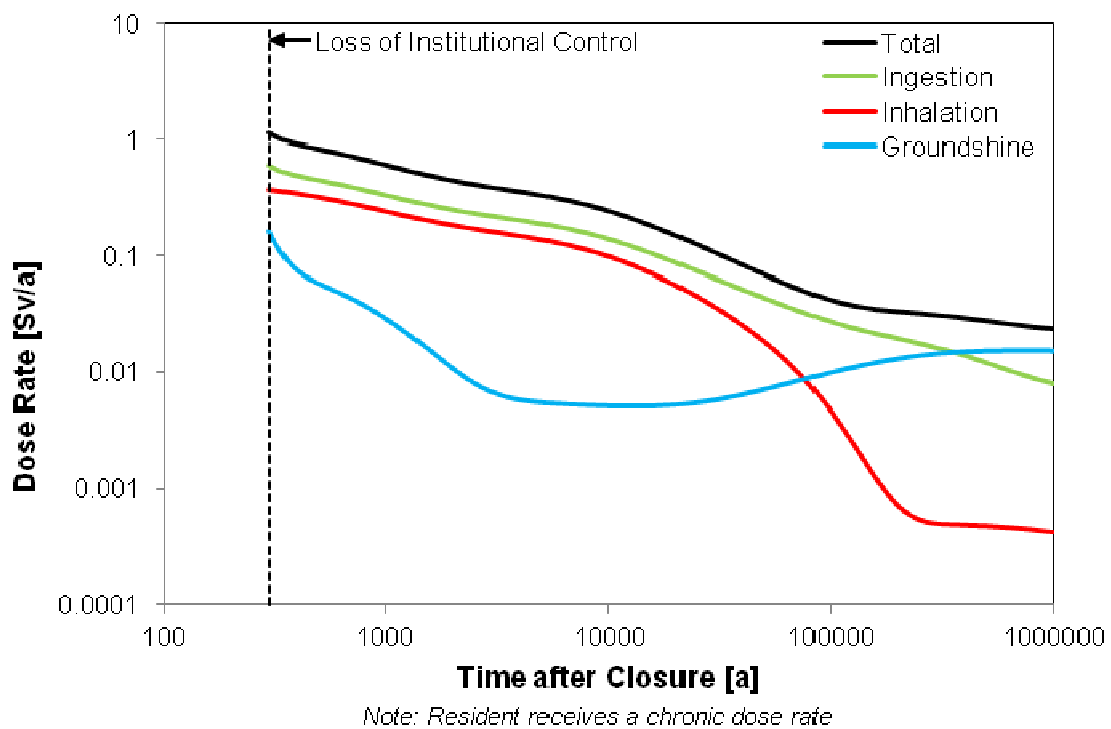


Figure 7-127: Inadvertent Human Intrusion - Exposure Pathway Dose Rates for Resident

For the Resident, the exposure could potentially occur any time after the used fuel is deposited on the surface, assuming the site is not remediated in the interim. Figure 7-128 shows the dose to the Resident as a function of arrival time at the site, assuming the intrusion occurs at the earliest possible time after closure (i.e., 300 years). The results show that leaching can cause a substantial reduction in dose at later times.

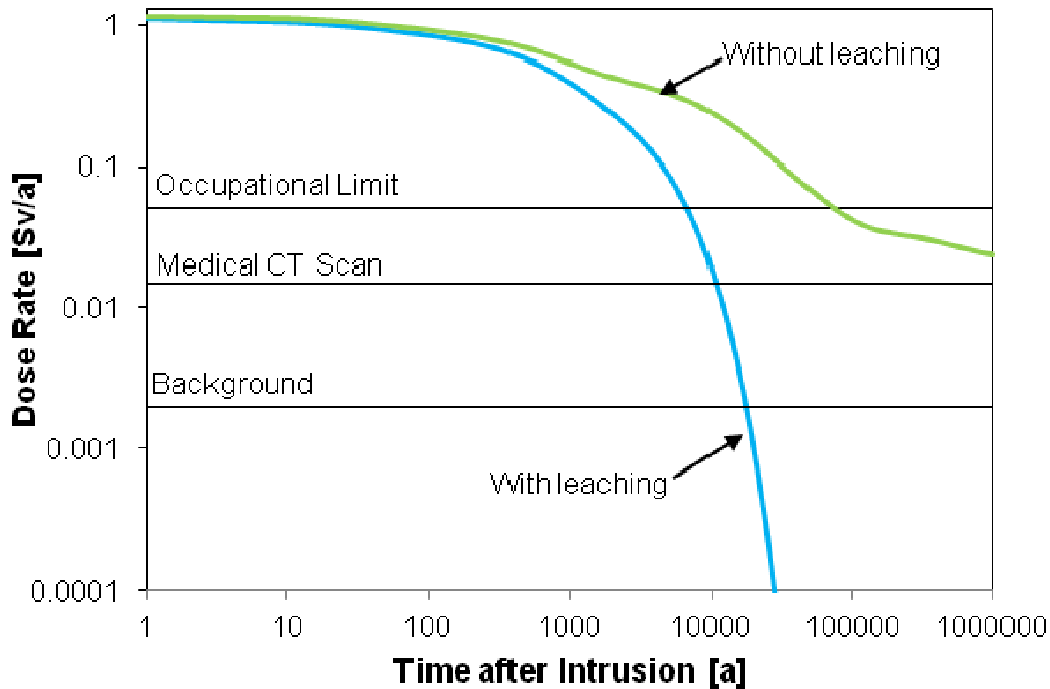
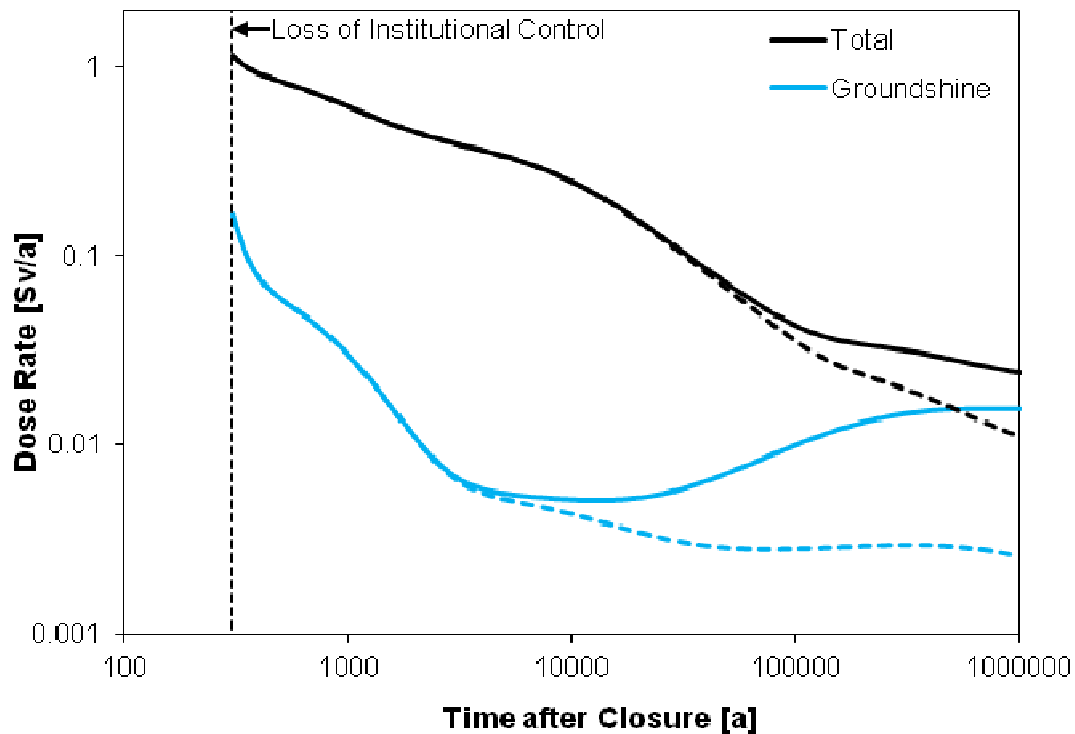


Figure 7-128: Dose Rate to Resident as a Function of Arrival Times Assuming Intrusion Occurs 300 Years after Closure

The results shown for the Resident dose in Figure 7-125 and Figure 7-127 conservatively assume all Rn-222 stays in the soil. In reality, because Rn-222 is a gas, much of it is likely to escape the soil and be dispersed in the atmosphere. Figure 7-129 shows the effect on the Resident dose of removing the groundshine contribution of Rn-222 and its short-lived daughters (i.e., Po-218, Pb-214, Bi-214 and Po-214) is significant at long times. The contribution from Pb-210 (a longer-lived daughter) is still included because Pb-210 formed underground would not quickly decay away when it reaches the surface.



Note: Dotted lines show the dose rates without Rn-222 and its short-lived daughters.

Figure 7-129: Effect of Rn-222 and Short-Lived Daughters in Groundshine Pathway on Resident Exposure

Annual Risk

To provide context for the dose rates, the annual risk to the most exposed individual can be estimated.

The risk to the Resident (R_R), which is the most exposed group, is determined via:

$$R_R = Y \cdot H \cdot P$$

Where:

Y is the total risk per Sievert for total cancer, non fatal cancer and severe hereditary effects, or 0.057 according to ICRP (2007);

H is the highest calculated dose in the time period of concern; and

P is the intrusion frequency.

While the intrusion frequency could be estimated by assigning numerical values to each of the events in Figure 7-123, in practice these values are to a large extent non-quantifiable.

Consequently, a more simplistic approach is adopted to illustrate the frequency with which an intrusion event may occur. This approach considers only the frequency of drilling.

Specifically, given that the area around the repository has no significant mineral resources, a deep drilling frequency to resurvey or update the geological information of about once every 100 years is estimated. Assuming this surveys an area of $10 \text{ km} \times 10 \text{ km}$, this is a drilling frequency of $10^{-10} \text{ m}^{-2}\text{a}^{-1}$. Since the repository consists of 160 rooms, with each room having a projected area of 2200 m^2 , the frequency of inadvertent human intrusion into a room can be estimated as $3.5 \times 10^{-5} \text{ a}^{-1}$. This does not account for the container area being substantially less than the room area.

With $Y = 0.057 \text{ Sv}^{-1}$, $H = 1.14 \text{ Sv}$ and $P = 3.5 \times 10^{-5} \text{ a}^{-1}$, the annual risk to the Resident from an inadvertent human intrusion event is $2.3 \times 10^{-6} \text{ a}^{-1}$. This is less than the risk target of $10^{-5}/\text{a}$ for disruptive scenarios identified in Section 7.1.1.

The intrusion probability does not take into account the beneficial effect of institutional memory. Institutional memory could decrease with time, but at earlier times when high doses are more likely, ongoing institutional memory would significantly reduce the intrusion probability (and the risk) of such an event.

The repository might also be detected through surface geophysical measurements, but not recognized as a used fuel facility. In this case exploration drilling would specifically aim for the repository and the intrusion probability could be higher than the above random drilling frequency. But since the drilling program would be specifically designed to explore the anomaly, it is also more likely that the repository would be recognized before or shortly after the repository level was reached and the consequences would therefore be less than those estimated above.

At long times, the cumulative probability of intrusion increases, but the consequences also decrease until eventually they are similar to those for inadvertent intrusion into a uranium ore body.

7.9.2 All Containers Fail

The long-lived used fuel containers are an important feature of the multi-barrier concept. The reference copper containers are anticipated to last for a period of time in excess of one million years, based on the copper material, sturdy mechanical design and favourable site attributes. Nevertheless, the All Containers Fail Scenario considers the hypothetical case in which all the containers fail early.

Since the containers are durable and there is no identified mechanism to fail all containers, the base case considers failure at 60,000 years. This corresponds, for example, to the likely timeframe for an ice sheet to cover the site, and it is possible that some unanticipated effect of the ice sheet might cause failure.

The sensitivity to earlier failure times is examined in a sensitivity case in which all containers are assumed to fail at 10,000 years.

The sensitivity to geosphere hydraulic conductivity is examined in three sensitivity cases, each of which assumes all containers fail at 10,000 years.

7.9.2.1 Model and Assumptions

The dose assessment is performed using the same SYVAC3-CC4 model described in Section 7.5.4. All model parameters are identical to those in the Reference Case of the Normal Evolution Scenario except that:

- All 12,778 containers fail simultaneously;
- The radionuclide release model takes no credit for the presence of the container. As such, the release of radionuclides from the slowly dissolving fuel to the near field is limited only by the buffer properties; and
- The potential presence of a few containers with small initial defects is not included. This modelling simplification does not affect the peak dose rate.

The sensitivity cases examining the effect of geosphere hydraulic conductivity on I-129 transport to the well are performed using the same FRAC3DVS-OPG model described in Section 7.5.3. All model parameters are identical to those in the Reference Case of the Normal Evolution Scenario except that:

- All 12,778 containers fail simultaneously at 10,000 years;
- The radionuclide release model takes no credit for the presence of the container. As such, the release of radionuclides from the slowly dissolving fuel to the near field is limited only by the buffer properties;
- The potential presence of a few containers with small initial defects is not included. This modelling simplification does not affect the peak dose rate; and
- The geosphere hydraulic conductivities are varied as shown in Table 7-4. The three sensitivity cases represent a factor of 10 increase, a factor of 10 decrease, and a factor of 100 decrease in hydraulic conductivity.

7.9.2.2 Results

All Containers Fail at 60,000 Years

Figure 7-130 shows the dose rate for the base case in which all containers fail at 60,000 years. Also included for comparison is the dose rate for the Reference Case. The peak dose rate is 5.8×10^{-4} Sv/a and the time of the peak is 7.87×10^4 years. The peak is about 1760 times that of the Reference Case.

The increase is about 2.4 times less than the increase in the number of failed containers. This difference occurs because not all of the groundwater passing through the repository discharges to the well (i.e., the dominant exposure pathway for the Self-Sufficient Farmer critical group).

The peak dose rate is about a factor of 1.7 below the interim dose acceptance criterion of 1×10^{-3} Sv/a.

Hydrogen gas is generated by the corrosion of steel and the overall volume of gas will increase with the number of containers postulated to fail. The discussion in Section 7.11.4 on the effects

of gas generation indicates that no adverse consequences are anticipated due to hydrogen generation.

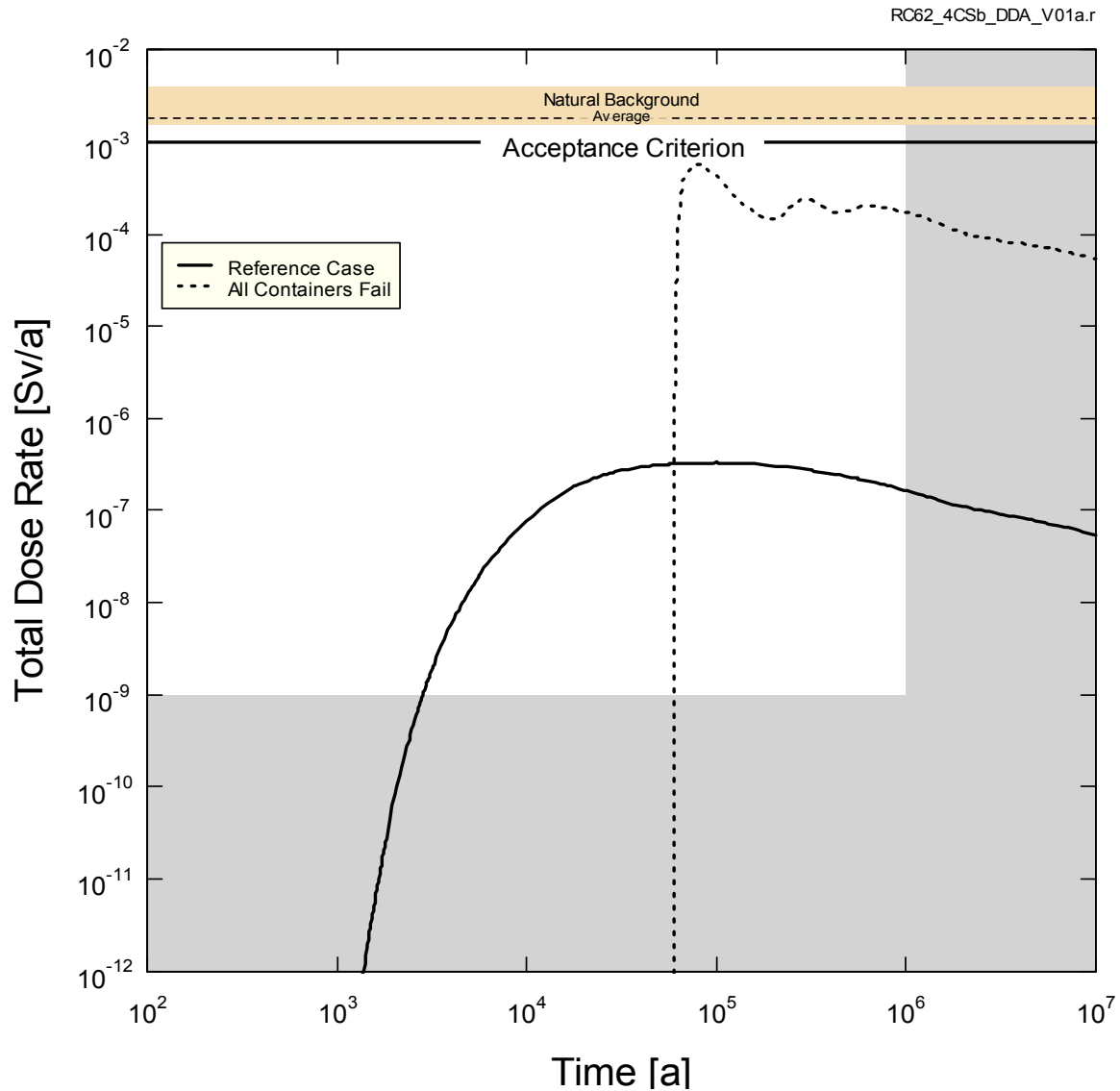


Figure 7-130: All Containers Fail at 60,000 Years - Dose Rate

Figure 7-131 shows the dose contributions from the most significant radionuclides. As in the Reference Case, I-129 is the dominant contributor. The apparently high contribution from Sn-126 and its daughter Sb-126 is due to the absence of a backfill pathway in many sectors of the system model as discussed in Section 7.8.1. This could be reduced in the future through further refinement of the model.

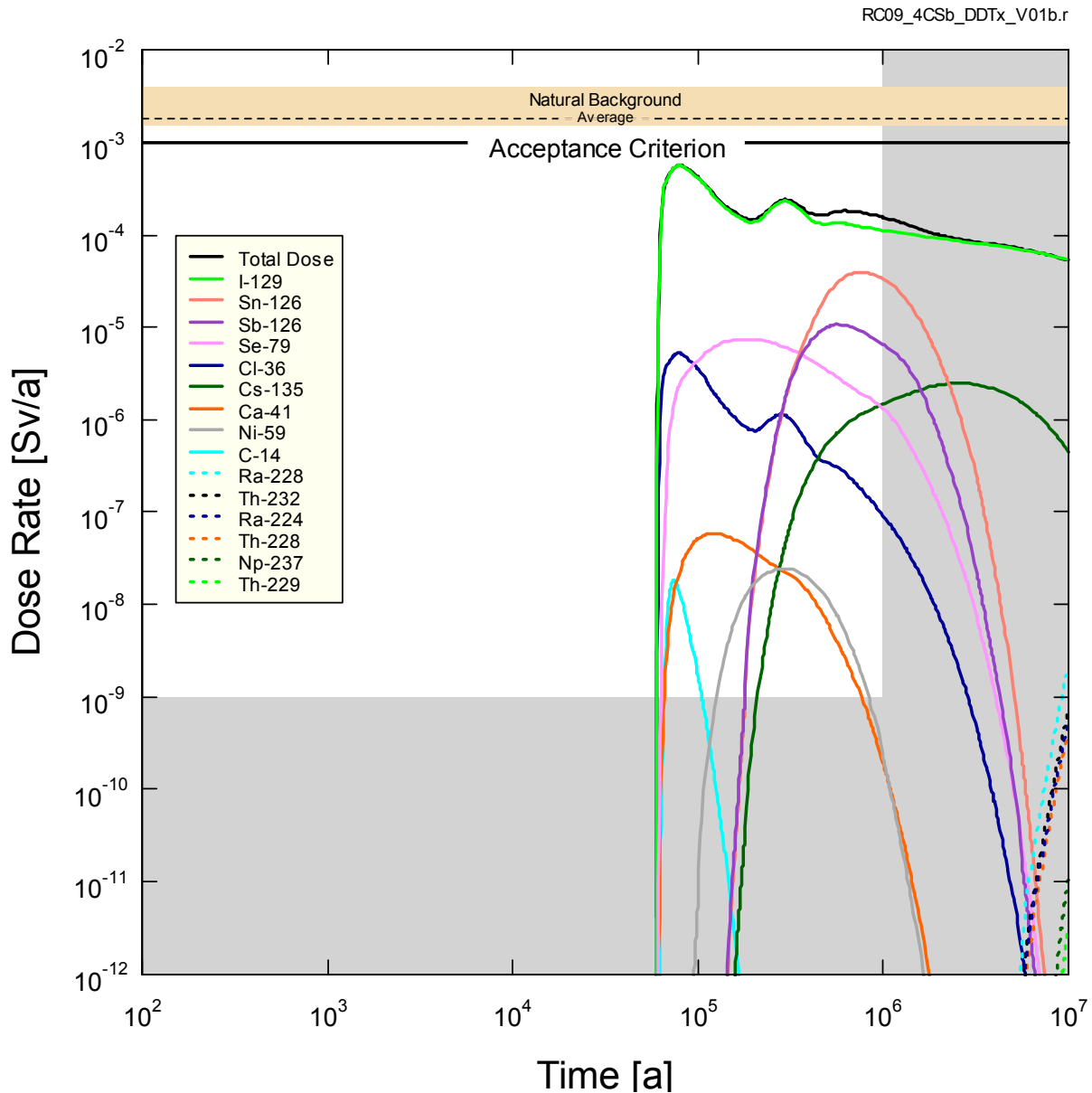


Figure 7-131: All Containers Fail at 60,000 Years – Contributing Radionuclides

All Containers Fail at 10,000 Years

Figure 7-132 compares the dose rate for the sensitivity case in which all containers fail at 10,000 years with results for the base case in which all containers fail at 60,000 years. The results are not substantially different, with a peak dose rate of 7.9×10^{-4} Sv/a occurring at 3.2×10^4 years. The increase in dose rate occurs as a result of less time being available for radioactive decay.

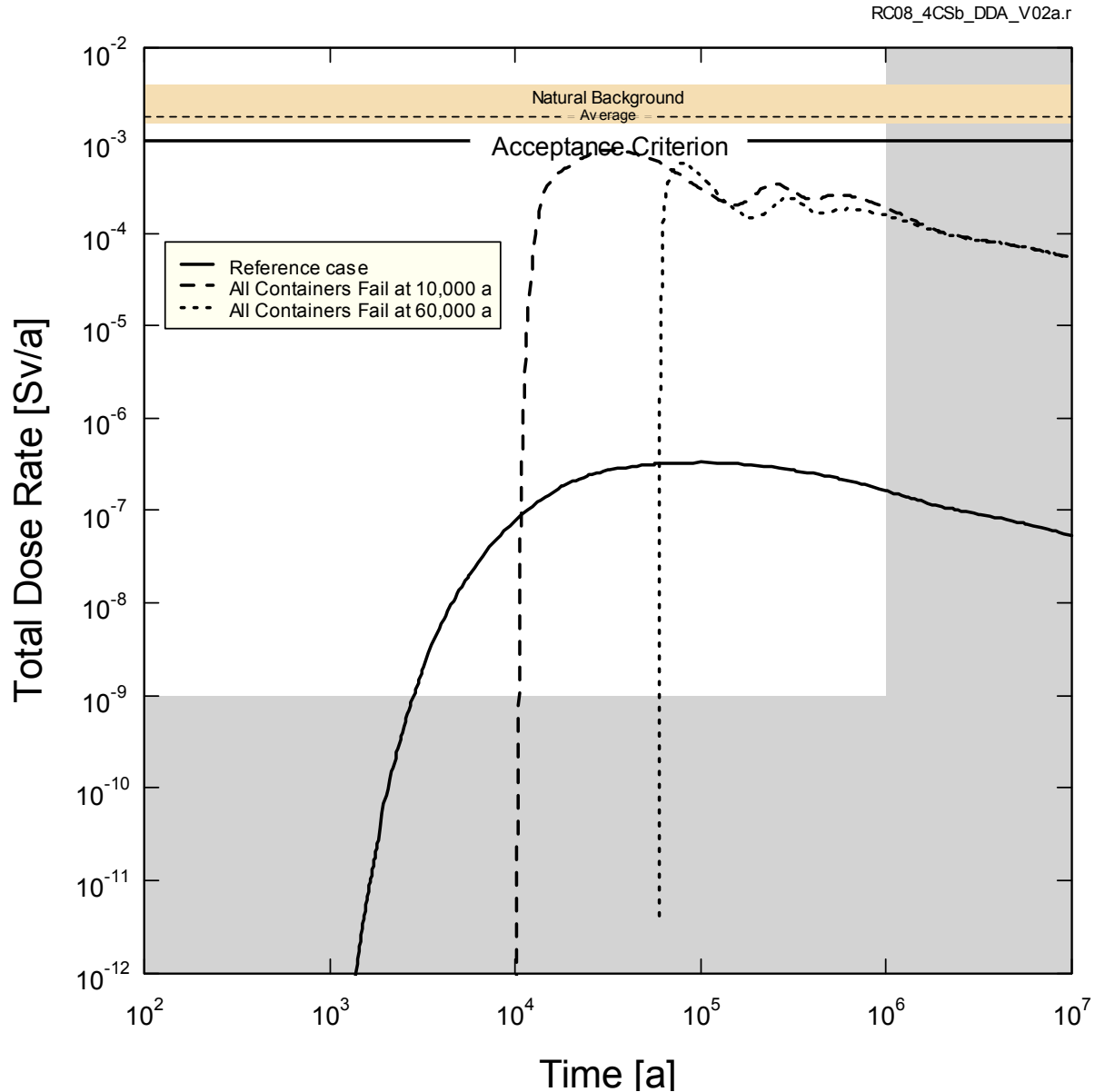


Figure 7-132: Sensitivity - All Containers Fail at 10,000 Years - Dose Rate

Effect of Geosphere Hydraulic Conductivity

Figure 7-133 shows the effect of varying the geosphere hydraulic conductivity on I-129 transport to the well for the case in which all containers fail at 10,000 years. Table 7-40 summarizes the peak values and the associated timing for each of the four cases illustrated.

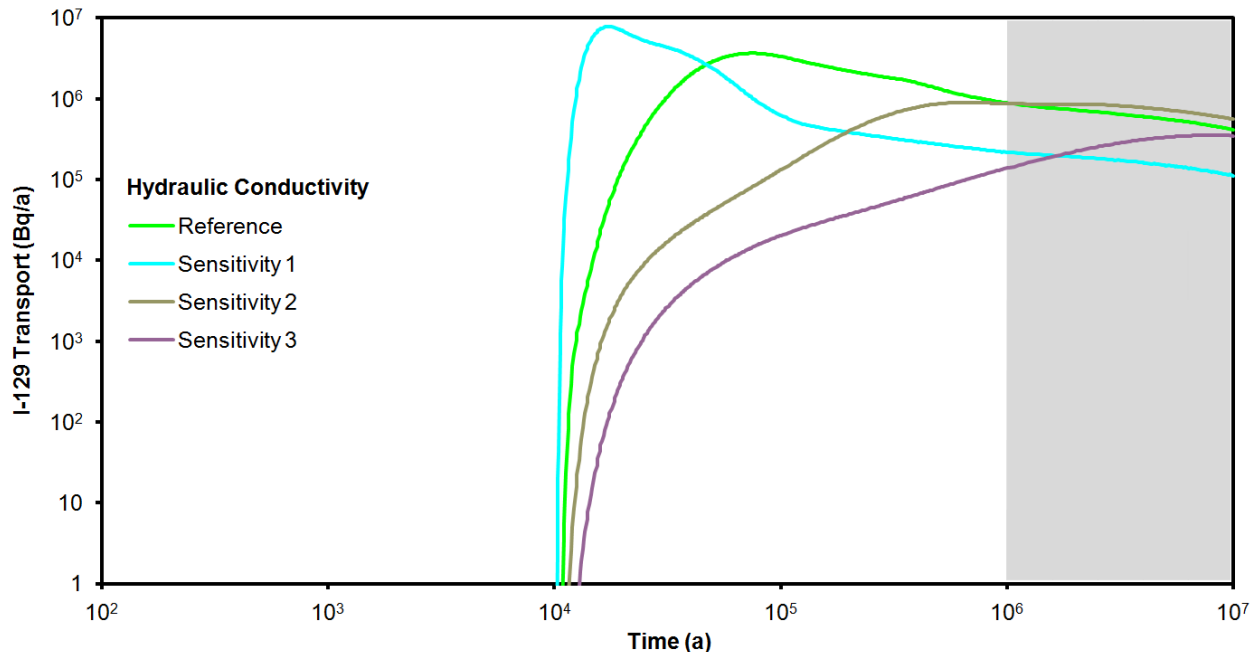


Figure 7-133: Sensitivity to Geosphere Hydraulic Conductivity - All Containers Fail at 10,000 Years - I-129 Transport to the Well

Table 7-40: Results for All Containers Fail at 10,000 Years - Sensitivity to Geosphere Hydraulic Conductivity

Hydraulic Conductivity	Peak I-129 Transport Rate at Well (Bq/a)	Time of Peak (a)
Reference	3.66×10^6	$75,000^4$
Sensitivity 1	7.81×10^6	17,100
Sensitivity 2	9.01×10^5	657,000
Sensitivity 3	3.54×10^5	8,000,000

⁴ This value differs from the 32,000 year value associated with Figure 7-132 because the Figure 7-132 result is generated using the SYVAC3-CC4 code. As noted in Section 7.8.1, the SYVAC3-CC4 code is conservative (i.e., earlier and higher releases) with respect to the FRAC3DVS-OPG code.

7.9.3 Shaft Seal Failure

The shafts represent a potentially important pathway for contaminant release and therefore the repository design includes specific measures to provide good shaft seals.

The Normal Evolution Scenario considers the likely behaviour of the shaft seals and the repository / shaft excavation damage zones. The Shaft Seal Failure Scenario considers the same evolution of the repository system and the same exposure pathways as the Reference Case of the Normal Evolution Scenario except that there is rapid and extensive degradation of the shaft seals. For conservatism, it is assumed that this degradation occurs at the time of repository closure.

7.9.3.1 Model and Assumptions

Analysis of the Shaft Seal Failure Scenario is performed using the same FRAC3DVS-OPG model described in Section 7.5.3. This model is used in lieu of the SYVAC3-CC4 system model because the groundwater flow field in the repository and near-field geosphere could be affected by the degradation of the shaft seals.

All model parameters are the same as in the Reference Case, except that the hydraulic conductivity of all shaft seal materials is set to a high value (i.e., 4.8×10^{-8} m/s).

The locations of the defective containers and the well have not been changed. This implies that the analysis may not result in the most conservative consequence and therefore the results should be considered illustrative only. For a real candidate site, these locations would be varied to ensure the most conservative locations are selected.

7.9.3.2 Results

The results for I-129 transport to the well are reported together with other FRAC3DVS-OPG sensitivity studies in Figure 7-83 in Section 7.7.2.2.6.

The results show no perceptible difference from the Reference Case. This is due to a combination of the distance to the shaft, the direction of groundwater flow and the effectiveness of the other intact seals.

7.9.4 Fracture Seal Failure

In this study a conductive fracture is assumed to intersect the repository footprint. This fracture is isolated during construction via a combination of grouting, cement and bentonite seals. As the repository is constructed, a number of tunnel seals and room seals of similar design are also put in place.

This section examines the effect of degraded fracture seals and the variant case in which all tunnel and room seals are degraded.

7.9.4.1 Model and Assumptions

The analysis of the Fracture Seal Failure Scenario is also performed using the same FRAC3DVS-OPG model described in Section 7.5.3. This model is used in lieu of the

SYVAC3-CC4 system model because the groundwater flow field in the repository and near-field geosphere could be affected by the assumed seal degradation.

The degraded seals are modelled by setting the hydraulic conductivity of the highly compacted bentonite in the keyed-in area of the seals to that of the inner EDZ (i.e., to 100 times that of the rock). For conservatism, it is assumed that this degradation occurs at the time of repository closure. The concrete is already set to degraded values in the Reference Case.

7.9.4.2 Results

The results for I-129 transport to the well for the Fracture Seal Failure Scenario and its variant case in which the degradation also occurs in all tunnel and rooms seals are reported together with other FRAC3DVS-OPG sensitivity studies in Figure 7-83 in Section 7.7.2.2.6.

The Fracture Seal Failure results show no perceptible difference from the Reference Case. This is due to the direction of groundwater flow and the effectiveness of other intact seals.

The variant case results show a slightly earlier arrival time at the well with a slightly higher peak transport rate (1677 Bq/a compared to 1675 Bq/a).

The absence of sensitivity is due to the hydraulic conductivity of the host rock supporting advective flow outside the repository together with the continuing presence of the buffer and backfill.

7.10 The Effects of Glaciation

The scenario identification discussion in Chapter 6 identifies glaciation as an important external factor influencing the behaviour of the Normal Evolution Scenario; however, for this pre-project review the dose assessment is performed assuming a constant temperate climate. The purpose of this section is to discuss the likely effects of glaciation on the calculated dose rates.

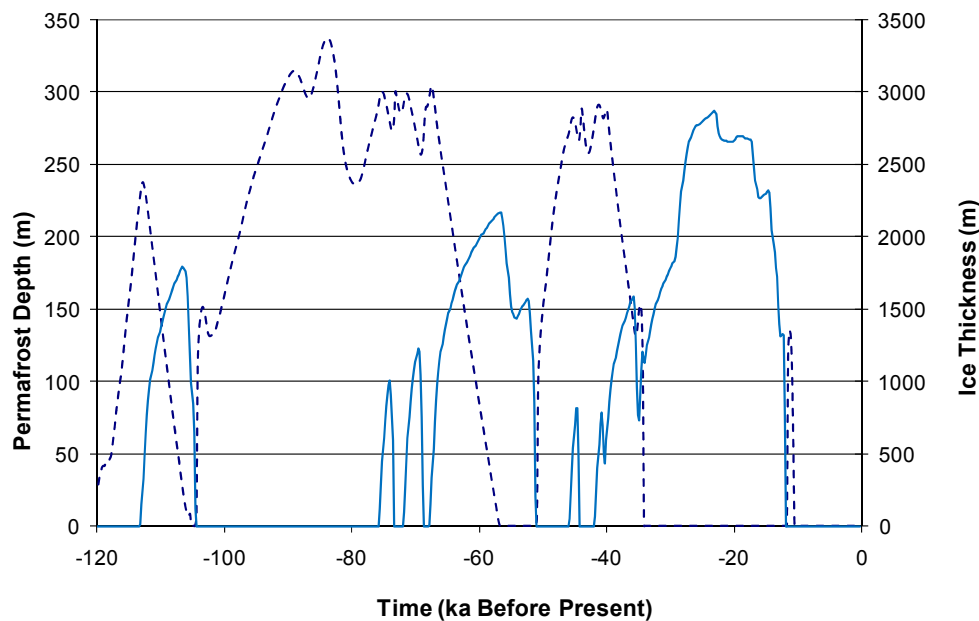
The impact of glaciation is discussed quantitatively based on the analysis of a glaciation scenario carried out as part of the Third Case Study (Garisto et al. 2010; Walsh and Avis 2010). The important features of this glaciation study are described and its applicability to the current study is discussed.

7.10.1 Description of the Glacial Cycle

During past glacial cycles, much of Canada has been covered by kilometre-thick ice sheets. The main factor that initiated these past glacial cycles (i.e., solar insolation variation due to Earth orbital dynamics) is still present. Current levels of greenhouse gases in the atmosphere are likely to delay the onset of the next glaciation (Berger and Loutre 2002); however, for the postclosure safety assessment it is assumed that glacial cycles reassert themselves in the long run.

To explore the possible effects of glaciation, a representative future glacial cycle has been defined in terms of climate and surface boundary conditions using models of past glacial behaviour (Peltier 2003, 2006).

Specifically, Peltier (2006) developed a set of reference glacial system models that were consistent with evidence from the past glacial cycle and the Laurentide Ice Sheet that covered Canada and northern United States. The model results include surface boundary conditions (e.g., ice thickness and permafrost depth) across North America on a scale of grid size 50-km on a side. Simulation nn2778 was selected for the glaciation study since it produced a “warm-based” glacier at the hypothetical site (i.e., liquid water is sometimes present at the base of the ice sheet that periodically covers the site). A warm-based glacier is of interest because there is a greater opportunity for deep groundwater flow to be affected by passage of the ice sheet. Data extracted from Simulation nn2778 for a location representative of the study site are shown in Figure 7-134. The last glacial cycle lasted about 120,000 years.



Note: Permafrost depth is represented by (---) and ice sheet thickness by (—).

Figure 7-134: Permafrost Depth and Ice Sheet Thickness for Simulation nn2778

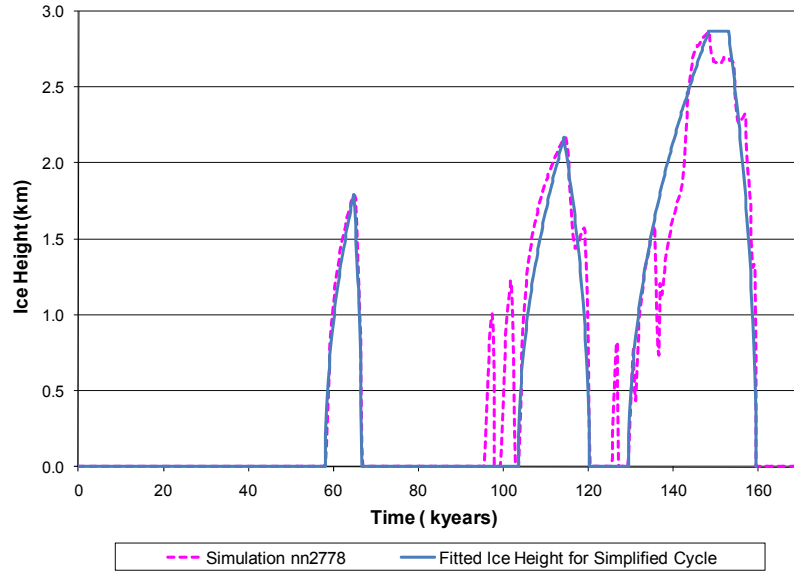
In the glaciation study, it is assumed that the present interglacial (temperate) period lasts a further 50,000 years. Following this long interglacial period, the climate at the repository site is represented by repeated cycles of a simplified version of Simulation nn2778 from Peltier (2006). A total of eight glacial cycles are assumed over the next million years.

A simplified glacial cycle was implemented to make the hydrogeological calculations feasible. This simplified cycle is shown in Figure 7-135 (ice height curves) and Figure 7-136 (permafrost depth profile). The time periods during which different glacial states occur at the study site are shown in Table 7-41.

The transient behaviour of the groundwater flow field during ice sheet movement across the site is of key interest. The time needed for the ice sheet to cross the model domain was estimated as follows:

- The ice sheet profile is specified by an analytical equation; and
- The ice height curves from Simulation nn2778 were fitted with the ice profile curve, assuming that the ice sheet travels at a constant speed over the site. The ice speed was varied until a good match was obtained.

The fitted ice height over the site is compared to Simulation nn2778 in Figure 7-135. The ice sheet advance and retreat speeds ranged from 50 to 60 m/a and from 100 to 200 m/a respectively, which compare well with literature field data (Garisto et al. 2010).



Note: The short periods of ice sheet cover at the site just before the 2nd and 3rd major ice sheet advances are neglected.

Figure 7-135: Comparison of Ice Sheet Height for the Reference Glacial Cycle with Simulation nn2778

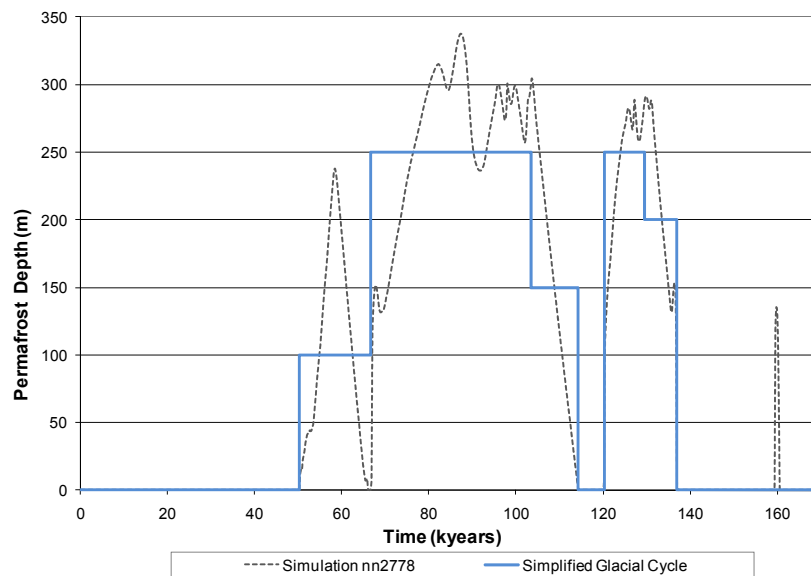


Figure 7-136: Comparison of Permafrost Depths for the Reference Glacial Cycle with Simulation nn2778

Table 7-41: Time History for Reference Glacial Cycle

Relative Time Period (years) ¹	Actual Times During First Cycle (years)	Duration of State (years)	Description of Glaciation State
-----	0 – 50,300		Temperate (current Interglacial)
0 – 7800	50,300 – 58,100	7800	Permafrost
7800 – 14,500	58,100 – 64,800	6700	Ice Sheet Advance, permafrost underneath
14,500 – 16,400	64,800 – 66,700	1900	Ice Sheet Retreat, permafrost underneath
16,400 – 53,200	66,700 – 103,500	36,800	Permafrost
53,200 – 64,000	103,500 – 114,300	10,800	Ice Sheet Advance, permafrost underneath
64,000 – 70,000	114,300 – 120,300	6000	Ice Sheet Retreat, no permafrost underneath
70,000 – 79,200	120,300 – 129,500	9200	Permafrost
79,200 – 86,600	129,500 – 136,900	7400	Ice Sheet Advance, permafrost underneath
86,600 – 102,700	136,900 – 153,000	16,100	Ice Sheet Advance, no permafrost underneath
102,700 – 109,200	153,000 - 159,500	6500	Ice Sheet Retreat, no permafrost underneath
109,200 – 110,400	159,500 – 160,700	1200	Proglacial Lake
110,400 – 121,200	160,700 – 171,500	10,800	Temperate

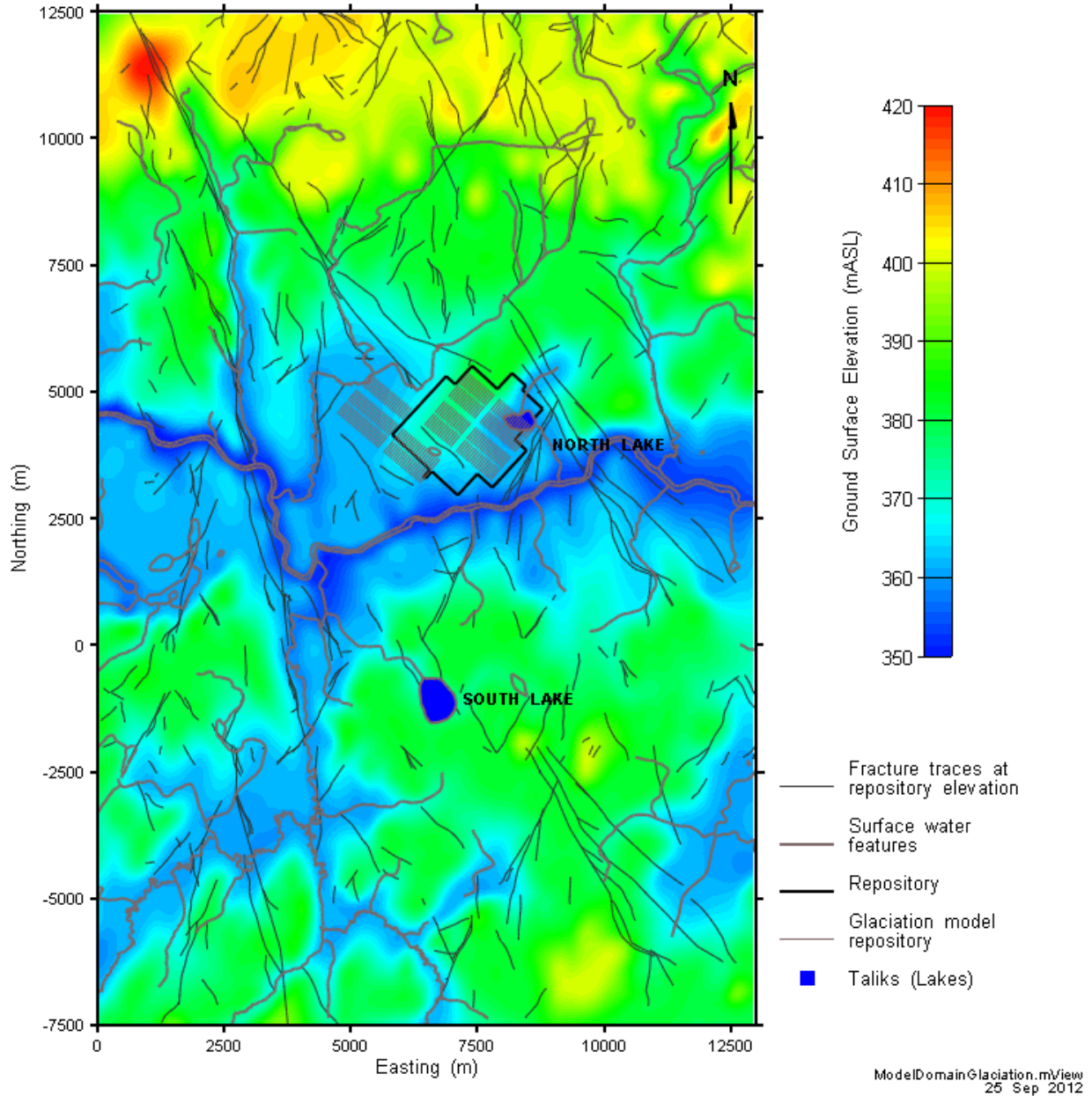
Notes: ¹ In the glaciation study the current interglacial period is assumed to extend 50,000 years into the future and immediately precedes the start of the first glacial cycle at 50,300 years. The glacial cycle repeats itself starting at: 171,500; 292,700; 413,900; etc. years.

7.10.2 Hydrogeological Modelling

The study area for the glaciation study is shown in Figure 7-137.

The hypothetical watershed is about 250 km², with a river crossing the domain and a topographic high along the northern boundary. The area is characterized by mild topographic changes. There are two major lakes within the model domain, the North and South lakes. The large scale (~100 m) fracture network was generated using a geostatistical fracture procedure, based on Canadian Shield lineament / fracture statistics and the results of a surface lineament analysis (Srivastava 2002).

Also shown for comparison purposes are the locations for the repository in the glaciation study and for the repository in this pre-project review.



Note: The Glaciation Study considered a repository at a depth of 670 m.

Figure 7-137: Hydrogeological and Transport Model Domain for Glaciation Study

The numeric flow modelling was performed using FRAC3DVS-OPG and included the 1-D hydromechanical (HM) coupling model, which is based on the work of Neuzil (2003) and assumes purely vertical strain. The modelling assumed constant density water flow. The absence of salinity is generally viewed as a conservative assumption (i.e., there is more flow at depth than would occur if salinity effects were included, Normani 2009).

The North Lake at the eastern edge of the repository was identified as a discharge zone and was the terminus of the shortest flow pathline from the radionuclide source (i.e., two defective containers which are located at the east corner of the repository). The North and South Lakes were designated as open taliks (i.e., there is no permafrost below the lakes at any depth during permafrost periods). A talik is a region of perennially unfrozen ground that may exist within a permafrost environment. Otherwise, the permafrost formed during the glacial cycle is assumed to be continuous across the study site.

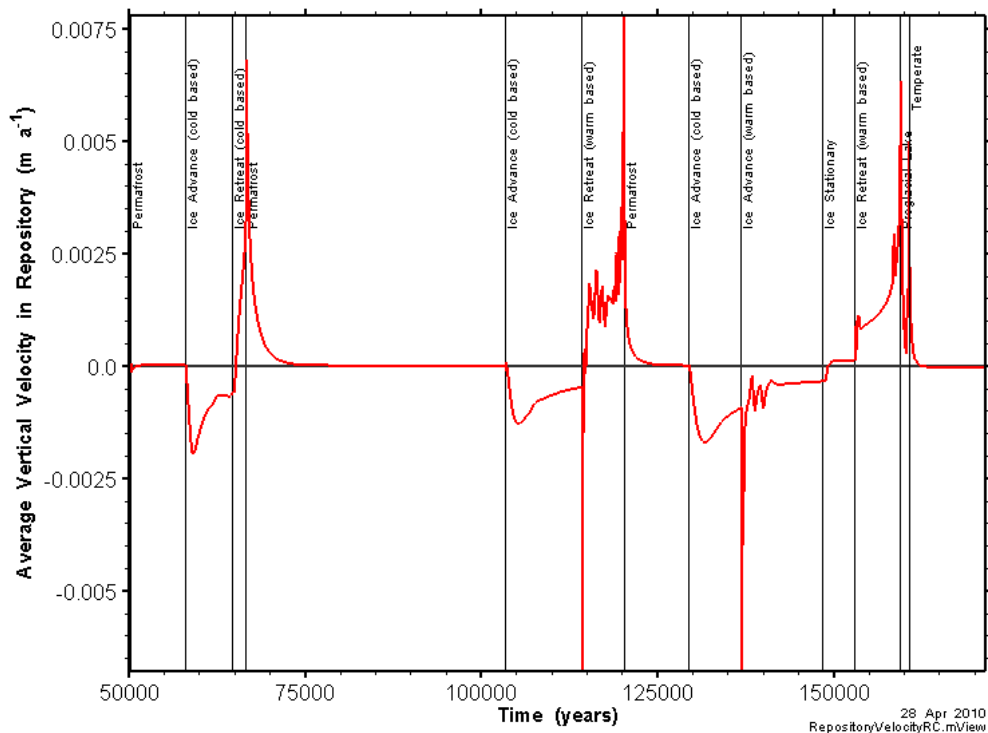
The groundwater modelling is described in detail in Walsh and Avis (2010), where a general approach is developed that captures the impact of glacial cycles on a complex, fractured flow system. The modelling was performed using a 50m grid model, which precluded direct incorporation of repository features and required use of a large dispersivity value (80 m). Even with these simplifications, execution time for eight glacial cycles (one million years) required more than six months. The main points are summarized below.

Unlike the constant climate case, the groundwater flow field is transient in the glaciation study due to the advance and retreat (along the north-south direction) of ice sheets over the model domain. Results of the simulations show the range of advective velocities that occur at the repository horizon. The modelling results indicated that the glaciation related changes to surface boundary conditions and permafrost formation had an extensive effect on the groundwater flow system, affecting direction and magnitude of flow.

In the glaciation flow model, the taliks were a dominant factor, focussing flow from a large portion of the model domain at discrete locations. These isolated gaps in the permafrost acted as pathways for the dissipation of hydraulic pressure generated from preceding glacial events. The system reached equilibrium after the stored glacial pressure was drained. The presence of additional taliks and / or formation of discontinuous permafrost could significantly reduce the duration of glacially induced overpressures and perhaps also the volume of water flowing through individual taliks, decreasing the influence of an individual talik.

The effect of glaciation on the groundwater velocities at the glaciation study repository level is illustrated in Figure 7-138 which shows how the average vertical component of the advective velocity within the repository footprint at repository depth changes with time and varying boundary conditions. The plot makes clear how the different hydraulic boundary conditions affect the flow field in the repository. Advancing glaciers lead to larger negative or downward vertical velocities. Retreating glaciers have the reverse effect, and this effect persists into the following permafrost stages, as the rapid retreat does not allow all the pressure stored during the glacial advance to dissipate.

Integrating the velocities shown in Figure 7-138 gives the average vertical travel distance within the repository footprint during one glacial cycle as shown in Figure 7-139. The cumulative vertical distance travelled is only about one meter after a 121,000 year long glacial sequence. This means that although the glacial cycling leads to increases in velocity and changes in flow direction, within the repository the hydraulic impacts of glacial advances and retreats almost cancel each other out. However, a caveat needs to be added. Although average velocities are very low within the repository, there is significant variation so that, at certain locations, particles need travel only a short distance from the repository before they encounter a fracture zone of higher permeability.



Note: Positive velocities are up, negative velocities are down.

Figure 7-138: Average Vertical Component of Velocity

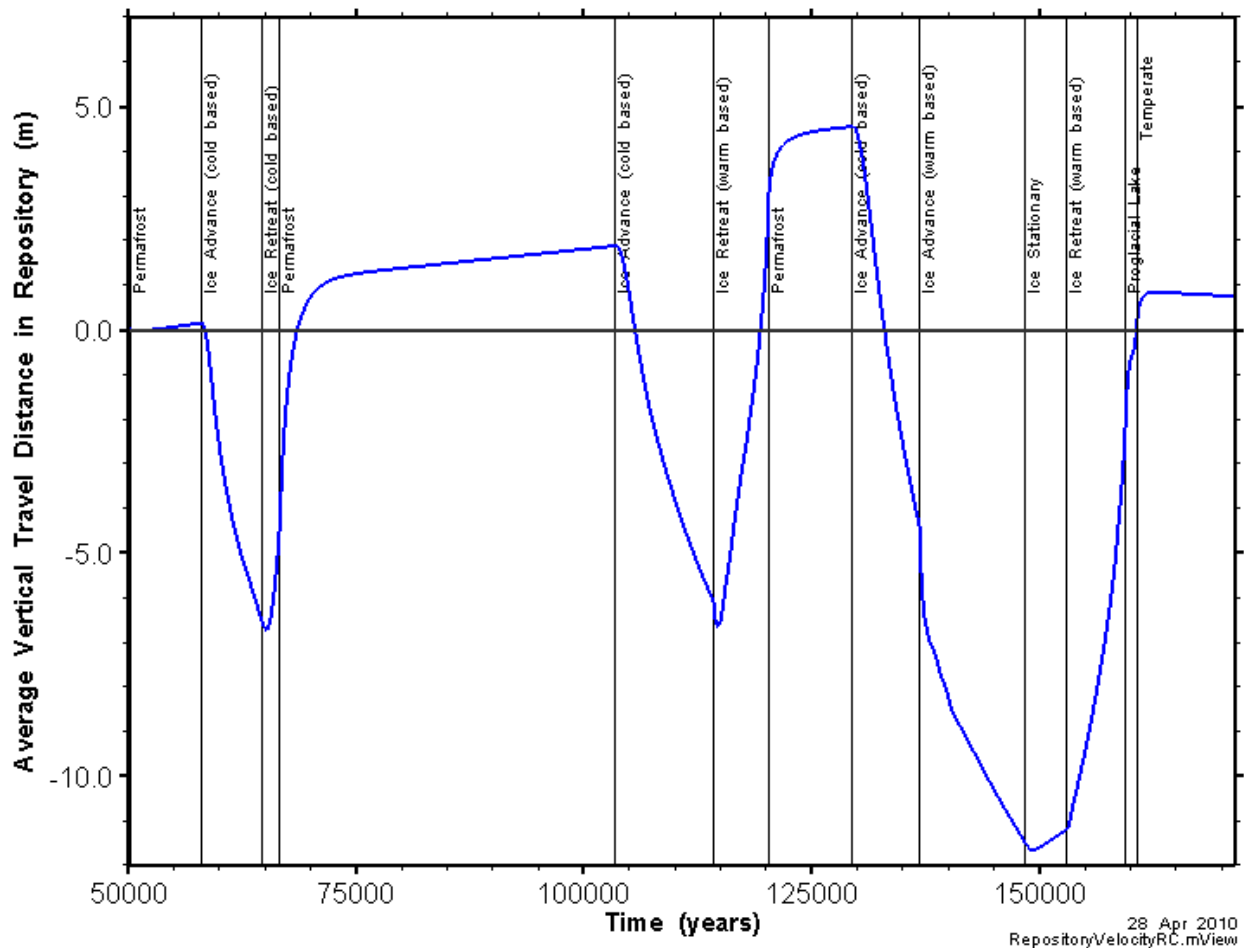


Figure 7-139: Cumulative Average Vertical Advective Flow Distance

7.10.3 Transport Modelling

The glaciation study further assumed that the repository was built to design specifications, except that two containers were unknowingly placed in the repository with small undetected defects in the copper shell (Garisto et al. 2010). The defective containers were assumed located at the repository location with the shortest groundwater travel time to surface based on the initial temperate climate flow field.

The dose consequences were determined using the SYVAC3-CC4 system model; however, unlike the constant climate case, the groundwater flow field is transient. Since the SYVAC3-CC4 model cannot handle transient flows, it was necessary to approximate the transient groundwater flow field using a series of fixed groundwater flow fields. A different fixed groundwater flow field was selected for each of the nine unique geosphere states defined in the

glaciation study (Garisto et al. 2010). Generally the groundwater flow field at around the mid-point of the state was used to represent the groundwater flow during the entire state.

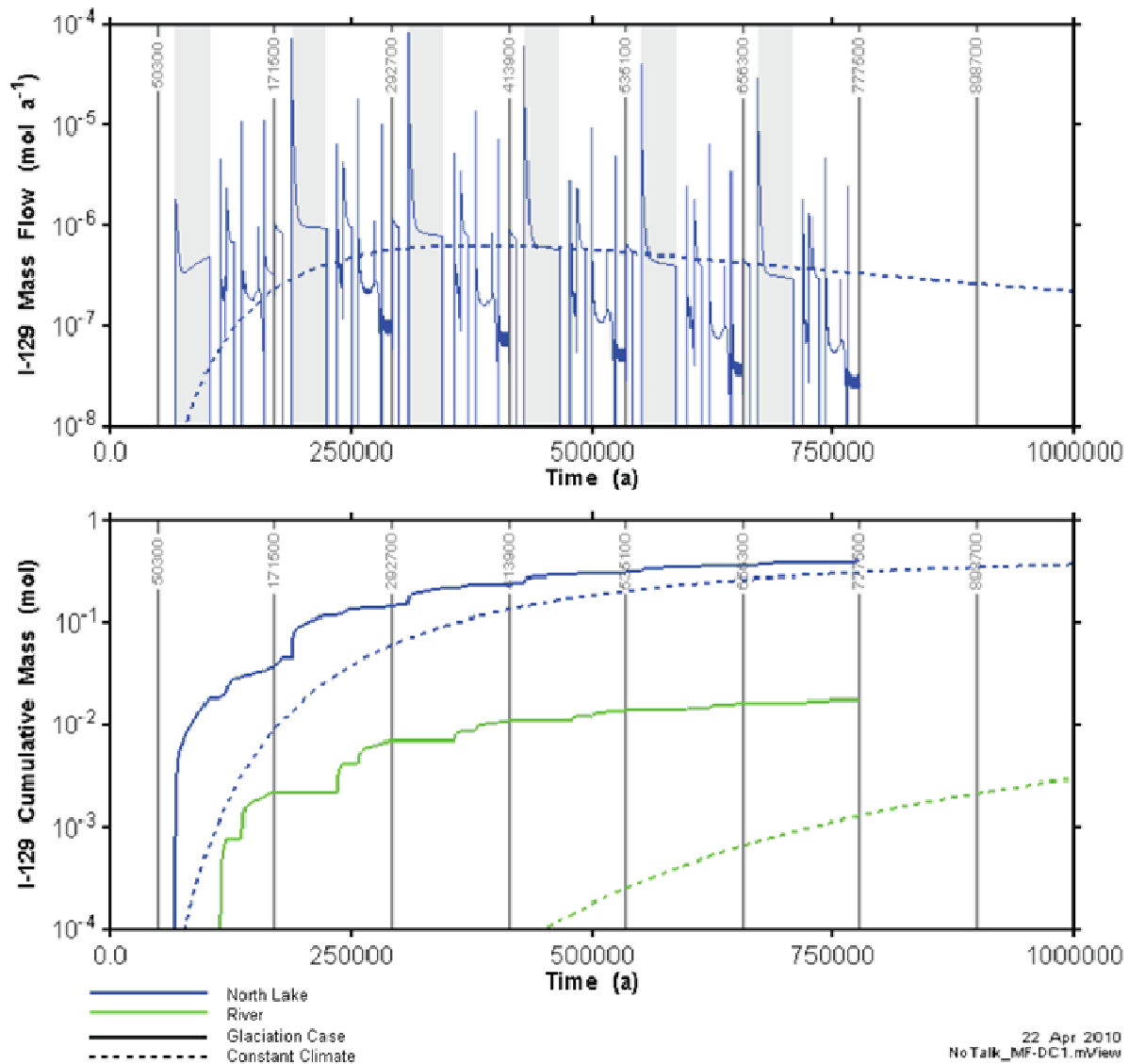
The groundwater flow field for each unique geosphere state was then used to generate the corresponding geosphere network model for each state using the same methodology described in Section 7.5.4.3. Comparison of the I-129 transport results and calculated dose rates obtained using FRAC3DVS-OPG and SYVAC3-CC4 indicated that the approximation of the transient groundwater flow field worked fairly well, given the differences in the models (Garisto et al. 2010, Appendix C). Furthermore, although the I-129 mass flow curves to the biosphere are quite different for the transient model compared to the constant climate case, the overall trend is similar and by the end of the simulation period the transient model shows roughly similar cumulative mass flows into, for example, the North Lake (Figure 7-140).

The effects of a typical glacial advance-retreat cycle on a contaminant plume were largely confined to the upper part of the plume in the more permeable, shallower units. The core of the plume remained relatively unaffected by the hydraulic perturbations induced by the advancing and retreating ice field (Walsh and Avis 2010, Garisto et al. 2010). This is largely due to the low permeability of the deeper geosphere, and the roughly equal and opposite effects of the glacial advance and retreat stages.

7.10.4 Biosphere Model and Dose Calculations

For the purposes of biosphere modelling, the glacial cycle was divided into temperate, permafrost, ice sheet and proglacial lake states. The occurrence of these states during the reference glacial cycle is shown in Table 7-41. Biosphere parameters are dependent on the climate (i.e., the glacial state (Garisto et al. 2010, Appendix A)). Because the biosphere is so different for these states, a different critical group was defined for each state.

In the temperate state, a Self-Sufficient Farmer household is the critical group. This group is assumed to spend their entire lives in the vicinity of the site and to obtain all their needs locally. All water needs (including irrigation and drinking) are met by a well that intercepts the contaminant plume from the repository. This is similar to the critical group assumed in this pre-project report.



Notes: Compared to equivalent constant climate case (without a well). Mass flow only plotted for North Lake to improve legibility of plot. The vertical lines indicate the start of a glacial cycle. Shaded regions show the second permafrost state in each glacial cycle.

Figure 7-140: I-129 Mass Flow Rate and Cumulative Mass Flow from the Glaciation Study

The biosphere features of the permafrost state are based on the Southern Arctic Ecozone (Environment Canada 2008). This region has a periglacial climate with soils underlain by continuous permafrost and active (thaw) layers that are usually moist or wet throughout the summer. Caribou herds graze in this area in the summers and use it as calving grounds. Migratory birds use this ecozone as a major breeding and nesting ground.

An open talik was assumed to exist below the North and South lakes during permafrost states. Therefore, these lakes become the primary discharge area for groundwater from the repository during permafrost periods. The North lake is assumed to be the primary water source for the critical group living during permafrost states.

During permafrost states, farming is not possible so a Self-Sufficient Hunter, characteristic of the inland tundra region, is the critical group. This group is assumed to spend their entire lives in the vicinity of the site and to obtain all of their needs from that area. Their diet consists mainly of caribou meat, augmented with wild birds and plants. Caribou eat lichens which grow near the repository and are contaminated via air deposition. (The atmosphere becomes contaminated due to aquatic degassing and aerosol suspension from the nearby lake.) Because lichens live for long periods of time and retain deposited radionuclides effectively, they can accumulate contamination over an extended period.

During ice sheet states, the region near the repository site is covered by an ice sheet and the area is assumed to be uninhabited. Dose rates during the ice sheet state are zero.

The proglacial lake state climate was assumed to resemble that of the permafrost state. The main difference is the presence of a large proglacial lake created by rapid melting of the retreating ice sheet which supplies the critical group with all its water needs. In the proglacial lake state, the critical group is a Self-Sufficient Fisher who moved into the area after the last glaciation. This group resembles the Hunter critical group in that it hunts local mammals such as caribou and wild fowl; however, due to the availability of fish in the proglacial lake, the self-sufficient Fisher diet contains a greater proportion of fish.

Dose rates were calculated up to a million years to determine the long-term impact of the repository. The dose pathways considered were climate state dependant and include water ingestion and immersion, plant ingestion, animal (fish, bird, milk, cattle, caribou, etc.) ingestion, and air inhalation and immersion.

The calculated I-129 dose rates are shown in Figure 7-141 for the reference case of the glaciation study and for the corresponding constant climate case. These doses were calculated using the FRAC3DVS I-129 mass flows to the biosphere and the SYVAC3-CC4 biosphere model. (Dose rates are zero during the ice sheet states, as discussed above.) Calculated total dose rates are shown Figure 7-142. These latter dose rates were calculated with the SYVAC3-CC4 system model.

Calculated dose rates were well below the ICRP-81 recommended dose constraint of 3×10^{-4} Sv/a (which is equal to the interim dose acceptance criteria for the pre-project review), and the average natural Canadian background dose rate (1.8×10^{-3} Sv/a).

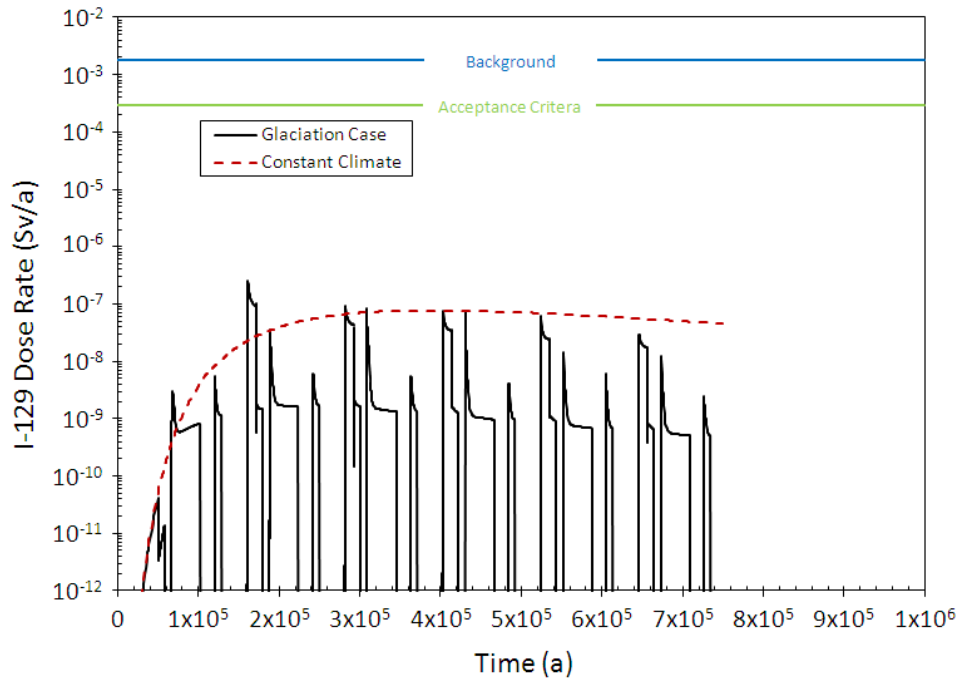


Figure 7-141: I-129 Dose Rate with Glacial Cycles

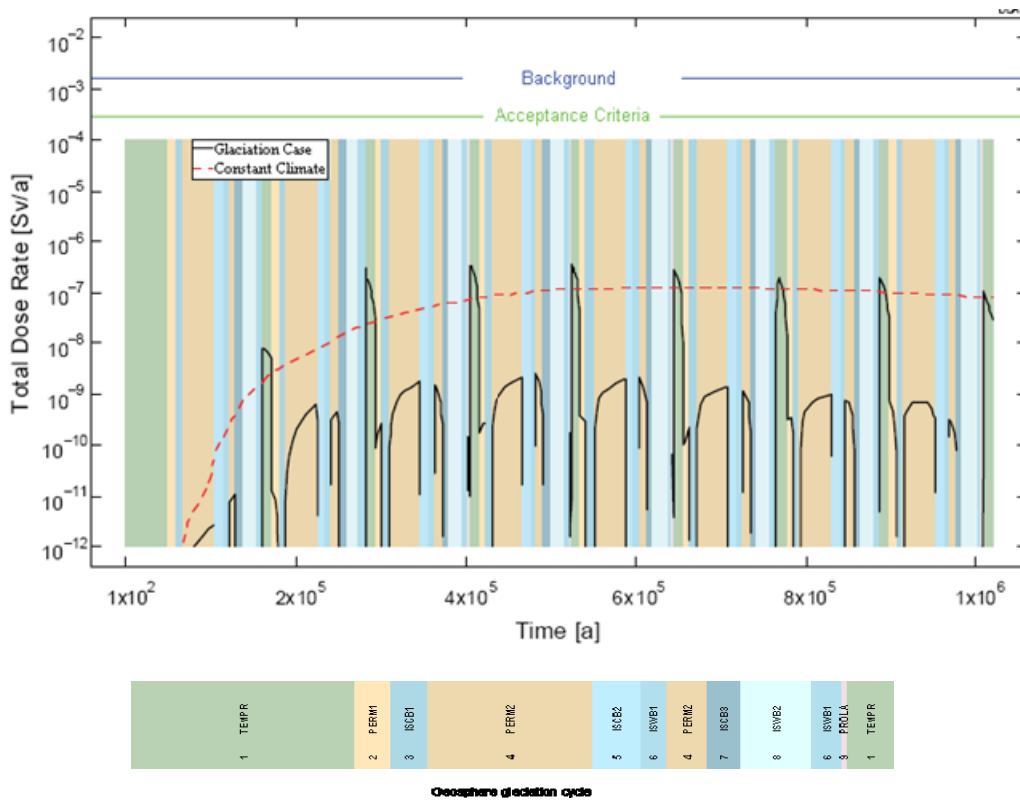


Figure 7-142: Total Dose Rate with Glacial Cycles

The two different models give similar results except for the sharp peaks in the FRAC3DVS-OPG dose rates that occur at the beginning of the second permafrost state of each glacial cycle. These sharp peaks are absent from the SYVAC-CC4 model because this model only uses snap-shots of the transient groundwater flow field as discussed above.

Dose rates during the temperate state are much higher than during the other states mainly because the Farmer critical group uses a well for its water needs whereas the other critical groups use lake water. Radionuclide concentrations in well water are much higher than in lake water because of the lower dilution.

The most important exposure pathway for the Hunter and Fisher critical groups is ingestion of caribou meat because caribou ingest large quantities of lichens which can be contaminated by air deposition.

Besides the reference glaciation case, various sensitivity cases and probabilistic cases were also examined in the glaciation study (Garisto et al. 2010), including an All Containers Fail case similar to that investigated in this pre-project review. For all sensitivity cases, except the All Containers Fail case, the calculated peak dose rate was well below 3×10^{-4} Sv/a. For the All Containers Fail case, the total dose rate was 4.1×10^{-4} Sv/a for a brief period of time; however, the peak is below the 1×10^{-3} Sv/a interim dose acceptance criterion for Disruptive Event Scenarios used in this pre-project review.

It can therefore be concluded that for the hypothetical glaciation study site, the impacts of a deep geological repository will be well below regulatory limits when the effects of glaciation are considered.

7.10.5 Applicability to the Pre-Project Review

The glaciation study illustrates the analysis methods and techniques that could be used in support of a quantitative discussion of the relative impacts of glaciation at a real repository site. While the pre-project review site is different from the glaciation site, there are some similarities which support a qualitative discussion of the potential effects on the dose results for the Normal Evolution Scenario. The pre-project review repository is located in the same watershed of the Canadian Shield as the glaciation study repository (see Figure 7-137). Consequently, for example, the fracture network used in the two studies is quite similar and will have a similar influence on groundwater flows. Also, the host rock properties are similar, although the pre-project review host rock has higher hydraulic permeabilities. At repository level, for example, the permeability of the host rock is 7×10^{-19} m² in the glaciation study versus 4×10^{-18} m² in the current study.

Because the repositories are located in the same watershed, the climate would evolve similarly and the glacial cycle described in Section 7.10.1 is representative of the future climate at the pre-project review site. This means that the critical exposure groups defined for the glaciation cycle are also appropriate. The Farmer critical group present during the temperate period of the glaciation study has similar characteristics to the critical group used to calculate exposure doses in the current study. In particular, both groups use water from a well for drinking, irrigation, etc. and this well captures most of the radionuclide plume from the repository.

Finally, the radionuclide release scenarios are essentially the same. That is, in both cases, it is assumed that the repository is built to design specifications; but a very small number of used fuel containers (two in the glaciation study and three in the current study) are placed in the repository with undetected defects. These defects are assumed to lead to early releases of radionuclides. Since the size of the defects is similar in both studies, the radionuclide source terms are similar, with differences arising due to changes in, for example, the assumed instant release fraction for I-129 and the larger number of defective containers.

There are some differences. The repository in the current study is at a shallower depth (500 m versus about 650 m) than in the glaciation study. This could lead to an increased impact of ice sheet retreat / advance over the repository site on the groundwater velocities in the repository. The repository design is also different in that in-floor container placement is used whereas horizontal borehole placement was used in the glaciation study. The pre-project review repository, although situated in a very similar location, also has a large water conducting fracture intersecting the repository footprint.

This latter difference means that groundwater from the repository discharges at different locations of the biosphere. For the glaciation study, the main discharge zone for groundwater from the repository is the North lake during both the temperate period and permafrost period. (During permafrost periods the North lake is treated as an open talik.) In contrast, for the current study, the River, Central Wetland, East Wetland and the Lake are the main discharge areas, where the Lake is the same physical location as the North lake in the glaciation study. The River may be large enough to support a talik. If the River is an open talik, then the available discharge area during permafrost periods would be much larger and the groundwater flows during permafrost periods would not be as focussed as they were in the glaciation study, likely causing dilution of the contaminant plume from the repository. Also, pressure gradients arising from the ice load imposed by the retreating ice sheet may be more readily dissipated if the discharge area is larger, perhaps muting the effects of ice sheet advance / retreat.

In spite of the differences outlined above, it is anticipated that the relative effects of glaciation will be similar given that the two repositories are located at the same site on the Canadian Shield. The glaciation study shows that the calculated peak dose rate could be an order of magnitude greater (depending on the glacial cycle) than the peak dose rate for a constant temperate climate case. Because the peak dose rate determined for the Reference Case of the Normal Evolution Scenario is well below the interim dose acceptance criterion (i.e., 3×10^{-4} Sv/a), it can be concluded that the anticipated dose consequences at the hypothetical site that is the subject of this pre-project review will also likely be well below regulatory limits when the effects of glaciation are considered.

A discussion of the potential effects of glaciation on the deep groundwater system for the pre-project review geosphere is provided in Chapter 2.

7.11 Other Considerations

This section presents results for complementary indicators for radiological assessment, results for the radiological protection of the environment, and results for the protection of persons and the environment from hazardous substances.

A discussion on the effects of gas generation and migration is also included.

7.11.1 Complementary Indicators for the Radiological Assessment

An “indicator” is a characteristic or consequence of a repository which can be used to indicate the overall safety or performance of the system. The most widely used indicator is the peak radiological dose rate, which is calculated from the characteristics of the waste and repository, the properties of the geosphere and biosphere, and the characteristics of the critical group.

The relevance of the calculated dose rates as indicators of potential exposure tends to decrease with time, in part because of uncertainties in the models used to calculate them. In particular, assumptions concerning the biosphere (e.g., climate), human lifestyles (i.e., critical group characteristics) and water flows in the near-surface environment become increasingly uncertain. The purpose of complementary long-term indicators is to supplement the dose rate indicator using system characteristics that are much less sensitive to such assumptions.

The types of complementary indicators used in this report address:

- Radionuclide concentrations in the biosphere; and
- Radionuclide transport to the biosphere.

Indicators of the first type avoid assumptions about biosphere pathways but make assumptions about flow rates in surface water bodies (i.e., dilution rates). Indicators of the second type avoid assumptions about surface water flows. Concentration type indicators are more useful on medium timeframes (about 10^4 to 10^5 years), while transport type indicators are more useful for very long timeframes ($> 10^5$ years) when there is more uncertainty about surface conditions.

The specific complementary indicators used in this study were selected based on the recommendations of the SPIN project (Becker et al. 2002). The indicators are:

- Radiotoxicity concentration in a water body, for medium time scales; and
- Radiotoxicity transport from the geosphere, for longer time scales.

Radiotoxicity concentration (in Sv/m^3) is the sum over all radionuclides of the activity concentrations in the water body (in Bq/m^3) multiplied by the corresponding radionuclide ingestion dose coefficient. The radiotoxicity transport from the geosphere (in Sv/a) is similarly defined.

Although these complementary indicators are expressed in units of Sv/m^3 or Sv/a , they do not represent a dose; rather, they are radiotoxicity-weighted concentration or transport indicators.

Reference Indicator Values

To make use of indicators, reference values are required for comparison purposes.

A reference value for the radiotoxicity concentration in a water body has been derived from present-day natural radionuclide concentrations in Canadian Shield surface water (Garisto et al. 2004, Section 8.2). The reference value for the radiotoxicity concentration is $2 \times 10^{-5} \text{ Sv}/\text{m}^3$. Dose impacts associated with these natural background levels are not likely of concern so it follows that any dose impacts from the repository that are small in comparison are also not likely of concern.

Natural transport processes carry small amounts of natural radioactivity from within the geosphere to the biosphere. The most important processes are groundwater flow and erosion (IAEA 2002). The natural radioactivity discharged to the biosphere with groundwater flow has been calculated from groundwater flow rates and radionuclide concentrations in groundwater. The result is a value of 700 Sv/a over a 100 km² sub-regional watershed area (Garisto et al. 2004, Section 8.2).

Alternatively, the radiotoxicity transport to the surface can be calculated from the elemental composition of Canadian Shield granites and the erosion rate of granite over long time periods. The radiotoxicity transport caused by erosion of the granite bedrock in a 100 km² sub-regional watershed area is about 600 Sv/a (Garisto et al. 2004, Section 8.2). This is slightly less than the 700 Sv/a radiotoxicity transport value for groundwater flow and is therefore adopted as the reference value.

Table 7-42 summarizes the reference values for the dose rate indicator and the complementary long-term indicators used in this report. The reference values proposed in the EC SPIN project (Becker et al. 2002) are also shown for comparison. The higher value for the transport indicator is due to the higher uranium content of Canadian Shield granite.

Table 7-42: Reference Values for Indicators

Indicator	Reference Value	
	Current Study	SPIN
Dose rate (Sv/a)	3×10^{-4}	1×10^{-4} to 3×10^{-4}
Radiotoxicity concentration in a lake (Sv/m ³)	2×10^{-5}	2×10^{-5}
Radiotoxicity transport from the geosphere (Sv/a)	600	60

Results

The radionuclide concentrations in the Lake just to the east of the repository are used to calculate the radiotoxicity concentration while the total radionuclide transport to the biosphere is used to calculate the radiotoxicity transport.

Figure 7-143 shows the indicator values for the Reference Case together with the dose rate indicator. The indicators have the same general shape because they all depend on radionuclide transport to the biosphere.

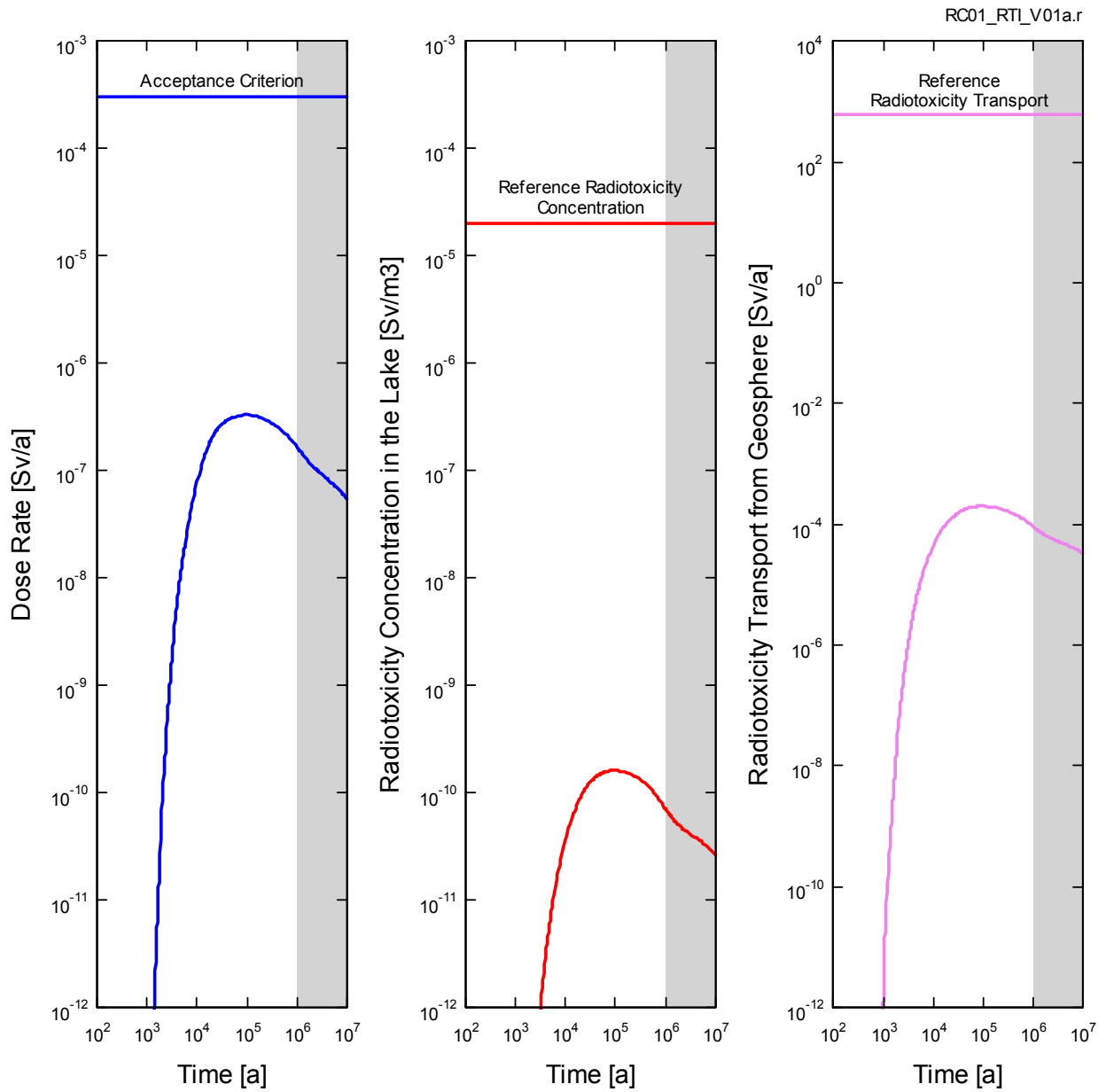


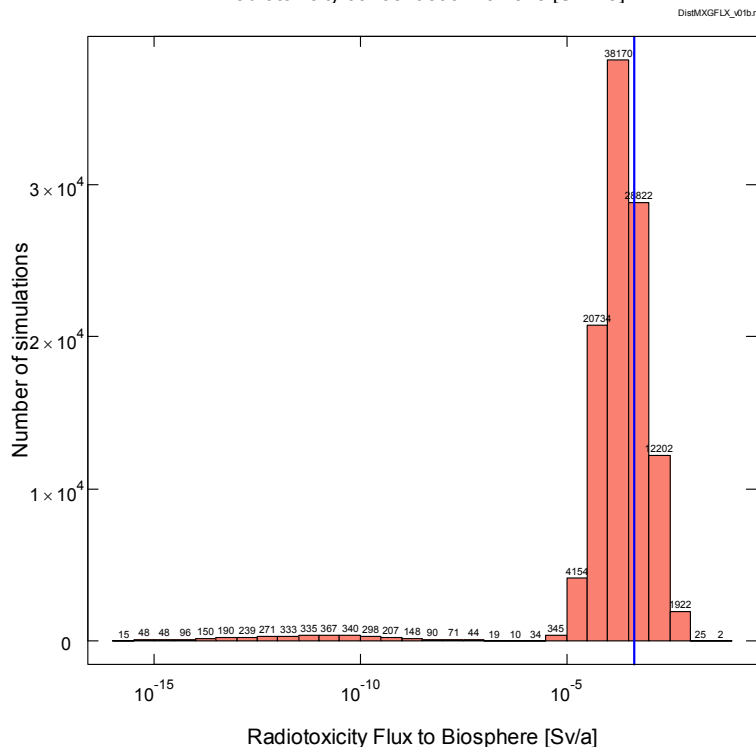
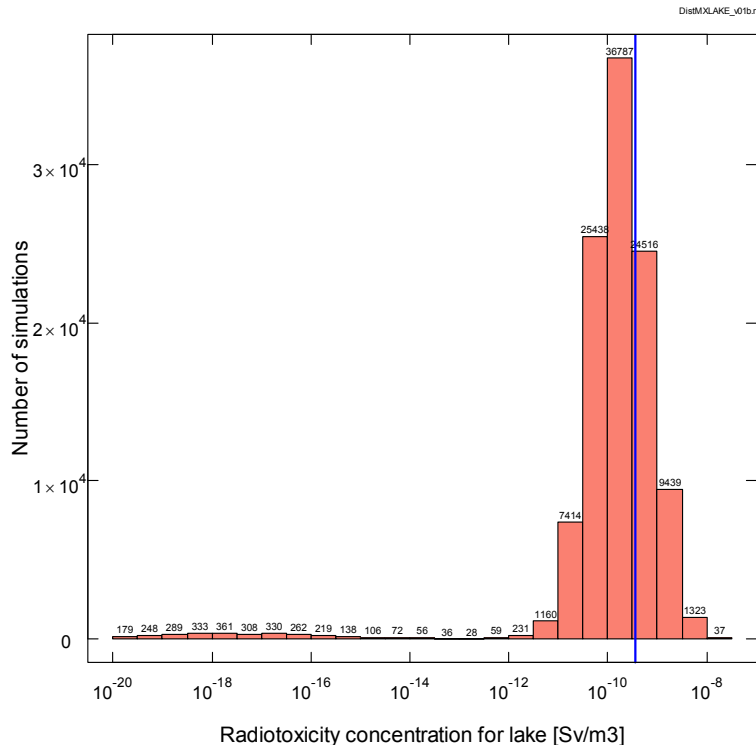
Figure 7-143: SYVAC3-CC4 – Reference Case Results for Complementary Indicators

The figure shows the radiological dose rate has the smallest margin to its associated criterion. The reasons for this are:

- The critical group uses well water, which has much higher radionuclide concentrations than surface waters; and
- The two radiotoxicity reference values are derived from the radionuclide concentrations in the natural environment while the dose rate acceptance criterion is not. The interim dose acceptance criterion is about six times lower than the natural background dose rate, thereby making it more restrictive.

Figure 7-144 shows the calculated distribution of indicator values over the 120,000 probabilistic simulations. The average radiotoxicity transport to the biosphere is 4.5×10^{-4} Sv/a and the average radiotoxicity concentration is 3.7×10^{-10} Sv/m³. The maximum radiotoxicity transport to the biosphere is 6.4×10^{-2} Sv/a and the maximum radiotoxicity concentration is 2.1×10^{-8} Sv/m³. These are orders of magnitude below the indicator reference values of 600 Sv/a and 2×10^{-5} Sv/m³ respectively.

Since both indicators are well below the acceptance / reference values, additional confidence is provided that at long times (i.e., when the dose rate is more uncertain) the impacts of the repository are likely to be very small.



Note: The vertical blue lines indicate the average values of the complementary indicators.

Figure 7-144: SYVAC3-CC4 – Distribution of Complementary Indicators

7.11.2 Radiological Protection of the Environment

The results presented in Section 7.7 and Section 7.8 address the potential radiological impact on persons. This section addresses the potential radiological impact on the environment.

The approach compares results obtained for the Reference Case of the Normal Evolution Scenario, its associated No Geosphere Sorption sensitivity case and the All Containers Fail Disruptive Event Scenario against the interim acceptance criteria established in Section 7.1.3 for the radiological protection of the environment. The No Geosphere Sorption sensitivity case is selected because this yields the highest dose of all Normal Evolution sensitivity cases considered. Similarly, the All Containers Fail at 60,000 years is a high dose Disruptive Event Scenario.

Table 7-43 shows this comparison for Reference Case of the Normal Evolution Scenario for I-129, C-14, Cs-135 and Cl-36. Figure 7-106 shows that these radionuclides are the top contributors to the total dose rate.

The comparison shows very large margins to the interim acceptance criteria. It is therefore concluded that the radiological effects on the environment associated with the Reference Case of the Normal Evolution Scenario are negligible within the time frame of interest.

Table 7-43: Comparison of Reference Case Concentrations with Interim Acceptance Criteria for the Radiological Protection of Non-human Biota

Radionuclide	Media					
	Surface Water (Bq/L)			Soil (Bq/kg)		
	Criterion	Calculated	Ratio	Criterion	Calculated	Ratio
I-129	3.2×10^0	1.5×10^{-6}	4.5×10^{-7}	2.4×10^3	9.6×10^{-3}	4.0×10^{-6}
C-14	2.7×10^{-2}	7.5×10^{-7}	2.8×10^{-5}	2.4×10^2	7.5×10^{-5}	3.1×10^{-7}
Cs-135	2.1×10^{-3}	8.9×10^{-7}	4.2×10^{-4}	8.5×10^0	4.8×10^{-1}	5.6×10^{-2}
Cl-36	2.8×10^0	9.6×10^{-7}	3.4×10^{-7}	3.8×10^{-1}	1.5×10^{-4}	4.0×10^{-4}
	Sediment (Bq/kg)*					
	Criterion	Calculated	Ratio			
	I-129	1.2×10^6	1.8×10^{-1}	1.5×10^{-7}		
C-14	2.8×10^5	1.6×10^{-1}	5.6×10^{-7}			
Cs-135	3.5×10^5	5.5×10^1	2.2×10^{-4}			
Cl-36	4.1×10^4	6.5×10^{-4}	1.6×10^{-8}			

Note: * Values are estimated using the well concentration and the sediment Kd because there is no discharge to the River or Lake in the Reference Case

Table 7-44 shows this comparison for the No Geosphere Sorption sensitivity case of the Normal Evolution Scenario for Po-210, Rn-222, Pb-210 and Ra-226. Figure 7-111 shows that these radionuclides are the top contributors to the total dose rate.

The comparison shows large margins to the interim acceptance criteria. It is therefore concluded that the radiological effects on the environment associated with this sensitivity case of the Normal Evolution Scenario are negligible.

Table 7-44: Comparison of No Sorption in Geosphere Sensitivity Case Concentrations with Acceptance Criteria for the Radiological Protection of Non-human Biota

Radionuclide	Media					
	Surface Water (Bq/L)			Soil (Bq/kg)		
	Criterion	Calculated	Ratio	Criterion	Calculated	Ratio
Po-210	7.0×10^{-3}	5.3×10^{-6}	7.6×10^{-4}	3.0×10^1	5.5×10^{-1}	1.8×10^{-2}
Rn-222**		5.4×10^{-6}			3.4×10^{-1}	
Pb-210	4.3×10^0	1.9×10^{-6}	4.4×10^{-7}	3.7×10^3	5.5×10^{-1}	1.5×10^{-4}
Ra-226	5.9×10^{-4}	9.1×10^{-6}	1.5×10^{-2}	2.5×10^2	4.1×10^{-1}	1.6×10^{-3}
	Sediment (Bq/kg)*					
	Criterion	Calculated	Ratio			
Po-210	5.6×10^3	2.5×10^1	2.0×10^{-3}			
Rn-222**						
Pb-210	6.3×10^3	1.0×10^3	1.6×10^{-1}			
Ra-226	9.3×10^2	2.9×10^0	3.2×10^{-3}			

Notes:

* Values are estimated using the well concentration and the sediment Kd because there is no discharge to the River or Lake in the Reference Case

** Criterion not established in Section 7.1.3

Table 7-45 shows this comparison for the All Containers Fail Disruptive Event Scenario of I-129, Sn-126, Sb-126, Se-79, Cs-135, and Cl-36. Figure 7-131 shows that these radionuclides are the top contributors to the total dose rate.

The comparison shows reduced margins as compared to the Normal Evolution Scenario (as would be expected due to the significantly greater source term) with Cs-135 exceeding its interim acceptance criterion for Soil. This exceedance is judged acceptable on the basis that the amount of the exceedance is small and that the likelihood of the scenario is low. It is unlikely that all containers would fail simultaneously, and a staggered failure could result in a significant broadening of the release and a subsequent reduction in the peak concentration.

In conclusion, the All Containers Fail Scenario could result in a small exceedance of the interim acceptance criteria for selected radionuclides. Considering the conservatism in the model and the low likelihood of the event, it is concluded that the hazard arising from this event is within acceptance risk bounds.

Table 7-45: Comparison of All Containers Fail at 60,000 years Disruptive Event Scenario Concentrations with Interim Acceptance Criteria for the Radiological Protection of Non-human Biota

Radionuclide	Media					
	Surface Water (Bq/L)			Soil (Bq/kg)		
	Criterion	Calculated	Ratio	Criterion	Calculated	Ratio
I-129	3.2×10^0	6.5×10^{-3}	2.0×10^{-3}	2.4×10^3	1.7×10^1	7.0×10^{-3}
Sn-126**		1.4×10^{-4}			9.0×10^0	
Sb-126**		1.7×10^{-4}			9.0×10^0	
Se-79**		8.5×10^{-4}			1.2×10^1	
Cs-135	2.1×10^{-3}	1.0×10^{-4}	4.9×10^{-2}	8.5×10^0	5.6×10^1	6.6×10^0
Cl-36	2.8×10^0	2.7×10^{-3}	9.6×10^{-4}	3.8×10^{-1}	3.3×10^{-1}	8.7×10^{-1}
	Sediment (Bq/kg)*					
	Criterion	Calculated	Ratio			
I-129	1.2×10^6	8.0×10^1	6.7×10^{-5}			
Sn-126**		1.7×10^1				
Sb-126**		1.7×10^1				
Se-79**		2.1×10^2				
Cs-135	3.5×10^5	5.8×10^0	1.7×10^{-5}			
Cl-36	4.1×10^4	6.1×10^2	1.5×10^{-2}			

Notes:

* Values are estimated using the well concentration and the sediment Kd because there is no discharge to the River or Lake in the Reference Case

** Criterion not established in Section 7.1.3

7.11.3 Protection of Persons and the Environment from Hazardous Substances

This section considers the potential non-radiological effects of contaminants arising from the used fuel bundles and from the container on the health and safety of persons and the environment.

The approach compares results obtained for the Reference Case of the Normal Evolution Scenario, its associated No Solubility Limits sensitivity case and the All Containers Fail Disruptive Scenario against the interim acceptance criteria shown in Table 7-1. The No Solubility Limits sensitivity case is selected because this yields the highest contaminant concentrations of all Normal Evolution sensitivity cases considered. Similarly, the All Containers Fail at 60,000 years is a high release Disruptive Scenario.

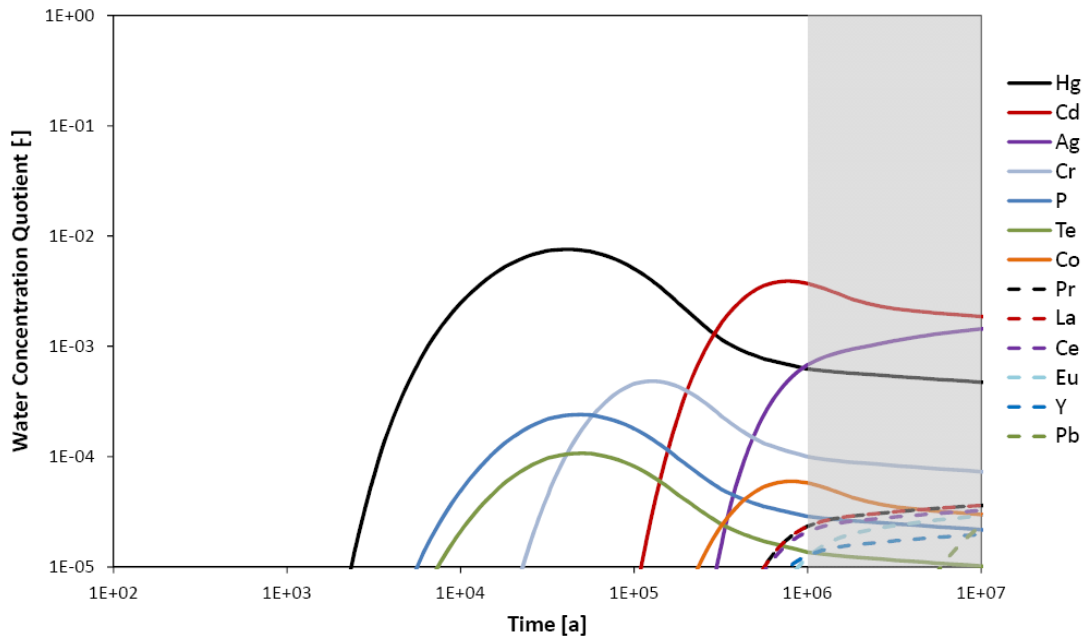
Table 7-1 shows different acceptance criteria for surface water and groundwater. Because the well is the primary source of water in the SYVAC3-CC4 model, well water concentrations are compared to the minimum of these two criteria to ensure conservative results are obtained. The ratio determined by dividing an element concentration by its acceptance criterion is the 'concentration quotient'. Concentration quotients less than 1.0 indicate the interim acceptance criterion is not exceeded.

7.11.3.1 Contaminants from the Used Fuel Bundles

Figure 7-145 shows the concentration quotients (computed using well water concentrations) as a function of time for the Reference Case. Table 7-46 shows numerical values computed using the Water, Soil, and Sediment interim acceptance criteria. The simulation is carried out to 10 million years and results shown beyond the 1 million year timeframe are indicative only.

The highest overall concentration quotient is 7.6×10^{-3} for Hg in Water. The highest concentration quotient in the Soil is 5.8×10^{-5} for Cr. There is no discharge through the sediment layer in the SYVAC3-CC4 Reference Case (with well) simulation and therefore the concentration in that compartment is zero.

All concentration quotients are well below 1.0, indicating that wide margins are available to the interim acceptance criteria.



Note: results for As, I, Nd and U are off-scale low

Figure 7-145: SYVAC3-CC4 - Concentration Quotients for the Reference Case

Table 7-46: SYVAC3-CC4 - Concentration Quotients for the Reference Case

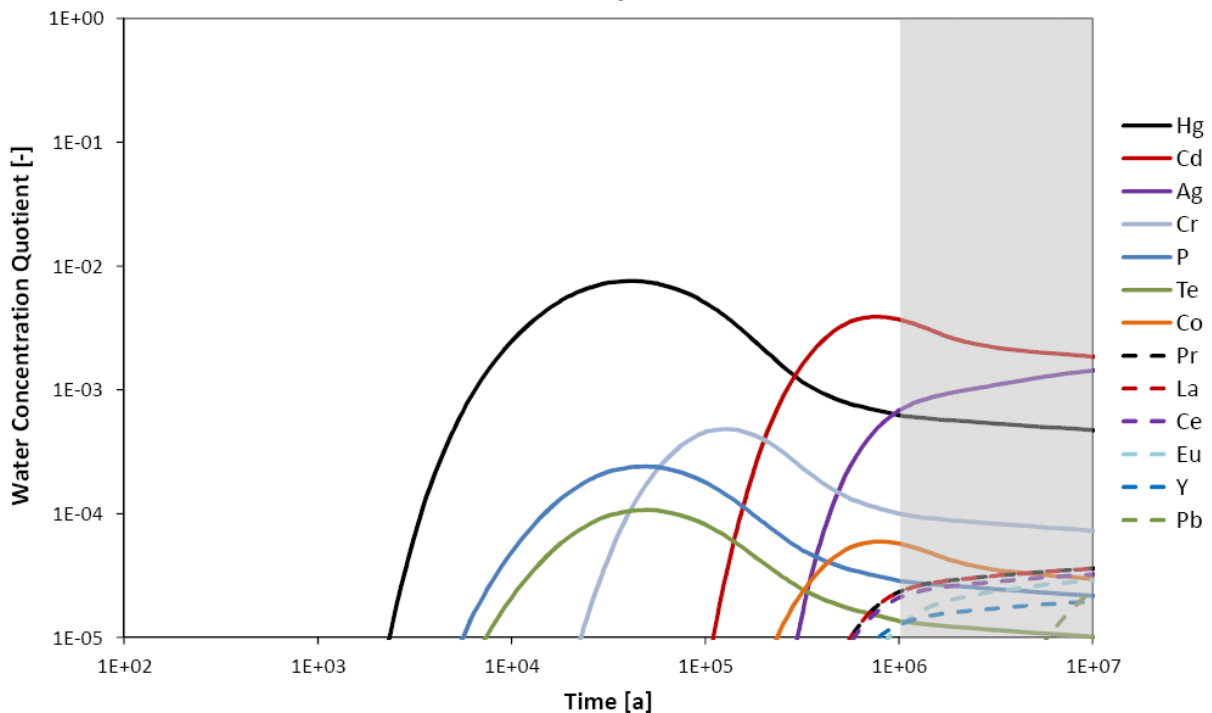
Element	Water	Soil	Sediment*
Ag	1.4x10 ⁻³	1.9x10 ⁻⁵	1.7x10 ⁻⁴
As	9.7x10 ⁻⁷	3.3x10 ⁻⁹	2.5x10 ⁻⁷
Cd	3.9x10 ⁻³	3.8x10 ⁻⁶	7.8x10 ⁻⁴
Ce	3.2x10 ⁻⁵	4.7x10 ⁻⁶	1.5x10 ⁻⁶
Co	6.0x10 ⁻⁵	1.2x10 ⁻⁷	7.0x10 ⁻⁶
Cr	4.9x10 ⁻⁴	5.8x10 ⁻⁵	2.8x10 ⁻⁶
Eu	2.9x10 ⁻⁵	5.0x10 ⁻⁷	1.3x10 ⁻⁷
Hg	7.6x10 ⁻³	2.2x10 ⁻⁶	4.9x10 ⁻⁵
I	3.8x10 ⁻⁶	4.6x10 ⁻⁷	-
La	3.6x10 ⁻⁵	8.8x10 ⁻⁷	2.3x10 ⁻⁷
Nd	0	0	0
P	2.4x10 ⁻⁴	-	-
Pb	1.3x10 ⁻⁴	5.4x10 ⁻⁷	3.2x10 ⁻⁴
Pr	3.6x10 ⁻⁵	4.7x10 ⁻⁷	1.0x10 ⁻⁷
Te	1.1x10 ⁻⁴	8.0x10 ⁻⁷	-
U	1.1x10 ⁻²⁶	8.8x10 ⁻²⁸	-
Y	2.0x10 ⁻⁵	3.1x10 ⁻⁷	3.2x10 ⁻⁷

Note: * Values are estimated using the well concentration and the sediment Kd because there is no discharge to the River or Lake in the Reference Case

Figure 7-146 shows the concentration quotients (computed using well water concentrations) as a function of time for the No Solubility Limits sensitivity case. Table 7-47 shows numerical values computed using the Water, Soil, and Sediment interim acceptance criteria.

The results are largely unchanged from the Reference Case because many species are already not solubility limited. One exception is U which has increased in concentration by approximately 4.5 times in the Water and by 44 times in the Soil at the end of the 10 million year simulation but remains below the figure scale.

Despite the increases, concentrations remain well below the interim acceptance criteria and no potential hazard exists.



Note: results for As, I, Nd and U are off-scale low

Figure 7-146: SYVAC3-CC4 - Concentration Quotients for the No Solubility Limits Case

Table 7-47: SYVAC3-CC4 - Concentration Quotients for the No Solubility Limits Case

Element	Water	Soil	Sediment*
Ag	1.4×10^{-3}	1.8×10^{-5}	1.7×10^{-4}
As	9.7×10^{-6}	3.3×10^{-9}	2.5×10^{-7}
Cd	3.9×10^{-3}	3.8×10^{-6}	7.8×10^{-4}
Ce	3.2×10^{-5}	4.7×10^{-6}	1.5×10^{-6}
Co	6.0×10^{-5}	1.2×10^{-7}	7.0×10^{-6}
Cr	4.9×10^{-4}	5.8×10^{-5}	2.8×10^{-6}
Eu	2.9×10^{-5}	5.0×10^{-7}	1.3×10^{-7}
Hg	7.6×10^{-3}	2.2×10^{-6}	4.9×10^{-5}
I	3.8×10^{-6}	4.6×10^{-7}	-
La	3.6×10^{-5}	8.8×10^{-7}	2.3×10^{-7}
Nd	0	0	0
P	2.4×10^{-4}	-	-
Pb	1.6×10^{-3}	6.7×10^{-6}	4.0×10^{-3}
Pr	3.6×10^{-5}	4.7×10^{-7}	1.0×10^{-7}
Te	1.1×10^{-4}	7.9×10^{-7}	-
U	4.9×10^{-25}	3.9×10^{-26}	-
Y	1.4×10^{-3}	1.8×10^{-5}	3.2×10^{-7}

Note: * Values are estimated using the well concentration and the sediment K_d because there is no discharge to the River or Lake in the Reference Case

Figure 7-147 shows the concentration quotients (computed using well water concentrations) as a function of time for the All Containers Fail Disruptive Scenario. Table 7-48 shows numerical values computed using the Water, Soil, and Sediment interim acceptance criteria.

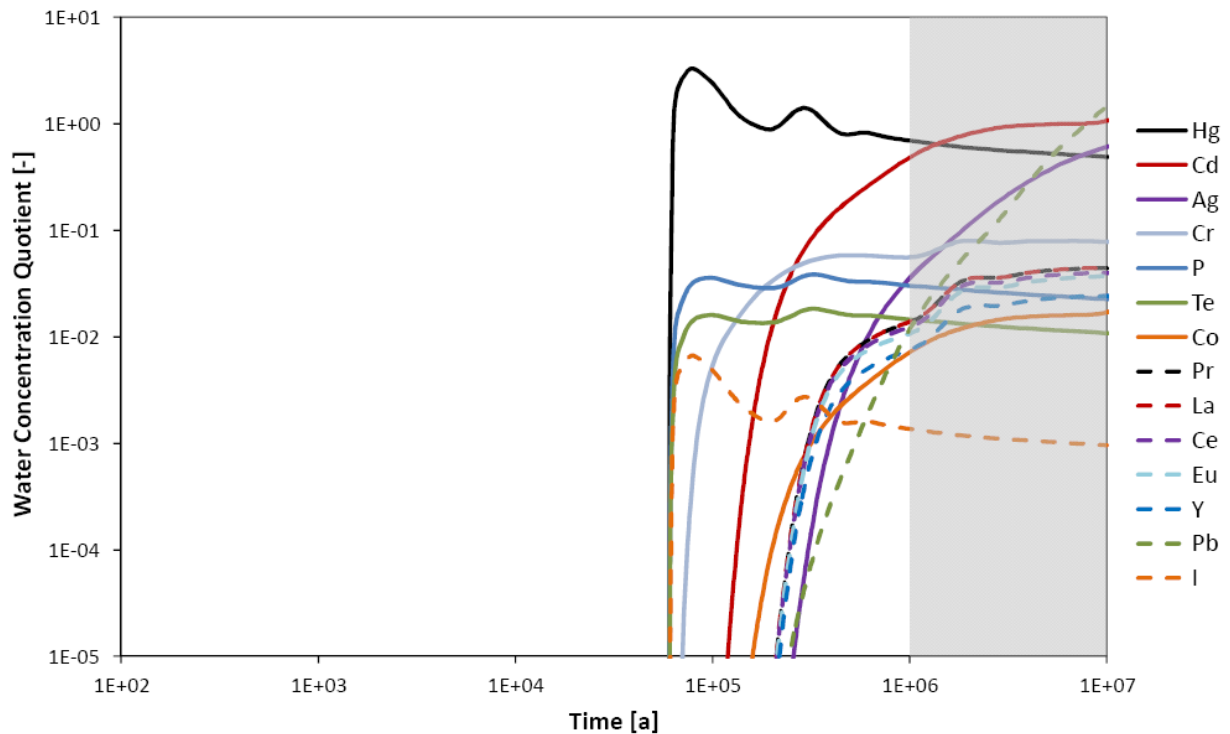
The concentration quotients are significantly higher than in the Normal Evolution Scenario (as expected due to the significantly greater source term), with Hg, Pb and Cd slightly exceeding the Water criteria with concentration quotients of 3.3, 1.6 and 1.1 respectively. The peak Hg concentration occurs relatively early due to its 4% instant release fraction, its high solubility and lack of sorption while the Cd and Pb values are still increasing at the end of the 10 million year simulation. Continuation of the simulation indicates peak values of 2.8 and 1.4 can be expected.

For the Soil and the Sediment criteria there are no exceedances and the highest concentration quotients are 9.0×10^{-3} for Cr and 1.7×10^{-1} for Pb in the Soil and Sediment respectively.

Although some species exceed criteria, the exceedances are judged acceptable on the basis that the amount of the exceedance is small and that the likelihood of the scenario is low. It is unlikely that all containers would fail simultaneously and a staggered failure could result in a significant broadening of the release and a subsequent reduction in the peak concentrations. It

is also possible that the assumed criteria are based on a conservative species assumption and the hazard is over-estimated.

In conclusion, the All Container Fail Scenario shows concentration quotients slightly greater than 1.0 for three species. Considering the conservatism in the model and the low likelihood of the scenario, it is concluded that the non-radiological hazard arising from this unlikely event is within acceptable risk bounds.



Note: results for As, Nd and U are off scale low

Figure 7-147: SYVAC3-CC4 - Concentration Quotient for the All Containers Fail Case

Table 7-48: SYVAC3-CC4 - Concentration Quotients for the All Containers Fail Case

Element	Water	Soil	Sediment
Ag	6.1×10^{-1}	7.8×10^{-3}	1.4×10^{-1}
As	1.5×10^{-3}	5.1×10^{-7}	5.2×10^{-6}
Cd	1.1	1.0×10^{-3}	6.9×10^{-3}
Ce	4.0×10^{-2}	5.8×10^{-3}	2.3×10^{-5}
Co	1.7×10^{-2}	3.5×10^{-5}	8.6×10^{-5}
Cr	7.6×10^{-2}	9.0×10^{-3}	1.9×10^{-4}
Eu	3.7×10^{-2}	6.4×10^{-4}	1.8×10^{-5}
Hg	3.3	9.4×10^{-4}	4.3×10^{-3}
I	6.6×10^{-3}	8.0×10^{-4}	-
La	4.4×10^{-2}	1.1×10^{-3}	3.2×10^{-5}
Nd	0	0	0
P	3.7×10^{-2}	-	-
Pb	1.6	6.8×10^{-3}	1.7×10^{-1}
Pr	4.4×10^{-2}	5.7×10^{-4}	1.5×10^{-5}
Te	1.7×10^{-2}	1.3×10^{-4}	-
U	2.3×10^{-23}	1.8×10^{-24}	-
Y	2.4×10^{-2}	3.8×10^{-4}	4.7×10^{-5}

7.11.3.2 Copper Container Chemical Hazard Assessment

Chemical elements of potential concern could also be released from the copper containers and the engineering sealing materials. While the hazard from the sealing materials is expected to be very low because the components tend to be natural clay materials, an assessment is needed to determine the hazard associated with the copper containers.

The rate of release depends on the copper corrosion rate. Although reducing conditions are expected after closure, a small amount of copper corrosion can still occur as discussed in Chapter 5. As this occurs, copper and any associated impurities are released into the buffer porewater.

In this assessment, a solubility-limited dissolution model is used to determine the corrosion rate of the copper shell and thus the corrosion rate is controlled by the rate at which copper diffuses away from the container / buffer interface. FRAC3DVS-OPG was used to model the transport of copper to the biosphere and to calculate the copper concentrations.

The transport was simulated by applying a constant concentration boundary condition of 1.4×10^{-4} mol/m³, which corresponds to the solubility limit increased by a factor of 10 to account for uncertainties in the temperature local to the container (Garisto et al. 2012), at every grid node intersecting the boreholes of the repository. This results in a continuous input of copper into the model over the course of the 10 million-year simulation.

Figure 7-148 shows the resulting copper concentration after 1 million years across the repository site. Figure 7-149 shows the transport of copper to the surface as a function of time.

To conservatively assess the concentration quotient, the maximum total flux to the surface (1.3×10^{-3} mol/a) is assumed to enter the well with the well pumping at a rate of $911 \text{ m}^3/\text{a}$. The resulting well concentration is 1.4×10^{-6} mol/ m^3 or 9.1×10^{-2} $\mu\text{g}/\text{L}$ resulting in a Water concentration quotient of 9.1×10^{-2} .

To estimate the maximum Sediment concentration the well concentration of 1.4×10^{-6} mol/ m^3 was multiplied by the sorption coefficient for Sediment. Sediment has a higher sorption coefficient than Soil for copper and Soil can therefore be expected to have a lower concentration. For copper, the Sediment K_d is $0.37 \text{ m}^3/\text{kg}$ and the Soil K_d is $0.03 \text{ m}^3/\text{kg}$ resulting in maximum concentrations of 3.3×10^{-2} $\mu\text{g}/\text{g}$ and 2.7×10^{-3} $\mu\text{g}/\text{g}$. This results in concentration quotients of 5.3×10^{-4} for Soil and 2.1×10^{-3} for Sediment.

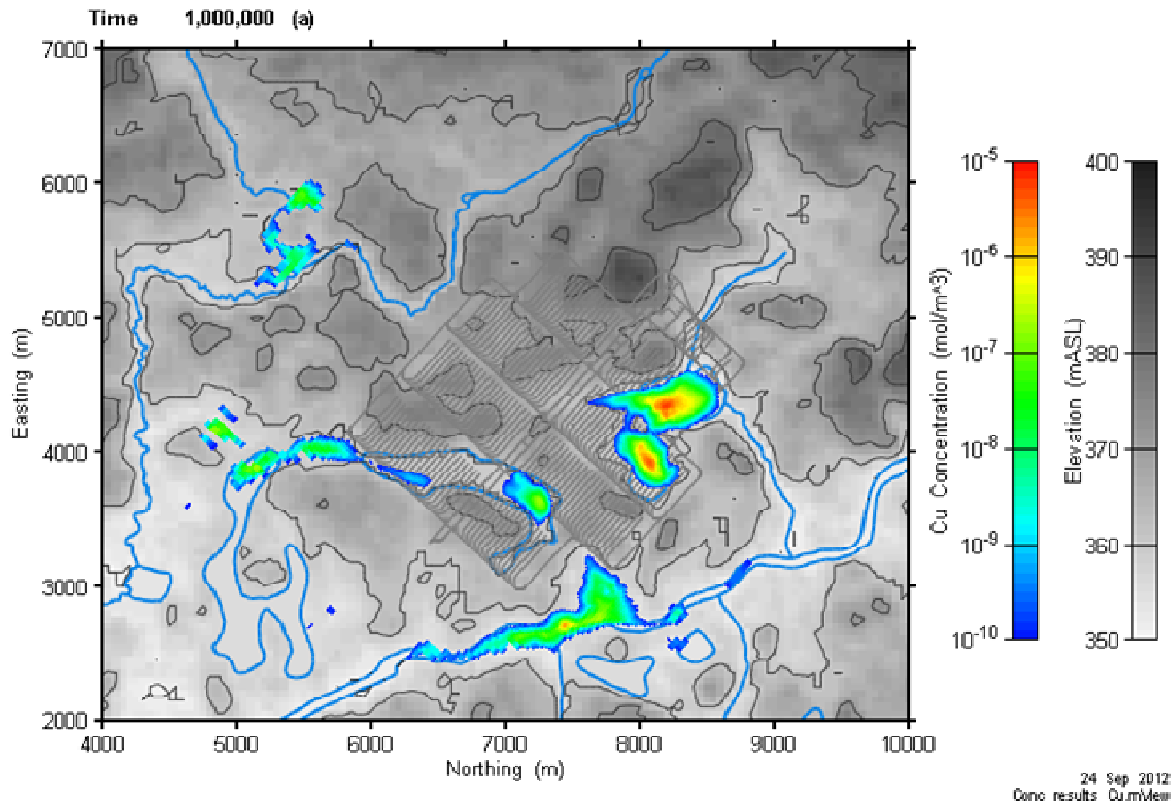


Figure 7-148: FRAC3DVS-OPG - Cu Concentration Over the Repository Site

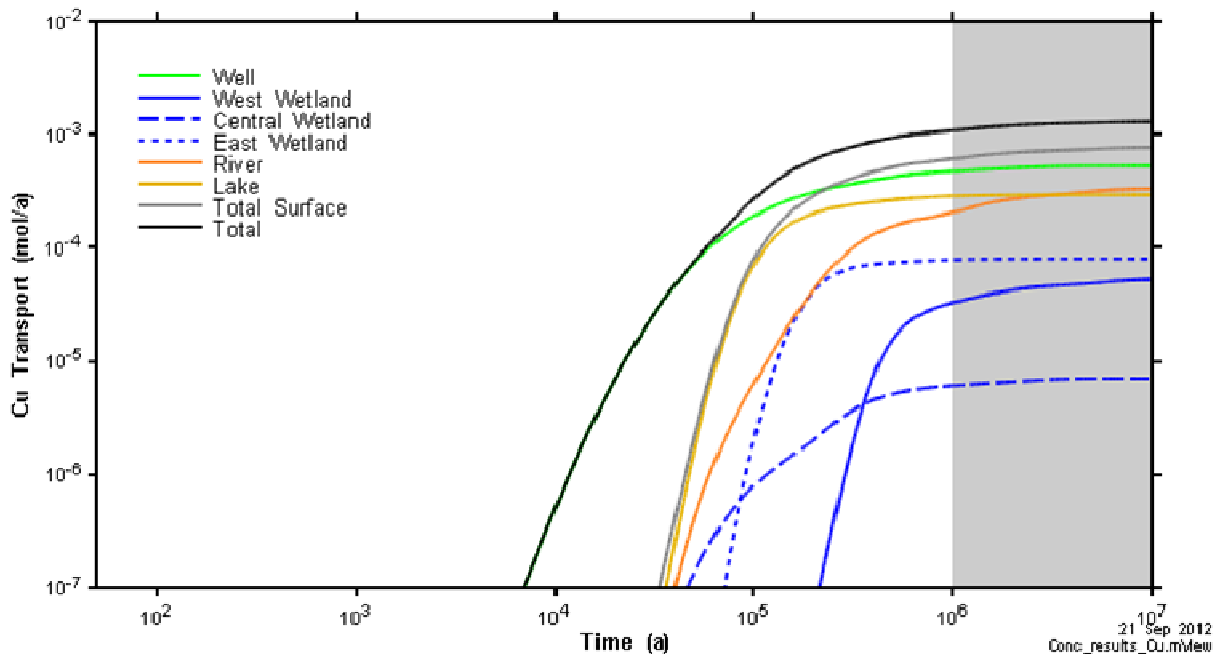


Figure 7-149: FRAC3DVS-OPG - Cu Transport to the Surface

Chemical element impurities are present in the copper at the levels shown in Table 7-49 (SKB 2010b and SKB 1998). These impurities are also released as the copper corrodes. The concentrations of these elements in well water and surface waters were estimated as the product of the concentration of copper in the water body. The calculation of copper impurity concentrations assumes the impurities are transported with the copper. Element specific K_d values in the buffer and geosphere for the impurities may produce some variation in the transport time but since the chemical species do not decay, peak impurity concentrations are largely independent of transport times.

The well water and surface water concentration quotients for the impurity elements were determined from the estimated well water concentration of these elements and are shown in Table 7-49. Since these concentrations quotients are all well below 1.0, it is concluded that these elements would not pose a health and safety hazard to persons or to the environment.

Several other impurities (Bi, Fe, S, Se, Ni, Si, Sn, and Zn) for which chemical toxicity criteria have not been defined are also present in the copper at concentrations ranging from 1 to 20 ppm. Based on the analysis of the other elements the effect of these impurities is expected to be negligible on the overall chemical hazard.

Table 7-49: SYVAC3-CC4 - Concentration Maximum Impurity Levels in Copper and Estimated Impurity Element Concentration Quotients for Well Water

Element	Maximum Impurity Level ¹ [ppm]	Impurity Level [mol/mol Cu]	Estimated Maximum Element Concentration in Well Water [mol/m ³]	Estimated Maximum Water Concentration Quotient
Cu	-	-	1.4×10^{-6}	8.9×10^{-2}
Ag	25	1.5×10^{-5}	2.1×10^{-11}	2.2×10^{-5}
As	5	4.2×10^{-6}	5.9×10^{-12}	8.9×10^{-8}
Cd	1	5.7×10^{-7}	7.9×10^{-13}	5.2×10^{-6}
Co	20	2.2×10^{-5}	3.0×10^{-11}	2.0×10^{-6}
Cr	15	1.8×10^{-5}	2.6×10^{-11}	1.3×10^{-6}
Hg	1	3.2×10^{-7}	4.4×10^{-13}	2.2×10^{-5}
P	100	4.6×10^{-5}	6.4×10^{-11}	8.8×10^{-7}
Pb	5	1.5×10^{-6}	2.1×10^{-12}	4.5×10^{-7}
Te	2	1.0×10^{-6}	1.4×10^{-12}	8.9×10^{-9}

Note: ¹ Impurity level for P is from SKB (2010b) others remain unchanged from SKB (1998).

7.11.3.3 Complimentary Indicators

Natural processes carry small amounts of naturally occurring chemical elements from within the geosphere to the surface. Reference values for natural chemical element fluxes to the biosphere can be obtained using the elemental composition of Canadian Shield granites and the erosion rate of granite over long time periods.

The average erosion rate on the Canadian Shield due to wind and water is estimated as 6.5×10^{-6} m/a (Merrett and Gillespie 1983). Assuming the erosion rate is constant over a watershed area of 16 km^2 (i.e., approximately the area encompassing the repository and its surface discharges) and using a granite density of 2700 kg/m^3 , an erosion rate of about $2.8 \times 10^5 \text{ kg/a}$ can be determined.

Table 7-50 lists the concentration of some of the chemical elements of potential concern in Canadian Shield surface granite. Using these values and the erosion rate, the chemical element fluxes from the geosphere can be calculated. The results of this calculation are shown in Table 7-50 for All Containers Fail Scenario Disruptive Scenario.

The results indicate that even under the conservative assumptions of the All Containers Fail Scenario, the element fluxes to the biosphere are generally much smaller than the corresponding erosion fluxes. The ratio of the calculated peak element flux is largest for Te (with a value of 0.84), mainly because the natural erosion flux of tellurium is the lowest. This adds confidence to the conclusion that the potential chemical hazard from the repository is not likely not significant even for the All Containers Fail Scenario.

Table 7-50: Erosion Fluxes out of the Geosphere

Element	Canadian Shield Surface Granite ¹ [g/Mg]	Canadian Shield Erosion Flux [mol/a]	All Containers Fail Flux to Surface [mol/a]	Ratio of All Containers Fail Flux to Erosion Flux
Ag	4.0x10 ⁻²	1.0x10 ⁻¹	2.0 x10 ⁻³	1.9 x10 ⁻²
As	1.5x10 ⁰	5.6x10 ⁰	3.5 x10 ⁻⁴	6.3 x10 ⁻⁵
Cd	9.0x10 ⁻²	2.5 x10 ⁻¹	6.8 x10 ⁻⁴	2.7 x10 ⁻³
Ce	1.7x10 ²	3.4 x10 ²	1.8 x10 ⁻²	5.2 x10 ⁻⁵
Co	9.1x10 ⁰	4.3 x10 ¹	1.1 x10 ⁻³	2.5 x10 ⁻⁵
Cr	8.1x10 ⁰	4.4 x10 ¹	5.2 x10 ⁻³	1.2 x10 ⁻⁴
Eu	8.7x10 ⁻¹	1.6 x10 ⁰	7.4 x10 ⁻³	4.6 x10 ⁻³
Hg	8.0x10 ⁻²	1.1 x10 ⁻¹	1.9 x10 ⁻⁴	1.7 x10 ⁻³
I	2.0x10 ⁻¹	4.4 x10 ⁻¹	1.6 x10 ⁻²	3.7 x10 ⁻²
La	1.0x10 ²	2.0 x10 ²	9.7 x10 ⁻³	4.8 x10 ⁻⁵
Nd	5.8x10 ¹	1.1 x10 ²	2.4 x10 ⁻⁷	2.2 x10 ⁻⁹
P	3.1x10 ²	2.8 x10 ³	1.7 x10 ⁻²	6.1 x10 ⁻⁶
Pb	1.2x10 ¹	2.4 x10 ¹	4.4 x10 ⁻²	1.8 x10 ⁻³
Pr	1.2x10 ¹	2.4 x10 ¹	8.7 x10 ⁻³	3.6 x10 ⁻⁴
Te	5.0x10 ⁻³	1.1 x10 ⁻²	9.3 x10 ⁻³	8.4 x10 ⁻¹
U	5.9x10 ⁰	7.0 x10 ⁰	5.2 x10 ⁻⁹	7.5 x10 ⁻¹⁰
Y	2.4x10 ¹	7.6x10 ¹	5.3x10 ⁻³	6.9x10 ⁻⁵

Note: ¹ Data are from Flavelle (1996) except Hg and Te which are from Bowen (1979).

7.11.4 The Effects of Gas Generation

Gas will be generated in the repository due to corrosion of metals, degradation of organic materials, radiolysis of water, and radioactive decay. The potential impacts of gas generation have been studied internationally (ANDRA 2005, NAGRA 2008, Mallants and Jacques 2004, SKB 1999). Among the potential impacts, the key ones are mechanical damage of the engineered barriers and host rock due to high gas pressures, modifications to groundwater flow and contaminant transport, gas release to the biosphere, and chemical effects of the gas on repository conditions.

This section describes calculations performed to estimate the potential effects of gas generation on the calculated dose consequences. The Reference Case of the Normal Evolution Scenario and the All Containers Fail Disruptive Event Scenario are considered. For these calculations the gas generated in a given placement room is conservatively assumed to be confined to only that room due to the presence of a seal at the end of the room. Additional void volume present in the tunnels and access drifts is assumed inaccessible and the gas generated is discussed on

a per room basis. The Reference Case examines the case with three containers failing in a single room while the All Containers Fail Scenario examines the case with 80 containers failing in every room.

7.11.4.1 Gas Generation from Metals and Organics

Approximately 51,000 kg of steel is available for gas generation in a placement room containing three defective containers. The three containers account for 74% of the total steel available for corrosion with the remainder due to rock bolts.

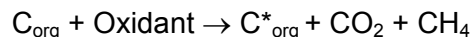
The steel surface area available for corrosion inside each container is approximately 29 m² (assuming both sides of the container insert are exposed to water) for a total of 86 m² for three failed containers. The rock bolt assemblies present in each placement room amount to a significant amount of steel and for conservatism the entire rock bolt is assumed available for corrosion. This results in an additional 282 m² available for corrosion due to the assumed presence of 843 rock bolt assemblies.

Under the anaerobic conditions expected in the repository, hydrogen is produced by corrosion of steel following the reaction:



Approximately 15,000 kg of organic carbon is also present, almost all of which is found in the buffer and backfill materials. The dense backfill is a 5:25:70 mix of MX-80 bentonite, Lake Agassiz glacial clay and granite sand while the gap fill consists of small MX-80 bentonite pellets. The organic carbon content of MX-80 bentonite is 2000 ppm (SKB 2004) and that of Lake Agassiz glacial clay is 1200 ppm by weight (Stroes-Gascoyne et al. 1997). Granitic sand is assumed to have 30 ppm organic carbon (Stroes-Gascoyne et al. 1996).

Organic materials will also degrade under anaerobic conditions. Degradation of organics in clay is modelled as:



where C_{org} and C^*_{org} denote initial organics and residual organics after degradation. For simplicity, equal amounts of CO₂ and CH₄ are assumed to be produced and for conservatism, it is assumed that all organic carbon is consumed (i.e., all the organics are decomposable and no residual organic is formed). This is conservative since most of these organics would have been present in the natural clay materials for millions of years, so are probably in a low decomposition form.

Gas generation rates are calculated assuming that steel corrodes at a rate of 1 μm/a and that the organic carbon in the bentonite and aggregate sealing materials degrade at a rate of 10⁻⁶/a and 10⁻⁴/a, respectively. The estimated initial (i.e., maximum) gas generation rates are therefore 69 mol/a H₂ from steel corrosion and a total of 113 mol/a of CO₂ and CH₄ from degradation of organics. The total maximum gas generation rate from corrosion and degradation of organics is therefore 182 mol/a or 4.4 m³/a at standard temperature and pressure (STP) in a placement room with three defective containers.

Gas generation is assumed to continue until all steel inside the placement room has corroded (after about 1.8×10^4 years) and all organic material has degraded (after 10^6 and 10^4 years for the organics in the bentonite and aggregate clay materials). The cumulative volume of gas generation is therefore about $9.1 \times 10^4 \text{ m}^3 @ \text{STP}$ with H_2 from steel corrosion contributing ~32% and CO_2 and CH_4 from organic degradation each contributing ~34% to the total gas volume.

In the event that all the containers fail the number of container inserts available for corrosion in the placement room increases from 3 to 80. In this case the total initial gas generation rate from corrosion and organic degradation increases to roughly 479 mol/a or $\sim 14 \text{ m}^3/\text{a} @ \text{STP}$ for one placement room. The total amount of gas generated in one placement room is approximately $6.5 \times 10^5 \text{ m}^3 @ \text{STP}$ with H_2 from corrosion contributing roughly 91% and CO_2 and CH_4 from degradation of organic carbon each contributing an equal share of the remainder (~4.5% each).

Note that this assessment conservatively ignores the methanogenesis reaction, $4\text{H}_2 + \text{CO}_2 > \text{CH}_4 + 2\text{H}_2\text{O}$. This exothermic reaction, used by methanogenic bacteria as energy source, reduces the total inventory of gas.

7.11.4.2 Gas Generation from Radiolysis and Decay

Radiolysis can also generate gas. Radiolysis of water inside the three defective containers could contribute a significant amount of hydrogen gas to the system at early times; however, due to diminishing radiation fields the production rate rapidly decreases with time. For example, 100 years after closure, radiolysis could contribute an additional 42 mol/a (roughly 23% of the maximum gas generation rate from corrosion and degradation of organics) while 1000 years after closure the gas generated by radiolysis would decrease to roughly 18 mol/a (approximately 10% of the maximum gas generation rate). By 60,000 years, radiolysis would contribute an additional 2.6 mol/a with three failed containers (1.4% of the maximum generation rate). If all containers fail at 60,000 years the rate would increase to 69 mol/a or 14% of the maximum gas generation rate for the all containers fail case.

Because the amount of gas generated by radiolysis is significant on times scales relevant for steel corrosion, the maximum gas generation rate from radiolysis is conservatively added to the total gas generation rate. As a result the maximum Reference Case gas generation rate is increased by 42 mol/a to 224 mol/a and the maximum All Containers Fail Case gas generation rate is increased by roughly 69 mol/a to 549 mol/a.

He and Rn are also generated by decay of actinides in the fuel; however, the amount of these gases is relatively small and they are neglected.

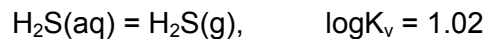
Outside the containers the radiation fields are low due to attenuation by the thick container walls. Gas generation by radiolysis occurring outside the containers is therefore neglected.

7.11.4.3 Volatilization of H_2S

While the primary contributors to the gas pressure in the repository are expected to be H_2 , CO_2 and CH_4 , it is possible that hydrogen sulphide could also be present. Hydrogen sulphide, H_2S , is slightly soluble in water and is formed by the reduction of sulphate in the groundwater by microbes. Sulphate reducing bacteria are unlikely to be present in the repository due to the high swelling pressure of the engineered sealing materials; however outside the engineered sealing

materials the concentration of H₂S could be up to 3 ppm (Tullborg et al 2010) and the contribution of H₂S to the gas pressure cannot be neglected outright. This section estimates the H₂S contribution to the total gas pressure in the repository.

The vapour pressure of H₂S(g) in equilibrium with a given concentration of H₂S(aq) can be determined by using the equilibrium constant for the reaction:



The values of the equilibrium constant K_v is taken from Hummel et al. (2002).

The volatility of an aqueous solution of hydrogen sulphide will be highest when H₂S(aq) is the dominate species in solution (i.e., at pH values less than about 6, based on the first reaction shown above. Based on the this reaction, the partial pressure of H₂S(g), p(H₂S(g)), at equilibrium with a given concentration of H₂S(aq), [H₂S(aq)], is given by the following equation

$$p(\text{H}_2\text{S(g)}) = 10^{1.02} [\text{H}_2\text{S(aq)}]$$

where the partial pressure p(H₂S(g)) is in units of bar (0.1 MPa) and [H₂S(aq)], the concentration of H₂S(aq) in solution, is expressed in units of mol/kg.

If the hydrogen sulphide concentration in solution is 3 ppm (3 mg/kg) or 9.1x10⁻⁵ mol/kg, then the partial pressure of H₂S(g) would be 9.5x10⁻⁴ bars or 9.4x10⁻⁴ atm. This vapour pressure is very small compared to the total gas pressure in the repository and can therefore be neglected.

7.11.4.4 Gas Release and Migration

A number of mechanisms exist by which the gas can escape into the host rock. To evaluate the relative importance of the different release mechanisms, scoping calculations have been done with results compared against the gas generation rates.

Gas Migration by Diffusion and Advection

Gas generated in the repository may dissolve in the groundwater and then diffuse or advect away. For the conceptual repository in this study, the engineered barrier system has a very low hydraulic conductivity and there is a small head differential across the repository.

The maximum amount of dissolved gas that can be removed by diffusion and advection can be estimated using Henry's Law. Based on a Henry's law constant for H₂ of 2x10⁻⁷ m³@STP/m³/Pa, and an effective diffusivity of 3x10⁻⁵ m²/a, the diffusive transfer rate can be estimated as 6x10⁻⁸ m³@STP/m²/a. The advective transfer rate is assumed to be zero due to the low hydraulic conductivity of the engineered barrier materials. The total gas generation rates (approximately 7.2x10⁻⁴ m³@STP/m²/a for the Reference Case and 2.1x10⁻³ m³@STP/m²/a for the All Containers Fail Case) are greater than the rate at which dissolved gases can escape and it is therefore concluded that a H₂ gas phase is likely to be formed. A similar conclusion can be drawn for the CO₂ and CH₄ gases generated by degradation of organics in the sealing materials.

This conclusion is consistent with other studies that show, in general, that diffusion of dissolved gas in groundwater does not provide a significant contribution to the bulk gas flux through the

near field and does not prevent gas phase formation (ANDRA 2005, NAGRA 2008, Mallants and Jacques 2004, and SKB 1999).

Gas Formation and Transport

Because the diffusive and advective fluxes are insufficient to remove the gases, a gas phase will form in the repository after the porewater becomes saturated with dissolved gas. The gas pressure could likely then build up until it is sufficient to overcome the threshold pressure of the repository engineered materials (buffer and backfill) and the surrounding host rock. The escaping gas could then enter the geosphere, and permeate (two-phase flow) through the rock.

Gas Transport through Bentonite

Gas transport through clay-based buffer and backfill materials is a complex process. It is known that a certain threshold pressure must be exceeded for gas to move through these materials. Gas propagation and penetration may be controlled by capillary retention, by the tension strength of the clay matrix, and by the swelling pressure (Pusch 2003). Early experiments and models suggested that the threshold pressure for water-saturated bentonite is approximately the sum of the hydrostatic and swelling pressures (SKB 1999).

While later experiments, such as LASGIT at the Äspö Hard Rock Laboratory in Sweden, have indicated this is too simple a model, the threshold pressure is in this range. Also, after the gas passes through the water-saturated bentonite buffer, evidence from laboratory tests suggest that the buffer will reseal (Hoch et al. 2004), with restoration of the hydraulic and transport properties that it possessed prior to the passage of gas.

Based on this information, it is anticipated that a gas transport pathway will be formed through the buffer annulus after the pressure around the container exceeds a threshold value. Once the gas passes through, the pressure near the container decreases significantly and the pathway is anticipated to close. If gas generation continues, a cycle may occur with successive pressure build ups and gas release.

Gas Transport through Host Rock

The host rock is a porous medium, with existing fractures and bulk rock porosity. Gas flow can occur in a porous medium if the following resistances are overcome:

- the capillary resistance as the gas-water interface moves through the pore or fracture constrictions, and
- the hydrostatic head and viscous resistances to water flow, so that water is displaced from the pathways.

For the bulk granitic rock at the repository level, the estimated threshold capillary pressure ranges from about 0.5 to 3 MPa, depending on the permeability (EC 2003). Given the permeability at repository depth a reference capillary pressure of 3 MPa is adopted. In contrast, the estimated threshold capillary pressure for fractures is of the order of a few kPa, substantially lower than for bulk rock. Therefore, fractures, if encountered, would be the dominant gas migration pathway.

If it is assumed that the gas travels vertically through the homogeneous rock from which water has been at least partially displaced, a simple model, based on Darcy's law, can be used to estimate the flux of gas (Rodwell and Nash 1992). If the repository gas pressure exceeds the threshold capillary pressure of the overlying rock, the estimated gas release flux through the host rock is approximately $3 \text{ m}^3\text{@STP}/\text{m}^2/\text{a}$ (assuming the Reference Case hydraulic conductivity). If the hydraulic conductivity is reduced to that of Sensitivity Case 3 (i.e., by a factor of 100) the gas flux through the host rock could be reduced to $0.03 \text{ m}^3\text{@STP}/\text{m}^2/\text{a}$. Even with this very conservative estimate, the gas release flux exceeds the estimated gas generation flux by a factor of 41 for the Reference Case and by a factor of 14 for the All Containers Fail scenario. It is therefore anticipated that most of the gas reaching the buffer / rock interface will escape via the host rock after the gas overpressure in the repository exceeds the gas threshold pressure.

The results from this assessment are consistent with other calculations that show that gas generated in a geological repository is likely to escape through most fractured crystalline rocks without an extreme gas pressure build up (SKB 1999).

It is therefore concluded that gas release via the host rock is sufficient to remove gas generated in the repository for both the Reference Case and the All Containers Fail Disruptive Event Scenario. Pressure outside the buffer and backfill will be limited by the threshold capillary pressure in the host rock. To damage the host rock the gas pressure will have to approach the lithostatic pressure which is estimated to be about 13 MPa. For this reason, it is also concluded that gas build up in the repository is insufficient to mechanically damage the host rock.

7.11.4.5 Evaluation of Potential Gas Generation Impacts

The possible impacts of gas generation in geological repositories have been previously identified in a number of review studies and safety assessments (EC 2003, Cool et al. 2004, Rodwell et al. 2000). Based on the assessment described above, some impacts are likely to be insignificant (e.g., mechanical damage to the host rock) so that only the potential impacts due to fires / explosions, releases of radioactive gases and the effect on container evolution need to be considered further.

Fire and Explosion Impact

If the repository pressure exceeds the capillary threshold pressure of the bulk granitic rock, gases could be released via the bulk rock / fractures to the surface. This assessment assumes that a direct path from the repository to the surface could be created and that a house is situated on top of the repository. Gases released to the surface can infiltrate into this house, which is assumed to have a volume of 228 m^3 , a floor area of 95 m^2 , and an air exchange rate of $7 \times 10^5 \text{ m}^3/\text{a}$ (Garisto et al. 2012).

Hydrogen and methane pose a potential explosion hazard in air if they accumulate to a level within the flammable range and if there is an ignition source. The flammable range in air (by volume) is between 4% and 74% for hydrogen (Air Product and Chemicals, 1994), and between 5% and 15% for methane (Air Products and Chemicals, 1999).

The gas inflow rate needed to achieve the lower limits of flammability is $2.8 \times 10^4 \text{ m}^3\text{@STP}/\text{a}$ for H_2 and $3.5 \times 10^4 \text{ m}^3\text{@STP}/\text{a}$ for CH_4 . These rates are substantially higher than the maximum

total gas generation rate from the placement rooms in the repository (about 639 m³@STP/a for the Reference Case and 2600 m³@STP/a for the All Containers Fail Disruptive Event Scenario).

It is therefore highly unlikely that significant flammable concentrations of hydrogen or methane would be produced and it is therefore concluded that a significant fire or explosion hazard in the biosphere does not exist.

Potential Dose Impact of Gas Release to Accessible Environment

The radiological impact of a release of C-14 gas (as CO₂ and CH₄) into the biosphere is considered here. The radiological impact of Rn-222 releases are not calculated because Rn-222 has a short half-life (3.8 days) and is expected to decay to negligible concentrations before reaching the surface.

To calculate the C-14 doses, radioactive decay and the transport time through the geosphere are ignored and it is conservatively assumed that all C-14 in the repository (496 moles or 1.15x10¹⁵ Bq) is released with the CO₂ and CH₄ gases and that the release rate of CO₂ and CH₄ into the biosphere is equal to their maximum production rates (i.e., 1×10¹¹ Bq/a). The gases are homogeneously released from the ~4 km² repository footprint and seep into the house resulting in an inhalation exposure pathway. As in the fire and explosion assessment, the house is assumed to have a volume of 228 m³, a floor area of 94 m², and an air exchange rate of 7x10⁵ m³/a (Garisto et al. 2012). The adult house dweller has a breathing rate of 0.96 m³/h and spends roughly 80% of the year (7000 hrs) indoors (Garisto et al. 2012). The adult inhalation dose coefficient for C-14 (as CO₂) is 1.2x10⁻¹¹ Sv/Bq (CSA 2008).

The equilibrium concentration of radionuclides in the house can be calculated from the floor area, the volume of the building, the flux of radioactive gases up through the geosphere and the building exchange rate. Based on these very conservative assumptions, the C-14 concentration in the house is estimated as 2.0 Bq/m³ and the C-14 inhalation dose rate for an adult living in the house is about 1.6x10⁻⁷ Sv/a. Since this dose rate is well below the interim dose acceptance criterion of 3x10⁻⁴ Sv/a the radiological impact of C-14 gas releases to the surface is deemed negligible.

Note that for the Reference Case, only three containers are assumed to fail and so the C-14 dose rates would be considerably lower.

Effect of Gas Generation on Container Evolution

Ingress of water into the failed containers will cause anaerobic corrosion of the inner steel vessel and generation of hydrogen (McMurry et al. 2004). If the gas pressure in the container becomes sufficiently high, it could affect the evolution of the container (i.e., the time needed for water to fill the container and for the defect in the copper shell to grow larger (SKB 1999, Section 9.6)). Experimental evidence also exists to show that the presence of hydrogen in the failed containers causes the dissolution rate of the used fuel to decrease (Shoesmith 2008, King and Shoesmith 2004, Spahiu and Sellin 2001, Spahiu et al. 2000).

These effects have been neglected in this report.

7.12 Summary and Conclusions

This section summarizes the postclosure safety assessment.

7.12.1 Scope Overview

The Normal Evolution Scenario represents the normal (or expected) evolution of the site and facility. Disruptive Event Scenarios consider the effects of unlikely events that lead to possible penetration of barriers and abnormal degradation and loss of containment.

Section 7.2 discusses the detailed scope of the assessment. Both Normal Evolution and Disruptive Event Scenarios are considered.

The containers are robust and there would be multiple inspection steps to ensure they are fabricated and placed correctly. However, with the large number of containers, it is possible that some containers could be placed with undetected defects. In particular, based on a simple estimate of the likelihood of failure in the copper shell welding and inspection process (i.e., 1/5000, Maak et al. 2001), statistically there could be three containers with undetected defects placed in the repository. For the assessment of the Normal Evolution Scenario, it is assumed that three containers with undetected defects are present in the repository at the time of closure.

Recognizing that the geosphere characteristics at a candidate site and the design of the repository may be different from the reference conditions assumed in this study, a number of sensitivity cases are also examined to illustrate the function of various engineered and natural barriers. Both deterministic and probabilistic simulations are conducted.

In the deterministic simulations, parameter variations are performed about a Reference Case of the Normal Evolution Scenario, where the Reference Case has the following attributes:

- Geosphere properties as per Chapter 2;
- Used fuel inventories as per Chapter 3;
- Repository design as per Chapter 4;
- Three containers each with an undetected defect placed in the repository at the location with the shortest groundwater transport time to the surface;
- Defect radius = 1 mm, no evolution of the defect size with time;
- No other container failures occur;
- Groundwater fills the defective containers 100 years after the containers are placed in the repository;
- Constant temperate climate and steady-state groundwater flow;
- Self-sufficient farming family growing crops and raising livestock on the surface above the repository;
- Drinking and irrigation water for the family obtained from a 100 m deep well located along the main pathway for contaminants released from the defective containers;
- The well is pumping at a rate of 911 m³/a. This is sufficient for drinking water and irrigation of household crops; and
- Input parameters that are represented by probability distributions are set to either the most probable value (when there is one) or to the median value otherwise.

The deterministic sensitivity cases are:

- Fuel dissolution rate increased by a factor of 10;
- Instant release fractions set to 0.10 for all radionuclides;
- Container defect area increased by a factor of 10;
- No solubility limits in the container;
- No sorption in the near field;
- Fracture location moved with respect to the nearest part of the repository;
- Geosphere hydraulic conductivity increased and decreased from the Reference Case value (3 cases investigated);
- No sorption in the geosphere;
- Hydraulic conductivity of the excavation damage zone and thermal damage zone increased by a factor of 10; and
- Low sorption in the geosphere with coincident high solubility limits in the container.

For the probabilistic simulations, random sampling is used to simultaneously vary all input parameters for which probability distribution functions are available.

These deterministic and probabilistic cases are described in detail in Table 7-3.

An assessment based on the results of an existing study performed for a similar crystalline rock geosphere is used to discuss the anticipated effects of glaciation.

Results are generated for two complementary indicators of radiological safety. Results are also generated to address the radiological protection of the environment, and the protection of persons and the environment from hazardous substances. A complementary indicator of safety for hazardous substances is also evaluated.

Finally, the consequences of gas generation caused by decomposition of organics and by corrosion of steel in the defective containers and rock bolts are determined.

The Disruptive Scenarios examined are:

- Inadvertent Human Intrusion;
- All Containers Fail at 60,000 Years (with a sensitivity case that has the failure occurring at 10,000 years);
- Fracture Seal Failure and its variant case in which the fracture seals and the repository tunnel and room seals degrade rapidly and extensively; and
- Shaft Seal Failure.

These scenarios are described in detail in Table 7-4. All Disruptive Scenarios are analysed with deterministic methods only.

The consequences of gas generation caused by corrosion of steel in the defective containers and rock bolts left in the repository at closure are discussed for the All Containers Fail Years scenario.

Some additional sensitivity cases were simulated in the course of the analysis as issues emerged that challenged the integrity of the simulations. These cases are listed below and further described in Table 7-5:

- Discrete Fracture Network (DFN) modelling compared with the Equivalent Porous Media (EPM) approach; and
- Increased spatial resolution and increased number of time steps to confirm model convergence.

Neither of the modelling choices had any material effect on the results and they are therefore not discussed further.

7.12.2 Results for the Normal Evolution Scenario

Reference Case

Section 7.8.2.1 reports the peak dose rate for the Reference Case of the Normal Evolution Scenario as 3.3×10^{-7} Sv/a occurring at 1.0×10^5 years. This is well below the average Canadian background dose rate of 1.8×10^{-3} Sv/a and is a factor of 910 times less than the 3×10^{-4} Sv/a interim dose acceptance criterion established in Section 7.1.1 for the radiological protection of persons.

The analysis shows that I-129 is the dominant contributor to dose rate in the timeframe of interest (i.e., up to one million years), followed by C-14 and Cs-135. This is because I-129 has a sizeable initial inventory, a non-zero instant release fraction, a very long half-life, is non-sorbing in the buffer, backfill and geosphere and has a radiological impact on humans. All other fission products and actinides either decay away, or are released very slowly as the fuel dissolves and are thereafter sorbed in the engineered barriers and geosphere.

Section 7.10 discusses the anticipated effects of glaciation. The discussion concludes that the peak dose rate could increase by an order of magnitude depending on the glacial cycle. Nevertheless, given the wide margin available, the dose rate would remain well below the interim dose acceptance criterion when the effects of glaciation are considered.

Section 7.11.1 presents results for the two complementary indicators determined using releases from the Reference Case. These indicators (i.e., radiotoxicity concentration in a water body) and radiotoxicity transport from the geosphere) supplement the dose rate indicator using system characteristics that are much less sensitive to assumptions regarding the biosphere and human behaviour. The discussion shows that both indicators are well below their reference values, thereby providing additional confidence that at long times the impact of the repository is likely to be very small.

Section 7.11.2 presents results addressing the radiological protection of the environment (i.e., on non-human biota). The discussion concludes that these effects are negligible for the Normal Evolution Scenario.

Section 7.11.3 discusses the protection of persons and the environment from hazardous substances. Such non-radiological hazards effects could arise due to release of copper and

other potentially hazardous elements from the containers and used fuel. The discussion concludes that the non-radiological hazard is negligible for the Normal Evolution Scenario.

Section 7.11.4 discusses the anticipated effects of gas generation and migration. Gas can be generated through corrosion of steel in the defective containers, through corrosion of rock bolts left in the repository at the time of closure and through the degradation of organic material in the buffer and backfill materials. The discussion concludes that no adverse consequences to either the repository or to persons living above the repository are anticipated.

Sensitivity Cases

Section 7.7.2.2 and Section 7.8.2 present radionuclide transport results for the deterministic sensitivity cases examining the effects of degraded physical barriers, degraded chemical barriers and increased geosphere hydraulic conductivity. These results are summarized in Table 7-51. The table shows the peak impacts (expressed in Bq/a I-129 or in Sv/a), the time of the peak impact, the effect of the parameter variation on the Reference Case result and the factor by which the result is below the interim dose acceptance criterion for the radiological protection of persons. Results are shown in Bq/a I-129 for FRAC3DVS-OPG simulations because this groundwater flow and transport model does not have biosphere and dose models. Inferences on dose impacts can be made from the I-129 transport results by comparison to cases for which both I-129 transport (In Bq/a) and dose rates (in Sv/a) are calculated.

Table 7-51: Result Summary

Case	Time of Peak Impact (a)	Peak Impact*		Ratio to Reference Case ⁺	Factor to Dose Limit
		I-129 (Bq/a)	Dose (Sv/a)		
Reference Case of the Normal Evolution Scenario	100,000	1675	3.3x10⁻⁷	-	910
Geosphere Sensitivity Cases					
Geosphere Conductivity (Sensitivity 1)	70,000	1083	8.6x10 ⁻⁷	2.6	350
Geosphere Conductivity (Sensitivity 2)	375,000	1318	-	0.8	1200
Geosphere Conductivity (Sensitivity 3)	1,150,000	602	-	0.4	2500
Fracture Location (10 m distance)	95,000	1692	-	1.0	900
EDZ and TDZ Conductivity 10 times Higher	88,000	1681	-	1.0	900
Degraded Physical Barrier Sensitivity Cases					
Fuel Dissolution Rate 10 times Higher	100,000	-	2.4x10 ⁻⁶	7.3	130
Container Defect Area 10 times Higher	45,000	-	8.6x10 ⁻⁷	2.6	350
Instant Release Fraction set to 10%	72,000	-	4.8x10 ⁻⁷	1.5	630
Degraded Chemical Barrier Sensitivity Cases					
No Sorption in the Geosphere	48,000	-	6.8x10 ⁻⁵	210	4.4
No Solubility Limits	100,000	-	3.9x10 ⁻⁷	1.2	770
No Sorption in the Near Field	84,000	-	6.2x10 ⁻⁶	19	48
Low Sorption in the Geosphere With Coincident High Solubility Limits	100,000	-	5.2x10 ⁻⁷	1.6	580
Probabilistic Simulations					
All parameters varied (95 th percentile)	-	-	1.3x10 ⁻⁶	4.0	230
Disruptive Event Scenarios					
All Containers Fail at 60,000 Years	79,000	-	5.8x10 ⁻⁴	N/A	1.7
All Containers Fail at 10,000 Years	32,000	-	7.9x10 ⁻⁴	N/A	1.3
Fracture Seal Failure	100,000	1675	-	N/A	3030
Fracture Seal Failure Variant Case	98,000	1677	-	N/A	3030
Shaft Seal Failure	100,000	1675	-	N/A	3030

Notes:

* The peak impacts are determined from simulations performed with either the FRAC3DVS-OPG code or the SYVAC3-CC4 code. The FRAC3DVS-OPG model does not have biosphere and dose models and therefore results are presented for I-129 transport to the surface. This is a reasonable surrogate for dose because SYVAC3-CC4 simulations show that I-129 is the dominant dose contributor.

** Inferred from I-129 (Bq/a) transport result

+ N/A: not applicable

Geosphere Sensitivity Cases

These cases examine the individual effects of increasing and decreasing the hydraulic conductivity of the host rock, reducing the distance between the repository and the nearest

conductive fracture and increasing the hydraulic conductivity of the EDZ and TDZ regions within the repository. Results indicate a relative insensitivity to these changes. Key features to note are:

- For the increase in geosphere hydraulic conductivity associated with “Sensitivity 1” (i.e., 10 times higher than the Reference Case at repository level), the Reference Case calculated dose rate is only increased by a factor of 2.6. This is because the 70,000 year transport time to the surface, although shorter than the Reference Case result of 100,000 years, remains sufficiently long that shorter-lived fission products have time to decay away. Actinides and most of the remaining longer-lived fission products are sorbed in the engineered barriers and geosphere and do not reach the surface biosphere. The increase in dose occurs because less time is available for decay C-14 and Sn-126.
- Despite the reduction in the assumed distance between the transmissive fracture and the nearest part of the repository (i.e., to 10 m from 25 m), the transport time is almost unchanged and the Reference Case result is essentially unaffected.

Degraded Physical Barrier Sensitivity Cases

These cases examine the individual effects of increasing the fuel dissolution rate, increasing the container defect area and increasing the instant release fractions. Key features to note are:

- Increasing the fuel dissolution rate by a factor of 10 increases the calculated dose rate by a factor of 7.3 compared to the Reference Case. Even with this increase, the dose consequence remains a factor of 130 times below the interim dose acceptance criterion; and
- The other sensitivity cases have less pronounced effects and their associated dose rates remain well below the interim dose acceptance criterion.

Degraded Chemical Barrier Sensitivity Cases

These cases examine the individual effects of not crediting sorption in the geosphere, not crediting sorption in the near field, not crediting solubility limits and the combined effect of crediting low sorption in the geosphere with coincided high solubility limits.

The two ‘No Sorption’ cases show the highest sensitivities, with the No Sorption in the Geosphere case resulting in a dose rate that is 210 times the Reference Case value. Even with this highly conservative assumption, the results remain below the interim dose acceptance criterion.

Probabilistic Cases

Table 7-51 presents summary results for the probabilistic case. In this case 120,000 simulations are performed in which all parameters represented by probability distributions are simultaneously varied. The 95th percentile peak dose rate of 1.3×10^{-6} Sv/a is 4.0 times that of the Reference Case. This is a factor of 230 times less than the interim dose acceptance criterion.

Section 7.8.3.1 discusses that the results also show six simulations (i.e., 0.004% of the total) have peak doses either above or very close to the interim dose acceptance criterion. This is attributed to an overly conservative estimate of the amount of Sn-126 that reaches the surface

when the failed container(s) are located in model sectors that do not include a backfill pathway. This aspect of the model may be further refined in subsequent work.

7.12.3 Results for the Disruptive Event Scenarios

Table 7-51 also presents summary results for five of the six Disruptive Event Scenarios. These scenarios examine the consequences of all containers failing and the effects of degraded fracture and shaft seals, as well as variant cases. Key features to note are:

- Failure of all containers at 60,000 years results in a peak dose rate of 5.8×10^{-4} Sv/a while failure of all containers at 10,000 years results in a peak dose rate of 7.9×10^{-4} Sv/a, indicating a slight sensitivity to the assumed failure time. While the time of failure remains sufficiently long that most fission products decay before reaching the biosphere, the earlier failure time means some fission products with intermediate half lives (such as C-14) reach the biosphere in greater quantities.
- The Fracture Seal Failure case has no effect on the dose consequence. This is because the integrity of the other tunnel seals is unaffected and because much of the radionuclide transport occurs outside the repository footprint due to the advective nature of the groundwater flow field.
- The variant case of the Fracture Seal Failure Scenario in which the fracture seals and all tunnel and room seals are degraded has essentially no effect on the dose consequence. This is because much of the radionuclide transport occurs outside the repository footprint due to the advective nature of the groundwater flow field.
- The Shaft Seal Failure Scenario also has no effect on the dose consequence. This is likely because the three failed containers are located some distance away from the degraded shaft seal (i.e., the failed container location was selected to maximize radionuclide transport to the well and not to the degraded shaft seal).

The discussion of the anticipated effects of gas generation and migration in Section 7.11.4 considers the All Containers Fail scenario. The discussion concludes that no adverse consequences to either the repository or to persons living above the repository are anticipated.

Section 7.9.1 presents a stylized analysis for the Inadvertent Human Intrusion Scenario. This scenario is not included in Table 7-51 because it is a special case, as recognized in Regulatory Document G-320. The assumed intrusion bypasses all barriers, and therefore the associated dose consequence exceeds the regulatory limit. The results show potential doses to the Drill Crew of about 1.06 Sv and to a site Resident of about 1.14 Sv assuming early intrusion, leaving contaminated material on the site, and a future resident living on the contaminated material. The risk of inadvertent human intrusion is minimized by placing the used fuel deep underground in a location with no mineral resources and no potable groundwater resources, and by the use of markers and institutional controls. The likelihood of this event occurring cannot be accurately determined; however, based on simple estimates of deep drilling rates, it is roughly estimated as 3.5×10^{-5} per annum, which implies a risk to the Resident of 2.3×10^{-6} per annum. This is less than the reference risk criterion 10^{-5} per annum.

Table 7-52 shows results illustrating the effect of geosphere hydraulic conductivity on the All Containers Fail at 10,000 Years Scenario. The results indicate that the dose rate for the Sensitivity 1 case (i.e., the case with conductivity 10 times greater than that in the Reference Case) exceeds the interim dose acceptance criterion. This suggests that a candidate site with a

hydraulic conductivity of the order of 4×10^{-10} m/s would have the potential to exceed the interim dose acceptance criterion for disruptive events.

Table 7-52: Effect of Geosphere Hydraulic Conductivity on the All Containers Fail at 10,000 Years Scenario

All Containers Fail at 10,000 Years	Time of Peak Impact (a)	Peak Impact*		Factor to Dose Limit
		I-129 (Bq/a)	Dose (Sv/a)	
Reference Hydraulic Conductivity				
FRAC3DVS-OPG Result**	75,000	3.66×10^6	-	-
SYVAC3-CC4 Result**	32,000	-	7.9×10^{-4}	1.3
Geosphere Sensitivity (Computed using FRAC3DVS-OPG)				
Sensitivity 1 (10 times higher)	17,000	7.81×10^6	1.7×10^{-3}	0.6
Sensitivity 2 (10 times lower)	657,000	9.01×10^5	2.0×10^{-4}	5.0
Sensitivity 3 (100 times lower)	8,000,000	3.54×10^5	9.7×10^{-5}	10.3

Notes:

* The peak dose impact for the sensitivity cases is determined by scaling the peak release in Bq/a to the results obtained using the Reference Hydraulic Conductivity. The dose rate for Sensitivity 1 is likely to be higher when other radionuclides are accounted for.

** The Time of Peak Impact differs because the SYVAC3-CC4 model produces conservative results (i.e., earlier and greater releases) when compared to the FRAC3DVS-OPG model.

7.12.4 Conclusion

The postclosure safety assessment shows, for the Normal Evolution Scenario and associated sensitivity cases, that all radiological and non-radiological interim acceptance criteria are met with substantial margins during the postclosure period.

7.13 References for Chapter 7

Air Products and Chemicals, Inc. 1999. *Methane Gas* [MSDS# 1070]

<http://avogadro.chem.iastate.edu/MSDS/methane.pdf> (Accessed Oct 26, 2012).

Allentown, PA, USA.

Air Products and Chemicals, Inc. 1994. *Hydrogen Gas* [MSDS# 1009].

<http://avogadro.chem.iastate.edu/MSDS/hydrogen.pdf> (Accessed Oct 26, 2012).

Allentown, PA, USA.

ANDRA. 2005. Evaluation de Sûreté du Stockage Géologique. Paris, France

Becker, D.-A., D. Buhmann, R. Storck, J. Alonso, J.-L. Cormenzana, M. Hugi, F. van Gemert, P. O'Sullivan, A. Laciok, J. Marivoet, X. Sillen, H. Nordman, T. Vieno and M. Niemeyer. 2002. Testing of Safety and Performance Indicators (SPIN). European Commission Report FIKW-CT2000-00081. European Commission, Brussels, Belgium.

Berger, A. and M.F. Loutre. 2002. An exceptionally long interglacial ahead? *Science* 297, 1287-1288.

Bond A.E., A.R. Hoch, G.D. Jones, A.J. Tomczyk, R.W. Wiggin, W.J. Worraker. 1997. Assessment of a spent fuel disposal canister. Assessment studies for a copper canister with cast steel inner component. Swedish Nuclear Fuel and Waste Management Company Report SKB TR-97-19. Stockholm, Sweden.

Bowen, H.J. 1979. *Environmental Chemistry of the Elements*. Academic Press Inc., London, England.

Brown, J.E., B. Alfonso, R. Avila, N.A. Beresford, D. Coplestone, G. Pröhl and A. Ulanovsky. 2008. The ERICA Tool. *J. Environ. Radioactivity* 99: 1371-1383.

CCME. 2007. *Canadian Environmental Quality Guidelines*. Canadian Council of the Environment. Originally issued in 1999 (including updates until September 2007). Canada

CNSC. 2006. *Regulatory Guide G-320: Assessing the Long Term Safety of Radioactive Waste Management*. Canadian Nuclear Safety Commission. Ottawa, Canada.

Cool, W., M. Cunado, L. Johnson, M. Mantynen, W. Muller, S. Norris, W. Rodwell. 2004. EC GASNET Project: Gas issues in the safety assessment of deep repositories for nuclear waste. *Material Research Society Symposium Proceedings Volume 807*, 19-24.

CSA. 2008. *Guidelines for Calculating Derived Release Limits for Radioactive Material in Airborne and Liquid Effluents for Normal Operation of Nuclear Facilities*. Canadian Standards Association. N288.1-08. Toronto, Canada.

Curti E. and P. Wersin. 2002. *Assessment of Porewater Chemistry in the Bentonite Backfill for the Swiss SF/HLW Repository*. NAGRA Technical Report 02-09. Wettingen, Switzerland.

DiCiccio, T.J. and B. Efron. 1996. Bootstrap Confidence Intervals. *Statistical Science* Volume 11(3), 189-228.

DOE. 2008. *Final Supplemental Environmental Impact Statement for a Geologic Repository for the Disposal of Spent Nuclear Fuel and High-Level Radioactive Waste at Yucca Mountain*. US Department of Energy Report DOE/EIS-0250F-S1. Nevada, USA.

EC. 2003. *GASNET: A Thematic Network on Gas Issues in Safety Assessment of Deep Repositories for Radioactive Waste*. European Commission Report. Luxembourg.

EC/HC. 2003. *Priority Substances List Assessment Report: Releases of Radionuclides from Nuclear Facilities (Impact on Non-Human Biota)*. Environment and Health Canada. Canadian Environmental Protection Act. Ottawa, Canada.

Environment Canada. 2008. *Southern Arctic Ecozone* (<http://www.ec.gc.ca/soer-ree/English/vignettes/Terrestrial/sa/default.cfm>, accessed 2008).

- Ferry, C., J.-P. Piron, A. Poulesquen, and C. Poinssot. 2008. Radionuclides Release from the Spent Fuel under Disposal Conditions: Re-evaluation of the Instant Release Fraction. Material Research Society Symposium Proceedings 1107, 447-454.
- Flavelle, P. 1996. Perspectives of the scale of the Canadian Nuclear Fuel Waste Disposal Concept. Atomic Energy Control Board Report INFO-0635. Ottawa Canada.
- Garisto, F. 1989. The Energy Spectrum of α -particles Emitted from Used CANDU Fuel, Annals of Nuclear Energy 16. 33-38.
- Garisto, F. 2001. Radionuclide Screening Model (RSM) Version 1.1 Verification and Validation. Ontario Power Generation Report 06819-REP-01300-10029-R00. Toronto, Canada.
- Garisto, F. and P. Gierszewski. 2001. Summary of Verification and Validation Studies for SYVAC3-PR4 and its Submodels. Ontario Power Generation Report 06819-REP-01200-10043-R00. Toronto, Canada.
- Garisto, F., J. Avis, N. Calder, A. D'Andrea, P. Gierszewski, C. Kitson, T. Melnyk, K. Wei, L. Wojciechowski. 2004. Third Case Study – Defective Container Scenario. Ontario Power Generation Report 06819-REP-01200-10126-R00. Toronto, Canada.
- Garisto, F., T. Kempe, P. Gierszewski, K. Wei, C. Kitson, T. Melnyk, L. Wojciechowski, J. Avis and N. Calder. 2005. Horizontal Borehole Concept Case Study: Chemical Toxicity Risk. Ontario Power Generation Report 06819-REP-01200-10149-R00. Toronto, Canada.
- Garisto, N.C., F. Cooper and S.L. Fernandes. 2008. No-effect Concentrations for Screening Assessment of Radiological Impacts on Non-human Biota. Nuclear Waste Management Organization Report NWMO TR-2008-02. Toronto, Canada.
- Garisto, F., J. Avis., T. Chshyolkova, P. Gierszewski, M. Gobien, C. Kitson, T. Melnyk, J. Miller, R. Walsh and L. Wojciechowski. 2010. Glaciation Scenario: Safety Assessment for a Used Fuel Geological Repository. Nuclear Waste Management Organization Report NWMO TR-2010-10. Toronto, Canada.
- Garisto, F., M. Gobien, E. Kremer and C. Medri. 2012. Fourth Case Study: Reference Data and Codes. Nuclear Waste Management Organization Report NWMO TR-2012-08. Toronto, Canada.
- Gierszewski, P., J. Avis, N. Calder, A. D'Andrea, F. Garisto, C. Kitson, T. Melnyk, K. Wei and L. Wojciechowski. 2004. Third Case Study - Postclosure Safety Assessment. Ontario Power Generation Report 06819-REP-01200-10109-R00. Toronto, Canada.
- Goodwin, B.W., P. Gierszewski and F. Garisto. 2001. Radionuclide Screening Model (RSM) Version 1.1 - Theory. Ontario Power Generation Report 06819-REP-01200-10045-R00. Toronto, Canada.
- Grambow, B., J. Bruno, L. Duro, J. Merino, A. Tamayo, C. Martin, G. Pepin, S. Schumacher, O. Smidt, C. Ferry, C. Jegou, J. Quiñones, E. Iglesias, N. Rodriguez Villagra, J. M. Nieto, A. Martínez-Esparza, A. Loida, V. Metz, B. Kienzler, G. Bracke (GRS), D. Pellegrini, G.

- Mathieu, V. Wasselin-Trupin, C. Serres, D. Wegen, M. Jonsson, L. Johnson, K. Lemmens, J. Liu, K. Spahiu, E. Ekeroth, I. Casas, J. de Pablo, C. Watson, P. Robinson, and D. Hodgkinson. 2010. MICADO Model Uncertainty for the Mechanism of Dissolution of Spent Fuel in Nuclear Waste Repository. European Commission Report EUR 24597 EN. Brussels, Belgium.
- Grasty, R.L. and J.R. LaMarre. 2004. The Annual Effective Dose from Natural Sources of Ionising Radiation in Canada. *Radiation Protection Dosimetry* 108, No 3, 215-226.
- Guo, R. 2009. Application of numerical modelling in choosing container spacing, placement-room spacing and placement-room shape for a deep geological repository using the in-floor borehole placement method. Nuclear Waste Management Organization Report NWMO TR-2009-28. Toronto, Canada.
- Guttman, I. and S.S. Wilks. 1965. *Introductory Engineering Statistics*. John Wiley & Sons. New York, USA.
- Hermann, O.W. and R.M. Westfall. 1995. ORIGEN-S - SCALE System Module to Calculate Fuel Depletion, Actinide Transmutation, Fission Product Buildup and Decay, and Associated Radiation Source Terms. In: *SCALE: A Modular Code System for Performing Standardized Computer Analyses for Licensing Evaluations*. Oak-Ridge National Laboratory NUREG/CR-0200, Rev.4 (ORNL/NUREG/CSD-2/R4) Volume II, Part I. Oak-Ridge, USA.
- Hoch, A. R., K.A. Cliffe, B.T. Swift and W.R. Rodwell. 2004. *Modelling Gas Migration in Compacted Bentonite: GAMBIT Club Phase 3 Final Report*, POSIVA Report 2004-02, Oikiluoto, Finland.
- Hummel, W., U. Berner, E. Curti, F.J. Pearson and T. Thoenen. 2002. *Nagra / PSI Chemical thermodynamic data base 01/01*. Universal Publishers. Parkland, U.S.A.
- IAEA. 2002. *Safety Indicators for the Safety Assessment of Radioactive Waste Disposal*. International Atomic Energy Agency TECDOC-1372. Vienna, Austria.
- IAEA. 2006. *Safety Requirements: Geological Disposal of Radioactive Waste*. International Atomic Energy Agency Safety Requirements WS-R-4. Vienna, Austria.
- ICRP. 2006. *Assessing Dose of the Representative Person for the Purpose of Radiation Protection of the Public*. International Commission on Radiological Protection Publication 101, *Annals of the ICRP*, 36 (3). Vienna, Austria.
- ICRP. 2007. *The 2007 Recommendations of the International Commission on Radiological Protection*. International Commission on Radiological Protection Publication 103, *Annals of the ICRP (W2-4)*. Vienna, Austria.
- JNC. 2000. H12: Project to Establish the Scientific and Technical Basis for HLW in Japan. Japan Nuclear Cycle Development Institute JNC TN1410 2000-004. Tokai, Japan.

- King, F. and M. Kolar. 2006. Simulation of the Consumption of Oxygen in Long-term in situ Experiments and in the Third Case Study Repository using the Copper Corrosion Model CCM-UC.1.1. Ontario Power Generation Report 06819-REP-01300-10084-R00, Toronto, Canada.
- King, F. and D. Shoesmith. 2004. Electrochemical Studies of the Effect of H₂ on UO₂ Dissolution. Swedish Nuclear Fuel and Waste Management Company Report SKB TR 04-20. Stockholm, Sweden.
- Kitson C.I., T.W. Melnyk, L.C. Wojciechowski, T. Chshyolkova. 2012. SYVAC3-CC4 User Manual, Version SCC409. Nuclear Waste Management Organization Report NWMO TR-2012-21. Toronto, Canada.
- Maak, P., P. Gierszewski and M. Saiedfar. 2001. Early Failure Probability of Used-Fuel Containers in a Deep Geologic Repository. Ontario Power Generation Report 06819-REP-01300-10022-R00, Toronto, Canada.
- Mallants, D. and D. Jacques. 2004. Performance Assessment for Deep Disposal of Low and Intermediate Level Short-lived Radioactive Waste in Boom Clay, SCK•CEN-R-3793. Mol, Belgium.
- McMurry, J., B.M. Ikeda, S. Stroes-Gascoyne, D.A. Dixon and J.D. Garroni. 2004. Evolution of a Canadian Deep Geologic Repository: Defective Container Scenario. Ontario Power Generation Report 06819-REP-01200-10127-R00. Toronto, Canada.
- Medri, C. 2012. Human Intrusion Model for the Fourth and Fifth Case Studies: HIMv2.0. Nuclear Waste Management Organization Report NWMO TR-2012-04. Toronto, Canada.
- Merrett, G.J. and P.A. Gillespie. 1983. Nuclear Fuel Waste Disposal: Long-term Stability Analysis. Atomic Energy of Canada Limited Report AECL-6820. Pinawa, Canada.
- MoE. 2011. Soil, Groundwater and Sediment Standards for Use under Part XV.1 of the Environmental Protection Act. Ontario Ministry of the Environment. Toronto, Canada.
- MoEE. 1994. Water Management Policies Guidelines Provincial Water Quality Objectives of the Ministry of Environment and Energy. Toronto, Canada.
- Muurinen, A. and J. Lehtikoinen. 1999. Porewater chemistry in compacted bentonite. *Engineering Geology* 54, 207-214.
- NAGRA. 2002. Project Opalinus Clay: Safety Report, Demonstration of the Disposal Feasibility for Spent Fuel, Vitrified HLW and Long-lived ILW. Nagra Technical Report 02-05. Wettingen, Switzerland.
- NAGRA. 2008. Effects of Post-disposal Gas Generation in a Repository for Low- and Intermediate-level Waste Sited in the Opalinus Clay of Northern Switzerland. Nagra Technical Report NTB 08-07. Wettingen, Switzerland.

- Neuzil, C. 2003. Hydromechanical coupling in geological processes. *Hydrogeology Journal*, 11, 41-83.
- Normani, S.D. 2009. Paleoevolution of pore fluids in glaciated geologic settings. Ph.D. Thesis, University of Waterloo, Department of Civil Engineering. Waterloo, Canada.
- NWMO. 2012. SYVAC3-CC4 Theory, Version SCC409. Nuclear Waste Management Organization Report NWMO TR-2012-22. Toronto, Canada
- Parkhurst, D.L. and C.A.J. Appelo. 1999. User's Guide to PHREEQC (Version 2) – A Computer Program for Speciation, Batch-Reaction, One-Dimensional Transport, and Inverse Geochemical Calculations. U.S Department of the Interior and U.S. Geological Survey Water-Resources Investigations Report 99-4259. Denver, USA.
- Peltier, W.R. 2003. A refined model of the last deglaciation event of the current ice-age: ICE-5G. International Union for Quaternary Research (INQUA), XVI INQUA Congress Paper No. 9-3. Reno, USA.
- Peltier, W.R. 2006. Boundary Conditions Data Sets for Spent Fuel Repository Performance Assessment. Ontario Power Generation Report 06819-REP-01200-10154-R00. Toronto, Canada.
- Pusch, R. 2003. The Buffer and Backfill Handbook. Part 3: Models for Calculation of Processes and Behaviour. Swedish Nuclear Fuel and Waste Management Company Report SKB TR-03-07. Stockholm, Sweden.
- Rodwell, W.R. and P.J. Nash. 1992. Mechanisms and Modelling of Gas Migration from Deep Radioactive Waste Repositories. Nirex Report NSS/R250. Dorchester, U.K.
- Rodwell, W.R., T.R. Lineham and M.P. Gardiner. 2000. Gas Migration in the Geosphere: Review of the Work Undertaken by the Nirex Safety Assessment Research Programme. Report Produced for UK Nirex Limited. AEA Technology Report AEAT/R/ENV/0295 Issue 1. Oxfordshire, U.K.
- Shoosmith, D. 2008. The Role of Dissolved Hydrogen on the Corrosion/Dissolution of Spent Nuclear Fuel. Nuclear Waste Management Organization Report NWMO TR-2008-19. Toronto, Canada.
- SKB. 1998. Design Premises for Canister for Spent Nuclear Fuel. Swedish Nuclear and Waste Management Company Technical Report TR-98-08. Stockholm, Sweden
- SKB. 1999. Deep Repository for Spent Nuclear Fuel: SR 97 - Post-closure Safety: Main Report - Volume 1, Volume 2, and Summary. Swedish Nuclear Fuel and Waste Management Company Report SKB TR-99-06. Stockholm, Sweden.
- SKB. 2004. Interim Main Report of the Safety Assessment SR-Can. Swedish Nuclear Fuel and Waste Management Report SKB TR-04-11. Stockholm, Sweden.

- SKB. 2010a. Handling of future human actions in the safety assessment SR-Site. Swedish Nuclear and Waste Management Company Technical Report TR-10-53. Stockholm, Sweden.
- SKB. 2010b. Design, Production and Initial State of the Canister. Swedish Nuclear and Waste Management Company Technical Report TR-10-14. Stockholm, Sweden
- SKB. 2011. Long-term Safety for the Final Repository for Spent Nuclear Fuel at Forsmark, Main Report of the SR-Site Project. Swedish Nuclear Fuel and Waste Management Company Report SKB TR-11-01. Stockholm, Sweden.
- Spahiu, K., L. Werme and U.-B. Eklund. 2000. The influence of near field hydrogen on actinide solubilities and spent fuel leaching. *Radiochimica Acta* 88, 507-511.
- Spahiu, K. and P. Sellin. 2001. SR 97: Spent Fuel Alteration/Dissolution and the Influence of Near Field Hydrogen. In: *Scientific Basis for Nuclear Waste Management XXIV*. Material Research Society Symposium Proceedings Volume 663.
- Srivastava, R.M. 2002. The Discrete Fracture Network Model in the Local Scale Flow System for the Third Case Study. Ontario Power Generation Report 06819-REP-01300-10061-R00. Toronto, Canada.
- Stroes-Gascoyne, S., L.M. Lucht, D.W. Oscarson, D.A. Dixon and S.H. Miller. 1996. Migration of Bacteria into Sterilized Compacted Buffer Material. Atomic Energy of Canada Limited Technical Report TR-754, COG-96-298. Pinawa, Canada.
- Stroes-Gascoyne, S., S.A. Haveman and P. Vilks. 1997. The Change in Bioavailability of Organic Matter Associated with Clay-based Buffer Material as a Result of Heat and Radiation Treatment. *Materials Research Society Symposium Proceedings* 465, 987-994.
- Sykes, J.F., S.D. Normani and E.A. Sudicky. 2003. Regional Scale Groundwater Flow in a Canadian Shield Setting. Ontario Power Generation Report 06819-REP-01200-10114-R00. Toronto, Canada.
- Tait, J.C., I.C. Gauld and A.H. Kerr. 1995. Validation of the ORIGEN-S Code for Predicting Radionuclide Inventories in Used CANDU Fuel. *Journal of Nuclear Materials* 223, 109-121.
- Therrien, R., R. G. McLaren, E. A. Sudicky, S.M. Panday and V. Guvanasen. 2010. FRAC3DVS-OPG: A Three-Dimensional Numerical Model Describing Subsurface Flow and Solute Transport. User's Guide, Groundwater Simulations Group, University of Waterloo. Waterloo, Canada.
- Tullborg E.L., J. Smellie, A. Nilsson, M.J. Gimeno, L.F. Auqué, V. Brüchert and J. Molinero. 2010. SR-Site – Sulphide Content in the Groundwater at Forsmark. SKB Technical Report TR-10-39, Stockholm, Sweden

Used Fuel Repository Conceptual Design and Postclosure Safety Assessment in Crystalline Rock

Document Number: NWMO TR-2012-16

Revision: 000

Class: Public

Page: 529

Walsh, R. and J. Avis. 2010. Glaciation Scenario: Groundwater and Radionuclide Transport Studies. Nuclear Waste Management Organization Report NWMO TR-2010-09. Toronto, Canada.

THIS PAGE HAS BEEN LEFT BLANK INTENTIONALLY

8. TREATMENT OF UNCERTAINTIES

All analysis calculations have an associated uncertainty. CNSC Regulatory Guide G-320 (CNSC 2006) expects that uncertainty will be taken into account.

8.1 Approach

Many organizations use the following three broad categories¹ to structure the analysis of uncertainties in postclosure safety assessments (e.g., Marivoet et al. 2008):

- **Scenario Uncertainty:** Arises from uncertainty in the evolution of the repository system and human behaviour over the time scales of interest;
- **Model Uncertainty:** Associated with uncertainty in the conceptual, mathematical and computer models used to simulate the behaviour of the repository system (e.g., due to approximations used to represent the system); and
- **Data Uncertainty:** Arises from uncertainty in the data and parameters used as input in the modelling (e.g., due to incomplete site-specific data or due to parameter estimation errors from interpretation of test results).

The following briefly discusses the approach adopted for uncertainties in this pre-project review.

Scenario Uncertainty

Uncertainty in the future evolution of the site is addressed by assessing a range of scenarios that describe the potential evolution of the system. The scenario identification process, described in Chapter 6, ensures that key uncertainties are identified and scenarios are defined to explore their consequences.

The scenarios defined include the Normal Evolution Scenario (which describes the expected evolution of the repository) and a series of Disruptive Event Scenarios that postulate the occurrence of unlikely events leading to possible penetration of barriers and abnormal loss of containment.

Section 7.2 describes the suite of scenarios considered in this postclosure assessment.

It is unrealistic to predict human habits and behaviour over the time scale of relevance to the repository system. Major changes to the surface and near-surface environment are likely to occur as a result of natural changes such as ice sheet advance / retreat or as a result of future human actions. Also, societal and technological changes are inherently unpredictable over such timescales.

¹ The boundaries between these categories can overlap in that, depending upon how models are formulated, an uncertainty may be classed as a model or a data uncertainty.

To estimate potential future impacts, a stylized representation² of the biosphere and human receptors is used to allow illustrative estimates to be made. It is assumed that future humans are generally similar to present day humans, and will adopt behaviors that would be consistent with current or past human practice. People are assumed to live on the repository site in the future in a manner that maximizes their potential dose from exposure to releases from the repository.

Since assumptions concerning the biosphere (e.g., climate), human lifestyles (e.g., critical group characteristics) and water flows in the near-surface environment become increasingly uncertain with time, two complementary long-term indicators are also used to supplement the dose rate indicator using system characteristics that are much less sensitive to such assumptions.

Model Uncertainty

Conceptual and mathematical model uncertainties are identified in the model development process. Key uncertainties are addressed by using alternative conceptual representations of the system. This is facilitated by the availability of a range of computer codes (e.g., FRAC3DVS-OPG and SYVAC3-CC4) that are capable of representing different conceptualizations and mathematical descriptions of the system³.

Some conceptual and mathematical model uncertainties are amenable to representation with parameter values, and these are investigated using the methods applied to data uncertainties. For example, uncertainties in the representation of sorption are treated by considering bounding cases in which the sorption values are set to zero.

Data Uncertainty

Data uncertainties are identified in Garisto et al. (2012). These are accounted for through:

- Deterministic Calculations – alternative sets of parameter values, each providing a self-consistent representation of the system. Results are compared to the Reference Case and the differences explored. A limitation of this approach is that there is often no systematic or complete coverage of the uncertainty space in parameter values.

Sensitivity cases in this pre-project review (discussed in Section 7.2) explore the effect of variations in key parameters affecting the performance of various physical and chemical barriers.

- Probabilistic Calculations – parameters are assigned probability distribution functions that describe their inherent uncertainty. The model is evaluated a large number of times, with each case using as input values randomly selected from the distribution functions. The model output is a distribution of results. The strength of the probabilistic approach lies in its

² A stylized representation of the biosphere, and human habits and behaviour is a representation that has been simplified to reduce the natural complexity to a level consistent with the objectives of the analysis using assumptions that are intended to be plausible and internally consistent but that will tend to err on the side of conservatism.

³ Uncertainties related to the codes themselves are reduced through validation.

ability to be comprehensive in exploring the space of the phenomena considered, and their associated model parameters. Its weakness is the need to make use of simplified models.

Conservatism

Throughout the assessment process, it is necessary to make various assumptions relating to scenarios, models or data. Assumptions are often categorized as 'realistic'⁴ or 'conservative'⁵, although care needs to be taken when using such terms. The key is to ensure that each major assumption used in the assessment is considered and documented, and that the potential implications are understood.

While it may appear sensible to adopt a conservative approach to ensure that potential impacts are not under-estimated, care is needed because the net effect of many conservative assumptions can be an unrealistic estimate of impacts. Nevertheless, the following conservative assumptions are incorporated in the Normal Evolution Scenario:

- Three defective containers are assumed present in the Normal Evolution Scenario, with the defects present at the time of container placement;
- The defective containers fill with water in the first 100 years;
- No credit taken for the presence of the fuel sheath in maintaining fuel integrity and in preventing contact of the fuel matrix with water that may enter the container;
- No credit taken for the effect of H₂ (produced by corrosion of the defective container) on the dissolution rate of the UO₂ fuel;
- No credit taken for the effect of iron oxides (produced by corrosion of the defective container) in reducing the container internal void volume and providing a high surface area for adsorption of some of the radionuclides released from the fuel;
- No credit taken for the likely filling of the defect with bentonite and / or corrosion products which could significantly increase the transport resistance;
- Positioning the defective containers in the repository location with the shortest contaminant travel time to the surface;
- Adoption of a 100 m deep well located in the position with the shortest transport time to the surface;
- Positioning the well so that it maximizes the capture of radionuclides released from the defective containers;
- All major fractures extending to depth have high hydraulic conductivity (10⁻⁶ m/s); and
- Defining conservative properties of the critical group (e.g., use of 90th percentile food ingestion rates, obtaining all food, fuel, water and building material locally, all drinking and irrigation water taken from the well).

⁴ Realism is defined as "the representation of an element of the system (scenario, model or data), made in light of the current state of system knowledge and associated uncertainties, such that the safety assessment incorporates all that is known about the element under consideration and leads to an estimate of the expected performance of the system attributable to that element" (IAEA 2006).

⁵ Conservatism is defined as "the conscious decision, made in light of the current state of system knowledge and associated uncertainties, to represent an element of the system (scenario, model or data) such that it provides an under-estimate of system performance attributable to that element and thereby an over-estimate of the associated radiological impact (i.e., dose or risk)" (IAEA 2006).

The postclosure safety assessment adopts scientifically informed, physically realistic assumptions for processes and data that are understood and can be justified on the basis of the results of research and / or site investigation. Where there are high levels of uncertainty associated with processes and data, conservative assumptions are adopted to allow the impacts of uncertainties to be bounded.

8.2 Key Uncertainties

The postclosure safety assessment summarized in Section 7.12, indicates that the deep geological repository in geologic settings similar to the assumed site could tolerate large changes in the properties of key chemical and physical barriers without challenging the interim dose acceptance criteria.

The most important uncertainties in terms of their importance to modify potential impacts are:

- **Fracture Characterization:** For a real site in a Canadian Shield setting, there will be uncertainty in the fracture network and in the properties of the fractures. Site characterization may also not identify all existing significant fractures. A local network of small-scale fractures may provide a potential faster pathway through the rock mass than modelled here. These uncertainties can be reduced through site selection and repository location and depth, and any residual uncertainties can be handled through the adoption of conservative assumptions within the postclosure analysis. A range of fracture networks or parameters may need to be considered.
- **Glaciation Effects:** Although geological evidence at a real site is expected to indicate the deep geosphere has not been affected by past glaciation events and that the deep groundwater system has remained stagnant, glaciation will have a major effect on the surface and near-surface environment that is not entirely predictable. Glaciation is likely to occur after 60,000 to 100,000 years, at which point the remaining hazard will be long-lived radionuclides.
- **Container Failure Mode:** The Reference Case of the postclosure safety assessment assumes the three containers fail via a small (1 mm radius) defect and that the defect does not evolve with time. Uncertainty in the defect size evolution is addressed deterministically in Section 7.8.2.2 and probabilistically in Section 7.8.3.1 by considering the effect of larger hole sizes. Other container failure modes may need to be considered, as identified in the description of the Container Failure Disruptive Scenario.

Note that the failure model used in the All Containers Fail Disruptive Scenario is one in which the container is no longer assumed present so the radionuclide release rate into the surrounding buffer does not depend on diffusion through a small hole.

8.3 References for Chapter 8

- CNSC. 2006. Regulatory Guide G-320: Assessing the Long Term Safety of Radioactive Waste Management. Canadian Nuclear Safety Commission. Ottawa, Canada.
- Garisto, F., M. Gobien, E. Kremer and C. Medri. 2012. Fourth Case Study: Reference Data and Codes. Nuclear Waste Management Organization Report NWMO TR-2012-08. Toronto, Canada.
- IAEA. 2006. Safety Requirements: Geological Disposal of Radioactive Waste. International Atomic Energy Agency Safety Requirements WS-R-4. Vienna, Austria.
- Marivoet, J., T. Beuth, J. Alonso and D.-A. Becker. 2008. Safety Functions, Definition and Assessment of Scenarios, Uncertainty Management and Uncertainty Analysis, Safety Indicators and Performance/Function Indicators. PAMINA Deliverable D-No. 1.1.1, European Commission. Brussels, Belgium.

THIS PAGE HAS BEEN LEFT BLANK INTENTIONALLY

9. NATURAL ANALOGUES

Natural analogues are natural features that have been under conditions or processes occurring over long periods of time that are similar to those expected to occur in some part of a deep geological repository. They provide understanding or demonstration of how a repository may behave over time scales ranging to many millions of years. Analogues exist for most key features of the repository system, including the durability of used fuel, engineered and natural containment systems, and transport of contaminants.

The use of natural analogues in supporting key assumptions in safety assessment and adding credibility to its findings is recommended in IAEA (1999) and in Regulatory Guide G-320 (CNSC 2006). G-320 states: "*Natural analogue information should be used to build confidence that the system will perform as predicted by demonstrating that natural processes will limit the long-term release of contaminants to the biosphere to levels well below target criteria.*"

The natural analogues presented here can assist in understanding many of the underlying principles and the long-term isolation and containment of used nuclear fuel.

9.1 Analogues for Used Nuclear Fuel

9.1.1 Natural Uranium Deposits

Natural uranium is relatively abundant. Like all other elements, it is cycled through biological and geological systems and tends to concentrate in some locations by natural processes. Uranium will slowly dissolve under oxidizing conditions and precipitate under reducing conditions. Most uranium ore bodies form by this process. Once formed, until local conditions change, a uranium deposit will remain in place. Uranium ore bodies that are being mined today were formed hundreds of millions of years ago.

Used fuel consists predominantly of uranium dioxide, with about 2% of the total being fission and activation products resulting from the nuclear reactions occurring in the fuel during power production. These are mostly incorporated within the solid matrix of the used fuel. Natural uranium minerals are comparable in that they consist of uranium dioxide along with uranium decay products.

One gram of natural uranium, as it is extracted from the earth in equilibrium with its progeny contains a bit less than 2×10^5 Bq of radioactivity. In comparison, after discharge from a reactor and 30 years of cooling, used fuel has an inventory of 2.7×10^9 Bq per gram of uranium, principally in the form of fission and activation products (Tait et al. 2000), and is considerably more radioactive than the original uranium ore. Due to the rapid decay of most of the fission product isotopes present in used fuel, radioactivity decreases to 2.3×10^7 Bq per gram after 1000 years while after approximately 1,000,000 years, radioactivity decreases a level similar to that in natural uranium.

The Cigar Lake uranium deposit found in Northern Saskatchewan (Figure 9-1) provides a Canadian example of an analogue for geological placement of used nuclear fuel. The Cigar Lake deposit is under development as a uranium mine and has been well studied as a natural analogue (Cramer and Smellie 1994; Miller et al. 2000).

The Cigar Lake uranium deposit is located about 430 m below surface, similar in depth to the repository considered in this pre-project review (i.e., 500 metres underground). The ore body formed about 1.3 billion years ago. It is similar in general composition to used fuel, and the ore is surrounded by a clay envelope somewhat similar to the clay buffer specified in the repository design. It can be considered analogous to a “worst case” simulation, as it lacks any specially designed engineered barriers and the host rock above the ore body is highly fractured sandstone.

Based on the Cigar Lake natural analogue study (Cramer and Smellie 1994), it was concluded that:

- uranium dioxide will remain stable over 100 million year time scales under the chemically-reducing conditions found adjacent to the Cigar Lake ore body, with very little uranium migrating from the deposit;
- the natural clay surrounding the ore has provided an effective long-term seal, preventing migration of radionuclides from the deposit;
- dissolved organic matter in groundwater migrating past the ore has not played a significant role in mobilizing radionuclides from the deposit; and
- natural hydrologic barriers and appropriate geochemical conditions found at the site are effective in preventing significant radionuclide migration from the deposit.

Insufficient radionuclide migration has occurred to produce any detectable concentration anomalies in the soil, surface water and lake sediments and waters overlying the ore body. Environmental and geological exploration in the area has shown no surface expression of the ore body, and it had to be discovered by geophysical techniques. Indeed, on a map of surface radioactivity in Canada, the area of the Saskatchewan deposits generally shows up as having below-average surface radioactivity (McKee and Lush 2004).

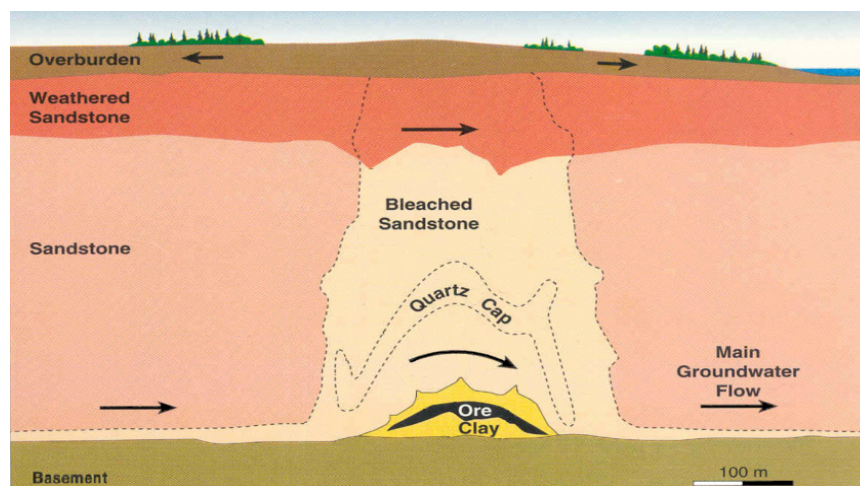


Figure 9-1: Cigar Lake Ore Deposit

9.1.2 Natural Fissioned Uranium

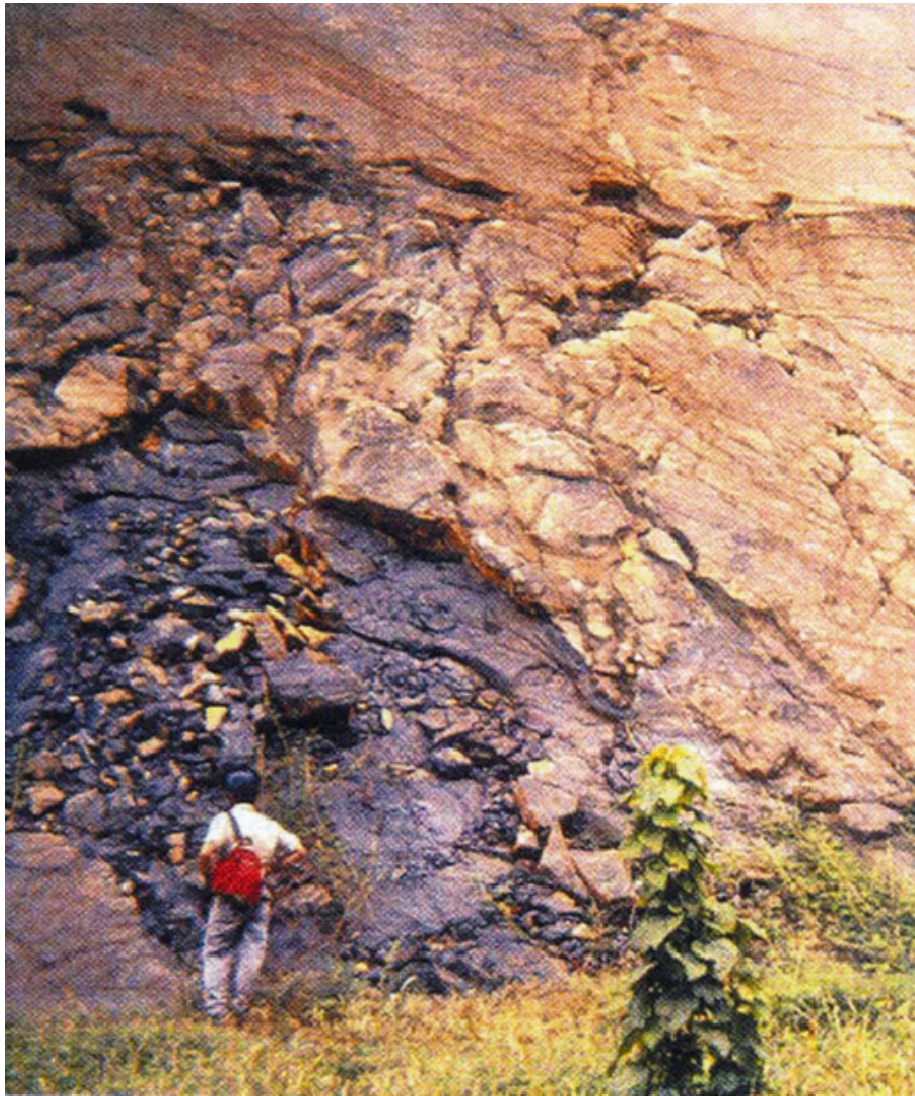
Nuclear fission occurred naturally on Earth over two billion years ago. In Gabon, Africa, there are 15 deposits of uranium ore that have acted as natural nuclear reactors (Miller et al. 2000), sometimes referred to as the Oklo fossil reactors (Figure 9-2). The remnants of natural uranium fission provide the closest natural analogue for used nuclear fuel over long time periods in a geologic environment.

The quantity of U-235 present in natural uranium ore bodies today is low at 0.7%. However, approximately two billion years ago, when the Oklo ore bodies formed, the fraction of U-235 present in natural uranium was much greater, comprising just over 5%. The Oklo reactors operated at low power over about one million years. Results of material sampling infers that approximately 6 to 12 tonnes of U-235 underwent fission, producing plutonium and generating temperatures in the natural reactors of up to 600°C.

Oklo reactor studies provide data regarding the stability of uranium dioxide in the presence of other fission products and the transport of radionuclides within the surrounding geology. These studies indicate that more than 90% of the uranium “fuel” present in the reactors 2 billion years ago has remained in place, including transuranic elements, most of the fission products and their decay products. The plutonium generated has moved less than 3 metres over two billion years. This is in the absence of the engineered barriers incorporated into a geological repository. The surrounding rock has proved to be a well sealed vault.

The stability of the Oklo used fuel has lasted through two billion years of continental drift and groundwater movement. This is additionally impressive considering the present day near-surface location of these natural reactors.

The Oklo fossil reactors provide a snapshot in time of the condition of a natural used fuel repository two billion years after decommissioning. Information is obtained through indirect evidence such as the quantity and location of fission products and their decay products, and the actinides that can still be found in association with these natural reactors. This evidence indicates that careful selection of the host rock formation for a used fuel deep geological repository will likely render many fission products and actinides largely immobile.



Notes: In Oklo, Gabon, the remains of an ancient natural nuclear reactor indicate the resulting plutonium has moved less than 3 metres over two billion years.

From Miller et al. (2000).

Figure 9-2: Naturally Occurring Fission Reactor

9.1.3 Roll-Front Uranium Deposits

Reducing conditions are expected in the repository due to buffering by the rock and engineered sealing materials; however, radiolysis of groundwater may produce oxidizing conditions locally. Redox conditions are critical because the geochemical behaviour of many elements strongly depends on their redox state. The long-term performance of the repository is therefore strongly dependent on the redox conditions assumed.

In some parts of the world, uranium found in permeable rocks is mined by “in-situ” mining methods. Some of the ore bodies mined in this manner are called roll-front ore bodies, as they are continuously migrating or rolling through the permeable host rock such as sandstone. The front of the ore body is in a reduced state, while the rear of the ore body is in a more oxidized state as a consequence of oxidizing groundwaters that are slowly driving the ore body through the rock formation. This creates a condition at the rear of the ore body in which the uranium becomes soluble and migrates to the front of the ore body where it again precipitates.

A well-studied example of a roll-front uranium deposit is the Osamu Utsumi mine in Brazil (Hofmann 1999). Measuring reducing materials such as iron or organic carbon provides an indication of how uranium and other radionuclides in used fuel will be immobilized in the repository.

Hoffman reported that migration of uranium, along with palladium and selenium, was strongly inhibited at a redox front, causing immobilization. Results indicated that reducing conditions inhibit transport of these elements under most natural low-temperature conditions.

9.1.4 Fractured Uranium Deposits

The Tono uranium ore body, located near Tokyo, has been the subject of analogue studies relating to transport of uranium (Miller et al. 2000). The ore body is approximately 3.4 km long; however, the area is tectonically active and between 5 and 10 million years ago, the ore body was split by a fault. This displaced a portion of the ore body 30 m upward. Despite this large fault, many other nearby faults, and the occurrence of frequent tremors, Miller et al. found that no significant uranium transport occurred from the ore body to the adjacent environment. The preferred location for a used fuel repository will be tectonically inactive, providing even greater physical stability and security than seen at this site.

9.2 Analogues for Barriers

The repository design uses multiple barriers, including materials such as iron, copper, and clays to inhibit or prevent movement of radioactive elements and other materials from the facility into the surrounding environment.

9.2.1 Metals

In the current study, used fuel bundles are placed into large, durable containers designed to hold 360 fuel bundles each. For the current reference container design, the inner vessel is made from 100 mm-thick carbon steel which provides the mechanical strength to withstand the pressures of the overlying rock and future glacial loading. The outermost layer of the container is corrosion-resistant copper, 25 mm thick, of which a few mm is required for corrosion

resistance over one million years. The used fuel container prevents water from contacting the used fuel bundles, preventing radionuclides in the fuel from escaping into the underground environment. The used fuel container is engineered to remain intact for at least 100,000 years, and is expected to last much longer, keeping the used fuel completely isolated from the surroundings.

9.2.2 Copper

Copper is one of the relatively few metals that naturally occur in their metallic state. Solid pieces of native copper have been found containing more than 99% copper. The largest known deposit of metallic copper is in the Keweenaw Peninsula of Michigan (Crissman and Jacobs 1982), where large pieces of almost pure copper were either mined or found in glacial outwash. Data from these natural analogues provide copper corrosion rates for both reducing and oxidizing environments, which are useful in assessing the longevity of the used fuel containers.

Copper “plates” found in the mudstones from south Devon (UK) (Figure 9-3) provide a natural analogue for the corrosion of used fuel containers placed in a clay backfill. These copper plates were formed 200 million years ago (lower Jurassic period) and show little corrosion since that time, due in part to the protection of the clay-rich mudstone (Milodowski et al. 2000).



Note: From Milodowski et al. (2000).

Figure 9-3: Copper Analogues

9.2.3 Iron

Recorded use of iron dates to Egypt in 1900 BCE (Miller et al. 2000). Johnson and Francis (1980) studied the corrosion of artefacts under a wide range of environmental conditions and reported annual corrosion ranging from 0.1 to 10 microns.

The large amounts of iron (carbon steel) in the used fuel containers may buffer redox conditions in the repository, preventing oxidizing conditions near the used fuel. The Inchtuthil Roman nails found in Scotland provide an interesting analogue for this. At a Roman fortress that was abandoned in 87 AD (Angus et al. 1962, Pitts and St. Joseph 1985), over 1 million nails were buried in a 5-m deep pit under 3 m of earth. When the nails were unearthed in the 1950s, the nails on the outside of the mass were found to have corroded and formed a solid crust of iron oxides (rust) around the remaining mass of nails. The outside layer of nails formed a sacrificial redox sink, consuming oxygen before it could penetrate to the interior of the mass of nails. The physical expansion of the rust also served to self-seal the remaining nails from intruding groundwater and water vapour. As a result, the nails inside the rusty barrier experienced minimal-to-no corrosion over nearly 2000 years.

Iron (II) minerals provide similar redox buffering in the clays surrounding the Cigar Lake ore body. The outer clay in contact with groundwater migrating past the ore body is a light reddish colour, indicating that the iron in the clay has oxidized. Deeper within the clay, the reddish colour disappears, suggesting that oxygen has been precluded and reducing conditions maintained. The result is a very stable ore body.

9.2.4 Clays

Bentonite (Figure 9-4) is a group of naturally occurring clays. Bentonite swells when exposed to water, minimizing water seepage and making an excellent sealing material when physically confined. It also has a high chemical sorption capacity, able to bind many elements to its crystalline surface, which greatly slows the migration of radionuclides. Bentonite is also very stable, typically formed millions to hundreds of millions of years ago. Clay materials can act as a very robust physical and chemical barrier, as illustrated in the discussion above of Cigar Lake where naturally formed clays acted as a protective barrier for geological time periods.



Note: From EUBA (2011).

Figure 9-4: Bentonite Clay

Bentonite is incorporated into the engineered sealing materials used in the repository. Each used fuel container is surrounded by compacted bentonite clay and all excavated spaces are filled with mixtures of clay, sand, and rock. As the closed and sealed repository is slowly infiltrated by groundwater, the bentonite will swell and fill any remaining void spaces. Radionuclides will only be able to move through the bentonite by diffusion, greatly restricting their migration. In addition, the clay's high adsorption capacity for many elements will significantly inhibit their movement.

The Dunarobba Forest in Italy (Figure 9-5) provides a natural analogue of the effectiveness of clays in minimizing groundwater movement (Benvegnú et al. 1988; Ambrosetti et al. 1992). The sequoia-like Dunarobba trees were buried in clay for 1½ million years. The clay minimized the flow of water to the trees and prevented oxygen from reaching the wood. This maintained reducing conditions around the wood, protecting the wood from bacterial or fungal decay or chemical oxidation. As a result, the trees did not decay. They also did not fossilize -- they are still made of wood.



Note: Retrieved Aug 25 2011 from <http://it.wikipedia.org/wiki/File:Dunarobba.jpg>.

Figure 9-5: 1.5 Ma Sequoia-like Tree Stumps at Dunarobba, Italy

In Canada, similar analogues have been found. During mining of diamondiferous kimberlite deposits in the Northwest Territories near the Arctic Circle and well above the current tree-line, many pieces of well-preserved wood have been recovered from the kimberlite ore and from shale (consolidated clay) deposits in the same region. Fifty million years ago, fragments of logs fell into volcanic ash and became encased as the ash lithified into kimberlite rock. This provided an effective barrier to oxygen and preserved the wood such that its cellular structure and most of its molecular structure remains intact.

9.3 Analogue for Geosphere

The site itself is an important analogue for the future behaviour of the geosphere. In particular, geoscientific evidence of the past history of the site provides a direct analog for future behaviour. This will be gathered for a real site as part of the site characterization, and presented in the geosynthesis. While this is not available for this hypothetical site, the Canadian Shield in general has low seismicity and no volcanism, with evidence that oxygen does not penetrate to any great depth during glaciation.

9.4 Natural Analogue Summary

Performance of repositories cannot be verified by experiment for time scales relevant to their long-term safety. Natural analogues provide qualitative and quantitative illustrations of

long-term behaviour, providing support for key model assumptions and for the identification of processes that need to be represented and those that can be excluded. The natural analogues identified here provide additional understanding of the materials and processes that influence the behaviour of radionuclides in a deep geological repository. They provide confidence in the long-term performance of the repository.

9.5 References for Chapter 9

Ambrosetti, P., G. Basilici, S. Gentili, E. Biondi, Z. Cerquaglia and O. Girotti. 1992. La Foresta Fossile di Dunarobba. Ediart, Todi, Italy.

Angus, N.S., G.T. Brown and H.F. Cleere. 1962. The Iron Nails from the Roman Legionary Fortress at Inchtuthil, Perthshire. *Journal of Iron and Steel Institute* 200, 956-968.

Benvegnú, F., A. Brondi and C. Polizzano. 1988. Natural Analogues and Evidence of Long-term Isolation Capacity of Clays Occurring in Italy: Contribution to the Demonstration of Geological Disposal Reliability of Long-lived Wastes in Clay. CEC Nuclear Science and Technology Report EUR 11896. Luxembourg.

CNSC. 2006. Regulatory Guide G-320: Assessing the Long Term Safety of Radioactive Waste Management. Canadian Nuclear Safety Commission. Ottawa, Canada.

Cramer, J.J. and J.A.T. Smellie. 1994. Final Report for the AECL/SKB Cigar Lake Analog Study. Atomic Energy of Canada Limited Report AECL-10851, COG-93-00147, SKB-TR-94-00004. Pinawa, Canada.

Crissman, D. and G Jacobs. 1982. Native Copper Deposits of the Portage Lake Volcanics, Michigan: Their Implications with Respect to Canister Stability for Nuclear Waste Isolation in Columbia River Basalts beneath the Hanford Site, Washington. Rockwell Hanford Operations Technical Report RHO-BW-ST- 26P. Hanford, USA.

EUBA. 2011. Fact Sheet on Bentonite. The European Association of the Bentonite Producers (EUBA: Member of IMA-Europe). Brussels, Belgium.

Hofmann, B.A. 1999. Geochemistry of Natural Redox Fronts – A Review. Nagra Technical Report NTB 99-05. Wettingen, Switzerland.

IAEA. 1999. Use of Natural Analogues to Support Radionuclide Transport Models for Deep Geological Repositories for Long Lived Radioactive Wastes. International Atomic Energy Agency TECDOC-1109. Vienna, Austria.

Johnson, A.B. and B. Francis. 1980. Durability of Metals from Archaeological Objects Metal Meteorites and Native Metals. Battelle Pacific Northwest Laboratory PNL-3198. Hanford, USA.

McKee, P. and D. Lush. 2004. Natural and Anthropogenic Analogues - Insights for Management of Spent Fuel. Nuclear Waste Management Organization Report APM-REF-06110-24105. Toronto, Canada.

Miller, W., R. Alexander, N. Chapman, I McKinley and J. Smellie. 2000. Geologic Disposal of Radioactive Wastes & Natural Analogues Volume 2. Elsevier/ Pergamon Press. Oxford, UK.

Milodowski, A.E., M.T. Styles and V.L. Hards. 2000. A Natural Analogue for Copper Waste Canisters: The Copper-uranium Mineralised Concretions in the Permian Mudrocks of South Devon, United Kingdom. Swedish Nuclear Fuel and Waste Management Company Report SKB TR-02-09. Stockholm, Sweden.

Pitts, L. and A. St. Joseph. 1985. Inchtuthil Roman Legionary Fortress Excavation 1952-1965. Society for the Promotion of Roman Studies. Britannia Monographs Series 6. London, England.

Tait, J.C., H. Roman and C.A. Morrison. 2000. Characteristics and Radionuclide Inventories of Used Fuel from OPG Nuclear Generating Stations Volumes 1 and 2. Ontario Power Generation Report 06819-REP-01200-10029-R00. Toronto, Canada.

THIS PAGE HAS BEEN LEFT BLANK INTENTIONALLY

10. QUALITY ASSURANCE

10.1 Introduction

This chapter describes how project activities important to safety in the APM Used Fuel Repository Conceptual Design and Postclosure Safety in Crystalline Rock were conducted under an appropriate quality assurance framework.

10.2 Used Fuel Repository Conceptual Design and Postclosure Safety

10.2.1 APM Safety Case Project Quality Plan

The APM Safety Case Project Quality Plan (PQP) APM-PLAN-00120-0002-R002 (NWMO 2012) was prepared by the NWMO Director, Quality Assurance and approved by the Project Manager for use during the preparation of the Used Fuel Repository Conceptual Design and Postclosure Safety in Crystalline Rock. This was an update to the APM Design and Safety Case Update Project Quality Plan (PQP) APM-PLAN-00120-0002-R001 (NWMO 2011a) which was established by the NWMO in 2009. This updated APM Safety Case PQP meets the requirements of both CAN/CSA-N286-05 and ISO 9001:2008.

The quality program applies to all organizational units with responsibilities for the preparation of the Used Fuel Repository Conceptual Design and Postclosure Safety in Crystalline Rock project. The following processes implement the program:

- A managed system consisting of governing documents that prescribe controls and responsibilities to ensure activities are carried out in a quality assured, effective manner by qualified personnel;
- Individual accountability for implementing and adhering to the managed system elements; and
- Evaluation and enhancement of the program elements through continuous improvement processes.

Selected vendors and suppliers are required to be qualified to appropriate quality assurance standards defined by the NWMO. Each of these vendors and suppliers selected is required to submit a detailed quality assurance and inspection plan, consistent with the APM Safety Case PQP, for approval.

The quality program includes provisions for systematic planned audits and assessments designed to provide a comprehensive, critical and independent evaluation of project activities. These audits and assessments cover the overall quality program, sub-tier programs, and interfaces between programs. The audits and assessments monitor compliance with governing procedures, standards and technical requirements, and confirm that quality program requirements are being effectively implemented. Audit and assessment results are documented, reported to and evaluated by a level of management having sufficient breadth of responsibility to assure actions are taken to address the findings.

Additional oversight of activities is provided through regular project monitoring and reporting, self-assessment and the non-conformance and corrective action program. In particular, the

corrective action program assures that non-conformance conditions are identified, documented, reported, evaluated and corrected in a timely manner.

The APM Safety Case PQP is supported by NWMO governance that establishes expectations for engineering and design, safety assessment, procurement, occupational health and safety, environmental protection, product and services approval, document control and records keeping.

The following are key elements of the APM Safety Case PQP:

- Project specific quality objectives are established.
- Each person working on the project is responsible for achieving and maintaining quality and management is responsible for providing adequate resources and evaluating the quality of the work.
- APM project work is performed in accordance with applicable NWMO governing documents and established processes and procedures.
- Specific requirements for design, safety assessment and technical studies involving computer modeling are described.
- All work is conducted by qualified individuals.
- When work within the scope of the APM project is performed by another organization, the consultant/contractor performs work in compliance with ISO 9001:2008 or CAN/CSA-N286-05 as appropriate and in compliance with an approved work specific quality plan and APM project-specific governing documents. When a consultant/contractor provides a specialized technical service, and their quality management system is not based on a recognized system, their quality management system may be accepted if it meets internal quality objectives and requirements.
- APM work is verified via verification processes and procedures. Furthermore for work conducted by contractors, project quality plans are approved and include appropriate verification procedures for deliverables including verification process documentation.
- NWMO APM project personnel have access to observe and verify consultants/contractors' quality processes and examine quality assurance documentation.
- Documents considered to be quality assurance records as per APM-LIST-08133-0001, Quality Assurance Documents (NWMO 2011b), are transmitted into NWMO records.
- Targeted periodic assessments of work are performed on the APM project. Work performed by NWMO project personnel is assessed for compliance with the APM PQP and applicable procedures. Work performed by consultants/contractors and their subcontractors are assessed to confirm that it is being performed in compliance with their work specific quality plans.

10.2.2 Examples of Peer Review and Quality Assurance

Experienced contractors worked with NWMO to carry out the illustrative postclosure safety assessments for the APM project under approved project specific quality plans. The contractors committed to provide high quality work through effective application of a quality system that fostered best practice and included processes for continual improvement. Safety assessments were conducted consistent with NWMO's governance, NWMO-PROC-EN-0003 Safety Assessment Procedure (NWMO 2010a). For this illustrative safety case formally accepted data clearance forms were used between the geosciences, engineering and safety assessment

teams. Software and reference datasets were procured, developed and maintained consistent with NWMO's governance, NWMO-PROC-EN-0002 Technical Computer Software Procedure (NWMO 2010b). NWMO and independent peer review of key results and conclusions in the illustrative postclosure safety assessment was planned by the NWMO and completed. The comments and suggested improvements provided by the independent reviewers have been addressed and incorporated as appropriate into the illustrative safety assessment prior to submission to the regulator.

10.2.3 Future Safety Case Quality Assurance

Once an actual repository site is selected, on-site work will commence to characterize the site in terms of its geophysical and environmental properties. Simultaneously the conceptual design will progress towards the detailed design required for licensing and ultimately construction. The project quality assurance plan will necessarily expand in scope to ensure that the site characterization, detailed design, associated preclosure and postclosure safety assessment and environmental assessment are prepared under a comprehensive and robust quality assurance regime.

10.3 References for Chapter 10

CAN/CSA-N286-05. Management System Requirements for Nuclear Power Plants. Canadian Standards Association. Canada.

ISO 9001:2008. Quality Management Systems Requirements. International Organization for Standardization.

NWMO. 2010a. Safety Assessment Procedure. Nuclear Waste Management Organization Procedure NWMO-PROC-EN-0003. Toronto, Canada.

NWMO. 2010b. Technical Computer Software Procedure. Nuclear Waste Management Organization Procedure NWMO-PROC-EN-0002. Toronto, Canada.

NWMO. 2011a. APM Design and Safety Case Update Project Quality Plan. Nuclear Waste Management Organization Plan APM-PLAN-00120-0002-R001. Toronto, Canada.

NWMO. 2011b. APM Deep Geological Repository Project Quality Assurance Documents. Nuclear Waste Management Organization List APM-LIST-08133-0001. Toronto, Canada.

NWMO. 2012. APM Safety Case Project Quality Plan. Nuclear Waste Management Organization Plan APM-PLAN-00120-0002-R002. Toronto, Canada.

THIS PAGE HAS BEEN LEFT BLANK INTENTIONALLY

11. SUMMARY AND CONCLUSIONS

11.1 Purpose of the Pre-Project Report

As stated in Chapter 1, this report presents an illustrative case study of a postclosure safety assessment methodology applied to examine the long-term safety of a reference multi-barrier deep geological repository design for Canada's used nuclear fuel within a hypothetical crystalline Canadian Shield setting. The purpose of this case study is to present a postclosure safety assessment methodology to illustrate how CNSC expectations, documented in CNSC Guide G-320 (CNSC 2006), subsequently referred to as G-320, are satisfied. Table 1-4 provides links between G-320 and sections of this report.

It should be recognized that this report is not intended to provide a full deep geological repository safety case as described in G-320. Aspects of G-320 that are relevant to this case study are extracted from this guidance document and included in grey 'text' boxes throughout this chapter. This text is intended to be complementary to this summary and to highlight how key aspects of G-320 have been addressed by the postclosure safety assessment methodology. In this regard, the work presented has focused on describing the appropriate selection and application of assessment strategies.

Developing a long-term safety case, G-320 Section 5.0:

Demonstrating long term safety consists of providing reasonable assurance that waste management will be conducted in a manner that protects human health and the environment. This is achieved through the development of a safety case, which includes a safety assessment complemented by various additional arguments...

It is noteworthy that in the context of a postclosure deep geological repository safety case, this illustrative case study does not include a Geosynthesis. The purpose of a Geosynthesis is to provide an understanding of the geosphere proposed to enclose the repository and its evolution as it relates to establishing confidence in a repository safety case. In the absence of a specific site, a hypothetical crystalline site was derived to encompass a range of characteristics that bound those expected in a potentially suitable site. The information was developed to inform the safety assessment on issues regarding strategies for the treatment of system uncertainties.

This summary chapter is intended to highlight the means by which a safety assessment methodology has been applied to evaluate the safety and the associated uncertainty in the performance of a repository for nuclear used fuel in a crystalline setting. The strategy adopted is based, in part, on a defense in depth approach consistent with current international practice. The results of the safety assessment provide useful insight into the performance of the multi-barrier repository design and specific features of the design that could influence long-term performance.

The request for a CNSC review of this repository design and illustrative safety assessment is consistent with the G-320 licensing considerations on determining methodology.

Licensing considerations, G-320 Section 4.3:

It is up to the applicant to determine an appropriate methodology for achieving the long term safety of radioactive waste based on their specific circumstances; however, applicants are encouraged to consult with CNSC staff throughout the pre-licensing period on the acceptability of their chosen methodology.

11.2 Repository System

Section 4 of G-320 identifies several methods for long-term waste management, including surface facilities, near-surface facilities and deep geological facilities. As previously mentioned, this report describes the currently envisioned deep geological multiple barrier repository design for the long-term safe management of used nuclear fuel in a crystalline rock setting. This design and waste management approach is commensurate with the waste's radiological, chemical, and biological hazard to the health and safety of persons and the environment.

The deep geological repository system is described in Chapters 2 through 5 of this report where:

- Chapter 2 describes the hypothetical geosphere setting;
- Chapter 3 describes the characteristics of the used nuclear fuel;
- Chapter 4 describes the repository design concept; and
- Chapter 5 describes how key components of the system will interact with each other and with the environment in the long term.

System description, G-320 Section 7.3:

It is recognized that the system description may be less complete and rigorous early in the licensing lifecycle, and that the information used in long term assessments of safety for the purpose of design optimization or to support an environmental assessment or a licence application may therefore need to use some default or generic data. As licensing progresses through the facility's lifecycle, as-built information and operational data are acquired, and the site characteristics become better understood. It is expected that assessments of long term safety that are made later in the licensing lifecycle will be based on updated and refined models and data, with less reliance on default, generic, or assumed information, resulting in more reliable model results.

These chapters are summarized in this section along with some key parameters that were assessed in this illustrative case study. G-320 recognizes that the system description may be less complete and rigorous early in the licensing lifecycle.

11.2.1 Geologic Description of the Hypothetical Site

Information related to the geologic characteristics of the site necessary to perform the illustrative safety assessment is presented in Chapters 1 and 2. Site characterization activities at a

candidate site would be designed to gather information on a broad range of geologic attributes necessary to support a repository safety case. For the purpose of this illustrative case study several key attributes have been assumed for the site as listed in Chapter 1 (Section 1.6.3.1). Such attributes that normally would be verified through site-specific investigation include:

- The repository is positioned nominally at a depth of 500 m below ground surface;
- The repository is located in an area of low seismic hazard;
- The repository location is not associated with potable groundwater resources;
- The repository location is not associated with economically viable natural resources;
- The groundwater system at repository depth is electrochemically reducing;
- The host rock formation can withstand transient thermal and mechanical stresses; and
- The rates of site uplift and erosion are sufficiently small not to influence the repository.

Specific site characteristics for the case study are described in Chapter 2. In particular, this chapter describes the spatial distribution: geologic, structural, physical and chemical hydrogeologic and geomechanical properties of the rock mass. The selection of these properties has been informed by historic work conducted within the Canadian Nuclear Fuel Waste Management Program. The information presented in Chapter 2 outlines the properties and long-term behaviour of the groundwater system for the reference case site. In addition to the reference case, alternative conceptual models are described with the intent of outlining a range of possible characteristics and properties at a crystalline site. The uncertainty associated with these alternative models is explored through sensitivity, bounding and 'what-if' simulations performed as part of the case study safety assessment.

11.2.2 Used Fuel

The characteristics of the used fuel are described in Chapter 3. The durability of used fuel and distribution of radionuclides within the fuel are identified as characteristics of the multi-barrier system. These characteristics contribute to the low dissolution rate of the fuel and hence the low release rate of radionuclides from the fuel matrix.

11.2.3 Design Concept

Licensing considerations, G-320 Section 4.3:

The design of a nuclear facility should be optimized to exceed all applicable requirements. In particular, a radioactive waste management facility should more than meet the regulatory limits, remaining below those limits by a margin that provides assurance of safety for the long term.

The repository design concept is presented in Chapter 4. As part of the multi-barrier system, two engineered barriers are included in this concept; a copper-shell container and a clay-based sealing system. The design will be further refined and optimized for a licence application. This approach is consistent with G-320, which identifies that the repository facility should more than meet the regulatory limits and remain below those limits by a margin that provides assurance of safety for the long term.

Waste management system, G-320 Section 4.1:

Waste management system for long term storage and disposal of waste refer to the combination of natural and engineered barriers and operational procedures that contribute to safely managing the waste. Long term assessment of these systems can provide information that can be used when making decisions concerning:

- 1. Selection of an appropriate site;*
- 2. Site characterization;*
- 3. Selection of suitable design options during planning;*
- 4. Optimization of selected design(s), including minimization of operational and post-operational impacts; and*
- 5. Development of construction, operation, and decommissioning strategies and plans.*

Key assumptions in this case study include:

- The repository was positioned at a depth of 500 m. In an actual siting process, the repository location and footprint geometry would be designed to improve safety based on site-specific host rock conditions.
- The repository was positioned such that 25 m of intact crystalline rock existed between the emplacement room and a transmissive (10^{-6} m/s) structural feature connected to the ground surface.
- A long-lived container with a 25 mm copper corrosion barrier. Research indicates that 1.3 mm would be sufficient for corrosion protection for 1 million years under reducing conditions. The assumed thicker copper-shelled containers provide a greater margin of safety and facilitate manufacturing and handling.
- Highly compacted low permeability bentonite encloses the containers.
- The low permeability of the sealing systems.

The influence of these design features and their properties on repository performance is explored through the safety assessment summarized in Section 7.12. For example, sensitivity and complementary bounding analyses are used to illustrate the effects of distance to a discrete transmissive fracture (i.e., 10 m), increased container failure, bentonite buffer thickness and buffer sorption.

Chapter 5 describes the repository system, and how key components of the system will interact with each other and the environment in the long term, consistent with the G-320 guidance.

The long-term safety assessment presented in this report provides information that can be used to support and inform future decision making as described in G-320.

11.3 Safety Assessment

A structured approach is used to conduct the postclosure safety assessment where two classes of scenarios are assessed, consistent with Sections 5 and 7 of G-320. More specifically, the expectation to demonstrate the understanding of the system through a well structured, transparent, and traceable methodology is described in this report.

Performing long term assessments, G-320 Section 7.0:

The CNSC expects the applicant to use a structured approach to assess the long term performance of a waste management system. Although long term assessments are done with different levels of detail and rigor for different purposes, the overall methodology for performing them should include the following elements:

- 1. Selection of appropriate methodology;*
- 2. Assessment context;*
- 3. System description;*
- 4. Timeframes;*
- 5. Assessment scenarios; and*
- 6. Development of assessment models.*

The approach uses a systematic scenario identification process that acknowledges the timeframes of interest and that identifies features, events, and processes, which could have an impact on the repository's safety features, as described in Chapter 6. The different assessment strategies, including key assumptions and rationale, are described and complementary indicators are presented in Chapter 7, and summarized in this section.

The **normal evolution scenario** is based on a reasoned extrapolation of the hypothetical site and repository features, events and processes. It accounts for the expected degradation of the site and repository over time, and addresses the effects of anticipated events. The computer models and key assumptions are discussed in Chapter 7 and analyses of impacts are presented for a Reference Case and a range of variant cases in which the effects of changes in physical and chemical conditions are examined.

Disruptive event scenarios examine the occurrence of unlikely events leading to the penetration of barriers and abnormal loss of containment. Chapter 7 presents the methods, assumptions and results associated with the analysis of disruptive events.

Criteria for protection of persons and the environment, G-320 Section 6.2:

The regulatory requirements for protection of persons and the environment from both radiological and non-radiological hazards of radioactive wastes lead to four distinguishable sets of acceptance criteria for a long term assessment:

- 1. Radiological protection of persons;*
- 2. Protection of persons from hazardous substances;*
- 3. Radiological protection of the environment; and*
- 4. Protection of the environment from hazardous substances.*

The results from the normal evolution scenario and disruptive events are compared against interim acceptance criteria in Chapter 7 consistent with the guidance of G-320. Interim acceptance criteria selected to meet the expectations in Section 6 of G-320 were initially proposed to the CNSC for the purpose of the pre-project report for each of the following categories:

- Radiological protection of persons;
- Protection of persons from hazardous substances;
- Radiological protection of the environment; and
- Protection of the environment from hazardous substances.

The interim acceptance criteria are updated in Section 7.1 for this case study.

11.3.1 Assessment Strategies

Use of different assessment strategies, G-320 Section 5.2:

The strategy used to demonstrate long term safety may include a number of approaches, including, without being limited to:

- 1. Scoping assessments to illustrate the factors that are important to long term safety;*
- 2. Bounding assessments to show the limits of potential impact;*
- 3. Calculations that give a realistic best estimate of the performance of the waste management system, or conservative calculations that intentionally over-estimate potential impact; and*
- 4. Deterministic or probabilistic calculations, appropriate for the purpose of the assessment, to reflect data uncertainty.*

Any combination of these or other appropriate assessment strategies can be used in a complementary manner to increase confidence in the demonstration of long term safety.

Key activities are included in the approach to provide relevant information to assess long-term safety, as follows:

- Identify radionuclides that are potentially significant so that subsequent assessments can focus on these radionuclides by completing a screening exercise.
- Conduct 3-dimensional hydrogeological modelling of the groundwater system(s) hosting the repository.
- Perform deterministic and probabilistic calculations of radionuclide transport from fuel to surface. This includes analysis of scenarios, along with sensitivity cases and bounding assessments.
- Estimate dose consequences for a critical group assumed to be farming above the repository.

11.3.2 Modelling Tools and Computer Codes

As discussed in Sections 7.3 and 7.4, appropriate modelling tools and computer codes are applied to assess key aspects of the repository's components and specific scenarios, consistent with the expectations in Section 7.6 of G-320.

The main computer models are FRAC3DVS-OPG v1.3 and SYVAC3-CC4 v4.08. These codes and the reference datasets are maintained under a NWMO software quality assurance system. They are the current generation of codes that have been in use for Canadian repository assessments for many years.

Developing and using assessment models, G-320 Section 7.6:

An assessment model should be consistent with the site description, waste properties, and receptor characteristics, and with the quality and quantity of data available to characterize the site, waste, exposure pathways, and receptors. A systematic process should be used to ensure that the set of data used for developing the assessment model is accurate and representative. Complex models should not be developed if there is not sufficient data to support them. The use of generic or default data in place of site-specific data in developing the conceptual and computer models may be acceptable when there is no site-specific data available, such as in early stages of development; however, with the acquisition of as-built information and operational data, and increased understanding of site characteristics throughout the facility lifecycle, site-specific data should be used.

Confidence in assessment models:

Confidence in the assessment model can be enhanced through a number of activities, including (without being limited to):

- 1. Performing independent predictions using entirely different assessment strategies and computing tools;*
- 2. Demonstrating consistency between the results of the long term assessment model and complementary scoping and bounding assessments;*
- 3. Applying the assessment model to an analog of the waste management system;*
- 4. Performing model comparison studies of benchmark problems;*
- 5. Scientific peer review by publication in open literature; and*
- 6. Widespread use by the scientific and technical community.*

The codes are used in a complementary manner, with FRAC3DVS-OPG providing detailed 3-dimensional flow and transport results for a limited number of cases, and SYVAC3-CC4 extending the results to a broad range of nuclides and sensitivity cases. The simplified SYVAC-CC4 model has been derived from the detailed FRAC3DVS-OPG transport results for I-129, and then verified for other specific radionuclides that represent a range of decay and transport parameters (i.e., C-14, Cl-36, Ca-41, Sn-126, Cs-135, U-238/U-234).

To explore uncertainties arising from variability in the data used in the assessment predictions, SYVAC3-CC4 is also used to carry out a probabilistic safety assessment of the entire repository system. Over 100,000 simulations are performed in which hundreds of input variables are simultaneously varied according to user defined parameter distributions.

11.3.2.1 Key Assumptions and Conservatisms in Modelling***Conservative over-estimates, G-320 Section 5.2.2:***

A conservative approach should be used when developing computer codes and models, and assumptions and simplifications of processes to make them more amenable for inclusion in computer models should not result in under-estimation of the potential risks or impacts.

Chapter 7 describes the key attributes for the Reference Case of the normal evolution scenario. The illustrative assessment presented in this report uses different strategies consistent with expectations in G-320. The assessment of the Reference Case includes the following conservatisms as described in Chapter 8:

- Three containers with undetected defects are assumed in the normal evolution scenario, with the defects present at the time of container placement;
- The defective containers fill with water in the first 100 years;
- No credit is taken for the presence of the fuel sheath in maintaining fuel integrity and in preventing contact of the fuel matrix with water that may enter the container;
- No credit is taken for the effect of hydrogen gas (H₂) (produced by corrosion of the defective container) on the dissolution rate of the uranium oxide fuel (UO₂) fuel;
- No credit is taken for the effect of iron oxides (produced by corrosion of the defective container) in reducing the container internal void volume and providing a high surface area for adsorption of some of the radionuclides released from the fuel;
- No credit is taken for the likely filling of the defect with bentonite and/or corrosion products which could significantly increase the transport resistance;
- Positioning the defective containers in the repository location with the shortest travel time to the surface;
- A 100 m deep well is included in the assessment. It is positioned in the location that maximizes the dose consequence;
- All major fractures extending to depth have high hydraulic conductivity (10⁻⁶ m/s) ; and
- Conservative properties of the critical group (e.g., daily energy need, obtaining all food, fuel, water and building material locally, all drinking and irrigation water taken from the well, etc.).

Since this Reference Case assumes a constant temperate climate, Section 7.10 also discusses the anticipated effects of glaciation on the assessment.

Analyzing uncertainties, G-320 Section 8.2:

A formal uncertainty analysis of the predictions should be performed to identify the sources of uncertainty. This analysis should distinguish between uncertainties arising from:

- 1. Input data;*
- 2. Scenario assumptions;*
- 3. The mathematics of the assessment model; and*
- 4. The conceptual models.*

These conservatisms are further described as part of the approach to assess uncertainties in Chapter 8. The division of uncertainties into scenario, model and data uncertainties is consistent with the guidance of G-320.

11.3.3 Normal Evolution Scenario

Normal evolution scenario, G-320 Section 7.5.1:

A normal evolution scenario should be based on reasonable extrapolation of present day site features and receptor lifestyles. It should include expected evolution of the site and degradation of the waste disposal system (gradual or total loss of barrier function) as it ages.

Depending on site-specific conditions and the timeframe for the assessment, a normal evolution scenario may need to include extreme conditions such as climate shifts or the onset of glaciations.

The normal evolution scenario is based on a reasoned extrapolation of the site and repository, consistent with the expectations in Section 7.5 of G-320. The containers are designed to be durable over very long times, and will be fabricated and placed under careful quality control.

For the Reference Case, the primary dose contributors from the defective containers are determined to be I-129, C-14, and Cs-135. These radionuclides are instantly released from the gap and grain boundary inventory in the fuel. They are relatively long-lived and mobile in the sub-surface environment. Other radionuclides, including actinides in particular, are only released by the very slow dissolution of the fuel and the sorption on the enclosing barrier systems.

Figure 11-1 illustrates how radionuclides from the assumed defective containers are expected to be transported through the system's barriers over time. Two timeframes (i.e., 1,000 years and 100,000 years) are used to illustrate the changes in activity for the following three types of radionuclides:

- I-129 is non-sorbing in the buffer, backfill and geosphere and is therefore expected to eventually be released to the surface biosphere, with a predicted peak contribution to dose occurring at around 100,000 years.
- Ca-41 is an intermediate sorbing fission product that is delayed by the buffer and backfill and hence its release to the surface biosphere is delayed.
- U-238 is strongly sorbing to the buffer and backfill and is never expected to be released to the surface biosphere.

The calculated peak total dose for this case is determined to be about 0.00033 mSv/year and occurs at about 100,000 years. As shown in Figure 7-106, I-129 is responsible for this dose consequence. The dose applies to a person living directly above the repository. It is about 910 times less than the dose constraint of 0.3 mSv/year, and is a small fraction of the average natural background dose.

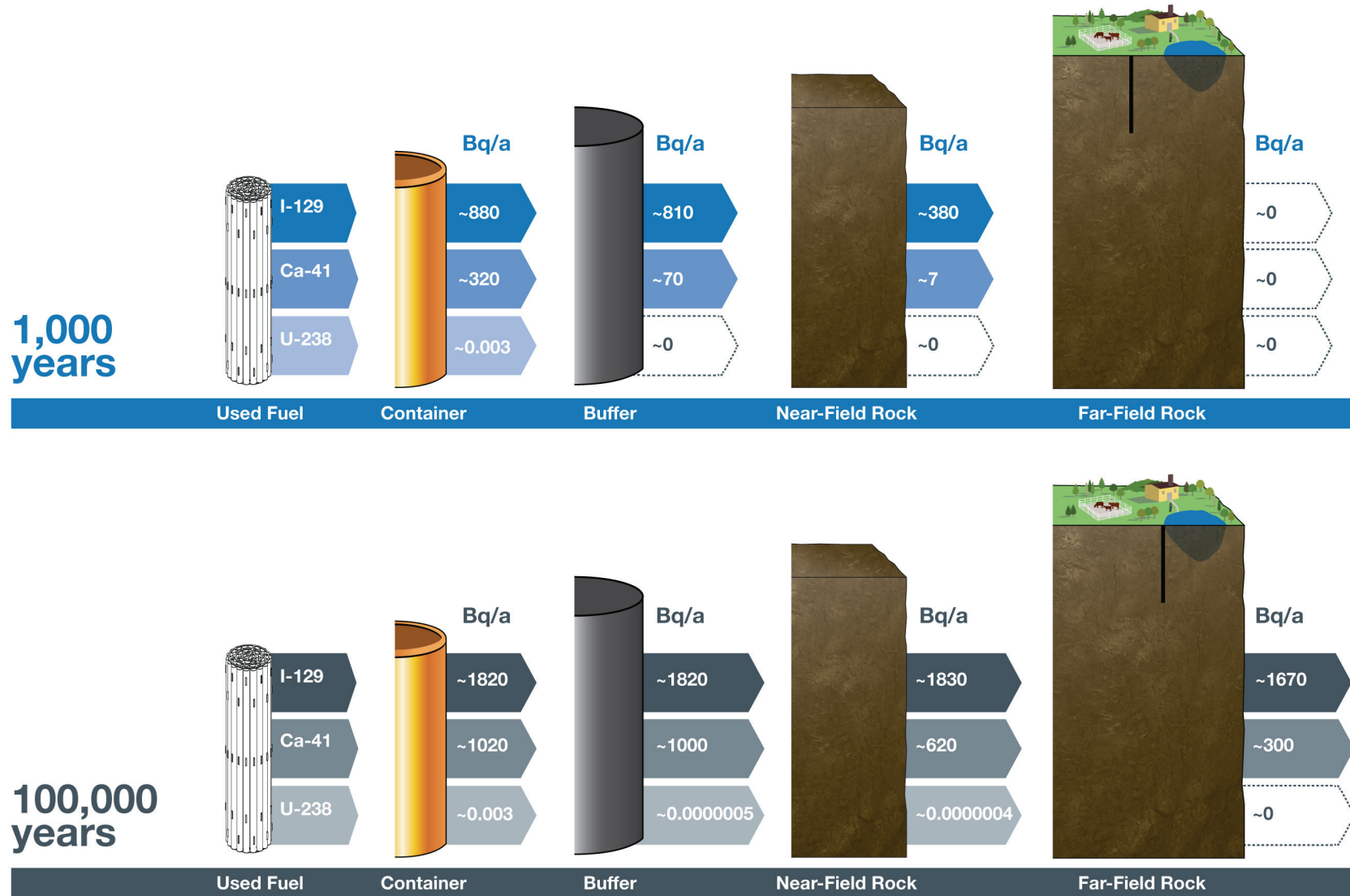


Figure 11-1: Illustration of Radionuclide Transport in the Repository System

11.3.3.1 Results from Sensitivity Analyses and Bounding Assessments

Deterministic calculations, G-320 Section 5.2.3:

The mathematical approach to analyzing the scenarios in the safety case is guided by the purpose of the long term assessment. A deterministic model uses single-valued input data to calculate a single-valued result that will be compared to an acceptance criterion. Variations in input data values are taken into account in these calculations. To account for data variability, individual deterministic calculations must be done using different values of input parameters.

This is the approach used for performing sensitivity analyses (determining the response of model predictions to variations in input data) and importance analyses (calculating the range of predicted values that corresponds to the range of input values) of deterministic models.

To account for the variation in key input data values used in the Reference Case, a number of sensitivity analyses are completed for key parameters as described in Section 7.2. Some parameters are also pushed beyond the reasonable range of variations by setting their values to zero or by removing limits and running a set of bounding assessments, where a specific parameter is completely ignored. The identified parameters, the variation in their values and the rationale for selecting these cases are summarized in Chapter 7, Table 7-3.

A summary of the cases, a comparison against the interim acceptance criterion and the key findings are presented in Table 11-1. This comparison of assessment results with interim acceptance criteria is consistent with the guidance in Section 8 of G-320.

The sensitivity analyses show that the impact on dose is small when key parameters are varied. The sensitivity analysis with the most significant impact on dose is from the dissolution of used fuel. The dose consequence when the fuel dissolution is increased by a factor of 10 is 7.3 times greater than the Reference Case. This remains 130 times below the interim dose acceptance criterion with the peak dose arrival time not materially changed from the Reference Case, i.e., at 100,000 years. Increasing the container defect area is found to have a minimal impact on dose and the impact from increasing the fuel's instant release fraction is negligible.

When the hydraulic conductivity of the rock mass enclosing the repository is varied, the peak dose consequence relative to the Reference Case generally remains the same with the exception of the higher conductivity case. In each of the hydraulic conductivity cases, the peak dose arrival time varies. For the highest case, the peak dose is 2.6 times greater than the Reference Case and occurs at 70,000 years. For the case where the hydraulic conductivity is set 100 times lower than the Reference Case, the peak dose occurs at 1,150,000 years.

Some sensitivity analyses are found to have a negligible impact on dose in this case study and these include: decreasing the distance between the repository and a major fracture, increasing the hydraulic conductivity value of the excavation damage zone, and reducing sorption in the geosphere at the same time as increasing solubility limits.

Table 11-1: Summary and Key Findings from Sensitivity Analyses and Bounding Assessments

Case	Description	Key Findings
Reference Case	Reference Case parameters	<ul style="list-style-type: none"> Peak dose occurs at 100,000 years Peak dose is 910 times lower than normal evolution dose acceptance criterion of 0.3 mSv/a
Degraded Physical Barrier Sensitivity Cases		
Fuel dissolution rate	Fuel dissolution rate increased by a factor of 10	<u>Impact of variation is noticeable</u> <ul style="list-style-type: none"> Peak dose rate occurs at the same time Dose consequence is 7.3 x Reference Case
Container defect area	Container defect area increased by a factor of 10	<u>Impact of variation is minimal</u> <ul style="list-style-type: none"> Peak dose rate occurs at \approx 45,000 years Dose consequence is 2.6 x Reference Case
Fuel Instant Release Fraction	Instant Release Fraction increased to 10%	<u>Impact of variation is negligible</u> <ul style="list-style-type: none"> Peak dose rate occurs at \approx 72,000 years Dose consequence is 1.5 x Reference Case
Geosphere Sensitivity Cases		
Rock conductivity (Sensitivity 1)	Hydraulic conductivity increased by approximately a factor of 10	<u>Impact of variation is negligible</u> <ul style="list-style-type: none"> Peak dose rate occurs at \approx 70,000 years Dose consequence is 2.6 x Reference Case
Rock conductivity (Sensitivity 2)	Hydraulic conductivity decreased by a factor of 10	<u>Impact of variation is negligible</u> <ul style="list-style-type: none"> Peak dose rate occurs at \approx 375,000 years Dose consequence is 0.8 x Reference Case
Rock conductivity (Sensitivity 3)	Hydraulic conductivity decreased by a factor of 100	<u>Impact of variation is minimal</u> <ul style="list-style-type: none"> Peak dose rate occurs at \approx 1,150,000 years Dose consequence is 0.4 x Reference Case
Location of major fracture	Distance from fracture to the repository reduced from 25 m to 10 m	<u>Impact of variation is negligible</u> <ul style="list-style-type: none"> Peak dose rate occurs at \approx 95,000 years Dose consequence is equal to Reference Case
Conductivity of excavation damaged zone	Hydraulic conductivity value increased by a factor of 10	<u>Impact of variation is negligible</u> <ul style="list-style-type: none"> Peak dose rate occurs at \approx 88,000 years Dose consequence is equal to Reference Case
Degraded Chemical Barrier Sensitivity Cases		
Coincident sorption and radionuclide solubility limits	Low sorption in the geosphere with coincident high solubility limits	<u>Impact of variation is negligible</u> <ul style="list-style-type: none"> Peak dose rate occurs at the same time Dose consequence is 1.6 x Reference Case
Bounding Assessments		
Sorption in the geosphere	Sorption in the geosphere is ignored	<u>Impact of variation is significant</u> <ul style="list-style-type: none"> Peak dose rate occurs at \approx 48,000 years Dose consequence is 210 x Reference Case
Radionuclide solubility limits	Radionuclide solubility limits are ignored	<u>Impact of variation is negligible</u> <ul style="list-style-type: none"> Peak dose rate occurs at the same time Dose consequence is 1.2 x Reference Case
Sorption in the near field	Sorption in the near field is ignored	<u>Impact of variation is noticeable</u> <ul style="list-style-type: none"> Peak dose rate occurs at \approx 84,000 years Dose consequence is 19 x Reference Case

As noted above, a set of bounding assessments are included to explore the effects of varying some parameters beyond the reasonable range of variations.

The bounding assessment with the most significant impact on dose is from ignoring sorption in the geosphere. When sorption is ignored, the dose consequence is assessed to be 210 times greater than the Reference Case. This remains 4.4 times below the interim dose acceptance criterion with the peak dose occurring at approximately 48,000 years. There is also a noticeable impact on dose when sorption in the near field is ignored. The dose consequence when sorption in the near field is ignored is assessed to be 19 times greater than the Reference Case. This remains 48 times below the interim dose acceptance criterion and this peak occurs at approximately 84,000 years.

The results from the bounding assessments show negligible impact when radionuclide solubility limits are ignored.

11.3.3.2 Results from the Probabilistic Analysis

Probabilistic calculations, G-320 Section 5.2.3:

Probabilistic models can explicitly account for uncertainty arising from variability in the data used in assessment predictions. Such models may also be structured to take account of different scenarios (as long as they are not mutually exclusive) or uncertainty within scenarios. Probabilistic models typically perform repeated deterministic calculations based on input values sampled from parameter distributions, with the set of results expressed as a frequency distribution of calculated consequences. Frequency multiplied by consequence is interpreted as the overall potential risk of harm from the waste management system.

The results from the probabilistic cases are presented in Chapter 7, consistent with the expectations of G-320 in Section 5.2 on the use of different assessment strategies, where all parameters represented by probability distributions are simultaneously varied. In this case study, relevant parameters for contaminant release and transport were varied whereas the parameters associated with groundwater flow were not.

The 120,000 simulations are performed and examined to identify a 95th percentile peak dose rate. The dose consequence in this case is assessed to be 4 times greater than the Reference Case. This remains 230 times below the interim dose acceptance criterion. The results also show that the peak doses in 5 simulations (i.e., 0.004% of the total) exceed the interim dose acceptance criterion. This is attributed to the use of overly conservative models for some aspects of the calculations. These overly conservative models will be revised in future postclosure safety assessments.

11.3.3.3 Results from Complimentary Indicators

Complimentary indicators of safety, G-320 Section 5.4:

Several other safety indicators, such as those that reflect containment barrier effectiveness of site-specific characteristics that can be directly related to contaminant release and transport phenomena, can also be presented to illustrate the long term performance of a waste management system. Some examples of additional parameters include:

- 1. Container corrosion rates;*
- 2. Waste dissolution rates;*
- 3. Groundwater age and travel time;*
- 4. Fluxes of contaminants from a waste management facility;*
- 5. Concentrations of contaminants in specific environmental media (for example, concentration of radium in groundwater); or*
- 6. Changes in toxicity of the waste.*

Complimentary indicators other than dose to an assumed human group are described in Section 7.11.1. Two indicators considered in this study are:

- Radiotoxicity concentration in a water body, for medium time scales; and
- Radiotoxicity transport from the geosphere, for longer time scales.

The results presented in Chapter 7 show that the indicators are well below reference values. The result for the lake concentration is approximately five orders of magnitude below the reference value and the radiotoxicity transport from the geosphere is approximately six orders of magnitude below the reference value. This provides additional confidence that the impacts of the repository would be very small.

11.3.4 Disruptive Events Scenarios

Disruptive event scenarios, including human intrusion, G-320 Section 7.5.2

Disruptive event scenarios postulate the occurrence of unlikely events leading to possible penetration of barriers and abnormal loss of containment.

Disruptive scenarios are assessed where barriers are assumed to fail due to unlikely failure mechanisms, as described in Section 6.2 of this report and consistent with Section 7.5 of G-320.

Chapter 6 also includes a review of the scenarios considered in assessments of deep repositories in other countries. The results, summarized in Table 6-5 of this report, show that most assessments have identified a limited number of additional scenarios that consider the degradation / failure of engineered and natural barriers by natural processes (e.g., earthquakes, climate change) and human actions (e.g., drilling, poor quality control). Although there are some scenarios identified that are not considered in the current study, these are either not

relevant to a Canadian Shield site or were identified as relevant but not analyzed in this case study.

The scenarios considered in this study and key findings are summarized in Table 11-2.

The peak impacts are determined from simulations performed with either the FRAC3DVS-OPG or the SYVAC3-CC4 codes. The FRAC3DVS-OPG code does not have a biosphere model and therefore its results are presented in terms of I-129 transport to the surface. This provides a reasonable estimate of potential impacts by comparison with the I-129 transport to surface for the normal evolution scenario, since SYVAC3-CC4 simulations show that I-129 dominates the dose consequence, by more than two orders of magnitude at its peak.

Table 11-2: Summary of Key Findings from Disruptive Events

Scenario	Key Findings
All Containers Fail at 60,000 Years	<p><u>Impact is significant</u></p> <ul style="list-style-type: none"> • Peak dose rate occurs at 79,000 years • Dose consequence is 1.7 times below the disruptive events dose acceptance criterion of 1 mSv/a
All Containers Fail at 10,000 Years	<p><u>Impact is significant</u></p> <ul style="list-style-type: none"> • Peak dose rate occurs at 32,000 years • Dose consequence is 1.3 times below the disruptive events dose acceptance criterion of 1 mSv/a
All Container Fail at 10,000 Years in the Geosphere with Higher Hydraulic Conductivity	<p><u>Impact is significant</u></p> <ul style="list-style-type: none"> • Peak dose rate occurs at 17,000 years • Dose consequence is 1.7 times above the disruptive events dose acceptance criterion of 1 mSv/a
Shaft Seal Failure	<p><u>Impact is negligible</u></p> <ul style="list-style-type: none"> • Peak dose rate occurs at 100,000 years • Dose consequence is 3030 times below the disruptive events dose acceptance criterion of 1 mSv/a
Fracture Seal Failure	<p><u>Impact is negligible</u></p> <ul style="list-style-type: none"> • Peak dose rate occurs at 100,000 years • Dose consequence is 3030 times below the disruptive events dose acceptance criterion of 1 mSv/a
Fracture Seal Failure Variant Case (in which all tunnel and room seals are degraded)	<p><u>Impact is negligible</u></p> <ul style="list-style-type: none"> • Peak dose rate occurs at 98,000 years • Dose consequence is 3030 times below the disruptive events dose acceptance criterion of 1 mSv/a

The results from the all container failure scenarios, identified in Table 11-2, indicate that the containers are an important part of the multiple barriers in crystalline rock. The total peak impact is roughly proportional to the number of failed containers (a little less as some containers have long pathways to release). However the peak results are not highly sensitive to the time of container failure beyond 10,000 years. This occurs since the container failure time in both cases is larger than the fission product decay time. The remaining actinides and most of any remaining fission products are retained and delayed in the other engineered and natural barriers so that the peak dose rate does not substantially change between these two cases. The peak results are found to be more sensitive when varying the geosphere hydraulic conductivity at the

same time as having all the containers fail at 10,000 years. When the hydraulic conductivity is increased by a factor of 10, the peak dose occurs at 17,000 years. This result suggests that a candidate site with a hydraulic conductivity of the order of 4×10^{-10} m/s would have the potential to exceed the interim dose acceptance criterion for disruptive events.

The various seal failure scenarios have shown no effect on the predicted dose consequence in this study due to the distance between the containers with undetected defects and the degraded seals.

Disruptive event scenarios, including human intrusion, G-320 Section 7.5.2

Scenarios assessing the risk from inadvertent intrusion should be case-specific, based on the type of waste and the design of the facility, and should consider both the probability of intrusion and its associated consequences. Surface and near-surface facilities (e.g., tailings sites) are more likely to experience intrusion than deep geological facilities.

Scenarios concerning inadvertent human intrusion into a waste facility could predict doses that are greater than the regulatory limit. Such results should be interpreted in light of the degree of uncertainty associated with the assessment, the conservatism in the dose limit, and the likelihood of the intrusion. Both the likelihood and the risk from the intrusion should therefore be reported.

As described in Chapter 7, Section 7.9.1 presents a stylized analysis for the Inadvertent Human Intrusion Scenario. This scenario is a special case, as recognized in Section 7.5.2 of G-320, since it bypasses all the barriers put in place, and therefore the associated dose consequence could exceed the regulatory limit.

The results from the human intrusion assessment show a potential dose to the drill crew of about 1,100 mSv, and to a site resident (i.e., someone farming on the site) of about 1,100 mSv, assuming early intrusion and improper management of the drill site.

This scenario is addressed through making it very unlikely; in part through placing the used fuel deep underground in a geologic setting with low mineral resource potential, poor prospects for potable groundwater resources, and by the use of institutional controls.

The likelihood of this event occurring is roughly estimated as 3×10^{-5} per year, which implies a risk of serious health effects of 2.3×10^{-6} per year. This is significantly less than the annual risk of 7×10^{-5} per year noted in G-320 for stochastic effects associated with the current regulatory limit of 1 mSv per year for dose to members of the public.

11.4 Future Work

The conceptual design and illustrative postclosure assessment presented in this report for a hypothetical site represent a single case study in crystalline rock. Other design concepts and other site conditions have been explored in other Canadian and international case studies.

Since this report is prepared for a hypothetical site and thus is not a full safety case, a number of aspects are not covered in detail. These are noted in Chapter 1. Also, the postclosure safety assessment illustrated the method and approach, but did not assess all scenarios or aspects of relevance for a full safety case (see Section 7.2.4).

There is ongoing work at NWMO to improve our understanding of key processes and uncertainties. These are described in the NWMO RD&D report (Villagran et al. 2011).

11.5 Conclusion

The purpose of the NWMO request for a review of this pre-project report is to obtain CNSC feedback on meeting general overall expectations of CNSC Guide G-320, Assessing the Long Term Safety of Radioactive Waste Management. The current case study work, done at a very early stage in the APM Project, supports the continuing development of a deep geological repository for used fuel in crystalline rock. The current repository design concept and a corresponding illustrative postclosure safety assessment methodology are included for review.

11.6 References for Chapter 11

CNSC. 2006. Regulatory Guide G-320: Assessing the Long Term Safety of Radioactive Waste Management, Canadian Nuclear Safety Commission, Ottawa, Canada.

Villagran, J., M. Ben Belfadhel, K. Birch, J. Freire-Canosa, M. Garamszeghy, F. Garisto, P. Gierszewski, M. Gobien, S. Hirschorn, N. Hunt, A. Khan, E. Kremer, G. Kwong, T. Lam, P. Maak, J. McKelvie, C. Medri, A. Murchison, S. Russell, M. Sanchez-Rico Castejon, U. Stahmer, E. Sykes, A. Urrutia-Bustos, A. Vorauer, T. Wanne and T. Yang. 2011. RD&D Program 2011 – NWMO’s Program for Research, Development and Demonstration for Long-Term Management of Used Nuclear Fuel. Nuclear Waste Management Organization Report NWMO TR-2011-01. Toronto, Canada.

THIS PAGE HAS BEEN LEFT BLANK INTENTIONALLY

12. SPECIAL TERMS**12.1 Units**

a	annum
Bq	becquerel
°C	degree Celsius
cm	centimetre
d	day
dm	decimetre
g	gram
Gy	gray
GPa	gigapascal
h	hour
K	Kelvin
kg	kilogram
kgU	kilogram of Uranium
kJ	kilojoule
km	kilometre
kW	kilowatt
L	litre
m	metre
mASL	metres above sea level
mBGS	metres below ground surface
mg	milligram
Mg	megagram
MJ	megajoule
mL	millilitre
mm	millimetre
mol	mole
MPa	megapascal
mSv	millisievert
mV	millivolt
mW	milliwatt

MW	megawatt
n	neutron (associated with neutron fluence)
nm	nanometre
Pa	pascal
ppm	parts per million
s	second
Sv	sievert
W	watt
wt%	mass percentage
µg	microgram
µm	micrometre
µSv	microsieverts

12.2 Abbreviations and Acronyms

1D	One Dimensional
2D	Two Dimensional
3D	Three Dimensional
AECL	Atomic Energy of Canada
ALARA	As Low as Reasonably Achievable
APM	Adaptive Phased Management
BCE	Buffer Container Experiment
BSB	Bentonite-Sand Buffer
CANDU	CANada Deuterium Uranium
CANLUB	Thin graphite coating between the fuel pellet and the fuel sheath
CC4	Canadian Concept Generation 4
CC	Constant Climate
CCM	Copper Corrosion Model
CEAA	Canadian Environmental Assessment Act
CNSC	Canadian Nuclear Safety Commission
CRT	Container Retrieval Test
C-S-H	In the C-S-H term, the "C" stands for Ca, "S" for Si, and "H" for H ₂ O. The hyphens indicate that no specific solid phases or proportions are implied.
CSA	Canadian Standards Association

DBF	Dense Backfill
DEM	Digital Elevation Model
DFN	Discrete Fracture Network
DGR	Deep Geological Repository
DGSM	Descriptive Geosphere Site Model
EBS	Engineered Barrier System
EBW	Electron-Beam Welding
EDZ	Excavation Damage Zone
Eh	Oxidation Potential
ENEVs	Estimated No Effect Values
EPM	Equivalent Porous Media
ERICA	Environmental Risks from Ionising Contaminants Assessment
FEPs	Features, Events and Processes
FP	Fission Product
FSW	Friction-Stir Welding
GM	Geometric Mean
GSD	Geometric Standard Deviation
HCB	Highly-Compacted Bentonite
HEPA	High-Efficiency Particulate Air
HIM	Human Intrusion Model
HM	Hydromechanical
IAEA	International Atomic Energy Agency
ICRP	International Commission on Radiological Protection
ID	Inner Diameter
Imp	Impurity
LBF	Light Backfill
LGM	Last Glacial Maximum
MIC	Microbiologically Influenced Corrosion
MLE	Mean Life Expectancy
NDT	Non-Destructive Testing
NTS	National Topographic System
NWMO	Nuclear Waste Management Organization
OD	Outer Diameter

O/M	Oxygen/Metal
OPG	Ontario Power Generation
PDF	Probability Density Function
PQP	Project Quality Plan
PWR	Pressurized Water Reactor
RSM	Radionuclide Screening Model
SCC	Stress Corrosion Cracking
SKB	Swedish Nuclear Fuel and Waste Management Company (Svensk Kärnbränslehantering AB)
SSM	Swedish Radiation Safety Authority
STP	Standard Temperature and Pressure
SYVAC3	System Variable Analysis Code
TDS	Total Dissolved Solids
TDZ	Thermal Damage Zone
THM	Thermal-hydraulic-mechanical
TWI	The Welding Institute
UFC	Used Fuel Container
UFPP	Used Fuel Packaging Plant
UofT GSM	University of Toronto Glacial Systems Model
URL	Underground Research Lab
WRA	Whiteshell Research Area